The geothermal activity and geology of the northern sector of the Kenya Rift Valley

British Geological Survey
Research Report SC/93/1
International Series

Kenyan Ministry of Energy

Overseas Development Administration

RESEARCH REPORT SC/93/1

International Series

The geothermal activity and geology of the northern sector of the Kenya Rift Valley

P N Dunkley, M Smith, D J Allen and W G Darling

BRITISH GEOLOGICAL SURVEY

RESEARCH REPORT SC/93/1

International Series

The geothermal activity and geology of the northern sector of the Kenya Rift Valley

P N Dunkley, M Smith, D J Allen and W G Darling

With contributions by H K Andambi, T K Ball, B A Barreiro, A Deino, S J Kemp, J Ndogo, J Ndolo, C C Rundle and N C Sturchio

The report was prepared on behalf of the Overseas Development Administration

Cover illustration
Basaltic maar at Kangirinyang at the southern end of the Suguta Valley, looking south-west. The lake is strongly alkaline and fed by hot springs along its western shores.

Geographic index
Kenya

Subject index
Geothermal exploration, geology, volcanism, hydrogeology

Bibliographic reference
Dunkley, P N, Smith, M, Allen, D J, and Darling, W G. 1993. The geothermal activity and geology of the northern sector of the Kenya Rift Valley. *British Geological Survey Research Report* SC/93/1

ISBN 0 85272 233 8

Keyworth, Nottingham British Geological Survey 1993

BRITISH GEOLOGICAL SURVEY

The full range of Survey publications is available through the Sales Desks at Keyworth and at Murchison House, Edinburgh, and in the BGS London Information Office in the Natural History Museum Earth Galleries. The adjacent bookshop stocks the more popular books for sale over the counter. Most BGS books and reports are listed in HMSO's Sectional List 45, and can be bought from HMSO and through HMSO agents and retailers. Maps are listed in the BGS Map Catalogue, and can be bought from BGS approved stockists and agents as well as direct from BGS.

This report may also be obtained from The Mines and Geological Department, Ministry of Environment and Natural Resources, Nairobi, Kenya.

The British Geological Survey carries out the geological survey of Great Britain and Northern Ireland (the latter as an agency service for the government of Northern Ireland), and of the surrounding continental shelf, as well as its basic research projects. It also undertakes programmes of British technical aid in geology in developing countries as arranged by the Overseas Development Administration.

The British Geological Survey is a component body of the Natural Environment Research Council.

Keyworth, Nottingham NG12 5GG

☎ 0602–363100 Telex 378173 BGSKEY G
Fax 0602–363200

Murchison House, West Mains Road, Edinburgh EH93LA

☎ 031–667 1000 Telex 727343 SEISED G
Fax 031–668 2683

London Information Office at the Natural History Museum, Earth Galleries, Exhibition Road, South Kensington, London SW7 2DE

☎ 071–589 4090 Fax 071–584 8270
☎ 071–938 9056/57

St Just, 30 Pennsylvania Road, Exeter EX4 6BX

☎ 0392–78312 Fax 0392–437505

Bryn Eithyn Hall, Llanfarian, Aberystwyth, Dyfed SY23 4BY

☎ 0970–611038 Fax 0970–624822

Windsor Court, Windsor Terrace, Newcastle upon Tyne NE2 4HB

☎ 091–281 7088 Fax 091–281 9016

Geological Survey of Northern Ireland, 20 College Gardens, Belfast BT9 6BS

☎ 0232–666595 Fax 0232–662835

Maclean Building, Crowmarsh Gifford, Wallingford, Oxfordshire OX10 8BB

☎ 0491–838800 Telex 849365 HYDROL G
Fax 0491–825338

Parent Body

Natural Environment Research Council

Polaris House, North Star Avenue, Swindon, Wiltshire SN2 1EU

☎ 0793–411500 Telex 444293 ENVRE G
Fax 0793–411501

Printed by Saxon Graphics Ltd. Derby

CONTENTS

FIGURES

PLATES

TABLES

ACKNOWLEDGEMENTS

The authors wish to express their gratitude to Mr J K Kinyariro of the Ministry of Energy for his support throughout the project.

Special thanks are extended to Benson Macharia, Paul Mwangi, David Lemu Siwarang and Joseph Kangogo, who provided unstinting support during field work under arduous conditions. The staff of Autair Helicopters Ltd. of Nairobi are gratefully acknowledged for their services, especially Gustav Martin, Captain William Silaa, Major Charles Wachira and the late Tim Ward-Booth. Thanks are extended to Mr and Mrs Art Davis of Orus Mission for their hospitality and for providing hydrogeological information on the Paka area.

Dr R O Fournier of the United States Geological Survey is thanked for advice and comments provided during a technical review of the Project in 1990. Professor R Macdonald and Drs L A J Williams and G J H McCall are thanked for providing unpublished information on Silali.

Paul Turner and Caron Simpson are gratefully acknowledged for drafting the figures for this report.

EXECUTIVE SUMMARY

It is generally recognised that geothermal energy is the least expensive form of electrical power generation available to Kenya, and therefore to meet increases in demand for electricity over the next two decades there are plans for a significant expansion in the country's geothermal power sector. To facilitate this proposed expansion the Government of Kenya has promoted a programme of regional geothermal resource assessment along the length of the Rift Valley to ensure that development is not hampered by a lack of proven reserves.

As part of this regional assessment programme, an exploration survey was jointly undertaken between 1988 and 1992 along the northern sector of the Rift Valley by the British Geological Survey, under the auspices of the Overseas Development Administration of the British Government, and the Ministry of Energy of Kenya. The main objective of this survey was to investigate the geothermal activity of six principal volcanic centres and a number of minor centres between Lake Baringo and Lake Turkana. In addition, reconnaissance surveys were undertaken on the islands and shores of Lake Turkana.

The results of the survey are described in the following report, which is accompanied by five coloured 1:50 000-scale geological maps and five companion geothermal maps of the principal volcanic centres.

The text of the report is divided into sixteen chapters.

Section One defines the objectives of the project and describes the general features of the surveyed area, such as its location, access and climate. Previous geological work in the region is briefly reviewed and the working methods employed by the survey are outlined.

Section Two describes the regional geological setting of the northern sector of the Rift and examines the geophysical and structural controls that have influenced its development.

Section Three provides a detailed description of the geomorphology of the region, relating major physiographic elements and drainage patterns to the underlying structural controls.

Sections Four to Twelve describe the geology and geothermal activity of the volcanic centres of the region. From south to north these are Ol Kokwe Island in Lake Baringo, Korosi, Chepchuk, Paka, Silali, Emuruangogolak, Namarunu, the Barrier Volcanic Complex (BVC), and South, Central and North islands in Lake Turkana.

The inner trough of the Rift between Lake Baringo and Lake Turkana subsided at the end of the Pliocene. In the south of the area a further major phase of subsidence occurred around half a million years ago, and the southern volcanoes of Ol Kokwe, Korosi, Paka and Silali were subsequently constructed along its axis. These are linked by a system of *en échelon* N-trending fractures which developed in an oblique rifting regime. Faulting was associated with basaltic activity and the fracture system is coincident with a positive Bouguer gravity anomaly believed to overlie a dyke swarm. In contrast, the three northern centres of Emuruangogolak, Namarunu and the Barrier Volcanic Complex show more prolonged activity extending from the Lower Pleistocene to historic times.

Regardless of their age and structural setting the volcanic centres show similar styles of evolution and activity. Low-relief peralkaline trachyte shields were constructed at early stages and were subsequently faulted. Later activity has been characterised by the eruption of trachytic lavas and pyroclastic deposits from summit areas, and of basaltic lavas from flank fissures. Subaqueous and phreatomagmatic activity took place in lacustrine environments at the three northern centres during wet palaeoclimatic periods when the inner trough was occupied by the former Lake Suguta.

Calderas formed at late stages in the evolution of four of the centres, and their collapses were triggered by various mechanisms. These include major pyroclastic eruptions at Paka and the Barrier Volcanic Complex, and voluminous flank eruptions of trachyte lavas at Emuruangogolak and basalt lavas at Silali.

Surface geothermal manifestations occur on the upper flanks and summit areas of the volcanic centres and take the form of fumarolic activity associated with hot, hydrothermally altered and steaming ground. The location of the activity is strongly controlled by N to NNE-trending faults and by caldera structures. Where calderas are developed these appear to overlie the upflow zones of the geothermal systems.

Hot springs do not occur on the volcanic centres, although silica sinters testify to former discharges of hot water on the flanks and summit areas of several centres. The radiometric ages of the sinters correlate with pluvial climatic periods when lake levels within the Rift were high. It is concluded that at various stages in the past elevated water tables and the increased availability of meteoric water associated with wetter climates, promoted greater transfer of heat to the surface from the deep, long-lived magmatic heat sources of the volcanic centres. Variations in the intensity and vigour of the geothermal activity within the region is therefore not simply a function of the availability of heat, but is modulated by climatic and hydrogeological conditions.

Section Thirteen describes the main petrological features of the volcanic centres of the region and inferences are made regarding the nature of the intrusive magmatic systems within the centres. It is concluded

that compositionally zoned central trachyte-basalt cupolas or intrusion complexes exist at shallow levels within the volcanoes and these have been periodically replenished by fresh influxes of magma from depth.

Section Fourteen summarises the physical hydrogeology of the region. It is concluded that the regional groundwater flow pattern is a combination of northerly axial flows along the floor of the inner trough as far north as Lake Logipi and lateral flows from the rift margins. Minor axial flow is also directed southwards from Lake Turkana towards Lake Logipi.

Recharge of groundwater occurs from a number of sources. Lateral groundwater flows are recharged from the higher and wetter rift margins. Subsurface outflow from Lake Baringo recharges groundwaters in the floor of the rift, and Lake Turkana also contributes towards recharge beneath the Barrier Volcanic Complex. The analysis of meteorological data also indicates that despite the semi-arid to arid climate of the region, direct infiltration of rainfall on the rift floor is likely to provide local recharge, especially on the higher ground of the volcanic centres themselves. It is concluded that geothermal exploitation on a scale similar to that of the existing geothermal power station at Olkaria would not greatly affect regional water resources.

Estimates of hydraulic properties of aquifers from shallow borehole data suggest that geothermal reservoirs are likely to have low permeability, although regional estimates derived from considering the subsurface outflow from Lake Baringo suggests significantly higher permeabilities.

Section Fifteen describes the chemical and isotopic compositions of the ambient and thermal fluids of the region.

The compositions of ambient spring and well waters within the rift floor indicate that they are mainly fed by meteoric water from the rift margins and the volcanic centres.

Hot springs are widespread along the floor of the inner trough, and important systems at Kapedo and Elboitong have high discharge rates indicating significant heat sources. However, none of the hot springs in the region show compositional evidence of outflow from high temperature geothermal systems, with the exception of minor occurrences on Ol Kokwe Island and Central Island. Instead they are believed to represent waters that have been heated by deep circulation along rift boundary faults.

The chemical composition of steam condensates provides an estimate of the relative strength of the geothermal systems at each volcanic centre. This indicates increasing strength in the order Korosi, Chepchuk, Silali, Kakorinya (BVC), Emuruangogolak and Paka, with Korosi and Chepchuk being very much the weakest systems. Stable isotope compositions of fumarolic steam accords with this, indicating that subsurface condensation takes place at all the centres but is particularly prevalent at Korosi and Chepchuk. The stable isotope compositions of fumarolic steam as far north as Emuruangogolak may be modelled in terms of derivation from a lakewater-meteoric water mixing series, which suggests that the fumaroles of Paka, Silali and Emuruangogolak contain decreasing amounts of lakewater, consistent with a progressive northward dilution of groundwater outflow from Lake Baringo. The stable isotope composition of fumarolic steam from Kakorinya may be modelled in terms of derivation from a mixture of Turkana lakewater and meteoric water from the rift margins, containing up to 40% lakewater.

The application of gas geothermometry is hampered by the general weakness of the fumaroles, although the new methane/ethane geothermometer, developed specifically for use in the East African Rift System, provides plausible temperature estimates. This indicates that Paka, Silali and Emuruangogolak are all associated with high temperature geothermal systems with reservoir temperatures in excess of 300°C. Kakorinya appears to be associated with a lower temperature geothermal system, but still with a maximum estimated temperature exceeding 300°C. Chepchuk and Korosi systems are markedly cooler with average temperatures of around 230°C and 200°C respectively.

Section 16 presents a synthesis of the geology of the region and summarises the main conclusions of the survey. It is concluded that the most important heat sources for the geothermal systems are compositionally zoned trachyte or trachyte-basalt cupolas which occur at shallow levels within the volcanic centres. Those centres that have experienced young trachytic activity and have calderas are considered to have the youngest and largest heat sources. Indications of the strength and temperature of the geothermal systems at depth, based on the chemical compositions of fumaroles, support these assumptions. Dyke-related basaltic activity does not appear to have provided significant long-lived heat sources for the geothermal systems of the region. At best this type of activity provides auxiliary heat sources, which may currently contribute to the heating of low enthalpy spring waters.

As an overall conclusion to the report, the principal geothermal prospects of the region are ranked in order of their considered potential and recommendations are made regarding future exploration strategy.

RANKING OF GEOTHERMAL PROSPECTS

Taking geological, hydrogeological and fluid geochemical criteria into consideration, and ignoring socio-economic factors, the main geothermal prospects of the region are ranked according to their considered potential as follows:

1 Silali
2 Emuruangogolak
3 Paka
4 Kakorinya
5 Korosi
6 Chepchuk

Silali, Emuruangogolak and Paka have high temperature geothermal systems associated with young trachytic

magmatic events, and should therefore be given priority in future exploration. Despite their ranking, there is little to choose between these three prospects and from a purely geological point of view they should be given approximately equal status in future exploration programmes.

Kakorinya is clearly ranked fourth in terms of estimated reservoir temperatures and the age of its youngest trachytic volcanic activity. However, it appears to be associated with a moderately hot geothermal system and is considered worthy of further exploration.

Korosi and Chepchuk have markedly weaker and lower temperature geothermal systems. On Korosi the youngest trachytic activity, which was also the last major phase of volcanism on the centre, occurred about one hundred thousand years ago. Although the geothermal system of Korosi is not vigorous, the area of surface activity is the largest in the region and therefore merits further exploration. Chepchuk is a much older volcanic centre, with an age of at least 1.1 million years, and the nature of its heat source is obscure. The area of surface activity on Chepchuk is small, but some additional exploration is recommended with the initial objective of ascertaining the subsurface extent of its geothermal system.

Namarunu is primarily a Pliocene volcanic centre on which Quaternary volcanic activity has been superimposed. Volcanic activity over the last half million years has been exclusively basaltic, and currently the centre is associated with extremely weak surface geothermal manifestations only. It is therefore considered to be a very poor prospect which does not merit further exploration.

RECOMMENDATIONS

1. On technical criteria it is proposed that all of the volcanic centres of the region merit further exploration, except for Namarunu. Priority should be given to Silali, Emuruangogolak and Paka.

2. Geophysical surveys should be undertaken to investigate broad aspects of the volcano-tectonic models of the volcanic centres. In particular, gravity, low-level aeromagnetic and seismic tomography surveys should be carried out to elucidate the form and nature of the intrusive bodies which provide the heat for the geothermal systems.

3. Detailed geophysical surveys should be carried out on individual prospects to delimit subsurface zones of geothermal activity and hydrothermal alteration. Resistivity methods should be applied wherever possible, although the remoteness of some centres and their extensive cover by young lava fields are likely to place operational constraints on the application of such techniques. In view of this, magneto-telluric and transient electromagnetic surveys should also be carried out to augment resistivity surveys.

4. At present there is an acute shortage of information on hydrogeological conditions under, or near, the main geothermal areas. It is recommended that boreholes be drilled to depths of at least a few hundred metres to obtain information on depth to water tables, temperature, heat flow and rock permeability, and to provide fluid samples for chemical analysis.

The ultimate objective of these proposed geophysical and hydrogeological surveys should be to delimit sites for the drilling of exploration geothermal wells at the most suitable prospects.

1 Introduction

This report describes the geothermal activity and geology of the northern part of the Kenya Rift Valley. It is based on a survey undertaken between 1988 and 1992 by phases II and III of the British Geothermal Energy Exploration Project — a Technical Co-operation project carried out jointly by the British Geological Survey (BGS), under the auspices of the Overseas Development Administration of the British Government, and the Ministry of Energy of the Government of Kenya.

1.1 OBJECTIVES OF THE SURVEY AND ITS ROLE IN GEOTHERMAL ENERGY DEVELOPMENT IN KENYA

In 1985 the first and only geothermal power station in Africa was commissioned at Olkaria, which is situated in the central sector of the Kenya Rift Valley. This has the capacity to generate 45 Mwe, although a second well-field has recently been drilled at Olkaria and sufficient reserves of steam have been proven for an additional 64 Mwe power plant.

Geothermal energy is considered to be the least expensive form of energy available to Kenya for the generation of electricity (Acres, 1987), and because of this there are plans to increase geothermal generating capacity by approximately 450 Mwe by the year 2010 (Gichuru, 1992). To facilitate this proposed expansion the Government of Kenya has promoted a programme of regional geothermal resource assessment along the length of the Rift Valley, to ensure that development is not hampered by a lack of proven reserves.

The first phase (Phase I) of the British–Kenyan geothermal exploration project was undertaken between 1985 and 1987, as part of the regional resource assessment programme. This survey investigated various aspects of the geology, geothermal activity and hydrogeology of the southern and central part of the Rift Valley as described by Allen et al. (1989) and Clarke et al. (1990). Phase I was carried out in collaboration with a more wide ranging geothermal exploration survey conducted by the United Nations Development Programme within the Rift Valley between Lake Magadi in the south and Lake Bogoria in the north.

The main objective of Phase II of the project was to extend the inventory of the Rift Valley's geothermal energy resources northwards from Lake Baringo, with particular emphasis on the four Quaternary volcanic centres of Korosi, Paka, Silali and Emuruangogolak. The work of the project included mapping the geology and geothermal manifestations of the four principal volcanic centres, undertaking regional hydrogeological investigations, and carrying out hydrochemical studies on the geothermal systems within the region. Following a review of this work in late 1990, the project was extended to cover the remainder of the rift to the north. The main objective of this extension, designated Phase III, was to investigate the geothermal potential of the young volcanic centres of Namarunu and the Barrier, and also to undertake regional recon-

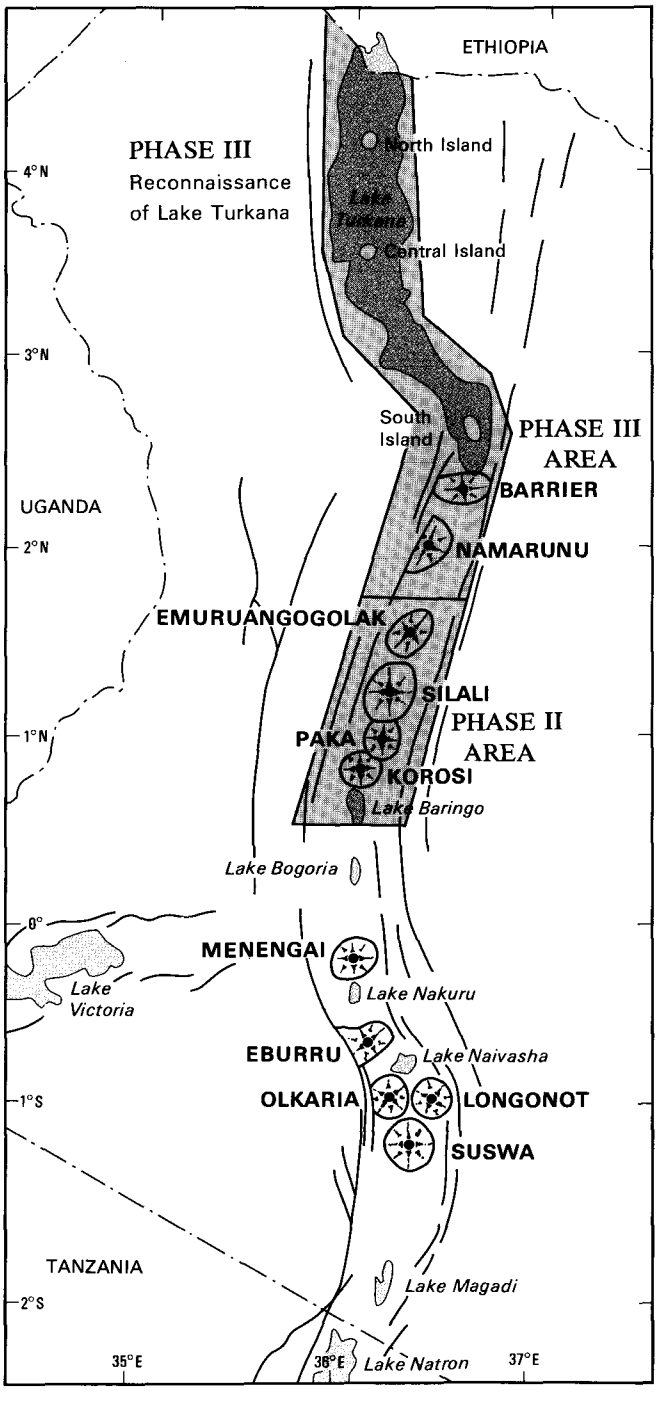

Figure 1.1 Kenya Rift Valley showing the location of major boundary faults, lakes and young volcanoes, and the location of the project area.

naissance surveys on the shores and islands of Lake Turkana.

A series of 1:50 000-scale geothermal maps and corresponding geological maps are enclosed at the back of this report. These cover the volcanic centres of Korosi-Paka, Silali, Emuruangogolak, Namarunu and the Barrier, and should be studied in conjunction with the relevant chapters of the report.

1.2 LOCATION OF THE SURVEYED AREA

The mapped area extends from the southern shores of Lake Baringo, at latitude 0°30' N, to the southern shores of Lake Turkana at latitude 2°30'N, and is confined principally to the inner trough of the Rift Valley, encompassing an area of approximately 7600 km^2.

The southern part of the area falls within the Baringo District, and the northern part within the Turkana and Samburu Districts of the Rift Valley Province. The area is sparsely populated. Kampi-ya-Samaki, on the western shores of Lake Baringo, is the largest settlement in the area, and further to the north there are small centres of population at Loruk, Nginyang, Chemolingot, Tangulbei, Churo, Kapedo and Lomelo. In the northern half of the area there is only one small mission station at Parkati, although there are important administrative settlements to the east of the rift at Baragoi and Maralal, and to the west at Lokori. The dominant ethnic groups within the region are the Pokot in the south and the Turkana in the north, both of which lead semi-nomadic existences. In the north of the area the Samburu occupy the eastern shoulder of the rift, and in the south the Njemps are found around the eastern shores of Lake Baringo and the Tugen around the south-western shores.

1.3 ACCESS

A good tar-sealed road provides access from Nakuru to the southern part of the area (Figure 1.2). This road skirts along the western shores of Lake Baringo and at the settlement of Loruk, situated at the north-west corner of the lake, the tar-seal ends and the road branches. One branch continues northwards as a poorly maintained dirt road which passes along the western side of the rift floor through Nginyang, Kapedo and Lomelo, and provides access via several poorly-defined and rough tracks to the low ground between the volcanic centres within the rift. The other branch is a good murram road which passes around the eastern side of Korosi to Tangulbei and then ascends out of the rift to join the main Nyahururu-Maralal road at Sukuta Mugie. The road from Nyahururu provides access along the high ground to the east of the rift and passes through Maralal and Baragoi to Loiyangalani on the south-east shores of Lake Turkana. From Baragoi there are two very rough tracks into the rift. One of these passes through the settlements of Tum and Parkati and leads to the eastern side of the Barrier volcano. The other track descends into the rift via the Gates of Samburu and from there it is possible to cross the floor of the rift and join with tracks from Lomelo and Lokori, although the route is very poorly defined

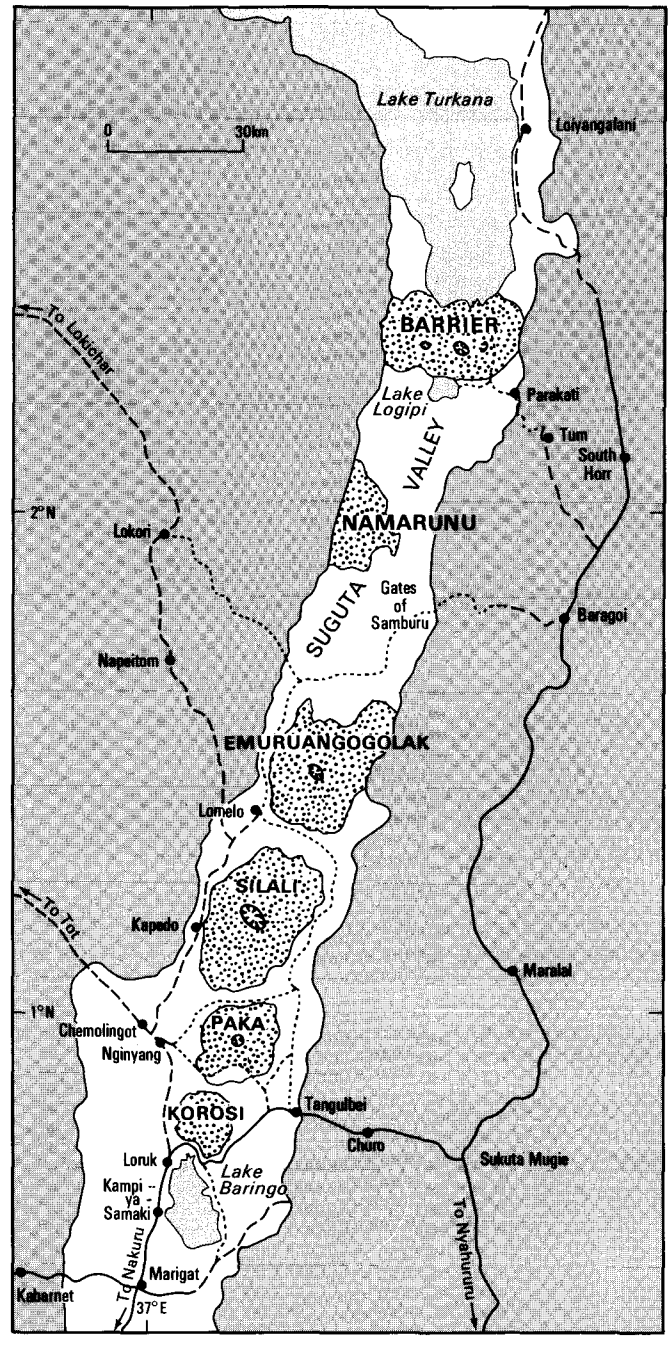

Important road (mostly dirt)

Poorly maintained dirt road

Bush tracks (dry weather only)

Settlement

Figure 1.2 Map of the northern sector of the rift, showing settlements, roads and tracks.

and is prone to be obscured by wind-blown sands and shifting braided river courses that are liable to flash-flooding.

All of the dirt roads and tracks become impassable during wet weather and are liable to be cut by flooded rivers. Off-the-road driving conditions for four-wheel drive vehicles are at best difficult, and in the northern part of the area are hazardous and should only be attempted during dry weather.

1.4 CLIMATE

Along the floor of the Rift Valley the climate varies from being semi-arid in the south to arid in the north, with mean annual rainfall ranging from about 650 mm around Lake Baringo to less than 200 mm around Lake Turkana where desert conditions prevail. The high ground to the west of the rift is wetter but also shows a marked decrease in precipitation northwards, with mean annual rainfall exceeding 1300 mm on the Kamasia Range decreasing to less than 300 mm at Lokori. Mean annual rainfall is lower on the high ground to the east of the rift and also decreases in a northerly direction from approximately 850 mm in the south to about 500 mm in the north around Baragoi. Rainfall is distinctly seasonal. In the south of the area two rainfall maxima occur around April and August and there is a dry season from September to March. In the north of the area the August maximum is not apparent and November is the wettest month.

Maximum daytime temperatures along the floor of the rift generally range from 30–35°C in the south up to about 45°C in the north, but are reported occasionally to reach more than 50°C in the northern part of the Suguta Valley. The higher areas to the east and west of the rift are cooler than the adjacent floor but also show increases in temperature northwards.

More detailed information on the climate of the region is provided in Section 14.2.

1.5 PREVIOUS GEOLOGICAL WORK

Some of the earliest systematic geological investigations were undertaken in the north of the area by Baker (1963) and Dodson (1963) of the Mines and Geology Department. They largely confined their surveys to the eastern margin of the rift in the Baragoi and South Horr areas, although Dodson's work also covered the Barrier volcano.

The geology of large parts of the northern sector of the Rift Valley was investigated in the late 1960's and 1970's by a number of research students working under the auspices of the East African Geological Research Unit (EAGRU) based at Bedford College, University of London. The results of this research is described in a series of Ph.D. theses (Martyn, 1969; Chapman, 1971; Webb, 1971; Carney, 1972; McClenaghan, 1972; Weaver, 1973; Sceal, 1974; Truckle 1977a and Golden, 1978) and was published in several geological maps at a scale of 125 000 (Chapman et al., 1973; Truckle, 1977b, 1979a and 1979b). At about this time, McCall of the Mines and Geology Department surveyed parts of Silali and the results of this were published in several papers (McCall, 1968a; McCall and Hornung, 1972) and incorporated into the EAGRU maps. As part of the EAGRU project, Rhemtulla carried out reconnaissance geological work to the north of Emuruangogolak, the findings of which were published as one of a collection of papers resulting from a Royal Geographical Society expedition to the South Turkana area (Rhemtulla, 1970). A considerable number of radiometric dates were also determined during the course of the EAGRU project and those covering the southern part of the region were compiled in a paper by Chapman and Brook (1978).

Between 1980 and 1986 a regional geological survey was undertaken over a large part of north-eastern Kenya by the Samburu–Marsabit Geological Mapping and Mineral Exploration Project, a joint technical co-operation project carried out by the British Geological Survey and the Mines and Geology Department of Kenya. Although the northern part of the Rift Valley fell within the Samburu–Marsabit project area no fieldwork was actually carried out in this ground, but the results of the EAGRU work on the rift were collated and incorporated into the project's reports and maps which were published at a scale of 1:250 000. Of specific interest to the present survey are the maps and reports for the areas of Baringo–Laikipia (Hackman, 1988), Maralal (Key, 1987) and Loiyangalani (Ochieng' et al., 1988), which provide a useful synopsis of the regional stratigraphy of the rift margins.

Since the late 1960's a considerable amount of geophysical research has been undertaken in the northern part of the Rift Valley to investigate its deep structure (Section 2). Of particular importance is a long-term programme of seismic research which was instigated by the University of Leicester in the 1960's and has been joined in recent years by researchers from Germany, France, Kenya and the United States to become known as the Kenya Rift International Seismic Project (KRISP). The earliest seismic refraction survey was carried out along the axis of the rift between Lake Bogoria and Lake Turkana in 1968 by Griffiths et al. (1971), and this indicated the presence of high velocity material within 3 km of the rift floor and a crustal thickness of 18.5 km. In 1975 seismic refraction studies were undertaken along a short line extending from Lake Baringo westwards across the Kamasia Range (Tugen Hills) to the Kerio Valley, with a view to confirming the presence and lateral extent of the high velocity material and to provide a control for the interpretation of gravity data (Swain, 1979; Swain et al., 1981). KRISP85 confined its experiments to the central and southern parts of the rift, extending as far north as Lake Baringo, and indicated a much greater crustal thickness along the axis of the rift than was deduced by the earlier studies to the north of Lake Baringo (Henry et al., 1990). To reconcile this discrepancy a major seismic refraction experiment was conducted in 1990 by KRISP90, and preliminary interpretations of the data confirm that the crust does in fact thin along the axis of the rift to the north of Lake Baringo (KRISP Working Group, 1991).

In addition to seismic refraction experiments, the University of Leicester has also undertaken several microseismic monitoring programmes in the northern part of the rift (Pointing et al., 1985; Young et al., 1991; Toungue and Maguire, in press), as well as gravity surveys by Khan and Mansfield (1971), Swain (1979) and Swain et al. (1981).

An EEC sponsored aeromagnetic survey was undertaken in 1987 for the National Oil Corporation of Kenya by Compagnie Generale de Geophysique (CCG, 1987). Although the entire rift was surveyed, interpretation of the results only covers the southern part of the project area as far north as 1°N. The main purpose of this survey was to locate target areas for geothermal exploration, by trying to find magnetic anomalies with signatures similar to the producing geothermal field at Olkaria (which has a negative anomaly). Only one such target anomaly was discovered in the entire area

surveyed by CCG. This occurs on the rift margin to the south-east of Lake Baringo and by virtue of its position is considered to be unprospective for geothermal energy.

Heat flow measurements were made by Morgan (1973) on boreholes drilled for water at Chemolingot, Tangulbei and in the low ground between Paka and Silali, the results of which are discussed in Section 2.2 and Section 14.7.

1.6 WORKING METHODS OF THE PROJECT

The two southernmost volcanic centres of Korosi and Paka were surveyed during the first year of the project by foot traverses supported by vehicular access. In the second and third years the larger and more remote volcanoes to the north were mainly surveyed with the support of helicopters.

Detailed photogeological interpretations of the volcanic centres were carried out prior to field work and these formed a basis for geological and geothermal survey work on the ground. During the course of field work, surface geothermal manifestations were located and mapped, and temperatures were measured with digital thermometers. Because of the low humidity and high air temperatures of the area, steam is rarely visible from a distance. Geothermal areas were therefore recognised from afar by the presence of hydrothermal alteration, which gives rise to reddened and bleached ground, and by marked changes in vegetation. Of particular assistance was the distinctive sedge *Abligaardia lispidula*, which colonises all the geothermal areas as far north as Emuruangogolak. In the more arid ground to the north this sedge was nowhere seen, and therefore the location of geothermal areas on Namarunu and the Barrier volcano depended entirely on the recognition of hydrothermal alteration.

After completing each phase of field work the air photographs were reinterpreted in the light of information gained on the ground, and geological and geothermal manuscript maps were then compiled on topographic base maps at a scale of 1:50 000. Landsat Thematic Mapper images were also used to assist with the interpretation of air photographs, particularly with respect to the delineation of large-scale structures.

Samples of representative lava types were collected from each volcanic centre for major and trace element chemical analysis, and for the preparation of microscope thin sections. The chemical analyses were used to classify rock types using the TAS system (Le Bas et al., 1986). Samples of hydrothermal alteration products were also collected for mineralogical analysis which was carried out at the laboratories of the BGS (Kemp, 1989 and 1990).

A comprehensive programme of radiometric dating was undertaken after the geological mapping had been completed, with the objective of dating the main events in the evolution of each of the volcanic centres. Most of the samples were dated at the Institute of Human Origins in Berkeley using the single-crystal laser-fusion $^{40}Ar/^{39}Ar$ technique described by Deino and Potts (1990). Some samples were also dated by $^{40}Ar/^{39}Ar$ step-heating and other ages were determined by the K/Ar method. Silica sinters deposited by former hot spring systems were also dated using the U-series methods of Sturchio and Binz (1988) at the Argonne National Laboratory, Illinois (Sturchio et al., 1993).

Systematic hydrochemical studies were carried out on completion of each stage of the primary mapping survey. Steam condensates and gases were collected from fumaroles, and water samples were collected from hot and cold springs, lakes, rivers and rainfall. Chemical and stable isotope analysis of the samples was undertaken at the BGS laboratories at Wallingford. In a parallel study, all the available hydrogeological, hydrological and meteorological information was compiled as part of an investigation into the physical hydrogeology of the region. The results of the hydrochemical and hydrogeological investigations have been integrated in order to gain an understanding of the nature and source of the fluids within the geothermal systems of the region, and of the cool ambient waters recharging these systems.

2 Regional structure and stratigraphy of the northern sector of the Kenya Rift

2.1 INTRODUCTION

The Kenya Rift is an integral part of the East African Rift System which extends for over 3000 km from southern Mozambique through Tanzania, Kenya and Ethiopia to join the Red Sea and Gulf of Aden rifts at the Afar triple junction (Figure 2.1). It is regarded as one of the best examples of an incipient or early stage in the formation of a constructive plate margin.

The Kenya Rift straddles a local region of crustal upwarping, about 1000 km in diameter, termed the Kenya Dome. Based on the recognition of a series of sub-volcanic erosional surfaces in eastern Kenya early workers postulated up to 1800 m of uplift for the Kenya Dome (Baker et al., 1972). Although much of the topographic expression of the dome is due to the construction of large volcanic edifices in the vicinity of the rift (e.g. King, 1978), long wavelength Bouguer gravity and apatite fission-track studies (Bechtel et al., 1987; Wagner et al., 1992) confirm the existence of a crustal dome, albeit on a much smaller scale (<500 km in diameter) than previously thought. There is no evidence to support the 1500 m of Pliocene uplift advocated by the early workers. The attitude of the basement-cover contact, the radial disposition of early Miocene flood lavas (Smith and Mosley, 1993) and studies of palaeo-drainage patterns (King, 1978) indicate that the formation of this dome largely preceded volcanism and rifting.

2.2 LITHOSPHERIC STRUCTURE AND HEAT FLOW

To account for the dome and its associated geophysical anomalies Baker and Wohlenberg (1971) proposed a model which has formed the basis for subsequent examinations of the lithospheric structure beneath the Kenya Rift. Their model and the early gravity studies of Fairhead (1976) and Swain et al.

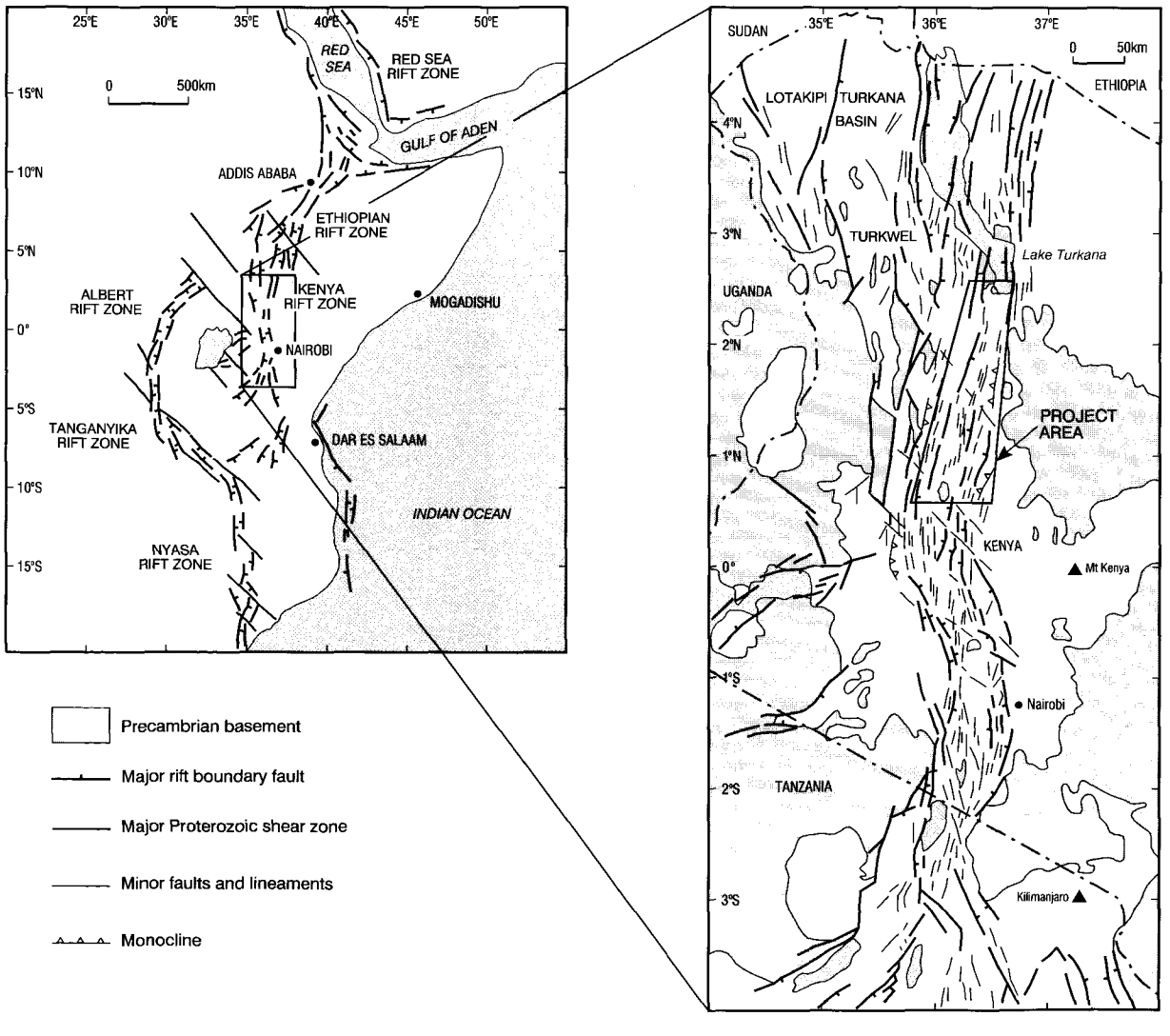

Figure 2.1 Location of project area and simplified structural map of the Kenya Rift.

(1981) indicate the presence of an axial intrusion along the line of the inner trough of the rift. This intrusion was considered to represent asthenospheric mantle intruding the crust, thereby implying that the process of rifting involved crustal separation (e.g. Mohr, 1987). However, more recent seismic refraction data obtained by the Kenya Rift International Seismic Project (KRISP, 1987; Henry et al., 1990) do not support this model. P-wave velocities beneath the rift do not indicate an axial intrusion near the base of the crust, although a model involving basaltic dyke intrusion within the basement rocks is not precluded. Instead a model involving normal, albeit thinned crust under the rift with replacement by layered igneous material is postulated. By analogy with other continental rifts the presence of a high velocity layer at about 22 km beneath the rift is interpreted as a mid-crustal magma body (Henry et al., 1990). Teleseismic delay times (Savage and Long, 1985; Dahlheim et al., 1989; Green et al., 1991) and electrical conductivities (Banks and Beamish, 1979) combine to show that at deeper levels (>35 km) the Kenya Dome is intimately associated with an anomalous low velocity and low density zone in the sub-crustal lithosphere. This anomalous zone is narrow and steep sided and considered to be a diapir or plume of asthenospheric melt forcibly intruded into the lithosphere.

Crustal thicknesses vary markedly both across and along the length of the rift. Seismic refraction data indicate that in the southern part of the project area crustal thickness varies from 42–44 km beneath the rift flanks to about 34 km beneath the rift floor. This implies only moderate amounts of crustal thinning, which is supported by estimates of surface extension of 8–10 km (King, 1978) and by the small amounts of partial melt required by interpretation of the geophysical data (Dahlheim et al., 1989). The most recent data from KRISP (1991) (Figure 2.2) indicate that in the Turkana area and under most of the northern part of the Kenya Rift, crustal thicknesses vary from 18 to 20 km. This contrast in crustal thickness between north and south is thought to relate to the nature of the lithosphere beneath the rift. Smith and Mosley (1993) argue that the margin of the Tanzanian craton was refoliated and buried during the Pan-African orogeny and lies some 100 km east and north-east of the exposed outcrop of Archaean rocks, beneath the central part of the Kenya Rift. The junction between the cold and mechanically rigid cratonic crust and thinned mobile-belt crust is marked by a major NW-trending Precambrian shear zone which passes immediately to the south of the surveyed area.

At present, knowledge of heat flow patterns and geothermal gradients within the Kenya Rift is limited. The available data, summarised in Battici (1987), Nyblade et al. (1990) and Wheildon et al. (in press) are mainly concentrated between latitudes 1°N and 1°S and indicate that the highest heat flow (>75 mW/m^2) is spatially associated with the Quaternary volcanism, faulting and geothermal activity of the inner trough. Heat flow values on the eastern and western rift flanks are low (40–60 mW/m^2) and typical of African mobile belt terrains. The absence of a broad surface heat flow anomaly suggests that at present heat transfer into the crust is accomplished by magmatic convection related to a narrow lithospheric-asthenospheric source located beneath the central part of the rift. This is supported by the relatively young tectonic development of the rift, the published apatite fission track data (Bechtel et al., 1987) and the lithospheric

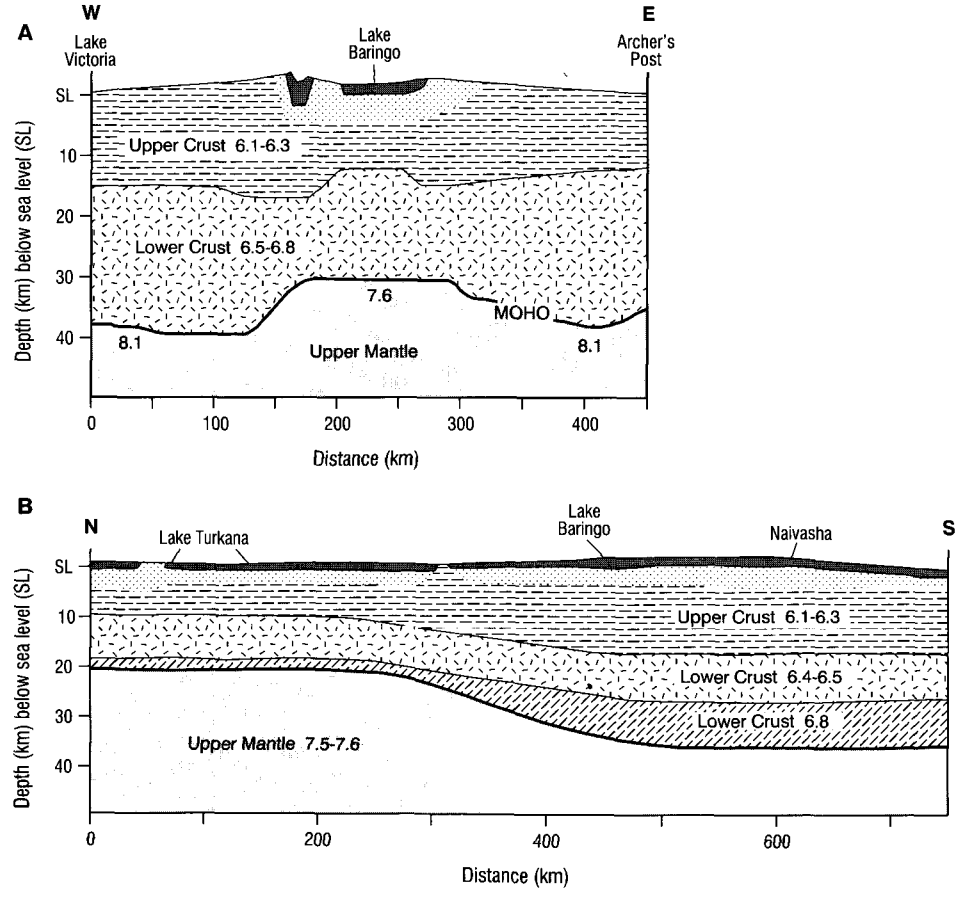

Figure 2.2 Schematic velocity models for (a) the cross profile and (b) the axial profile along the Kenya Rift, after KRISP, 1990 and Keller et al. (1992). Velocities are shown in kilometres per second.

seismic anomalies. Thermal conduction time constants (Wheildon et al., in press) suggest that this process is relatively young and that the age of heating of the mantle at the moho may be no older than 10 Ma.

2.3 STRUCTURAL OUTLINE

The Kenya Rift consists of a linear graben structure which extends for 900 km from the Turkana depression in the north to the central Tanzanian plateau in the south (Figure 2.1). In the north and south it passes laterally into 250 km wide zones of splayed, faulted and tilted blocks. Although morphologically similar, initiation of rifting in these two zones took place at markedly differing times. Rifting between 2°N and 5°N extends back into Upper Oligocene times (Morley et al., 1992), whereas in northern Tanzania rifting only commenced in Pliocene times.

Variations in orientation and contrasting styles of morphology, volcanism and structure conveniently subdivide the Kenya Rift into three main graben sectors. The project area lies within the northern graben sector and is dominated by N and NNE-trending structures (Figure 2.3). Summaries of the tectonic evolution and fault patterns of parts of the project area are contained in Hackman (1988) and Key (1987).

The northern sector of the Kenya Rift displays marked changes in structural style along its length. At the latitude of Baringo (0°35'N) it is an asymmetric deep graben structure with a double western margin delineated by the Elgeyo and Saimo boundary faults (Figure 2.4a) (Chapman et al., 1978; Morley et al., 1992). Exposures of Precambrian gneisses in the footwalls of both these faults combined with a thick westerly-dipping sequence of sediments and volcanics and a large negative (-200 mgl) Bouguer gravity anomaly in the hanging wall indicate substantial vertical displacements. Estimates of the displacement on the Elgeyo fault range from 3–9 km depending on how the gravity anomaly is modelled. Recently, Swain (1992) has suggested that the anomaly could represent a granitic intrusion at depths of around 5 km.

In contrast, the eastern margin at the latitude of Lake Baringo is cut by a zone of distributed faulting up to 20 km wide, characterised by anastomosing *en échelon* synthetic and antithetic faults. These faults delineate a series of horst and graben and back tilted fault blocks connected by low-angle ramps. No basement rocks are exposed and cumulative displacements are uncertain, but throws of up to 1500 m occur on the larger faults (Carney, 1972). Immediately east of Lake Baringo a broad tilted platform, the Mukutan platform, is delineated by the Karau and Aruru faults (Figure 2.3). Similarly, east of the Saimo fault the outcrop of Pliocene basalts define a broad arch or anticlinal structure, the Kaparaina Arch, which is cut by a dense swarm of dykes and normal faults. The Karau fault and the eastern margin of the Kaparaina Arch define the limits of an inner trough.

To the north, at the latitude of Silali volcano (1°20'N) the rift margins display a gradual change in structural style (Figure 2.4b). The boundary faults along the western margin lose their topographic expression and with decreasing displacements pass laterally into broad symmetrical arches and asymmetrical anticlinal flexures with steep east-facing limbs. Similarly on the eastern margin the complex pattern of faulting passes northwards into a major west-facing monoclinal downwarp, the Samburu Monocline (Shackleton, 1946; Baker, 1963). The hinge of this monocline lies near to the crest of the present day rift margin and is marked by a change from flat-lying to westerly dips (locally up to 45o) within Miocene and Pliocene strata. The steep limb of the monocline is intensely faulted and locally offset by NW-trending structures. Landslipping is widespread and further north is an important feature of both rift margins. At the northern end of the Suguta Valley the rift margins are no more than 7 km wide and take the form of gentle downwarps characterised by tilted strata, extensive landslips and tensional faults (Figure 2.4). Displacements on individual faults are not large.

The change in structural style along the rift margins is also reflected in the patterns and width of faults in the inner trough. At the latitude of Lake Bogoria the inner trough is 70 km wide and broken up by a dense array of closely spaced faults. Northwards, this faulting is lost beneath the alluvium south of Lake Baringo. The main zone of tectonism than passes through Lake Baringo before transferring eastwards across the rift floor via an *en échelon* array of normal and oblique-slip faults. Between Paka and Emuruangogolak volcanoes the inner trough is fractured by a 12 km wide zone of complexly linked normal faults. This zone is slightly oblique to the regional trend of the rift margins. North of 2°N the inner trough narrows to less than 30 km, and where exposed, faulting is restricted to narrow linear zones associated with the most recent volcanism. The inner trough is also spatially associated with a pronounced positive Bouguer gravity anomaly and high seismic velocities (6.0–6.1 km/s) indicating high density rocks at depth. These anomalies may be explained by a model in which the whole of the inner trough is underlain by Precambrian basement intruded by a swarm of basic dykes (KRISP, 1987; Swain, 1992).

2.4 INFLUENCE OF BASEMENT STRUCTURES

The basement of the area consists of gneisses, schists and metasediments of the 'Mozambique-Belt' of Pan-African age (Key, 1987; Hackman, 1988). The tectonic grain of these rocks is predominantly NNE–SSW and broadly parallels the rift structures. NW and ENE-trending structures are also important though less well understood. The importance of NW-trending basement structures during the evolution of the Kenya rift has been demonstrated by Smith and Mosley (1993). In particular, these authors emphasise the control exerted by a number of widely spaced ductile-brittle shear zones which effectively segment the rift into its component graben sectors and control the location of the main accommodation or transfer zones in the Cenozoic cover rocks.

In the vicinity of Baringo the major boundary faults (Elgeyo and Saimo) may root down into older Proterozoic NNE and N-trending thrust structures. Further north the location of downwarps and monoclines is spatially related to the faulted margins of upstanding basement blocks. The Cenozoic sediments and volcanic rocks are deformed into a series of drape folds above the margins to these blocks. The influence of NW-trending structures in the surveyed area is at present unclear. The Lake Baringo basin is bounded

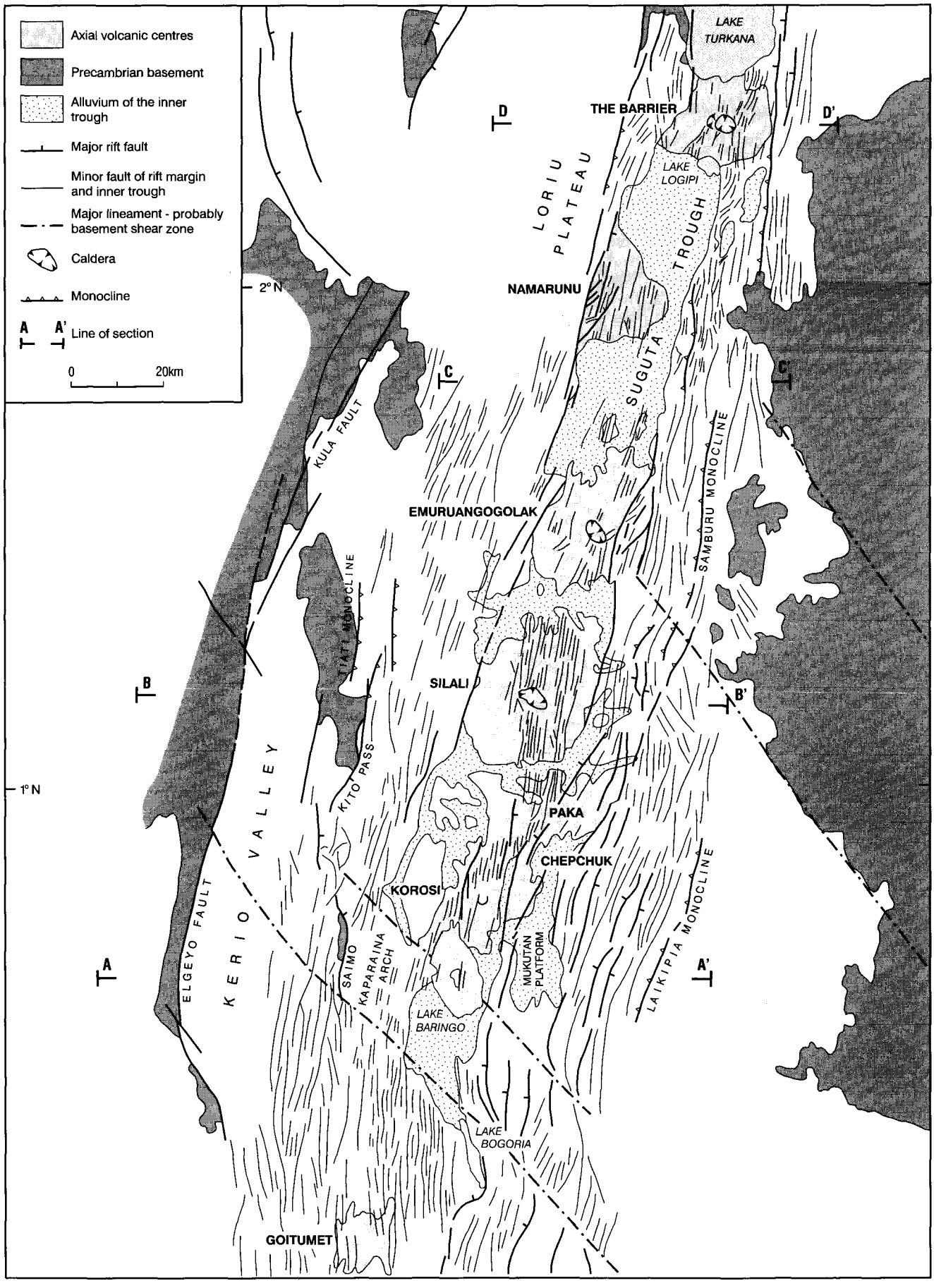

Figure 2.3 Regional structure of the northern sector of the Gregory Rift.

Figure 2.4 Schematic cross-sections across the northern Gregory Rift along lines indicated on Figure 2.3. Vertical exaggeration ×2. Note change in scale between sections (b) and (c).

by NW-trending faults which pass along strike into synthetic transfer zones (Morley et al., 1992) and a pull-apart model has been proposed for this basin by Tiercelin and Vincens (1987). The marked change in structural style along the rift margins from a deep asymmetric graben structure with clearly defined boundary faults to a symmetric downwarp with monoclinal structures may correlate with a NW-trending lineament in the basement which extends under Emuruangogolak volcano (Figure 2.3).

2.5 FAULTING, SEISMICITY AND STRESS FIELD ORIENTATIONS

Steeply inclined (>60°) normal dip-slip faults predominate at the surface. However the amounts of throw and fault kinematics are difficult to ascertain due to insufficient exposure. According to Bosworth et al. (1986), Jones (1988) and Bosworth (1989) analysis of stratal dips and section balancing suggest that the major rift boundary faults may be listric in profile and sole-out

into a basal detachment at depths of between 10–15 km. This depth is within the ductile-brittle transition boundary determined from earthquake data (Young et al., 1991). However, it should be noted that to date no listric geometries have been proven by geophysical methods. Furthermore, as magma intrusion and dyke injection are significant within the rift, then estimates of depth to detachment based on section balancing alone may be subject to large degrees of error. Further doubt on the applicability of these techniques in the Kenya Rift is strengthened by current geophysical investigations in the Kerio Valley which indicate the presence of a buried symmetrical graben structure located beneath the centre of the valley (Figure 2.4a), (D Pope and M R Strecker, personal communication, 1993).

The zones of faulting and volcanism along the axis of the inner trough are microseismically active (Pointing et al., 1985; Tongue et al., in press). Monitoring of local and teleseismic events in the Lake Baringo and Lake Bogoria areas indicates a large number of events located at depths of between 5–12 km. The shallower events correlate closely with areas of geothermal activity and at depth are underlain by a seismic high velocity zone (Tongue et al., in press). Focal mechanism analysis of the Baringo data suggests that the seismic activity is occurring on steep vertical tensile fractures down to depths of between 3.5–6.5 km. At the surface these events also coincide with the zones of normal faulting and basaltic volcanism which extend down the southern flanks of Korosi volcano to Ol Kokwe island (Section 5.2.4). Elsewhere, for example between Silali and Emuruangogolak, and at Namarunu, microseismic activity (Pointing et al., 1985) appears to be broadly associated with young basaltic volcanism and fracturing of the inner trough. Although the exact locations and depths of these events are poorly delimited they may be related to dyke injection and magma movement at shallow levels in the crust.

Analysis of regional fault kinematic and borehole break-out data (Strecker et al., 1988; Bosworth et al., 1992), and shear wave data for the Baringo area (Tongue et al., in press) indicate that today, and extending back to at least 0.5 Ma, the least principal stress field is orientated NW–SE. This orientation favours strike-slip reactivation of the NW-trending basement structures and implies that the tectonism and volcanism of the inner trough has thus occurred within an oblique rifting regime. Prior to 0.5 Ma the principal stress field is thought to have been orientated E–W.

2.6 STRATIGRAPHIC OUTLINE AND EVOLUTION

The purpose of this section is to provide a brief review of the regional stratigraphy and evolution of the northern sector of the Kenya Rift. This provides a framework within which the detailed stratigraphies of the Quaternary volcanoes may be viewed. Useful summaries and further details may also be found in Baker et al. (1972), King (1978), Williams (1978), Williams and Chapman (1986) and Smith and Mosley (1993) and in the reports of the Samburu-Marsabit Geological Mapping and Mineral Exploration Project, (Hackman, 1988; Key, 1987; Ochieng' et al., 1988).

The stratigraphic relationships within the rift are complex. There are problems in correlating the Miocene and Pliocene strata of the rift margins, and these combine with along-strike changes to produce a complex three-dimensional picture which varies through time. Fortunately, a large number of radiometric age dates now exist to constrain the main stratigraphic units, but there remains a need to rationalize and formalize the stratigraphic nomenclature. The stratigraphy and evolution of the northern rift is summarised in Table 2.1.

2.6.1 Miocene developments

During Oligocene to Lower Miocene times a series of deep (5–7 km) half-graben were initiated west and south-west of Lake Turkana (Morley et al., 1992). These basins are associated with voluminous tholeiitic basalt volcanism (Bellieni et al., 1981) which extended southwards from southern Ethiopia.

At around 20 Ma alkaline basaltic flood eruptions, represented by the Samburu Basalts, marked the commencement of volcanism in the central part of the Kenya Rift. Miocene volcanic rocks and sediments record the development of a shallow NNE-trending axial depression with contemporaneous volcanism and faulting both within the trough and along its margins. Tilting and uplift along a NW-trending axis in the Tiati and Bogoria areas is indicated by local unconformities and the development of sedimentary basins. The Samburu Basalts were erupted from a series of basalt shields and fissures located in the southern part of the project area (Golden, 1978; Griffiths, 1977). Contemporaneous trachyte and basalt shields also formed on the western margin of the rift (Weaver, 1973). All these volcanoes are now deeply eroded and partially covered by younger deposits. The ensuing Plateau Phonolites, volumetrically and areally represent one of the most important units of the Kenyan Rift. Low viscosity flows were erupted over a relatively short period (Lippard, 1973) from a number of low relief shield volcanoes located within the subsiding axial depression and along its margins (Williams and Chapman, 1986). Lavas overspilled from these centres to mantle the flanks of the Kenya Dome.

By about 11 Ma volcanism was much reduced, and widespread subsidence and downwarping commenced along the major faults to produce a series of down-to-the-west asymmetric basins adjacent to the Elgeyo, Saimo and Kito Pass faults. Further north a significant phase of basaltic activity is represented by the Kamolingaran basalts (12–9 Ma) (Truckle, 1979a; Tatsumi and Kimura, 1991). The Upper Miocene is marked by a return to flood style volcanism with the eruption of the Kabarnet trachytes and the continuing development of sedimentary basins in the Baringo-Elgeyo sector. Regional upwarping of the rift margins culminated in a major phase of faulting, tilting and erosion at 7 Ma. This period of tectonism is thought to correspond with a marked change in magma composition. A final phase of Miocene volcanism is represented by fissure-style eruptions of transitional basalts of the Eron, Kaparaina and Nathelot Formations.

2.6.2 Pliocene developments

During the Pliocene, faulting and downwarping migrated into a narrower zone along the axis of the rift where subsidence increased and graben formed.

Table 2.1 Summary of the regional stratigraphy of the northern sector of the Kenya Rift

AGE	VOLCANIC GROUP+	VOLCANIC STYLE	WESTERN RIFT MARGIN North	WESTERN RIFT MARGIN South	INNER TROUGH	EASTERN RIFT MARGIN North	EASTERN RIFT MARGIN South	TECTONIC EVOLUTION
	V	Trachyte-basalt volcanoes and lake sediments			South Island (?–0) Barrier (1.37–0) Namarunu East (0.87–0) Emuruangogolak (0.9–0) Silali (0.3–0.01) Paka (0.39–?0) Korosi (0.38–?0) Ol Kokwe (?) Lacustrine and fluvial sediments of the Suguta Valley and Baringo Basin (?0.5–0)			Faulting syn-post volcanism associated with dyke intrusion
		basalts Flood Trachy-phonolites and trachytes Basalts	Loriu basalts Kamuge Basalt (0.8) Murgisian basalt (<0.8)	Chemikilani basalts (2.0–1.8)	Goituimet Basalt Baringo Basalt Mistoni Basalt Hannington T/P (0.5) Baringo Tr. (0.58) Loyamarok T/P (0.5) Kapthurin Fm (0.6–0.8)	Logipi basalts Latarr basalts	Karau (0.54) Chepchuk (1.2–1.1)	Major phase of faulting to define inner trough flexuring on the west and landslipping on east margin
	IV	Trachyte shield volcanoes with basalts and sediments	Lomi (3.0) Lorikipi basalt (4.0–1.86) Namurunu (>4.5) Kalokopon (4.4) Nathelot basalt (4.5)	Olyamur (2.7) Jamkana Fm (3.4) Kajamamuk Lokwaleibit basalts Kafkandal/Ribkwo (5.2) Kachila/Nasaken (5.7) Chemron Fm		Tirr Tirr (4.2–2.74) Ejuk (4.5) Parkati basalts (>4.2)	Emuruagiring Trachytes (3.1) Orus (3.2)	Main graben features formed, arching of rift margins and tilting into proto-Suguta Trough
	III	Basalts	Tirioko basalts (6.6–4.5)	Kaparaina/Eron Basalts (5.5)		Sipili-Losiolo Phonolites Kamolingaran basalt (12–7)	Narokwe Basalts (5.6) uplift and formation Kabarnet Trachyte (7.0) Lopogno Trachyte (9.0) Ewalel Phonolite Nasarut Basalt (9.4)	Major phase of faulting with flank
	b	Phonolites and trachytes						
	II a	Phonolite flood lavas and pyroclastics	Kasorogol/Tiati Shiro Phonolites (11–9) Lokwanamur basalts (15) Kowun (15)	Ngorora Fm (13–10.5) Uasin Gishu/Timm Phonolites (14–9.4)		Losogol Alengerr (10.6) Seronut (13–12) Katomuk (12.15)	Marmanet (11.6) Uaso Narok Ngelesha Towana (12.0)	of axial trough, main activity in SW Saimo and Elgeyo structures active Tilting on western margin along NW axes
	I	Fissure basalts	Kapcherat Basalts (15.7)	Tambach Beds Chof/Sidekh Phonolites (15–6) Elgeyo Fm (15.1) Kamego Fm BASEMENT		Samburu Basalts (21–16)	Lopet Phonolites Murgomol Chembalo (16–14) BASEMENT	Downwarping and tilting — protorift depression uplift to the south

+ Modified after King and Chapman, 1971. Figures in brackets are ages in Ma

Volcanism continued along the western margin of this graben with the construction of a number of low-angle trachyte shield complexes (Webb and Weaver, 1975; Key, 1987) on a tilted and faulted platform of Miocene basalts. The faulted remnants of a series of trachyte shields and plateaux are preserved along the eastern side of the rift. These include the Tirr Tirr and Emuruagiring plateaux, the eroded plugs of Lopogno and Nakali and the Orus Trachyte. They all rest with marked unconformity on older Miocene strata and thicken westwards into the rift, and are thus likely to form the foundation strata of the Quaternary volcanoes in the inner trough. In the north, the proto-Suguta trough was the site of voluminous eruption of basalt flood lavas in the Upper Pliocene, which became ponded in the trough and later overflowed its margins (Figure 2.4d).

2.6.3 Quaternary developments

During the Pleistocene the Kenya Rift evolved into a full graben with the localisation of tectonism and faulting in an inner trough. In the south, early to middle Pleistocene trachyte and trachyphonolite volcanoes erupted along the eastern side of the rift and rest unconformably on older Plio-Miocene strata. In the southern part of the project area and extending southwards to Lake Bogoria, fissure-controlled trachyphonolites and basalts of the Hannington Group, Loyamarok Trachyphonolite, and the Baringo Trachyte were erupted in the period 1.3–0.5 Ma. An important phase of faulting post-0.5 Ma downfaulted these volcanoes by as much as 0.5–1 km into the inner trough. On the rift margins in the north, adjacent to Silali and Emuruangogolak, widespread faulting, tilting and landslipping of the Plio-Pleistocene strata is probably related to this phase. In the far north renewed subsidence formed the Suguta trough and the southern basin of Lake Turkana.

Subsequently, large shield volcanoes of late Pleistocene age were constructed along the axis of the inner trough and these are the main subject of this report.

3 Physiography

3.1 INTRODUCTION

The region is divisible into three main physiographic zones which are broadly coincident with the main tectonic elements of the Rift. These are the inner trough, the western margin and the eastern margin.

3.2 THE INNER TROUGH

The inner trough of the rift is a NNE-trending zone of Quaternary volcanism and sedimentation, varying in width between 35 km in the south and 17 km in the north, which is bounded to the west and the east by escarpments that are controlled by faults and monoclinal warps. In the south of the area the trough is an asymmetrical graben structure, delimited on the west by the impressive escarpment of the Saimo fault system, and in the east by a series of smaller escarpments which step-up to the Laikipia Plateau. The major faults die-out towards the north where the inner trough takes on the form of a symmetrical valley bounded by escarpments that are mainly controlled by monoclinal folds.

The floor of the trough has a marked northward gradient. Lake Baringo in the south of the area has an altitude of approximately 1000 m and from here the floor descends gradually towards the north, reaching an elevation of about 270 m at Lake Logipi, which is the lowest part of the Kenya Rift Valley. The average gradient of the floor of the inner trough between Lake Baringo and Lake Logipi is 4.3 m/km although locally it exceeds 10 m/km, as in the Emuruangogolak sector. Lake Logipi is separated from Lake Turkana to the north by the Barrier volcanic complex. The shoreline of Lake Turkana fluctuates around 365 m and at its southern end the lake reaches depths of about 100 m (Johnson et al., 1987), indicating that the floor of the lake is at a similar elevation to Lake Logipi.

Between Lake Baringo and Emuruangogolak the floor of the inner trough also has a marked westerly tilt. Thus, the Komol River, which flows from east to west between Korosi and Paka, drops 300 m across the floor of the trough. Similarly, the Amaya River falls 200 m across the floor of the trough between Paka and Silali, and the Sekut River drops approximately 100 m across the trough between Silali and Emuruangogolak. The combination of the northerly and westerly gradients in the rift floor results in an overall north-westerly tilt vector which has strongly influenced the development of the volcanoes within the trough, giving rise to asymmetry in the gross morphology of the volcanic shields. To the north of Emuruangogolak the inner trough is symmetrical in cross profile and only has a slight northward gradient.

For the purpose of description the physiography of the inner trough is subdivided into three elements. These are the axial volcanoes, alluvial-lacustrine areas and the Baringo–Loyamarok platform.

3.2.1 Axial volcanoes

The volcanic centres of Ol Kokwe Island, Korosi, Paka, Silali, Emuruangogolak, Namarunu and the Barrier are located along the axis of the inner trough. They take the form of large, low-angle, multi-vent shields which are composed predominantly of trachytic and basaltic lavas and pyroclastic deposits. Volcanic landforms are generally less-well preserved and more vegetated in the south of the area than in the north, and there is a general increase in the occurrence of very young volcanic features towards the north. Thus, Korosi appears to be extinct and is densely vegetated, whereas Emuruangogolak and the Barrier are largely covered by young, pristine volcanic features, including lavas that were erupted late in the last century and possibly during the present century.

Ol Kokwe Island is situated in the centre of Lake Baringo and consists of a small volcanic complex covering an area of about 4 km^2. The main part of the island consists of a group of coalesced basaltic scoria cones and in the east there is a N-trending peninsula bounded by faults.

Korosi is the smallest of the main volcanic centres, rising between 450 and 500 m above the surrounding floor of the trough and covering an area of about 260 km^2. Volcanic landforms are degraded and the shield is broken by a set of prominent NNE-trending fault scarps. No major crater is developed, unlike the other volcanoes of the area.

Paka covers an area of approximately 280 km^2 and rises between 600 and 700 m above the floor of the trough. Volcanic features appear to be more juvenile than on Korosi, and a small, well-preserved caldera, 1.5 km in diameter is developed on the summit area. A large part of the volcano is blanketed by young pyroclastic deposits upon which a radial drainage pattern is developed. The eastern and north-eastern flanks of the volcano are intensely faulted by NNE-striking faults giving rise to a series of stepped and tilted escarpments separating the volcano from the eastern margin of the Rift.

Silali, the largest volcano in the area, is a low-angle shield covering an area of 850 km^2 and rising almost 760 m above the floor of the trough. The summit area is occupied by a spectacular caldera measuring 7.5 km by 5 km, which is elongated in a north-westerly direction and bounded by vertical cliffs 300 m high. Several NNE-trending fracture zones cross the central and eastern parts of the shield, producing numerous open fissures, scarps and narrow graben structures. Many of the lava flows have well- preserved morphological features, especially on the eastern flanks where there is a series of young trachyte domes aligned along NNE-trending fissures.

Emuruangogolak covers an area of approximately 525 km^2 and is situated in the narrowest part of the inner trough, which it almost completely straddles. It rises between 700 and 1000 m above the floor of the rift and its summit area is occupied by an elliptical shaped caldera measuring 5 km by 3.5 km which is elongated in a north-westerly direction. The eastern and western flanks represent the slopes of an old

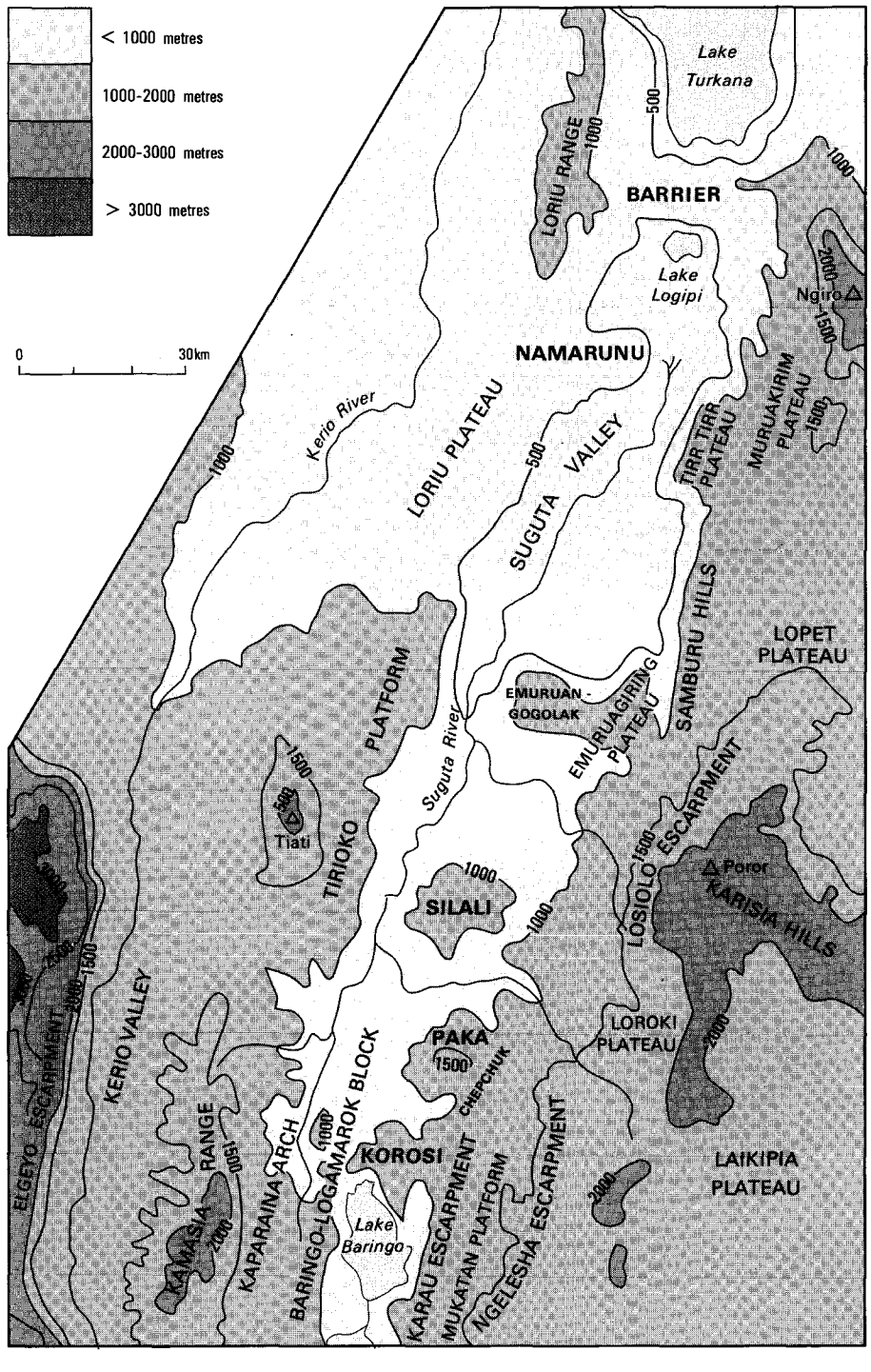

Figure 3.1 Simplified physiographic map of the region.

trachyte shield which are broken by NNE-trending fault scarps and graben, whereas the northern and southern flanks are mantled by young trachyte and basalt lava fields with associated pyroclastic cones.

Namarunu is a hilly volcanic complex which abuts the western margin of the inner trough. It has the form of a broad shield-like edifice which rises approximately 540 m above the surrounding floor of the trough. Despite its position in the floor of the rift, the bulk of the volcanic edifice represents a Pliocene volcanic shield that has been partially down-faulted into the inner trough. Quaternary activity along the axis of the inner trough has superimposed extensive basaltic lava fields, scoria cones, tuff cones and tuff rings upon the older fractured volcanic shield.

The Barrier Volcanic Complex has the form of an east-west trending whale-back ridge which forms a complete barrier across the inner trough at the southern end of Lake Turkana. The ridge is about 20 km in length and 15 km wide, and is a composite structure composed of four coalesced volcanic centres which decrease in age from the margins of the inner trough towards the axis. The older marginal volcanoes are faulted and eroded, whilst the youngest axial volcano of Kakorinya has the form of a low-angle basalt-trachyte shield with a well-preserved summit caldera. Young trachyte and phonolite lava domes partially infill the caldera, and pristine basalt fields and associated pyroclastic cones cover large areas of the northern and southern flanks.

The Suguta Valley, which is synonymous with the northern part of the inner trough between Emuruangogolak and the Barrier, was occupied at various stages in the Quaternary by a large lake known as Lake Suguta.

Stand lines related to this former lake are preserved around the margins of the valley and occur on Namarunu, the southern flanks of the Barrier and the northern flanks of Emuruangogolak. Much of the youngest volcanism on these three centres took place within the lake or upon its shores, resulting in the eruption of subaqueous lavas and the formation of phreatomagmatic features such as tuff cones, tuff rings and maars.

3.2.2 Alluvial-lacustrine areas on the floor of the inner trough

Extensive plains occur on the floor of the trough between the axial volcanoes. These are mainly covered by alluvial deposits laid down by seasonal rivers and sheet wash during periods of flooding. Along the western side of Korosi, Paka and Silali, large areas of low ground are underlain by horizontally bedded pumiceous volcaniclastic deposits, some of which have been reworked by fluvial and lacustrine processes.

Alluvial fans occur along the margins of the inner trough at the base of the bounding escarpments. In the south of the area these are not common and tend to be small. Northwards they increase in size and frequency, and in the Suguta Valley coalesced fans form extensive and almost continuous aprons along both sides of the inner trough. These aprons slope gently towards the axis of the trough and are covered with coarse gravels.

Lacustrine sediments deposited by the former Lake Suguta occur in the Suguta Valley between Emuruangogolak and the Barrier. They comprise horizontally bedded diatomites, conglomerates, sands and volcaniclastic deposits which are dissected and deeply gullied by stream channels. Down-wasting of the deposits has resulted in *remanié* gravel veneers being preserved upon the interfluves. Gravel clasts are coated with desert varnish giving the deposits a dark-brown to black colour, which on air photographs and satellite images masks the underlying pale coloured lake sediments.

In the more arid northern part of the inner trough the alluvial and lacustrine deposits are redistributed by wind action. The most extensive aeolian deposits occur to the south and south-west of Namarunu where large sand dune fields have formed on the western side of the inner trough in response to the prevailing easterly wind.

3.2.3 Baringo–Loyamarok platform

To the west of Lake Baringo a low platform occurs along the western margin of the inner trough and extends northwards into the Loyamarok Hills. This is underlain by Upper Pleistocene trachyte and trachyphonolite flood lavas which have been faulted along a NNE trend and broken into a series of blocks with prominent fault scarps. Small graben and tilted fault blocks on the platform have acted as depositional basins for fluvio-lacustrine sediments.

3.3 EASTERN MARGIN OF THE RIFT

The eastern margin of the Rift is mainly composed of Neogene volcanic rocks. Several high plateau areas flank the margins of the Rift and are separated from the inner trough by a complex shoulder made up of a series of westerly facing escarpments controlled by a combination of steeply dipping faults and west-facing monoclines.

In the south of the area the trough is bounded along its eastern margin by a broad zone of faulting approximately 20 km wide which gives rise to a stepped shoulder to the rift. Several major fault systems occur within this zone and are manifested by prominent west-facing escarpments. To the east of Lake Baringo and Korosi the boundary of the inner trough is delimited by the Karau-fault scarp, and approximately 10 km further to the east a second fault system gives rise to the Ngelesha escarpment, the crest of which rises more than a 1000 m above the trough floor. A platform of intermediate elevation, the Mukutan platform, occurs between these two fault systems and is underlain by Pleistocene trachyte and trachyphonolite lavas and pyroclastic deposits which were erupted from a number of small volcanoes including Chepchuk, Karau, Ereni and Paratello. These volcanoes are aligned along the Karau–Nagoreti fault system and have well-preserved eastern flanks and summit craters, but their western flanks have been downfaulted into the trough and buried beneath younger fill. The Mukutan platform is tilted towards the north-east and dies out at the latitude of the Komol River. Back-tilting of the platform has given rise to the development of a basin along the base of the Ngelesha escarpment, which has acted as a trap for fluvio-lacustrine sedimentation.

The main Ngelesha escarpment exposes Miocene basalts capped by flood phonolites which dip gently to the east and form the extensive and monotonous Laikipia Plateau. Further to the north the high-level Loroki and Lopet plateaux are also underlain by horizontal Miocene flood phonolites. The plateau areas of Emuruagiring, Tirr Tirr, Muruakirim and Ejuk are situated at lower elevations closer to the margin of the inner trough, and are composed of Pliocene lavas. The general form of the marginal plateaux is controlled by a sub-Miocene erosional surface on Precambrian basement, upon which the Neogene flood lavas were erupted. In the north, inliers of basement gneisses crop-out on the highest points around Poror and Ng'irio, and also in downfaulted blocks close to the margin of the inner trough along the eastern side of the Suguta Valley.

The importance of the major boundary fault systems along the eastern margin of the inner trough diminishes northwards, and to the north of Silali the shoulder of the rift is made up of complexly faulted west-facing monoclinal warps. The hinges of these monoclines mark the crest of the rift shoulder. Volcanic sequences capping the plateaux to the east are horizontal or dip gently eastward, whereas to the west of the monoclinal hinges there is an abrupt tilting of fault blocks into the trough, with dips of up to 45°. Poorly consolidated sediments intercalated within the volcanic sequences of the rift shoulders have acted as zones of weakness facilitating widespread and large-scale landslipping into the trough along fault lines. The combined effect of faulting, tilting, landslipping and erosion in the north of the area has produced very rugged topography along the shoulder of the rift, and this is accentuated where intrusive plugs have been exposed by erosion to

produce steep pinnacles such as Nakali and Losogol in the area adjacent to Silali.

3.4 WESTERN MARGIN OF THE RIFT

In the south of the area the rift has a double western margin controlled by the Elgeyo and Saimo faults, both of which give rise to impressive east-facing escarpments that expose metamorphic basement rocks overlain by Neogene phonolites and trachytes. The Elgeyo escarpment forms the western margin of the rift system and rises more than 2000 m above the floor of the Kerio Valley, which is a major graben structure parallel to the inner trough but separated from it by the intervening westerly-tilted fault block of the Kamasia Range. The escarpment of the Kamasia Range rises approximately 1000 m above the inner trough floor and is controlled by the Saimo fault. The Kaparaina arch separates the Kamasia block from the inner trough and is composed of strongly faulted and upwarped Pliocene volcanics and sediments which give rise to a dissected, low ridge approximately 10 km in width.

Northwards the Elgeyo fault displays a rapid decrease in displacement, bifurcating and passing into the Kula fault which has no topographical expression. The Kamasia block gives way to an asymmetrical anticline with basement rocks exposed in its core, upon which the prominent Miocene basalt-phonolite massif of Tiati is developed. The Kaparaina arch also appears to die-out northwards and passes into an area dominated by eastward dips. From the latitude of Silali northwards the western shoulder of the inner trough is marked by a complex zone of large, low-relief, trachytic volcanic shields of Pliocene age which rest on a gently easterly dipping plateau of Miocene volcanic rocks. Faulting combined with preferential erosion of pyroclastic deposits in the cores of these volcanic shields has given rise to very chaotic and rugged terrain. The flanks of the shields form featureless plateaux which are cut by NNE-trending river gorges aligned along faults.

The Loriu Plateau is underlain by Pliocene and Pleistocene lavas which form an extensive and gently undulating region extending northwards from the area of Pliocene shield volcanoes to the south-western shores of Lake Turkana. The shoulder between the southern part of the Loriu Plateau and the inner trough is represented by a series of easterly facing fault scarps, but northwards these pass into a single large escarpment which is largely controlled by an easterly facing monocline that has been locally modified by large-scale landslips. To the west of the rift shoulder the surface of the plateau dips gently westwards down to the Kerio River. The N-trending Loriu Range rises above the general level of the plateau in the north-east and is composed of an inlier of Precambrian basement rocks. The eastern side of the range is marked by the Mugor fault scarp, the crest of which rises about 360 m above the floor of the inner trough.

3.5 DRAINAGE

Most of the rivers within the region are seasonal, except for the Suguta, Kerio, Molo, Pekera, Endau and Mukutan which flow throughout the year.

Drainage is strongly controlled by the main structural elements of the region. The crest of the eastern shoulder of the rift acts as a watershed between rivers that flow westwards through steep gorges into the inner trough, and rivers with gentler profiles that drain the high plateau areas and flow eastwards to the Ewaso Ng'iro which eventually discharges into the Indian Ocean.

The crest of the western shoulder of the rift is marked by a line extending along the summit ridge of the Kamasia Range through Tiati to the Loriu Plateau. This acts as a drainage divide between the Kerio system to the west, and short, steep water courses draining into the inner trough to the east.

Within the inner trough there are two main drainage systems, namely the Lake Baringo catchment in the south and the Suguta in the north. Lake Baringo is fed by several rivers flowing from the south, south-east and west. The main feeder is the Molo which rises far to the south on the Mau escarpment but is joined by numerous tributaries flowing off the eastern flanks of the Kamasia range. The Pekera and Endau also drain the Kamasia range and flow into the west side of the lake, whilst the Mukutan and Ol Arabel drain the Ngelesha escarpment and flow into the south-east side. Lake Baringo has no surface outflow but is a freshwater lake, and therefore must have a significant subsurface outflow (see Section 14.3.3).

The Suguta River is the main drainage system within the inner trough. It is strongly influenced by the northwesterly tilt of the inner trough floor and the location of the axial volcanoes. As a result, the overall direction of drainage is to the north, and the main drainage channels are located on the western side of the inner trough. The Suguta sensu stricto rises at Kapedo where it is fed by hot springs issuing from the base of the western flanks of Silali. During wet periods it is joined from the south by the seasonal Nginyang River which is fed by various water courses draining the eastern and western shoulders of the rift and the volcanoes on the floor of the inner trough. The Nginyang and Suguta rivers flow along the western side of the inner trough, but north of Emuruangogolak, where there is no westerly tilt in the valley floor, the Suguta passes into a braided river system located along the axis of the trough. After passing through the narrowest part of the inner trough in the vicinity of Namarunu, the Suguta splits into a complex system of distributaries which feed a small group of highly saline and ephemeral lakes known collectively as Lake Alablab. Several hot spring systems also feed into this distributary system.

The lowest part of the inner trough is occupied by the highly saline Lake Logipi, which is situated immediately to the south of the Barrier Volcanic Complex and effectively acts as a sump. It is fed by hot springs along the base of the southern flanks of the Barrier, but the main source of water is the Suguta River, which inundates large areas of the Suguta Valley when it floods, causing Lake Alablab to expand northwards and coalesce with Logipi. Such flooding events are short-lived and the water is quickly lost by evaporation and by percolation into the porous deposits of the trough floor. During drought periods Lake Logipi shrinks to a narrow strip along the base of the southern flanks of the Barrier.

Lake Turkana is situated to the north of the Barrier and is by far the largest lake in the Kenya Rift, having

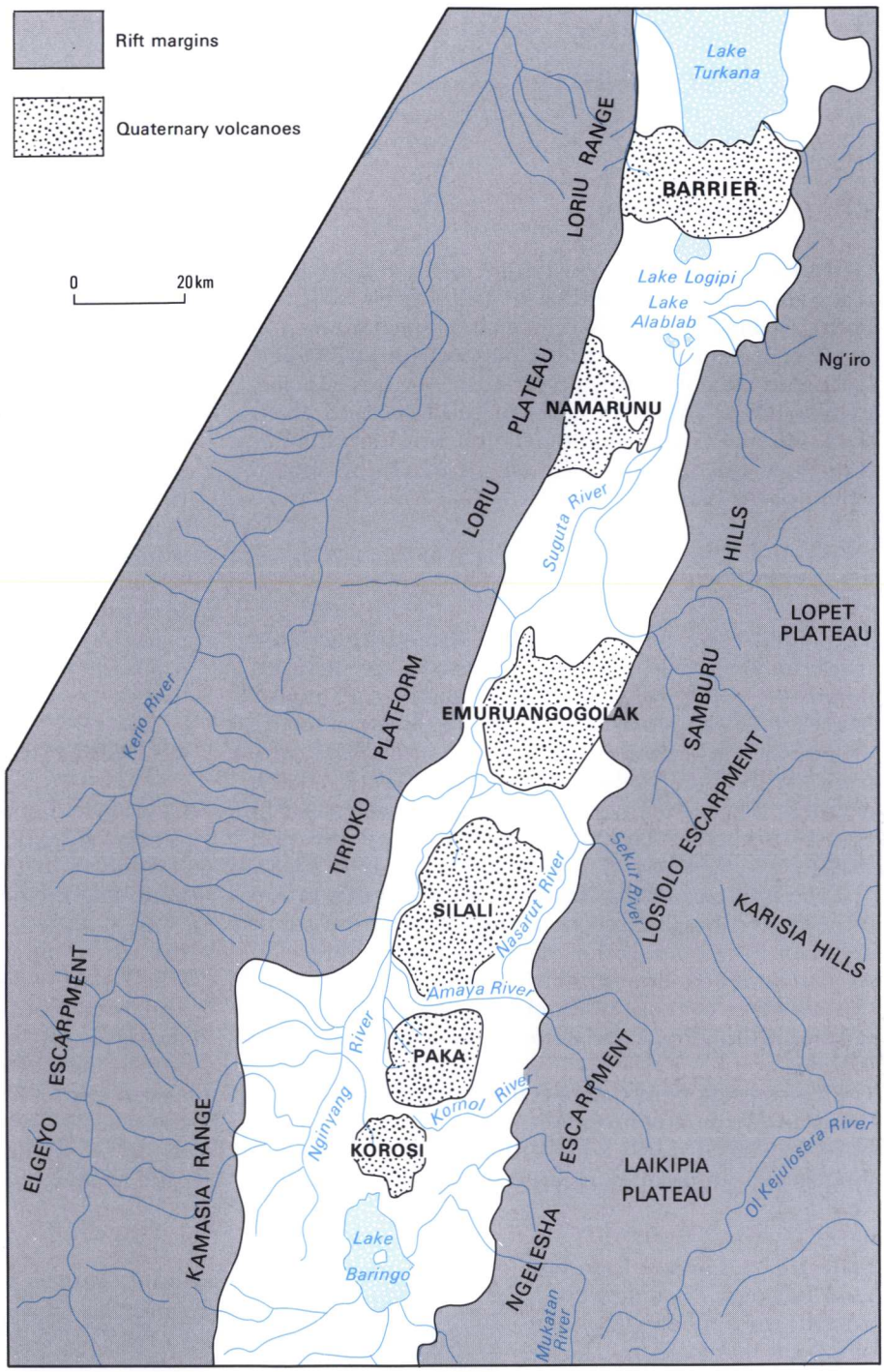

Figure 3.2 Simplified drainage map of the region.

a length of 250 km and a width of between 15 and 30 km. The lake is mainly fed by the Omo River which drains the Ethiopian highlands to the north. The Kerio and Turkwel rivers discharge into the lake in the south-west but provide less than 10% of the inflow.

4 The geology and geothermal activity of Ol Kokwe Island

4.1 INTRODUCTION

Ol Kokwe Island is a low-lying, multi-vent, basalt-trachyte complex situated in the centre of Lake Baringo (Plate 4.1). It is the smallest Quaternary volcanic centre in the northern part of the Rift Valley, having an area of slightly under 4 km^2. It rises approximately 130 m above the level of the lake, and given that the lake is very shallow, being nowhere deeper than 6 m, the shores of the island mark the spatial extent of the complex.

4.2 GEOLOGY

The oldest rocks on the island are strongly brecciated trachyte lavas which form a narrow, steep-sided peninsula in the south. The small island of Parmalok [AL 1720 0670], situated approximately 2 km to the west of Ol Kokwe, consists of a breached trachyte cone from which a steep sided button-shaped lava has been erupted. These trachytes are probably equivalent in age to the Lower Trachyte Lavas of Korosi (Section 5.2.3).

The main part of the island is composed of a group of coalesced basaltic scoria cones which in the south are seen to rest upon the trachyte lavas and breccias. At least seven cones or crater features are preserved in various states of erosion. Blocky basalt lavas have been erupted from a breached cone in the south-east of the island.

A N-trending fault system separates the main part of the island from a peninsula in the east, which is composed of basalt lavas with subordinate amounts of mugearite and basalt-mugearite breccias. The faulting has uplifted and tilted the lavas of the peninsula, producing a prominent west-facing scarp with a moderately steep dip-slope to the east.

The fault system is inferred to be an extension of the main fault-fissure zone of Korosi. On Korosi the faulting and fissuring was intimately associated with the widespread eruption of scoria cones and basalt lava fields which extend from the summit down to the shores of the lake. The lake floor between Ol Kokwe and Korosi is underlain by solid rock, and the intervening islands of Longicharo [AL 1765 0715] and Samatiany [AL 1740 0710] are composed of basalts which are also faulted along N-trending lines. The basalts of Ol Kokwe are therefore considered to represent an extension of the basaltic activity that took place on Korosi, for which an Ar/Ar date of 121±37 ka has been obtained (Section 5.2.4).

4.3 GEOTHERMAL ACTIVITY

Geothermal activity on Ol Kokwe occurs around the shores of the peninsula in the north-east of the island. It appears to be controlled by the N-trending faults bounding the peninsula.

An intense area of activity occurs on the shore on the north-eastern side of the peninsula [AL 1752 0695]. At this locality hot springs, boiling mud pools and fumaroles extend along a 60 m length of the shoreline. They occur on the flat muddy foreshore and in the bouldery talus backing the shore up to an elevation of about 2 m above the lake. Gas bubbling in the lake indicates that activity also occurs for a short distance offshore. This area is visited regularly by tourists and reports indicate that the activity is prone

Plate 4.1 Ol Kokwe Island in Lake Baringo. Looking west towards the Saimo escarpment of the rift margin. The lake is permanently brown due to suspended sediment.

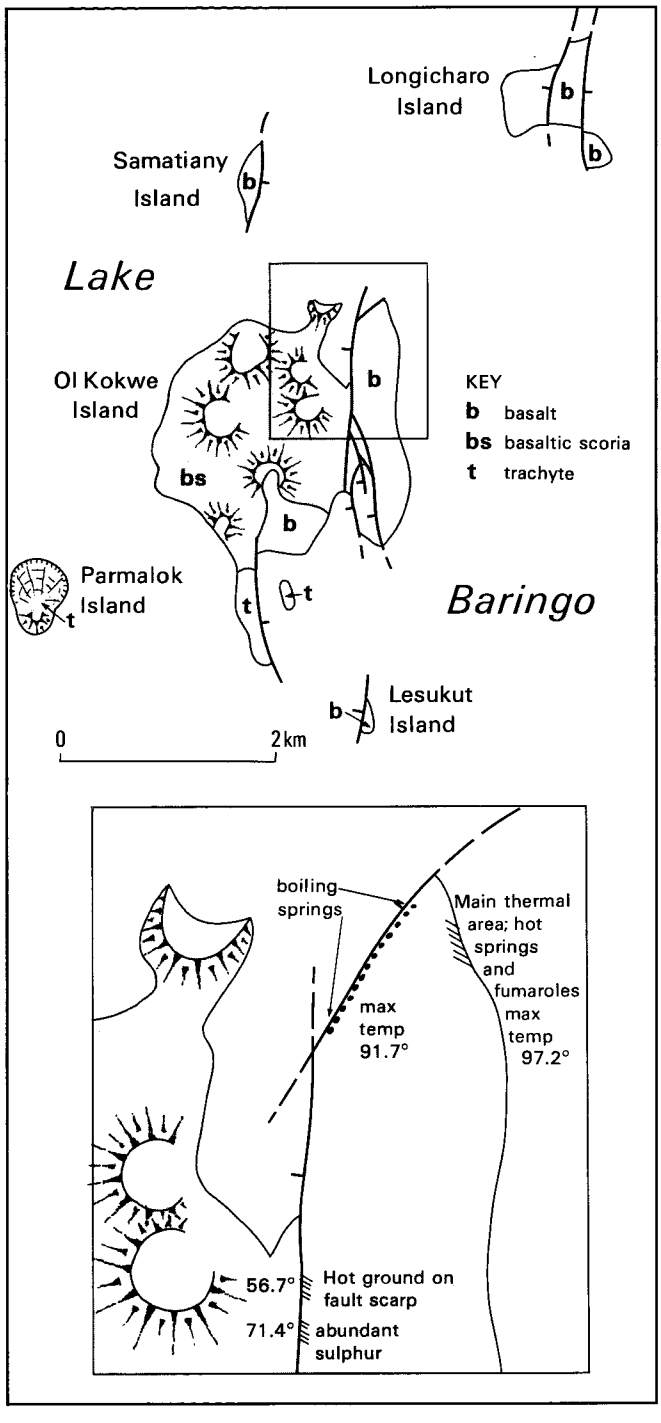

Figure 4.1 Simplified geological map of Ol Kokwe Island with the location of geothermal activity inset.

to change in intensity over relatively short periods. At the time when the locality was surveyed, in September 1988, the activity was vigorous. Recorded fumarole temperatures range between 70.5 and 96.5°C, whilst the springs and mud pools are slightly hotter with temperatures ranging up to 97.2°C, which is approximately the local boiling point. There is a high gas-flow from the springs accompanied by the smell of H_2S. Calcite and amorphous silica deposits are associated with the activity and trace amounts of sulphur occur. A report by Kemp (1989) indicates that the amorphous silica around one of the largest hot springs is admixed with a significant proportion of diatoms.

Hot springs, vigorously bubbling pools, and fumaroles are common over a length of 300 m along the north-western shore of the peninsula around [AL 1750 0697]. This activity occurs within bouldery talus up to 3 m above the level of the lake. Recorded temperatures range up to 91.7°C. Carbonate encrustations on the talus boulders surrounding the springs indicate that the elevation of the activity fluctuates with seasonal variations in the level of the lake.

Two small areas of hot ground occur within talus at the base of the westerly-facing fault scarp on the west side of the peninsula. The northernmost area [AL 17480 687] has ground temperatures up to 56.7°C and is associated with strong pervasive silicification and relatively large amounts of coarsely crystalline green sulphur. The southern of the two areas [AL 1748 0685] has ground temperatures up to 71.4°C and has lesser amounts of sulphur.

5 The geology and geothermal activity of Korosi Volcano

5.1 INTRODUCTION

Korosi is a trachyte-basalt volcanic complex situated immediately to the north of Lake Baringo, at approximately 00°45'N, 36°05'E. It occupies an area of about 260 km^2 and rises between 450–500 m above the surrounding floor of the inner trough, reaching a maximum height of 1446 m on the summit cone of Kotang in the north-east.

The geology of Korosi was first mapped and described by Carney (1972), but no mention was made of geothermal activity upon the volcano. Subsequently a summary of the geology was provided by Hackman (1988), based upon Carney's work.

5.2 GEOLOGY OF KOROSI

5.2.1 Introduction

Korosi is a multi-vent complex composed predominantly of trachyte lavas which have built up a low volcanic shield, upon which lesser amounts of basalt, mugearite and pyroclastic deposits have been erupted. The minimum thickness of the volcanic pile is 450–500 m, based upon the height of the volcano above the surrounding floor of the inner trough. Korosi is fractured by a zone of *en échelon* NNE-trending faults which steps progressively eastward across the volcanic complex onto the flanks of Paka. This faulting has superimposed a horst and graben topography upon the volcanic shield.

In the south-west and west, the volcanic pile of Korosi rests upon flood lavas of the Loyamarok Trachyphonolite which have yielded a K/Ar date of 0.58 Ma (Chapman and Brook, 1978). On the outermost northern flanks, in the Adomeyan area [AL 1830 0930], there are pristine and unvegetated basalt lavas and spatter cones. Although the precise age of this basaltic activity is unknown, it appears to be very young. Activity on Korosi therefore falls within the broad time span of 0.5 Ma to Recent.

Carney established a stratigraphy for the volcano, based partly upon the relative ages of faulting episodes with respect to the various eruptive phases. Because faulting has progressively taken place throughout the evolution of Korosi, the relative ages of some rock units and their relationships to faulting episodes is uncertain. In particular, it is difficult to distinguish between Carney's lower and middle trachytes, and it is also apparent that the pyroclastic rocks of the complex appear to be of more than one age. The volcanic succession is therefore described using the revised scheme presented in Table 5.1.

5.2.2 Pumiceous deposits (K^v)

The oldest exposed rocks of the volcanic complex are pumiceous deposits which cover a large area to the west and south-west of Korosi, on the flat ground around Loruk [AL 1695 0790] and extending northwards to the plain of Korkore [AL 1730 0950]. Here the deposits rest upon flood lavas of the Loyamarok Trachyphonolite. They consist of poorly consolidated, well-bedded pumice lapilli deposits and pumice lapilli ashes. Individual beds are laterally extensive and cross-cutting structures are not common.

The most instructive section exposed in these pumiceous deposits occurs approximately 3.5 km north-east of Loruk, in a roadside cutting on the road to Tangulbei at [AL 1715 0818]. Here the deposits rest sub-horizontally on Loyamarok Trachyphonolite and are unconformably overlain by Lower Trachytes. At this locality the deposits have a thickness of approximately 22 m, although the overlying trachyte lava cuts down through the sequence towards the west. The section consists of poorly consolidated, pale buff-brown to grey, bedded pumice lapilli deposits and pumice lapilli ashes. Lapilli range up to 5 cm in size and are sub-angular to subrounded. Individual beds range from a few centimetres up to about 2 m in thickness and show moderate degrees of sorting. Normal grading is common but not well-developed, although some units show gradation from basal pumice lapilli deposits through to ash at the top. Slightly cross-cutting bedforms occur in some of the thicker units. Poorly developed reddened zones, possibly representing palaeosols, occur at the top of several units and suggest that significant time lapses may have occurred between some of the eruptive events.

These pumiceous deposits are interpreted as air-fall deposits. Their well-stratified nature, moderate sorting, and rapid transitions from coarse pumice to ash suggest that they are more likely to represent the product of sub-plinian eruptions rather than more vigorous plinian activity. The wide extent of the deposits to the west of Korosi probably results from dispersal of the eruptive columns by prevailing winds from the east. Similar westerly dispersal patterns are preserved in the pyroclastic deposits of all the other volcanoes of the region.

Ar/Ar dating of alkali feldspar crystals separated from the pumice deposits exposed in the road section north-east of Loruk at [AL 1715 0818] has yielded an age of 380±7 ka.

5.2.3 Lower Trachytes (K^l)

Lower Trachytes, corresponding to Carney's lower and middle trachytes, are exposed in a peripheral apron around the outer flanks of Korosi. On the south-west flanks they rest upon the pumiceous deposits described in the previous section, and elsewhere on the southern and northern flanks are overlain by basalts and Upper Trachytes.

Lower trachyte lavas are mid grey-green in colour, weathering to buff or pale red-brown. They are sparsely to moderately porphyritic and are compositionally oversaturated peralkaline pantelleritic and comenditic trachytes. Compared with the Upper Trachytes, the

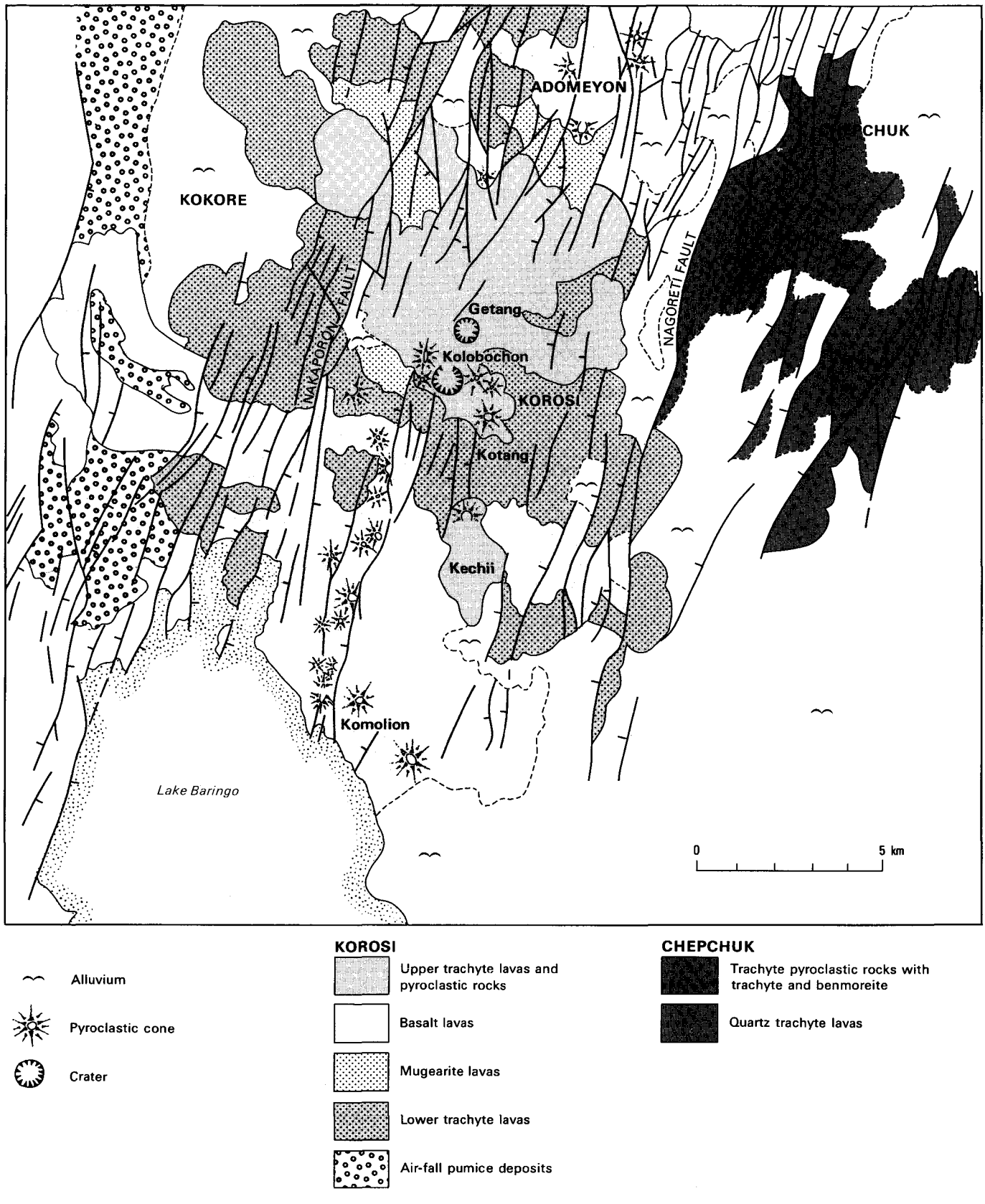

Figure 5.1 Simplified geological map of Korosi and Chepchuk.

Table 5.1 Summary of the stratigraphy of Korosi

Young Basalts (b^y)		
Upper Trachytes (K^{tu})	104 ± 2 ka	
Basalt and Mugearite ($K^b + K^m$)	121 ± 37 ka	FAULTING AND FISSURE ACTIVITY
Lower Trachytes (K^{tl})	307 ± 8 ka	SHIELD FORMATION
Pumiceous deposits (K^v)	380 ± 7 ka	

Lower Trachytes are more intensely faulted and have less well-preserved flow features. Individual flows are lobate or button-shaped with steep flow fronts. On air-photographs concentric pressure ridges are recognisable on the surface of flows and less commonly radial fractures are seen. Some flows are blocky and others are composed of agglutinated scoriaceous clasts, termed froth flows by Carney (1972). Flow banding is commonly developed and many of the trachytes have a strong fissility resulting from the flow alignment of microscopic mineral laths.

The eruption of the Lower Trachytes resulted in the formation of an early volcanic shield approximately 14 km across from east to west and 19 km from south to north. Although disrupted by faulting and partly covered by younger lavas, the disposition and morphology of the Lower Trachytes indicates that they were erupted from numerous sources on the shield and generally flowed radially off its flanks. Although the precise position of many of the eruptive sites has been obscured by later events, several source vents are preserved, and these are described below. Carney (1972) maintained that some of these vents acted as eruptive centres on more than one occasion.

The best preserved Lower Trachyte eruptive centre is Kotang [AL 1800 0845] which forms the summit of the Korosi volcanic complex. Kotang is a trachytic pyroclastic cone approximately 100 m in height with a small parasitic cone low on its western flanks. Two small trachytic cones also occur immediately to the north of the main cone. Kotang is composed of an alternating sequence of unconsolidated pumice deposits and agglutinated trachytic scoria and spatter. This is typical of the trachytic pyroclastic cones of Korosi, in which all gradations exist between highly vesicular, low-density pumice and almost non-vesicular trachyte spatter. The summit of Kotang has a shallow crater rimmed by agglutinated trachyte spatter and scoria, which is breached on the eastern side by a steeply dipping trachyte lava with high lateral spatter ramparts. This lava flowed down the steep eastern flanks of Korosi for a distance of 5 km and eventually came to a halt in a prominent lobate flow-front at the foot of the volcano. The spatter ramparts adjacent to the breach on Kotang indicate that the trachyte magma was very fluid and that eruption of the lava was accompanied by fire-fountaining.

Other Lower Trachyte vents are preserved a kilometre to the south of Kotang, at Majarikolong [AL 1801 0829], where according to Carney (1972) there is a complex of small pumice cones and lava domes aligned along a N-trending fissure system.

On the western side of Korosi the best preserved Lower Trachyte centre is the cone of Kesitoi [AL 1768 0849]. The cone is composed of pumice lapilli deposits and has a breach on its western side from which a steeply dipping trachyte lava was erupted. A short distance to the north-east is the eroded pumice cone of Lemu [AL 1775 0855] which Carney suggested may have been the source of several of the Lower Trachytes occurring on the north-west flanks of Korosi.

A Lower Trachyte lava exposed along the Loruk-Tangulbei road at [AL 1716 0818] has given an Ar/Ar age of 307±8 ka.

5.2.4 Basalts and mugearites ($K^b + K^m$)

Carney (1972) maintained that a minor episode of faulting took place after the Lower Trachyte activity and prior to the eruption of basalts and mugearites. Whilst the work of the present survey can neither

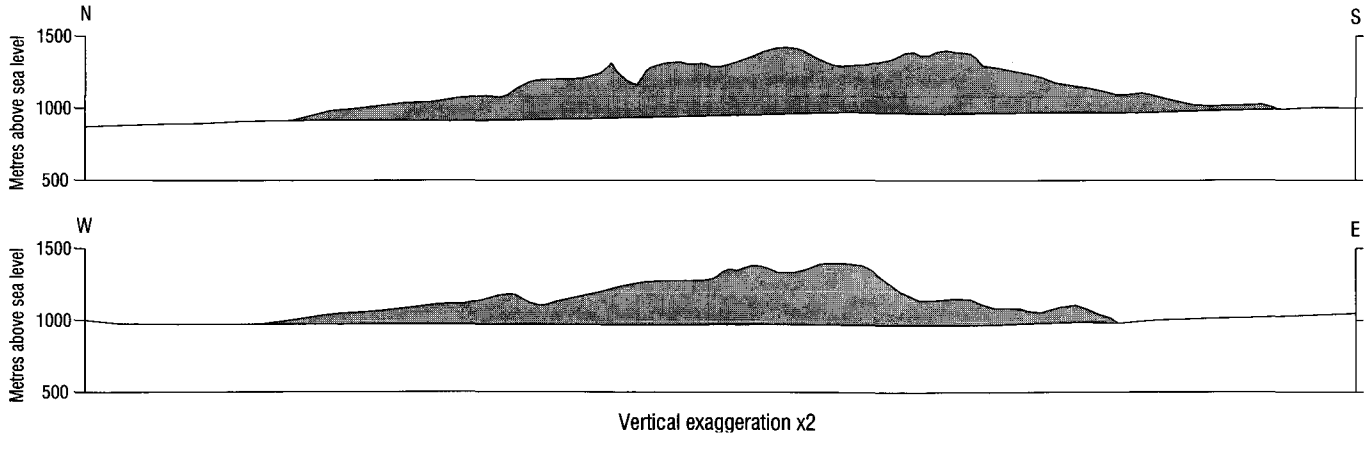

Figure 5.2 Topographic profiles across Korosi.

refute nor confirm this, it appears that a major episode of fissuring and faulting accompanied and controlled the basaltic activity.

Basaltic and related intermediate lavas occur in three main areas. They cover a large part of the southern and south-western flanks of Korosi and extend southwards into Lake Baringo. Extensive basalts and mugearites also occur on the peripheral northern flanks and in the low ground of the Nagoreti–Nginyat–Tilam area between Korosi and Paka. A third and minor occurrence of mugearite is found on the western side of summit area, in the vicinity of Lemu [AL 1775 0855].

The basaltic lava field on the southern flanks covers an area of approximately 100 km^2, excluding that which probably underlies much of the north-eastern part of Lake Baringo. A prominent line of basaltic cones is situated upon the main NNE-trending fault zone which extends along the axis of the volcanic complex from the summit area to the shores of Lake Baringo. This is interpreted as a fissure zone from which highly fluid basalt lavas were erupted, largely by fire-fountaining. The cones at higher elevations along the northern part of the fissure zone are mainly composed of agglutinated spatter, whereas those on the lower flanks in the south around Komolion and Chesoro [AL 1770 0768] are composed predominantly of poorly consolidated scoria. In places spatter ramparts are preserved along the crests of fault escarpments, indicating that these faults reactivated earlier eruptive fissures. Basalts erupted from the main fissure zone flowed to the south and west, and were channelled to some extent by the topography of the Lower Trachytes. The basalts that flowed westwards off the high ground of the axial fissure zone eventually reached the foot of the volcanic shield around Kokwomow [AL 1710 1840], and then veered northwards as two large flows with high flow-fronts. This veering to the north was a result of the north-westerly tilt on the floor of the inner trough.

A second NNE-trending fissure zone was active approximately 3 km to the east of the main zone near Kechii [AL 1805 0815]. This erupted a separate basaltic field which flowed down the eastern flanks of Korosi to the Tangulbei River. This second fissure zone can be traced across the basalts in the low ground to the south-east of Korosi and may control the location of the basaltic pyroclastic cone of Lemuyet [AL 17830 0750].

Original tensional fissures are still preserved within the basalts at a few localities, as for example between the cone of Kuraiswa [AL 1720 0810] and its neighbouring cone to the south. An open fissure also occurs within basalt lavas on the south side of the Loruk-Tangulbei road at [AL 1787 0780] and is reported to extend southwards to Lake Baringo.

On the northern flanks of Korosi, olivine basalts occupy the low ground of the Nagoreti plains [AL 1840 0910] and partly infill fault controlled valleys around the northern end of Chepchuk (Section 6). These basalts are associated with a line of basaltic scoria cones located upon NNE-trending faults that extend northwards from Korosi to the southern flanks of Paka. Low on the northern flanks at Nginyat [AL 1820 0910] and also to the south of Lake Tilam [AL 1790 0935] there are two extensive areas of mugearite and hawaiite lavas. These overlie Lower Trachytes and are inturn overlain by Upper Trachytes. A chemical analysis from Carney (1972) indicates that at least one of the flows in the Nginyat area is of benmoreitic composition.

A small lava, reported by Carney to be mugearitic, was erupted from the main fissure-fault zone on the western side of the summit area. This flowed down the north-western flanks, splitting into two flows around the older trachyte cone of Lemu [AL 1775 0855], and continued down the flanks as a long narrow flow channelled between the flow-fronts of Lower Trachytes.

The basalts of Korosi are transitional alkali basalts which include both weakly nepheline normative and weakly hypersthene normative compositions. A lava from the southern flanks, exposed in a fault scarp at [AL 1766 0774] near Komolion, has given a step-heating Ar/Ar date of 121±37 ka.

5.2.5 Upper Trachytes (K^{tu})

Upper Trachytes cover a large part of the northern flanks of Korosi, where they overlie Lower Trachytes, basalts and mugearites.

The Upper Trachytes are generally less faulted than the Lower Trachytes and basalts. Carney (1972) concluded that a faulting episode took place prior to the eruption of the Upper Trachytes, resulting in the formation of a horst and graben topography. He postulated at least two phases of faulting, with the first movements taking place towards the end of the basaltic fissure activity. The mapping of the present survey indicates that the main phase of faulting was broadly contemporaneous with the basaltic activity. However, some Upper Trachyte lavas are more faulted than others, suggesting that faulting continued throughout this later phase of trachytic volcanism.

Upper Trachytes are similar to the Lower Trachytes but have better preserved morphology and flow features which are clearly discernible on air-photographs. Several of the longer trachyte lavas have the form of narrow ribbon-like flows with well-developed levees on the upper flanks of the volcano, but pass into laterally extensive lobate flows on the lower flanks and surrounding flat areas. To some extent the ribbon nature of these lavas on the upper flanks is a result of channelling by pre-existing topography, although steepness of slope has also influenced morphology. The length of the ribbon-like flows, in proportion to their narrowness, suggests that at the time of eruption these trachytes were relatively fluid.

Extrusive domes also occur, particularly on the periphery of the northern flanks of the volcano. Lavas have been extruded from breaches on the flanks of several of these domes, as for example at [AL 1790 0892]. Other domes of similar form occur at the base of the northern flanks at [AL 1810 0900] and [AL 1829 0899], and also on the upper flanks, as for example on the north-west side of the summit area [AL 1781 0860].

Small parasitic domes also occur on the surfaces of several of the Upper Trachyte flows. For example, a NE-trending line of small domes is situated a short distance to the north-east of Getang (Kinyach) crater [AL 1805 0878] and a parallel line occurs a short distance to the north-west [AL 1803 0885]. These small parasitic domes were probably extruded upon the surface of their host flows at a late stage in their cooling history, and their orientation parallel to the main faults in the

Plate 5.1 Getang crater on the northern side of the Korosi summit area.

vicinity suggests they have been controlled by underlying fractures.

The Upper Trachytes were erupted from various locations on the northern flanks of Korosi. Some were erupted from breached domes and a few were erupted from breached trachytic pyroclastic cones, as can be seen in the area immediately to the south of Lemu on the north-western flanks [AL 1775 0875]. Many of the larger flows on the northern flanks can be traced back to sources in the general region of Getang crater [AL 1797 0867], although the precise nature and position of these sources is obscured by later tephra.

Getang is a large cylindrical pit crater approximately 600 m in diameter at the rim, and 120 m deep (Plate 5.1). The floor of the crater is flat and has a diameter of about 200 m. The upper walls of the crater are almost vertical and expose massive trachyte lava, but the lower walls are covered by extremely coarse boulder talus. No pyroclastic deposits are exposed in the crater walls. The crater rim is surrounded by a low-relief circular rampart composed of coarse, poorly sorted, angular to subrounded, lithic blocks of trachyte and syenite. No juvenile magmatic pyroclasts have been identified within these deposits. Getang is considered to have formed by piston-like collapse, presumably in response to the lateral drainage of magma, accompanied by the explosive removal of trachyte country rock by gas coring.

A tuff ring, thought to be of Upper Trachyte age, occurs on the summit region at Kolobochon [AL 1793 0855]. The structure is a shallow circular crater feature approximately 800 m in diameter, with a low rim composed of trachytic pumice and scoria. A small trachytic pumice cone occurs in the centre of the tuff ring, but the nature of the deposits in the floor of structure is obscured by hydrothermal alteration.

Only one Upper Trachyte lava occurs on the southern flanks of Korosi, at Kechii [AL 1798 0818]. This was erupted from a breach on the southern side of a large, well-preserved, pyroclastic cone composed of agglutinated trachyte scoria and spatter. The lava flowed southwards over faulted basalts and Lower Trachytes, and on its eastern side abuts against a prominent N-trending fault scarp in Lower Trachytes.

Compositionally the Upper Trachytes are all peralkaline and oversaturated, including both pantelleritic and comenditic types. A lava from the Upper Trachytes on the north-western flanks of Korosi at [AL 1815 0585] has yielded an Ar/Ar age of 104±2 ka.

5.2.6 Young Basalts (B^y)

Young basalt lavas were erupted from a series of scoria and spatter cones aligned along a N-trending fault-fissure system in the Adomeyon area, situated in the low ground between Korosi and Paka. The basalts appear to have been highly fluid and were ponded by the flow-fronts of Upper Trachytes. These basalts are unvegetated and have pristine morphological features, and are therefore considered to be very young.

5.3 SUMMARY OF EVOLUTION AND STRUCTURE

Korosi is a multivent volcanic shield built largely of oversaturated peralkaline trachyte lavas with lesser amounts of transitional alkali basalts, mugearites and pyroclastic deposits. The volcano is constructed upon a basement of Loyamarok Tracyphonolite flood lavas which have an age of 0.5 Ma.

The oldest exposed rocks are trachytic pumice deposits and pumice lapilli ashes of air-fall origin which have an age of 380±7 ka. These are overlain by Lower Trachyte lavas which built up an early volcanic shield and have yielded an age of 307±8 ka. Eruption of the Lower Trachytes took place from vents on the upper flanks and summit area of the volcanic shield, many of which are the sites of trachytic scoria-spatter cones.

The Lower Trachytes were intensely fractured by NNE-trending faults which superimposed a horst and graben topography upon the early volcanic shield. This main phase of faulting was accompanied by the

voluminous eruption of fluid basalt and mugearite lavas and pyroclastic cones from a NNE-trending fissure zone located along the axis of the shield. Radiometric dating indicates an age of 121±37 ka for this phase of activity.

The main phase of faulting and basaltic activity was followed by the eruption of Upper Trachyte lavas, domes and pumice-scoria cones which are aligned along NNE-trending faults. The majority of the lavas were erupted from the northern part of the summit area and flowed down the northern flanks of the volcano. At a late stage during this phase of activity the large pit crater of Getang formed on the northern side of the summit area. Radiometric dating of the Upper Trachyte lavas indicates an age of 104±2 ka.

Activity within the area continued until relatively recent times, with the eruption of young basalts in the low ground between Korosi and Paka.

Faulting took place throughout the evolution of Korosi, although the most important episode appears to have been closely associated with the main phase of basaltic volcanism (*cerca* 120 ka). The faults have a right-stepping, *en-échelon* pattern, and form part of a regional zone that extends in a north-easterly direction from the western side of Lake Baringo across Korosi and Paka to the eastern margin of the rift adjacent to Silali. This fracture system links the major boundary faults on the western side of the inner trough adjacent to Lake Baringo, with boundary faults on the eastern side of the trough adjacent to Silali and Paka.

The majority of faults on Korosi appear to have relatively minor displacements, although there are several important faults to the east and west of the complex which define a broad graben in which the volcanic shield has been constructed. The Nagoreti fault system extends along the whole of the eastern side of Korosi and has a downthrow to the west. The displacement on the Nagoreti fault is considerable, because the entire western flank of the older volcano of Chepchuk, situated to the north-east of Korosi, has been downfaulted along it and buried within the floor of the inner trough (Section 6). The Nakaporon fault system occurs low on the western flanks and throws down to the east. It has a complex pattern of interconnecting and diverging splays which give rise to an east-facing scarp along most of the western side of the volcano. The Nakaporon fault is particularly important because it acts as the western boundary to surface geothermal activity on Korosi.

5.4 GEOTHERMAL ACTIVITY ON KOROSI

5.4.1 Introduction

Surface geothermal manifestations on Korosi take the form of hot ground, steaming ground and fumaroles. Hydrothermal alteration is associated with active manifestations and with extinct thermal areas now at ambient temperatures.

The surface geothermal manifestations on Korosi are confined within an area of approximately 33 km^2.

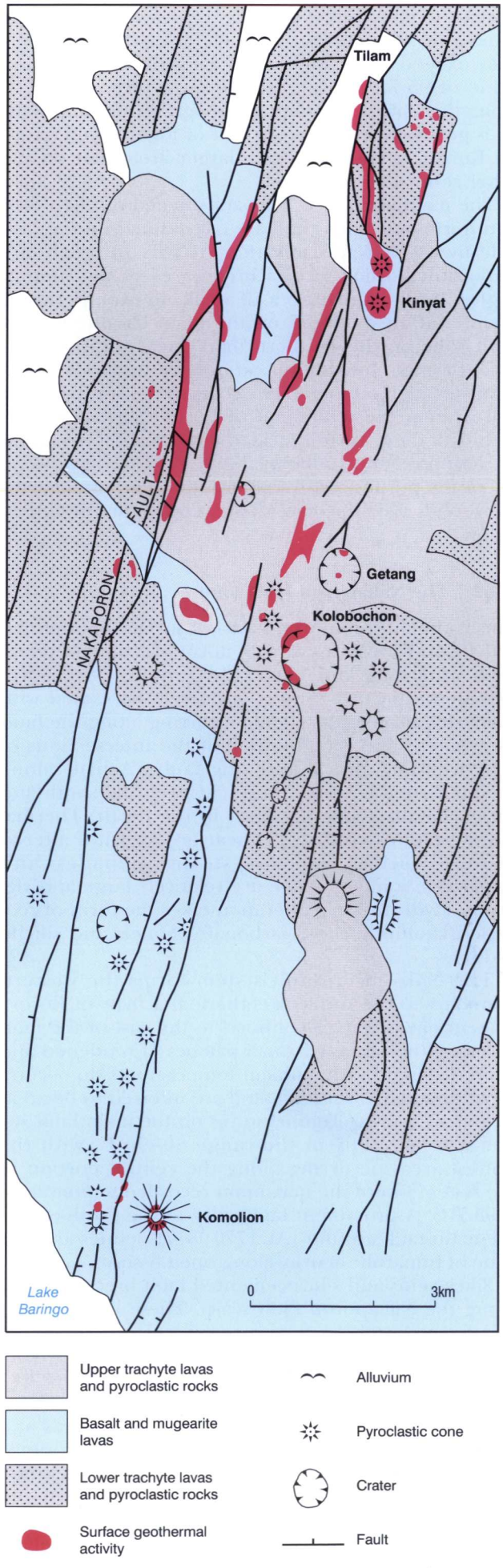

Figure 5.3 Location of surface geothermal activity on Korosi.

Surface temperatures are generally lower than on the other volcanic centres of the region, although locally they exceed 90°C, and reach a maximum recorded value of 95.7°C in the area of most intense activity along the Nakaporon fault. Although geothermal activity is generally less vigorous and of lower temperature on Korosi, it encompasses a larger area than on the other centres of the region.

The main areas of activity are situated on the north and north-west flanks and are constrained on the west side by the Nakaporon fault. Activity of secondary importance occurs over a broad area of the summit region, and a third area of weak, low-temperature manifestations is found on the main basaltic fissure-fault zone on the southern flanks near the shores of Lake Baringo. In addition, an isolated fumarole with a relatively high temperature occurs to the south-west of Korosi near the settlement of Loruk. Surface activity within all these areas is located upon faults, or is found in close proximity to them.

For the purpose of description the geothermal activity is subdivided into several areas which are described below.

5.4.2 The Nakaporon fault zone

This is the most important area of surface geothermal activity on Korosi. It takes the form of a narrow linear zone 6 km long and 1 km wide trending N to NNE. Activity within this zone is intimately associated with the Nakaporon fault system, occurring along the fault escarpment and hanging wall at the intersections of NNE-trending and SE-trending faults. Activity along the fault zone is hosted in trachytes in the south and within basalts and mugearites in the north. Thermal manifestations consist of linear areas of hot altered ground with numerous steam seepages and fumaroles, some of which are relatively large and vigorous. Hydrothermal alteration takes the form of reddened kaolinitic clays, carbonate veinlets and silicification.

The Nakaporon fault system forms the western boundary to the surface geothermal activity of Korosi. Present day activity is confined to the east of the fault system, although a few small patches of reddened and altered ground with ambient temperatures do occur a short distance to the west, and are inferred to be areas of extinct activity. Temperatures on the main fault system are generally in the range 80–90°C, with the hottest areas occurring along the central portion of the system where the maximum recorded temperature is 95.7°C. A prominent fault splay to the south-east of the main fault around [AL 1770 0877] defines another zone of fumarolic activity along open fissures.

Silica veins and silica cemented fault breccias occur along the Nakaporon fault scarp. These have a finely laminated internal structure typical of hot spring sinters. U-series dating of two sinter samples from Nakaporon indicates depositional ages of 11.8±0.8 ka and 12.7±0.8 ka respectively. This corresponds with a climatically wet period when Lake Baringo was at a high level of around 985 m (Tiercelin & Vicens, 1987). The sinters at Nakaporon occur at an elevation of approximately 1000 m and are therefore believed to have been deposited by hot spring activity when water tables and lake levels were high (Sturchio et al., 1993).

5.4.3 The summit area of Korosi

The summit area of Korosi has a number of scattered areas of geothermal activity which are mainly associated with NNE-trending faults, or occur upon trachytic eruptive centres which are themselves controlled by faults of this orientation. Surface manifestations consist of hot ground, steaming ground and weak fumaroles, with temperatures generally in the range 40–70°C. Hotter areas occur around the northern rim of the trachytic tuff ring of Kolobochon [AL 1785 0848], where fumaroles have recorded temperatures of up to 95.5°C, and on the south-east side of the trachyte cone of Lemu [AL 1776 0855], where temperatures reach 91.4°C. The main crater of Getang (Kinyach) [AL 1797 0867] has a few small patches of warm ground with weak steam seepages on its northern rim. These are located upon minor N-trending faults and have a maximum recorded temperature of 47.6°C.

5.4.4 The northern flanks of Korosi

Several disparate linear zones of activity occur along faults and lines of volcanic cones on the northern and north-western flanks.

On the upper flanks activity takes the form of hot ground with isolated fumaroles, aligned along N to NNE-trending faults. Vigorous fumaroles occur in shattered trachyte lavas at [AL 1793 0901]. Ground and fumarole temperatures are generally lower than at Nakaporon and mostly range between 50°C and 70°C, reaching a maximum recorded value of 91°C. Sites of extinct activity along many of the fault lines are indicated by reddened ground with ambient temperatures and silica sinter float.

On the lower northern flanks, fumaroles and hot ground occur in a series of linear zones to the south and south-east of Lake Tilam [AL 1795 0935], extending up to the basalt and trachyte pyroclastic cones at Kinyat [AL 1801 0906]. These zones are aligned along, or parallel to, a number of N to NNW-trending faults, and are mainly hosted in trachyte lavas. Temperatures range from less than 40.0°C up to a maximum recorded value of 90.1°C, and are generally higher than those on the upper northern flanks. The ground is altered to red and white kaolinitic clays with traces of alunite, and silica veins occur to the east of Tilam. The highest temperatures and strongest fumaroles are present on the basalt cone at Kinyat. The lava flow from this cone also hosts fumaroles which have temperatures of 50–60°C.

To the north-east of Kinyat, near to the Komol River [AL 1810 0926], hot ground with numerous steam seepages and weak fumaroles occurs upon shattered trachytes and basalt lavas. Here the activity is controlled by NNW-trending fractures, and the maximum recorded temperature is 77.8°C.

5.4.5 The southern flanks of Korosi

Minor geothermal activity occurs low on the southern flanks of Korosi around Komolion [AL 1765 0775]. This consists of warm ground with weak steam seepages occurring upon basalt scoria cones and NNE-trending fissures and faults cutting basalt lavas. Temperatures are low, reaching a maximum of 48.7°C.

Minor carbonate alteration occurs around steam seepages within scoria.

5.4.6 Loruk

A small, isolated zone of hot and altered ground with a single weak fumarole occurs close to the main road to the south of Loruk at [AL 1679 0737]. This isolated occurrence is several kilometres to the south-west of Korosi, but for convenience is described here because it is located upon a continuation of the same fault system that controls the activity on Korosi. Despite its isolated occurrence and low flow rate the fumarole has a relatively high recorded temperature of 91.6°C. The activity occurs upon a N-trending fault within lavas of the Baringo Trachyte.

6 The geology and geothermal activity of Chepchuk

6.1 INTRODUCTION

Chepchuk is the name given to the highest point (1380 m) of a series of prominent north to south trending ridges that rise 220 m above the plains to the north-east of Korosi and south-east of Paka. These ridges mark the faulted remnants of a large Lower Pleistocene trachyte volcanic shield. The remnants of the volcano crop-out over an area of about 100 km^2, although the original edifice was considerably larger.

6.2 GEOLOGY

The geology of the Chepchuk complex has been described by Carney (1972) and summarised by Hackman (1988). The western part of the complex is intensely fractured by N-trending faults and consists predominantly of pyroclastic deposits with interbedded trachyte and benmoreite lavas. The eastern part is composed of strongly faulted, easterly dipping trachyte lavas. A central caldera structure is discernable on air-photographs in the north of the complex, but on the ground is largely obscured by younger basalt lavas and the effects of later faulting.

The cross-sections and reconstructions of Carney indicate that the preserved volcanic sequences on Chepchuk represent the eastern sector of a major shield volcano. The remains of this volcano, thought to have had dimensions similar to Paka, are preserved to the east of the Nagoreti fault and in an outlier at Longiro [AL 1846 0888]. The western half of the volcano has been downfaulted along the Nagoreti fault and completely buried in the floor of the inner trough by younger extrusive rocks of Paka and Korosi (Figure 5.1).

Carney et al. (1971) report four K/Ar dates for trachyte lavas and feldspar separates from the pyroclastic deposits of Chepchuk. These ages are in the range 1.13 ± 0.06 to 1.22 ± 0.06 Ma, and are consistent with the magnetism data of Dagley et al. (1978) which indicates that the Chepchuk trachytes have a reversed polarity.

The disposition of the volcanic units and the fault patterns indicate the presence of two eruptive centres, one of which is centred on Lotiamaleh [AL 1875 0925] and the other to the west of Longiro [AL 1846 0888]. The eastern half of a caldera structure is preserved at Lotiamaleh, the western part of which has been downfaulted along the Nagoreti fault and buried. From these centres trachyte lavas flowed eastwards across the Tangulbei plain. Stratal dips exceed 10° in the centre of the complex but decrease eastwards until they are sub-horizontal at the periphery. Trachyte lavas are the dominant lithology of Chepchuk. These are more siliceous than the younger trachytes of Korosi and Paka and were termed quartz trachytes by Carney (1972). On the upper flanks they occur as narrow leveed flows which pass down slope into laterally extensive lobate flows with well preserved concentric pressure ridges and flow fronts.

The pyroclastic deposits (C^v)are exposed in sections along the escarpment of the Nagoreti fault and on Longiro Hill. They comprise stratified, welded and non-welded pumiceous tuffs, interbedded with streaky, fissile, trachyte lavas. Benmoreites (C^i) are intercalated with the uppermost pyroclastic rocks on the southern flanks. Carney (1972) recognised a cyclical repetition within the succession which led him to propose that pyroclastic activity was contemporaneous with lava extrusion. According to Carney a typical cyclical

Plate 6.1 The geothermal area of Chepchuk. Reddened areas with sparse vegetation are hydrothermally altered and have ambient and elevated temperatures.

Plate 6.2 Specimen of silica sinter from Chepchuk.

sequence consists of a basal unit of pumice lapilli tuffs passing up into streaky porcelaineous welded tuffs which are overlain by vesicular trachyte lavas.

Younger basaltic lavas (C^{bu}), related to later activity on Paka and Korosi, were erupted from the Lotiamaleh centre. These lavas partly infilled the old caldera structure and locally overflowed its margins.

6.3 GEOTHERMAL ACTIVITY

Geothermal activity occurs on the northern part of Chepchuk where it is located upon a number of N-trending fault-bounded ridges parallel to the main Nagoreti Fault. The manifestations are confined to an area of about 2.5 km^2 (Plate 6.1).

Activity consists of hot altered ground and fumaroles. Some of the fumaroles are relatively vigorous and temperatures commonly exceed 90°C, reaching a maximum recorded value of 96.1°C, which is approximately the local boiling point. The principal areas of activity are located where the main N-trending faults are intersected by E-trending minor faults. Anomalous ground temperatures also occur in the caldera floor [AL 1877 0925], indicating that this area may be associated with a larger thermal anomaly than is evident from the surface manifestations.

Silica sinters and calcite veins are associated with areas of hydrothermal alteration which have ambient temperatures. These occur well to the south of the active geothermal areas, but are situated on the same controlling faults, suggesting that activity was previously more extensive or may have migrated northwards with time. The silica sinters are interpreted as fossil hot spring deposits (Plate 6.2). Two samples have been dated by U-series methods, giving ages of 430 ± 120 ka and 350 ± 60 ka (Sturchio et al., 1993) indicating that the geothermal activity at Chepchuk has been long-lived.

7 The geology and geothermal activity of Paka Volcano

7.1 INTRODUCTION

Paka is a well-defined volcano situated 25 km north of Lake Baringo and 15 km east of Nginyang village at 00°55'N, 36°12'E. It rises 600–700 m above the rift floor to reach a maximum altitude of 1697 m, and in plan view has an irregular outline covering an area of 280 km^2 (Figure 7.1). North to south topographic profiles indicate a symmetrical shield-like form, whereas east to west profiles show a more irregular, asymmetrical outline with steeply dipping western flanks (Figure 7.2). The rift floor around Paka has a pronounced west to north-west tilt falling from 1200 m in the Komol Valley in the south-east to less than 860 m at Nginyang village in the north-west. Whilst the eastern flanks overlie a faulted platform of Pliocene strata, the western flanks rest on the unfaulted floor of the inner trough.

The summit area of Paka is dominated by a NW-trending fault-bounded ridge. This ridge is a constructional feature formed by a series of coalesced eruptive centres, upon which several craters and a circular caldera 1.5 km in diameter have developed (Plate 7.1). On the upper northern and north-eastern flanks the base of this ridge is indicated by a prominent break of slope.

Paka is composed of trachytic and basaltic lavas and pyroclastic deposits. The geology was first described by Sceal (1974) and is summarised in reviews by Williams et al. (1984) and Hackman (1988). The work of Sceal (1974) is incorporated in the published 1:125 000-scale EAGRU geological map (Truckle, 1977b) and details of the geochemistry and petrology are discussed in Sceal and Weaver (1971). Prior to the present survey there were no radiometric age determinations for the rocks of Paka. A lower age of 0.5 Ma was generally assumed because the Nginyang Basalt overlies the Loyamarok Trachyphonolite dated at 0.53–0.50 Ma (Chapman and Brook, 1978). New dates obtained by the present survey indicate that activity had commenced by 390 ka and culminated at around 10 ka with the collapse of the summit caldera. The presence of unvegetated pristine basalt flows and scoria cones on the lower northern flanks suggests that activity may have continued into the last few millennia.

The evolutionary history of Paka may be broadly separated into two periods of trachytic volcanism separated by basaltic activity and faulting. The early history of the volcano is uncertain as the older shield-forming lavas are mantled by trachytic pyroclastic deposits which cover much of the northern, western and southern flanks of the volcano. Dissection of these deposits has produced a radial drainage pattern and an irregular topography of gullies and ridges densely vegetated by acacia and grass. The summit and upper flanks of Paka are characterised by short trachyte flows that can be discerned beneath the mantle of younger pyroclastic deposits. Basalt lavas were erupted from fissures and cones located along N-trending fractures on the northern and southern flanks, and contemporaneous normal faulting led to the formation of a N-trending linear zone of rifting which extends down the northern flanks. This rift zone is defined by two faults, the Eastern and Western Boundary faults (Figure 7.1) which controlled the dispersion of lavas and pyroclastic flows during the final stages of eruption and caldera collapse, and also constrain the geothermal activity of Paka. Trachyte and basalt lavas were erupted in the caldera and flowed out through a breach and down the northern flanks (Plate 7.1).

Paka is surrounded by a number of smaller satellite volcanic centres, which are linked to the main volcano by linear zones of basalt and trachyte cones and eruptive fissures (Figure 7.1). Activity on these centres is considered to have been broadly contemporaneous with that of Paka. To the north, Gulungul [AM 1900 1100] comprises a faulted trachyte shield mantled and surrounded by younger basalt flows. To the north-west, Napokoriatom [AM 1830 1100] is marked by a number of large discoid trachyte flows, associated with subordinate basalts and mugearites. In the south, at Adomeyan [AL 1810 0940] faulted trachyte lavas of uncertain source are overlain by younger basalt flows erupted from N-trending fissure zones extending between Paka and Korosi.

The tectonics of Paka are dominated by a zone of intense normal faulting and fissuring located on the eastern and north-eastern flanks. This faulting has downfaulted older Pleistocene and Pliocene strata of the rift margin against the younger lavas of Paka, and forms part of a larger belt of deformation which extends northwards onto Silali and southwards to Korosi. In contrast, there is no evidence for faulting nor fissuring to the west of Paka on the Natan Plains.

7.2 GEOLOGY AND EVOLUTION OF PAKA

The stratigraphy of Paka is summarised in Table 7.1. The terminology and sequence generally follows that of Sceal (1974) and Golden (1978) but has been modified in light of evidence gained during the present survey. Place names are derived from the published 1:50 000 topographical map.

7.2.1 Lower Trachytes (P^{tl})

The Lower Trachytes are the oldest rocks exposed on Paka and correspond to Sceal's Older Trachytes. They are overlain by the Lower Basalts and the Upper Trachytes. The base is rarely exposed, but to the north-east and east of Paka trachyte flows overstep onto the Orus Trachyte (3.2 ± 0.2 Ma, Golden, 1978), and in the south rest on trachytes of Chepchuk (Section 6). The Lower Trachytes form lobate or button-shaped flows which are distinguished on air-photographs by monotonous grey photo-tones, and by their faulted, eroded and vegetated appearance. They are microporphyritic, weakly silica-oversaturated, pantelleritic trachytes.

Prior to this survey the age and stratigraphical position of the trachyte lavas exposed in the faulted terrain

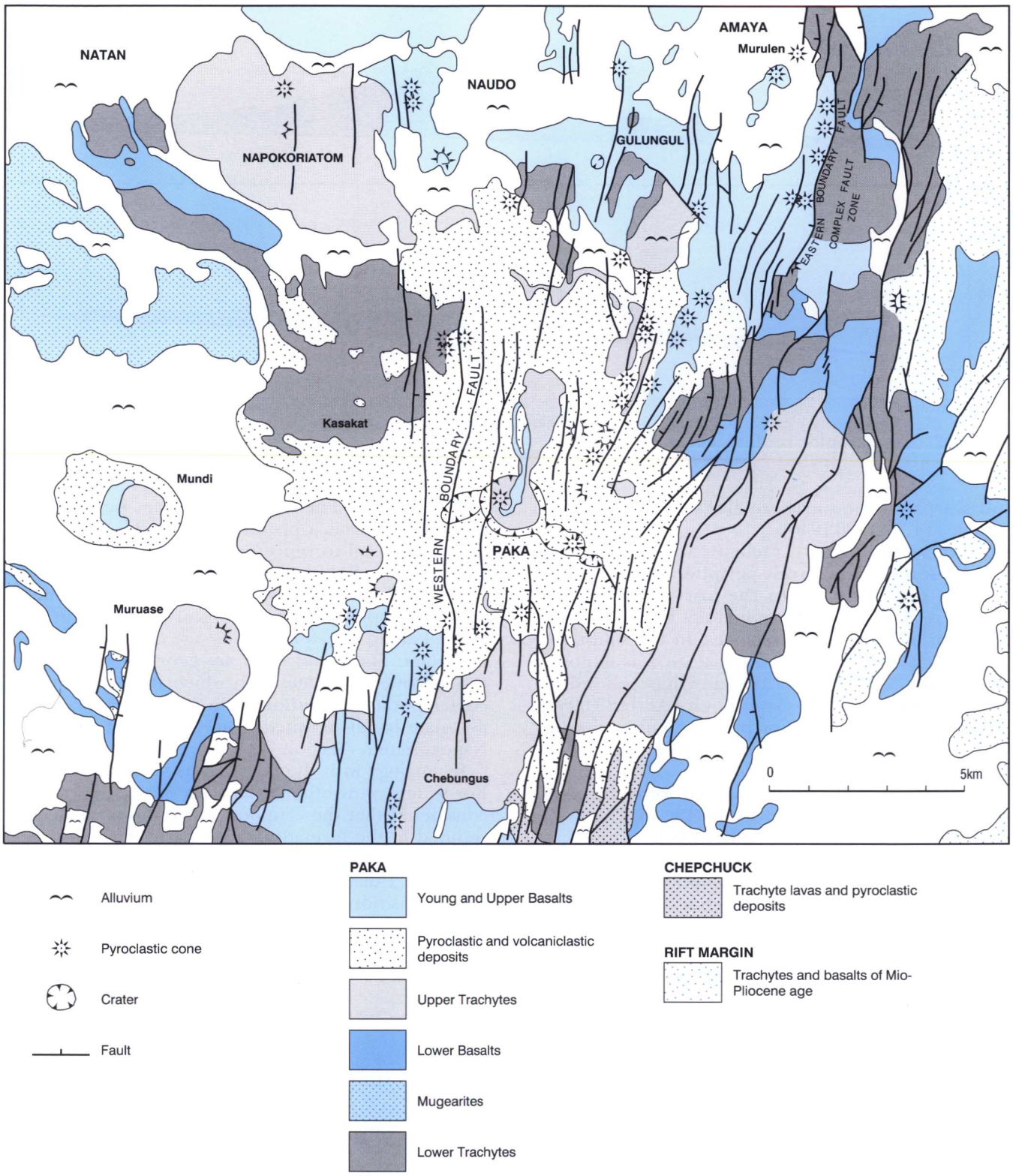

Figure 7.1 Simplified geological map of Paka volcano.

to the north-east of Paka was uncertain. These lavas, shown on the accompanying geological map as the Secuminus Trachytes (Sct), were previously designated as Pliocene (Truckle, 1977b; Golden, 1978) or Pleistocene (Sceal, 1974) in age. The present survey has obtained an Ar/Ar age of 390 ± 6 ka for one sample at [AM 1962 1097] indicating that the Secuminus Trachyte is part of the Lower Trachyte lavas of Paka. These lavas are largely confined to a faulted, narrow trough, 15 km long and 3 km wide, but they also extend northwards to the Amaya river and eastwards to rest on landslipped blocks of Orus Trachyte. Stratal dips and flow directions indicate that prior to faulting they formed a low relief, north-easterly-dipping sheet which can be traced upslope across the lower flanks of Paka. At Secuminus Hill [AM 1953 1130] Sceal recorded up to 74 m of porphyritic trachytes and interbedded mugearites, and similar lavas are exposed in

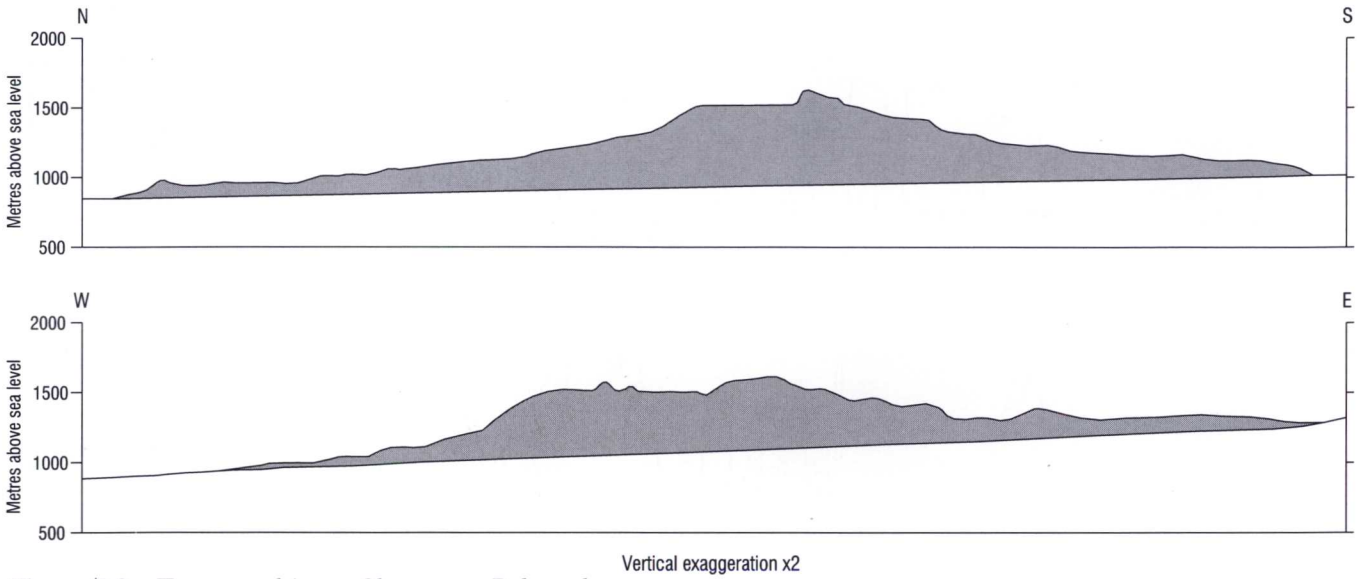

Figure 7.2 Topographic profiles across Paka volcano.

fault scarps on the northern flanks of Paka, as for example at [AM 1920 1046].

Elsewhere the Lower Trachytes are exposed in a series of scattered outcrops peripheral to the lower flanks of the volcano. On the northern flanks at Jamokatan [AM 1883 1093] an inlier of faulted trachyte is overlain by basalts and trachytes. In the south and south-west a single lobate trachyte flow is exposed beneath the Upper Trachytes and has yielded an Ar/Ar age of 219 ± 4 ka. At Tapogh [AL 1885 0950] altered trachytes, overlain by pyroclastic deposits and the Upper Trachytes, are exposed in a series of N-trending fault scarps.

A number of cones and unfaulted lobate trachyte flows, provisionally assigned to the Lower Trachytes, occur on the north-western flanks of Paka. These pass upslope into narrow flows with levees, which are overlain by younger trachyte lavas. Eruptive sources take the form of a series of volcanic cones aligned along N–S fractures. The largest of these, Kasakat [AM 1835 1040], forms a prominent hill which was interpreted by Sceal to represent an eroded centre from which most of the pyroclastic deposits have been removed. To the north-east of Kasakat, three minor centres composed of trachyte scoria and pumice are aligned along a N–S fault. The age of these centres is uncertain. The oldest flows are geochemically similar to the Lower Trachytes with which they are probably contemporaneous, although the youngest flows clearly post-date basalts erupted from the satellite centre of Napokoriatom (Section 7.2.8.2).

By analogy with the contiguous volcanic centre of Korosi and with other volcanoes of the region, it is considered that the eruption of the Lower Trachytes resulted in the formation of an early volcanic shield. The size of this shield is uncertain, but it appears to have had a diameter of about 15 km, as indicated by the disposition of the younger flows and featuring

Plate 7.1 Aerial view of Paka volcano looking south-east over the summit area. The faulted terrain of Chepchuk is visible in the distance.

within the overlying pyroclastic deposits.

7.2.2 Lower Basalts (P^{bl}) and faulting

As on Korosi, Sceal (1974) believed that the two main phases of trachyte activity on Paka were separated by a period of faulting and basaltic volcanism. The Lower Basalts correspond to Sceal's Older Basalt unit and are exposed in faulted sections on the north-eastern and south-eastern flanks where they are overlain by the Upper Trachytes. Also included in this group are small faulted inliers and scoria cones at Jamokatan and south of Cheptomas [AM 1875 1102]. The distribution of scoria and spatter in both of these areas suggests eruption of fluid lava along fissures with localised strombolian activity.

The older Lower Basalts are faulted, eroded and thickly vegetated. Source areas are obscured by younger deposits, with one exception being a small scoria cone at [AM 1938 1042]. Compositionally, they are predominantly weakly undersaturated basalts although picritic basalts and rare occurrences of ankaramites were also recorded by Sceal (1974).

A sequence of basalt lavas, indicated on the accompanying map as the Kokwabangà Basalt (K^{kb}), outcrop in a narrow strip on the east side of Paka and north of the Komol valley. They overlie the Secuminus and Orus trachytes and are thought to be contemporaneous with the Lower Basalts on Paka. These basalts were erupted from a N-S trending fissure zone upon which a number of basalt scoria cones are aligned. From these cones, basalt lavas up to a 10 m thick flowed northwards and westwards over the Orus Trachyte and infilled small graben within the Secuminus Trachyte. At the most northerly of the scoria cones [AM 1970 1075] Sceal (1974) recorded scoria containing xenoliths of banded gabbro and syenite.

By comparison with adjacent centres, Sceal (1974) considered it likely that faulting and fissuring accompanied the eruption of the Lower Basalts. However on Paka it is difficult to substantiate this. The ponding of basalt lavas on the lower southern flanks against the Nagoreti fault, and within graben in the Lower Trachytes to the east, indicates that movements had taken place along the rift margin faults, but the exact timing of this faulting relative to the basaltic activity is unknown.

The Nginyang Basalt forms a large lava field which covers the plain to the west of Paka and extends as far as Nginyang. On the geological map (enclosed), these lavas are included within the Upper Basalts. However, no contact relationships are seen between the Nginyang Basalt and other volcanic units, and therefore its age is open to speculation. Following publication of the geological map, chemical analyses were obtained which indicate the Nginyang Basalt to be hypersthene-normative, whereas all the other basalts of Paka are nepheline-normative. Hypersthene-normative basalts are not common within the volcanic centres of the inner trough, but where they do occur they are usually the oldest basalts and in some cases may pre-date the volcanoes. The Nginyang Basalt is partly buried by superficial deposits and is vegetated, and in this respect does not resemble the Upper Basalts. On the available evidence, albeit circumstantial, it is now considered more logical to include the Nginyang Basalt within the Lower Basalts.

Table 7.1 Summary of the stratigraphy of Paka

Young Basalts (b^{y})		
Trachytes and mugearites	11 ± 3 ka	INTRA-CALDERA LAVAS
		CALDERA FORMATION
Pyroclastic Deposits (P^{v})	8 ± 4 ka	
Upper Basalts (P^{bu})		
Upper Trachytes (P^{tu})		
Lower Basalts (P^{bl})		
Lower Trachytes (P^{tl})	219 ± 4 ka 390 ± 6 ka	SHIELD FORMATION

7.2.3 Upper Trachytes (P^{tu})

The Upper Trachytes were erupted from the summit area and from numerous parasitic centres located on the eastern and southern flanks (Figure 7.3), and are volumetrically the most important rocks on Paka. They rest on the Lower Trachytes, except on the north-east flanks where the Lower Basalts intervene. The Upper Trachytes are characterised by pancake-like flows with well preserved morphological features and high flow fronts. On air-photographs they show pale grey mottled photo-tones and at outcrop are fissile, grey lavas with up to 30% phenocrysts of alkali feldspar. Compositionally, they include both weakly nepheline normative and weakly quartz normative peralkaline trachytes.

The outcrops of Upper Trachytes may be conveniently described in terms of three sectors as follows.

The trachytes of the eastern and south-eastern flanks define a broad apron extending from Cheptuyun [AM 1950 1030] in the north to Chebungus [AL 1860 0960] in the south. They were erupted from sources high on the eastern flanks and cover an area of about 6 km^2, swamping the faulted Lower Basalts and Lower Trachytes. Small button-shaped flows and extrusive domes indicate eruptive centres at [AL 1890 0990] and [AM 1920 1011]. Initially the fault scarp topography of the eastern flanks impeded the flow of lava, but as the topography was progressively buried, flows were able to spread laterally across the Lower Trachytes and Lower Basalts. Subsequently, many of the early faults were rejuvenated. The Chebungus flow dominates the southern flanks. It extends for 5 km and has well developed levees, pressure ridges and radiating tension cracks.

The apparent lack of trachyte lavas exposed on the western and south-western flanks led Sceal (1974) to suggest that the Western Boundary Fault created a topographic barrier restricting flow into this area. However, there is widespread evidence of button-shaped flow-fronts and levees beneath the pyroclastic deposits that mantle this area, indicating that trachyte activity was extensive on the south-western and western flanks. This sector includes the flow of Moruatabka which was extruded from a parasitic trachyte pumice cone at [AM 1835 1008], and Murase [AL 1795 0985], a spectacular button-shaped flow 100 m thick that was erupted from a breached trachyte scoria cone on the rift floor.

Trachytes on the northern flanks are exposed as a series of ribbon-like outcrops marking the flow-fronts of large lobate flows now buried by pyroclastic

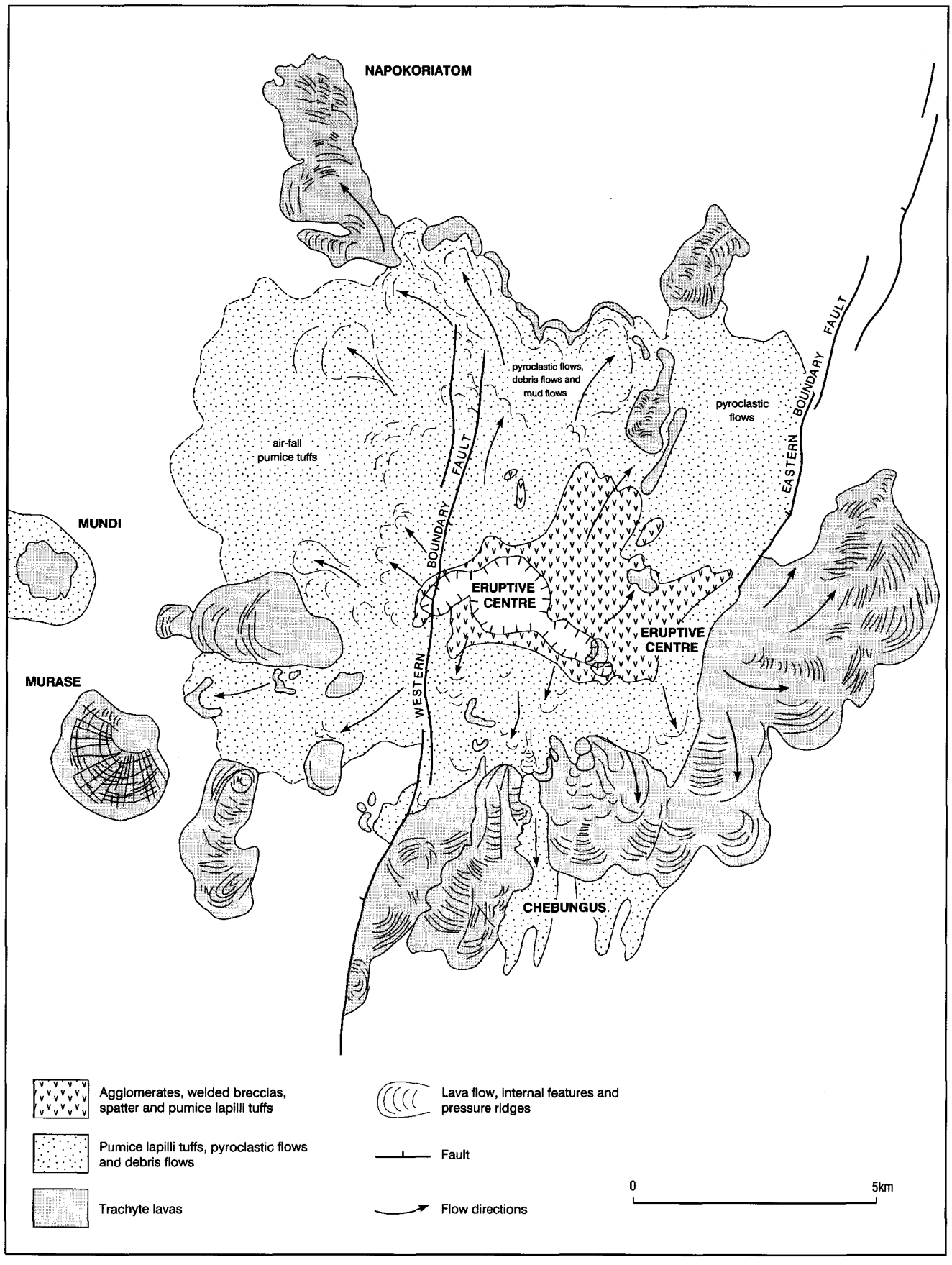

Figure 7.3 Distribution of Upper Trachytes and pyroclastic rocks on Paka volcano.

deposits. Sporadic exposures occur in stream sections and fault scarps on the upper flanks, and on the summit area these flows are overlain by numerous short trachyte lavas that are cut by the summit caldera. The uppermost flows were erupted from fissures along the line of the Western Boundary Fault and from trachyte cones on the upper flanks that were contemporaneous with the pyroclastic deposits described below in Section 7.2.5.

7.2.4 Upper Basalts (P^{bu})

The Upper Basalts were erupted from a series of NNE-trending fissures and scoria cones on the southern and north-eastern flanks. They consist of weakly undersaturated basalts and hawaiites that appear to have been very fluid at the time of eruption. They are generally less vegetated than the Lower Basalts.

On the southern flanks, basalts were erupted from two NNE-trending fissures marked by lines of spatter and scoria cones at Chepkatamai (or Lokukus) [AL 1850 0983]. Elsewhere basalt flows infilled the low ground between Paka and Korosi and flooded southwards. Later faulting has produced a series of N–S graben and horsts within these basalts. Fissure-controlled scoria cones and spatter ramparts also extend north-eastwards from the summit area of Paka and were the source of fluid basalts which flowed across the plains between Silali and Paka.

The main phase of faulting on Paka was probably contemporaneous with the Upper Basalts. Major movements along the Western Boundary Fault and the Eastern Boundary Fault formed a broad axial rift across the summit area and northern flanks of the volcano. Along the Eastern Boundary Fault swarms of minor faults with displacements of less than 10 m are associated with open fissures, basalt scoria and spatter cones, and hornitos. These include the cones of Copanomorule [AM 1906 1065], Luweat [AM 1921 1075] and Morulen [AM 1940 1134] which are breached to the north and north-east. These are post-dated by pristine, sparsely vegetated basalts which were erupted from fissures located in the fault zone to the north-east.

7.2.5 Pyroclastic and Volcaniclastic Deposits (P^{v})

Trachytic pyroclastic deposits form a thick mantle over the summit area and large parts of the western and northern flanks of Paka. The deposits overlie the Upper Basalts and Upper Trachytes, and are cut by the caldera. They were erupted from pumice cones on the summit area and upper north-eastern flanks (Plate 7.2), and were carried to the west on the prevailing easterly wind. This has resulted in a strong asymmetry to their distribution. To the east they have only been mapped up to 1 km from the summit, but to the west they extend at least 17 km to Nginyang (Figure 7.3).

In the following sections the pyroclastic deposits of the summit and flank areas are described separately.

7.2.5.1 Summit area

The summit area of Paka is dominated by a number of craters and a small caldera, which are aligned in a north-westerly direction. The caldera is circular in plan with a diameter of 1.5 km, has vertical walls up to 120 m high, and is breached on its northern side. To the south-east there is a second large crater, the eastern crater, referred to by Sceal (1974) as the 'explosion crater'. The eastern crater measures 1 km by 0.5 km and has a degraded trachyte pumice cone which forms a ridge across the centre, effectively splitting the crater into two. An older crater with a long axis trending NNE is also present to the west of the main caldera and exposes sections through stratified pumice-rich breccias and lapilli deposits, and another old crater feature also occurs to the south-east of the eastern crater.

The deposits are well exposed in the caldera walls where they overlie a thick sequence of trachyte lavas and lithic breccias. They consist predominantly of stratified pumice lapilli tuffs interbedded with poorly sorted, polymictic agglomerate and matrix-supported breccia units containing lithic clasts of trachyte and

Plate 7.2 Aerial view of trachytic pumice cones on the upper north-eastern flanks of Paka, looking south-east. Areas of brown vegetation are geothermally active.

microsyenite up to half a metre in size. Strongly welded obsidian-like glassy zones occur within the tuffs and the breccias. Ar/Ar dating of alkali feldspar crystals from the youngest lapilli tuff exposed in the south-west wall has given an age of 8 ± 4 ka.

The dominant feature exposed in the west wall of the caldera is a NNE-dipping discontinuity within the lower beds (Plate 7.3). The upper beds attenuate towards, and appear to be draped over this structure. The present survey agrees with the interpretation of Sceal (1974) who suggested that this structure and the underlying beds represent an oblique section through a trachyte cone complex. A similar structure on a smaller scale is exposed at the northern end of the west wall and is indicated by steep dips and local unconformities in the sequence. A small intrusive plug occurs low in the south-west wall within the lower sequence of welded breccias.

In the south-east wall, well-jointed trachyte lavas and lithic breccias are exposed, the uppermost beds of which contain abundant obsidian fragments. Westwards, the sequence becomes more heterogeneous with intervening beds of pumice and agglomerate with well-rounded trachyte bombs. The east wall comprises a cyclical sequence of poorly-sorted, heterolithic breccias and pumice breccias containing strongly welded obsidian-like layers. The beds undulate gently and have local intraformational unconformities.

Exposure in the eastern crater is poor due to intense hydrothermal alteration and down-wasting. The wall at the eastern end of the crater is about 60 m high and is composed of massive trachyte lava overlain by welded trachyte scoria. Elsewhere around the crater, trachyte lavas are overlain by welded scoria and poorly consolidated pumiceous deposits. Vent agglomerates composed of well-rounded lithic clasts are patchily exposed in the north-western wall and on the western half of the crater floor.

7.2.5.2 Flank deposits

The dissected lower western flanks have numerous sections exposed in poorly-consolidated, pumice lapilli tuff overlying trachyte lava. Similar tuffs also drape Mundi Hill and extend westwards to overly the Nginyang Basalt. The well-bedded nature of these pumiceous deposits and the manner in which they drape the topography suggests an air-fall origin from plinian-style eruptions on the summit area. On the upper western flanks these tuffs are overlain by coarser-grained, more proximal sequences of alternating lithic breccias and pumice lapilli tuffs. Typical is a section in the scarp of the Western Boundary Fault at [AM 1855 1014] which exposes 70 m of interbedded, lithic breccias and pumice lapilli tuffs. The breccias are clast-supported and poorly sorted. They contain large angular clasts of trachyte lava and syenite set in a finer matrix of lithic and pumice lapilli. Thin irregular beds of fine tuff commonly mantle the tops of the breccia units, but where these are absent the contacts with overlying pumice lapilli tuffs are sharp and planar. The lapilli tuffs consist of fine to medium-grained pale brown pumice with fine lithic clasts. They are crudely stratified and some beds are inversely graded. Thin zones of welding and beds of agglutinated trachytic spatter are common throughout. The overall impression imparted by these deposits is one of a rhythmical series of events.

The upper northern slopes reveal sections in the pyroclastic cones from which the deposits were erupted. These consist of trachyte spatter, scoria, pumice breccias and well-bedded pumice lapilli tuffs and ashes. In places, spectacular drapes of agglutinated spatter and strongly welded obsidian-like beds mantle the flanks of these cones, resting unconformably on the underlying deposits, as for example at [AM 1893 1028] (Plate 7.4).

Stream sections on the lower northern flanks reveal a wide range of pyroclastic and volcaniclastic deposits. These include massive and stratified pumice lapilli tuffs and breccias of pyroclastic-flow and mass-flow origin. These deposits have distinctive white photo-tones and are deeply dissected. Mudflow deposits occur on the lowest flanks and are composed of pumice and polymictic lithic clasts supported by reddened clay-rich matri-

Plate 7.3 Western wall of Paka caldera showing bedded trachytic tuffs with zones of welding, draped against massive lavas and welded breccias.

Plate 7.4 Trachytic spatter mantling bedded pumice lapilli deposits on the north-eastern flanks of Paka. Looking north-east.

ces. At several localities, pumice lapilli within the mudflow deposits are surrounded by voids, which are interpreted as representing original steam carapaces formed by the interaction of hot clasts with a wet matrix. The disposition of these pyroclastic deposits indicates that they were erupted from the summit region and flowed down the northern flanks where they were constrained in a trough-like depression bounded in the west by the Western Boundary Fault and in the east by a NNE-trending ridge of Lower Trachyte. Interpretation of air-photographs indicates that pyroclastic flows also passed through breaches in the scarp of the Western Boundary Fault and flowed down the western flanks between Kasakat and Moruatabka.

7.2.6 Caldera formation

The limited accumulation of talus deposits and lack of degredation indicates that the caldera of Paka is a relatively young feature. Formation of the caldera was preceded by large-scale eruption of the trachytic pyroclastic flow and fall deposits described in the previous section, which are cut by the caldera wall. The youngest of these deposits in the caldera wall has an age 8 ± 4 ka, and a resurgent trachyte lava ponded on the caldera floor has an age of 11 ± 3 ka. Collapse of the caldera must therefore have occurred around 10 ka and was triggered by the eruption of the voluminous Pyroclastic Deposits.

The eastern crater also post-dates the Pyroclastic Deposits and probably formed at approximately the same time as the main caldera.

7.2.7 Post-caldera activity—basalts and trachytes

Post-caldera activity on Paka has been limited to the eruption of a trachyte and a mugearite lava within the caldera.

A blocky trachyte lava covers most of the caldera floor and has poured out through the breach in the north wall of the caldera to extend 2.5 km down the northern flanks (Plate 7.1). This trachyte has pronounced concentric pressure ridges and multi-lobate flow-fronts up to 40 m high. Ar/Ar dating of alkali feldspar phenocrysts indicates an age of 11 ± 3 ka for this flow.

The final stage of activity on Paka is marked by the eruption of fluid mugearites from a scoria cone within the western half of the caldera. Fire-fountaining from the cone produced agglutinated spatter, and directed blasts gave rise to spatter and scoria drapes on the south-west wall of the caldera. Lavas from this cone flowed southwards and eastwards across the trachyte on the caldera floor before flowing out of the breach and down the northern flanks. The rapid drainage of magma from the conduit feeding this cone has formed a cylindrical vent 30 m deep within the cone. The walls of the vent expose sections through the scoria cone and show that it rests on 10–20 m of well-bedded pumice lapilli tuffs which in turn rest on porphyritic trachyte lava.

7.2.8 Satellite volcanic centres

7.2.8.1 Gulungul and Cheptomas

On the Amaya plains to north of Paka, the low hills of Cheptomas [AM 1880 1100] and Gulungul [AM 1900 1100] represent the remnants of a small satellite trachyte shield with an area of 10.5 km^2. The older trachyte lavas (P^{tl}) of the shield are exposed in a number of fault bounded sections on Cheptomas Hill [AM 1884 1103] and further east as inliers within younger basalt flows (b^{y}). A crater, 200 m in diameter, is exposed at [AM 1895 1111] and was probably the central source for these flows. Short, steeply dipping trachyte flows and partly eroded cones are preserved along fault scarps on Gulungul and suggest fissure type eruptions occurred on the flanks of the shield. The age of the Cheptomas satellite shield relative to the main volcanic edifice of Paka is uncertain, although it is overlain by lavas and pyroclastic deposits of the Upper Trachytes suggesting contemporaneity with the Lower Trachytes of Paka.

The overlying, young, unvegetated basalts of Gulungul and Cheptomas were erupted from a series of N–S fissures indicated by lines of hornitos, tumuli

and spatter ramparts. Spatter and scoria cones are also present to the south and east. From these fissures and cones pahoehoe flows spread northwards and westwards to the Amaya valley, covering the faulted topography of the early trachyte shield. To the north of Gulungul the tops of two basalt cones protrude through the alluvium and indicate a link with the Flank Fissure Basalts of Silali (Section 8.3.8).

7.2.8.2 Napokoriatom

Four large trachyte flows are present at Napokoriatom, located on the periphery of the north-western flanks of Paka. Sceal (1974) considered that the lavas were derived from Kasakat, but their spatial distribution and flow features indicate they were erupted from a single source, possibly a fissure at [AM 1835 1095], now largely buried by younger flows. Two distinct ages of trachyte lava are present. The older flows are lobate and discoid with well preserved pressure ridges and levees. These are silica-oversaturated pantelleritic trachytes which closely resemble the Discoid Trachytes of Silali (Section 8.3.5). The overlying trachytes are strongly porphyritic and nepheline-normative. They have well-preserved flow features similar to the Upper Trachytes on Paka.

On the east side of Napokoriatom, basalt and hawaiite lavas were erupted from the scoria cone of Lokawatch [AM 1846 1130]. The age of these flows is unknown, although they appear to be older and more vegetated than the nearby basalts of Gulungul.

7.2.8.3 Katalim and Hill of Mundi

The Katalim mugearite is a single lava flow which was erupted from a NE-trending fissure at [AM 1795 1072]. It spread across the Natan plains to overly the Jamkana Formation and the Jarota (Murgisian) Basalts of Plio-Pleistocene age. The lava, a dove-grey vesicular rock, covers an area of about 26 km^2. Further south, in the Tilam area, Sceal (1974) records a single fissile mugearite lava outcropping below the Nginyang Basalt. Similar mugearite lavas are exposed in the Hill of Mundi [AM 1780 1023], where three flows were erupted from a central vent. These dip gently westwards and are overlain by a thin layer of pumice capped by a trachyte lava (Sceal, 1974).

7.3 SUMMARY OF EVOLUTION AND STRUCTURE

Paka is a small shield volcano constructed largely of trachyte lavas and pyroclastic deposits. Basalt, hawaiite and mugearite lavas were erupted from a series of fissure and fault zones located on the lower north-eastern and southern flanks. Volcanic activity commenced by 390 ka and has continued to within the last 10 ka. Broadly contemporaneous trachytic and basaltic activity occurred on a number of small satellite centres peripheral to the main volcanic edifice.

The oldest exposed rocks are the Lower Trachytes which constructed an early volcanic shield. Subsequent fracturing of the early shield by NNE-trending faults was accompanied by eruption of the Lower Basalts from fissure sources on the eastern flanks of the volcano.

Faulting was followed by the eruption of the Upper Trachytes which formed a broad apron of discoid trachyte lava around the flanks of the volcano. These lavas were erupted from numerous domes and cones located along N-trending and NNE-trending fissures on the upper flanks and summit area. Further faulting and fracturing across the shield led to the formation of an axial rift zone defined by two important faults, the Eastern and Western Boundary faults. Rifting was probably contemporaneous with a second phase of basaltic activity that produced the Upper Basalts, which were erupted from fissures on the lower northern and southern flanks of the volcano.

At around 10 ka large volumes of trachytic pyroclastic deposits were erupted from a complex of cones on the upper northern flanks and summit area. These cones constructed a NW-trending ridge across the summit area. Pyroclastic-flows and mud-flows from the summit cones were topographically constrained by the rift zone and flowed down the northern flanks, and also locally flowed through breaches in the Western Boundary Fault scarp to cover the western flanks. Airfall pumice deposits and tuffs were dispersed on the prevailing easterly wind and extend for more than 17 km to the west. This pyroclastic activity finally resulted in the collapse of the summit area to form a series of craters and the caldera. These craters are aligned on a north-westerly trend, similar to the orientation of the calderas on Silali and Emuruangogolak.

Resurgent activity gave rise to the eruption and ponding of a trachyte lava within the caldera soon after its formation, and subsequently this was followed by the eruption of a mugearitic scoria cone and lava. Young basalt and hawaiite lavas have also been erupted from fissures low on the northern and southern flanks.

The structure of Paka is dominated by a broad zone of normal faulting, 7.5 km wide, which shows a right-stepping *en échelon* arrangement across the volcano. This zone forms part of a regional fault pattern which extends southwards to Korosi and Chepchuk and northwards onto the southern flanks of Silali. On the southern flanks of Paka the faults trend N–S but as they cross the summit area they show an arcuation into a NNE to NE trend. This refraction across the volcano and the general absence of faulting in the summit area suggests that a magma body may have existed at a high structural level within the volcanic centre at the time of faulting.

The main locus of faulting is restricted to this axial zone of rifting which largely formed during Upper Basalt times. Within this zone displacements across individual faults are minor (<10 m), although the cumulative displacement across the boundary faults may be considerable; for example, the cumulative throw across the Eastern Boundary Fault is estimated to be in excess of 250 m. Subsidence and faulting continued during the eruption of the pyroclastic deposits and some movements along the Western Boundary Fault post-dated the formation of the caldera.

7.4 GEOTHERMAL ACTIVITY OF PAKA

7.4.1 Introduction

Surface geothermal activity, manifested in the form of hot ground, steaming ground and fumaroles associated with hydrothermal alteration, is widely developed on Paka within the summit craters and upon the northern

flanks (Figure 7.4). There are no hot springs on Paka, although pools of warm water form locally within the summit craters by condensation from fumaroles on near-vertical rock surfaces. In many of the thermal areas maximum temperatures are at, or slightly exceed, the local boiling point, and the maximum recorded value of 97.8°C is several degrees above this. The highest temperatures are found within areas of steaming ground, often characterised by white, purple and red clays. Areas of extinct activity are indicated by hydrothermally altered ground with ambient temperatures.

Geothermal activity on Paka is dispersed over a broad NNE-trending zone covering an area of approximately 32 km^2, extending from high on the southern flanks northwards across the summit area and down the northern flanks. In addition, there is an isolated occurrence further to the north-east on the basaltic cone of Murulen [AM 1939 1135]. Surface activity within the main zone is strongly controlled by NNE-trending faults, and on a more local scale is associated with scoria and pumice cones aligned along these fractures. The activity is bounded on the west by the Western Boundary fault, to the west of which there are no surface manifestations. The eastern limit of thermal activity is less well defined, but is constrained by a number of west-facing faults cutting the north-east flanks of the volcano.

For the purpose of description the thermal activity on Paka is divided into seven sub-areas.

7.4.2 Caldera

Geothermal activity is widespread within the summit caldera (Figure 7.4), and is most intense on and around the basaltic scoria cone in the western half of the caldera floor [AM 1869 1022]. Hot ground with weak to moderately strong fumaroles occurs on the north-western and south-eastern flanks of the cone, and is continuously developed around the rim. Recorded ground temperatures range from 50.2°C to 94.5°C, and fumarole temperatures between 74°C and 93.7°C. The hottest ground and strongest fumaroles are situated on the south-western rim of the cone, where the basalt spatter and scoria has in places been thoroughly altered to purple, red and white clays with yellow sulphates, and where there is a sulphurous smell. Hot and steaming ground also occurs within the deep cylindrical vent of the scoria cone; near the base of the southern wall of the vent two moderately strong fumaroles issue from joints within massive trachyte, and condensation gives rise to a small pool of water.

The activity surrounding this scoria cone forms part of a broad northerly trending zone which extends across the floor of the western half of the caldera, and down the north-western flanks of the volcano (see below). Within this zone on the caldera floor there are numerous fumaroles with temperatures above 80°C and many exceeding 90°C. The largest and hottest fumaroles occur at the southern end of the zone where it intersects the base of the caldera wall around [AM 1868 1017). Here, weak to strong fumaroles with temperatures up to 96.2°C issue from trachyte which is strongly altered to white clays consisting dominantly of kaolinite with alunite.

Immediately to the east and south-east of the scoria cone there are patches of hot ground with numerous fumaroles developed upon basalt lavas. Ground and fumarole temperatures range up to 96.3°C and there is intensive alteration to kaolinitic clays with alunite and some carbonate. Passing eastwards across the caldera floor, the intensity of the activity declines and temperatures are considerably lower. Activity in the eastern half of the caldera floor is confined to small, sporadic patches of hot and altered ground with a maximum recorded temperature of 61.9°C.

Activity is also developed around the caldera walls, particularly within the porous pyroclastic deposits on the north-western side. Several vigorous fumaroles are located along a small N-trending fault, and a maximum temperature of 95.8°C was recorded. Activity on the southern wall of the caldera is limited due to the presence of relatively impermeable massive trachyte lavas and breccias. Several small patches of hot ground occur in talus at the base of the wall, and in one of these [AM 1875 1014] a maximum temperature of 97.1°C was recorded.

7.4.3 Eastern Crater

Intense geothermal activity occurs in the Eastern Crater around the southern and south-eastern walls, and on the eastern side of the central trachyte cone. The activity includes hot ground, steaming ground and fumaroles, hosted in scree and pumiceous deposits which are intensely altered to white and purple-red kaolinitic clays containing alunite. Fumaroles have moderate to strong flows and temperatures commonly exceed 90°C, ranging up to a maximum of 95.9°C. The largest fumarole on Paka is located on the highest point of the south-eastern rim of the crater, and produces a prominent steam plume which is often visible from a distance of several kilometres. Around the eastern and north-eastern wall temperatures are generally lower, although several fumaroles and areas of steaming ground have temperatures close to boiling point.

Geothermal activity in the western part of the crater is less intense and is indicated by a number of patches of hot ground and sporadic fumaroles with temperatures generally in the range 40–80°C. In the floor of the western part of the crater there is a small area of flat ground surrounded by hummocks of agglomerate. These are the sites of vigorously steaming ground with temperatures at boiling point (maximum recorded 95.2°C).

7.4.4 North-western flanks

To the west of the young trachyte flow breaching the caldera, geothermal activity occurs within a broad zone extending for a distance of 4 km down the north-western flanks. A prominent NNE-trending fault scarp, exposing trachyte lava, marks the western margin of this zone. Steaming and altered ground is developed along this fault over a length of 2.5 km from [AM 1868 1036] to [AM 1875 1057]. Ground and fumarole temperatures commonly exceed 90°C, and the highest temperature of 97.5°C (local boiling point 95.5°C) was recorded from an area of intense alteration at the southern end of the zone [AM18671035].

Within the lower ground to the east of the fault scarp and along the western margin of the young trachyte lava flow there are a number of patches of hot and reddened ground developed upon pumiceous


Area of hot ground
and / or fumarolic activity
Fumarole
Fault
Volcanic cone
Trachyte lava
Basalt lava
WESTERN BOUNDARY FAULT
ZONE A
ZONE A
ZONE B
ZONE B
ZONE C
EASTERN
CRATER
0
1km

Figure 7.4 Location of geothermal activity on Paka and its relationship to faulting and volcanic activity.

pyroclastic deposits. Temperatures within this low ground commonly exceed 90°C and reach a maximum recorded value of 96.2°C (Plate 7.5). Several of the patches are linearly disposed and controlled by northerly trending minor faults. At the northern end of this zone a fault scarp in pumiceous pyroclastic deposits extends in a NNE direction from the NW corner of the young trachyte lava [AM 1878 1056]. Fumaroles with moderate to strong flow rates are present along this scarp, but temperatures are generally low due to the ingestion of air, reaching a maximum recorded value of only 81.6°C.

7.4.5 North-eastern flanks

Activity on the north-eastern flanks extends from the rim of the eastern crater downslope for a distance of 7 km and is concentrated in three linear zones which have slightly divergent northerly trends down the flank of the volcano. These zones, designated A, B and C (Figure 7.4) are coincident with separate fracture lines upon which trachytic and basaltic pyroclastic cones are developed.

Zone A, the westernmost of the three zones, extends over a length of 4.5 km and for most of this distance is constrained by two parallel northerly-trending faults. Hot ground, steaming ground and discrete fumaroles are located upon the inner rims and upper flanks of trachytic pumice-scoria cones and ridges. Temperatures are highest along the central part of the zone where they reach a maximum of 96.1°C. Fumarole flows range from weak to strong. Alteration takes the form of red, purple and white clays, with carbonates and sulphates in the more porous deposits.

Zone B extends in a NNE direction for a distance of 7 km from [AM 1892 1021] on the upper flanks of the volcano down to the basalt cone near Gulungul [AM 1908 1079]. Within this zone, hot ground, steaming ground and weak fumaroles are developed upon a prominent line of trachytic pumice and basaltic scoria cones. In the upper (southern) parts of the zone temperatures within thermal areas generally exceed 90°C and reach a maximum of 96.1°C. Activity is less intense in the lower ground at the northern end of the zone and temperatures are lower, with maximum recorded values for individual thermal areas ranging from 46.7° to 93°C. Alteration takes the form of red and purple clays with secondary carbonates and sulphates.

Zone C extends downslope in a NNE direction for a distance of 5 km from [AM 1896 1021] to the basaltic cone at [AM 1914 1058]. This zone is less well defined and comprises a number of separate *en échelon* fault-controlled areas, underlain by a variety of lithologies. Activity is mostly manifested as patches of hot ground with occasional weak to moderate-strength fumaroles. Temperatures are generally low with maximum recorded values for individual thermal areas ranging from 35.5°C to 96.3°C. Of particular interest is the fact that the highest temperatures occur at the northern end of this zone [AM 1912 1056], well away from the summit area. Red, purple and white clays are common in the southern part of the zone. Silica veins within this zone at [AM 1907 1036] have yielded U-series dates of 81 ± 7 ka and 64 ± 4 ka (Sturchio et al., 1993).

7.4.6 Western flanks and old crater

On the western flanks of Paka, geothermal manifestations are confined to a NNE-trending linear zone along the Western Boundary Fault, and to the inner side of the northern rim of the old crater feature to the west of the caldera.

Reddened patches of hot ground with weak to moderate fumaroles extend along the trace of the Western Boundary Fault for a distance of 4 km from [AL 1855 1000] in the south to [AL 1861 1028] in the north. Maximum recorded temperatures on individual areas of hot ground range between 48.7°C and 77.5°C. In the old crater to the west of the caldera [AM1860 1020], patches of reddened and hot ground with weak

Plate 7.5 Area of hydrothermal alteration and geothermal activity in pumice deposits on the northern flanks of Paka.

fumaroles and steam seepages occur in an E–W trending belt along the inner side of the northern rim. At the western end this zone merges with the NNE-trending zone controlled by the Western Boundary Fault, and at the eastern end it merges with the activity of the caldera. Temperatures are lowest in the west and increase in an easterly direction towards the caldera, with maximum recorded values of 67.7°C in the west and 88.9°C in the east.

7.4.7 Southern flanks

Patches of hot ground, some of which are associated with weak fumaroles, are scattered over the uppermost southern flanks of Paka. All are developed upon pyroclastic deposits which are altered to red clays. There appears to be no obvious structural control on the manifestations, except at [AL 1878 0997] where two faults intersect. Temperatures are generally lower than on the other areas of the volcano, with maximum recorded values for individual patches of hot ground ranging from 42.7°C up to a maximum of 77.5°C.

7.4.8 Murulen

Isolated geothermal activity is found on the basaltic scoria cone of Murulen [AM 1939 1135] on the low ground between Paka and Silali. This takes the form of warm ground within the crater and upon the western flanks of the cone. A maximum temperature of 39.9°C was recorded.

Further to the west, Sceal (1974) recorded silica sinter and small fumaroles around the summit area of Cheptomas at [AM 1885 1105]. Although the lavas in this area are reddened and altered, no geothermal activity was observed at this locality during the present survey.

8 The geology and geothermal activity of Silali Volcano

8.1 INTRODUCTION

Silali is one of the largest and most spectacular volcanoes of the Kenya Rift. It is situated on the border of the Baringo and Turkana districts, 50 km north of Lake Baringo at 1°10'N, 36°12'E.

It is a broad shield that rises 760 m from the rift floor to reach an altitude of 1528 m on the summit, which is located to the west of a large caldera (Figure 8.1). In profile, Silali is morphologically comparable with the basaltic shields of the Galapagos Islands (Nordlie, 1973). The shield is elongated in a N–S direction, having basal dimensions of 36 km by 25 km and an areal extent of 850 km^2. North to south topographical profiles (Figure 8.2) indicate the shield is broadly symmetrical with gently dipping flanks (dips <5°). In contrast, east to west profiles show a pronounced asymmetry with steep slopes and a step-like profile on the western flank. There is a significant NW-directed tilt to the rift floor in the vicinity of Silali. Over a distance of 30 km the rift floor drops from 1000 m on the south-eastern side to 540 m on the north-western side of the volcano.

Textural and tonal contrasts on satellite thematic-mapper images highlight the presence of a blister-like area around the summit. This measures 12 km × 10 km, and is a constructional feature which coincides with the outcrop of late-stage trachyte and basalt lavas. On the western and northern areas of the summit these lavas also define a number of flat benches. The centre of the blister-like area is dominated by the caldera which is perfectly preserved (Plate 8.1). The caldera is elliptical in plan with a long axis of 7.5 km, trending north-west, and a short axis of 5 km. The walls of the caldera are unbreached and in the south and south-eastern sectors reach a maximum height of 340 m. The northern and western walls are lower with heights of 180–200 m. The caldera floor is virtually flat but broken by a series of low ridges and volcanic cones which trend NNE–SSW.

Silali is a complex, multi-centre, shield volcano composed predominantly of basalt and trachyte with minor volumes of hawaiite, mugearite, benmoreite and phonolite. Mixed magmas are also present. In the exposed parts of the volcano the ratio of trachytic to basic rocks is estimated to be approximately 4:1. Basalt and trachyte lavas cover most of the shield and summit area and were erupted from pyroclastic cones, fissures and arcuate fractures located on the summit area and the upper western and eastern flanks. Pyroclastic deposits and intermediate lavas are largely restricted to sections in the caldera walls. Air-fall pyroclastic deposits erupted from Silali cover large parts of the western flanks and are dispersed as far as the western margin of the rift where they mantle older Miocene strata. The lower northern and southern flanks are cut by a N to NNE-trending volcanic rift zone, 10 km wide and up to 30 km in length. This zone, characterised by numerous faults, tension cracks, fissures and minor graben, is intimately associated with extensive basalt lava fields which mantle the flanks of the shield. The total thickness of strata on Silali volcano is considered to be in excess of 700 m, of which nearly half is exposed in the caldera walls.

Thick alluvial deposits obscure the foundation rocks around Silali volcano. To the west, sections in the Suguta River expose pyroclastic deposits from Silali resting on basalts of unknown age. In the east, basalts from Silali overlie or are faulted against westward-dipping trachytes and basalts of Miocene age.

8.2 PREVIOUS WORK

A reconnaissance survey of Silali was carried out by McCall in 1965 and 1967 but the results of this were not published. The original maps and accompanying rock analyses were made available to the present survey and are also incorporated into the 1:125 000-scale EAGRU geological map (Truckle 1979a). Aspects of the geology and geochemistry of Silali are briefly discussed in McCall (1968 a, b and 1970) and McCall and Hornung (1972). Brief reviews of the geology and possible evolution of Silali have also been presented by Williams et al., (1984) and Key (1987).

In 1987 Macdonald and Williams of Lancaster University visited Silali, and they provided an unpublished manuscript paper and geochemical analyses to the present survey.

8.3 STRATIGRAPHY

8.3.1 Introduction

McCall and Hornung (1972) outlined a crude stratigraphy for Silali which has been adopted by subsequent workers. This stratigraphy has been found to be essentially correct during the present survey and is supported by eleven new Ar/Ar dates.

Prior to the present survey no radiometric dates were available for Silali. McCall assumed that basalts on the southern flanks were contemporaneous with the Upper Basalts of Paka, and therefore a lower age of 0.5 Ma was implied. Ar/Ar dates obtained during the present survey indicate that construction of the original volcanic shield was completed by 225 ka and that caldera collapse probably occurred around 64 ka. The youngest dated trachyte lavas have an age of 4 ± 2 ka, although basaltic activity on the northern flanks has probably continued to within the last few thousand years.

During the present survey, three sections in the caldera walls were logged in detail and combined with photographs to provide the basis for some of the descriptions and interpretations given below. The geology of the caldera is summarised in Figure 8.3, which is enclosed in the back of this report. The stratigraphical classification used in this report is summarised in Table 8.1. Place names are taken from the

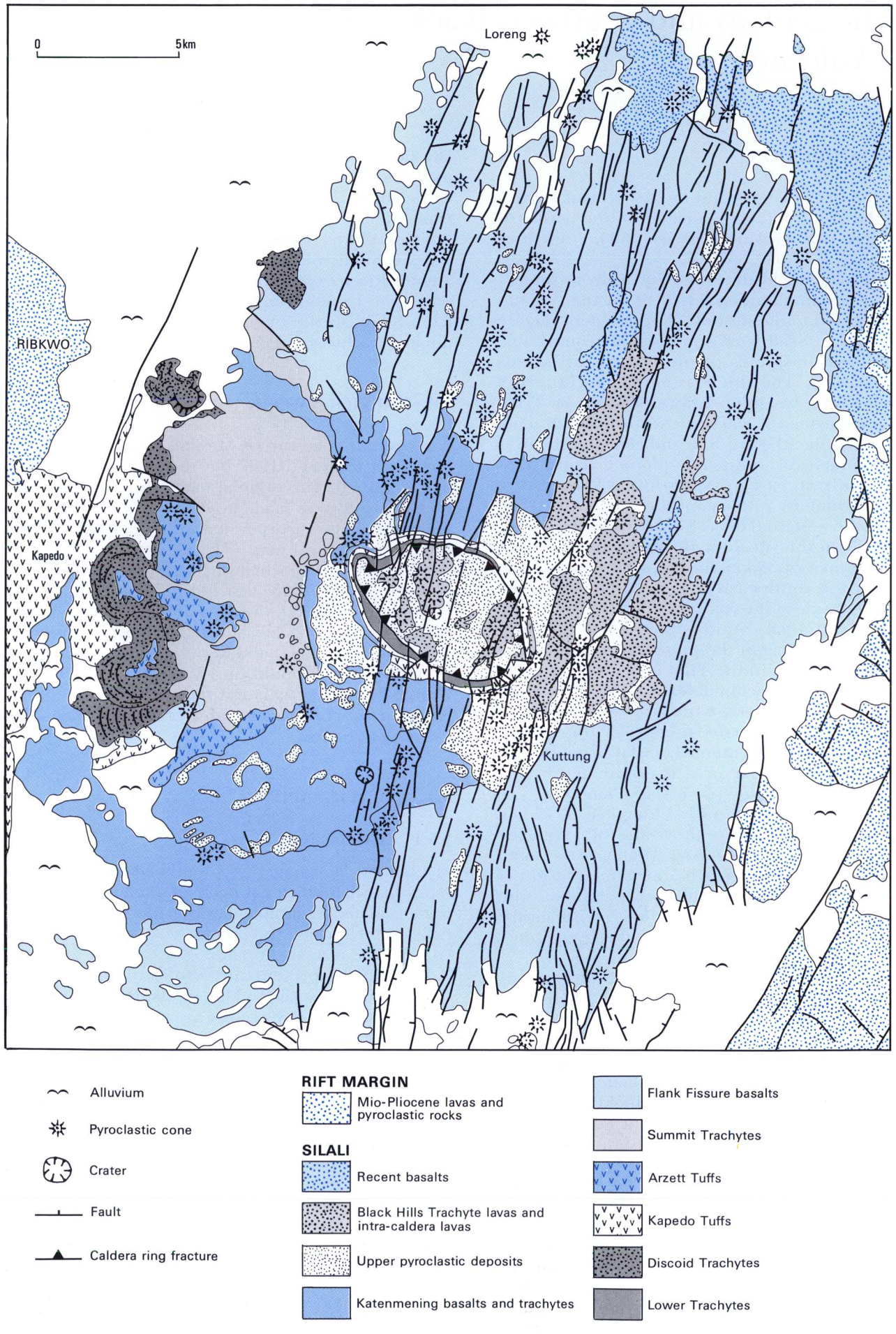

Figure 8.1 Simplified geological map of Silali volcano.

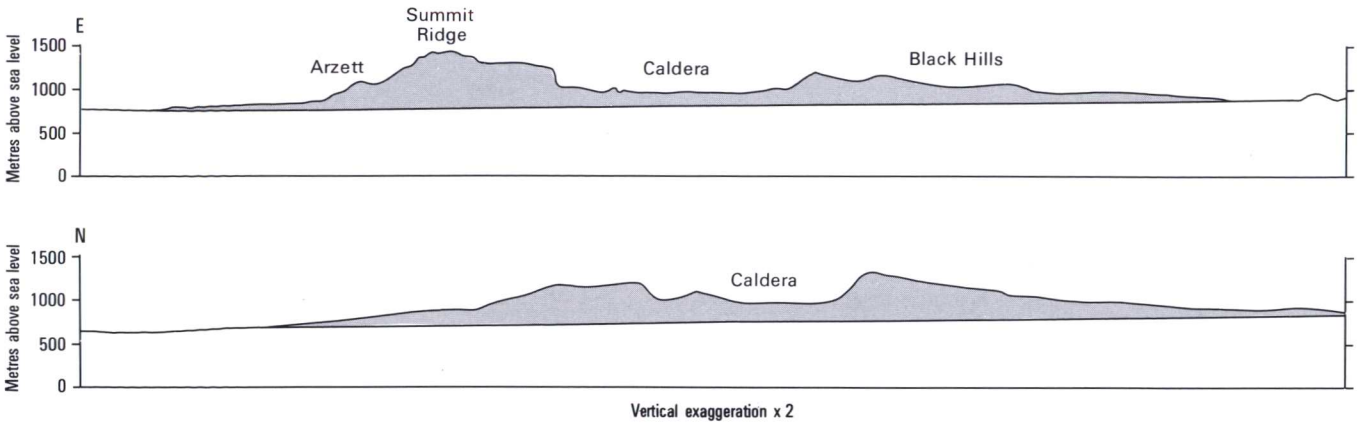

Figure 8.2 Topographic profiles across Silali volcano.

published 1:50 000 topographical maps or from McCall (1970) and McCall and Hornung (1972).

8.3.2 Mission Basalt (M^b)

The Mission Basalt outcrops along the base of the western flank of Silali and is exposed in several sections in the Suguta River around Kapedo at [AM 1781 1312], [AM 1776 1305] and [AM 1767 1292]. Petrologically and geochemically similar basalt flows are also exposed along the banks of the Suguta River up to 10 km north of Kapedo.

The Mission Basalt is a fine to medium-grained, aphyric to sparsely phyric basalt lava with scattered olivine and feldspar phenocrysts. A thickness of 30 m is present at the Kapedo waterfall, but nowhere is the base exposed. The contact with the overlying Kapedo Tuffs is abrupt and around Kapedo village is marked by a line of hot springs and seepages.

The lateral extent of the Mission Basalt under Silali is unknown. The Nasorut basalts exposed on the eastern side of Silali have been dated at 9.4 Ma (Golden, 1978) and are chemically different to the Mission Basalt. A borehole on the south flanks at Losikirimoi [AM 1899 1152] proved 137 m of basalt flows separated by thin rubbly zones. These flows may correlate with the Mission Basalt and may underly Silali. To the south-east of Silali, the Murgisian basalt of probable Lower Pleistocene age crops out (McCall and Hornung, 1972). This is petrologically similar to the Mission Basalt and is also overlain by the Kapedo Tuffs.

8.3.3 Lower Trachyte Lavas (t^l)

Trachyte lavas, considered to be the oldest exposed on the volcano, crop-out along the base of the southern wall of the caldera and in gullies in the lower eastern wall. A maximum thickness of only 33 m of outward dipping (<5°) lavas is exposed. These are nepheline-normative and contain scattered microphenocrysts of anorthoclase. They are grey, weathering to a reddish-brown colour, and are streaky and fissile. Ar/Ar dating of feldspar phenocrysts from two samples collected from [AM 1888 1281] has yielded ages of 228 ± 7 ka and 224 ± 9 ka for these lavas.

By analogy with the other volcanoes of the region it is believed that the Lower Trachyte Lavas represent the remnants of an early volcanic shield. Outside the caldera,

Plate 8.1 Aerial view of Silali caldera, looking north-west.

Table 8.1 Summary of the stratigraphy of Silali

Young basalt lavas (b^y)		
Black Hill Trachyte lavas (BH^t)	$4 \pm 2 - 10 \pm 2$ ka	
Late Pyroclastic Deposits (P^{vl})		
Upper basalt and trachyte lavas ($b^u + t^u$)	7 ± 3 ka	
CALDERA FORMATION		
Katenmening Lavas (KT^b+KT^t)	64 ± 2 ka	
FAULTING AND SUBSIDENCE		WESTERN FLANK ACTIVITY
Flank Fissure Basalts (b^f)		Summit Trachytes (S^t)
Upper Pyroclastic Deposits (K^{vu})	133 ± 3 ka	Arzett Tuffs and Lavas (A^v) 117 ± 5 ka Discoid Trachytes
FAULTING		
Intermediate Lavas (K^I)		
Lower Pyroclastic Deposits (K^{vl})		Kapedo Tuffs (K^t)
Lower Trachyte Lavas (t^l)	224 ± 9 ka	
Mission Basalt (M^b)		

this shield is completely covered by younger strata and its dimensions can only be estimated by consideration of the topographic profiles and dips of the overlying strata. These suggest that the early shield was of low relief, rising to a maximum altitude of about 1300 m, and was elongated along a NNW-trending axis with a length of about 25 km. By analogy with Emuruangogolak, the early shield is likely to be composed of trachyte lavas with subordinate pyroclastic deposits.

8.3.4 Kapedo Tuffs (K^t)

Within the caldera walls the Kapedo Tuffs locally make up to 80% of the section and comprise three distinct units. The Upper and Lower Pyroclastic Deposits are separated by a layered sequence of trachytic, benmoreitic and basaltic lavas termed the Intermediate Lavas. Extensive pyroclastic deposits are also present to the west of Silali around Kapedo and mantle the western margin of the rift.

8.3.4.1 Lower Pyroclastic Deposits (K^{vl})

The Lower Pyroclastic Deposits are well exposed in the southern and eastern sectors of the caldera wall (Figure 8.3a, b). They comprise a lower sequence (<45 m) of rubbly breccias interbedded with thin trachyte lavas, conformably overlain by an upper unit of more massive, welded pyroclastic breccias with thin pumice-rich layers. This upper unit forms a wedge-shaped pile up to 139 m thick, which gives rise to distinctively jointed buttresses in the lower and middle sections of the caldera wall. The breccias are stratified and show cross-cutting and irregular contacts. They are poorly sorted and contain sub-rounded clasts of trachyte up to 1 m in diameter, set in a matrix containing flattened and contorted obsidian and finer lithic clasts, including syenite.

The lithology and overall morphology of the Lower Pyroclastic Deposits and their mantling by later eruptive deposits indicates that they represent oblique sections through a series of large trachyte pyroclastic cones. These cones, with basal dimensions of 0.8–1.2 km and moderately dipping (<30°) slopes appear to have developed mainly on the eastern half of the early shield. The Lower Pyroclastic Deposits are not exposed in the north wall of the caldera, but steep dips in the overlying pyroclastic deposits in the north-western sector (Figure 8.3b) suggest mantling over a buried structure analogous to the cones described above.

8.3.4.2 Intermediate lavas (K^I)

The Intermediate Lavas are exposed in the southern, northern and western walls of the caldera and include hawaiites, mugearites, bemoreites and trachytes. In the west they rest conformably on the Lower Trachyte Lavas but eastwards thin and wedge out against the Lower Pyroclastic Deposits.

In the central-south wall, east of the main area of Lower Pyroclastic cone deposits (Figure 8.3a), a distinctive layered sequence of thin trachyte and benmoreite lavas is exposed. The outcrop of these lavas is lens shaped with the lavas thinning laterally and onlapping onto the eastern flanks of the older cone. Their eastward extent is masked by scree and colluvial deposits. The lower part of the sequence comprises up to 27 m of vesicular, blocky flows of undersaturated hawaiite. Further west, in the south-western wall of the caldera, similar layered flows of benmoreite, mugearite and trachyte form a unit up to 95 m thick, which tapers eastwards and dips westward beneath the screes at the base of the west wall. Individual flows are rarely more than 1 m thick and weather to a dark brown to buff colour. They are fissile and microporphyritic and typi-

cally contain small cognate xenoliths of amphibole and pyroxene. The top of the Intermediate Lavas is capped by up to 30 m of microporphyritic trachyte lavas with thin heterolithic breccias containing gabbroic bombs.

In the north-east wall of the caldera up to 35 m of layered trachyte and mugearite lavas are exposed immediately above the scree line. The lower part of the section comprises massive trachytic lithic breccias interbedded with thin mugearite and trachyte flows. The upper part consists of reddened, blocky, vesicular flows of trachyte. Further west the upper flows reach a maximum total thickness of about 75 m and are capped by one or two massive, lens-shaped flows of trachyte lava (Figure 8.3b). The basal unit in the north wall at [AM 1903 1315] is reported to be of basaltic composition (R Macdonald, personal communication, 1990).

The thin and regularly layered aspect of the Intermediate Lavas suggests frequent eruptions, possibly from fissures located across the summit of the early volcanic shield. The lateral thickness variations indicate ponding and infilling of an irregular topography on the summit area.

8.3.4.3 Faulting

Prior to the eruption of the Upper Pyroclastic Deposits the summit area of the early shield underwent a period of faulting and erosion. A prominent unconformity in the eastern wall of the caldera (Figure 8.3b) indicates a break in activity between the Upper and Lower Pyroclastic Deposits. During this period the pyroclastic cones of the Lower Pyroclastic Deposits were eroded and faulted to produce a series of small asymmetrical graben and broad synclinal structures which were subsequently infilled by deposits of the next phase of explosive volcanism.

8.3.4.4 Upper Pyroclastic Deposits (K^{vu})

More than half of the caldera wall sections consist of an alternating sequence of welded and non-welded trachytic pumice tuffs, of pyroclastic-flow and air-fall origin. These deposits vary dramatically in thickness where they drape over and infill irregularities in the former topography of the summit region. The thickest sequences (>150 m) are preserved in the northern and eastern half of the caldera and are associated with the dissected remnants of a series of pyroclastic cones visible around the northern, eastern and southern rim of the caldera. Westwards, these deposits dip beneath younger basalt and trachyte lavas.

In the north wall (Figure 8.3b) up to 115 m of strata are exposed. The basal unit consists of up to 10 m of polymict, lithic-rich breccia. This is overlain by up to 100 m of buff-coloured, stratified, pumice-rich deposits with welded zones. Non-welded pumice units vary between 5–10 m in thickness and typically have a lithic-rich base grading up into normally-graded and crudely stratified pumice lapilli deposits, which pass up into poorly-sorted, inversely-graded pumice with large clasts at the top. Welded zones, up to 15 m thick, consist of streaky, grey-green and black glassy fiamme, in a matrix of finer pumice and lithic clasts. The fiamme are flattened and deformed around lithic clasts. Towards the top of the section the deposits are generally coarser and have larger fiamme and contain gabbroic bombs.

Elsewhere around the caldera, the Upper Pyroclastic Deposits consist of well-bedded pumice lapilli tuffs, resting upon the Lower Pyroclastic Deposits and Intermediate Lavas. Cross-bedding and normal grading are present in these beds. The upper part of the section is dominated by poorly consolidated pumice beds with sub-rounded lithic clasts of trachyte and more rarely agglutinated basalt. Dense, obsidian-like, welded zones occur throughout the sequence. These are mostly thin, but can be traced laterally for several kilometres, although the most spectacularly developed zone near the top of the section in the west wall reaches a thickness of 33 m (Figure 8.3c). Ar/Ar dating of feldspars indicates an age of 133 ± 3 ka for the youngest deposits exposed in the southern rim of the caldera at [AM 1886 1276].

Immediately east of Kapedo village [AM 1780 1300] up to 10 m of bedded pumiceous tuffs mantle the topography of the underlying Mission Basalt and are in turn overlain by trachyte lavas. Individual beds are up to 0.75 m thick, are internally stratified, and contain sub-rounded lithic clasts of trachyte and obsidian. A sample from this locality has yielded an Ar/Ar date of 131 ± 3 ka. Further south, sections in the Suguta and Kapedo Rivers expose up to 20 m of well-bedded trachytic pumice-lapilli tuff and ash. These deposits are locally intercalated with, and cut into by, fluvial conglomerates and sandstones, as for example upstream from the bridge at [AM 1765 1288]. Cross-bedding, parallel lamination and slumps are common. These features indicate that in this area the Kapedo Tuffs were deposited within a fluvio-lacustrine environment and were probably reworked. It should be noted that these sections are also likely to contain fall-out from the overlying Arzett cones (Section 8.3.6), which in the field is indistinguishable from the Kapedo Tuffs.

On the rift margin to the west of Kapedo, pumiceous tuffs from Silali mantle an irregular topography on the Murgisian Basalt and older Pliocene and Miocene strata (McClenaghan, 1972; Truckle, 1979a). This wide dispersal to the west suggests that easterly winds prevailed during eruption, as appears to have been the case for major pyroclastic eruptions at all the other volcanic centres of the region.

In summary, the Kapedo Tuffs were probably produced by plinian-style eruption from a series of cones located over the eastern half of the former summit area of Silali. The more massive and inversely graded pumice units exposed in the north wall of the caldera are interpreted as pyroclastic-flow deposits. The relatively coarse grain size and presence of bombs suggests they represent proximal deposits to the remnant cones exposed in the east wall of the caldera. In contrast, the well-bedded deposits which drape the pre-existing topography in the southern and western parts of the caldera are interpreted as air-fall deposits. Thick zones of welding within these air-fall deposits may be attributed to high rates of deposition (Mahood, 1984). The prevailing easterly wind dispersed the tephra over a wide area to the west, as far as the rift margins.

8.3.5 Discoid Trachyte Lavas (t^d)

On the western flanks of Silali the Kapedo Tuffs are overlain by an alternating sequence of trachytic lava flows and pyroclastic deposits. These rocks are not exposed in the caldera.

East of Kapedo village up to six large discoid-shaped pantelleritic trachyte lava flows occur. Further north at the edge of the Suguta plains the flow-fronts of several other trachytes crop-out beneath a cover of basalt and have been provisionally assigned to this group also. The Discoid Trachytes have lobate flow-fronts up to 50 m high, which pass upslope (eastwards) into narrow flows with prominent levees, indicating sources buried beneath the Arzett cones. They have prominent pressure ridges and show morphological and compositional similarity to the discoid flows at Napakoriatom, north-east of Paka volcano (Section 7.2.9.2). In outcrop the Discoid Trachytes are aphyric, strongly fissile and pale green in colour.

Kaveterang [AM 1815 1365] is a tuff ring from which a pancake-like flow of Discoid Trachyte was erupted. The tuff ring has a broad shallow crater, breached in the west, and is composed of pale brown bedded pumiceous tuff and breccia deposits. It is believed to have formed by phreatomagmatic eruption of trachyte magma in a shallow lacustrine environment or upon a wet sediment substrate. This evidence, and that from the Kapedo Tuffs described above, indicates that during part of its evolution at least, Silali was flanked in the west by ephemeral lakes.

8.3.6 Arzett Tuffs and Lavas (A^v)

The Arzett Tuffs and Lavas were erupted from a number of pyroclastic cones situated mid-way up the western flanks of Silali (Plate 8.2). The main Arzett cones have basal diameters of about 0.5 km and heights up to 220 m. They are deeply dissected by radial drainage systems and are surrounded and partly buried by the younger Summit Trachytes. Flow directions in these overlying lavas indicate the presence of at least one other buried Arzett cone at [AM 1838 1317].

The eruptive products from these cones consist of up to 40 m of well-stratified, poorly-consolidated, trachytic pumice-lapilli deposits and breccias, interbedded with welded breccias and welded air-fall tuffs. The deposits coarsen and thicken upslope where they grade into poorly sorted breccias and agglomerates around the cones. The lower flanks of the cones are deeply dissected and show numerous sections through well-bedded, fine to medium-grained pumice lapilli deposits with small droplet-like achneliths of obsidian and clasts of syenite. Fine-grained, fissile, microporphyritic trachyte lavas are exposed within the tuffs, and according to McCall one such flow was extruded from a breach on the western side of the most northerly cone [AM 1828 1292]. McCall also reports the occurrence of obsidian dykes in the vicinity of the Arzett cones. An Ar/Ar age of 117 ± 5 ka was obtained from feldspar crystals within the Arzett tuffs at [AM 1817 1288].

8.3.7 Summit Trachytes (S^t)

The Summit Trachytes form an arcuate ridge, 8 km in length and 300 m high, about a kilometre to the west of the caldera. Lavas erupted from the ridge form a broad apron that mantles the western flank of the volcano. The summit ridge is bound in the west by a series of prominent linear and arcuate break-of-slope features (Figure 8.4). Morphology and flow directions point to a series of arcuate fissures and domes on the ridge crest as the eruptive sources for these lavas. This arcuate zone is not a continuous structure, but is composed of three distinct segments which trend 150°, 020° and 040° and bifurcate at their northern and southern terminations (Figure 8.4). The ridge is a constructional feature composed of discrete linear zones of small, discoid-shaped domes and short digital lava flows with high-aspect ratios, associated with short normal faults and open fractures (Plate 8.3). It is the flow-fronts of these lavas and domes which have coalesced to form the break-of-slope features.

The Summit Trachytes are fissile, streaky, fine-grained pantelleritic trachyte lavas with autobreccias. The earliest trachyte lavas, although largely obscured by later flows, are exposed on the lower slopes where they form low-relief flows with medium-grey photo-tones. Flow-fronts are generally less than 10 m in

Plate 8.2 Aerial view of the Arzett cones, western flanks of Silali, looking north-east. Note vegetated trachyte lavas of the Summit Trachytes surrounding and partly burying the cones and the prominent break-of-slope feature in the background.

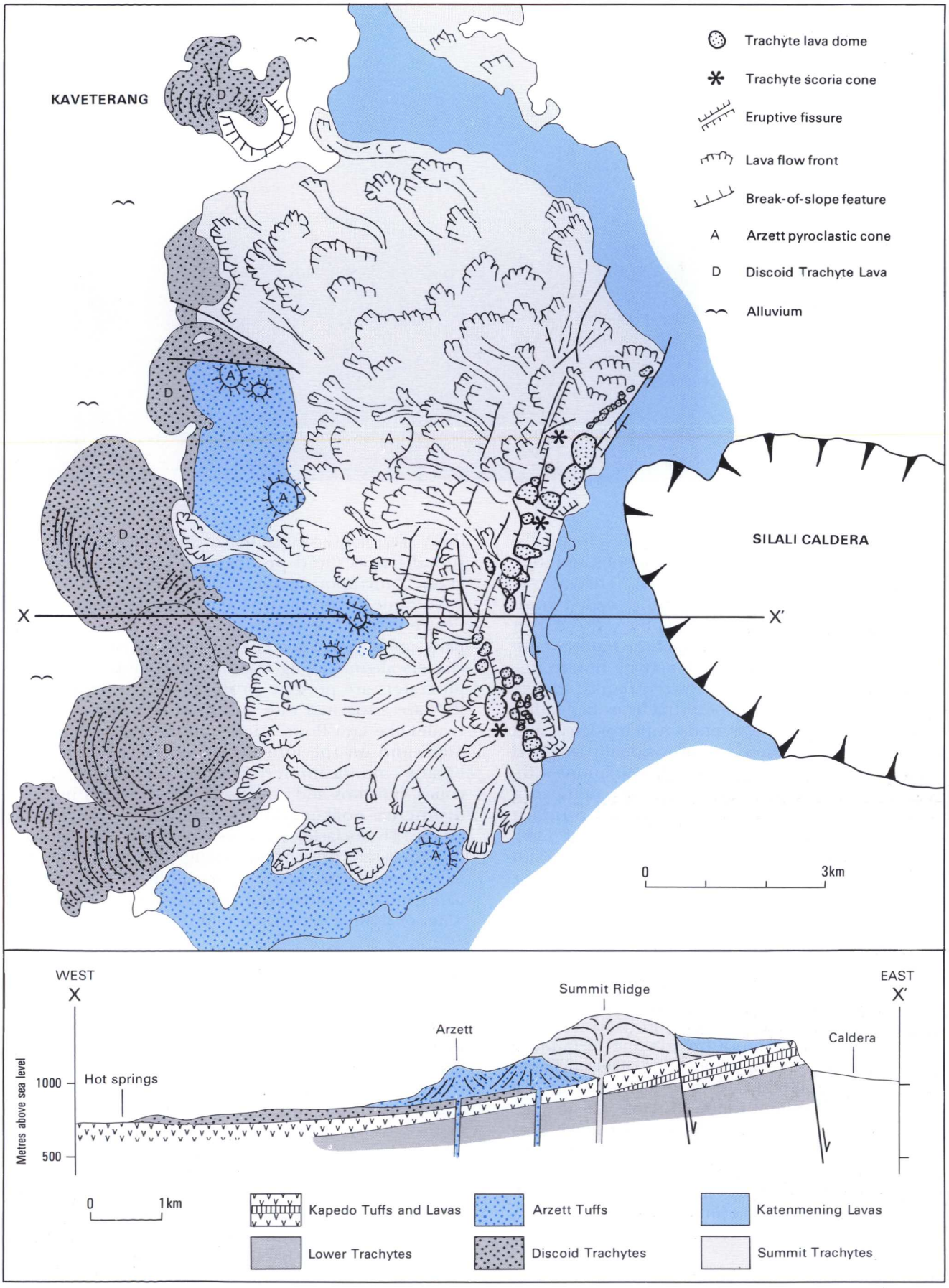

Figure 8.4 Flow patterns and eruptive centres in the Summit Trachytes, west flank of Silali. Cross section along X-X' shows the correlation of the Kapedo Tuff sequence in the wall of the caldera with tuffs at Kapedo.

Plate 8.3 Aerial view of summit ridge of Silali, looking north. Note the short digital trachyte flows of the Summit Trachytes.

height and pressure ridges are rarely developed. In contrast, later flows have darker photo-tones and well-developed pressure ridges and levees. These flows were fluid at the time of eruption and cascaded down the western slopes to encircle and bury the Arzett cones, eventually reaching the base of the flanks where they built up a series of low-relief, arcuate flow-fronts. Stream sections on the south-western flanks, for example at [AM 1855 1206], expose trachytes beneath a cover of Katenmening Lavas, and on petrological and geochemical grounds these are provisionally assigned to the Summit Trachytes. Upslope, dip variations within the younger Katenmening Lavas define a number of breaks of slope indicating that buried Summit Trachytes extend around the southern flanks of Silali. In the north-west, the Summit Trachytes are overlain by the Flank Fissure Basalts and the Katenmening Lavas.

8.3.8 Flank Fissure Basalts (b^f)

Prior to the formation of the caldera a major phase of basaltic activity occurred across the volcano. Highly fluid basalts were erupted from numerous fissures and scoria cones located within a broad zone of faulting which cuts the summit area and upper flanks. These mantle the earlier shield lavas and Kapedo Tuffs on the northern, eastern and southern flanks (Plate 8.4). Evidence for the eruption of basalt on the western flank is limited to a small outcrop [AM 1820 1250] which overlies the Summit Trachytes. Contact relationships on the northern flanks indicate that the Flank Fissure Basalts overlie the Summit Trachytes and are in turn overlain by trachyte and basalt lavas of Katenmening age.

The basalts form sheet-like, gently dipping lobate and branching flows which typically show dark to medium-grey photo-tones. Individual flows are up to 6 km long but are rarely more than 5 m thick. Up to 50 m of thinly layered flows is exposed in the walls of a graben structure south-east of Kuttung [AM 1945 1245] but the base is not seen. Elsewhere, tiered basalt flows are exposed in numerous faulted sections, tensional fissures and pit craters. The lavas are fine-grained microporphyritic olivine basalts.

Volcanic landforms typical of Hawaiian-style basaltic fissure activity are common. Basaltic cones and ramparts composed of scoria and spatter occur singly or as clusters aligned along fractures and faults. Numerous pit craters are present on the northern flanks where they are associated with collapsed lava tubes and thin rivulet-like lava flows. Along the northern margin of Silali and on the alluvial plains to the north, the basalts contain numerous small pit craters, spatter cones, hornitos and collapsed tumuli which impart a distinctive pock-marked appearance on air-photographs. Hyaloclastite textures have been observed, and tuff cones are present at Loreng [AM 1943 1500] and to the north and west of Lake Kalnang'i. These features indicate phreatomagmatic activity in shallow water or upon a water-saturated substrate.

8.3.9 Faulting and subsidence

The structure of Silali is dominated by a N- to NNE-trending median zone of brittle deformation, 12 km wide and 30 km in length. This zone contains a number of linear belts of intense deformation separated by relatively undeformed areas. These linear belts are characterised by swarms of open tensile fractures and fissures associated with normal faults and minor horst and graben structures. Field relationships indicate much of this deformation was concomitant with eruption of the Flank Fissure Basalts and probably continued during the eruption of the overlying Katenmening Lavas. This deformation style is typical of crustal dilation associated with basaltic fissure eruption and dyke injection (cf. Opheim and Gudmundsson, 1989).

The absence of the Summit Trachytes within the caldera walls and evidence for ponding of the younger Katenmening Lavas over the former summit region, indicate that between the eruption of these two units the summit area of Silali underwent a period of faulting and subsidence. This subsidence was probably con-

Plate 8.4 Faulting in the Flank Fissure Basalts, aerial view, looking south up the northern flanks of Silali. Note vegetated pools of Kalnangi along fault scarp to left of centre.

temporaneous with the widespread faulting described above and was controlled by a series of arcuate or circumferential fractures on the western and northern parts of the summit area.

8.3.10 Katenmening Lavas (KT^t, KT^b)

The term Katenmening was originally used by McCall (1970) for all the basalts exposed on the flanks of Silali, and was based on the section in the Katenmening pit crater [AM 1882 1230]. McCall recognised that the Katenmening included trachyte lavas and that the uppermost basalt flows locally contain abundant gabbroic xenoliths. The present survey restricts usage of the term Katenmening to the younger pre-caldera basalt and trachyte lavas which cover the upper flanks of the volcano and are exposed in the caldera walls (Figure 8.3a,b).

The Katenmening Lavas were erupted from an important fissure zone which cuts the western half of the summit area, and from a number of circumferential fissures and cones located around the upper northern and southern flanks. Two members are recognised. The Lower Trachyte Member is exposed in the upper sections of the western walls of the caldera and on the upper north-western and southern flanks. The Upper Basalt Member includes the youngest lavas exposed in the caldera walls and flows of basalt which extend down the south-western and north-western flanks. On air-photographs the Katenmening basalts may be distinguished from the Flank Fissure Basalts by their more youthful morphology, multi-lobate flow-fronts and their thin, fluid-like aspect. However, where the two basalt sequences are juxtaposed, differentiation can be difficult.

The **Lower Trachyte Member** consists of two or three flows of fissile, fine-grained and strongly jointed, pantelleritic trachyte lava. Marked lateral thickness variations (10–37 m) indicate that these lavas were ponded within a series of NNE-trending summit depressions bound by the topography of the earlier eruptive cones of the Kapedo Tuffs.

On the upper southern flanks at [AM 1885 1261] trachyte lavas are exposed in a series of N-trending fault scarps. They were erupted from a number of centres, including NNW-trending fissures, lava domes and pumice cones. Lavas from these sources flowed southwards and westwards over an irregular topography and are exposed at the base of the northern wall of the Katenmening pit crater. On the northern flanks, NE-trending lines of eruptive cones and fissures define a number of source areas. Lavas from these are discernible beneath a blanket of younger basalt lava and pyroclastic deposits as far east as the Black Hills area. A single flow exposed around the eastern rim of the caldera (Figure 8.3 b, d) is shown on the accompanying map as part of the Black Hills Trachyte Lavas. A K/Ar date of 115 ± 0.012 ka obtained by UNOCAL (Thompson, 1991), indicates that this flow is not part of the Black Hills group, and geochemical evidence suggest it has more affinities with the Katenmening Trachytes.

The **Upper Basalt Member** consists of up to 20 m of layered flows, each 1–2 m thick, of basalt, benmoreite and in places trachyte. Eruptive sources are indicated on the northern flanks by E-trending fissures with spatter ramparts and scoria cones, and in the south by NW-trending fissures and clusters of scoria cones aligned along N–S axes. Flows from these sources were highly fluid as indicated by their morphology and length. Flow directions suggest a significant topography existed at this time with high ground on the west and east margins of the summit area, restricting the lateral flow of lava. Thus, thin basalt flows erupted on the summit area initially ponded and infilled a summit depression before overflowing down the south-western and north-western flanks to bury the older lavas of the Summit Trachytes and Arzett Tuffs. The youngest eruptions of the Katenmening lavas were flank eruptions from small isolated centres located on the lower flanks. In the south, a small bocca at [AM 1892 1226] is the source for a large volume flow of basalt (about 2 km^3) which first flowed south-east and then northwards to reach Kapedo village some 19 km from

source. In the north, basalt flows erupted from small pyroclastic cones at [AM 1869 1347] extend for 6 km to the Suguta alluvial plains.

Pit craters are common within the Katenmening basalts. The largest of these, the Katenmening pit crater [AM 1880 1230], is a circular crater 0.6 km in diameter and 40–50 m deep. The crater walls expose a section dominated by layered basalt flows dipping gently to the south. At the base of the section 5–6 m of trachyte lava, intercalated with rubbly autoclastic breccias is present. The uppermost flow around the crater rim is a basalt covered with agglutinated spatter containing abundant nodules of syenite and gabbro up to 6 m in diameter (McCall, 1970, section 13.7). Agglutinated spatter locally drapes the north and east walls and also occurs in landslip deposits on the crater floor. The presence of pit craters and the morphology of the eruptive centres described above is typical of Hawaiian-style activity.

In the west wall of the caldera, rubbly, flow-folded comenditic trachyte lavas are intercalated with the Upper Basalt Member (Figure 8.3c). On the caldera rim these trachytes can be traced laterally into a series of lava cones (the 'Three Hills'), one of which has been dissected by the caldera ring fault [AM 1873 1307] to expose a massive, radially jointed intrusive plug immediately beneath the extrusive cone. Lavas from these cones extend 5 km down the north-western flanks and display a distinctive pattern of pressure ridges and surface ribbing. Step-heating Ar/Ar dating indicates an age of 64 ± 2 ka for the youngest of these trachytes cut by the caldera wall.

8.3.11 Caldera formation

The collapse of the summit area to produce the caldera occurred late in the evolution of Silali. The timing of this collapse is constrained by the radiometric ages of the Katenmening Lavas exposed in the caldera wall and Upper Trachyte Lavas on the caldera floor (Section 8.3.12), and thus occurred between 64 ± 2 ka and 7 ± 3 ka. The caldera has a regular outline and vertical walls, suggesting that it was formed by a piston-like collapse. Subsequently, minor landslipping has locally modified its regular form. The prominent scalloped embayment in the western corner of the caldera [AM 1876 1305], associated with drapes of spatter and agglutinate on the inner walls, indicates that in this area collapse may have incorporated an earlier pit crater.

The absence of significant volumes of pyroclastic deposits associated with, or post-dating the Katenmening Lavas, indicates that caldera collapse was not triggered by explosive activity. Instead, the evidence for Hawaiian-style activity within the Katenmening Lavas, associated with the formation of pit craters and linear fissure swarms on the upper flanks, indicates that collapse was probably triggered by magma withdrawal accompanied by lateral dyke injection beneath the volcano (cf. Sigurdsson and Sparks, 1978, Opheim and Gudmundsson, 1989). Assuming a depth of 350 m, the present day volume of the caldera is about 8 km^3. The volume of the Flank Fissure Basalts is greatly in excess of this figure and their eruption is unlikely to be related to caldera collapse. However, for an average thickness of 45 m, the volume of the Katenmening Lavas is approximately equivalent to that of the caldera.

It has been proposed that nested calderas are a feature of Quaternary volcanoes in the northern part of the rift (Williams et al., 1984). In the example of Silali it was considered that the break-of-slope features on the northern and western flanks marked the trace of an earlier caldera structure (Section 8.3.7). A plot of all the eruptive centres and topographic features for the summit area of Silali (Figure 8.5) clearly defines a series of arcuate structures which extend around the northern, western and southern flanks. However, within the exposed stratigraphy there is no evidence to support the existence of an earlier caldera.

Firstly, neither the break-of-slope features nor the lines of eruptive centres are contemporaneous with each other around the volcano. At different locations they relate to either the Summit Trachytes or to the Katenmening Lavas. Secondly, as noted by Williams et al. (1984), if these features represent ponding within an early caldera then some mechanism of topographic inversion is required. Such a process seems unlikely and cannot be substantiated by analogy with adjacent volcanoes (see Section 9.3.5). Thirdly, the caldera wall sections cannot be regarded as infill to an earlier caldera, because the Kapedo Tuffs exposed within the caldera wall and at the base of the western flanks have almost identical ages, of 133 ± 3 ka and 131 ± 3 ka respectively.

Instead, it is proposed that the arcuate structures on the upper flanks represent a series of circumferential fissures or a ring feeder zone around the western half of Silali. Volcanic activity along this zone alternated with incremental subsidence of the summit area and pre-dated the collapse of the caldera. Subsidence of the summit area of Silali was initiated during Kapedo Tuff times, as indicated by ponding of the Upper Pyroclastic Deposits, and activity along the ring feeder zone later erupted the Summit Trachytes. This was followed by renewed subsidence, contemporaneous with the eruption of Flank Fissure Basalts. A second phase of activity on the ring feeder zone occurred immediately prior to caldera collapse with the eruption of the Katenmening Lavas around 64 ka. These circumferential fissures are morphologically similar to those developed on the basalt shield volcanoes of the Galapagos Islands (Simkin and Howard 1970; Nordlie, 1973; Chadwick and Howard, 1991) and of Iceland and Hawaii, where caldera formation has been linked to the lateral drainage of magma.

8.3.12 Post-caldera lavas and pyroclastic deposits

Upper Trachyte Lavas (t^u) were erupted on the eastern half of the caldera floor from a prominent NE-trending fissure. Ramparts of trachytic lava, spatter, pumice and scoria occur along the fissure. Small pumice and spatter cones are located upon the fissure part of the way up the caldera wall, and clearly post-date movements on the caldera ring fault. This zone of activity is continuous with a line of pumice cones and fissures outside the caldera on the northern and south-eastern flanks. Young trachyte lavas were also erupted from the caldera ring fracture at the northern end of a downfaulted platform on the eastern wall of the caldera [AM 1938 1272]. Ar/Ar dating indicates an age of 7 ± 3 ka for trachytes erupted from the fissure on the caldera floor.

In contrast, the western half of the caldera floor is underlain by basalts and hawaiites of the **Upper Basalt Lavas (b^u)**. These lavas were erupted from several N-trending fissures and scoria cones. Two pit craters at

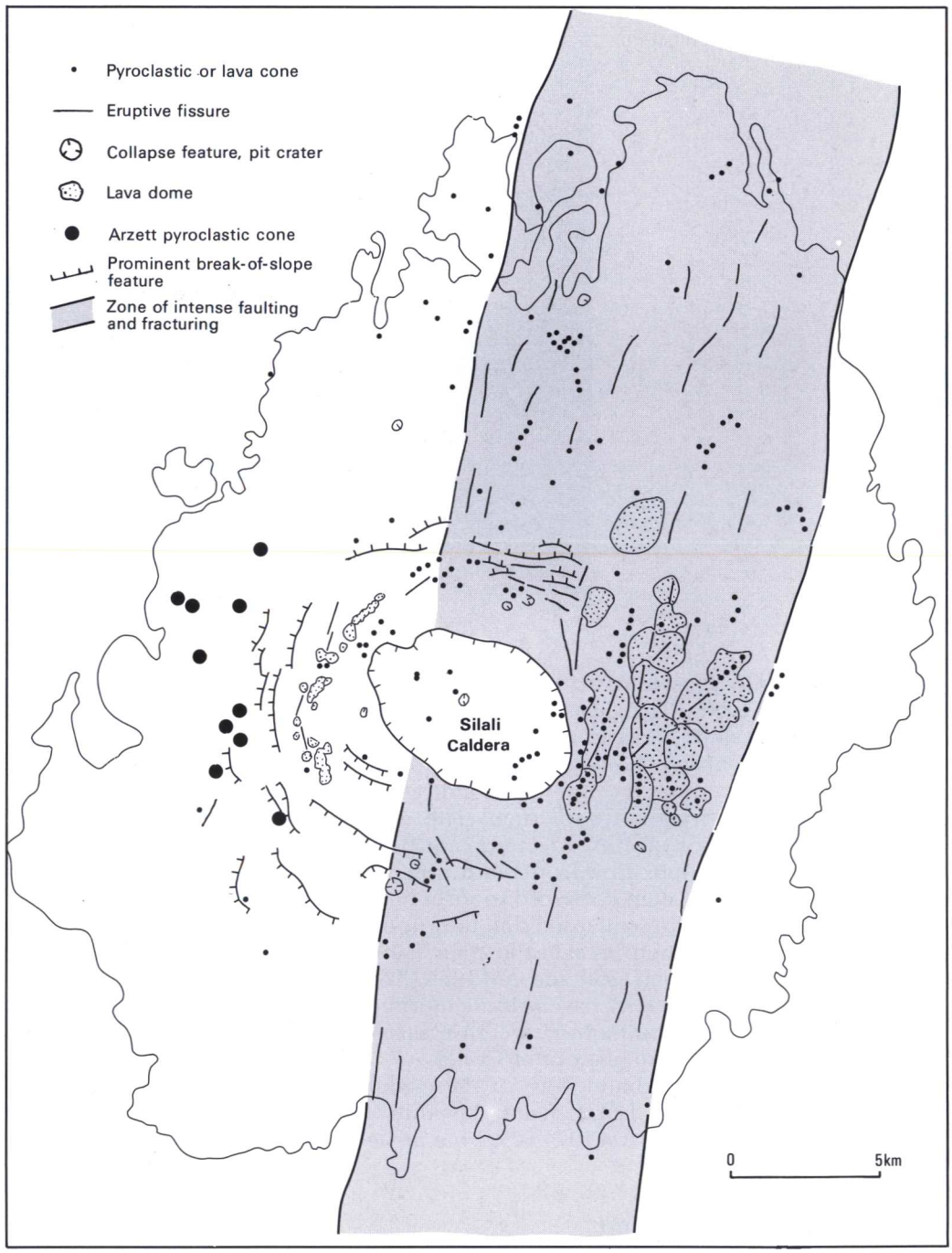

Figure 8.5 Summary of volcano-tectonic lineaments, eruptive centres, break of slope features and faulting across Silali volcano.

[AM 1905 1295] expose 30 m of massive, coarsely porphyritic basalts and hawaiites.

The contact between the two lava groups on the caldera floor is obscured by the **Late Pyroclastic Deposits (P^{vl})**. These consist of 1–1.5 m of unconsolidated trachytic pumice deposits and pumiceous lapilli ash which cover most of the caldera floor. The deposits also occur around the caldera rim and upper flanks. Thickness variations and dispersal patterns indicate the main source was located on the upper eastern flanks, although some pumice may have been erupted from the trachyte fissure on the caldera floor.

8.3.13 Black Hills Trachyte Lavas (BH^t)

The Black Hills Trachyte Lavas are exposed on the upper eastern flanks of Silali where they form a linear belt 9 km long and 4.5 km wide. Within this belt three distinct linear zones of lava domes, fissures, craters and pyroclastic cones are developed. Also included in this group are isolated trachyte flows on the northern and north-eastern flanks at [AM 1960 1350].

The Black Hills lavas include a range of compositions. Undersaturated peralkaline trachytes predominate, although benmoreites, phonolites and lavas of mixed composition also occur.

The lavas are rough and clinkery with vesiculated glassy surfaces. They form low relief, elongate domes up to 20 m high (Plate 8.5), often breached and surmounted by linear chains of collapse features including blow holes and craters, or constructional features including small button-shaped lava flows and pumice cones. These linear chains define two trends. The dominant orientation is N to NNE (020°) and parallels the axial rift zone in the Flank Fissure Basalts. A sec-

Plate 8.5 Breached trachyte lava dome, Black Hills, eastern flank of Silali.

ond set of volcanic alignments and fractures link the main set and trends NE (045°).

Contact relationships between the domes are complex, although they may be broadly subdivided into an older group and a younger group, which indicate an easterly migration of activity with time. The older domes have pale photo-tones due to a mantle of pumice which buries their flow-fronts and obscures surface detail. They are often coalesced to form linear ridges, some of which have collapsed due to eruption of blocky lava flows through breaches in their flanks, as for example at [AM 1960 1350 and AM 1975 1323]. In contrast, the younger domes have pristine morphology. They have no mantle of pumice, are unvegetated, and on air-photographs have black photo-tones.

The oldest dome immediately east of the caldera has yielded an Ar/Ar age of 10 ± 2 ka, and the morphologically youngest dome at [AM 1974 1252] has an age of 4 ± 2 ka.

8.3.14 Young Basalt Lavas (b^y)

The youngest activity on Silali erupted porphyritic olivine basalts on the north-eastern flanks from a series of small scoria cones. The lack of vegetation and juvenile appearance of the cones suggest activity may have taken place only a few hundred years ago. Similar flows on the southern flanks of Emuruangogolak are known to have erupted within the last 200–300 years (Section 9.3.10). Contemporaneous eruptions of basalt also occurred along the adjacent rift margins at [AM 2006 1378] and from a centre at Lokoyamama (Golden, 1978), situated slightly to the east of the mapped area.

8.4 INTRUSIVE ROCKS

Twelve dykes have been observed cutting the south and west walls of the caldera (Figure 8.3a). These are predominantly of trachyte, although composite dykes of basalt and trachyte showing evidence of magma mixing also occur. The dykes are up to 2 m wide, trend 010° to 015°, and are closely related to a set of normal faults associated with post-emplacement brecciation and hydrothermal alteration. They are curvilinear and some pass laterally into irregular apophyses and sill-like bodies along the contact between the lavas and pyroclastic deposits. Two phases of dyke injection are recognised. Early dykes intrude the Lower Pyroclastic Deposits and were feeders to the uppermost trachytes of the Intermediate Lavas. Later dykes cut the Upper Pyroclastic Deposits and were feeders to the overlying Katenmening Lavas.

In the north wall, immediately west of the trachyte cones on the caldera floor, an intrusive plug of trachyte has been identified (Figure 8.3b). This plug has a distinctive radial pattern of columnar joints similar to the dissected lava cones of the 'Three Hills' exposed in the west wall. Although no samples were collected, its stratigraphical position and intrusive relationship with the Upper Pyroclastic Deposits indicates this plug is probably of Katenmening age.

8.5 SUMMARY OF EVOLUTION AND STRUCTURE

The oldest rocks exposed on Silali are trachyte lavas, which by analogy with neighbouring volcanoes are believed to represent part of an early trachyte shield, now mantled by younger rocks. The age range of this early activity is unknown, but construction of the shield was probably completed by about 225 ka.

The Kapedo Tuffs were erupted during the next volcanic episode. Three distinct phases of activity are recognised within this stratigraphic group. The first phase of activity, represented by the Lower Pyroclastic Deposits, constructed a number of trachytic pyroclastic cones across the summit area. These are overlain by the Intermediate Lavas which were erupted from NNE-trending fissures and dykes located in the central and western parts of the summit area. Subsequently the summit area underwent a period of erosion and frac-

turing by N and NNE-trending faults to form a series of horst and graben structures. Pyroclastic activity recommenced with the eruption of the Upper Pyroclastic Deposits from a series of trachyte pyroclastic cones located mainly on the eastern half of the summit area. Pyroclastic flows from these cones ponded and infilled an irregular topography over the summit area and locally flowed down the northern and southern flanks. In the west, welded air-fall and pumice lapilli deposits draped over the earlier cones and accumulated in fault-controlled depressions. Air-fall pumice deposits and tuffs from these cones were dispersed by the prevailing winds to mantle the western flanks of Silali and the floor and margins of the rift further to the west. The youngest deposits of this activity have an age of around 130 ka.

The next phase of activity took place on the western flanks. Initially the Discoid Trachyte Lavas were extruded, and these were superseded by the Arzett Tuffs and Lavas which were erupted around 117 ka from a series of large pyroclastic cones on the middle flanks.

The subsequent phase of activity, which culminated in the collapse of the caldera, commenced with the eruption of the Summit Trachytes from an arcuate feeder zone on the western half of the summit area. This activity was followed by, and probably overlapped with, the eruption of large volumes of fluid Flank Fissure Basalts from a volcanic rift zone which cuts the northern and southern flanks. The association of numerous tensile structures, eruptive centres and collapse pits within the rift zone is typical of many large basaltic shield volcanoes and indicates the lateral injection of dyke swarms to shallow levels within the volcanic edifice. Subsidence and contraction over the summit area in response to this magma movement created a series of circumferential and NNE-trending fissures from which the Katenmening Lavas were erupted at around 64 ka. Rapid eruption of these fluid and voluminous lavas triggered the collapse of the summit region to form the caldera.

Post-caldera magmatism is represented by resurgent activity within the caldera floor along NNE-trending fissure lines. In the west of the caldera hawaiite and basalt lavas were erupted along the line of the Katenmening fissure, and in the east the Upper Trachytes were erupted from a series of pyroclastic cones and fissures. The latest evolutionary phase of Silali is represented by the eastward migration of activity into the Black Hills area where a series of trachyte lava domes associated with minor amounts of benmoreite, phonolite and basalt were erupted between 10 ka and 4 ka along NNE and NE-trending fractures. Subsequently very young looking basalts have been erupted from fissures on the northern and north-eastern flanks.

The axial rift zone which has played such an important part in the younger phases of volcanism on Silali, shows a change in orientation across the volcano. In the north, it is parallel to the rift margin and trends NNE–SSW at 018°, whereas in the south individual deformation belts become narrower, trend more N–S, and are oblique to the rift margins. Southwards this zone passes into a region of intense faulting on the north-eastern flanks of Paka. The faults and fractures in this rift zone are curvilinear with strike lengths of up to 5 km, and are often composed of a series of smaller *en échelon* segments linked by short up-faulted horsts or by obliquely-trending relay or transfer faults. Downthrow directions are distributed equally between east and west and displacements vary from 10–20 m. Changes in displacement directions along individual faults are not uncommon, particularly on the northern flanks. Post-caldera activity within this zone is also indicated by numerous faults which cut the caldera walls and the lavas on the caldera floor.

Preliminary interpretation of the available gravity data for Silali (Swain, 1976) indicates the presence of a narrow, linear, positive anomaly extending southwards from Silali to Paka volcano. This anomaly, which is spatially coincident with the zone of fracturing described above may reflect the presence of an axial dyke swarm intruded into the Precambrian basement at depths of 2–3 km (Swain, 1992). It has been modelled as a steep-sided dense (?basaltic) body, 11 km by 6 km, intruded to within 2 km of the surface and flanked by a considerable thickness of low density rocks. Gravity modelling suggests that a small cupola may overlie this intrusion directly below Silali caldera (Swain, 1976).

8.6 GEOTHERMAL ACTIVITY

8.6.1 Introduction

Hot, steaming and altered ground with fumaroles occur in the eastern half of the caldera and on the upper eastern flanks of Silali. At the base of the western flanks around Kapedo there is an extensive hot spring system, and a separate spring system occurs 9 km further north at Lorusio. Warm alkaline springs also occur along several fault lines at the periphery of the northern flanks.

The highest surface temperatures occur in the eastern half of the caldera floor, where the maximum recorded value is 96.8°C (the local boiling point). Generally, the temperatures are lower outside the caldera, although in places they are close to boiling point. In total, the geothermal activity in the caldera and upper eastern flanks falls within an area of about 20 km^2. Within this area, activity appears to be closely associated with the youngest phase of trachytic volcanism in the eastern half of the caldera and Black Hills area. Surface manifestations within these areas are controlled by NNE to NE-trending faults, fissures, and the caldera ring fracture.

8.6.2 Geothermal activity within the caldera

The most extensive and hottest geothermal activity on Silali occurs in the eastern half of the caldera floor, where it is largely concealed by a thin mantle of pumice. Hot altered ground and fumaroles also occur around the walls of the eastern half of the caldera. The western half of the caldera appears to be geothermally inactive, although hydrothermally altered areas with ambient temperatures on the western walls testify to former activity.

8.6.2.1 Activity around the caldera walls

Hot and steaming ground with red and white clays and isolated fumaroles occurs around the south-east and eastern walls of the caldera. The activity extends from the base to near the top of the caldera wall and occurs

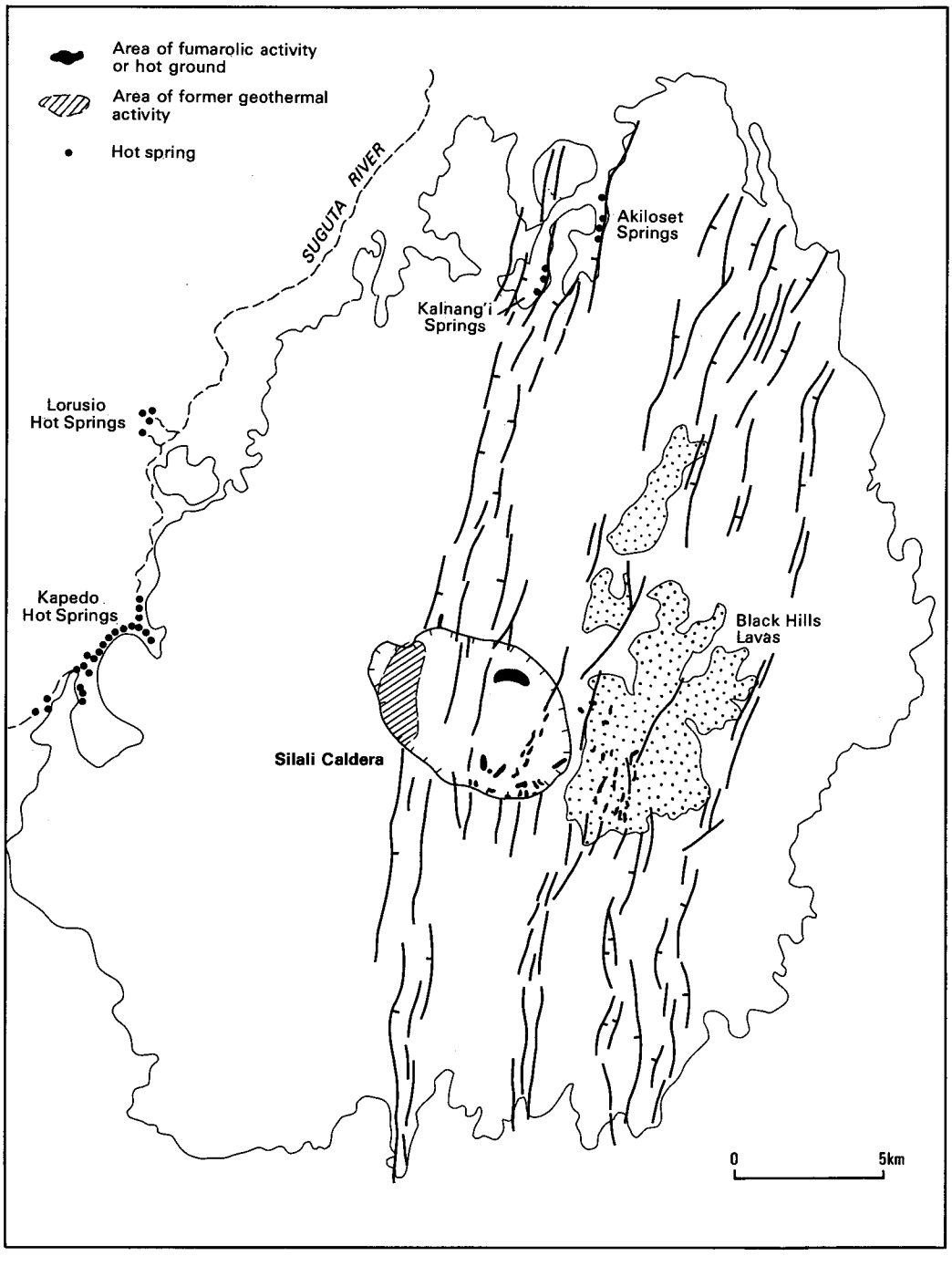

Figure 8.6 Summary of geothermal activity on Silali volcano.

on NNE or NNW-trending fractures. Some leakage may be associated with the caldera ring fracture but this structure is everywhere obscured by talus deposits. The host rocks consist of porous, pumiceous deposits of the Kapedo Tuffs. Near the base of the caldera wall activity occurs within pumiceous scree deposits and fractures cutting the Lower Trachyte Lavas.

The most extensive and hottest activity is located near the base of the wall and in erosional gullies in the south-east corner of the caldera at [AM 1925 1263]. Here fumarole and ground temperatures reach a maximum of 96.8°C. At this locality the lavas are deeply altered to red, white and purplish clays, composed dominantly of kaolinite with alunite (Kemp, 1990). Some silicification occurs, and fine acicular crystals of sulphur are present around the hottest fumarole. Fumaroles are weak and have high CO_2 and Rn concentrations and smell of H_2S.

Isolated fumaroles and hot ground occur on the southern sector of the caldera wall where it is cut by N-trending faults. Fumarole temperatures here range up to 96.3°C and ground temperatures reach 96.7°C. At the northern end of the downfaulted platform on the eastern wall of the caldera [AM 1938 1272], weak fumaroles with temperatures up to 84.2°C occur along a series of NNW-trending faults. Analysis of the alteration products indicates the presence of clays and alunite, amorphous silica, jarosite and haematite, (Kemp, 1990). To the north of the platform there is an isolated area of activity located high on the caldera wall. Here, reddened kaolinitic clays are associated with veins of amorphous silica and ground temperatures reach up to 84.2°C.

The western half of Silali caldera is devoid of geothermal activity, but hydrothermal alteration in the south-west and north-west walls indicate this area was

geothermally active in the past. In several places on the south wall this alteration is associated with NNE-trending faults and dykes, which when projected onto the caldera floor coincide with the post-caldera basalt fissure zone. Just outside the north-western rim of the caldera a small area of hot altered ground with steam seepages occurs upon this fissure zone at [AM 1895 1320]. This activity occurs within trachytic pumice tuffs and breccias and is restricted to a narrow linear zone along a fault scarp. Recorded temperatures range up to 57.6°C.

The prominent buttress in the north-western wall of the caldera [AM 1885 1309] shows extensive hydrothermal alteration which is associated with faults and dykes. Here silicification and brecciation of the trachyte lavas is widespread and associated with fibrous growths of gypsum and anhydrite (Kemp, 1990).

8.6.2.2 Activity on the caldera floor

Surface geothermal activity is associated with the trachyte fissure line in the east of the caldera, and is manifested by weak fumaroles and steam seepages at [AM 1926 1285]. Ground temperatures range up to 95.8°C and the highest recorded fumarole temperature is 78.3°C. Trachyte lavas in the immediate vicinity of the fissure are haematitised and silicified.

The caldera floor is covered by a thin mantle of trachytic pumice which supports a cover of thick grass with scattered thorn bushes. A number of areas characterised by sparse vegetation (Plate 8.6) with occasional clumps of *Abligaardia lispidula* are associated with small depressions and low mounds with scattered silicified blocks. Elevated temperatures occur at shallow depths (0.5 m) beneath the surface and a series of traverses were carried out to locate the sub-surface extent of this activity (Figure 8.7). These indicate that the ground temperature over most of the caldera is between 30–35°C, except in the north-west where temperatures are less than 30°C. The sub-surface geothermal activity is located exclusively within the eastern half of the caldera and is largely confined to a series of narrow, NNE-trending linear zones.

These narrow high-temperature zones correlate closely with the main NNE-trending faults exposed in the caldera walls and with lineaments crossing the caldera floor. One exception is the geothermal area in the central northern sector of the floor at [AM 1920 1305]. This area trends NE and appears to be located at the intersection of the buried caldera ring fault and the regional fault trend.

The high temperature linear zones are up to 200 m wide and range in length from 0.5 km to 2 km. White, red and purple clays composed predominantly of kaolinite with minor amounts of alunite occur at the base of the pumice cover. Holes made into the pumice to a depth of 0.5–1 m result in the emission of steam smelling of H_2S. The thermal gradient profiles show pronounced increase in temperature beneath the pumice cover illustrating its efficiency as a thermal insulator. Soil-gas concentrations within these areas vary rapidly across the high temperature zones, with CO_2 concentrations ranging from less than 1% to 36% and radon values reaching up to 1622 Bq/l. The highest radon and CO_2 concentrations are coincident with the zones of maximum temperature. Steam emitted from holes made into the pumice over the hottest areas contains high CO_2, with concentrations of up to 98% in the non-condensable fraction. The asymmetry of the soil temperature and gas anomalies may reflect a dip on the controlling fractures.

8.6.3 Geothermal activity on the eastern flanks

Geothermal manifestations are developed along a series of N to NNE-trending faults and open fissures which cut the trachyte lava domes and pumice cones of the Black Hills Trachyte Lavas. Maximum recorded temperatures for individual areas of hot ground within this zone range from 56.8°C to 86.0°C and for fumaroles from 56.4°C to 94.6°C.

In the cool of the early morning or after rain, a series of steam plumes is visible along a zone of open fissures and faults and indicates the hottest and most

Plate 8.6 Silali caldera floor and eastern wall. Pale areas of vegetation indicate main areas of surface geothermal activity.

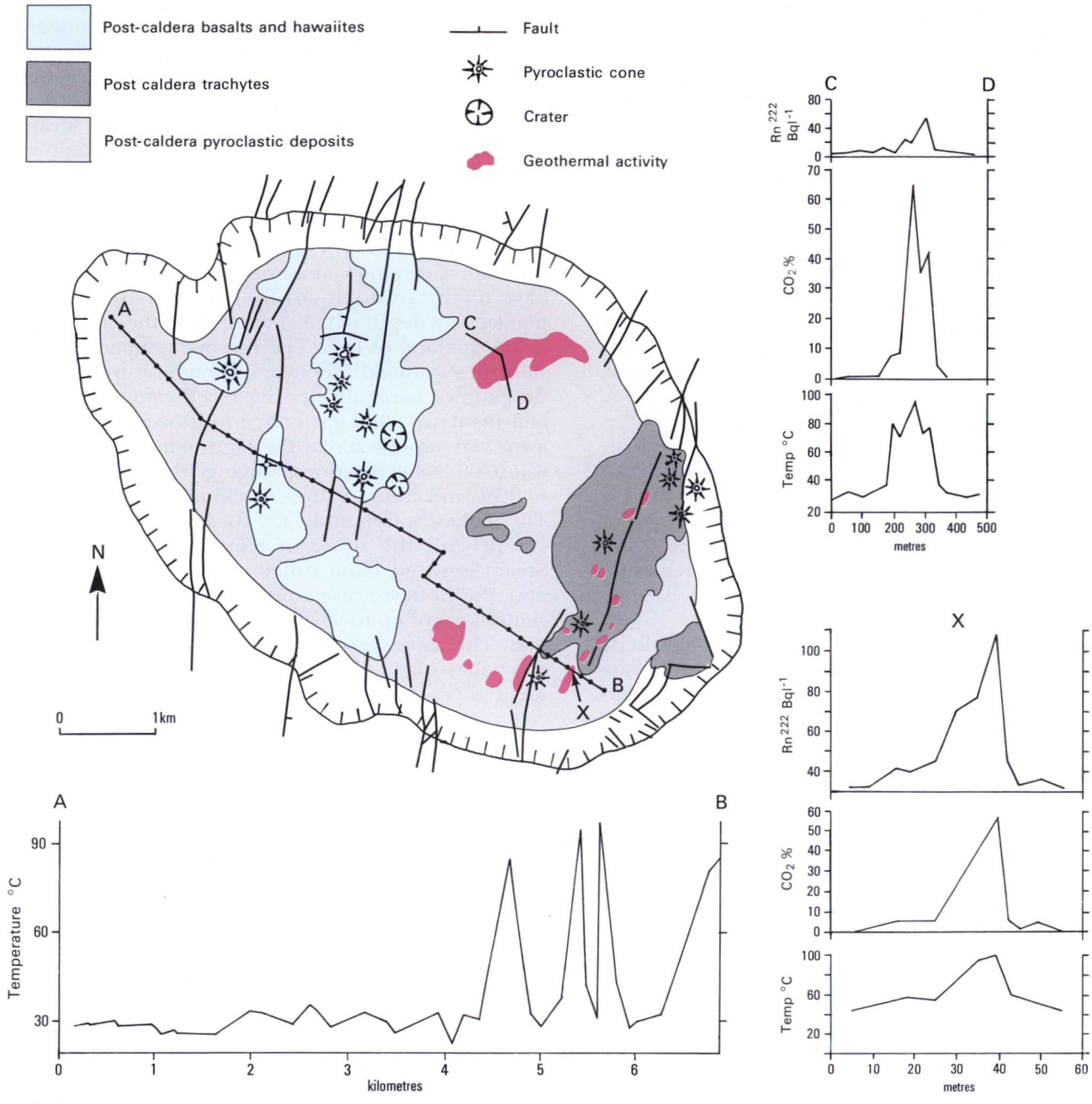

Figure 8.7 Location of geothermal activity and associated temperature and soil gas anomalies on the floor of Silali caldera.

vigorous activity in this area. The zone extends for over 2 km, and occurs largely within trachytic pumice overlying lava. Numerous collapse pits occur and open fissures up to 50 m deep have steam condensing on their walls. Many of the fumaroles in this fractured zone show evidence of cooling due to ingestion of air, and a maximum temperature of 94.6°C was recorded at [AM 1955 1266]. Soil gases over this general zone of fissuring have high CO_2 and Rn.

Elsewhere geothermal activity in the form of isolated weak fumaroles and seepages is located along the flanks or rims of trachyte pumice cones and on the crests of lava domes. The pumice is reddened and altered to clays. Fissures cutting the youngest trachyte domes are in places lined with a white, brittle, botryoidal mineral. This has been identified as villiaumite (NaF), and is associated with minor amounts of kogarkoite (Na_3SO_4F) and trona ($Na_3H(CO_3)_22H_2O$) (Kemp, 1990).

8.6.4 Kapedo hot springs

The Kapedo hot springs are the source of the Suguta River. They occur along a 5 km strip on the eastern side of the Suguta River at the base of the western flanks of Silali. The most southerly (upstream) area of springs occurs in the vicinity of Kapedo bridge [AM 1768 1292]. Here a series of weak springs and seepages with temperatures in the range 35–40°C are marked by beds of reeds and algae. They bubble up from joints and cracks within the Mission Basalt and at the contact of the basalt with overlying superficial and pyroclastic deposits. Carbonate deposition is common along joints within the basalt lava.

Plate 8.7 Hot waterfall at Kapedo village.

Plate 8.8 Carbonate travertine at Lorusio hot springs. Looking west towards the rugged topography of the rift wall.

At Kapedo village there is a major discharge of hot water into the Suguta River where a 30 m high waterfall, with a temperature of 45°C, cascades over a fault scarp in the Mission Basalt (Plate 8.7). The source of the waterfall and the hot stream, known locally as Adoketabolun, is located to the south-east at [AM 1779 1292]. Here, four bubbling springs with temperatures in the range 45–55°C issue along the contact between a young basalt flow of the Katenmening Lavas and bedded pyroclastic deposits of the Kapedo Tuffs. Between these springs and the waterfall, innumerable springs and seepages add to the flow of the Adoketabolun. Individual springs have flow rates greater than 10 l/sec and cumulatively give an estimated flow of around 1000 l/sec at the waterfall (Burgess, 1986). To the north-east of the main springs, a prominent clump of doum palms around a low mound at [AM 1781 1304] marks the location of another set of hot springs and seepages which form the Chaburwas hot stream. Temperatures here vary from 45 to 50°C and individual springs have flow rates of around 5 l/sec. The Chaburwas stream flows over the Mission Basalts 250 m north of the main waterfall and has been harnessed by the Kapedo mission in a small hydro-electric scheme.

The Kapedo spring system extends another 1.5 km downstream with numerous springs and seepages adding to the flow of the Suguta River. These springs rise along the east bank at the basalt-tuff contact, but also discharge within the river bed. Flow rates are generally low, being typically only a few litres per second with temperatures in the range 37–53°C. Old travertine deposits indicate former spring activity up to 2 m above the present level.

The temperature of the Suguta River varies along its length. Near Kapedo village it is in the range 42–45°C decreasing down to 32°C just before the Lorusio springs enter (Section 8.6.5). Temperature also varies with the degree of dilution by seasonal flood water coming from the Nginyang and Kapedo tributaries upstream from the spring area.

8.6.5 Lorusio springs

Nine kilometres to the north of Kapedo village on the east side of the Kapedo to Lomelo track, there is a gently sloping flat pan with sparse vegetation and a covering of white salts. Within this area reed mounds mark the site of hot springs and seepages which flow east to join the Suguta River. The springs occur within colluvial and alluvial deposits overlying Kapedo Tuffs near the base of the western wall of the rift at [AM 1790 1394]. Spring discharge covers an area of 2 km^2.

The largest of these springs has a small travertine terrace (Plate 8.8) covered with dark green and orange algae. This spring has a recorded temperature of 82.2°C and an estimated flow rate of 15 l/sec. (Burgess, 1986). It bubbles vigorously and emits CO_2.

The Lorusio springs probably represent deeply circulated fluids that are upwelling along a boundary fault marking the edge of the inner trough.

8.6.6 Warm springs on the northern periphery of Silali

Around the periphery of the northern flanks of Silali, within the Flank Fissure Basalts there are a number of cool and warm alkaline springs. These springs are clearly visible on air-photographs and satellite images as a series of coloured ponds occurring within N-trending fault-bounded graben. They drain northwards to Loreng and then westwards to join the Suguta River at [AM 1893 1494]. The pools vary in colour from green to pinkish-red and brown reflecting the growth of algal blooms and the degree of evaporation at the time. They contain abundant small fish (*Tilapia.* sp.) and are surrounded by lush green reed beds which support an abundant and varied wildlife including crocodiles, snakes, flamingoes, pelicans and numerous wading birds.

The largest springs are located at the base of the west-facing fault scarps at Alikoset [AM 1954 1466] and around the ephemeral Lake Kalnang'i [AM 1930 1439]. Temperatures range from ambient to a maximum of 38.2°C. Individual flow rates are low, but in aggregate may be high judging from the volume of water entering the Suguta River to the west. The mud flats surrounding Lake Kalnang'i have a thin crust of trona with minor amounts of halite (Kemp, 1990).

9 The geology and geothermal activity of Emuruangogolak Volcano

9.1 INTRODUCTION

Emuruangogolak is a large basalt-trachyte volcano situated in the narrowest part of the inner trough of the Rift Valley between latitudes 1°25'N and 1°40'N. Some confusion surrounds the naming of the volcano, and several names are in common use. On the published 1:50 000 topographical map (series Y731, sheet 77/2) the eastern flank is covered by the name Moruagikokolak Plateau and the western part of the summit area is designated as the Kagimoging'olei Plateau, but on smaller scale maps the area is referred to as Emurua Kirig West or as Emuruagiring. The name Emuruangogolak is preferred in this work because it is entrenched in the geological literature and has parlance amongst the local Turkana.

Emuruangogolak almost completely straddles the inner trough, abutting against Pliocene trachytes of the Emuruagiring Plateau along the eastern margin and against a faulted and tilted sequence of older Plio-Pleistocene trachytes and basalts in the west. The volcano reaches an elevation of 1328 m on the summit cone of Emuruepoli, and has a broad shield-like form that is elongated in a north-north-east direction along the axis of the trough. The main volcanic edifice covers an area of approximately 525 km^2, having a length of 33 km and a width of 20 km, although to the north of the main shield a chain of fissure-controlled scoria cones, tuff rings and maars extends for a further 9 km in a north-north-east direction onto the rift floor.

The floor of the rift in the vicinity of Emuruangogolak has a marked tilt towards the north, with an average gradient of 1:100. As a result of this, the summit of the volcano rises 700 m above the base of the southern flanks, but is about 1000 m higher than the periphery of the northern flanks. Similarly, the eastern margin of the volcano has an altitude of 950 m where it is juxtaposed against the fault scarp of the Emuruagiring Plateau, but the base of the western flank at the same latitude has an elevation of only 550 m. This may be due to the westerly tilt in the floor of the trough, but may also partly result from ponding of Emuruangogolak lavas against the escarpment of the Emuruagiring Plateau. The combined tilting of the rift floor to the north and west has imparted an asymmetry to the volcano, with the summit region being located south and east of centre.

A large part of the volcanic pile consists of an old trachyte shield, the lavas of which crop out over much of the eastern and western flanks of Emuruangogolak. These older trachytes are vegetated by sparse to moderately dense thorn scrub. In contrast, almost all of the northern flanks and most of the southern flanks are covered by extensive spreads of young basalt and trachyte lavas with pristine morphological features and little vegetation. High on the western side of the volcano there is a cluster of trachytic pumice cones from which an apron of pyroclastic deposits extends down to the base of the western flanks. These pyroclastic deposits are deeply gullied on the upper flanks but on the lower slopes are characterised by gently dipping surfaces that are sparsely vegetated.

The summit region of the shield is occupied by a caldera which is elliptical in plan, having a long-axis measuring 5 km in a north-west direction and a short axis of 3.5 km (Plate 9.1). Post-caldera trachyte lavas infill much of the caldera and form a thick pile which has overflowed the rim in the south-west, north-west and north-east, so concealing large parts of the ring structure. A well-developed vertical caldera wall up to 70 m high is preserved around the eastern, south-eastern and western side of the caldera, and is manifested by several short scarps in the north.

Extensive alluvial plains occur around the southern periphery of the volcano in the ground extending southwards to Silali. The Suguta River drains this region and flows northwards in a valley confined between the western flanks of Emuruangogolak and the western margin of the inner trough. To the north of the volcano, the Suguta opens out into a braided drainage system along the axis of the inner trough. This northern part of the trough is floored by a large expanse of fluvial, lacustrine and windblown deposits, and was once occupied by the former Lake Suguta. The massif of Emuruangogolak effectively formed a barrier across the trough and dammed the southern end of the lake. Lavas were erupted into the lake and phreatomagmatic activity took place upon its shorelines, and during periods of high lake levels lacustrine sediments were deposited on the northern flanks of the volcano.

9.2 GEOLOGY OF THE RIFT MARGINS ADJACENT TO EMURUANGOGOLAK

The Emuruagiring Plateau forms the eastern margin of the rift adjacent to Emuruangogolak and is faulted against the eastern flank of the volcano (Plate 9.7). The plateau is upfaulted from the rift floor along a series of scarps controlled by NNE-trending faults. The surface of the plateau reaches a maximum elevation of about 1380 m in the south-east and slopes gently to the north and west.

Williams (1978) reported an age of about 3.5 Ma for the lavas of Emuruagiring. However, this date is erroneous because it does not pertain to Emuruagiring (Williams, personal communication, 1990) but to trachytes dated by Baker et al. (1971) from the Tirr Tirr Plateau situated about 50 km to the north (Section 10.2.2). During the present survey three sets of duplicate samples from different stratigraphical levels within the lava pile were dated by the K/Ar method and these gave a range of ages from 2.36–3.01 Ma, with the more reliable and preferred dates falling close to 3 Ma (Rundle, 1991). Williams et al. (1984) provisionally regarded the Emuruagiring lavas as upfaulted parts of the Emuruangogolak volcanic shield. However, the Pliocene dates obtained by the present survey clearly indicate that the Emuruagiring lavas are significantly

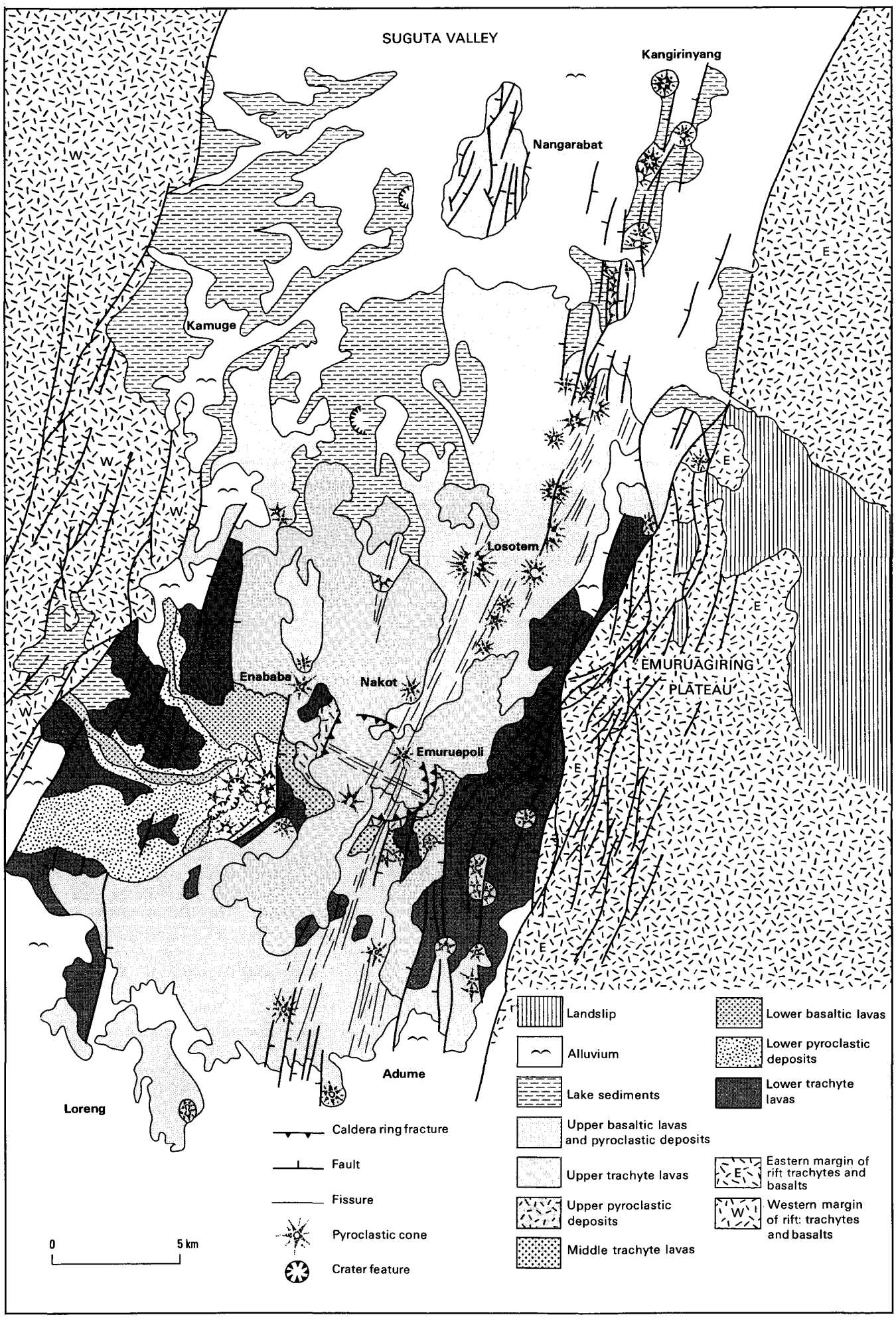
SUGUTA VALLEY
Kangirinyang
Nangarabat
Kamuge
Losotem
Enababa
Nakot
Emuruepoli
EMURUAGIRING
PLATEAU
Adume
Loreng
W
E
0
5 km
Caldera ring fracture
Fault
Fissure
Pyroclastic cone
Crater feature
Landslip
Alluvium
Lake sediments
Upper basaltic lavas and pyroclastic deposits
Upper trachyte lavas
Upper pyroclastic deposits
Middle trachyte lavas
Lower basaltic lavas
Lower pyroclastic deposits
Lower trachyte lavas
Eastern margin of rift trachytes and basalts
Western margin of rift: trachytes and basalts

Plate 9.1 Aerial view of Emuruangogolak caldera looking north. The trachyte lava cone of Emuruepoli and its associated dome on the east are visible on the northern rim of the caldera.

older than Emuruangogolak, which is of Upper Pleistocene to Recent age. It is therefore a reasonable assumption that the Emuruagiring Trachytes underlie Emuruangogolak, at least in the east.

Compositionally the lavas of the Emuruagiring Plateau are strongly silica-oversaturated peralkaline trachytes and rhyolites which are considerably more siliceous than the trachytes of Emuruangogolak. They occur as thick, laterally extensive, massive flows which rest unconformably on older Miocene volcanic and sedimentary sequences exposed around the northern and eastern margins of the plateau. Key (1987) reported a thickness of 80–100 m for the lavas along the eastern margin of the plateau and suggested that they thicken westwards towards the inner trough. The maximum thickness in the west is unknown because the lavas are heavily faulted and the base of the pile is not exposed. During the present survey a section was examined in a fault scarp in the central part of the plateau [BM 2164 1725]. At this locality the sequence is approximately 200 m thick, although the base is not exposed, and consists of three massive porphyritic trachyte lavas overlain by a massive rhyolite flow forming a capping to the plateau.

The underlying Miocene volcanic and sedimentary rocks exposed around the northern and eastern edge of the Emuruagiring Plateau have undergone large-scale landslippage. These strata are designated Samburu Basalts on the Emuruangogolak geological map accompanying this report. However, subsequent to the publication of this map, additional survey work in the Namarunu area has indicated that these are probably correlatives of the Kamolingaran basalts (Section 10.2.1) which are younger than the Samburu Basalts.

The western margin of the rift adjacent to Emuruangogolak is composed of a sequence of faulted trachytes and basalts which have not been studied during the present survey. The trachytes were erupted from the volcanic centres of Kanatim (4.3 Ma) and Kaptagani (3.3 Ma), which form part of a series of Pliocene volcanic shields along the western margin of the rift (Webb and Weaver, 1975). The basalts of this area were mapped by Truckle (1977a) as Lorikipi and Kamuge basalts of Pleistocene age, and in the map accompanying this report they are grouped together as Pleistocene basalts. However, subsequent to the publication of this map, additional survey work in the Namarunu area has shown that the Lorikipi Basalts are of Pliocene age (Section 10.3).

Figure 9.1 Simplified geological map of Emuruangogolak.

9.3 GEOLOGY OF EMURUANGOGOLAK

9.3.1 Introduction

Weaver (1977) described the geology and petrology of Emuruangogolak, based on a brief expedition undertaken by several members of the EAGRU research group in 1974. He formulated an evolutionary model for the volcano in which two episodes of summit collapse produced nested calderas, and he postulated the presence of an incipient ring fracture that might be the precursor of a third collapse event. Truckle surveyed the area to the north and west of Emuruangogolak and provided a brief description of the lacustrine sediments and the history of the former Lake Suguta (Truckle, 1976 and 1977a). Various synopses of the geology of Emuruangogolak and surrounding areas have subsequently been published (e.g. Williams et al., 1984; Key, 1987) but these are based on the earlier descriptions of Weaver and Truckle.

Emuruangogolak is of Upper Pleistocene to Recent age. Weaver (1977) reported a K/Ar age of 900±100 ka for the oldest exposed lavas on the south-east flanks, which form part of the early trachyte shield. Charcoal obtained from the youngest basalt flow on the southern flanks yielded a ^{14}C age of 250 ± 100 years (Shotton et al., 1974). Skinner et al., (1975) used

Table 9.1 Summary of the stratigraphy of Emuruangogolak

Lacustrine sediments (l)	>120 ka – 3 ka?	
Upper Basaltic Lavas (b^u)	>38 ka? – 250 ± 100 yr	LAKE SUGUTA
Upper Trachyte Lavas (t^l)	38 ± 3 ka – c.1900 AD	
		CALDERA FORMATION
Upper Pyroclastic Deposits (p^u)	38 ± 6 ka	
Middle Trachyte Lavas (t^m)		
Lower Basaltic Lavas (b^l)	185 ± 11 ka	
Lower Pyroclastic Deposits (p^l)	205 ± 4 ka	
		MAJOR FAULTING
Lower Trachyte Lavas (t^l)	>900 ka – 500 ka	SHIELD FORMATION

some of the younger flows on Emuruangogolak to construct secular magnetic variation curves for Kenya. These investigations suggest that basalt lavas on the northern flanks are 700–900 years old, whilst the youngest trachyte flow on the southern flanks, which overlies the youngest basalt, may only be about 95 years old. The very young age of this flow is corroborated by reports from Turkana elders that earlier generations of their tribe observed volcanic eruptions in the area which were accompanied by ground tremors.

A generalised sequence of events in the evolution of Emuruangogolak is summarised in Table 9.1 and forms the basis for the geological description given in the following sections. It should be noted that during the more recent development of the volcano the Upper Trachytes and Upper Basalts were erupted during the same broad time period, with some centres having erupted both magma types at different times. It should also be stressed that the complex multi-caldera model of Weaver (1977) is considered to be untenable in the light of evidence obtained during the present survey.

9.3.2 Lower Trachyte Lavas (t^l)

Lower Trachyte Lavas crop-out over large parts of the eastern and western flanks, and are exposed in small inliers within younger lavas on the southern and northern flanks.

They are pantelleritic in composition and are generally sparsely microporphyritic, although strongly porphyritic flows also occur.

The lower trachytes are pale to dark green in colour, weathering to buff or pale brown. In outcrop the majority are flow-banded and have a fissility parallel to the banding. Original flow features are reasonably well-preserved on the eastern flanks of the volcano and can be seen on air-photographs. Most flows are lobate to discoid in shape with steep flow-fronts, and small domes also occur. The disposition of flow-features indicates that the lower trachytes were erupted from numerous sources on the eastern flanks, and flowed radially away from the summit area of the volcano.

In contrast, original flow morphology is rarely preserved in the lower trachytes on the western and southern flanks. An exception to this is a large, coarsely porphyritic flow which has been exhumed from beneath a cover of Lower Pyroclastic Deposits on the lower part of the western flanks [AM 1929 1669]. This trachyte was erupted from a source on the middle part of the flanks and flowed down slope for several kilometres as a narrow linear flow with prominent levees, which spread-out into a broad flow-head at the base of slope.

A broad tongue-like flow of benmoreitic composition occurs on the lower south-western flanks, to the west of Naturtur at [AM 1910 1620]. This flow is faulted and is assumed to have been coeval with the lower trachytes, although no field relationships are seen between the two, nor with the Lower Pyroclastic Deposits. In outcrop the flow is strongly brecciated, and in thin section is seen to be a mixed lava, composed of blebs of partly assimilated vesicular basalt in a trachyte groundmass.

During the course of the present survey no pyroclastic rocks were recognised within the lower trachytes, although Weaver (1977) reports uncommon occur-

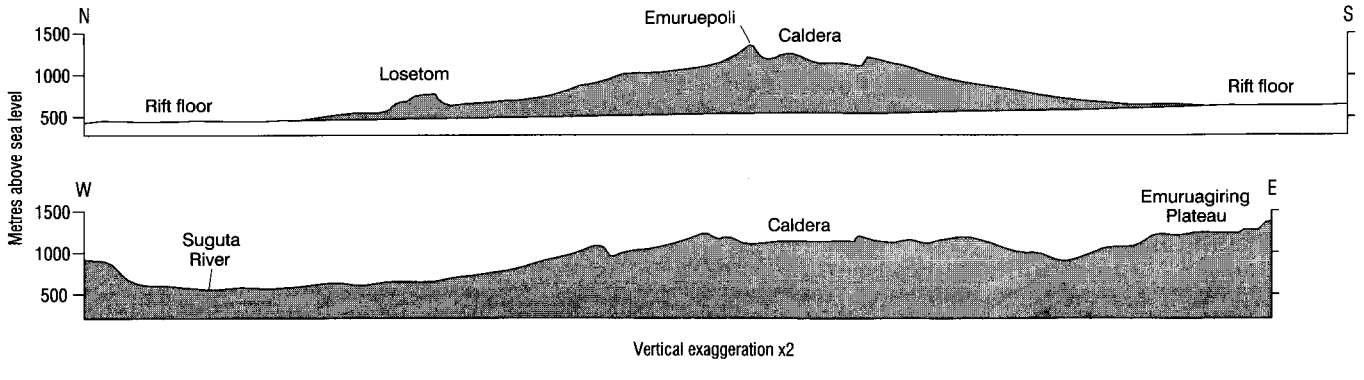

Figure 9.2 Topographic profiles across Emuruangogolak.

rences of thin ignimbrites (*sic*) intercalated within them on the eastern flanks.

The eruption of the Lower Trachyte Lavas constructed an early volcanic shield on which later activity has been superimposed. The distribution of present day exposures of lower trachyte lava suggest that this early volcanic shield was between 20 and 25 km in length along the axis of the rift and about 20 km wide. The flanks of this shield generally sloped between 3 and 4 degrees away from the summit region, although the gradient on the lower parts of the western flanks appears to have been less. Extrapolation of the slopes indicates that the early shield probably reached an elevation of approximately 1300 m, and was therefore of similar height to the present day volcano. Basaltic activity appears to have been absent during the growth of the early trachyte shield, a feature also noted by Weaver (1977), although the occurrence of the mixed benmoreitic lava on the south-western flanks does indicate the presence of basaltic magma at the time.

Weaver (1977) reports K/Ar ages of 900 ± 100 ka for the oldest exposed trachytes and 500 ± 100 ka for trachytes thought to represent the youngest part of the early volcanic shield. In keeping with this age span, a Ar/Ar date of 864 ± 7 ka was obtained by the present survey from the well-featured porphyritic trachyte low on the western flanks at [AM 1930 1672]. This date relates to the outer flanks, which implies that the bulk of the early trachyte shield must be older.

9.3.3 Faulting

The early trachyte shield was subject to an episode of faulting, prior to the eruption of the Lower Pyroclastic Deposits. This faulting generally trends NNE, although on the south-eastern flanks several important faults are orientated almost N–S, and in the north-east a number of minor splays or linking faults trend NE. Two faults in particular appear to have played an important role in controlling the distribution of later lava flows, and for reference purposes these are given informal names. The NNE-trending Enababa fault runs along the upper western flanks for a distance of 5 km and has a downthrow to the east. It has a prominent east-facing scarp which at its northern end is buried beneath the Upper Trachyte Lava cone of Enababa [BM 2014 1694]. On the eastern flanks there are several N-trending faults which downthrow to the west. The most important of these, the Eastern boundary fault, is manifested by a prominent fault scarp which extends from beneath alluvium near Nadume in the south [BM 2070 1550] and can be traced northwards for a distance of 10.5 km before passing beneath Upper Trachyte Lavas at [BM 2074 1656]. The Enababa and Eastern boundary faults define a broad axial graben structure over the summit region of the volcano.

9.3.4 Lower Pyroclastic Deposits (p^l)

Lower Pyroclastic Deposits, of trachytic composition, form a thick and extensive apron on the western flanks of the volcano. They overlie faulted Lower Trachyte Lavas and are overlain by Lower Basaltic Lavas and Upper Trachyte Lavas.

The pyroclastic apron on the western flanks is composed of a very well-bedded sequence of unconsolidated to poorly consolidated, yellow-buff, pumice lapilli ashes, tuffs and pumice lapilli deposits. Obsidian clasts and lithic clasts of trachyte and microsyenite also occur within the deposits. Bedding generally dips westwards and is approximately conformable with the slope of the flanks, although local variations in dip occur where beds drape pre-existing topographical features on the underlying faulted surface of the lower trachytes. Originally the pyroclastic apron covered an area of at least 65 km^2, although subsequently parts have been removed by erosion to expose inliers of lower trachyte.

The deposits were erupted from a cluster of trachytic pumice cones high on the western flanks. Nine cones or coalesced crater features are preserved within the deposits. The two largest cones are approximately a kilometre in diameter and have shallow craters that have undergone some degradation by erosion. Because they were built upon a slope these two cones are asymmetrical in profile, having short flanks on the up-slope side, and long western flanks which merge down-slope into conformity with the stratification of the pyroclastic apron. They are composed of poorly stratified pumice lapilli deposits, trachytic scoria and spatter, with layers of welded or agglutinated obsidian. It is concluded from the wide distribution of these deposits, their well-bedded nature, and the manner in which they mantle the pre-existing topography, that they represent air-fall deposits produced by plinian-style eruption. The strongly asymmetrical distribution of the deposits on the western flanks is the result of redistribution by easterly prevailing winds. Weaver (1977) concluded that the deposits have a maximum thickness of 150 m. Whilst such thicknesses may occur on the source cones, the pyroclastic apron is considered to be generally thinner, ranging in thickness between 20 to 80 m.

The positions of the source cones appear to have been controlled by NNE-trending fractures, that were probably reactivated faults in the underlying lower trachytes. Two cones are located upon NNE-trending faults and are breached on their south-west sides, and another five craters are coalesced to form a NNE-trending chain. Faults within the underlying lower trachytes do not appear to cut the pyroclastic deposits, indicating that little or no movement took place upon the faults during or subsequent to eruption of the deposits.

Ar/Ar dating of K-feldspar crystals has yielded ages of 212 ± 22 ka and 205 ± 4 ka for the Lower Pyroclastic Deposits. Thus a significant period of dormancy appears to have occurred between the formation of the early trachyte shield (by 500 ka) and the eruption of the pyroclastic deposits.

9.3.5 Arguments against the formation of an early caldera

Weaver (1977) and Williams et al. (1984) postulated that the trachytic pyroclastic activity on the western flanks preceded and triggered the formation of an early caldera, concluding that the Enababa fault is the only surviving remnant of a ring fracture related to this caldera.

The concept of an earlier caldera as proposed by Weaver is considered to be a speculative complication in the evolutionary model of the volcano, and is not accepted in the present work. The main objection to this idea is that it is impossible to extrapolate a ring

structure around the volcano starting from the Enababa fault on the western side. Even Weaver admits that his proposed structure is difficult to identify around the eastern flanks and that it is completely buried beneath younger lavas on the northern flanks. On the southern flanks Weaver concludes that the hypothetical ring structure is buried, but that it probably runs along a line between two young trachyte cones at [BM 2063 1633] and [BM 2026 1622] which is coincidental with a marked break in slope. However this break in slope cannot be reconciled with the proposed caldera for a number of reasons. Firstly, the feature is the reverse of that expected for a caldera, in that the break of slope faces away from the summit area. Secondly, it trends obliquely across the southern flanks of the volcano in a north-westerly direction and continues well to the west of the line of the Enababa fault, and consequently extends outside the confines of the postulated caldera. Thirdly, the break in slope is in places preserved in Lower Trachytes Lavas and these show no signs of fracturing coincident with the feature, which implies that the structure responsible for the break of slope must lie buried beneath the lower trachytes exposed at the surface, and therefore pre-dates Weaver's postulated episode of early caldera formation by a significant period of time (at least 300 ka).

9.3.6 Lower Basaltic Lavas (b^l)

Lower Basaltic Lavas, which include hawaiites and mugearites, occur on the western flanks of the volcano. The lavas take the form of thin planar flows, in most cases only a few metres thick, which form an extensive and nearly conformable westerly-dipping cap over the Lower Pyroclastic Deposits. Erosion of the underlying unconsolidated pyroclastic deposits has resulted in extensive gullying with cappings of the lava preserved on interfluves. Upper Trachyte Lavas erupted from Enababa unconformably overlie the Lower Basaltic Lavas and infill erosional gullies incised within them and the underlying Lower Pyroclastic Deposits [BM 2008 1688].

Most of the lower basalts were erupted along the crest of the Enababa fault scarp, possibly from fissures parallel with the fault, and they flowed westwards down the flanks over the Lower Pyroclastic Deposits. Towards the northern end of the line of eruption the lavas drape the eastern face of the fault scarp, which at this point is a low feature, but they appear not to have flowed for any distance to the east of the scarp. The uniformly thin but extensive nature of the lavas suggests that they were very fluid at the time of eruption. This is exemplified by a hawaiite lava that was erupted from a breached lower pyroclastic cone high on the western flanks [AM 1991 1660], and which extends as a thin, ribbon-like flow for more than 8 km down the flanks of the volcano to the Suguta River.

A breached mugearitic scoria cone is juxtaposed against the eastern side of the Enababa fault scarp at its northern end [BM 2011 1687]. This is partly overridden by a Middle Trachyte lava, the flow-front of which is ramped-up over the eastern side of the cone. From this it is concluded that the Lower Basaltic Lavas pre-date the Middle Trachyte Lavas.

Step-heating Ar/Ar dating of an hawaiite from low on the western flanks at [AM 1933 1674] has yielded an age of 185 ± 11 ka.

9.3.7 Middle Trachyte Lavas (t^m)

Middle Trachyte Lavas occur on the uppermost flanks of the volcano around the outside of the caldera rim. They overlie Lower Trachyte Lavas, and evidence presented in the previous section indicates that they also post-date the Lower Basaltic Lavas on the western flanks. They are overlain by the Upper Pyroclastic Deposits and the Upper Trachyte Lavas, and are cut by the caldera, but are otherwise virtually unfaulted.

Most middle trachytes are small, lobate, steep-sided flows which appear to have been viscous at the time of eruption. However, a group of flows situated immediately to the south-east of the caldera rim have less steep flow-fronts and cover a relatively large area, and were probably more fluid. Small domes also occur, and to the east of the caldera at least ten are coalesced in a single NE-trending line.

The middle trachytes were erupted from multiple sources on the uppermost flanks and former summit area, which is now occupied by the caldera. They are confined to a zone bounded by the Enababa fault in the west and the Eastern boundary fault in the east. Flows radiate away from the summit area and the fronts of several abut against the scarps of the Enababa and Eastern boundary faults which acted as barriers at the time of eruption.

9.3.8 Upper Pyroclastic Deposits (p^u)

Upper Pyroclastic Deposits, of trachytic composition, are preserved on the upper flanks of the volcano around the western, southern and eastern rim of the caldera. They overlie the Middle Trachyte Lavas and are cut by the caldera. Field relationships demonstrate that they pre-date most of the Upper Trachyte Lavas, although radiometric dating indicates that the oldest upper trachytes, which were erupted from Enababa, are virtually the same age as the Upper Pyroclastic Deposits.

Poorly stratified Upper Pyroclastic Deposits rest upon trachytes in the western wall of the caldera. An accessible section is exposed through these in the south-west corner at [BM 2020 1665]. Here the sequence consists of approximately 8 m of strongly welded, dark green, lapilli tuffs, overlain by 2 m of poorly consolidated grey to buff-weathering pumice, which grades up into a capping of trachytic agglutinate. The entire sequence is rich in feldspar crystals and the welded tuffs at the base contain abundant subrounded and rounded bombs of syenite. Ar/Ar dating of anorthoclase crystals indicates an age of 38 ± 6 ka for the uppermost deposits at this locality.

To the west, patches of unconsolidated trachyte scoria and pumice rest upon middle trachytes in the ground between the caldera rim and the Enababa fault. These are the remnants of a relatively thin and impersistent pyroclastic layer that is contiguous with the deposits exposed in the western wall of the caldera. The deposits in this ground are exposed in a pit crater at [BM 2010 1651], where they consist of approximately 5–10 m of stratified, green-grey, buff-weathering pumice. A small trachyte scoria cone occurs a short distance to the south-west of the caldera rim [BM 2010 1651] and the ground in this area is strewn with trachytic scoria bombs.

Upper Pyroclastic Deposits occur in scattered patches on the upper southern and south-eastern flanks of the volcano, and are preserved as a thin layer around much of the southern rim of the caldera. In the south-east at [BM 2058 1643] a small trachytic pumice cone has been cut by the ring fracture and the remnants, including part of the vent, remain perched on the caldera edge. In the vicinity of this cone the surface is strewn with syenitic bombs, similar to those occurring within the deposits exposed around the western rim of the caldera.

In summary, it is concluded that the Upper Pyroclastic Deposits were erupted from a number of trachyte pumice-scoria cones on the former summit area of the volcano, of which only the remnants of a few are preserved around the caldera rim. Subsequent collapse of the summit area and the infilling of the caldera with younger lavas has masked the extent of the deposits, although their patchy and thin nature around the outside of the caldera suggests they are unlikely to represent a major phase of explosive activity.

9.3.9 Caldera formation

The caldera post-dates the Middle Trachyte Lavas and Upper Pyroclastic Deposits, both of which are cut by the caldera ring fault. Upper Trachyte Lavas infill much of the caldera and overflow its rim in the south-west, north-west and north-east, so concealing large sectors of the ring fracture. Formation of the caldera took place between 38 ± 6 ka and 27 ± 5 ka; the former date being the age of the Upper Pyroclastic Deposits exposed in the caldera wall, and the latter being the age of a relatively early intra-caldera Upper Trachyte Lava which overflowed the south-western rim of the caldera.

The caldera has an area of about 13 km^2 and is elliptical in plan, having a NW-trending long axis measuring 5 km and a NE-trending short axis of 3.5 km. The caldera wall is up to 70 m high around the eastern and south-eastern margins and bifurcates in the north-east before passing beneath upper trachytes erupted from the summit cone of Emuruepoli. Elsewhere remnants of the caldera wall are manifested by a prominent N-trending scarp 10–40 m high along the west side of the caldera, and by several short easterly trending fault scarps in the north.

The original depth of the caldera cannot be estimated with confidence, because the thickness of infill is uncertain. In the south-east and east the caldera floor is flat and does not appear to have been infilled by resurgent trachytes, although basalts of minor thickness do occur in these areas. Assuming that the infill in the east and south-east is negligible, then the 70 m height of the adjacent caldera wall provides an estimate of the original depth of the caldera in this area. In the west, however, resurgent trachyte lavas are banked against the caldera wall, and therefore its present height of 40 m can only be taken as a minimum estimate for the original depth of the caldera in this sector.

For an area of 13 km^2 and an estimated depth of 70 m, the original volume of the caldera would have been about 0.9 km^3, assuming that subsidence was uniform around the structure. The volume of Upper Pyroclastic Deposits is considered to be much too small to account for caldera collapse by a Krakatoan-style mechanism alone. Alternatively, lateral drainage of upper trachyte magma from a high-level chamber beneath the summit is a plausible triggering mechanism. The Upper Trachyte Lavas of Enababa are of more than sufficient volume to account for the collapse of the caldera, and their radiometric age of 38 ± 3 ka indicates that they were erupted either shortly before or at approximately the same time as the collapse of the caldera. However, whilst the extrusion of Enababa trachytes may have been the dominant factor triggering summit collapse, the eruption of the Upper Pyroclastic Deposits (38 ± 6 ka) may have been a contributing factor also.

9.3.10 Upper Trachyte Lavas (t^u)

Upper Trachyte Lavas occur as small steep-sided coulées and domes within the caldera, and as voluminous linear flows on the northern and southern flanks which were erupted from large lava cones situated on the caldera ring fracture and upper flanks of the volcano (Figure 9.3). Some of the lavas on the northern flanks show evidence of having flowed into the former Lake Suguta.

Although the bulk of the Upper Trachyte Lavas post-date the caldera, the oldest were erupted from Enababa either shortly before, or contemporaneously with its formation (Section 9.3.9). The age range of the Upper Trachyte Lavas is 38 ± 3 ka to approximately 100 years, which is broadly the same as that of the Upper Basalt Lavas. Generally, the trachytes pre-date the basalts, and several vents that initially erupted trachyte were the sites of later basaltic activity. However, there are exceptions to this general relationship between the two lava groups; for example, on the north-western flanks the oldest basalts appear to pre-date the oldest trachytes, and on the southern flanks the youngest trachyte post-dates the youngest basalt.

The total volume of Upper Trachyte Lavas is estimated to be approximately 5.5 km^3. All of these lavas are silica-oversaturated and the majority are pantelleritic, although some flows are comenditic.

The trachytes infilling the caldera occur as small domes and steep-sided flows that were erupted along intersecting NNE and ESE-trending fissure zones. Prolonged activity along these zones has resulted in numerous flows becoming stacked upon one another to form ridges, and at the intersection of the two main fissure zones in the centre of the caldera the lavas are piled 60 m higher than the caldera rim. The oldest flows in the caldera are vegetated and on air-photographs appear to have a thin and sporadic 'dusting' of pyroclastic material, whilst the younger flows are pristine. The main locus of activity is an ESE-trending fissure line which cuts across the middle of the caldera and extends for a short distance outside its western and eastern margins. Activity along this zone has built up a broad ESE-trending ridge of trachyte domes and small button-shaped flows, the crest of which is marked by a system of ESE-trending *en échelon* open fissures. Weaver (1977) designated these lavas as 'arc trachytes', believing they were erupted along an arcuate fracture which he speculated to be part of an incipient ring fracture; this supposition is not accepted in the present study. The main NNE-trending fissure line that extends across the volcano has also acted as an

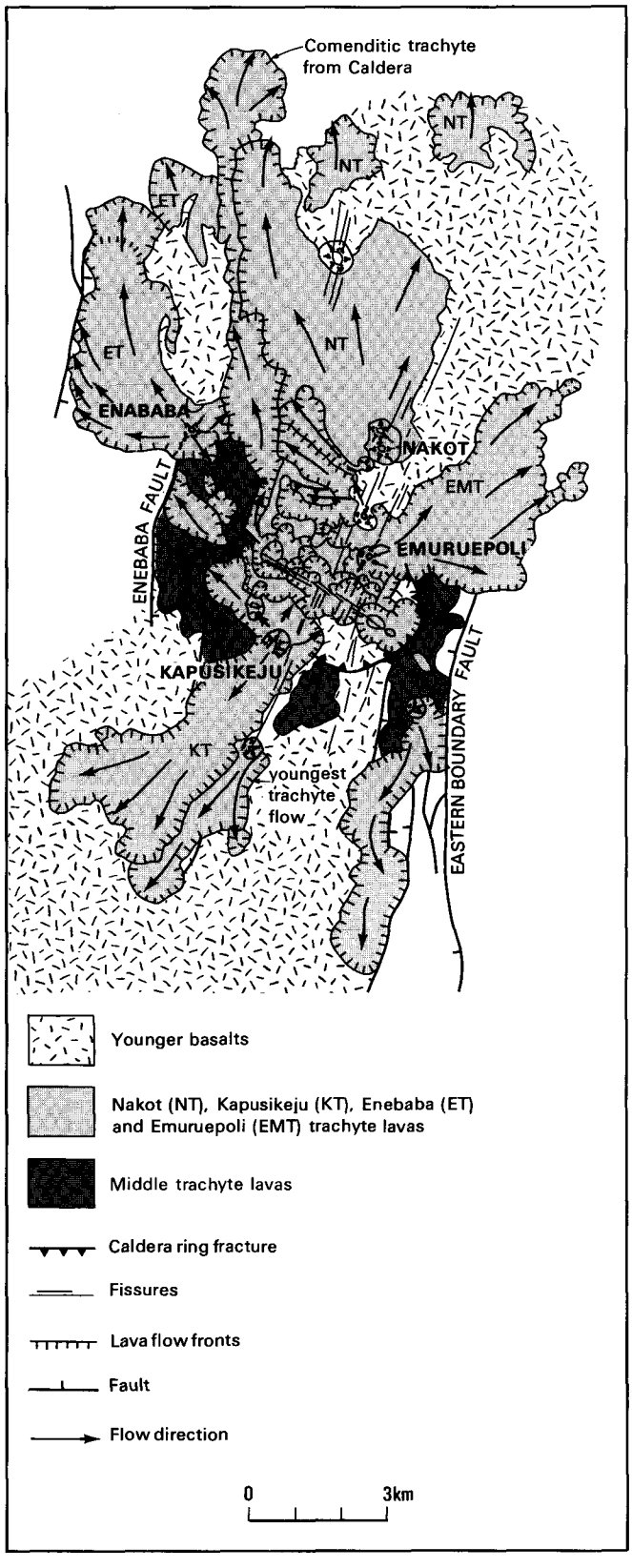

Figure 9.3 Distribution of Middle and Upper Trachyte Lavas.

important feeder zone for trachyte lavas within the eastern half of the caldera. This has given rise to the formation of a ridge of trachyte domes and small discoid flows upon which the summit cone of Emuruepoli (Plate 9.8) has been built. A more poorly defined NNE-trending line of upper trachyte domes is aligned along a weaker fissure system across the centre of the caldera, and a third line of this orientation occurs along the western side.

The Upper Trachyte Lava fields on the flanks were erupted from six lava cones and several minor sources. The cones of Emuruepoli [BM 2054 1665] and Kapusikeju [BM 2032 1647] are located on the caldera ring fracture, and those of Nakot [BM 2055 1690], Enababa [BM 2014 1694] and the two unnamed cones on the southern flanks at [BM 2063 1633] and [BM 2026 1622] are situated upon NNE-trending fissures or faults.

Enababa is a steep-sided lava cone located upon the Enababa fault (Plate 9.2). It rises about 180 m above the surrounding flanks of the volcano and has a narrow cylindrical summit vent. The flows erupted from Enababa extend down the northern flanks for up to six kilometres and form a lava field covering an area of approximately 20 km^2. In the proximal part of the lava field the flows appear to have been fluid and are long, narrow and sinuous with well-developed levees. On the lower flanks these coalesce to form larger and more massive flows with high flow-fronts. A number of flows that were erupted down the western flanks of Enababa abutted and ramped-up against an older N-trending fault scarp in lower trachytes which channelled them northwards. The north-western part of the Enababa lava field is represented by a single large trachyte lava which may have flowed into lake water. This has a double-stepped flow-front more than 100 m high and prominent pressure ridges between which diatomaceous sediments are preserved. The north-eastern lobe of the Enababa field [BM 2005 1745] has a low aspect ratio and an unusual surface pattern formed of large-scale, concentrically arranged lava ropes with chilled carapaces, which are thought to have formed as a result of subaqueous flow over the flat floor of Lake Suguta (Plate 9.3). A younger parasitic basaltic cone occurs high on the northern slopes of Enababa and has erupted basaltic flows which cover the central and eastern part of the trachyte lava field. Ar/Ar dating of a lava at AM 1996 1737 indicates an age of 38 ± 3 ka for the trachytes of Enababa, which coincides with the age of the Upper Pyroclastic Deposits.

Nakot is situated upon the main NNE-trending fissure zone and is the source of the most extensive trachyte lava field. It is a very steep-sided lava cone which rises approximately 180 m above the surrounding flanks of the volcano and has two narrow cylindrical vents at the summit. A large number of blocky trachyte flows were erupted from the cone and flowed radially down the northern flanks of Emuruangogolak for up to 8 km to form a delta-shaped lava field covering an area of more than 50 km^2 with steep terminal flow-fronts 40–50 m in height. Ar/Ar dating indicates an age of 16 ± 5 ka for the trachytes of Nakot.

The summit lava cone of Emuruepoli is located just inside the caldera upon the main NNE-trending fissure zone and is similar in form to Enababa and Nakot. It has two cylindrical summit vents from which steeply dipping rivulet-like trachyte flows have been erupted. A large trachyte dome is juxtaposed against the north-eastern flank of Emuruepoli and is situated upon the caldera ring fracture. This dome is very steep-sided, with slopes of up to 60°, and is highly fissured, brecciated and flow-banded. It is uncertain whether the dome was extruded from the caldera ring fracture or from a breach at the base of Emuruepoli. Numerous blocky trachyte flows were erupted from

Plate 9.2 Aerial view of Enababa trachyte lava cone on the north-west flanks of Emuruangogolak. Note the large number of narrow rivulet-like trachyte lavas that were erupted down its flanks.

Plate 9.3 Aerial view of subaqueously erupted trachyte lavas on the north-western flanks of Emuruangogolak. Field of view is approximately 250 m across.

the sides of the dome and flowed down the north-east flanks of the volcano for up to 5.5 km to cover an area of approximately 12 km^2.

A short distance to the north of Emuruepoli a small trachyte scoria cone is situated upon the intersection of the caldera ring fault and the main NNE-trending fissure zone [BM 2054 1670]. A tongue-shaped, blocky trachyte was erupted from a breach on the north-west side of the cone, and flowed north-westwards out over the caldera rim. Subsequently the cone was the source of basaltic activity, resulting in the deposition of spatter and the eruption of very fluid basalt lavas on top of the trachytes.

The youngest and longest trachyte flow on the northern flanks is comenditic in composition and was erupted from a small vent in the south-west corner of the caldera [BM 2028 1670]. It flowed northwards along the western side of the caldera floor, over the caldera rim, and down the northern slopes as a narrow valley-flow along the contact between the Enababa and Nakot lava fields. At the base of the northern flanks it spread laterally over lake sediments to form a lobate flow-head with a low flow-front terminating more than 11 km from the source. The length of the lava and the low-aspect ratio of the flow-head suggests that it was relatively fluid at the time of eruption. The head of the flow is overlain by diatomites and shows signs of having flowed into water. Numerous protrusions, resembling tubular pillows or large-scale pahoehoe toes extend from the base of the flow-front, and have caused wet-sediment deformation in the underlying diatomites.

The largest upper trachyte lavas on the southern flanks were erupted from the vicinity of Kapusikeju, which is situated on the intersection of the caldera

ring fault with a NNE-trending fissure zone. The oldest exposed trachyte at Kapusikeju was extruded along the ring fault and mainly flowed south-westwards down the flanks of the volcano, although parts also flowed into the caldera and buried the caldera wall. Ar/Ar dating of this flow where it overrides the caldera wall at [BM 2020 1665] indicates an age of 27 ± 5 ka. This early flow is more than 80 m thick in the source area where it forms a platform on which domes and small flows of intra-caldera trachytes were erupted and on which the cone of Kapusikeju was built. Subsequently, an extremely blocky trachyte with prominent levees was erupted from a breach on the south-west side of Kapusikeju and flowed down the southern flanks of the volcano for 6 km to terminate in steep flow-fronts more than 100 m in height.

The youngest trachyte on Emuruangogolak is a comenditic flow that was erupted from a small lava cone situated upon a NNE-trending fissure zone at the base of the main break in slope on the southern flanks [BM 2063 1633]. The source cone is approximately 50 m high and is composed of ropy lava and spatter. The main lava issued from a breach at the base of the cone and flowed south-westwards for 4 km. The proximal part of the flow has a ropy surface with well-developed levees, whereas the more distal part has an extremely blocky surface and terminates in high, steep-sided, flow-fronts. Secular magnetic variation studies suggest that the flow was erupted around the turn of the century (Skinner et al., 1975), and therefore probably represents the youngest volcanic activity in Kenya.

9.3.11 Upper Basaltic Lavas (b^u) and associated pyroclastic deposits

Upper Basaltic Lavas, of basalt and hawaiite composition, cover large parts of the northern and southern flanks of the volcano and partly infill the caldera. They mostly post-date the Upper Trachyte Lavas, although on the southern flanks the youngest trachyte overlies the youngest basalt. The age of the oldest basalts exposed on the low ground around the northern periphery of the volcano is uncertain because contact relationships are nowhere to be seen. However, these older basalts are intercalated with lake sediments and together these form a pedestal-like area peripheral to the volcano, on which trachytes erupted from Enababa and Nakot appear to rest. On the basis of this geomorphological evidence these older basalts are considered to pre-date the Upper Trachyte Lavas.

The earliest basalts on the northern flanks were erupted into the former Lake Suguta. Basalt lavas erupted subaerially from a scoria cone near the summit of Enababa pass down-slope into a thick pile of pillow lavas below an elevation of about 560 m at [BM 2010 1735]. The remnants of two tuff cones occur low on the north-western flanks [AM 1990 1755] and have three wave-cut benches at elevations of between 480 m and 520 m preserved upon their flanks. A spectacular pile of tubular-pillow basalts has been extruded from the lower part of the westernmost of these two cones (Plate 9.4), and very long tubular protrusions extend from the base of the pillow pile onto the surrounding diatomites.

The tuff cone of Losetom is situated on a NNE-trending fissure zone at [BM 2078 1738]. It is approximately 1.5 km in diameter, rises more than 200 m above the surrounding flanks of the volcano, and has a central crater. It was formed by phreatomagmatic activity on a former shoreline of Lake Suguta and has a prominent wave-cut notch around its base at an elevation of 575 m (Plate 9.5). This corresponds to the highest stand of Lake Suguta, which occurred at about 10 ka (Section 9.3.12). The cone is buff coloured and composed of planar-bedded, cross-bedded and massive palagonitised tuffs and fine scoriaceous breccias, which dip radially outwards at angles of 30° or more. Within the summit crater a basaltic 'tide mark' bears evidence to a former lava lake which drained laterally as small flows through breaches in the northern and southern flanks of the cone.

A line of tuff cones occurs upon the main NNE-trending fissure zone on the north-eastern flanks. The best preserved of these is an unnamed cone situated 2.5 km to the east of Losetom at [BM 2104 1736]. This

Plate 9.4 Pile of basalt pillow lavas north-west periphery of Emuruangogolak.

Plate 9.5 Aerial view of Losetom tuff cone, northern flanks of Emuruangogolak. The cone rises more than 200 m above the surrounding ground and has a prominent wave-cut notch around its base, which formed during the highest stand of the former Lake Suguta.

is breached on its eastern side and has a wave-cut notch around its base at an elevation of about 575 m. A small pit crater occurs within the main crater of the cone and is surrounded by ramparts of agglutinated spatter. Fire-fountaining from this pit crater produced a lava which flowed out through the breach on the side of the cone to form a small, steep-fronted delta of basalt pillows below the level of the wave-cut notch. The remnants of another tuff cone occur upon the main fissure zone approximately 1.5 km further down the flanks of the volcano at [BM 2108 1750]. The top of this has been planed-off by erosion during a regression or transgression of Lake Suguta. Three wave-cut benches are preserved upon the remnants of the cone at elevations of between 520 m and 560 m, and these have been faulted and displaced by subsequent movement along the fissure zone.

To the north-east of Emuruangogolak the main fissure zone passes on to the floor of the inner trough in the Kangirinyang area [BM 2150 1900]. Here it is manifested by a NNE-trending ridge of intensely faulted lake sediments and lavas upon which numerous tuff rings and maars are developed (Plate 9.6 and Frontispiece). Most of the tuff rings and maars are situated directly upon faults, some of which have undergone post-eruptive movement. The morphology and bedforms of these craters are consistent with subaerial phreatic and phreatomagmatic activity, caused when magma moving along the fissure-fault system came into contact with groundwater or wet sediment. The two best preserved maars occur at the northern end of the zone at [BM 2155 1924] and [BM 2150 1897] and have steep-sided craters occupied by saline lakes. Low-angle ramparts occur around the craters and are com-

Plate 9.6 Aerial view of maars and tuff rings aligned along faults in the Kangirinyang area, north-east of Emuruangogolak. The features are composed of a mixture of basaltic tephra and lake sediment.

posed of crudely stratified and cross-stratified units containing varying amounts of sediment and juvenile basaltic material. Tephra composed of sediment includes bombs, blocks and lapilli of marl and diatomite, and generally occurs in greater proportion than juvenile basaltic material. Some beds are composed almost entirely of sedimentary material, and others are composed mainly of basaltic tephra, although the majority of beds are composed of mixtures of the two. Basaltic ejecta include cauliflower bombs and composite bombs formed of concentric layers of basalt nucleated on cores of sediment. Another maar occurring at the southern end of the fault zone at [BM 2132 1853] has a deep cylindrical crater with near vertical sides and is surrounded by a low-angle cone composed almost entirely of cobbles and pebbles derived from underlying fluvial sediments.

The young subaerial basalts of Emuruangogolak cover large areas of the northern and southern flanks. They were very fluid and were erupted from fissures which are associated with spatter ramparts indicative of fire-fountaining. Young basalts were also erupted from scoria cones and fissures located upon the rift boundary faults along the edge of the Emuruagiring Plateau. These cascaded down the escarpment of the plateau onto the floor of the inner trough (Plate 9.7).

The youngest basalt lava field on the northern flanks covers an area of more than 70 km^2. It was erupted from several sites on the upper flanks, although the primary source appears to have been at the intersection of the main NNE-trending fissure zone with the caldera ring fracture at [BM 2055 1675]. These young basaltic lavas flowed down the northern flanks, passing around and over the older tuff cones and pillow lavas, before coming to rest on the floor of the rift more than 18 km from source. They have pristine morphology and according to the magnetic variation studies of Skinner et al. (1975) were probably erupted between 900 and 700 years ago.

Fluid basalts were erupted from the main fissure zone in the caldera and became ponded on the floor in the east and south. Lavas were also erupted on the southern rim of the caldera where it is cut by the fissure zone. Some of this lava flowed down the southern flanks, and some cascaded down the wall of the caldera and became ponded at its base. In the northern half of the caldera, basalts occur as long, narrow, valley-flows between the steep-sided trachyte domes. Basalt 'tide marks' occur well above the floors of the narrowest valleys, indicating that at the time of eruption the valleys were almost full, suggesting high rates of eruption of fluid magma. In places vertical tree moulds are found within these basalts.

Extensive basalt lava fields cover the southern flanks of the volcano. A small flow was erupted by fire fountaining from the southern end of a fissure at [BM 2030 1635] and has yielded a ^{14}C date of 250 ± 100 years (Shotton et al., 1974). This is post-dated by the youngest Upper Trachyte Lava which was erupted from the same fissure immediately downslope. At the foot of the southern flanks there is a large scoria cone [BM 2009 1566] surrounded by an extensive basalt lava field. Ash from this cone is found upon the surrounding basalts and the Upper Trachyte Lavas, except for the youngest trachyte flow. All of the basalts on the southern flanks were erupted subaerially, although on the flat ground to the south and south-west of the volcano, in the Loreng area, some show evidence of having flowed onto wet alluvial sediment or possibly into shallow water. Here the surfaces of these lavas are covered by numerous irregularly distributed hornitos, dribblet spires, and shallow crater-like depressions, many of which are occupied by small lakes, as for example around [AM 1960 1530] and [AM 1985 1550]. These lavas were clearly very fluid and the rootless vents on the surface are believed to have formed as a result of mild phreatomagmatic activity caused by steam generated from the wet substrate beneath the flows.

9.3.12 Lacustrine sediments and stand lines of Lake Suguta

Lacustrine sediments of the former Lake Suguta underlie most of the floor of the inner trough to the

Plate 9.7 Aerial view looking south along the faulted margin of the Emuruagiring Plateau with the eastern flanks of Emuruangogolak on the right. Note the young basalt lavas in the foreground that have been erupted along the rift boundary faults.

earliest Upper Trachyte Lavas from Enababa. Eruption of the Upper Pyroclastic Deposits at approximately the same time is likely to have been a contributory triggering mechanism for caldera formation.

Voluminous eruption of the Upper Basalt Lavas occurred at a late stage in the history of Emuruangogolak. The majority of the basalts post-date the Upper Trachyte Lavas, although there was some overlap in activity between the two lava groups. The oldest basalts may pre-date the upper trachytes of Enababa, whilst the youngest basalt, with an age of 250 ± 100 years, is post-dated by the youngest trachyte. The earliest basalts on the northern flanks were erupted into Lake Suguta, resulting in the formation of pillow lavas. Phreatomagmatic activity also took place on shorelines at various times, giving rise to the formation of tuff cones. The younger basalts form very extensive lava fields on the northern and southern flanks and partly infill the caldera. These were highly fluid and were erupted subaerially from NNE-trending fissures.

9.5 GEOTHERMAL ACTIVITY ON EMURUANGOGOLAK AND NEARBY AREAS

9.5.1 Introduction

Surface geothermal manifestations on Emuruangogolak are almost exclusively confined to the summit caldera. The only known exception to this is an ephemeral fumarole situated a short distance to the south of the caldera rim. Hot springs occur to the north of the volcano within several of the basaltic maars in the Kangirinyang area, and there are warm springs at Nangarabat. Hot springs also occur to the north-west of Emuruangogolak in the valley of the Kamuge River, where they are located upon a major fault bounding the western margin of the inner trough.

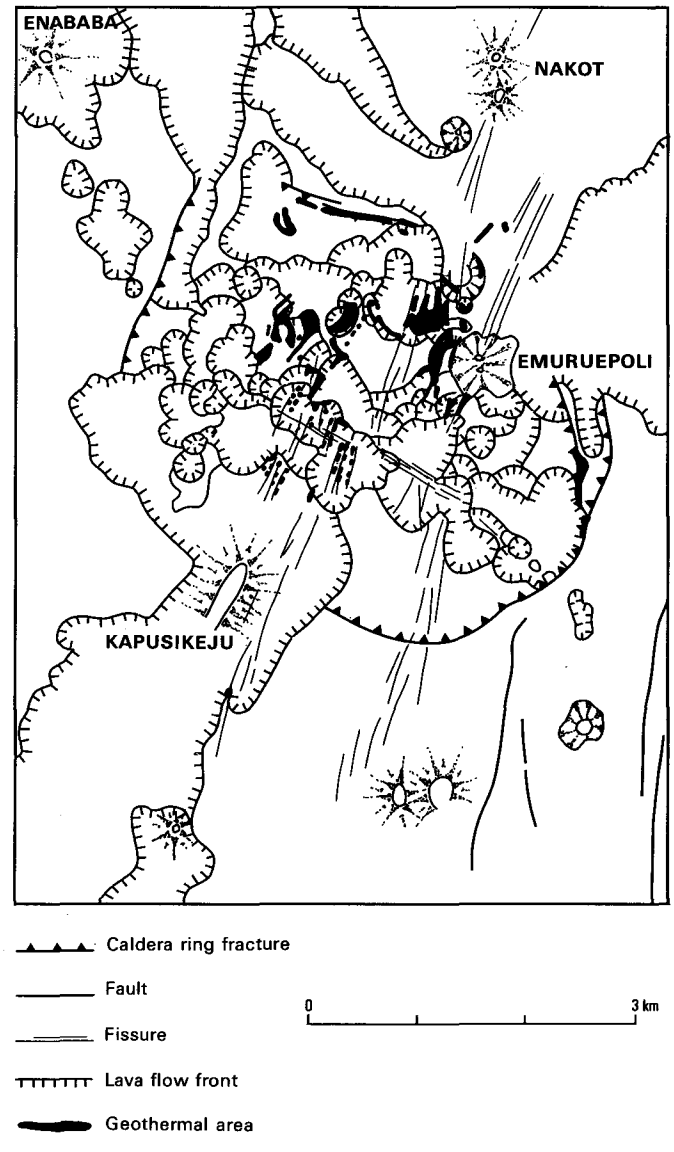

Figure 9.4 Distribution of surface geothermal activity on Emuruangogolak.

9.5.2 Caldera of Emuruangogolak

Fumaroles and hot, steaming, hydrothermally altered ground cover an area of approximately 8 km^2 within the caldera. The main areas of activity occur in the central and north-eastern parts of the caldera and are controlled by NNE-trending fissures, although the highest temperatures and most intense alteration are found in a relatively small area located upon the ring-fracture on the eastern side of the caldera. Several small patches of steaming and hot ground, with relatively low temperatures, also occur close to the northern margin of the caldera. For the purpose of description the activity within the caldera is subdivided into the following areas.

9.5.2.1 Eastern rim of caldera

Steaming and altered ground with numerous fumaroles occurs in two patches on the ring fracture on the eastern side of the caldera at the point where it bifurcates.

The larger of the two patches occurs a short distance to the north of the bifurcation at [BM 2064 1657]. It covers the steep slopes of the caldera wall from top to bottom and extends for a short distance onto the adjacent caldera floor. The entire slope is steaming and has numerous small to moderate sized fumaroles which issue under pressure and emit a quiet hissing sound. Ground and steam temperatures are mostly above 80°C and range up to a maximum recorded value of 96.0°C, which is approximately the local boiling point and the highest temperature recorded on Emurangogolak. The trachytes of the caldera wall are intensely altered to red, purple and white clays with thin surface encrustations of carbonate and sulphates. Silica veins occur within the altered trachytes, and on top of the caldera rim a small area is covered by silica sinter. These sinters have a laminated fabric and are interpreted as fossil hot spring deposits. U-series dating yielded an isochron age of 29±4 ka for these sinters (Sturchio et al., 1993). This corresponds with a climatically wet period when the lakes in the rift where at high levels (Casanova, 1986), and when water tables would have been correspondingly high.

The smaller area of activity occurs at the point where the caldera ring-fracture bifurcates [BM 2063 1650]. It is characterised by reddened and altered ground with weak steam seepages at the base of the caldera wall. Recorded temperatures are relatively low, being in the range 42.2°C to 51.5°C.

north and north-west of Emuruangogolak. They also occur as isolated patches on the northern flanks of the volcano and in the re-entrant that extends southwards between the north-eastern flanks and the Emuruagiring Plateau. The highest lacustrine sediments in these areas occur at elevations of approximately 575 m, which corresponds to the highest lake stand lines preserved around the Suguta Valley.

Six stand lines of different elevations ranging from 480 m up to 575 m are recognisable on the various tuff cones on the northern flanks of Emuruangogolak. The highest preserved stand has been dated on Namarunu at 9660 ± 210 years (Truckle, 1976) which corresponds to a climatically wet period when East African lakes reached their highest levels (Hillaire-Marcel, 1986). This is also corroborated by ^{14}C ages of 11–9 ka obtained on shell material from sediments on the northern flanks of Emuruangogolak (Bishop, personal communication in Weaver, 1977).

Truckle (1976 and 1977a) described the lake sediments of the area between Emuruangogolak and Namarunu, and collectively referred to them as the Suguta Beds. One of the best sections exposed in the sediments occurs in the prominent cliff line that runs along the eastern bank of the Suguta River near its confluence with the Kamuge River [AM 1987 1819]. Here approximately 20 m of horizontally bedded diatomites are capped by a massive basalt lava. The basal part of the section consists of 7 m of white diatomite paper shales with a thin sandy band containing calcareous nodules near the base. These are overlain by 6–7 m of finely bedded white-buff diatomites with calcareous nodules, which are overlain by a similar thickness of buff coloured silty diatomites. At the top of the section 1–2 m of reddened grits overlie the diatomites and are capped by basalt. Fish remains are found throughout the diatomites of the Kamuge-Suguta confluence area and Truckle reports the occurrence of crocodile teeth. A short distance to the south-west, near the waterfall on the Suguta River [AM 1973 1772], the massive basalt capping the section overlies about 25 m of poorly stratified and cross-stratified sands and pebbly sands with thin beds and lenses of gravel, which are cross-cut by large channels infilled with coarse conglomerates. The rapid lateral facies variations, cross-bedding, and cross-cutting channel deposits suggest a fluvial origin for these sediments. Truckle describes similar coarse clastic sediments with intercalations of diatomite (his member B) in the ground extending north-westwards to the Kamuge River. It is concluded here, that at this stage in its development Lake Suguta was extensive but relatively shallow, and that in the Kamuge area alluvial fans and deltas carried coarse clastic detritus into the lacustrine diatomites.

The age range of the lake sediments is unknown. However, the highest lake stand occurred at about 10 ka, and the trachytes of Enababa, which flowed into water, indicate a minimum age of 38 ka for underlying diatomites found around the north-west periphery of the volcano.

9.4 SUMMARY OF EVOLUTION AND STRUCTURE

Emuruangogolak is a large volcanic shield with a summit caldera. It is composed of oversaturated peralkaline trachyte lavas and pyroclastic rocks, and mildly undersaturated basalts, in which the proportion of trachyte to basalt is approximately 10:1. Two broad phases of activity are recognised in the evolution of the volcano. These occurred during the approximate periods extending from before 900 ka to 500 ka, and from 205 ka to the present, and were separated by a period of apparent inactivity.

Eruption of the Lower Trachyte Lavas during the period >900–500 ka constructed an early shield of similar extent and height to the present day volcano. This early shield subsequently underwent a period of N–S faulting which resulted in the formation of a number of prominent fault scarps and a broad axial graben across the summit region. The axial graben, defined by the Enababa fault in the west and the Eastern boundary fault in the east, influenced the distribution of younger lavas erupted from the upper parts of the volcano, tending to channel them to the north and south.

Following what appears to have been a long period of quiescence, the Lower Pyroclastic Deposits of trachytic composition were erupted around 205 ka. These deposits were erupted by plinian-style activity from a series of pumice cones located upon N- to NNE-trending fractures on the upper western flanks. The easterly prevailing wind carried the tephra westwards to form a thick apron of well-stratified pumice deposits which drapes the pre-existing faulted topography of the early trachyte shield.

Very fluid Lower Basaltic Lavas, with an age of 185 ± 11 ka, were next erupted from fissures high on the western flanks in the vicinity of the Enababa fault. These lavas form a uniformly thin but extensive capping to the Lower Pyroclastic Deposits.

Renewed trachytic activity resulted in the eruption of the Middle Trachyte Lavas from a number of sources on the summit area and uppermost flanks. These lavas flowed radially away from the summit and were confined by the axial graben. The Upper Pyroclastic Deposits rest upon the Middle Trachytes and form a thin discontinuous covering of trachytic pumice on the uppermost flanks. These deposits have an age of 38 ± 6 ka and were erupted from pyroclastic cones on the summit region. Following eruption of the Upper Pyroclastic Deposits, the summit area collapsed to form a caldera. However, the volume of the pyroclastic deposits is too small to have caused this collapse alone.

The Upper Trachyte Lavas were erupted during the period from 38 ± 3 ka to the present day, and form extensive lava fields on the northern and southern flanks. They were erupted from prominent lava cones on the upper flanks and summit area. All of these cones occur upon NNE-trending fissures or faults, and several are located where these intersect the caldera ring fracture. Some of the trachytes on the northern flanks show evidence of having flowed into the former Lake Suguta. Resurgent activity also took place along NNE-trending and NW-trending fissure zones within the caldera, resulting in the eruption of trachyte domes and small steep-sided flows. Whilst the bulk of the Upper Trachyte Lavas clearly post-date the caldera, those erupted from Enababa, dated at 38 ± 3 ka, were contemporaneous with, or pre-dated its formation. It is concluded that the caldera formed as a result of summit collapse in response to the flank eruption of the

9.5.2.2 North-eastern-central area of the caldera

The main area of activity in the caldera is situated slightly to the north-east of centre. Steaming ground with a large number of fumaroles occurs immediately to the west of the summit cone of Emuruepoli and is confined to a 2 km long N-trending zone, in places reaching over 300 m in width, characterised by bare rock and areas of red clay vegetated by *Abligaardia lispidula*. Activity is virtually continuous along the southern 1.5 km of the zone and is intermittent in the north. This is visually the most impressive area of fumaroles in Kenya, and can be seen in cool weather from a considerable distance (Plate 9.8). The manifestations are located upon small domes and steep-sided trachyte lavas which are cut by NNE-trending fissures. Manifestations are primarily controlled by the fissures, although the lavas are extensively fractured and steaming ground and fumaroles are distributed on the crests and sides of the domes. The fumaroles are relatively strong and issue under some pressure accompanied by a quiet hissing sound. Ground and steam temperatures mostly range between 60°C and 90°C, tending to be highest in the south of the zone where a maximum value of 90.7°C was recorded. These temperatures are relatively low considering the vigorous nature of the steam emissions over such a large area. However, the strongly fractured and steep-sided form of the trachyte domes promotes the ingestion of air which causes cooling. This has been confirmed by field-based analytical methods, which indicate that oxygen is present in atmospheric proportions even within the hottest fumaroles.

9.5.2.3 Western-central part of the caldera

Geothermal manifestations are extensively developed in the central and western-central part of the caldera, and are spatially separate from the north-eastern zone described above.

The primary structural control on this activity is a set of NNE-trending fissures. Surface manifestations are dispersed about these fissures, on the margins and crests of fractured trachyte flows, and are characterised by altered, steaming ground which is sparsely vegetated by *Abligaardia lispidula*. Temperatures range from around 40°C to over 90.0°C. The most intensive activity occurs on the western side of the zone around [BM 2036 1667] and is coincident with the highest temperatures, which commonly exceed 90°C and reach a recorded maximum of 94.0°C. In the hotter areas the fumaroles are moderately vigorous and the ground is intensely altered to red, purple and white clays with thin surface encrustations of carbonate and sulphates. Analysis indicates that the fumaroles in this area are strongly contaminated with air, which presumably has a cooling effect.

Numerous fumaroles occur along the NNE-trending fissure zone where it cuts the youngest trachyte lava flows in the central part of the caldera around [BM 2037 1657]. These fumaroles are sporadically developed and issue silently from large crevices in the lavas. They are strongly contaminated with air, resulting in relatively low temperatures that are generally in the range 40°C to 70°C. The young trachyte lavas have extremely rough, unvegetated surfaces. They show no signs of hydrothermal alteration, so that the thermal activity can only be recognised by the presence of steam plumes, which are only apparent in the early morning after prolonged rain.

9.5.2.4 Northern part of the caldera

Small patches of geothermal activity occur on the ring fracture along the northern rim of the caldera. The ring fracture is represented by two E–W trending fault scarps which are exposed over a length of about 1 km [BM 2042 1679]. Hot ground and weak steam seepages occur on the degraded inward facing scarps and crests of these faults and recorded temperatures range up to 73.3°C. A short distance to the south of the ring fracture two small areas of hot ground occur on the flow-fronts of trachyte lavas on the floor of the caldera. Both areas have many fumaroles, several of which are relatively vigorous. Recorded temperatures reach up to 81.2°C on the westernmost of these two patches [BM 2035 1677] and up to 62.5°C on the eastern patch.

Plate 9.8 The summit trachyte lava cone of Emuruempoli on the northern side of Emuruangogolak caldera, looking north-east. The main zone of fumarolic activity is located upon north-east trending fissures and can be seen in front of the cone.

Plate 9.9 Area of hot steaming ground in Emuruangogolak caldera. The activity occurs on the sides of trachyte lava domes and is vegetated by the sedge Abligaardia lispidula which gives a distinctive brown colour.

9.5.3 Ephemeral fumarole on the upper southern flanks

The only geothermal manifestation discovered outside the confines of the caldera is an ephemeral steam plume situated approximately 1.5 km south of the caldera rim at [BM 2029 1631]. This was observed during a low-level reconnaissance helicopter flight, undertaken early in the morning after a period of prolonged and very heavy rainfall. The steam emanated from a deep NNE-trending fissure, which was the source of the youngest basalt flow on the volcano. On visiting the site during dry weather several days later no steam nor elevated temperatures were detected, although delicate acicular crystals of sulphur were observed on the edge of the fissure a short distance to the north. These crystals showed no sign of weathering to sulphates, and this together with their delicate and well-formed nature suggests that they could only have been deposited shortly before the visit. This is the only locality on Emuruangogolak where sulphur has been observed.

9.5.4 Basaltic maars in the Kangirinyang area

A salt lake occurs in the crater of the largest basaltic maar on the main NNE-trending fissure zone in the Kangirinyang area at [BM 2140 1897] (see Frontispiece). The lake is approximately 200 m in length from east to west and 100 m wide from north to south. It is blue-green in colour, although around its southern margin there are several highly alkaline shallow pools with surface encrustations of trona, that are deep red due to the presence of algae. Slightly above the lake on its southern margin, several water-holes have been dug to depths of 1.5–2 m to exploit a perched aquifer of clear fresh water. Recorded water temperatures in the lake are around 27°C, whereas the fresh water in the water-holes has recorded temperatures of 23.9°C to 26.6°C. Elevated temperatures of between 30°C and 56°C are found in the mud underlying reeds that fringe the lake, and many hot springs issue from just below the water-line around the northern and western shores. The water of these springs is fresh. The springs and seepages on the west side of the lake are weak and have temperatures between 43.1°C and 55.9°C, whereas those on the northern side have greater flow-rates and are much hotter, with temperatures ranging between 63.8°C and 69.2°C.

The northernmost basaltic maar on the fissure zone at Kangirinyang, situated at [BM 2155 1923], is occupied by a small, highly saline lake. The lake is deep red in colour due to the presence of algae, and it has extensive but thin surface encrustations of carbonate, and a slight sulphurous smell pervades the air. An analysis of the surface encrustation indicates that it is composed of burkeite ($Na_6CO_3(SO_4)_2$) and halite (Kemp, 1990). Blocks of coarsely crystalline rock salt also occur in scree at the base of the north-west wall of the crater, but no source outcrop is evident. Temperatures of the lake water range between 30.6°C and 35.5°C, and those recorded in mud around the edge of the lake range from 31.1°C up to 51.3°C, with the highest temperatures occurring on the west side. Slightly up-slope from the lake, but still on the crater floor, a water-hole has been dug to a depth of about 3 m to exploit a perched aquifer. The water in the hole is fresh and has a recorded temperature of 26.1°C. Elevated temperatures ranging between 35.1°C and 42.9°C, were also recorded from the tephra in the eastern wall of the maar. Some caution should be exercised in the interpretation of the elevated temperatures in this maar because air temperatures in the afternoon usually exceed 45°C and surface ground temperatures are considerably higher due to incident sunlight. However, the ground and water temperatures quoted above were recorded in the early morning before the maar was in direct sunlight, and therefore at least some of the elevated temperatures are likely to result from geothermal activity.

A third maar occurs several kilometres to the south at [BM 2143 1866]. Within this maar there is a deep crater lake with an intense green colour. The water is cold (24.4°C) and slightly alkaline with a pH of 8.5. A small water-hole is situated slightly above the lake with-

in the steep sides of the crater and this has fresh water with a pH of 6.5.

9.5.5 Suguta River hot springs

Hot springs occur on the western bank of the Suguta River, a short distance downstream from the main waterfall on the periphery of the north-western flanks of Emuruangogolak at [AM 1974 1776]. At least 15 springs occur in three small clusters along a half kilometre stretch of the river bank. They are aligned in a NW direction and issue from lacustrine and alluvial sediments close to a contact with basalt and trachyte lavas. Flow rates are high and each cluster of springs feeds a small stream that flows into the river. Recorded temperatures range from 40.2°C to 69.7°C and the water is neutral to slightly alkaline. Each set of springs is surrounded by carbonate precipitates and dark green algal growths.

9.5.6 Nangarabat springs

Two warm springs and two seepages were discovered around the southern margin of the large whale-back outcrop of basalts in the floor of the Suguta Valley at Nangarabat. These occur at the contact between the basalts and surrounding alluvial sediments [BM 2087 1868] and are close to a prominent N-trending fault within the basalts. The springs were discovered after several weeks of very wet weather, but during a later visit following a month of drought they were found to be dry. At the time of their discovery the two springs issued fresh water, had low flow rates, and temperatures of 32.2°C and 38.1°C respectively.

A short distance to the south of Nangarabat a series of springs issue from beneath basaltic lavas around the northern periphery of Emuruangogolak at [BM 2080 1850]. These were visited after a prolonged period of rainfall, when flow rates were high and the waters were mildly alkaline and cold. A series of alkaline pools with surface encrustations of trona are associated with these springs.

9.5.7 Amuge hot springs

A set of hot springs occurs at Amuge [AM 1955 1862], which is situated at the entrance to the gorge on the Kamuge River approximately 7 km upstream from its confluence with the Suguta. The springs occur on the south side of the river and are located upon a major NNE-trending boundary fault along the western side of the inner trough. The springs are fresh, have high flow-rates, and feed a small stream that issues into the Kamuge River. Temperatures are consistently above 40°C and reach a maximum recorded value of 50.4°C.

Low-level aerial reconnaissance was undertaken along the fault-line extending to the south-west of the Amuge springs. Numerous small clusters of doum palms occur at the base of the fault scarp, suggesting the presence of water at a shallow depth, but no surface springs were observed.

10 The geology and geothermal activity of Namarunu and adjacent areas

10.1 INTRODUCTION

Namarunu is a basalt-trachyte volcanic complex situated on the western side of the inner trough of the Rift Valley between latitudes 1°50'N and 2°05'N.

The inner trough at this latitude is bounded on the west by the Loriu Plateau and on the east by the Tirr Tirr Plateau. Namarunu is a hilly area which abuts the Loriu Plateau in the west and juts out into the inner trough (Figure 10.1).

The floor of the inner trough is approximately 20 km wide to the north and south of Namarunu, but narrows to 2 km in an area known as the Gap, situated between the eastern flanks of Namarunu and the escarpment of the Tirr Tirr Plateau. In this area the floor of the trough has an elevation of approximately 300 m and has a slight northward gradient. The axial part of the trough is occupied by the flood plain of the Suguta River, on either side of which alluvial fans, covered by coarse gravels, slope gently up to the feet of the bounding escarpments. After flowing through the Gap, the Suguta River branches into a complex system of distributaries where the water either evaporates, infiltrates the sandy floor of the trough, or eventually reaches the small alkaline lakes of Lake Alablab. Extensive sand dune fields occur on the floor of the valley to the south of Namarunu.

The Tirr Tirr Plateau is highest in the south-east, where it reaches an altitude of 1264 m. From this point the plateau slopes gently north-westwards to an elevation of between 700 and 800 m along its western edge, where it is bounded by a major escarpment between 400 and 500 m high, which overlooks the inner trough. This escarpment is characterised by a continuous zone of complex and large-scale landslips along which large portions of the plateau have slipped into the inner trough. In the north, the surface of the plateau slopes down to an elevation of about 400 m where it is bounded by a large re-entrant in the rift margin at Losergoi. The eastern edge of the Tirr Tirr Plateau is bounded by a smaller, easterly-facing escarpment which separates it from the Muruakirim Plateau to the north-east, and from the Samburu and Napung Hills to the south-east.

The surface of the Loriu Plateau dips gently westwards. In the vicinity of Namarunu it has an altitude of between 600 and 800 m, although locally exceeds 900 m, and is bounded by an easterly-facing escarpment which marks the edge of the inner trough. To the north of Namarunu the escarpment is between 400 and 500 m high. Passing southwards the feature is less prominent, consisting of several small, parallel escarpments which step down to the western flanks of Namarunu. To the south-west of Namarunu the faults along the plateau margin bifurcate, resulting in the separate fault-bounded, westerly-tilted massif of Nakitoekirion, which is juxtaposed between the south-western flanks of Namarunu and the main escarpment of the Loriu Plateau.

Namarunu reaches an elevation of 817 m on its summit, which is approximately 520 m above the surrounding floor of the inner trough. The northern, southern and western flanks have long, relatively gentle slopes covered by basaltic lava fields. On the western side there is a broad saddle-like region formed where the western flanks abut against the easterly-facing escarpment of the Loriu Plateau. The summit region of Namarunu is composed of faulted and dissected trachytic volcanic rocks and is bounded on the east by strongly faulted flanks which step steeply down to the floor of the inner trough. Along the base of the eastern flanks there is a NNE-trending line of young basaltic scoria cones, tuff cones and tuff rings, from which young lava flows have been erupted onto the floor of the Suguta Valley.

Previous researchers assumed Namarunu to be a Quaternary volcano (Truckle, 1977; Key, 1987) by virtue of its position within the inner trough. However, the work of the present survey indicates that this is not the case, and has shown that the edifice is mainly composed of a downfaulted Pliocene volcanic sequence, similar to that of the adjacent rift margins, upon which later Quaternary volcanic activity has been superimposed. An appraisal of the geology of Namarunu must therefore be taken in context with that of the rift margins, as adopted in the following pages.

10.2 GEOLOGY OF THE EASTERN MARGIN OF THE RIFT ADJACENT TO NAMARUNU

The Tirr Tirr Plateau is composed of Pliocene basalt and trachyte lavas of the Tirr Tirr Series, which unconformably overlie Miocene basalts and sediments of the Kamolingaran basalts, which in turn rest upon Precambrian gneisses. Young deltaic-lacustrine sediments overlie the Tirr Tirr Series in the re-entrant around Losergoi.

10.2.1 Kamolingaran basalts (KB)

The term Kamolingaran basalt is used in this report for a sequence of Middle to Upper Miocene basaltic lavas with intercalated tuffs and volcaniclastic fluvio-lacustrine deposits, which outcrops to the east and south-east of the Tirr Tirr Plateau.

Baker (1963) mapped porphyritic olivine and augite basalts around the southern and eastern margins of the Tirr Tirr Plateau, and a short distance to the south mapped lake beds containing volcanic intercalations.

In the early 1980's the geology of the Samburu Hills was re-examined by a joint team of researchers from Japan and the National Museum of Kenya, primarily with an interest in fossil hominoid sites (Makinouchi et al. 1984; Pickford et al., 1984). The lacustrine sediments mapped by Baker were renamed the Namurugule Formation, and the porphyritic basalts were subdivided into the Aka Aiteputh, Kongia and Nagubarat formations. In aggregate these four formations have a total thickness of 710 m. Basalts from the

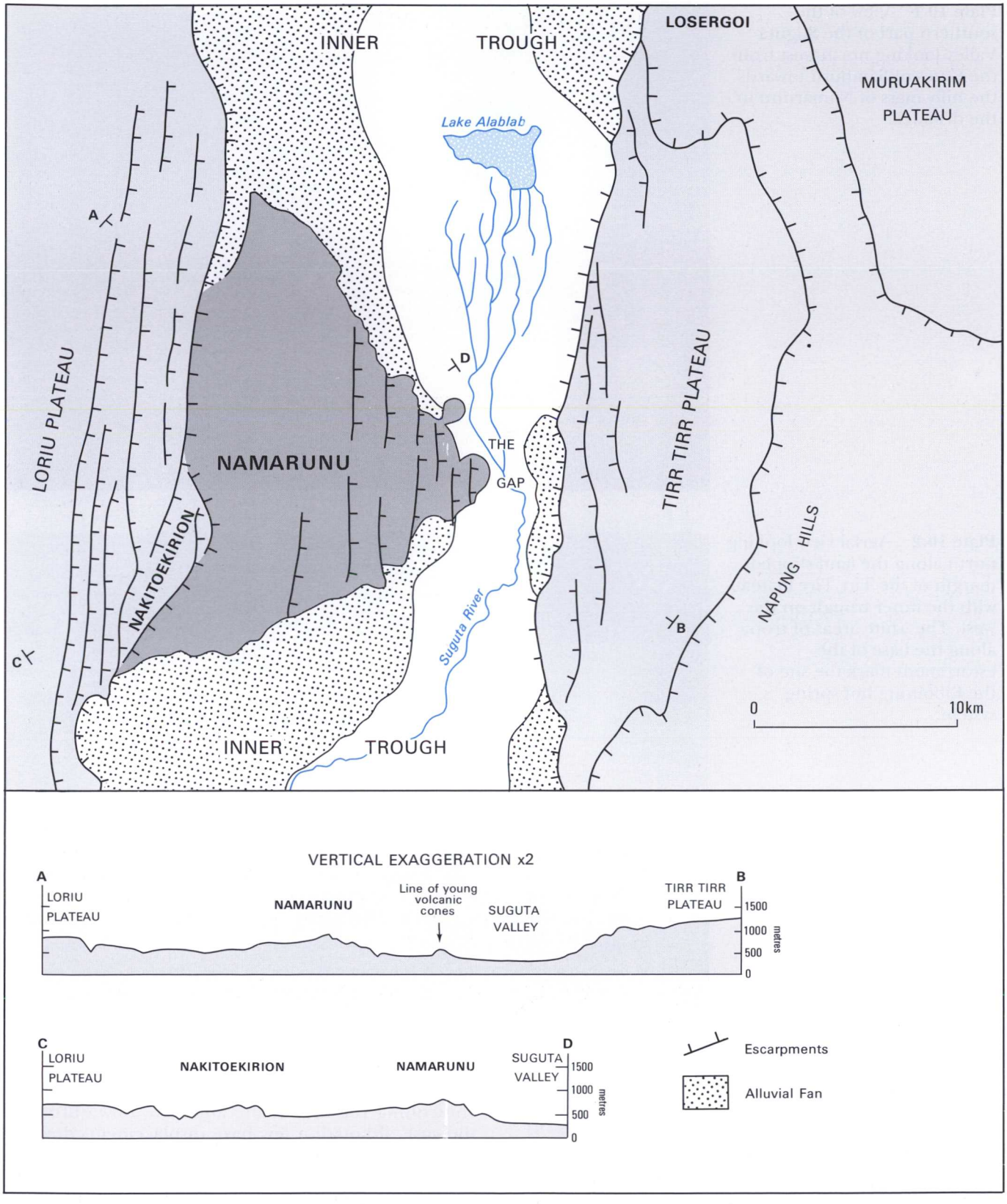

Figure 10.1 Simplified map of the main physiographic elements of the rift in the vicinity of Namarunu.

Aka Aiteputh Formation have yielded K/Ar dates of between 14.9 ± 0.5 Ma and 9.76 ± 0.52 Ma, and those from the Kongia Formation have given dates of between 7.19 ± 0.52 Ma and 4.53 ± 0.35 Ma (Tatsumi and Kimura, 1991). Although a number of sections were examined, the individual formations were not mapped by the Japanese team. However, as a broad group the basalts and sediments of these formations can be traced south-westwards into the Kamolingaran basalts of Truckle (1979a, b), and following the practice of Key (1987) this name has been retained in the present survey.

Plate 10.1 View of the southern part of the Suguta Valley looking north-west from the Gates of Samburu towards the hilly mass of Namarunu in the distance.

Plate 10.2 Aerial view looking north along the land-slipped margin of the Tirr Tirr Plateau with the inner trough on the west. The white areas of trona along the base of the escarpment mark the site of the Elboitong hot spring system.

10.2.2 Tirr Tirr Series (TT)

Baker (1963) originally used the term Tirr Tirr Series for trachytic and basaltic lavas which make up the Tirr Tirr Plateau and Muruakirim Plateau, and which lie unconformably upon older (Kamolingaran) basalts and Precambrian gneisses.

The surface of the Tirr Tirr Plateau approximates to a dipslope which is fractured by NNE- and NNW-trending faults and tensional fractures. The lavas are horizontal to very gently dipping on the highest parts of the plateau in the south-east, but dips gradually increase towards the north-west and west, reaching values of about 30° close to the zone of landslipping along the western edge of the plateau (Plate 10.2). Broadly, the western part of the plateau has a monoclinal structure, of which the steep western limb has been largely removed by major landslips into the inner trough. Most faults close to the western margin of the plateau are antithetic to the deeper seated structure controlling the monocline and have downthrows to the east, although a few have displacements down to the west. On the central and western-central part of the plateau some faults have sectors that show little or no displacement, and are in effect large open tensional fractures along the line of monoclinal flexuring.

Baker (1963) believed that most of the lavas are trachytic and that basalts are subordinate, whilst Makinouchi et al. (1984) reported that the surface of the plateau is capped by an alkali rhyolite in the south-east, but thought that elsewhere it may be underlain by basalts. In the present survey large tracts of the plateau were reconnoitred by helicopter and several sections were examined. From these investigations it is concluded that the series is predominantly basaltic with relatively minor amounts of trachyte.

The series is best exposed in the escarpment overlooking the Suguta Valley where it consists predominantly of a well-layered sequence of basaltic lavas approximately 300 m thick. A section through the succession near Elboitong [BN 2255 2218–BN 2263 2218] exposes 70 m of thinly layered basalt lavas, which are overlain by a prominent, columnar jointed, feldsparphyric trachyte lava, approximately 30 m thick. This trachyte can be traced southwards within the face of the escarpment for a few kilometres before being lost in landslides, and northwards it appears to thin and die out within a few kilometres. Above the trachyte there are 120–140 m of poorly-exposed, horizontally layered basalts with autobreccias, and at the top of the escarpment these are capped by a more resistant unit, consisting of approximately 30 m of thinly layered basalts.

Further north, in the area between [BN 2290 2330] and Losergoi, thin intercalations of poorly-consolidated sands, conglomerates, volcaniclastic sediments and hyaloclastites are interbedded within the basaltic lavas exposed in the Tirr Tirr escarpment. In this area the succession is intruded by NW-trending trachyte dykes. To the north and south the sediment intercalations die out rapidly.

Most of the lavas of the series are fine grained and sparsely microporphyritic or aphyric, although coarsely porphyritic varieties also occur. Compositionally they are slightly nepheline-normative transitional alkali basalts. Many of the fine-grained basalts are flow-banded and have a fissility, which in the absence of other criteria gives them the appearance of being trachytic. This may explain why Baker overestimated the proportion of trachytes in the series.

The series is thickest in the escarpment overlooking the Suguta Valley and thins rapidly eastwards. According to Baker (1963) the series is only about 30 m (100 ft) on the Muruakirim Plateau, where it is represented by two flows which rest directly on Precambrian gneisses. From the contact relationships and thickness variations of these basalts on the Tirr Tirr and Muruakirim plateaux, it is concluded that the main source of the lavas was located within a depression situated in the same position as the present day inner trough. As the lava pile grew in thickness, successive flows overstepped the higher ground to the east and eventually overflowed the margin of the depression.

A number of radiometric dates exist for the Tirr Tirr Series. A sample of basic trachyte (27/301) collected by Baker (1963) from a locality 4 miles south-east of Lowoi (approximately BN 2260 2170) gave K/Ar ages of 3.6 ± 0.4, 3.8 ± 0.4, 3.9 ± 0.4 Ma (Baker et al., 1971). Although the precise locality for this sample is unknown, it must have been collected from near the highest part of the plateau in the south-east. Tatsumi and Kimura (1991) report a similar K/Ar date of 3.94 ± 0.74 Ma for a basalt from the series, although no locality details are provided.

Several K/Ar dates were obtained by a collaborative research project undertaken in the northern part of the Suguta Valley by a consortium of oil companies (Bosworth and Maurin, 1993). Basalts from the Losergoi area (approximately BN 2295 2330) have given dates of 3.8 ± 0.2, 3.1 ± 1.2 and 4.2 ± 0.3 Ma, the latter result being obtained from an altered sample. Trachyte dykes intruding these basalts yielded ages of 3.8 ± 0.7 and 4.2 ± 0.7 Ma. Another basalt at Losergoi gave a date of 2.3 ± 0.4 Ma. Bosworth reported that this youngest flow was unconformable upon the older basalts and dykes. The topmost basalt on the plateau above Losergoi at [BN 2259 2112] was dated by the Ar/Ar step-heating method during the present survey and yielded a date of 2.74 ± 0.02 Ma.

Bosworth and Maurin also dated samples of trachyte at the base of the escarpment a short distance to the south of the Gap [BN 2235 2115], and obtained ages of 2.7 ± 0.2, 2.7 ± 0.2 and 2.6 ± 0.4 Ma from sanidine concentrates. These samples were taken from the toe of a major landslip and presumably represent lavas that have slipped from higher parts of the plateau. The examination of Landsat thematic mapper satellite images supports this assumption, indicating that the very edge of the plateau adjacent to the landslip at this locality is capped by trachyte, as are large coherent rafts of rock within the landslip itself.

10.3 THE GEOLOGY OF THE LORIU PLATEAU AND NAKITOEKIRION

10.3.1 Previous work in the Loriu Plateau area

Truckle (1977) investigated the geology of the Loriu Plateau and his findings were subsequently incorporated into the work of the Samburu–Marsabit Geological Mapping Project (Key, 1987; Ochieng' et al., 1988). Only part of Truckle's stratigraphy is considered to be directly relevant to a discussion of the geology of Namarunu, and this is summarised below.

The **Nathelot Basalts** outcrop on the western side of the Loriu Plateau and have yielded a K/Ar age of 4.5 ± 0.4 Ma. These are unconformably overlain by the **Loriu Trachyte Group** comprising the three quartz trachyte volcanoes of **Lopogut**, **Lomi** and **Kalakopon**, which are aligned parallel to the edge of the inner trough. Lopogut is well outside the area considered in this report, but Kalakopon lies on the western edge of the mapped area, and Lomi is situated a short distance to the south-west.

Kalakopon [BN 2030 2230] consists of a flat-lying to gently easterly-dipping sequence of trachytic lavas and volcaniclastic deposits. Truckle reported a single K/Ar date of 4.4 ± 0.2 Ma for a trachyte from Kalakopon.

Lomi [BN 2030 2230] is situated close to the eastern edge of the plateau and its eastern flanks have been down-faulted into the inner trough. It has a caldera with well-preserved western and northern walls, but with eastern and southern margins that have been destroyed by faulting and erosion. A single K/Ar date of 3.0 ± 0.2 Ma is reported by Truckle for a trachyte from Lomi.

The **Lorikipi Basalts** cover large areas of the Loriu Plateau. They rest unconformably upon the trachytic rocks of Kalakopon and have flowed into the caldera of Lomi. Truckle obtained a K/Ar date of 4.0 ± 0.1 Ma from the Lorikipi Basalts but rejected this because he believed the basalts to be younger than Lomi and to be of Quaternary age. However, the work of the present survey indicates that the Lorikipi Basalts are in fact of Pliocene age and contain important trachytic volcanic intercalations, which include the products of Lomi volcano.

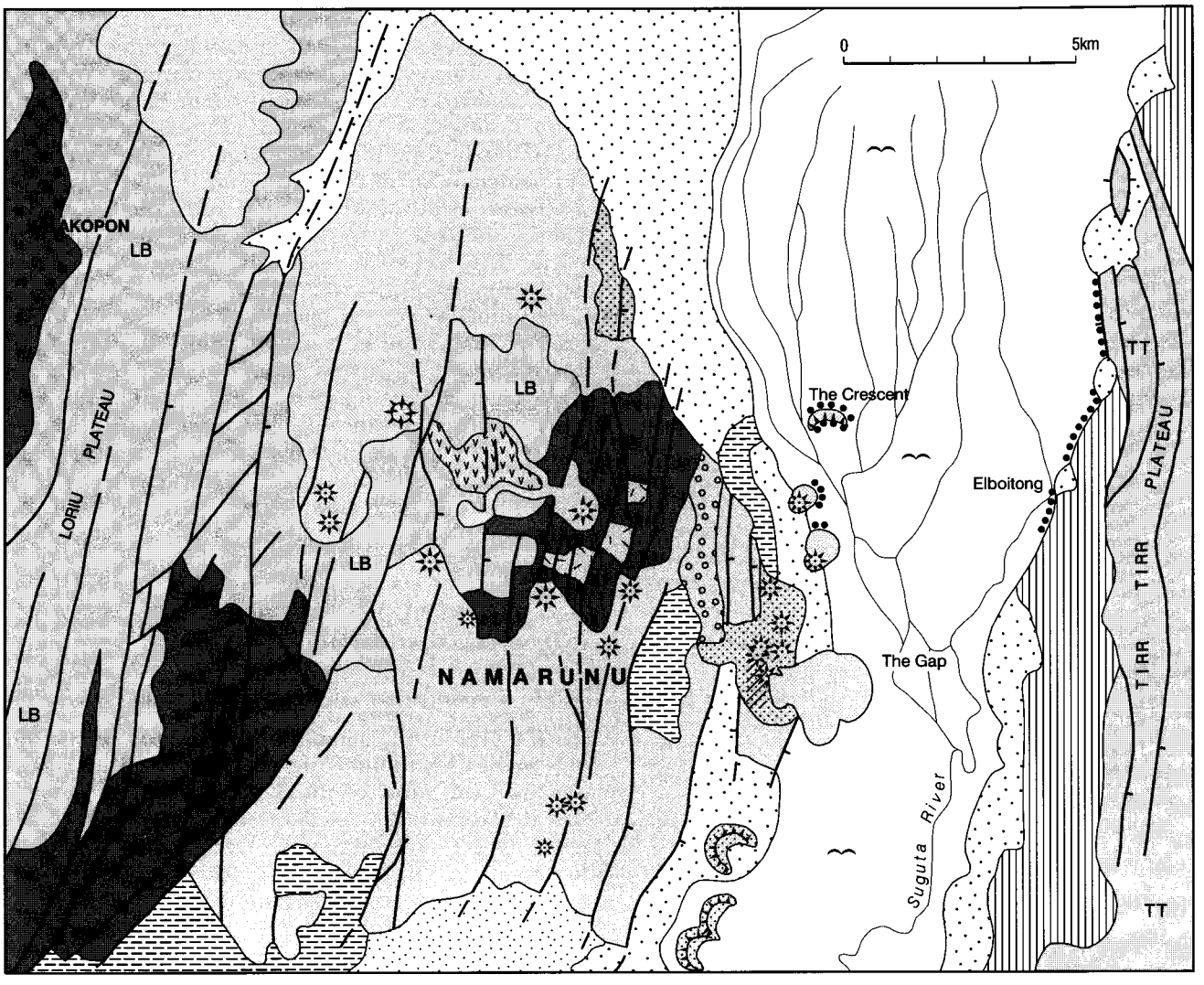

Figure 10.2 Simplified geological map of Namarunu and adjacent areas showing the location of surface geothermal activity.

10.3.2 Present survey of the Loriu Plateau

Five sections were examined in the Loriu escarpment and the entire length of the escarpment was reconnoitred by helicopter. The three most instructive sections are described below.

10.3.2.1 The Loriu escarpment south-west of Namarunu

An almost complete section is exposed through the Loriu escarpment in the valley of the Nalio River to the south-west of Namarunu, commencing at [BN 2045 2155] and ending on top of the plateau at [BN 2041 2156]. Four main rock units totalling approximately 230 m in thickness are exposed. From the base to the top these are layered basalts, trachytic tuffs, layered basalts and melanocratic trachytes. The basalts at the base and in the middle of the section are the Lorikipi Basalts of Truckle (1977; 1979b).

At least 60 m of basalt lavas are exposed at the base of the escarpment. These consist of alternating flows of fine-grained aphyric basalt and coarsely feldspar-

phyric basalt. Individual flows are laterally persistent and range in thickness from 30 cm up to about 5 m. Many of the flows are dominated by scoriaceous autobreccias, and reddened palaeosols are developed on top of the lowest three flows.

The basalts are overlain by approximately 50 m of trachytic pyroclastic rocks, consisting of buff-brown, poorly-sorted and poorly-stratified pumiceous deposits with zones of intense welding. The deposits are interpreted as the product of pyroclastic flows, possibly with an air-fall component. Ar/Ar dating of anorthoclase crystals indicates an age of 2.52 ± 0.02 Ma for a welded tuff within this unit.

The trachytic pyroclastic rocks are overlain conformably by about 80 m of horizontally layered basalts. These are identical to the basalts at the base of the section, consisting of alternating flows of aphyric and coarsely feldspar-phyric basalt with relatively thick scoriaceous autobreccias.

At the top of the escarpment the basalts are overlain by two massive flows of feldspar-phyric melanocratic trachyte, which together are approximately 17 m thick. These are dark grey, weathering black, and contain abundant coarse glassy anorthoclase phenocrysts and moderately abundant micophenocrysts of olivine. Ar/Ar dating indicates an age of 2.74 ± 0.02 Ma for the uppermost trachyte.

A similar succession is exposed in the Loriu escarpment 3 km to the south-west at [BN 2036 2124] (Plate 10.3). Here the Lorikipi Basalts form a single unit which rests with strong angular unconformity upon altered trachyte lavas, tuffs and breccias. The trachytic volcanic rocks are intruded by E-trending dykes and small plugs of trachyte with complex intrusive contacts. The unconformity surface at the base of the basalts dips steeply to the east.

10.3.2.2 The Loriu escarpment north-west of Namarunu

An instructive section through the Loriu escarpment occurs to the north-west of Namarunu. It begins in the main river valley between Namarunu and the base of the escarpment at [BN 2080 2252] and ends on top of the plateau at [BN 2060 2255].

Deeply weathered, pale green-buff trachytic lavas and breccias outcrop within the river bed and along the base of the escarpment. These have an irregular upper surface with a well-developed reddened palaeosol, upon which horizontally layered Lorikipi Basalts rest with marked unconformity. The basalts are at least 150 m thick and consist of alternating flows, mostly 1–5 m thick, of aphyric, sparsely feldspar-phyric, and strongly olivine-pyroxene-phyric lavas.

On the upper parts of the escarpment, around [BN 2065 2252], the horizontally layered Lorikipi Basalts are preserved as a thin veneer resting with strong angular unconformity upon altered trachytic lavas and breccias. The basalt flows show overlapping relationships and overstep the steeply dipping unconformity surface in a westerly direction. At several localities along the escarpment to the south, trachytic rocks are exposed as small inliers poking through the horizontally layered basalt cover. From these relationships it would appear that an older easterly-facing scarp was developed in the trachytes and was gradually buried by the Lorikipi Basalts, which were erupted from a source to the east. Subsequent faulting along the approximate line of this old buried scarp resulted in the formation of the existing escarpment (Figure 10.3).

A single basalt lava caps the plateau and drapes the face of the escarpment, in places resting with marked angular unconformity upon the Lorikipi Basalts. This younger basalt contains abundant coarse phenocrysts of olivine and clinopyroxene, and clearly post-dates the formation of the inner trough (see Section 10.3.2.3 below).

10.3.2.3 The Loriu escarpment north of Namarunu

The Loriu escarpment to the north of Namarunu exposes about 300 m of Lorikipi Basalts with thin trachytic volcaniclastic intercalations. Valleys incised into the escarpment provide almost complete sections, which indicate that the major structure between the plateau and the inner trough in this area is a mono-

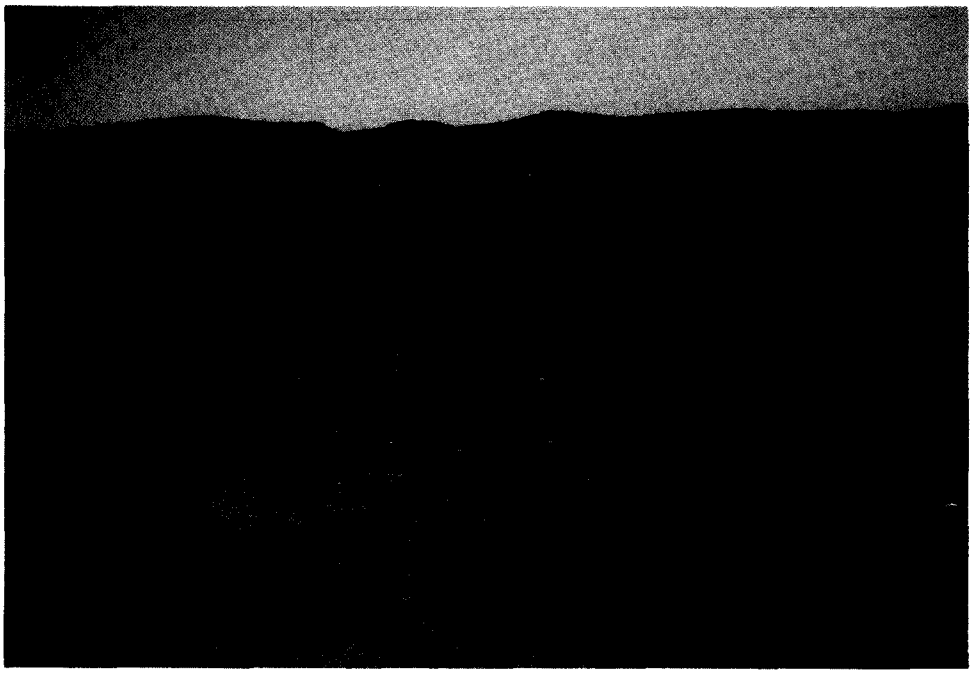

Plate 10.3 Lorikipi Basalts exposed in the escarpment of the Loriu Plateau to the south-west of Namarunu.

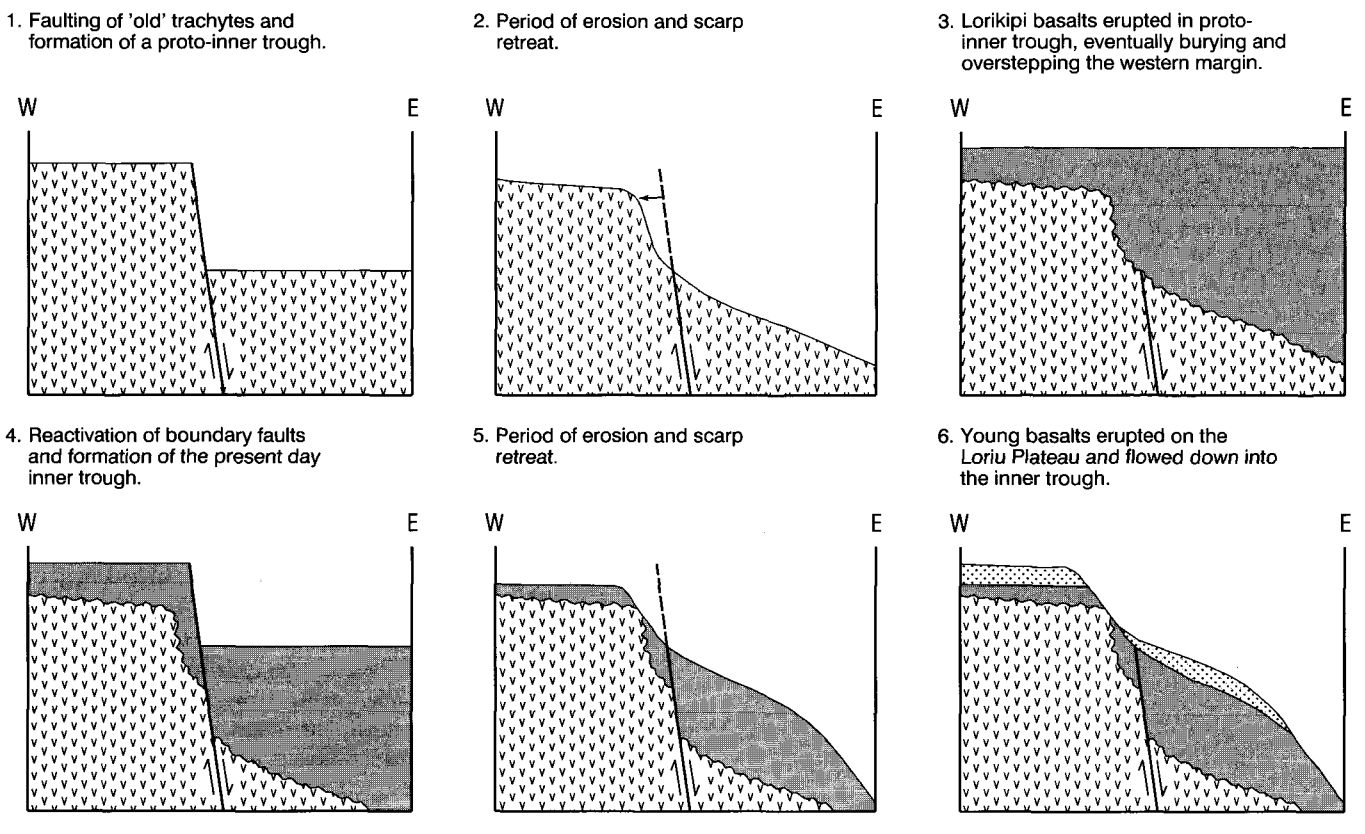

Figure 10.3 Evolution of the Loriu escarpment north-west of Namarunu.

clinal downwarp. Strata are horizontal at the top of the plateau, but on passing down the escarpment they progressively dip with increasing inclination to the east, reaching dips at the base of the escarpment of about 40°. The succession is faulted by minor antithetic faults with throws down to the west, but there are no easterly down-throwing faults.

The young basaltic cone of Kailongoleiko [BN 2085 2327], situated on top of the plateau, post-dates the formation of the inner trough. Basalt flows erupted from a breach on the north-west side of the cone cover large areas of the plateau to the west and south, and in several places have flowed over the Loriu escarpment and down into the inner trough. On the face of the escarpment these young flows rest with marked unconformity on the older Lorikipi Basalts.

The young lavas of Kailongoleiko contain abundant olivine and pyroxene phenocrysts and are nepheline-normative, and in this respect are similar to the Quaternary basalts of Namarunu. In contrast, the underlying Lorikipi Basalts are all hypersthene-normative.

10.3.3 The succession at Nakitoekirion

The westerly-tilted massif of Nakitoekirion is juxtaposed against the Loriu escarpment to the south-west of Namarunu. The succession exposed in the fault escarpment on the east side of Nakitoekirion was examined in a section commencing at the base [BN 2073 2130] and ending at the top [BN 2069 2131].

A small fault-bounded outcrop of microsyenite is exposed in the river bed at the base of the escarpment. Intrusive contacts are not seen, but a syenitic intrusion is inferred to be present at a shallow depth beneath the volcanic succession of Nakitoekirion.

The escarpment exposes approximately 255 m of trachytic volcanic rocks. The lower part of the succession is composed of pale green, altered, trachyte lavas and pyroclastic rocks containing several reddened palaeosols. The lavas are fissile and aphyric to sparsely microporhyritic. The pyroclastic rocks consist of pumice lapilli tuffs and breccias with intense zones of welding, and are interpreted as pyroclastic flows. These altered rocks are overlain by approximately 100 m of fresh, massive, feldspar-phyric melanotrachyte which cap the escarpment. At least four flows are present, and between the top two flows there is a 7 m thick band of trachytic scoria which is strongly welded near the top. These lavas are dark grey, weathering to black, and contain abundant fresh anorthoclase phenocrysts and moderately abundant olivine microphenocrysts. Ar/Ar dating indicates an age of 2.33 ± 0.02 Ma for the topmost flow.

During the course of aerial reconnaissance, several dykes trending approximately E–W were observed within the escarpment on the east side of Nakitoekirion.

The northern end of Nakitoekirion is partly buried by Lorikipi Basalts, which also extend around the western side of the massif where they rest upon the lower parts of the dipslope. Near the base of the escarpment at the north-east end of Nakitoekirion, at [BN 2081 2165], horizontal basalts rest with marked angular unconformity upon altered trachytic volcanic rocks of Nakitoekirion. The unconformity surface dips at 25–30° to the east and has a red palaeosol developed upon it. The basalt flows overstep the unconformity surface and show overlapping relationships in a westerly direction. These relationships indicate that the altered trachytic rocks forming the lower part of

Nakitoekirion formed a positive feature when the Lorikipi Basalts were erupted.

10.4 THE GEOLOGY OF NAMARUNU

10.4.1 Introduction

Namarunu is composed predominantly of a Pliocene volcanic sequence which may be broadly correlated with the succession of the rift margin. Quaternary volcanic rocks with pristine morphological features are superimposed on this older volcanic pile.

The succession of Namarunu, as mapped during the present survey is summarised in Table 10.1.

10.4.2 Trachyte lavas and pyroclastic rocks (N^{tv})

The oldest exposed parts of Namarunu consist of trachyte lavas, tuffs and breccias, which make up the bulk of the volcanic edifice (Plate 10.4). These generally dip away from the summit area and are overlain by Lorikipi Basalts on the western flanks. In many places these trachytic rocks are strongly hydrothermally altered.

Sections are exposed through these older rocks in valleys on the northern and western flanks. The lower part of the volcanic pile consists of massive, green and red, weathered, fissile, microporphyritic trachyte lavas. Thicknesses cannot be estimated because the base of the volcanic pile is not seen, but approximately 100 m of lavas are exposed in the most deeply incised valleys in the north.

The lavas in the lower part of the pile pass up into an alternating sequence of poorly-stratified trachytic pyroclastic rocks and lavas. The pyroclastic rocks consist of poorly-sorted, buff, red and green weathered pumice lapilli tuffs and lapillistones with intensely welded glassy bands exhibiting rheomorphic features. The thickness of these alternating lavas and pyroclastic deposits is difficult to estimate because of faulting, but is at least 200 m.

Melanocratic lavas of benmoreitic and mugearitic composition occur in minor amounts on the upper flanks of Namarunu, and are intercalated with the trachytic lavas and pyroclastic rocks.

The morphology of Namarunu and the radial dip of strata away from the summit area suggest that the old trachyte pile had the form of a volcanic shield. Truckle (1977) reported a K/Ar date of 6.8 ± 0.5 Ma for a trachyte on the western flanks of Namarunu, but rejected this on the assumption that the volcanic complex was of Quaternary age. However, the present survey has recognised that the western flanks of the early trachyte shield are overlain by Lorikipi Basalts of Pliocene age. This places an upper limit on the age of the early trachytic activity of Namarunu, with which Truckle's date is compatible.

10.4.3 Lorikipi Basalts (LB)

Basaltic lavas cover almost all of the southern, western and northern flanks of Namarunu, and parts of the eastern flanks. Truckle (1979b) mapped these basalts as a single lithological unit of Quaternary age, but observations made during the present survey indicate that they are of two distinct ages. The basalts on the northern, southern and eastern flanks are of Quaternary age and are younger than those on the western flanks. The older basalts on the western flanks are contiguous with the Lorikipi Basalts of the Loriu area and are compositionally identical to them, being hypersthene-normative; whereas the Quaternary basalts are nepheline-normative.

In the low ground between the western flanks of Namarunu and the easterly facing Loriu escarpment, the Lorikipi Basalts comprise a horizontally layered pile of flood lavas. The sequence thins and oversteps in an easterly direction onto the higher parts of Namarunu, but does not extend as far as the summit area. On the lower western flanks the basalts can be seen resting unconformably upon older trachyte lavas and pyroclastic rocks, and on the north-west flanks they are in turn unconformably overlain by younger rhyolitic and trachytic lavas and pyroclastic rocks. As described in Sections 10.3.2 and 10.3.3, the Lorikipi Basalts unconformably overstep the older trachytic rocks of Nakitoekirion and the Loriu Plateau to the west. From these relationships it is concluded that the basalts were erupted and ponded

Table 10.1 Summary of the stratigraphy of Namarunu

Lacustrine sediments (l)		
Upper Basalts (b)	500 – ?3 ka	LAKE SUGUTA
Trachytic pumice lapilli (N^{tp}) tuffs and breccias	509 ± 5 ka	
Melanocratic trachyte lavas (N^{tm})	840 ± 5 ka	
Rhyolitic and trachytic lavas (N^{rt}) and pyroclastic rocks	871 ± 5 ka	
		FORMATION OF INNER TROUGH
	unconformity	
Lorikipi Basalts (LB) with trachytic intercalations	2.33 ± 0.02 Ma – 4.0 ± 0.1 Ma	FLOOD LAVAS ERUPTED IN PROTO-INNER TROUGH
	unconformity	
Trachyte lavas and (N^{tv}) pyroclastic rocks		PLIOCENE VOLCANIC SHIELD FORMATION

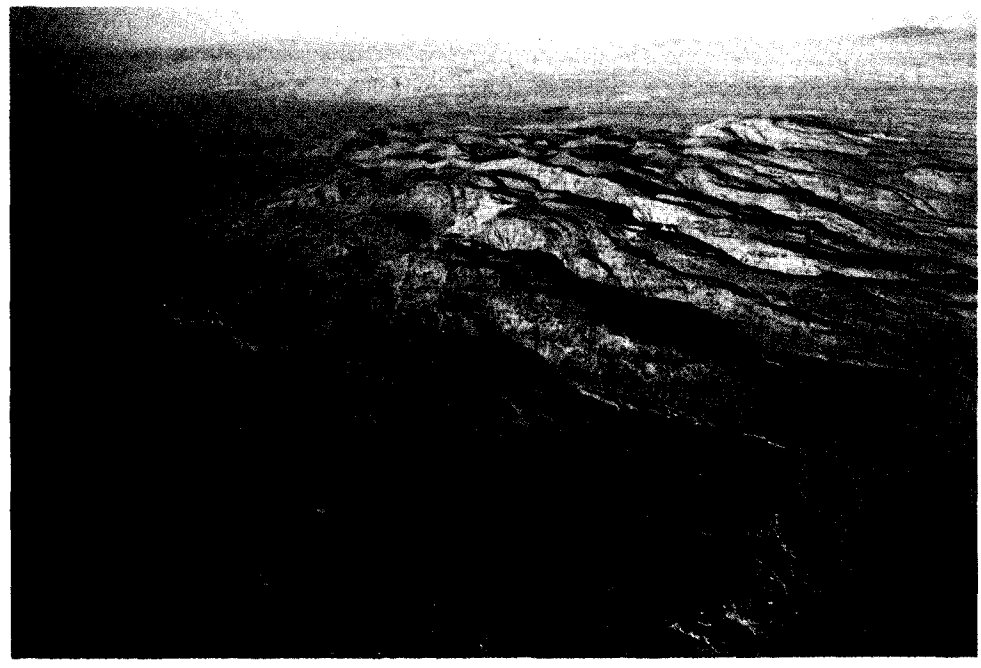

Plate 10.4 Aerial view of Namarunu looking south-west. The pale areas consist of Pliocene trachyte lavas and pyroclastic rocks fractured by north trending faults.

in a topographic depression bounded by the early trachyte shield of Namarunu on the east and by an upstanding trachytic volcanic terrain in the Loriu region to the west. As the basaltic pile grew in thickness, successive flows overstepped the trachytic shield of Namarunu to the east and the margins of the depression to the west.

The Lorikipi Basalts are fine-grained, aphyric to sparsely microporphyritic basalts and hawaiites, many of which are strongly flow-banded and fissile so as to resemble trachytes in the field. An unusual flow of highly feldspathic basalt is intercalated within the Lorikipi Basalts in the area between Namarunu and Nakitoekirion. This has a coarse granular texture and weathers to produce a distinctive hummocky surface pattern.

On the lower western flanks of Namarunu, well-bedded, air-fall trachyte pumice deposits are intercalated with the layered basalts. These deposits are generally thin, although a section at [BN 2111 2205] exposes 15 m of pumice lapilli deposits. At this locality the pumice deposits are cut by a vertical basaltic plug that flares upwards into a funnel-shaped conduit that acted as a feeder to an overlying basalt flow.

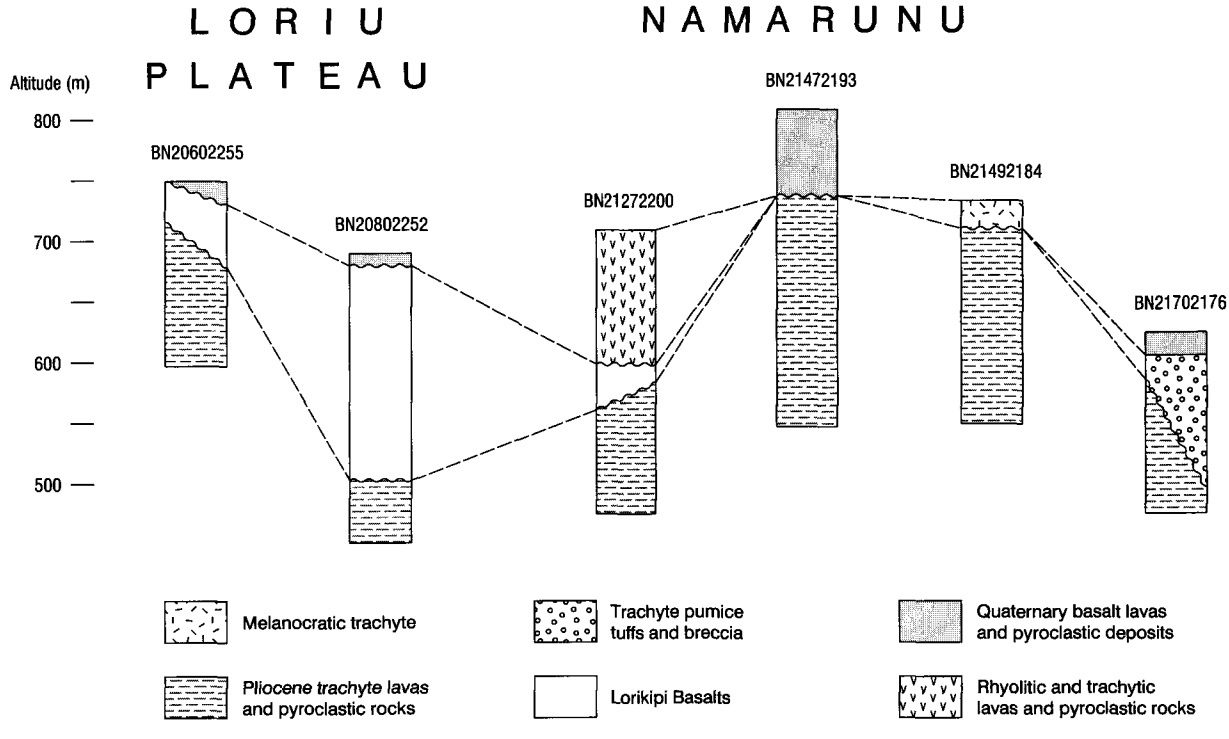

Figure 10.4 Generalised vertical geological sections in the Loriu escarpment and Namarunu areas.

flanks and parts of the eastern flanks of Namarunu. Basaltic activity also took place at the foot of the eastern flanks, where a prominent NNE-trending ridge of scoria cones, phreatomagmatic deposits and lava flows has been constructed along the western edge of the Suguta Valley.

Large areas of the northern flanks are covered by fine-grained aphyric and microporphyritic basalts that were erupted from fissures. In the north around Kangolenyang [BN 2115 2295] these fine grained basalts flowed into water, producing pillow lava and hyaloclastite deltas. Elsewhere on the northern flanks, several incised valleys expose pink to buff coloured palagonitised tuffs and hyaloclastites beneath the basalt cover.

Coarsely porphyritic lavas containing olivine and clinopyroxene phenocrysts were erupted from a number of spatter cones and spatter rings situated to the north and west of the summit area [BN 2138 2228] [BN 2109 2212] [BN 2093 2195]. These strongly porphyritic lavas are younger than the fine grained varieties and show evidence of having been highly fluid at the time of eruption. Very fluid and highly porphyritic olivine basalts were also erupted from a breached scoria cone forming the summit of Namarunu [BN 2147 2192]. These flowed westwards and became ponded against a pre-existing easterly-facing fault scarp on the western side of the summit area, before flowing down valleys to the west and north-west where they are preserved as narrow linear flows.

Most of the lavas on the southern and south-western flanks are fine grained aphyric or microporphyritic basalts. These were mainly erupted from scoria and spatter cones on the upper-middle flanks, although flows on the lower flanks may have been erupted from fissures. The basalts on the south-eastern flanks are strongly porphyritic, containing abundant coarse phenocrysts of plagioclase in addition to olivine and clinopyroxene.

The basalts of the southern flanks are more faulted than those on the northern flanks, particularly in the south-east where fault scarps cutting the lavas reach heights of 50 m. Movement along these faults must have been broadly contemporaneous with the basaltic activity, as is evident where fault scarps cutting certain lavas are buried or mantled by later flows.

In many places on the southern flanks, patches of diatomite rest upon the basalts and lake stand lines are preserved upon their surfaces. On the lowermost south-western flanks pillow lavas and hyaloclastites are intercalated with diatomites [BN 2058 2094].

Aruba Rock is a deeply eroded tuff cone composed of palagonite tuffs, situated low on the south-eastern flanks [BN 2138 2118]. This remnant cone is post-dated by younger basalt lavas which flowed around it and overlie its eroded margins. Lake stand lines are preserved upon the surfaces of these younger lavas at higher elevations on the flanks of Namarunu. It is concluded from this, that the tuff cone of Aruba Rock was erupted on a shoreline when the lake was at a relatively low-level, and that subsequently it was eroded, surrounded by younger lavas, and then submerged during a later transgression of the lake.

To the east of Namarunu, in the vicinity of the Gap, a NNE-trending line of young basaltic centres extends along the axis of the inner trough. The central portion [BN 2185 2157] of this line of basaltic centres culminates in a ridge of coalesced tuff and scoria cones that rises more than 200 m above the floor of the valley (Plate 10.5). This is composed predominantly of palagonitised tuffs and breccias, upon which a line of scoria cones is superimposed along the spine of the ridge. Poorly consolidated and unconsolidated fresh basaltic ash and scoria from these cones drapes the flanks of the ridge and overlies the palagonitised deposits. The ridge is considered to have been constructed largely by phreatomagmatic activity within Lake Suguta, and it eventually grew high enough above the water level for subaerial strombolian-style activity to take place. Lake stand lines are preserved upon the ridge, even on the summit scoria cones, indicating that at one stage the ridge was completely submerged by the lake.

Several young scoria cones occur on the upper eastern flanks of the ridge. These do not have lake stand

Plate 10.5 Young basaltic lavas, scoria cones and tuff cone deposits along the eastern base of Namarunu, looking south. The rift margin escarpment of the Tirr Tirr Plateau can be seen in the distance.

The remains of a Lorikipi basalt scoria cone occur on the western flanks of Namarunu at [BN 2120 2198], and are unconformably overlain and partly buried by the younger rhyolitic lavas and pyroclastic rocks described below.

10.4.4 Rhyolitic and trachytic lavas and pyroclastic rocks (N^{rt})

Rhyolitic and trachytic lavas, tuffs and breccias form the prominent hill situated 2 km north-west of the summit region of Namarunu at [BN 2125 2201]. On air-photographs this hill appears to have the approximate form of a volcanic cone, about 2 km in diameter, with a vague crater feature on its summit. This crater-like feature is believed to result from the fortuitous arrangement of later faults and is not thought to be a volcanic crater.

Silicic lavas and breccias can be seen resting unconformably upon Lorikipi Basalts at several localities around the base of the hill, as for example at [BN 2128 2208] and [BN 2120 2198]. A thickness of about 120 m is estimated for these silicic volcanic rocks, this being the height of the summit of the hill above the unconformity surface.

The hill is composed of gently dipping lavas, trachytic scoria, and pumice lapilli tuffs with strongly welded zones. The summit and flanks of the hill are draped by intensely welded, flow-folded and flow-brecciated rhyolitic tuffs. The orientation of the flow-folds and the manner in which the tuffs drape the slopes of the hill, suggest that these are welded air-fall deposits that were rheomorphosed and flowed after deposition. Ar/Ar dating of feldspars crystals from the welded rhyolitic tuffs on the summit of the hill at [BN 2127 2202] has yielded an age of 871 ± 10 ka.

Welded air-fall tuffs also drape small areas on the southern and eastern flanks of Namarunu, as for example at [BN 2131 2169] and [BN 2148 2179]. These are correlated with the rhyolitic tuffs on the main hill to the north-west of the summit.

10.4.5 Melanocratic trachyte lavas (N^{tm})

Massive outcrops of fresh melanocratic trachyte lavas occur on the uppermost eastern and southern flanks of Namarunu. These rest upon the altered trachytic lavas and pyroclastic rocks of the early shield, and are recognisable on air-photographs by distinctive, dark to almost black, photo-tones. They contain abundant coarse glassy phenocrysts of anorthoclase and microphenocrysts of olivine. Ar/Ar dating of anorthoclase phenocrysts from a melanocratic trachyte on the upper eastern flanks at [BN 2149 2184] indicates an age of 840 ± 5 ka for these lavas.

10.4.6 Trachytic pumice lapilli tuffs and breccias (N^{tp})

Poorly consolidated trachytic pumice lapilli tuffs and breccias, which weather to a distinctive bright ochreous-yellow colour, form a thick apron on the lowermost eastern flanks of Namarunu. Here they rest unconformably upon, or bank against, faulted lavas and pyroclastic rocks of the early trachyte shield.

The deposits consist of a crudely stratified, subhorizontal to eastward dipping pile of poorly-bedded pumice lapilli deposits and massive breccias, approximately 100 m thick. Individual breccia beds are up to 3 m thick and are composed of poorly-sorted pumice with matrix supported lapilli and blocks of trachyte and syenite up to a metre in diameter. In places the pumice deposits exhibit poorly developed cross-stratification. Bomb sags are commonly associated with the lithic blocks, indicating ballistic emplacement, although many blocks do not exhibit any impact structures. These deposits are interpreted as proximal pyroclastic fall deposits that underwent some post-depositional mass movement. Ar/Ar dating of feldspars separated from pumice indicates an age of 509 ± 5 ka for the uppermost deposits at this locality.

At the top of this sequence, ochreous coloured trachytic tuffs containing abundant accretionary lapilli grade up into 5 m of red-brown pumice-scoria lapilli tuffs, which in turn grade up into a few metres of basaltic scoria. The scoria is capped by a fine-grained aphyric basalt lava which forms several near-horizontal mesas halfway up the eastern flanks of Namarunu, as for example around [BN 2167 2193]. The gradational change from trachytic to basaltic composition in these deposits is taken as evidence for eruption from a compositionally stratified magma chamber.

The ochreous-yellow pumice deposits extend for several kilometres to the south-east and occupy much of the low ground between the eastern flanks of Namarunu and the ridge of young scoria cones along the margin of the Suguta Valley. A good section is exposed in the deposits in a prominent hill at [BN 2175 2165]. Here the lowest exposed part of the sequence consists of 30–40 m of sub-horizontally bedded, yellow, trachytic pumice lapilli deposits, which grade up into 30 m of red-brown palagonitised basaltic tuffs containing scoria. The deposits are planar-bedded and cross-bedded and contain angular to subangular lithic clasts of syenite and trachyte, some of which display bomb sags. At the top of the section the palagonite tuffs are capped by a thin layer of scoria. The deposits at this locality are generally much finer than those exposed on the eastern flanks of Namarunu, but they show the same gradational change from trachytic to basaltic composition. Nearby, at [BN 2175 2170] the pumice deposits are strongly cross-bedded and contain lag deposits composed of coarse lithic gravels and fish bones.

In summary, these pumiceous deposits are interpreted as the eruptive products of a compositionally zoned magma chamber. Initially trachytic tephra was erupted, but at a late stage this gradually changed to basaltic composition and finally basaltic lavas were erupted. The deposits are believed to have accumulated in a subaerial to lacustrine environment at the base of the eastern flanks of Namarunu, and at least some of the eruptive activity in this low ground was phreatomagmatic in style. The change from trachytic to basaltic compositions recorded in these deposits heralded the onset of a major phase of basaltic volcanism which is described in the following section.

10.4.7 Upper Basalts (b)

Widespread subaerial and subaqueous basaltic activity took place at a late stage in the evolution of Namarunu.

Basalt lava fields, with associated scoria and spatter cones, cover virtually all of the northern and southern

lines preserved upon their flanks and therefore post-date the high lake level that submerged the ridge. Basalts were erupted from breaches in these young cones and flowed down the eastern flank of the ridge to spread out as lobate flows on the floor of the Suguta Valley. These lavas have pristine morphology with well-preserved flow features. They include microporphyritic and coarsely porphyritic feldspar-phyric and olivine-clinopyroxene-phyric basalts, although the youngest flow is a fine grained aphyric basalt. These were erupted subaerially and post-date Lake Suguta, and must therefore be very young.

The southern end of the line of young basaltic centres is marked by three tuff rings situated on the edge of the Suguta flood plain to the south-west of the Gap at [BN 2177 2117], [BN 2175 2104] and [BN 2170 2095]. Each tuff ring is asymmetrical and crescentic in plan. They are open on their eastern sides, whilst their western flanks are high and steep sided. The northernmost tuff ring is cut by several N-trending basaltic dykes, and is partly mantled by fresh scoria which is overlain on the northern side by a glassy basalt lava. These tuff rings have lake stand lines preserved upon the inner slopes of their craters which indicate that at some stage after formation they were completely submerged by Lake Suguta (Plate 10.6).

The northern end of the line of young basaltic centres is marked by the remnants of a tuff ring, known as the Crescent [BN 2198 2215], which is partly buried within the flood plain of the Suguta.

The age range of the upper basaltic volcanism on Namarunu is not precisely known. However, the episode was heralded by eruption of the trachytic pumice tuffs, with an age of 509 ± 5 ka, which grade rapidly up into basaltic deposits on the eastern flanks (Section 10.4.6). The youngest scoria cones and basalt lavas on the ridge to the east of Namarunu post-date Lake Suguta, which probably did not dry out until 3 ka. On the available evidence, it is therefore concluded that the Upper basalts were erupted during a period from about 500 ka through to Recent times.

10.4.8 Lacustrine sediments and stand lines of Lake Suguta

Lacustrine sediments are widely preserved on and around the flanks of Namarunu. In many low-lying areas they are covered by gravel veneers left by surface down-wasting and wind erosion.

The most extensive lake sediments and best exposed sequences occur on the lowermost south-western flanks, where the Nalio River flows into the Suguta Valley. Here the Nalio has cut into the sediments and several good sections are exposed in cliffs and river bluffs. One such section at [BN 2063 2095] exposes approximately 17 m of sediment overlying pillow lavas and hyaloclastites (Plate 10.7). The sequence comprises diatomites with trachytic pumice beds and thin basalt flows. Some of the pumiceous beds are cross-bedded and have irregular cross-cutting bases, and the diatomites show evidence of loading and dewatering in the form of convolute bedding and small-scale clastic dykes. Mass-flow breccias occur at the base of the section and are composed of large clasts of diatomite supported within a diatomaceous-pumiceous matrix. Fish remains occur throughout the section, and complete fossil fish are preserved within paper shales near the top of the sequence. A thin algal limestone, indicative of shallow to emergent conditions, caps the sequence. This is overlain by a basalt that has oxidised and baked the topmost sediments and caused silicification of the algal limestone. Feldspar crystals separated from pumice at this locality have yielded an Ar/Ar date of 826 ± 6 ka. This may not represent the age of the lacustrine sedimentation, because the pumice was deposited by epiclastic processes and could therefore be significantly older than the sediments in which it occurs. However, this date does indicate that trachytic pyroclastic activity took place in the vicinity of Namarunu around 826 ka.

Stand lines testifying to former high lake levels occur extensively on Namarunu, Nakitoekirion and the Loriu escarpment, and are clearly visible on air-photographs. The highest are at an altitude of approximately 575 m, which is the same elevation as the high-

Plate 10.6 Aerial view of a tuff ring on the floor of the Suguta Valley south-east of Namarunu. Note the prominent lake stand lines and the wind-blown sand deposits.

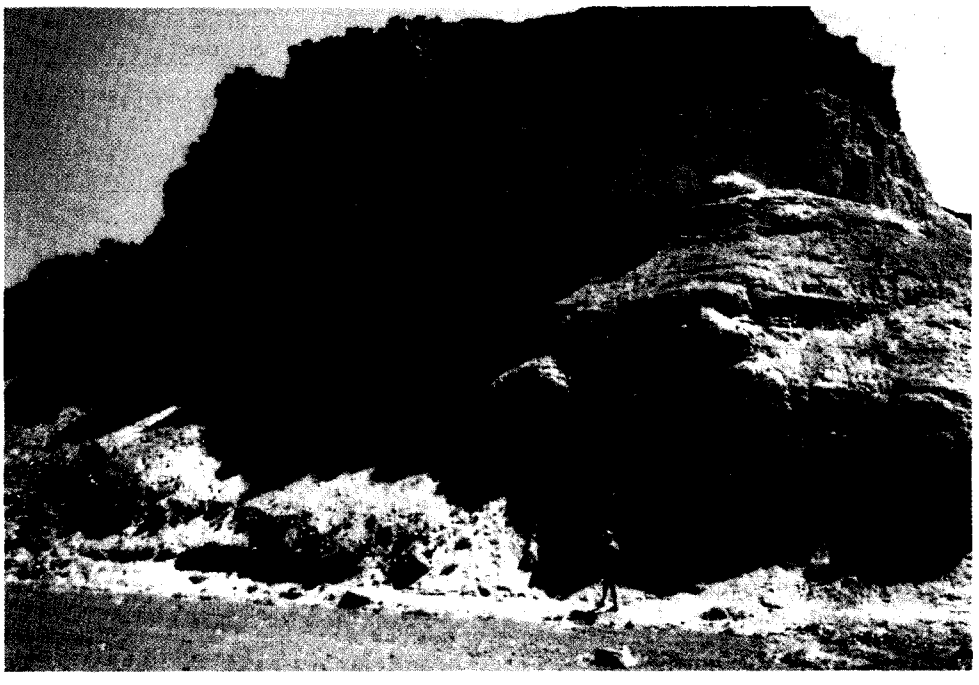

Plate 10.7 Diatomaceous sediments capped by a basalt lava, Nalio River, south-west of Namarunu.

est stand lines on Emuruangogolak and the Barrier volcano. This highest stand line is manifested on Namarunu by a wave-cut notch around the base of a scoria cone on the western flanks [BN 2120 2198] and by shelly deposits preserved on erosional benches on the upper southern flanks [BN 2145 2173]. Shell material from this highest shoreline on Namarunu has given a ^{14}C date of 9 660 ± 210 years (Truckle, 1976), which corresponds with a pluvial climatic period at the end of the last glaciation, when all the East African lakes were at their highest levels.

Truckle (1979b) indicated the presence of algal limestones on the upper south-western flanks of Namarunu. These were not seen during the present survey, although at many places where stand lines are preserved, stromatolitic coatings occur on water worn cobbles and boulders, as for example around [BN 2115 2215] on the western flanks and [BN 2167 2186] on the eastern flanks. Casanova (1986) undertook detailed studies on stromatolites related to former lake shorelines in the Suguta Valley at elevations of between 406 m and 460 m. He obtained a $^{230}Th/^{234}U$ date of 121 ± 20 ka from stromatolites associated with these shorelines in the Kangolenyang area, which is situated immediately to the north of Namarunu. This date corresponds with the last interglacial period when wet climatic conditions prevailed in inter-tropical Africa, resulting in high lake levels throughout the rift (Hillaire-Marcel et al., 1986).

Apart from the radiometric dates of circa 10 ka and 120 ka obtained from lake stand lines, there is additional evidence to suggest that Lake Suguta had a more prolonged history. This is provided by the trachytic pumice tuffs at the foot of the eastern flanks of Namarunu (Section 10.4.6) which have an age of 509 ± 5 ka. These have a phreatomagmatic origin and contain fish remains, suggesting that lacustrine conditions prevailed at this time.

10.4.9 Intrusions

Porphyritic microsyenite crops out over an area measuring 1.5 km by 0.75 km on the periphery of the north-eastern flanks of Namarunu around [BN 2155 2235]. Intrusive relationships are not seen, because the syenite is partly bounded by NNE-trending faults, and is unconformably overlain by upper basalt lavas in the south and west, and by superficial deposits of the Suguta Valley in the east. This indicates that the intrusion was faulted and unroofed prior to eruption of the Upper Basalts.

The syenite is a pale grey rock with a fine equigranular texture, which gives rise to massive outcrops with rectilinear joints. On the eastern side of the outcrop, massive syenite is cut by numerous vertical syenite dykes which trend NNE and ESE. These appear to have acted as lines of weakness along which hydrothermal fluids have passed, giving rise to pervasive silicification and thin veins of silica along the margins of the dykes.

Trachyte dykes occur at several localities on the upper eastern and western flanks of Namarunu, but are not common. Some trend NNE and others approximately E–W. Trachyte dykes trending approximately E–W also intrude the trachytic volcanic successions of Nakitoekirion and the Loriu escarpment to the south-west of Namarunu. In the Losergoi area [BN 2300 2320] NW-trending trachyte dykes intrude the Tirr Tirr Series.

Basalt dykes intrude the trachytic pumice tuffs on the lower eastern flanks and acted as feeders to the overlying upper basalt lavas. They trend in two directions, one trend being NE and the other being SE. Several N-trending dykes also intrude the tuff ring on the floor of the Suguta Valley at [BN 2176 2116].

10.5 SYNTHESIS OF THE GEOLOGY AND EVOLUTION OF NAMARUNU AND THE ADJACENT RIFT MARGINS

The earliest phase of volcanism on Namarunu constructed a volcanic shield composed predominantly of trachyte lavas, breccias and tuffs, with minor amounts of mugearite and benmoreite. The rocks of this early

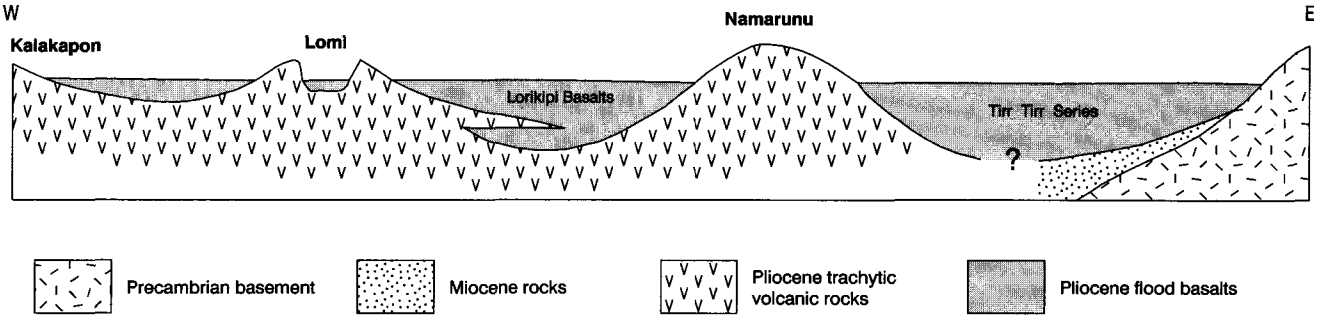

Figure 10.5 Schematic cross section across the rift in the vicinity of Namarunu during the late Pliocene.

trachyte shield are unconformably overlain on the western flanks by flood lavas of the Lorikipi Basalts, which extend westwards onto the rift margin in the Loriu Plateau area.

The Lorikipi Basalts of the Loriu area have yielded a radiometric date of 4.0 ± 0.1 Ma, and melanotrachyte lavas at the top of the basalts in the rift margin escarpment have an age of 2.74 ± 0.02 Ma. In the Loriu Plateau area, the Lorikipi Basalts unconformably overlie trachytic volcanic rocks at Kalakopon which have been dated at 4.4 ± 0.2 Ma. Important trachytic volcanic intercalations also occur within the Lorikipi Basalts along the rift margin, and Lomi volcano, which has yielded a date of 3.0 ± 0.2 Ma, is considered to be one such intercalation.

The age of the early trachyte volcanic shield of Namarunu is uncertain. It must be at least Pliocene in age because it is overlain by the Lorikipi Basalts, and could be a correlative of the trachytic volcanic sequence of Kalakopon. Truckle (1977) rejected a K/Ar date of 6.8 ± 0.5 Ma obtained from a trachyte on Namarunu, but according to the findings of the present survey such an age is acceptable in principle.

On the eastern margin of the rift, the Tirr Tirr Series comprises a layered sequence of flood basalts with subordinate trachytes. The series has yielded radiometric dates in the range 4.2 ± 0.3 Ma to 2.74 ± 0.02 Ma and is therefore correlated with the Lorikipi Basalts.

The Lorikipi Basalts are thickest in the area between the western flanks of Namarunu and the Loriu escarpment, where they rest with strong angular unconformity on altered and faulted trachyte lavas and pyroclastic rocks. The basalt pile thins rapidly to the west and only the uppermost flows extend westwards onto the Loriu Plateau. The basalts also thin eastwards and overstep onto the early trachyte shield of Namarunu. On the eastern margin of the rift, the Tirr Tirr Series is thickest in the escarpment overlooking the inner trough and thins rapidly eastwards. It is concluded from these relationships that the Lorikipi and Tirr Tirr flood lavas were erupted within a faulted depression located over the position of the present day inner trough. The basalt pile eventually infilled this depression and the youngest lavas overflowed its margins. The early (extinct) trachyte volcanic shield of Namarunu was a positive feature within this depression, and younger trachyte volcanoes, such as Lomi, were active along its western margin, locally erupting trachytic intercalations within the Lorikipi Basalts.

The present day inner trough subsided by a combination of downfaulting and monoclinal downwarping, accompanied by large-scale landslipping along its eastern margin. The formation of the inner trough must have postdated the youngest lavas capping the fault block of Nakitoekirion, dated at 2.33 ± 0.02 Ma, and the youngest Lorikipi Basalt lava capping the Loriu Plateau to the north, which has an age of 1.86 ka (Section 11.3.1).

Renewed volcanism commenced on Namarunu in the Upper Pleistocene. Initially rhyolitic and trachytic lavas, tuffs and breccias were erupted, including welded air-fall tuffs. These rhyolitic rocks rest unconformably upon the Lorikipi Basalts and have yielded an age of 871 ± 10 ka. Melanocratic trachyte lavas, which have yielded an age of 840 ± 5 ka, were next erupted on the summit area and upper flanks. Further trachytic pyroclastic activity occurred in the vicinity at about 826 ± 6 ka, as indicated by pumice of this age found in lacustrine sediments on the southern flanks. The next known eruptions were of trachytic pumice deposits and breccias which have an age of 509 ± 5 ka. These accumulated on the lower eastern flanks and on the floor of the inner trough, where they show indications of phreatomagmatic activity within a lacustrine environment. At the top these trachytic pumice deposits grade up into basaltic tuffs and scoria capped by basalt lavas. The gradational compositional change recorded in these deposits is taken as evidence for eruption from a compositionally zoned magma chamber. Voluminous basaltic activity then ensued on Namarunu. Extensive basalt fields were erupted on the northern, western and southern flanks, and include pillow lavas and hyaloclastites that were erupted in the former Lake Suguta. Phreatomagmatic activity took place within the lake to the east of Namarunu, resulting in the formation of a series of tuff rings, tuff cones and scoria cones aligned along the axis of the inner trough. The youngest basaltic activity is of Recent age and post-dates Lake Suguta.

Diatomaceous sediments were deposited within Lake Suguta and are found on the floor of the inner trough and flanks of Namarunu, where they are intercalated with basalt lavas and hyaloclastites. The lake fluctuated in depth in response to climatic changes. Numerous stand lines related to former high lake levels are preserved upon Namarunu, two of which have been dated at 121 ± 20 ka and 10.66 ± 0.2 ka. These correspond with wet palaeoclimatic periods when other lakes in East Africa were also at high levels.

10.6 GEOTHERMAL ACTIVITY

10.6.1 Introduction

Surface geothermal activity within the area is restricted to two zones. By far the most important manifestations are the Elboitong hot springs, which are situated on the eastern side of the Suguta Valley at the base of the Tirr Tirr escarpment. The other zone of activity is associated with the NNE-trending line of young basaltic centres situated along the western side of the Suguta Valley in the vicinity of the Gap.

Extensive areas of hydrothermal alteration and silica veining occur on the upper flanks and summit area of Namarunu. These are no longer geothermally active and have ambient temperatures. There are also reports of relict geothermal features to the north of the Tirr Tirr plateau at Losergoi.

10.6.2 Elboitong hot springs

Hot springs occur along the eastern side of the Suguta Valley around Elboitong [BN 2243 2188] and further north. They include the hottest surface geothermal manifestations in Kenya, with temperatures locally exceeding 100°C.

Although the Elboitong spring system is extensive and vigorous, it would appear to have been more active at the time of its discovery in the 1930's. Champion visited the Suguta Valley in 1932, and on descending from the Loriu Plateau in the west he saw steam at the foot of the escarpment on the eastern side of the valley in the vicinity of Elboitong. Champion estimated that he was 20 miles from the activity, but with the aid of binoculars concluded that he could see a 'large steam-jet' (Champion, 1935). Baker Beall visited the springs in 1932 and observed a geyser named Lokippi, which was surrounded by a well-formed basin of sinter (sic) from which boiling water surged up at regular intervals to a height of 4 feet. The volume of water is reported to have been large and to have been a major source of recharge to the Suguta River, which at this point had almost dried-up (Champion, 1937). From these descriptions, and also from a photograph of Baker Beall's which was reproduced by Champion (1937), it is evident that at the time of these visits the hot springs at Elboitong were very vigorous indeed.

The springs form an almost continuous line of activity along the base of the Tirr Tirr escarpment, extending for a distance of 5.5 km from Elboitong northwards. The only breaks within the spring line occur where two small alluvial fans are built-out from the base of the escarpment onto the floor of the Suguta Valley. These fans divide the spring system into three segments, which for the sake of description are termed the northern, central and southern segments. The spring system is recognisable from the air by the presence of a continuous surface coating of white trona (Plate 10.2). The trona is thin and in the vicinity of the springs overlies waterlogged muds, which render walking conditions difficult and hazardous (Plate 10.8).

The northern part of the system is manifested by seepages and springs which issue along the base of a fault-bounded cliff-line, between [BN 2257 2239] in the north and the alluvial fan at [BN 2260 2224] in the south. Activity is weakest and temperatures are lowest in the north, where only warm seepages and feeble springs occur with temperatures ranging from 30°C up to about 55°C. The strength of the springs gradually increases southwards, although flow-rates are low throughout all of this northern segment. Temperatures increase southwards reaching a maximum recorded value of 89.3°C at the southern end of the section. Gas bubbling occurs within the seepages and springs, increasing in vigour southwards.

The central portion of the spring system extends over a distance of 2 km from [BN 2259 2218] in the north to [BN 2250 2200] in the south, being delimited at both ends by alluvial fans. Here the springs occur along the toe of a major landslip at the base of the escarpment, and extend out onto the alluvium of the valley floor for approximately 50 to 60 m. Activity

Plate 10.8 Part of the Elboitong hot spring area. Looking south towards the Gap, with the landslipped margin of the Tirr Tirr Plateau on the east and Namarunu on the west.

throughout this stretch is vigorous and includes boiling springs, cauldrons and mudpots, all of which are characterised by strong gas bubbling. Temperatures are high throughout this part of the system, reaching local boiling point in most places, and a maximum temperature of 97.2°C was recorded.

The hottest and most vigorous activity occurs in the southern sector of the spring system around Elboitong itself. Here the springs are located along the toe of a major landslip at the base of the escarpment, and also occur on the valley floor in front of the south-west corner of the alluvial fan around [BN 2246 2195]. Activity in this area consists of vigorously boiling springs, many having the form of deep pools. Gas bubbling occurs in all the springs and in the intervening wet ground. Temperatures are mostly around the local boiling point, although in several springs they exceed this, and reach a maximum recorded value of 100.2°C. This is the hottest known surface geothermal activity in the Kenya Rift. At the southern end of the system the springs gradually weaken and pass into an area of hot bubbling seepages before dying out completely at about [BN 2242 2187].

There are signs that ephemeral spring activity occurs sporadically along the base of the escarpment for several kilometres to the south of Elboitong. However, the present survey of this area was undertaken during a drought period and no actual spring activity was observed, so that it is not known whether these ephemeral springs have elevated temperatures.

10.6.3 Geothermal activity on the eastern side of Namarunu

A zone of geothermal activity is associated with the NNE-trending line of young basaltic centres located along the western side of the Suguta Valley, at the base of the eastern flanks of Namarunu. Several patches of hot ground occur at the southern end of this zone and there are a number of hot springs in the north.

Two small areas of hot ground occur upon the ridge of scoria cones. The largest patch occurs at the southern end of the ridge [BN 2187 2147] and comprises a NNE-trending linear zone of reddened and altered scoria, approximately 200 m in length. The ground temperatures in this zone are not particularly high, ranging from ambient up to a maximum recorded value of 60.3°C. At the southern end of this zone several small, very weak fumaroles occur, with temperatures up to 55.1°C. A separate and very small patch of warm ground occurs on the south-west side of the crater rim of the scoria cone on the summit of the ridge at [BN 2185 2157]. A maximum temperature of only 42.2°C was recorded at this locality.

Several hot spring systems are associated with the northern part of the line of young basaltic centres, where it extends across the floor of the Suguta Valley. The activity occurs on the flat alluvium around the flow-front of a small lava flow associated with the remnants of an eroded tuff cone at [BN 2196 2194]. At this locality numerous small bubbling springs issue from the base of the lava front on its eastern and south-eastern side. The hot water discharges into a distributary of the Suguta River and in aggregate flow-rates are high. Recorded temperatures range between 53.5°C and 69.0°C, with the majority of springs being hotter than 60°C. A kilometre to the south of this locality, two warm springs issue on to the alluvium from the base of another basalt lava flow-front at [BN 2196 2186]. One spring is very weak and has a recorded temperature of only 30.0°C, whilst the other has a moderate flow and a recorded temperature of 37.2°C.

An isolated occurrence of warm springs is located on the north-west side of the line of young basaltic centres at [BN 2179 2181]. At this locality two weak springs with recorded temperatures of 32.0°C and 35.0°C are situated upon a minor NNE-trending fault in basalt lavas.

Numerous hot springs are associated with the Crescent tuff ring [BN 2200 2160], which is partly buried in the floor of the Suguta Valley. These issue from the contact with the alluvium on all sides of the tuff ring. Low temperature seepages occur at the western end of the Crescent, but flow rates and temperatures increase towards the eastern end where there are several moderately strong, gas-rich, bubbling springs. Recorded temperatures range from 30.4°C at the western end of the Crescent to 65.5°C at the eastern end. Access to this locality is difficult and should only be attempted during dry periods from the south. Walking conditions around the base of the tuff cone are hazardous at all times because of the hot-waterlogged condition of the surrounding alluvial muds.

10.6.4 Hydrothermal alteration and silica veining on Namarunu

Areas of intensive hydrothermal alteration, now at ambient temperature, are widely distributed on the upper flanks and summit area of Namarunu, and testify to former geothermal activity.

The alteration is exposed in incised valleys on the northern and southern flanks, and at several areas on the upper eastern flanks (Plate 10.9). Extensive areas are partially altered and reddened, but where alteration is advanced the rocks have been converted to red, purple and white kaolinitic clays. Pervasive silicification is found in association with the advanced clay alteration, and some of the reddened rocks have been converted to jasperoid.

Silica veins are widespread and very common on the upper parts of Namarunu. They range in size from small irregular veinlets to massive veins reaching more than a metre in thickness. The veins are composed predominantly of amorphous silica which is laminated parallel to vein margins, and they are interpreted as the conduits of former hot spring systems. No in situ surface spring sinters were recognised during the survey, except possibly in the area just to the south of the summit [BN 2145 2185] where the rocks are pervasively silicified and the ground is strewn with loose blocks of laminated sinter. Four silica vein samples have been dated by U-series methods (Sturchio et al., 1993). One sample gave an age of 133 ± 11 ka, which corresponds with a wet palaeoclimatic period (135 ± 10 ka) when lake levels in the rift were high (Hillaire-Marcel et al., 1986). The remaining three samples were found to be too old to be dated by the method, giving dates of ≥380 ka, ≥440 ka and ≥670 ka, but their high $^{234}U/^{238}U$ values suggest maximum ages of around 1 Ma. These dates indicate that hot spring activity occurred on Namarunu over a long

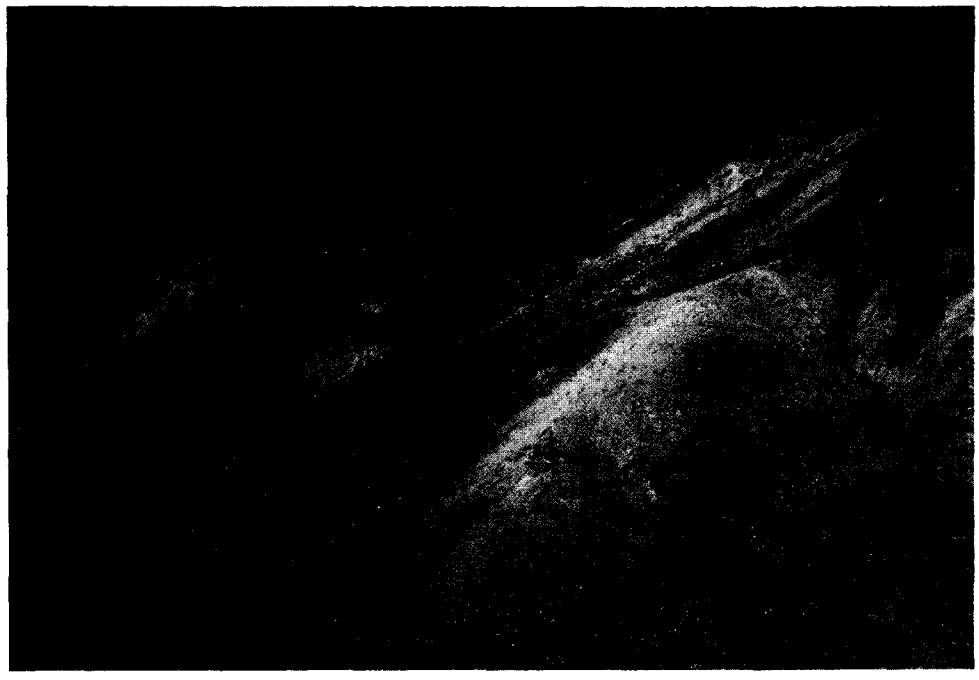

Plate 10.9 Hydrothermal alteration on the upper eastern flanks of Namarunu.

period, and that at least one phase of activity coincided with high lake levels when water tables would have been high.

10.6.5 Travertine at Losergoi

Calcareous travertine deposits are reported to occur on basaltic lavas at an elevation of about 450 m in the Losergoi area, at approximately [BN 2305 2330] (Bosworth and Maurin, 1993). From the descriptions of these deposits they appear to represent travertine mounds that may have developed around former hot springs.

11 The geology and geothermal activity of the Barrier Volcanic Complex

11.1 INTRODUCTION

The Barrier Volcanic Complex (BVC) is situated at 2°20'N, 36°37'E. It forms an E–W trending whale-back ridge, 20 km in length and 15 km wide, which forms a natural dam across the inner trough separating Lake Turkana from the Suguta Valley (Figure 11.1). North to south topographic profiles show this ridge to be a broad symmetrical feature with gently sloping flanks (Figure 11.2). In contrast, east to west profiles display a more rugged outline of coalescing hills, valleys and craters.

This survey recognises, for the first time, that the BVC is a composite structure composed of four distinct volcanic centres. From west to east these are, Kalolenyang, Kakorinya, Likaiu West and Likaiu East (Figure 11.1). They are composed of a wide spectrum of lava types including basanite, basalt, hawaiite, mugearite, benmoreite, trachyte and phonolite. Trachytic pyroclastic deposits cover much of the western slopes of Kakorinya and the summit area of Likaiu West. An estimate of volumes suggests an overall ratio of trachytic to basaltic rocks of about 10:1 (Section 13.2).

The Pliocene foundation rocks of the BVC are well-exposed in the adjacent rift margins. The oldest lavas of the BVC are basalts which occur in the faulted ground east of Lake Logipi and on the north-east flanks at Latarr. Early phases of trachytic volcanism constructed the centres of Kalolenyang and Likaiu East. Kalolenyang volcano rises 828 m above Lake Turkana and abuts against faulted and tilted Pliocene lavas of the Loriu Plateau in the west. To the east of the summit (1193 m) there is a shallow crater, 2 km wide and 50 m deep, which is breached on its northern side. Likaiu East (1197 m) represents the faulted remains of a volcanic shield, 4 km in diameter, which rests with marked unconformity on tilted and landslipped rocks of the eastern margin of the rift. Reactivation of the rift margin faults has produced a westward tilt of 10° to the western flanks of Kalolenyang and downfaulted the greater part of Likaiu East into the inner trough.

The centre of Likaiu West is less well-defined. It forms a low ridge, 5 km in length, which in the west is overlain by younger lavas from Kakorinya and in the east terminates against the fault scarps defining the western limits of Likaiu East. A series of arcuate break-of-slope features on the upper flanks crudely defines the outline of a volcanic shield. This shield is capped by low hills rising to a maximum height of 1134 m at [BN 2370 2572], composed of faulted lava domes and associated pyroclastic deposits. Numerous scoria cones cover the upper flanks of Likaiu West and were the source of extensive flows of basalt and hawaiite which mantle the northern and southern flanks.

Kakorinya volcano forms the central part of the BVC. It is the youngest of the four centres and forms a low shield rising 666 m above Lake Turkana to reach a maximum height of 1031 m on its summit, located on the western side of the volcano (Plate 11.1). Topographic profiles indicate that the shield is broadly symmetrical and has a basal diameter of about 15 km. However, in plan view Kakorinya is slightly elongated in a north-south direction, as a result of the topographic control exerted on the disposition of its eruptive products by the older centres of Likaiu West and Kalolenyang on either side.

The summit of Kakorinya is dominated by a well-preserved circular caldera to the west of which there are two arcuate ring fractures. The caldera, 3.75 km in diameter, is unbreached and partly infilled with lavas and pyroclastic deposits which produce a rough topography on the caldera floor. A number of breached lava domes obscure much of the northern wall of the caldera, and flows from these partly infill the caldera and locally extend down the northern flanks.

Extensive basalt lava fields cover the northern and southern flanks of Kakorinya and include the scoria cones known as Teleki's and Andrew's volcanoes. Teleki's volcano is located at a prominent break of slope on the northern flanks at [BN 2333 2620] and Andrew's volcano is situated immediately south of the caldera at [BN 2307 2550]. Basalts erupted from Teleki's cone extend north to the shores of Lake Turkana, and flows from Andrew's cone extend south to Lake Logipi.

Tuff cones are prominent on both the northern and southern flanks of the BVC. These, together with preserved stand lines and lacustrine deposits, provide evidence for high levels of Lake Turkana and the former Lake Suguta which infilled the inner trough to the south. The likelihood of there having been a hydrographic connection between these two lakes is discussed in Section 11.5.

The BVC is cut by a complex pattern of faulting. Adjacent to the rift margins N-trending faults produce tilted escarpments and affect Likaiu East and Kalolenyang. The central part of the BVC is transected by a series of curvilinear N- to NE-trending normal faults which extend in an *en échelon*, right-stepping fashion across the volcano, from the south-western flanks of Kakorinya to the northern flanks of Likaiu West.

11.2 PREVIOUS WORK

The BVC and the parasitic scoria cone of Teleki's volcano were discovered in 1888 by Count Samuel von Teleki during his expedition to lakes Turkana (Rudolph) and Stephanie (Von Hönel, 1894). At this time volcanic activity was observed on Teleki's volcano and on South Island in Lake Turkana. Subsequent expeditions to the south Turkana area failed to locate Teleki's volcano and confusion arose over its existence and supposed location (Cavendish, 1898; Welby, 1900). In the 1930's Teleki's volcano was rediscovered (Champion, 1935, 1937; Fuchs, 1934, 1939) and a similar cone, Andrew's volcano, was discovered on the southern flanks above the shores of Lake Logipi. The term 'volcano', as used by the early explorers for these

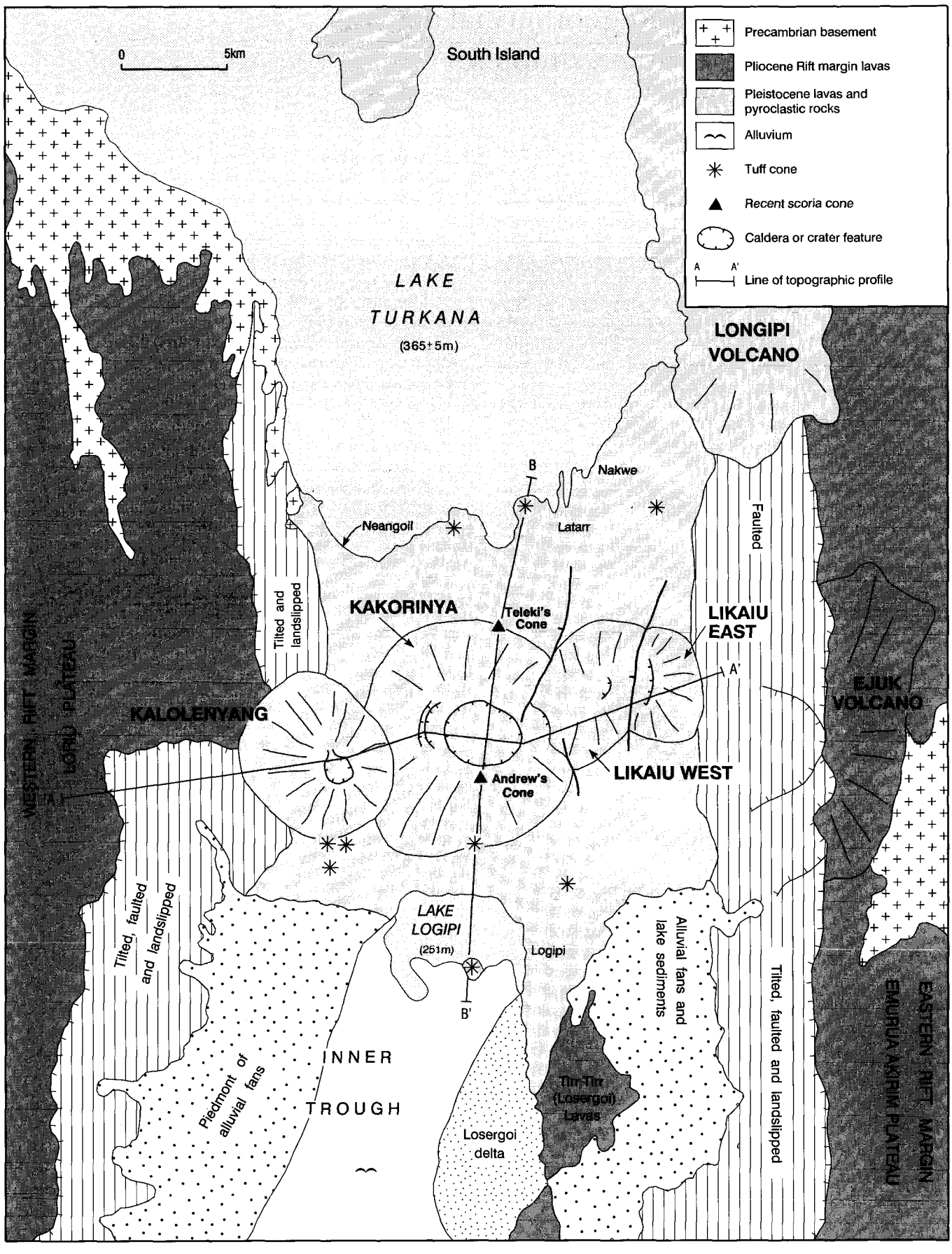

Figure 11.1 Physiography of the Barrier Volcanic Complex and adjacent rift margins.

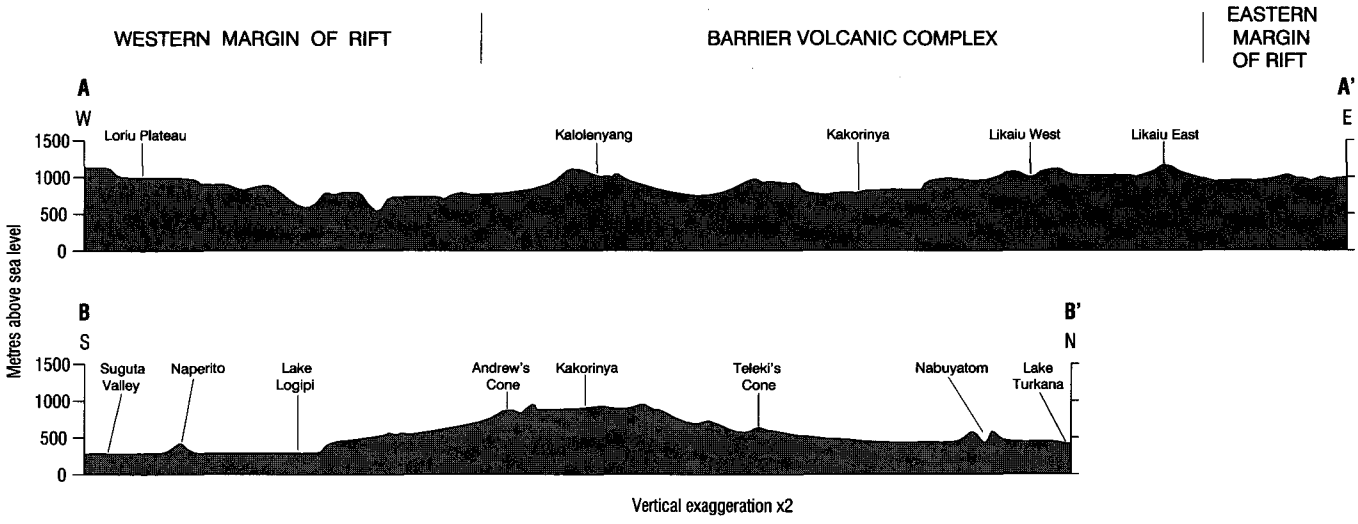

Figure 11.2 Topographic profiles across the Barrier Volcanic Complex.

two scoria cones is considered to be misleading and inappropriate. Neither cone is sufficiently large to merit the term, and the only feature that distinguishes them from numerous other parasitic cones scattered over the BVC is their pristine state of preservation. For this reason, the terms Teleki's cone and Andrew's cone are recommended for future use and will be used in the following account.

The first geological map of the BVC was produced by Dodson (1963). This map, based on a reconnaissance survey, contains many inaccuracies and has been completely revised. Dodson subdivided the succession of the BVC into four. His first phase of subaerial 'agglomerates' were erupted from a central edifice which cut off Lake Turkana from the former Lake Suguta. Later phases erupted basaltic ash cones on the lower flanks and phonolites and pyroclastic deposits on the upper slopes. Dodson's final phase resulted in the eruption of basalts and basanites which mantle the lower flanks. In a more recent review of the BVC using Dodson's map and augmenting it with air-photograph interpretation, Williams et al. (1984) proposed that an older, outer caldera may exist on Kakorinya.

Petrological studies of the lavas of the BVC commenced with the descriptions of the specimens collected by Champion (Campbell Smith, 1938). Basalts, trachytes and phonolites in the vicinity of Teleki's cone have also been described and analyzed by Brown and Carmichael (1971) and more recently by Bloomer et al. (1989).

Geophysical data for the area are sparse. A gravity profile was measured by Khan and Swain (1978) across the Suguta Valley immediately south of the BVC, and a more recent traverse has been carried out by AMOCO from the north-west of the map area along the shores of Lake Logipi towards Parkati village. However, no interpretation of these data is currently available. Finally, the southern Turkana basin and the northern Suguta Valley are areas of intense microseismic activity (Pointing et al., 1985). Up to 11 microearthquakes a day have been recorded in the area between Lake Alabalab and Lake Logipi.

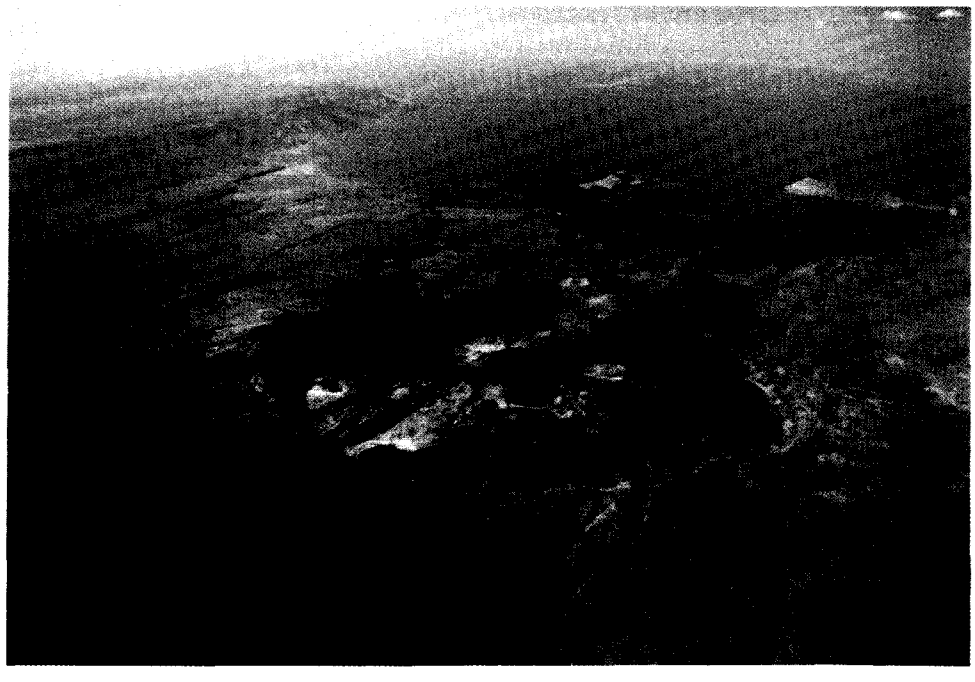

Plate 11.1 Aerial view looking north across Kakorinya caldera towards the southern shores of Lake Turkana. The outer ring fractures are visible to the west of the caldera. The young lavas in the caldera are phonolites. Andrew's cone can be seen to the south of the caldera rim.

11.3 STRATIGRAPHY OF THE RIFT MARGINS IN THE VICINITY OF THE BARRIER VOLCANIC COMPLEX

11.3.1 Western margin of the rift

Precambrian basement (Pc) is exposed in a series of linear outcrops forming the western shores to Lake Turkana and extends as far south as [BN 2243 2685]. No visits were made to these outcrops during the present survey, but according to Ochieng' et al. (1988) they consist of biotite gneisses with a steep easterly dipping foliation trending NNE–SSW.

The overlying **Lorikipi Basalts (LB)** make up a large part of the Loriu Plateau along the western margin of the rift. They are exposed in numerous stream sections dissecting the eastern margin of the plateau, and thin northwards as they overstep onto Precambrian basement. During the present survey a section was logged through the escarpment to the west of the BVC, starting at [BN 2157 2580]. At the base of this section an intrusive microsyenite with xenoliths of basement gneiss is exposed. Above, are 70 m of strongly microporphyritic basalt lavas with phenocrysts of olivine, pyroxene and feldspar and cognate xenoliths of gabbro. Midway up the section a thin trachytic welded tuff is underlain by buff to brown pebbly grits and sandstones. This band forms a prominent marker which can be traced around the adjacent valley sides. The remainder of the section comprises about 100 m of thin, sparsely microporphyritic to aphyric basalts. The topmost flow capping the plateau at [BN 2150 2580] is a hypersthene-normative hawaiite which has yielded a step heating Ar/Ar age of 1.86 ± 0.04 Ma.

North-west of Kalolenyang the Lorikipi Basalts are overlain by a distinctive reddish-orange weathering cap composed of rhyolitic and benmoreitic lavas, interbedded with thin bands of pumice and crystal-rich tuff. These lavas, termed the **Loriu Plateau Trachyte (LP^t)** were observed at [BN 2227 2601] where they rest conformably on the Lorikipi Basalts and can be traced northwards as a cap rock to tilted strata overlying Precambrian basement. Scattered outcrops occur as far south as [BN 2205 2570] and are overlain by lavas from Kalolenyang and by the younger basalts of the Loriu Plateau. In the Naitai area of the Loriu Plateau, 12 km south-west of the map area, Ochieng' et al. (1988) recorded pyroclastic deposits and phonolitic trachytes associated with a number of intrusions (their Naitai Trachytes). These trachytes may be contemporaneous with the Loriu Plateau Trachyte. The hill of Emuruanyangan [BN 2148 2555] is an alkaline intrusive body of foyitic affinity (Ochieng' et al. 1988) associated with NNE-trending dykes.

Locally the surface of the Loriu Plateau is mantled by thin basalt flows. These lavas clearly post-date the Lorikipi Basalts and the Loriu Plateau Trachytes but cannot be distinguished everywhere and are therefore not differentiated on the accompanying 1:50 000-scale geological map. They were erupted from small scoria cones on top of the Loriu Plateau, which are cut by E–W and N–S trending dykes. On air-photographs and in outcrop, these lavas have a fresh, unvegetated appearance. They flowed both westwards into the Kerio Valley, and eastward over the faulted rift margin into the Suguta Valley. These lavas are nepheline-normative and are of Quaternary age (see Section 10.3.2.3).

11.3.2 Eastern margin of the rift

The eastern margin of the rift is also dominated by a thick pile of layered basalts termed the **Parkati Basalts (P^b)**. The informal name for these lavas is derived from the gorge section south-east of Parkati village at [BN 2450 2425], where in excess of 300 m of layered basalt lavas with thin scoriaceous bands and reddish altered tuffs are exposed. Eastward, the sequence thins rapidly and oversteps onto Precambrian basement. The Parkati Basalts correspond to Dodson's 'Porphyritic basalts' which he considered to be broadly equivalent to the Samburu Basalts of Miocene age (Dodson, 1963). However, the morphology, petrography and chemistry of these basalts is unlike the Miocene basalts and shows more affinity with the Pliocene lavas of the Loriu Plateau. Exposures in stream sections north-east of Likaiu East reveal gently dipping sequences of fine-grained, sparsely microporphyritic, weakly nepheline-normative basalts (0.12–0.17% *ne*). Several ENE-trending dykes were observed at the base of the sections. A sample of altered basalt collected in the Losergoi river immediately to the south of the area has yielded a K/Ar date of 4.2 ± 0.3 Ma (Bosworth and Maurin, 1993). The basalts of the Tirr Tirr Series (Section 10.2.2) to the south of Losergoi are thought to be correlatives of the Parkati Basalts to the north.

To the east of the BVC, the crest of the eastern margin of the rift is dominated by the deeply dissected remnants of a large Pliocene shield volcano. This volcano, called Ejuk (Iyuk), is composed of coarse-grained, feldspar-phyric trachytes, glassy rhyolites and pyroclastic deposits (**Ejuk Trachytes (E^t)**) which have flowed radially away from a summit area located immediately to the east of the map. On air-photographs and satellite images these rocks have a distinctive high reflectance. Originally Ejuk volcano had a basal diameter in excess of 15 km and may have contained a summit caldera, but all of the western part of the volcano is now landslipped and downfaulted into the inner trough and partly buried by younger rocks. An Ar/Ar date of 4.53 ± 0.03 Ma was obtained from an outlier of Ejuk rhyolite lavas at [BN 24962428] which are intercalated with the upper parts of the Parkati Basalt sequence.

Northwards, the eastern margin of the rift consists of young basalt lavas that were erupted from Longipi volcano, located on the eastern shores of Lake Turkana. The **Longipi Basalts (LO^b)** outcrop in the extreme north-east corner of the accompanying 1:50 000-scale map but were not visited by the present survey. Here they consist of olivine basalt lavas interbedded with lacustrine sediments and thin tuffs, and further north contain pillow lavas and tuff cones. Key (1987) thought the Longipi Basalts are overlain by lavas from Kulal volcano dated at 1.91 ± 0.21 Ma. However, air-photograph interpretation indicates that lavas from Longipi overlie the Kulal basalts, and they also post-date the Parkati Basalts and the Ejuk Trachytes. Sections in the Serima gorge described by Fuchs (1939, p.256, figure 13) expose two sequences of olivine basalt lava separated by 1–2 m of gravel and

conglomerate composed of fragments of lava and fossiliferous limestone. By comparison with other lake deposits around Lake Turkana (300 ft level) a Middle Pleistocene age seems more likely. The uppermost 76 m of basalt lava oversteps eastward onto Precambrian basement and is intruded by N-trending dykes.

At the Nakwe delta [BN 2415 2700] a small outcrop of basalt lava with two eroded scoria cones is tentatively assigned to the Longipi Basalts and appears to be morphologically younger than the faulted Latarr basalts immediately to the south.

11.3.3 Tectonics and landslips of the rift margins

Volcanicity and rifting in the area commenced with the eruption and ponding of the Lorikipi and Parkati Basalts in a gentle downwarp which had formed by about 4 Ma (Section 10.6). The boundaries to this downwarp were defined by incipient monoclinal structures located above faults in the Precambrian basement which had a considerable topography at this time. In response to regional extensional stresses this downwarp rapidly subsided to form the inner trough. As subsidence took place the steep limbs of the monoclines were faulted and the beds tilted by up to 40° into the inner trough (Plate 11.2). Intimately associated with this tilting and faulting was the widespread development of landslip deposits.

Landslips are present along the escarpments of both margins of the rift and affect all strata of the Loriu Plateau, the Parkati Basalts and the Ejuk Trachytes. The younger strata of the BVC and the Longipi Basalts are unaffected. A maximum age for the collapse of the inner trough is given by an Ar/Ar date of 1.86 ± 0.04 Ma from the topmost Lorikipi Basalt on the Loriu Plateau (Section 11.3.1). The landslips contain coherent rafts of strata and completely chaotic deposits. Disruption is most intense across the faulted, steep limbs of the monoclinal folds, particularly where intercalations of poorly consolidated lacustrine sediments and volcaniclastic deposits occur within the basaltic lavas.

11.4 THE STRATIGRAPHY OF THE BARRIER VOLCANIC COMPLEX

11.4.1 Introduction

The older rocks making up the bulk of the BVC are not exposed, although dissection of the flanks of Kalolenyang and Likaiu East, and exposures around the caldera of Kakorinya provide sections in the upper parts of these centres. The stratigraphy of the BVC is summarised in Table 11.1.

Prior to this survey no age determinations had been carried out on the rocks of the BVC. Eight Ar/Ar dates obtained by the present survey indicate that volcanic activity commenced shortly after the formation of the inner trough and has continued to within the last century. The age of certain volcanic events is further constrained by lake stand lines, which suggest that much of the volcanic complex had been constructed by about 121 ka. Palaeomagnetic studies (Skinner et al., 1975) also provide additional information, indicating ages in the range 1050 ± 150 to 1883 ± 5 AD for basalts on the northern flanks, which is in good agreement with the historical evidence for activity.

Some confusion surrounds the naming of features on the BVC, but where practicable this survey uses the names shown on the published 1:100 000 topographical map. Originally the BVC was named Likaiu (or Likaiyo, or Likaiyiu) by Champion (1935), but this name has also been applied to a small basalt scoria cone on the southern flanks. The term Likaiu was later used by Dodson for the eastern part of the BVC and is also shown there on the published topographic map. Dodson preferred to use 'Nagaramsainia' or 'The Barrier' both of which are shown on his map at Kalolenyang. The word 'Lugugugut', meaning 'place that is burnt' in Turkana, has been used for both Teleki's and Andrew's cones but is not used here. Other prominent geological features and their alternative names are: Abili Agituk (Wargess); Andrew's cone (Likaiu); Lake Logipi (Namakat, Lukula); Nabuyatom (Naboiyoton); Namurinyang (Murniau); Naperito

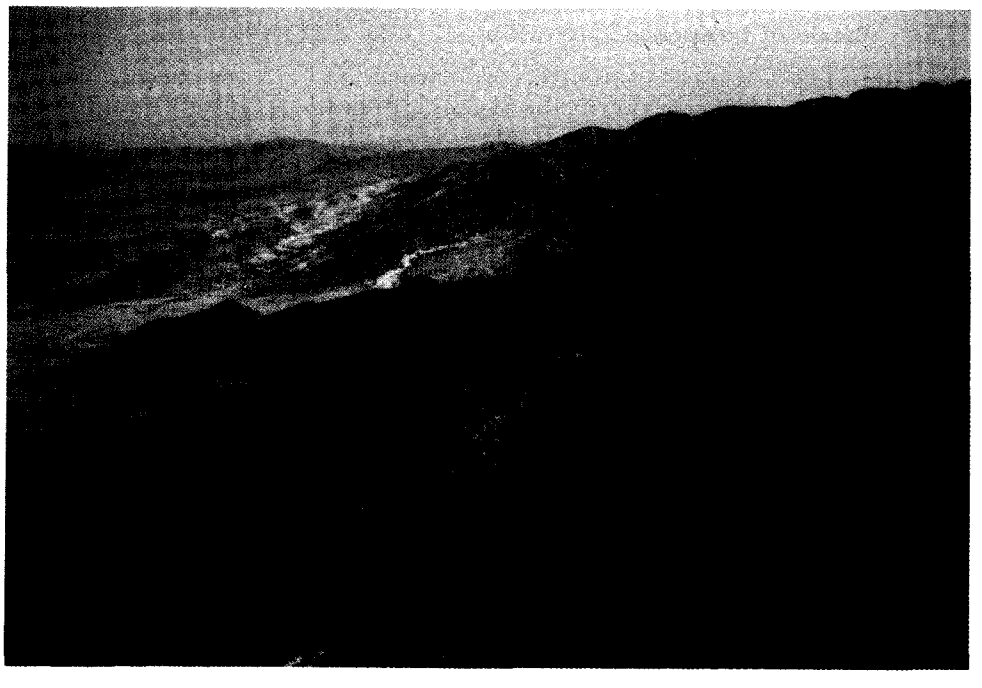

Plate 11.2 Parkati Basalts tilted into the inner trough along the eastern margin of the rift, south-east of the Barrier Volcanic Complex.

Table 11.1 Stratigraphy of the Barrier Volcanic Complex

KAKORINYA VOLCANO	
Recent Basalts and Mugearites (K^{by}, K^{my})	1 ka – 1888 AD
Recent Phonolites (K^{py})	
Upper Basalts (K^{bu})	
Trachyte lavas and domes (K^{t})	58 ± 4 ka
CALDERA FORMATION AND FAULTING	
Pyroclastic deposits (K^{vu})	92 ± 2 ka
Trachyte lava domes (K^{td})	
RING FRACTURE AND FAULTING	
Lower Basalts (K^{bl})	
Upper Trachytes (K^{tu}) including pyroclastic deposits	221 ± 4 – 97 ± 3 ka
Lower Trachytes (K^{tl}) including pyroclastic deposits	
FAULTING	
LIKAIU WEST VOLCANO	
Hawaiite lavas (LW^{h}) and Basalt lavas (LW^{b})	
Trachyte and phonolitic pyroclastic flow and breccia deposits (LW^{v})	
Trachyte, phonolitic and benmoreite lavas (LW^{t}) with pyroclastic deposits (LW^{tv})	
Basalts of Namurinyang tuff cone (N^{b})	
FAULTING	
KALOLENYANG VOLCANO	
Mugearite lavas (KL^{m})	
Basalt lavas (KL^{b})	
Trachyte lavas (KL^{t}) and pyroclastic flow deposits	773 ± 7 – 707 ± 6 ka
LIKAIU EAST	
Trachyte lavas (LE^{t}) and pyroclastic flow deposits	1.37 – 1.34 Ma
FOUNDATION ROCKS	
Basalt lavas of Logipi and Latarr (B^{b})	

(Lengerungi or 'Cathedral Rock'); Teleki's cone (Nagira Mwaiten, Luburrua).

11.4.2 Basalts of Logipi and Latarr (B^{b})

The oldest exposed rocks of the BVC are porphyritic olivine basalts which crop-out in the faulted ground immediately to the east of Lake Logipi and in the region of Latarr, south-east of Lake Turkana.

East of Lake Logipi, dark grey basalts form a series of sheet-like flows which are faulted and have a westerly tilt of between 5 and 10° (Plate 11.3). Individual flows are 5–10 m thick and a total thickness of about 50 m is exposed, although scree deposits obscure the base of the sequence so that contact relationships with the underlying rocks have not been observed. On air-photographs the dip slopes typically show a uniformly smooth, pale grey texture, which results from a thin veneer of lacustrine and pyroclastic flow deposits. Thin beds of yellow volcaniclastic deposits and reddened fluviatile sandstones are intercalated with the lava flows.

Further east, sections in the Lenchukuti stream bed at Lotipe [BN 2373 2468] expose olivine-phyric and pyroxene-phyric basalt lavas. Downstream, where these lavas overlie a small buried fault scarp at [BN 2373 2466] they are tilted gently to the south and pass into one of the most spectacular sequences of pillow basalts seen in the Kenya Rift (Plate 11.4). These flows can be traced northwards where they form the oldest rocks exposed in a fault scarp due east of Namurinyang tuff cone (Section 11.4.3). A number of small eroded and faulted basaltic scoria cones to the south-west of Namurinyang may represent source areas for these flows. Further west, basalt flows associated with degraded scoria cones are exposed beneath the younger trachyte lava and pyroclastic deposits which cover the south-western flanks of Kakorinya (Figure 11.7b). These are petrologically similar to the Logipi basalts but their age is uncertain.

On the north side of the BVC the Latarr basalts are morphologically and geochemically identical to the Logipi basalts. Here too, they are faulted and tilted to the west. They are overlain by hawaiitic lavas of Likaiu West and historic flows from Teleki's cone.

The age of the Logipi and Latarr basalts is poorly constrained. South of the Lenchukuti river the Logipi basalts interdigitate with lacustrine and fluvial sediments and rest conformably on basalts of the Tirr Tirr Series which in the Losergoi area have yielded dates in the range 3.8 ± 0.2 to 2.3 ± 0.4 Ma (Bosworth and Maurin, 1993). The division between the two groups of

Plate 11.3 Tilted and faulted Logipi Basalts along the eastern margin of the inner trough south-east of the Barrier Volcanic Complex.

Plate 11.4 Pillowed Logipi Basalts in the Lenchukuti stream, south-east of the Barrier Volcanic Complex.

basalts is supported by a marked compositional contrast; the Logipi basalts are strongly undersaturated, having between 4.5% and 7.5% normative nepheline, whereas the Tirr Tirr Series consists of transitional basalts with less than 0.3% normative nepheline. The oldest lavas from Likaiu East, dated at 1.37 Ma, are nowhere seen in contact with the Logipi basalts but on the northern flanks they overlie the Latarr basalts. This suggests that the Logipi and Latarr basalts were erupted before 1.37 Ma, but after the formation of the inner trough which has a minimum age of 1.86 Ma (see Section 11.3.3).

11.4.3 Basalts of Namurinyang tuff cone (N^b)

Namurinyang [BN 2345 2495] is one of the oldest tuff cones on the southern flanks of the BVC. It is a deeply eroded, symmetrical cone, 1.4 km in diameter, which rises 188 m above the Logipi basalts to reach a maximum height of 734 m. The inner crater of the cone is infilled with a distinctive dark porphyritic olivine basalt lava which flowed out through a breach in the southern wall. This lava rests conformably on the Logipi basalts and is tilted up to 10° to the west. Both the cone and the underlying lavas are dissected by N-trending normal faults.

In the fault scarp immediately to the east of the cone, beds of palagonite tuff derived from Namurinyang are interbedded with baked and disrupted fossiliferous silts and clays, locally overlain by up to 2 m of gravel containing shell fragments (Dodson, 1963 p.32). Overlying these beds is a welded pyroclastic flow from Likaiu West. The oldest exposed trachyte lavas from Kakorinya abut against and flow around the

northern flanks of the cone. These relationships suggest that Namurinyang pre-dates both Likaiu West and Kakorinya.

11.4.4 Kalolenyang volcano

The western side of the BVC was originally mapped by Dodson as 'pumice and ash' which post-dated his third phase of basaltic activity. However, the morphology of Kalolenyang and disposition of lava flows clearly indicate that it is a separate volcanic centre (Plate 11.5). Kalolenyang is composed mainly of comenditic trachytes, mantled by basalt and mugearite lavas (Figure 11.3).

11.4.4.1 Trachytes and pyroclastic flow deposits (KL^t)

Dissection of the southern and northern flanks of Kalolenyang has exposed sections through the early trachyte lavas and pyroclastic flows. The trachytes weather to a reddish-brown colour and on air-photographs are distinguished as a series of thin flows with lobate flow-fronts. Individual flows have rubbly scoriaceous bases and irregular tops and extend for up to 2.75 km down the flanks. The majority of flows contain abundant feldspar phenocrysts and locally, syenitic xenoliths. One of the oldest trachytes exposed on the lower southern flanks at [BN 2241 2536] has yielded an Ar/Ar date of 773 ± 7 ka.

The interbedded pyroclastic flow deposits extend from the summit area down the southern flanks to the Suguta Valley, where they are overlain by alluvial gravels and lake sediments. On the northern flanks, isolated outcrops in valley floors indicate that pyroclastic flows also flowed across the faulted and landslipped topography at the foot of the Loriu Plateau. The deposits mantle the irregular surface of the underlying lavas and consist of grey-green, welded and non-welded tuffs up to 40 m thick, with coarse, lithic-rich bases.

The radial disposition of the lavas and pyroclastic flows indicates a central source located on the summit of Kalolenyang. Parasol-type drainage patterns and pale photo-tones indicate a small parasitic cone immediately to the west of the summit area. Collapse of the summit area to form a crater, 1.75 km in diameter, followed soon after the final trachyte eruptions. The original depth of the crater is unknown as it is largely infilled with younger air-fall deposits from Kakorinya. The crater walls reach a maximum height of 50 m in the west and south-east where they expose the youngest welded pyroclastic flows and trachyte lavas. One of the youngest lavas exposed in the south wall at [BN 2244 2558] has yielded an Ar/Ar date of 707 ± 6 ka. A single trachyte dyke trending N–S was observed on the upper northern slopes [BN 2225 2595] and may have been a feeder to one of the uppermost flows.

11.4.4.2 Basalts and mugearites (KL^b, KL^m)

Later events on Kalolenyang were dominated by basaltic activity. Olivine-phyric and feldspar-phyric basaltic lavas were erupted from small scoria cones on the south-eastern, north-eastern and upper western flanks (Figure 11.3). Within the summit crater, basalts erupted from a small scoria cone located close to the north-western wall flowed out through a breach to mantle the northern flanks. Immediately to the north-west of the summit crater, a prominent hill capped by younger air-fall tuffs may represent a separate eruptive centre. Thin rivulet-like flows of vesicular basalts from this centre extend down the west flanks. The south-western flanks of Kalolenyang are covered by an extensive field of mugearite lava which was erupted from a complex of scoria cones west of the summit area at [BN 2220 2560]. These lavas mantle the early trachytic rocks and extend westwards to rest unconformably on the Lorikipi Basalts.

The youngest phase of activity on Kalolenyang is represented by a cluster of eroded and faulted tuff cones which occur low on the southern flanks at heights of between 400–460 m. These cones are associated with raised beach deposits and lacustrine sediments and are correlated with a high stand of the former Lake Suguta dated at 121 ± 20 ka (Section 11.4.9).

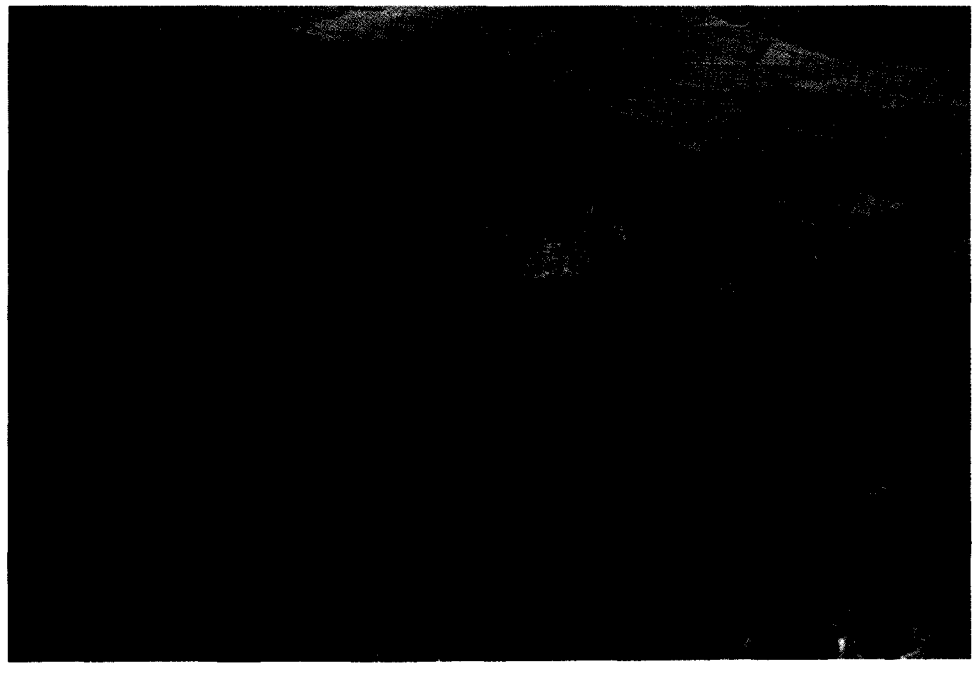

Plate 11.5 Aerial view of Kalolenyang volcano, looking north.

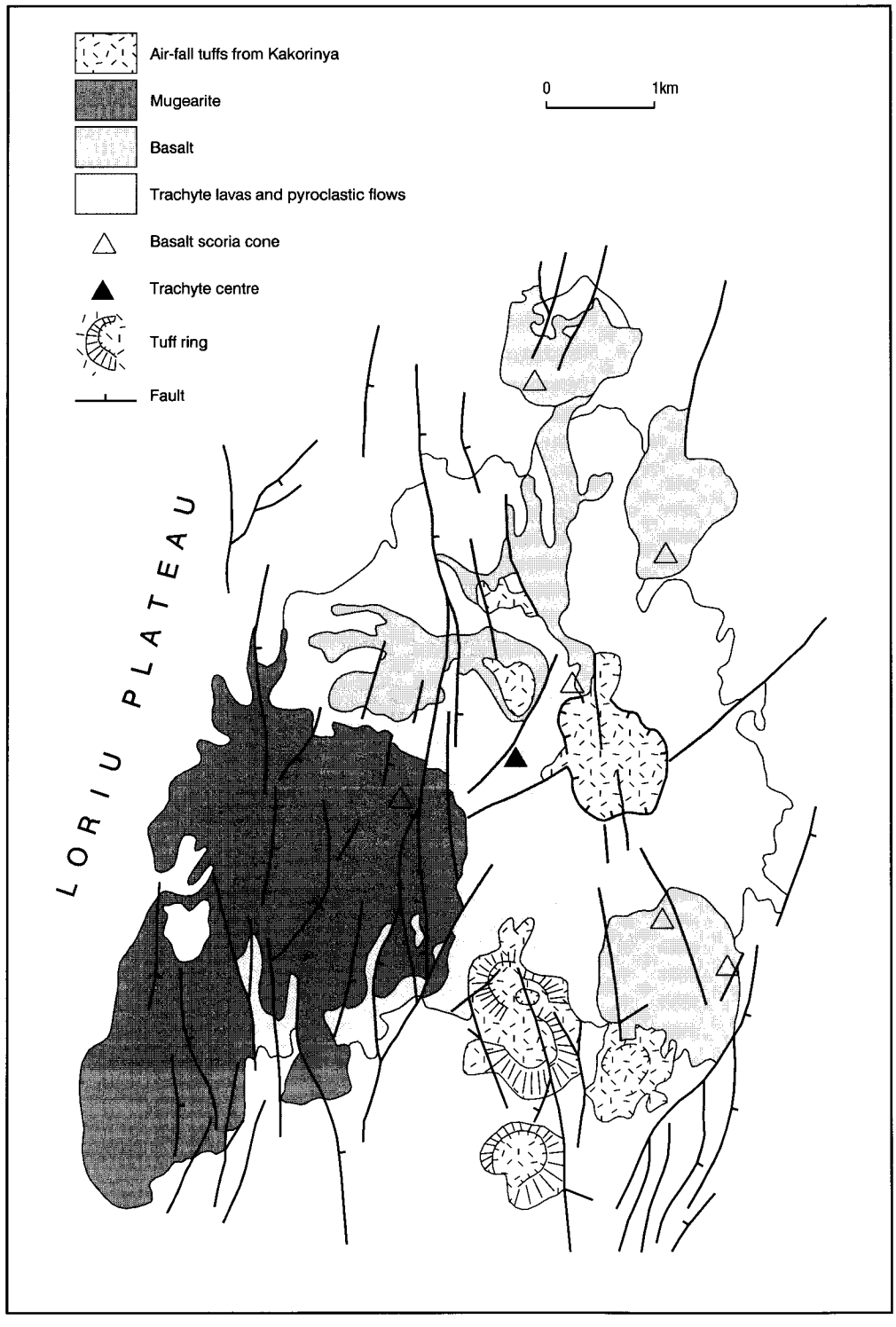

Figure 11.3 Simplified geological map of Kalolenyang volcano.

11.4.5 Likaiu East

The volcanic centres of Likaiu East and West (Figure 11.4) were mapped by Dodson as agglomerates (sic), overlain by later basalts and basanites. Likaiu East is morphologically similar to Kalolenyang but much of its original form is now obscured by faulting and by a cover of younger deposits from Likaiu West.

Likaiu East is composed of weakly silica-undersaturated trachyte lavas and pyroclastic-flow deposits (LE^t). They are exposed in numerous stream sections which dissect the southern and northern flanks, and in the east they rest with marked unconformity on tilted Parkati Basalts. In the middle and upper parts of the volcano the trachyte lavas are flow-folded and display a distinctive banded or streaky and clotted texture suggestive of mixing of two trachyte magmas. The lavas are overlain by, and interbedded with, welded pyroclastic flows, locally up to 30 m thick. These contain coarse blocks of lithic material including syenite. The bases of individual flows are strongly welded, whereas the upper parts are often non-welded.

The radial disposition of the pyroclastic flows and lavas suggests that Likaiu East had an original basal diameter of about 4 km. The oldest exposed trachyte lava in the lowermost stream sections on the southern flanks at [BN 2400 2562] has an Ar/Ar age of 1.37 ± 0.02 Ma, and on the summit area the youngest trachyte

Figure 11.4
Simplified geological map of Likaiu East and Likaiu West volcanoes.

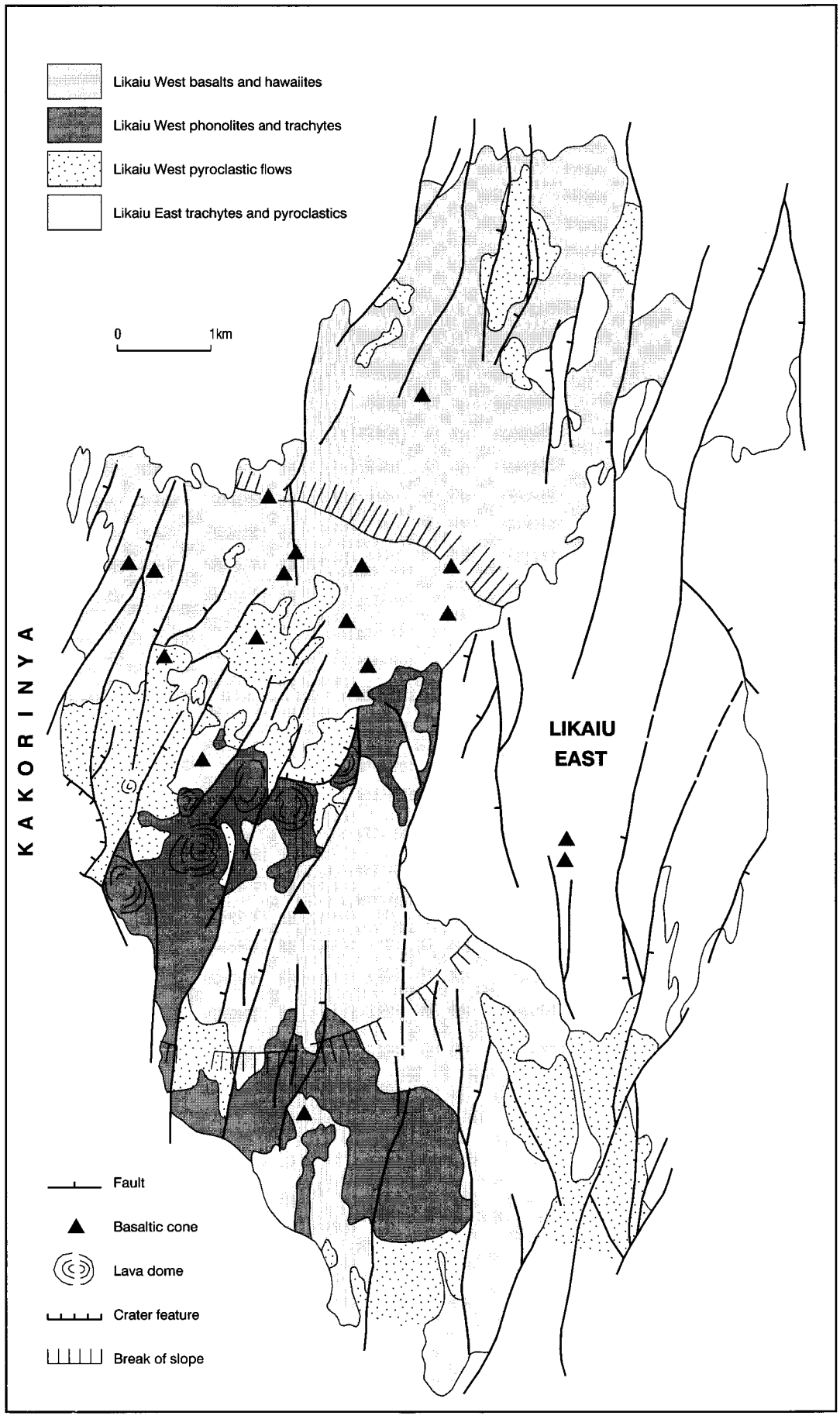

at [BN 2399 2580] has an Ar/Ar age of 1.34 ± 0.01 Ma. The bulk of the volcanic edifice is not exposed and must be older.

11.4.6 Faulting

Both Kalolenyang and Likaiu East post-date the formation of the inner trough, but were subsequently affected by renewed movement along the rift margin structures and are cut by N-trending normal faults. This period of movement downfaulted the western half of Likaiu East prior to the eruption of Likaiu West and may have been contemporaneous with faulting of the basalts of Latarr and Logipi.

11.4.7 Likaiu West

The geology of Likaiu West is poorly understood because its flanks are relatively undissected and its succession is poorly exposed. Field relationships combined with air-photograph interpretation show that it post-dates the faulting which cuts Likaiu East, and was itself faulted before the Upper Trachytes of Kakorinya were erupted. However, the youngest phase of basaltic activity post-dates the faulting of the Upper Trachytes and is probably contemporaneous with the Upper Basalts of Kakorinya.

11.4.7.1 Pyroclastic flows (LW^{tv})

The oldest exposed deposits of Likaiu West occur on the lower southern slopes where a series of non-welded and welded pyroclastic flows and debris flow deposits ('agglomerates' of Dodson, 1963) outcrop beneath the lava fronts of the younger trachytes from Kakorinya. In the south and east these flows rest on fluvial conglomerates and lake sediments and extend up to 3.5 km south of Namurinyang. Eastward they overlie the Parkati Basalts but their westward extent beneath Kakorinya is unknown.

The pyroclastic flows consist of sheet-like units, 3–5 m thick, of yellow, grey and brown, welded pumice lapilli tuffs with abundant lithic clasts. In total the deposits are exposed over an area of about 60 km^2. Arcuate faults surround a 1 km wide depression on the eastern side of Likaiu West at [BN 2377 2580] (Figure 11.4) which may represent the remnants of a crater feature associated with the eruption of these pyroclastic flows.

On the lower south-eastern flanks there is evidence that the pyroclastic flows either entered into water or flowed over a water saturated substrate. Sections in the Lenchukuti river near Lotipe [BN 2370 2476] expose a welded pyroclastic flow resting on fluvial conglomerates, and 1.5 km upstream the same flow is intercalated within diatomaceous sediments. The lower part of the flow has incipient welding fabrics, vertical gas segregation structures and chilled rims to pumice clasts attesting to its hot state during emplacement. The upper parts are strongly welded and overlain by a thin, stratified band of pumice lapilli deposits and ash. The same flow is exposed in the fault scarp east of Namurinyang. Here the base of the flow is highly irregular and contains sub-vertical pipes of welded tuff, up to 10 m in length, which extend down into the underlying lacustrine sediments (Figure 11.7a).

The age of these pyroclastic flows is unknown. They post-date Likaiu East (1.34 Ma) and Namurinyang tuff cone, and are overlain by trachytes and pyroclastic deposits from Kakorinya dated at 221 ± 4 ka.

11.4.7.2 Trachyte lavas, lava domes (LW^{t}) and pyroclastic flows (LW^{v})

Later events on Likaiu West constructed a series of lava domes and short viscous flows across the summit area. These domes, 0.5–1 km in diameter and up to 120 m high, comprise benmoreites, trachytes and phonolites. They are associated with friable pyroclastic flow and mass-flow deposits which extend for 7 km down the northern flanks. The domes are considered to represent resurgent activity on a series of trachytic pyroclastic cones which define the main eruptive centre of Likaiu West. Contemporaneous eruptions from a parasitic centre on the lower southern flanks produced a number of viscous trachyte lavas with high flow-fronts and prominent pressure ridges.

An important phase of faulting affected Likaiu West and the eastern margin of the BVC prior to the eruption of younger basalt and hawaiite lavas and the initiation of activity on Kakorinya. A 4 km-wide zone of N-trending normal faults, showing complex interlinking patterns, affected the Logipi Basalts and summit area of Likaiu West, and extends northwards to the Latarr Basalts. Strata were tilted westwards by up to 10° and displacements are generally less than 30 m.

11.4.7.3 Basalt (LW^{b}) and hawaiite (LW^{h}) lavas

During the final phase of activity on Likaiu West, fluid basalts and hawaiites were erupted from scoria cones located on the summit and upper northern flanks. The summit trachyte domes were intruded by ENE-trending basaltic dykes, and scoria cones were constructed upon them. These basaltic lavas post-date the Upper Trachytes of Kakorinya, and may therefore be equivalent to the Upper Basalts of that centre.

Basaltic lavas cascaded northwards over the faulted terrain of the Latarr basalts towards Lake Turkana to cover an area of more than 30 km^2. The southern and eastern flanks of Likaiu West are mantled by contemporaneous hawaiites which cover an area of more than 20 km^2. These were erupted from the faulted eastern half of the summit area and from minor centres on the southern flanks, and they extend for 10 km downslope where they rest on the Parkati basalts north-west of Parkati village.

11.4.8 Kakorinya Volcano

11.4.8.1 Lower Trachyte Lavas (K^{tl})

Scattered outcrops of the Lower Trachyte Lavas are exposed around the lower flanks of the volcano (Figure 11.5) and consist of silica-undersaturated trachytes interbedded with thin ash-flow and air-fall tuffs. On the southern flanks north of Namurinyang one of the oldest exposed trachytes rests directly on the Logipi Basalts. Morphologically and geochemically similar trachytes outcrop from beneath basalts on the lower north-western flanks of Kakorinya. Here, they occur in a number of arcuate outcrops which represent the fronts of a series of lobate flows which can be traced as far east as Teleki's cone. Further west, these lavas are down-faulted and buried by pyroclastic deposits.

The Lower Trachytes are composite lavas with flow-fronts 30–50 m high. They are fissile and sparsely

Figure 11.5 Simplified geological map of Kakorinya volcano.

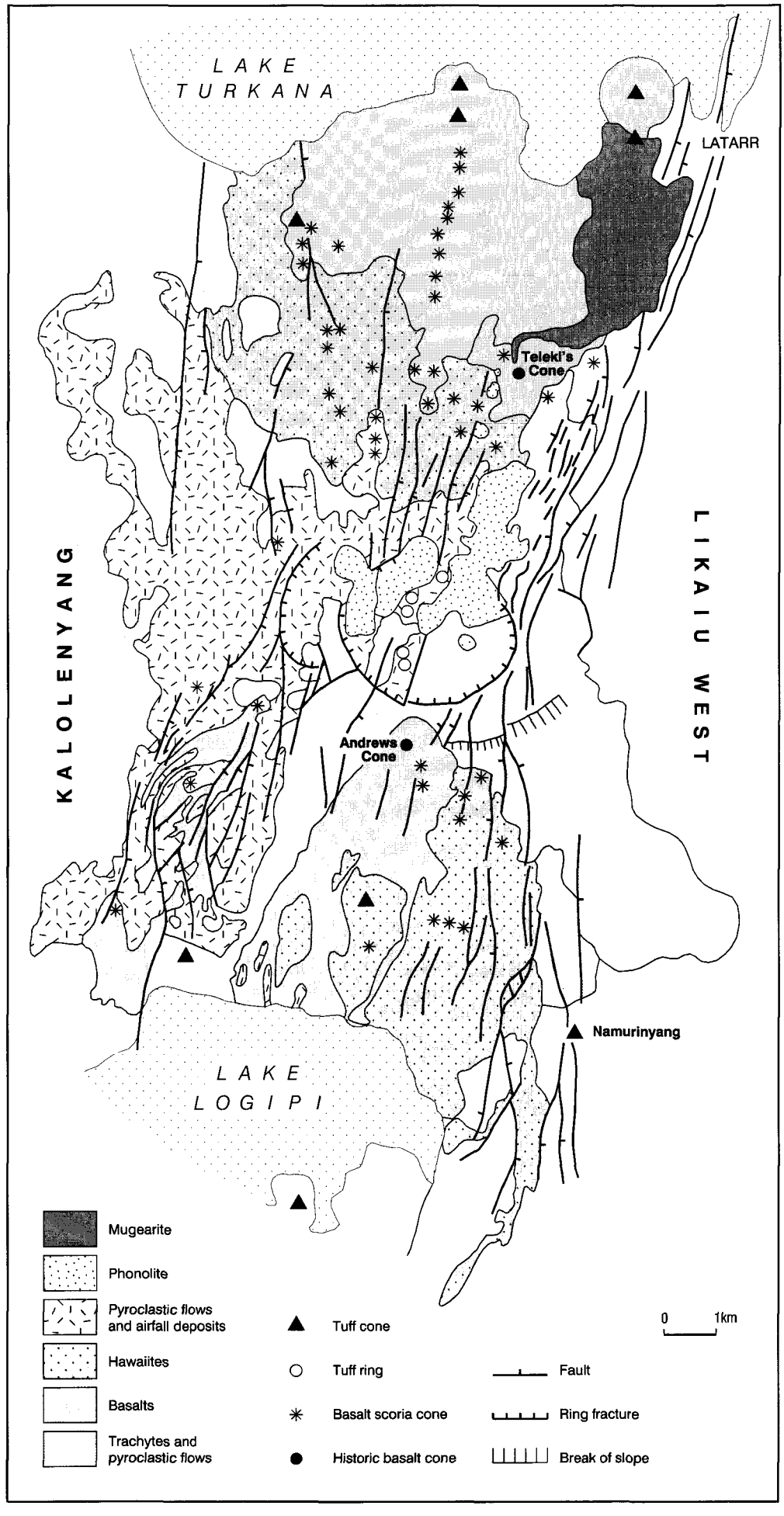

feldspar-phyric. The interstratified pyroclastic deposits form units 2–5 m thick, consisting of buff-yellow, poorly sorted, pumice-rich breccias and tuffs, of mass-flow and pyroclastic flow origin.

Isolated trachyte flows with prominent pressure ridges and levees are also exposed north of the col separating Kakorinya and Kalolenyang at [BN 2260 2619] and [BN 2250 2630]. A cover of younger pyroclastic flow deposits and a lack of contact relationships precludes any estimates of the relative age of these trachytes, but here they are arbitrarily grouped with the Lower Trachytes.

11.4.8.2 Upper Trachyte Lavas (K^{tu}) and Pyroclastic Deposits (K^{vl})

The Upper Trachytes are well-featured lavas, interbedded with air-fall and pyroclastic flow deposits. They account for more than 75% of the volume of Kakorinya and have a total thickness of 400–500 m. The trachyte lavas were erupted from the summit area and flowed radially to the north, east and south. Associated pyroclastic activity on the summit area gave rise to westerly-directed pyroclastic flows and air-fall tuffs, which on the south-western flanks were reworked in a lacustrine environment.

On the south-western and south-eastern flanks the Upper Trachytes occur as a series of prominent lobate and well-featured lavas. Stream sections and fault scarps expose the contacts between individual lavas which are often marked by thin bands of yellow pumice lapilli tuff. From the rim of the caldera a prominent flow extends for 6.5 km down the south-eastern flanks. On the steep upper slopes it is a narrow flow with prominent levees, and on crossing a break in slope at [BN 2353 2536] it broadens into a 3 km wide multi-lobate flow which rests on the Lower Trachytes and on strata of Likaiu West. Similarly, on the south-western flanks another prominent, leveed, and coarsely porphyritic flow extends from the rim of the caldera to the northern shores of Lake Logipi. Exposures on the northern flanks are limited by the cover of younger basalts and trachytic pyroclastic deposits but several sections are present in east-facing fault scarps south-west of Teleki's cone.

Overlying these lavas are a series of small, lobate, porphyritic trachyte lavas which form an apron around the summit area and are exposed in the southern and eastern walls of the caldera. The contrast in morphology between the upper and lower flows is also reflected in their chemical composition. The upper flows are weakly oversaturated whereas the lower flows are weakly undersaturated. The uppermost trachyte in the south-eastern wall of the caldera at [BN 2321 2560] has yielded an Ar/Ar age of 97 ± 3 ka.

On the western flanks of Kakorinya and in the south-western wall of the caldera the Upper Trachytes interdigitate with trachytic pyroclastic deposits (K^{vl}). These have a thickness of more than 100 m and consist of welded and non-welded pyroclastic flow deposits, breccias and air-fall pumice lapilli tuffs. Flow deposits extend up to 8 km from the summit area, reaching Lake Logipi in the south and Lake Turkana in the north, and they mantle the flanks of Kalolenyang to the west. The deposits also underlie the younger basalts of the northern flanks of Kakorinya and are exposed in fault scarps immediately to the west and south-west of Teleki's cone. On the northern and south-western flanks the pyroclastic deposits overlie the Upper Trachytes and on the summit area are in turn overlain by younger air-fall tuffs.

The most instructive sections occur in the western wall of the caldera and in the two outer ring fractures (Figure 11.6). In the caldera wall up to 90 m of welded and non-welded pyroclastic deposits are exposed. The inner ring fracture exposes about 60 m of greenish-grey, welded pyroclastic breccias, overlain by a heterogenous sequence of pale yellow and grey pumice lapilli tuffs with bands of coarse lithic breccia containing obsidian bombs. Low-angle cross-bedding and cross-cutting channel structures are common, and the tuffs contain abundant accretionary lapilli. Feldspar crystals from a pumice sample taken from the tuffs in the middle of the section at [BN 2287 2573] have yielded an Ar/Ar age of 221 ± 4 ka. The outer ring fault section is composed largely of stratified, yellow pumice lapilli tuffs with a thin unit of welded tuff infilling depressions on the upper surface.

On the lower south-western flanks the Upper Trachyte Lavas and youngest pyroclastic flow deposits are interbedded with diatomaceous lacustrine sediments and epiclastic deposits (Figure 11.7b). The epiclastic deposits include volcaniclastic sandstones and siltstones intercalated with beds of finer ash and silt. The deposits display trough cross-bedding, low angle cross-stratification, scour and fill channels and festoon cross-bedding, and show evidence of soft sediment deformation in the form of convolute lamination and slump folds. Coarse debris-flow breccias occur near the base of the section and contain lithic blocks up to 1.5 m in diameter. These volcaniclastic and lacustrine sediments are overlain by trachyte lavas with broken and fragmented flow-fronts. They occur at altitudes of between 400–460 m and are correlated with a high stand of the former Lake Suguta, dated by Casanova (1986) at 121 ± 20 ka.

11.4.8.3 Lower Basalts (K^{bl})

To the north-west of Lake Logipi, thin flows of basalt and basanite are intercalated with the youngest lavas and pyroclastic deposits of the Upper Trachytes. These basalts were erupted from a number of small scoria and spatter cones at [BN 2270 2541] and [BN 2271 2560], now largely buried by younger strata. Although these flows are thin (<5 m) they extend for at least 5 km to the western shores of Lake Logipi.

On the upper northern flanks of Kakorinya, basalt flows associated with spatter and scoria are intercalated with, and locally overlie, the topmost upper trachyte tuffs. They can be traced westwards as a thin cap to the outer ring fault and to the interfluves extending down the western flanks. The scarp face of the inner ring fault is in places draped by a thin veneer of basaltic spatter. These relationships suggest that limited basaltic activity was associated with the final phases of upper trachyte activity and overlapped with the formation of the ring fractures.

11.4.8.4 Ring fracture formation and faulting

Kakorinya has two outer ring fractures located approximately 1 and 1.3 km west of the main caldera (Plate 11.1). These fractures are manifested by prominent east-facing scarps that can be traced through about 40° of arc, and they have their greatest apparent displacements in the middle of the arc where the scarps are at

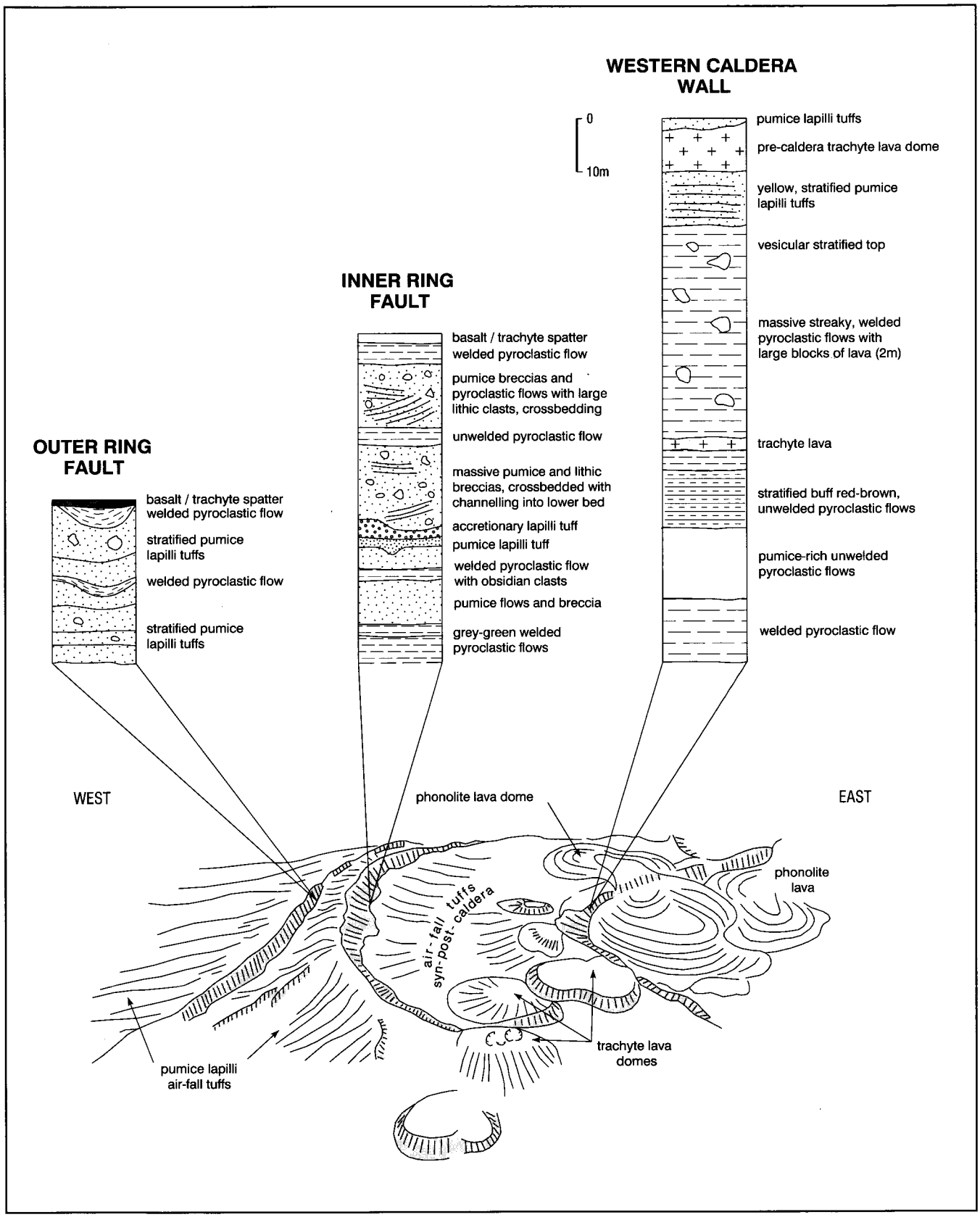

Figure 11.6 Generalised vertical sections in the caldera wall and outer ring faults of Kakorinya volcano.

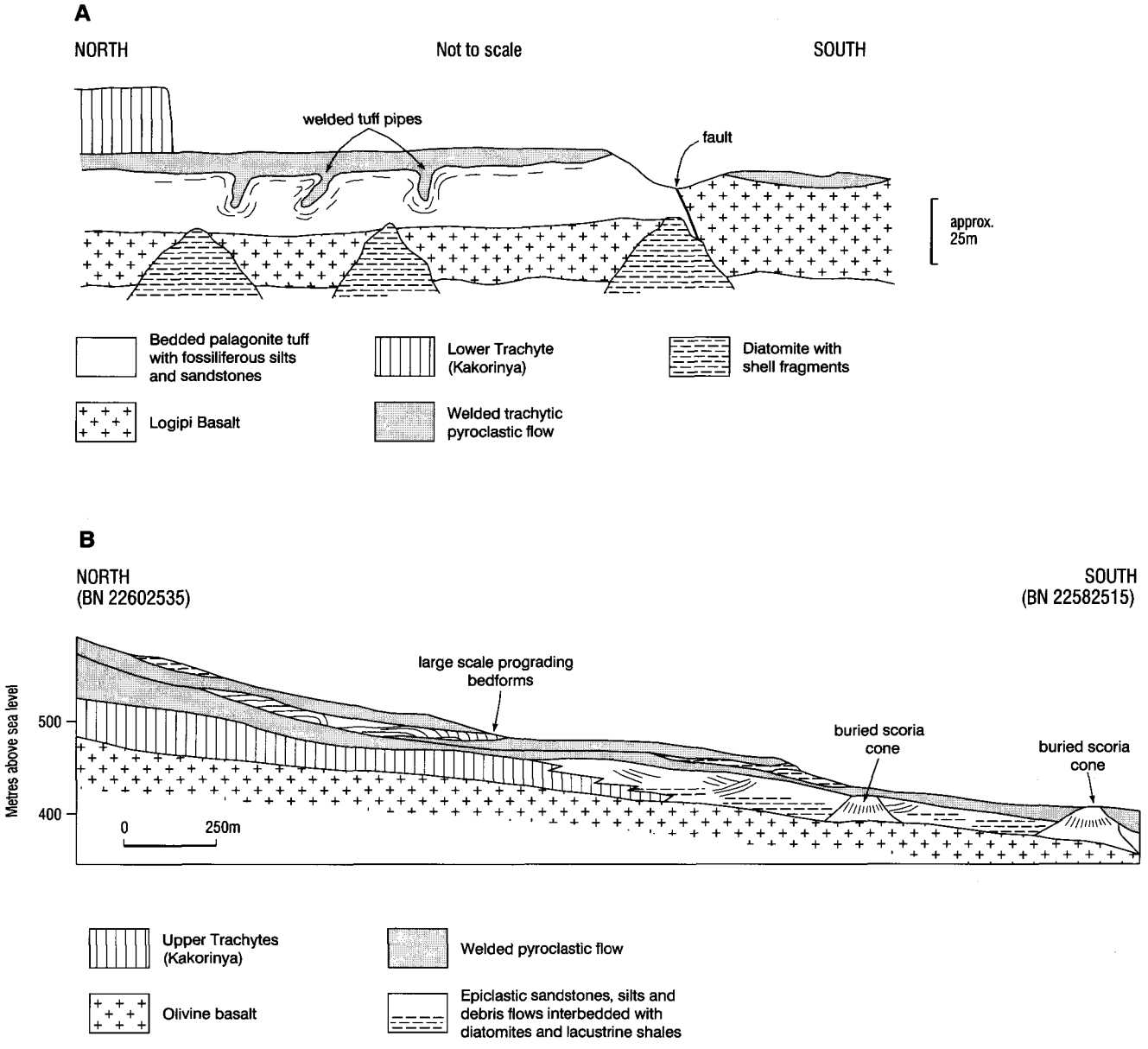

Figure 11.7 a) Sketch of geology in the fault scarp immediately east of Namurinyang tuff cone. b) Composite profile of lower south-western flanks of Kakorinya showing relationships between the Upper Trachytes, epiclastic deposits and lake sediments.

their highest. The inner ring fracture scarp reaches a maximum height of 60 m and the outer scarp about 30 m. The strata in the footwall are tilted and dip westwards at 10–15°. The natural continuations of the ring fault escarpments are marked on the northern and southern flanks by outward-facing breaks of slope, but dissection of these features shows that they represent the buried morphology of lava flow-fronts and there is no evidence for buried fault scarps.

The outer ring fractures cut the pyroclastic deposits of the Upper Trachytes dated at 221 ka. Younger air-fall tuffs dated at 92 ka drape the ring-fracture scarps and are in turn cut by the caldera (see Section 11.4.8.6). From these relationships it is clear that the ring fractures pre-date the formation of the main caldera.

An important phase of faulting affected the BVC, and in particular Kakorinya volcano, prior to formation of the caldera. This faulting is manifested as a series of *en échelon*, NNE-trending normal faults which extend from the south-west flanks near Lake Logipi, across Likaiu West to Latarr in the north-east. The faults have measurable displacements of 10–20 m and link into the ring fractures on the summit area. They cut all the trachytes and basalts described above, and are post-dated by the Trachyte Lava Domes on the west side of the caldera. On the eastern half of Kakorinya, reactivation of the faults in the Latarr and Logipi basalts produced a number of N-trending faults which link into the eastern side of the caldera fracture.

11.4.8.5 Trachyte lava domes (K^{td})

Prior to formation of Kakorinya caldera a number of small trachyte lava domes were erupted around the western half of the summit area. These domes overlie the outer ring fractures and are well-exposed in the upper parts of the south-west wall of the caldera. Their location was partly controlled by the intersection of the zone of NE-trending faults with the ring fractures. The domes are symmetrical, up to 0.5 km in diameter,

and in places coalesce to form irregular outcrops. They typically have carapaces of glassy, vesicular breccia. Small pyroclastic cones and a thin dusting of pumice lapilli tuff mantle the upper surfaces of several domes, and one dome at [BN 2283 2557] is mantled by basalt lava.

11.4.8.6 Pyroclastic deposits (K^{vu})

The youngest trachytic pyroclastic deposits on Kakorinya are air-fall pumice lapilli tuffs. These are best exposed in a thick wedge which infills the west dipping slope between the caldera rim and the outer ring fractures. Here, up to 20 m of pale buff-yellow, well-bedded pumice lapilli tuffs are intercalated with thin breccias. The sequence is capped by pale coloured tuffs containing abundant accretionary lapilli, which are exposed around the western rim of the caldera [BN 2303 2565]. These deposits bank against and mantle the ring fracture escarpments and the pre-caldera domes. They are cut by the caldera wall in the west and bury the northern wall. These relationships indicate that the eruption of these trachytic tuffs was broadly contemporaneous with caldera collapse, with some deposits pre-dating and others post-dating its formation. The pumice lapilli tuffs west of the caldera at [BN 2296 2571] have yielded an Ar/Ar age of 92 ± 2 ka.

The source of these deposits was a series of trachytic tuff rings, cones and pit features exposed on the central and northern parts of the caldera floor and on the northern rim of the caldera. On the caldera floor these eruptive sources are intimately associated with a NE-trending zone of faulting and fissuring and are overlain by later trachyte lavas. Trachytic cones and associated pyroclastic deposits occur outside the caldera on the northern flanks and are overlain by young phonolite lava domes which were extruded on the caldera rim. On the western flanks of Kakorinya similar thin pumiceous deposits form a capping to the older pyroclastic flow deposits (Kvl) and extend across to the eastern flanks and summit of Kalolenyang. On Kalolenyang, the summit crater is infilled with up to 10 m of air-fall pumice lapilli tuffs interbedded with fine ash bands.

The eruption of these deposits from tuff rings within the caldera indicates phreatomagmatic activity, and the occurrence of beds containing abundant accretionary lapilli also suggests wet conditions. This may indicate the presence of standing water or an elevated water table at the time of eruption.

11.4.8.7 Caldera formation

Kakorinya caldera covers an area of 8.25 km^2 and is slightly ellipsoidal in plan, having a long axis of 3.75 km trending north-west and a short axis of 3 km. The thickness of the caldera infill and the original depth of the caldera are unknown, but the present dimensions indicate a volume of 0.83 km^3. The caldera wall reaches a maximum height of about 100 m in the west, and progressively declines in height via a series of normal faults to about 10 m in the south wall, before increasing again to between 50–60 m in the east wall. The north wall of the caldera has low relief and is poorly defined and largely obscured by younger phonolite lavas and pyroclastic deposits. Thus the form of Kakorinya caldera can be likened to two opposing ring fractures, with displacements reaching a maximum on the central portions of the fractures and decreasing towards the ends.

The timing of caldera formation is moderately well-constrained. It post-dated the eruption of the Upper Trachyte Lavas and the Trachyte Lava Domes, and was in turn post-dated by intracaldera trachyte lavas. The field relationships described in the previous section indicate that the collapse was probably triggered by explosive trachytic activity dated at around 92 ± 2 ka. The preservation of tuff rings on the caldera floor suggests that pyroclastic activity continued during collapse. A minimum age limit for the caldera is indicated by a date of 58 ± 4 ka for the main intracaldera trachyte lava.

11.4.8.8 Intra-caldera trachyte lavas and lava domes (K^{t})

The eastern half of the caldera is covered by a coarsely feldspar-phyric trachyte lava. This lava has a thickness of 30–50 m and its surface is marked by arcuate pressure ridges cut by numerous fissures and minor faults. The morphology of this lava indicates that it was probably erupted from a source located in the eastern half of the caldera at [BN 2323 2567], which is now the site of a small phonolite dome. A sample collected near the south wall of the caldera at [BN 2320 2562] has yielded an Ar/Ar age of 58 ± 4 ka.

A series of coalesced trachyte lava domes and cones trend NNE–SSW across the central part of the caldera floor (Figure 11.8) and were probably contemporaneous with the trachyte flow in the east of the caldera. These domes are cut by numerous open fissures and small graben. Locally, the upper surfaces are covered by a thin dusting of basaltic ash and scoria with scattered bombs from Andrew's cone (Section 11.4.8.11).

11.4.8.9 Upper basalts (K^{bu})

The Upper Basalts cover an area of about 75 km^2 on the northern and southern flanks of Kakorinya and consist of basalts and hawaiites. They were erupted from fissures and numerous scoria cones which litter the landscape to the west of Teleki's cone, and to the south and east of Andrew's cone.

The northern flank basalts mantle the pre-existing topography of the Lower Trachytes and Upper Trachytes and are restricted in the east by a major fault scarp cutting the Upper Trachytes and Latarr basalts. They were erupted from a series of fissures which radiate away from a focal point located near the northern wall of the caldera. Individual fissures extend for up to 5.5 km and are the locus of scoria cones, spatter cones and collapse pits. Varying degrees of degradation and vegetation cover indicate that activity has continued over a considerable period of time.

Phreatomagmatic activity is indicated by the eroded and faulted remnants of tuff cones. Abili Agituk [BN 2320 2675] is an eroded complex of overlapping and nested craters cut by N-trending faults. A prominent wave-cut notch on the side of the cone occurs at an elevation of 440 m and correlates with the last high stand of Lake Turkana around 10 ka (Section 11.4.9). At [BN 2330 2643] pillowed and brecciated hawaiite lavas are surrounded by younger subaerial basalts from Teleki's cone. These sub-aqueous lavas occur at an altitude of 425–455 m, indicating that their eruption was broadly contemporaneous with the last major high stand of Lake Turkana.

On the southern flanks basaltic lavas extend over a broad triangular area south of the caldera to the

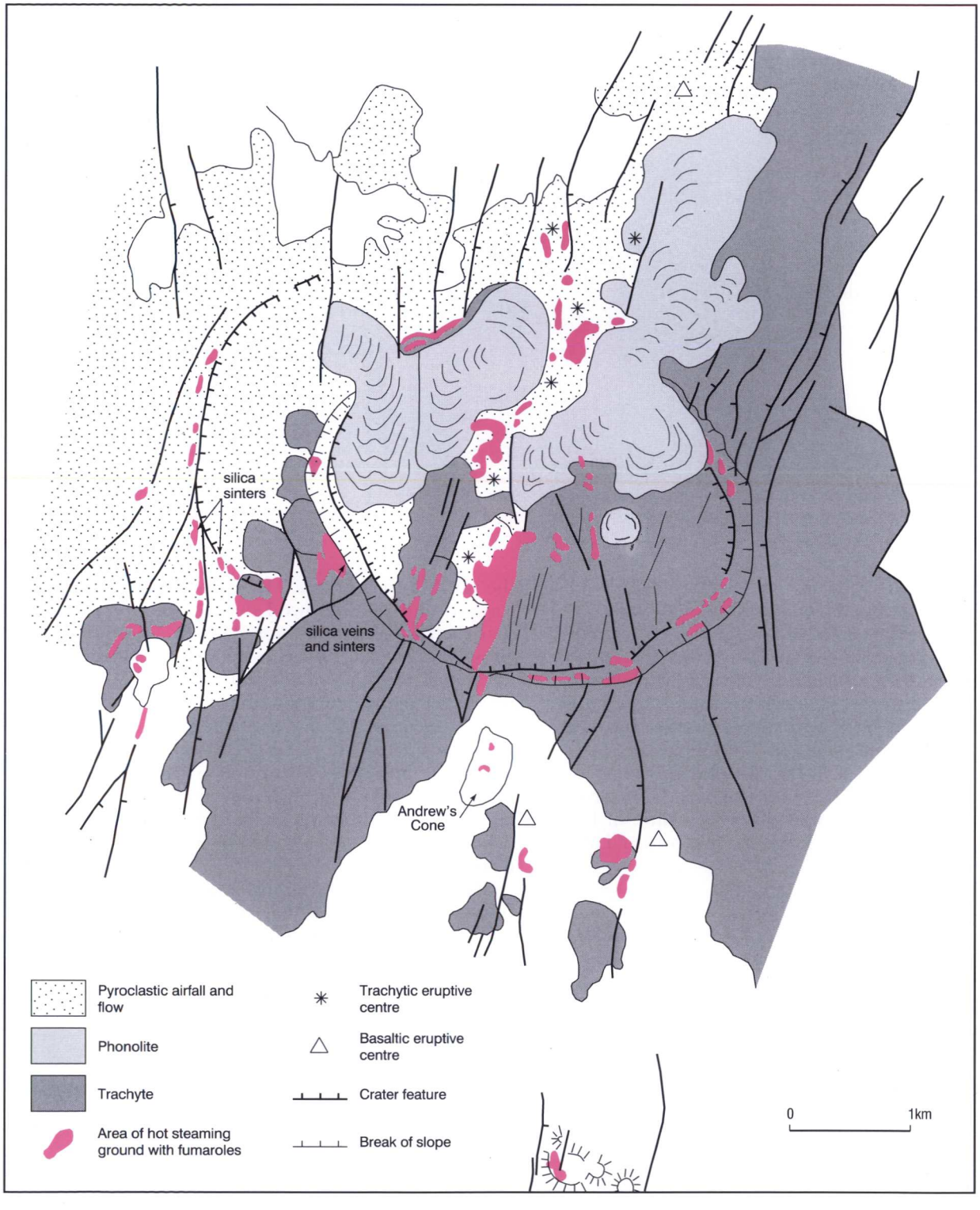

Figure 11.8 Location of geothermal activity on the summit of Kakorinya.

shores of Lake Logipi. On the upper slopes they were erupted from numerous scoria cones located along N-trending fractures. Downslope the scoria cones are replaced by tuff cones and large spatter cones. The older lavas flowed into the former Lake Suguta where they built a delta of pillow lavas, breccias and hyaloclastites (Plate 11.6). Sections through this delta are exposed in several gullies which cut the cliff line above Lake Logipi, as for example at [BN 2305 2498]. As these flows passed over the lava delta front they formed tubular pillows which fragmented to form a pile of hyaloclastite breccias. These pillow lavas are overlain locally by steeply dipping (20–35°S) beds of coarse-grained pumiceous sandstones, channelled and truncated by lenses of gravel and fine conglomerate containing rounded lava fragments. These beds are interpreted as steep delta front deposits formed by a fluvial system entering the former lake. The altitude of the sub-aqueous lavas (of about 460 m) suggests that this basaltic activity occurred during the last high stand of Lake Suguta at around 10 ka.

Plate 11.6 Aerial view of Lake Logipi and the southern flanks of the Barrier Volcanic Complex, looking east with Mount Ngir'o in the far distance. The terrace feature is constructed of pillow basalt and hyaloclastite, over which young subaerial basalts from Andrew's cone have flowed. The photograph was taken during a drought period when the lake was considerably reduced in size.

The youngest tuff cone on the southern flanks sits on a platform above the former shoreline of Lake Suguta. Its base height of 520 m suggests that it probably formed during the last high lake stand. It has two craters separated by a low ridge. Wave-cut notches and small aprons of reworked tuff within the craters indicate that they were filled with water during the last high lake stand. Naperito on the southern shores of Lake Logipi (251 m) is a deeply eroded tuff cone of unknown age (Plate 11.7). Its position on the floor of the inner trough suggests formation at a time of low lake levels, probably during the drying out of Lake Suguta after 3 ka.

11.4.8.10 Recent Phonolites (K^{py})

One of the most striking features of Kakorinya caldera are three large, low-relief, phonolite domes located on the northern rim (Plate 11.1). Flows from breaches in these domes have flowed over the caldera rim and down onto the caldera floor. They are highly vesicular, glassy and blocky lavas with steep flow-fronts and well-developed pressure ridges, and on aerial photographs have a distinctive dark photo-tone and rough texture. The easternmost flow was erupted just inside the low point on the caldera rim. Flows from this dome spread into the caldera and also out over the rim and down the northern flanks where they amalgamate with similar lavas erupted from a series of smaller domes. Some of the domes are surrounded by a low rim of pyroclastic deposits.

The age of the phonolites is unknown. They clearly post-date the intra-caldera trachytes (dated at 58 ka) and probably also the Upper Basalts with an age of around 10 ka. Their fresh and pristine appearance sug-

Plate 11.7 Naperito or 'Cathedral Rock' an eroded tuff cone on the southern shores of Lake Logipi, looking west to Loriu Plateau.

gests they may have been broadly contemporaneous with the Recent basalts described below. Immediately west and south-west of Teleki's cone there is a line of five small phonolite domes. Their older and more vegetated appearance suggests that they may be older than the summit phonolites.

11.4.8.11 Recent Basalts and Mugearites (K^{by}, K^{my})

Recent basalt lavas form a triangular apron covering an area of 25 km^2 on the lower northern flanks of Kakorinya. A prominent fissure line extends southwards from the eroded tuff cone of Abili Agituk [BN 2325 2675] and is marked by a line of pristine and unvegetated scoria cones, spatter cones, hornitos and collapse pits. Subaerial aa-type lavas were erupted from this fissure and flowed northwards towards Lake Turkana. Within 2 to 0.5 km from the present shores of the lake, below the 400 m contour, the basalts develop well-formed pillows indicating passage into a subaqueous environment. Palaeomagnetic data suggest an age of between 1050 and 1030 ± 150 AD for these flows (Skinner et al., 1975). Further west of the main fissure line, young basalt lavas have built out a platform from the scoria cone at [BN 2300 2645], and the lavas around the margins of this platform are also pillowed. In the fault scarp at [BN 2292 2660] these pillowed basalts are seen to rest on subaerial lavas of the Lower Basalts.

Nabuyatom is a beautifully preserved symmetrical tuff cone (Plate 11.8) located on the shoreline of Lake Turkana at [BN 2355 2670]. Its striking appearance has meant that it is often mistaken for Teleki's cone. Nabuyatom rises 217 m above the lake and has a basal diameter of 1.4 km. The northern flanks drop directly into the lake, whereas the southern flanks rest on an older eroded tuff cone and on the faulted basalts of Latarr. It has a steep-sided crater with a rim diameter of 0.75 km and a depth of 200 m. Nabuyatom is composed of buff-brown, bedded palagonite tuff with darker-grey bands of basaltic scoria. Large-scale, cross-cutting packages of tuffs and breccias are exposed in the eastern and western walls of the crater. The flanks of the cone and crater rim are draped by thin layers of steeply dipping (40° to 44°) tuff with accretionary lapilli up to 3 cm in diameter, and are littered with large bombs of scoria and spatter.

Within the crater, triangular aprons of reworked deposits occur above the crater floor and indicate that Nabuyatom once contained a small lake. These match similar aprons of beach deposits around the outside of the cone, 15 m above the present level of Lake Turkana (Plate 11.8) and may correlate with the 1870's level of the lake (cf. Butzer, 1971). The age of Nabuyatom is uncertain, although the lack of dissection and absence of erosion gullies on the flanks suggests it is very young. It pre-dates some of the older flows from Teleki's cone dated at 1870 ± 50 AD, although the account of Cavendish (1898) suggests that it may have been active in historic times.

Teleki's cone is a basalt scoria cone complex approximately 1.5 km in diameter, situated on the northern flanks of Kakorinya at [BN 2335 2615]. The main cone is about 100 m high and is asymmetrical, having a long gently inclined northern flank and a short steep southern flank. A small symmetrical cone is juxtaposed against the north-west flank of the main cone. The complex is dissected by two parallel fissures associated with small vents, craters and collapse pits. Sections in these fissures and in the crater walls show Teleki's cone is constructed largely of agglutinated spatter. Oxidation and alteration by hot gases have turned the spatter into friable red, white and yellowish ash which now covers the upper flanks and infills the craters and fissures. Lavas have been erupted from the fissures and have flowed northwards to Lake Turkana. The lavas around the fissures are of pahoehoe-type and are covered with 'cow-pat' bombs, but downslope they pass into blocky aa-type flows. On the lower flanks, blister-like surfaces and tumuli are developed, possibly caused by the volatilisation of groundwater, and in the vicinity of Lake Turkana the flows are broken into a mass of shattered fragments with anastomosing pahoehoe toes resembling rudimentary pillows.

The most recent eruptions took place from two vents. To the south of the main cone a deep vent, 3 m

Plate 11.8 Nabuyatom tuff cone on the southern shores of Lake Turkana, looking north with South Island in the far distance.

in diameter, is located upon a N-trending fissure at [BN 2328 2610]. Champion (1935) was of the opinion that the flow from this vent was that observed erupting by Teleki in 1888. The youngest flow, which was probably erupted in 1895 (Cavendish, 1898), is a mugearite which emanated from a similar pipe located at the northern end of a fissure at [BN 2332 2623]. This flow has been dated by palaeomagnetic methods by Skinner et al. (1975) who obtained an age of 1883 ± 5 AD, which is in good agreement with the historical evidence.

Andrew's cone is morphologically and structurally similar to Teleki's cone. It is a scoria cone complex located on the upper southern flanks of Kalolenyang, about 0.75 km south of the caldera rim at [BN 2310 2545]. It consists of an elongated cone approximately 65 m high, along the axis of which there are three main craters. Several minor vents are also located on the flanks. Like Teleki's cone it is composed largely of agglutinated spatter. The outer flanks have dips of up to 28° and are coated in basaltic ash and scoria scattered with bombs. Very fluid basalt lavas were erupted from Andrew's cone and extend in a broad triangular apron down to Lake Logipi. The youngest flow was erupted from a breach on the south-west flank and is one of the most undersaturated basalts encountered during the project, having 6.15% normative nepheline.

From their pristine and unvegetated appearance it is clear that Andrew's cone and its associated lavas are very young. Champion concluded that eruptions on Andrew's cone commenced sometime after those on Teleki's but ceased sometime before, as no activity was observed by Teleki's expedition. There is, however, no evidence either to substantiate or repudiate this view.

On the upper south-western flanks of Kakorinya a single flow of basalt was erupted from a scoria cone at [BN 2283 2561]. This basalt extends downslope in a series of thin rivulet-like lava flows confined to fault-bounded valleys in the underlying trachyte lavas and pyroclastic deposits. At [BN 2261 2538] the basalts rest on lake sediments. These sediments are associated with the youngest high stand of Lake Suguta, which indicates the basalt is younger than 9.5–7.5 ka (see Section 11.4.9 below).

11.4.9 Lacustrine sediments (l) and lake stands

Lacustrine sediments provide evidence for the existence of the former Lake Suguta which infilled the inner trough northwards from Emuruangogolak. They underlie the inner trough and are patchily exposed beneath the gravel fans along its western margin, and also occur on the lower southern flanks of the BVC. To the south-east of Lake Logipi, between the base of the rift margin and the faulted terrain of the Logipi basalts, thick sequences of lake sediment are intercalated with fluvial sediments. These mark the site of a major re-entrant in the rift margin, where a delta system, known as the Losergoi delta, was built out into Lake Suguta. Similar sequences of lake sediments also occur on the north-western and north-eastern flanks of the BVC where they are related to former high stands of Lake Turkana.

11.4.9.1 Suguta basin

An older phase of lake sedimentation is represented by ashy diatomites, siltstones and clays interbedded with pumice-rich epiclastic sandstones and mass-flow deposits. These beds are exposed in stream sections on the south-western flanks of Kakorinya (Section 11.4.8.2) and occur at elevations of between 400 and 450 m. They are correlated with a series of fossil beaches and stromatolitic limestones exposed further south in the Suguta Valley which have yielded a $^{230}Th/^{234}U$ date of 121 ± 20 ka (Casanova, 1986).

The youngest phase of lake sedimentation is represented on the BVC by beds of pure, white, diatomite with thin darker bands of impure diatomite, and fine pumiceous ash. Shelly beds with fish remains are also present, and the deposits have intercalations of cross-bedded sands and gravels. In places, polygonal desiccation cracks are also preserved on bedding surfaces, as for example in the diatomites around Namurinyang tuff cone. These younger sediments attain a maximum elevation of 575 m and are related to the last high stand of Lake Suguta, dated in the Namarunu area (Section 10.4.8) at 9 660 ± 210 yr BP (Truckle, 1976). Wave-cut notches related to this highest stand are preserved on all the tuff cones and indicate that the depth of the lake was greater than 300 m on the south side of the BVC.

The sediments exposed in the basin east and north of the Losergoi delta have not been studied in detail. They are up to 18 m thick and consist of fossiliferous beds of diatomite, including paper shales, interbedded with sands, silts, clays and gravel lenses. These beds overlie the pyroclastic flow deposits from Likaiu West and the Logipi basalts, and are capped by wind-blown sand.

11.4.9.2 Lake Turkana basin

On the northern flanks of the BVC lake sediments are exposed at Neangoil [BN 2273 2636], at Nakwamosin [BN 2448 2677], and in the faulted terrain of the Latarr basalts up to 2 km south of the shores of Lake Turkana. These isolated exposures suggest that the sediments were at one time laterally extensive and may have been removed by wind erosion. Their maximum elevation of about 440 m corresponds to the 220 ft mark recognised by Fuchs (1939) on the northern flanks of the BVC and preserved around the shores of Lake Turkana.

At Neangoil, diatomaceous silts and paper shales, 1.5–10 m thick, are interbedded with basalt lavas which have thin stromatolitic coatings and oyster (?*Aetheria elliptica*) clusters. Overlying diatomaceous silts and clays contain abundant shells (*Melanoides tuberculata* and *Corbiculina*) and fish bones which form winnowed layers at the base of individual beds.

11.4.9.3 The relationship between Lake Suguta and Lake Turkana

The possibility of a hydrographic connection between Lake Turkana and the former Lake Suguta was first proposed by Champion (1935). Later studies by Truckle (1976) in the southern Suguta Valley and the discovery of *Lates sp.* support a connection with the Nile basin.

The oldest lake sediments and tuff cone (Namurinyang) on the south-western flanks of Kakorinya occur at an elevation of between 510–515 m. The altitude and stratigraphic position of these sediments cannot be correlated with any other preserved lake stand lines in the Suguta Valley and it is therefore possible that they may be older than 121 ka. Age dating of tuffs

interbedded with lake sediments on Namarunu (Section 10.4.6) support the presence of a lake at around 509 ka. At this time lakes Turkana and Suguta were probably connected, prior to the construction of Kakorinya.

Butzer et al. (1972) indicate that at about 130 ka Lake Turkana had a high stand of around 460 m, which was virtually the same as the high level reached by Lake Suguta at this time, thus providing persuasive evidence for a connection between the two lakes during this period. However, dating shows that by this time the BVC was largely constructed, and therefore the connection between the two lakes was probably restricted to a narrow channel between Kalolenyang and Kakorinya.

The period corresponding with the last glaciation (21–12 ka) was a time of great aridity across Africa. It is likely that many of the lakes, including Turkana and Suguta, dried up or shrank at this time. With the onset of warmer and wetter climatic conditions following glaciation, the lakes rose rapidly to attain their highest stands in the period between 9.5–7.5 ka. At this time the level of Lake Suguta rose to an elevation of 575 m, some 115 m above the equivalent Lake Turkana stand. This indicates that the BVC had dammed the inner trough and the lakes were no longer connected. Drier conditions gradually returned after about 7 ka, and with the exception of two possible periods of high stand at around 6.6 ka and 3.5 ka it appears that Lake Suguta progressively evaporated and dried up.

11.5 SUMMARY OF THE EVOLUTION AND STRUCTURE OF THE BARRIER VOLCANIC COMPLEX

After formation of the inner trough of the rift in uppermost Pliocene—basal Pleistocene times, volcanism within the region of the BVC commenced with the eruption of strongly undersaturated flood basalts from a series of fissures along the eastern margin of the trough. These basalts probably covered the entire floor of the trough and form a platform to the BVC.

The BVC consists of four distinct volcanic centres which broadly decrease in age towards the axis of the inner trough. These centres are composed predominantly of trachytic and basaltic lavas and pyroclastic rocks, although intermediate lavas are not uncommon. At each centre initial trachytic activity built up small volcanic shields, the coalescing nature of which defines the broad morphology of the Barrier.

Trachytic volcanism commenced with the eruption of lavas and pyroclastic flows from Likaiu East and Kalolenyang volcanoes in the period extending from at least 1.37 Ma to 0.7 Ma. These eruptions built up steep sided edifices, the summits of which later collapsed to form craters. Small volumes of basalt were erupted at a late stage. Rejuvenation of rift margin structures faulted and tilted these centres before the next phase of volcanic activity.

Likaiu West (?0.5–0.2 Ma) is poorly exposed. The summit area is covered by small trachyte and phonolite lava domes and associated pyroclastic deposits. Several small crater features on the summit area are now largely obscured by faulting and younger deposits.

Volcanism on the BVC culminated with the formation of Kakorinya volcano (>0.2 Ma to Recent). The construction of a trachyte lava shield was accompanied by the eruption of extensive pyroclastic flow deposits and air-fall tuffs on the western flanks of the volcano. Collapse of the summit area of Kakorinya took place in two stages. Two outer ring faults formed immediately after the Upper Trachytes were erupted and were associated with limited basaltic activity on the summit area. These fractures are post-dated by trachyte lava domes and widespread air-fall tuffs, the eruption of which triggered the formation of the caldera at about 92 ka. Resurgent activity within the caldera is marked by trachyte lavas dated at 58 ka. Later events were dominated by the widespread eruption of basalt and hawaiite lavas from numerous radiating fissures and scoria cones on the northern and southern slopes. This was accompanied by phreatomagmatic and subaqueous activity during the last high stands of lakes Suguta and Turkana, dated at around 10 ka, and subaerial activity has continued into historic times. The most recent activity erupted a series of large phonolite domes and lavas around the caldera, and was also marked by basaltic flank eruptions from Andrew's and Teleki's cones which continued until the end of the last century.

Faulting and volcanism have occurred throughout the evolution of the BVC and have migrated towards the axis of the rift with time. The main phase of *en échelon* faulting appears to have been closely associated with the start of the collapse of the summit area of Kakorinya and the formation of the outer ring fractures.

11.6 GEOTHERMAL ACTIVITY ON THE BARRIER VOLCANIC COMPLEX

11.6.1 Introduction

Geothermal activity has only been observed on Kakorinya, the youngest of the volcanic centres of the BVC. Fumaroles and hot hydrothermally altered ground occur in the caldera and on the upper western and southern flanks. Silica veins and sinters indicative of former hot spring activity also occur at a number of sites on the rim and floor of the caldera. Only minor occurrences of weak steam seepages occur on Andrew's cone, and Teleki's cone appears to be geothermally inactive. The highest temperatures occur in the caldera, where a maximum value of 98.6°C (1.4°C above the local boiling point) was recorded. Temperatures are high outside the caldera, with recorded values reaching up to 97.3°C. The fumaroles and hot ground on Kakorinya are in total contained within an area of 20.5 km^2.

Lake Logipi is fed by numerous, weak, alkaline hot springs and seepages which issue along the base of the southern flanks of the BVC (Plate 11.6). The eroded tuff cone of Naperito is also fringed on the northern and eastern sides by weak hot springs and seepages which flow into Lake Logipi.

Nowhere on the BVC was the sedge *Abilgaardia lispidula* observed. This is in marked contrast to the other Quaternary volcanoes further south where it is ubiquitous in geothermal areas.

The locations of the geothermal activity on the BVC are summarised in Figure 11.8. For the purpose of description the activity is subdivided into three main areas.

11.6.2 Kakorinya caldera

Geothermal manifestations are present along a series of NNE-trending faults and fissures on the caldera floor, and also occur around the caldera walls in the east and south-east.

On the caldera floor two parallel fault-fissure systems are the loci of the main activity.

The western fault-fissure line cuts trachyte lava domes in the south [BN 2306 2560] and extends northwards into the deposits of the trachytic tuff rings. The most vigorous and hottest areas occur along the faults which cut the trachyte lavas, especially near the southern wall of the caldera where several strong fumaroles were recorded with temperatures up to 92.8°C. The fumaroles tend to be located where N-trending joints or minor faults cut the main NE-trending faults. Alteration of the trachyte lavas to reddened kaolinitic clays with silica veins is accompanied by ground temperatures of up to 94.1°C. Soil gases at this site contain relatively high concentrations of CO_2 (38.5%) and radon. Activity is reduced northwards to a series of weak fumaroles and seepages within reddened trachyte lavas containing silica veins. Further north, weakly steaming ground with fumaroles occurs within pumiceous deposits. The deposits are altered to kaolinitic clays and recorded temperatures range up to 90.3°C.

The eastern fault-fissure line contains the most visible geothermal activity on Kakorinya. A series of small collapse pits (Plate 11.9) are aligned along N-trending fissures [BN 2315 2560] which cut the flow-front of the trachyte lava infilling the eastern half of the caldera. The pits emit steam which is visible from a distance of up to 1.5 km. Fumarole temperatures range up to 96.1°C. Further to the east, a NW-trending fault cutting the same trachyte has a series of fumaroles and patches of hot altered ground aligned along it. Here fumarole temperatures range up to 94.6°C and ground temperatures reach 95.0°C.

Immediately to the north-west of the trachyte lava an extensive area of hot altered ground occurs upon a cluster of tuff rings [BN 2315 2575], and here the highest temperatures on the BVC were recorded. Temperatures reach up to 98.6°C and the ground is deeply altered to white, red and purple clays, which when penetrated emit steam with a gentle hissing sound. Soil gases in this area have high concentrations of CO_2 (26%) and radon.

Geothermal activity occurs where the **caldera rim** is cut by faults. The most important area occurs on the south-west rim where a pre-caldera trachyte dome is cut by the ring fault and by N-trending faults which extend across the caldera floor [BN 2295 2565]. The lava dome is strongly fractured, riddled with quartz veins and altered to red kaolinitic clays. Maximum recorded temperatures reach 92.8°C for the fumaroles and 94.1°C for the hot ground.

Elsewhere on the caldera rim, reddened and altered ground with elevated temperatures occurs in the north between the two young phonolite lavas which flow into the caldera [BN 2307 2584]. Here pumiceous pyroclastic deposits have ground temperatures up to 95.8°C. On the southern rim of the caldera a small area of hot steaming ground with temperatures up to 80.6°C is located along a NNE-trending fault which cuts the caldera wall [BN 2312 2555] and is a continuation of the main activity on the western side of the caldera floor.

Several areas of geothermal activity related to the caldera ring fracture are found around the **caldera walls**. The strongest activity occurs in the scree deposits of the south-east wall [BN 2325 2556] where recorded temperatures reach a maximum of 95.8°C. Small areas of hot ground also occur on the caldera floor in the 'moat' separating the caldera wall from the flow-front of the main trachyte lava [BN 2331 2564]. Invariably these sites are located where N-trending faults cut the caldera wall.

Silica sinter is common at many of the geothermal sites on Kakorinya and indicates former hot spring activity. It mainly occurs as scattered float around areas of hot ground and fumaroles, and also as thin irregular veins along faults. The most spectacular develop-

Plate 11.9 Steaming collapse pit on the floor of Kakorinya caldera.

ment of sinter occurs on the trachyte lava domes cut by the south-west wall of the caldera at [BN 2598 2568]. Here numerous silica veins range in thickness from 0.2–0.75 m. They have sub-vertical dips, strike 008–028° and are parallel to a series of open fissures and faults. The veins extend up to the top surface of the lava domes where mounds of botryoidal sinter occur. These sinter mounds are typical of hot spring sinters. The veins have been dated by the $^{230}Th/^{234}U$ method and yielded ages in the range 9.0 ± 0.7 to 7.4 ± 0.4 ka (Sturchio et al., 1993). This corresponds to a pluvial climatic period when lakes Turkana and Suguta were at their highest levels (Section 11.4.9), and when water tables would have been elevated.

11.6.3 The flanks and summit area outside the caldera

Outside the caldera, geothermal activity occurs on the outer ring fractures to the west, and on the upper northern, south-western and southern flanks. It is structurally controlled by the pre-caldera ring faults and by post-caldera faults which link with Teleki's and Andrew's cones.

The hottest and most vigorous activity is associated with the ring fractures and trachyte lava domes to the west of the caldera. On the inner ring fracture extensive alteration occurs along the contact between the fault scarp and younger pyroclastic deposits. Fumaroles are few, and due to air ingestion have relatively low temperatures of up to 78.2°C. The trachyte lava domes which post-date the inner ring fracture and extend down the south-western flanks are extensively altered. They contain several large fumaroles and abundant silica sinter. Fumaroles and strongly steaming ground at [BN 2295 2564] have recorded temperatures of up to 93.4°C. The outer ring fracture has less activity. Chalcedonic silica veins occur at several localities and where the ring fracture meets a NE-trending fault at [BN 2284 2573] weak fumaroles and steaming ground occur with recorded temperatures of up to 75.6°C.

On the northern flanks, immediately outside the caldera, fumaroles and steaming ground occur upon small trachyte scoria cones cut by normal faults. Recorded temperatures reach up to 93.2°C.

Geothermal activity on Teleki's cone has declined since its eruption in 1888, and only minor emissions of steam and sulphurous gases were recorded by Champion (1935, 1937) and Fuchs (1939) at the time of their visits in the 1930's. During the present survey no fumarolic activity nor elevated ground temperatures were detected around Teleki's cone, although deposits of sulphur and sulphates along the fissure attest to activity in the recent past.

On the southern flanks, geothermal activity is restricted to a series of faults which extend southwards from the caldera. At [BN 2322 2540] a small trachyte lava dome is pervasively altered and contains several moderate to strong fumaroles with temperatures of up to 75.0°C and hot altered ground with a maximum temperature of 85.3°C. Activity extends southwards from this dome along a fault, which is marked by red and purple clays and weak steam seepages in the scree deposits at the base of the fault scarp. The most southerly activity occurs 4 km south of the caldera and is located along the southern rim of a large basaltic cone at [BN 2317 2515]. Here hot ground and weak steam seepages with temperatures up to 69.3°C are associated with carbonate alteration.

Geothermal activity on Andrew's cone is restricted to several very small and almost imperceptibly steaming patches of scoria with recorded ground temperatures in the range 41.1–51.1°C.

11.6.4 Lake Logipi hot springs

Lake Logipi is fed by numerous hot springs located around its northern shores and around the eroded tuff cone of Naperito. During the wet season Lake Logipi may expand and many of the springs become inundated.

In total, 22 sites of hot spring activity were located by the survey. They range in temperature from 40.6°C to 71.1°C and generally occur as seepages and weak springs along the shorelines of the lake. Subsurface springs in the bed of the lake are indicated by the presence of passive upwellings of hot water, marked by dark green and black mats of algae up to several metres in diameter. Two moderately vigorous springs with temperatures of 71.1 and 69.9°C were located at the eastern end of the lake at [BN 2315 2480]. An area of widespread spring activity occurs on the north-western side of the lake where the sloping beach face is covered by numerous weak springs with temperatures in the range 64.4 to 66.2°C. These springs have clear, salty water and dark green to black algal mats.

Around the northern and eastern shores of Naperito, numerous hot springs and seepages occur on the sloping beach face and are associated with trona deposits and mats of red and dark green algae. A maximum temperature of 79.9°C was recorded on the northern shores from a series of small clear springs. The full extent of spring activity around Naperito is difficult to assess due to the inaccessibility of many of the areas of flowing water. Weak fumaroles with temperatures of below 60°C have also been reported on the summit of Naperito (G. Watson, personal communication, 1992).

12 The geology and geothermal activity of the volcanic islands of Lake Turkana

12.1 INTRODUCTION

The Lake Turkana Basin is generally regarded as the northernmost segment of the Kenya Rift. It has been tectonically active since at least Oligocene times, although the lake did not form until the Upper Pliocene. The site of the lake overlies a complex region of N–S and NNW–SSE trending rifts of Oligo-Miocene and Pliocene age (Key and Watkins, 1988; Wilkinson, 1988; Ochieng' et al., 1988 and Morley et al., 1992).

The present project undertook a reconnaissance geothermal survey of the three young volcanic islands of Lake Turkana which are described below. In addition, the two main areas of hot spring activity on the shores of Lake Turkana, at Loiyangalani in the south-east and at Eliye Springs in the west were surveyed and sampled (Figure 12.1).

South Island does not appear to be geothermally active, but Central and North Island have vigorous fumarolic and solfataric activity. The surface activity on these two islands is stronger and hydrothermal alteration is more intense than at any of the other geothermal areas in the Kenya Rift. The vigorousness of the surface activity on the islands, and in particular the presence of solfataric activity, is believed to be a function of high water tables (see Section 15.8).

Prior to the survey, unpublished geological maps and descriptions of the geology and petrography of the islands were provided to the project by Karson and Curtis of Duke University (Karson and Curtis, 1990).

12.2 SOUTH ISLAND

South Island is the southernmost and largest of the islands in Lake Turkana. It is situated at 2°38'N 36°36'E, 20 km north of the Barrier Volcanic Complex, and lies midway between the western and eastern shores of the lake. The island has an area of about 40 km^2 and is elliptical in plan, with a long axis trending N–S (Figure 12.1). It rises 320 m above the lake to an altitude of 800 m, and the water depth around the island reaches 114 m, thus giving a total height for the volcanic complex of about 430 m. Multichannel seismic data (Dunkleman et al., 1989) indicate that the island is part of a larger horst block which extends for about 10 km to the north beneath a cover of lake sediment.

South Island has a rugged topography dominated by a N-trending axial ridge composed mainly of coalesced basaltic scoria cones aligned along a fissure zone. To the east of this ridge the island is covered with young basalt lavas. In contrast, the western half of the island is composed of older pyroclastic deposits that were erupted from a series of tuff cones and tuff rings which are now faulted and deeply eroded. The lavas of the island range in composition from alkali olivine basalt to mugearite and phono-tephrite.

The oldest exposed rocks are basalts, including pillow lavas and hyaloclastites, that are found on the north-east shores of the island and the neighbouring islet of Enwoiti. These form a platform upon which phreatomagmatic activity constructed the tuff cones and tuff rings found along the western side of the island. This phreatomagmatic activity produced stratified, yellow-buff and pale-grey palagonite tuffs and scoria, containing basaltic bombs. The largest of the tuff cones occurs in the north-west. It is about 250 m high and contains a crater 100 m deep, the rim of which is capped by a small basaltic spatter cone. The tuffs are locally interbedded with fossiliferous lake sediments (Fuchs, 1939). A prominent stand line and cliff line marked by pillowed lava flow-fronts extends around the northern and much of the western side of the island. It marks the line of a former high lake level, approximately 50 m above the present surface of the lake.

Later phases of activity were dominated by sub-aerial eruptions of aphyric and porphyritic olivine basalt from a number of breached scoria cones aligned along the axial fissure zone. Lava flows from these cones completely mantle the eastern flanks of the island and flow-fronts form a prominent cliff line along the eastern shores. Similar flows infill and mantle the earlier tuff cones in the west. The most recent eruptions took place from several pristine spatter and scoria cones located along the northern half of the main fissure zone.

The volcanic succession exposed on South Island records a transition from subaqueous basaltic activity through emergent phreatomagmatic activity to sub-aerial eruption of lavas and scoria cones. The youthful appearance of the island undoubtedly indicates a Quaternary age. The eroded and faulted nature of the tuff cones and the presence of a stand line at 415 m suggest this activity may have been contemporaneous with Abili Agituk on the northern flanks of the Barrier, dated at around 10 ka (section 11.4.8.9). The ensuing subaerial activity clearly post-dates the last high stand in Lake Turkana, dated at around 3.2 ka (Ferguson and Harbott, 1982). An eruption on South Island was witnessed from the eastern shores of the lake by Count von Teleki's expedition in 1888. According to Von Hönel (1894, p.101), 'we counted five craters, from only one of which, however, was yellowish smoke issuing'. Today South Island is associated with microseismic activity (Pointing et al., 1985) and active faulting on the lake floor.

No geothermal activity has been reported by any of the previous visitors to South Island and none was observed by the present survey during low-level reconnaissance flights over the island.

Figure 12.1 Geology and geothermal activity of the volcanic islands of Lake Turkana and adjacent areas.

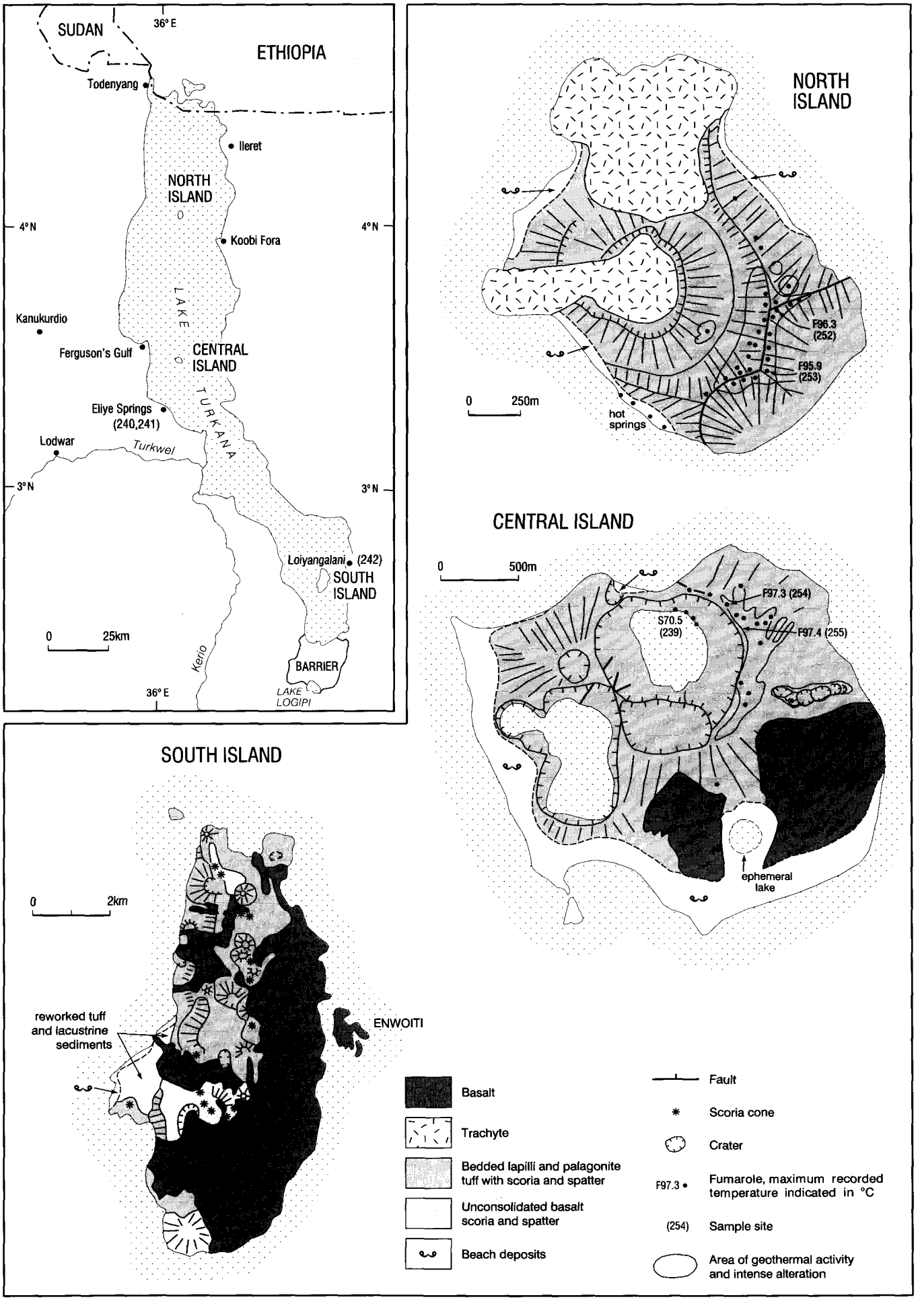
SUDAN
36° E
ETHIOPIA
Todenyang
Ileret
NORTH ISLAND
4° N
Koobi Fora
LAKE TURKANA
Kanukurdio
Ferguson's Gulf
CENTRAL ISLAND
Eliye Springs (240,241)
Lodwar
Turkwel
3° N
Loiyangalani (242)
SOUTH ISLAND
0 25km
Kerio
BARRIER
LAKE LOGIPI
NORTH ISLAND
F96.3 (252)
F95.9 (253)
0 250m
hot springs
CENTRAL ISLAND
0 500m
F97.3 (254)
S70.5 (239)
F97.4 (255)
ephemeral lake
SOUTH ISLAND
0 2km
reworked tuff and lacustrine sediments
ENWOITI
Basalt
Trachyte
Bedded lapilli and palagonite tuff with scoria and spatter
Unconsolidated basalt scoria and spatter
Beach deposits
Fault
Scoria cone
Crater
F97.3 • Fumarole, maximum recorded temperature indicated in °C
(254) Sample site
Area of geothermal activity and intense alteration

12.3 CENTRAL ISLAND

Central Island is a sub-circular island covering an area of approximately 9 km^2. It is located in the middle of the lake at 3°29'N 36°04'E and rises 170 m above the lake to reach a maximum altitude of about 550 m. The bathymetry of the lake in the region of Central Island (Ferguson and Harbott, 1982) shows that the volcanic edifice widens to a diameter of about 5 km at a depth of 45 m. The island is composed of a series of coalesced tuff cones and tuff rings (Plate 12.1). Two large craters with central lakes dominate the island (Figure 12.1). These are up to 1 km in diameter and 80 m deep and are associated with two smaller breached and dry craters immediately to the north and south. The altitude of the floors of these craters is approximately the same as the lake level. An ENE-trending chain of small explosion craters occurs within pyroclastic deposits on the eastern side of the island, and the morphology of these suggest a phreatic origin.

The island is composed of stratified, palagonitised lapilli tuffs, ashes and breccias with minor lava flows in the east and south-east. Reported compositions are variable, and include basanites, basalts, benmoreites and phono-tephrites (Bloomer et al., 1989; Wilkinson, 1988).

The three small islands immediately to the south represent the remnants of other volcanic cones and are considered to be part of the same volcanic complex (Karson and Curtis, 1990). Interpretation of multi-channel seismic reflection data collected by project PROBE (Dunkleman et al., 1989 and Rosendahl et al., 1992) indicates a number of other volcanic cones and plugs beneath the lake bed in the vicinity of Central Island.

Central Island is clearly a young volcanic centre, although its exact age is unknown. Wave-cut shorelines are present at several places around the island at altitudes between 370–377 m and probably relate to recent changes in lake level.

There is vigorous geothermal activity on Central Island. Fumaroles and solfataras were first reported by Worthington (1932) and later by Fuchs (1939) who noted sprays of sulphur from numerous large craters on the north-eastern side of the island. Eruptions were witnessed for several days during July 1974 by scientists stationed at Ferguson's Gulf when 'one unusually intense emission of molten sulphur occurred, together with clouds of white smoke, which were clearly visible from the mainland'. (Ferguson and Harbott, 1982, p.26). A report of another eruption witnessed in 1975 by a scientist 55 km to the north at Koobi Fora (Karson and Curtis, 1990) is unconfirmed. At present, the geothermal activity is located along a broad N-trending zone immediately to the east of the main crater (Figure 12.1). It consists of numerous vigorous fumaroles and solfataras associated with hot, steaming, altered clayey ground. Delicate sulphur chimneys are common (Plate 12.2) and are associated with sulphate salts. Recorded temperatures range up to a maximum of 97.4°C.

Innumerable hot springs and seepages with recorded temperatures up to 70.5°C bubble up within the main crater lake which is markedly more alkaline than Lake Turkana. Photographic evidence from previous visitors to the island suggests that the water level in this crater fluctuates. In contrast the crater lake immediately to the east has the same composition as Lake Turkana and no hot spring activity has been recorded there.

12.4 NORTH ISLAND

North Island is situated along the axis of Lake Turkana at 4°04'E 36°04'E. It is 2 km in diameter and is the smallest of the three islands in the lake. It is a trachytic volcano which rises 140 m above the level of the lake, which in the vicinity of the island is 80 m deep, giving a total height of 220 m for the volcano.

North Island is composed predominantly of phreatomagmatic deposits erupted from several tuff cones or tuff rings now preserved in various stages of erosion.

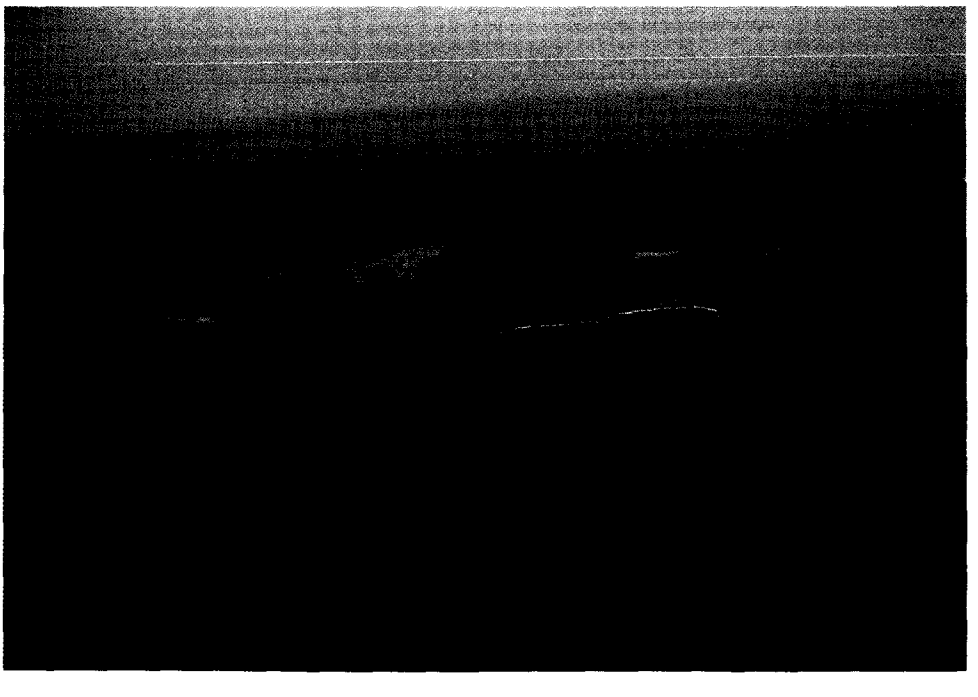

Plate 12.1 Aerial view of Central Island, looking south-east.

Plate 12.2 Sulphur chimney on eastern side of Central Island.

The remnants of an old cone or possibly two cones, are exposed along the southern shores. These consist of friable lapilli tuffs with thin flows of basalt and mugearite. According to Key and Watkins (1988) a dioritic plug is exposed in these deposits in the south-west. A young tuff ring, approximately a kilometre in diameter, occupies much of the central part of the island and appears to be nested inside the remnants of a much larger and older tuff ring. It is composed of planar-bedded and cross-bedded lapilli tuffs, ashes and agglutinated spatter. Lava bombs showing impact structures are common. A trachyte lava infills the shallow crater of the tuff ring and extends out through a breach on the west side (Plate 12.3). Another young trachyte lava covers much of the northern part of the island and was erupted from a breach at the base of the outer flank of the tuff ring on its northern side. Both lavas are dark brown in colour and have blocky surfaces with well-preserved pressure ridges and flow-fronts.

The petrography and chemistry of North Island rocks have been described by Brown and Carmichael (1971), Key and Watkins (1988), Bloomer et al. (1989) and Karson and Curtis (1990).

North Island is clearly a young volcanic centre. The presence of a lake stand line 76 m above the present day lake level has been correlated with the last high stand of Lake Turkana dated at 3 250 ka (Brown and Carmichael, 1971). The young trachyte lavas from the northern cone post-date this bench mark. K-Ar whole-rock dates suggest an age of less than 300 ka for the diorite plug (Key and Watkins, 1988).

Geothermal activity on North Island is vigorous and located in the southern half of the island, mainly along a prominent curvilinear ridge, trending approximately NE–SW (Plate 12.4). According to Karson and Curtis (1990) this ridge is controlled by a number of linked faults (see Figure 12.1). Alternatively, the geomorphology of the ridge may be interpreted as the rim of the deeply eroded remnants of two coalesced pyroclastic cones. Numerous strong fumaroles and solfataras are associated with widespread areas of altered red, white and yellow clays with abundant sulphur,

Plate 12.3 Aerial view of North Island, looking south.

Plate 12.4 Aerial view of the main area of geothermal activity on North Island, looking east.

gypsum and other sulphates. Temperatures range up to a maximum of 96.3°C at the north-eastern end of the ridge. Several small fumaroles and hot springs were also noted by Karson and Curtis (1990) on the wave-cut platforms and beaches on the south-western side of the island.

13 Petrology

13.1 INTRODUCTION

In this section the main petrological features of the Quaternary volcanic centres of the region are described. These features are used to make inferences regarding the nature of magmatic processes operating within the volcanic centres, which in turn have bearing on their geothermal potential.

A total of 269 samples were collected from the surveyed area for major and trace element analysis and petrographic examination. These were mostly of lavas from the volcanic centres within the inner trough, although a small number of rift margin samples were also collected. The major element data were supplemented with additional analyses from Carney (1972), Sceal (1974), Weaver (1977), Campbell-Smith (1938), Brown and Carmichael (1971) and Bloomer et al. (1989). In addition, Sr, Nd, Pb and O isotopic compositions were also determined on selected lavas from the youngest parts of Emuruangogolak and Kakorinya.

13.2 GENERAL COMPOSITIONAL FEATURES

Samples were classified using the TAS system of Le Bas et al. (1986), as shown in Figure 13.1. These diagrams illustrate the bimodal composition of the volcanic centres, in which basalts and trachytes predominate.

At Paka and Korosi, intermediate lavas are more common than at the other centres, although the overall compositional distribution is still strongly bimodal. Figure 13.1 shows that the trachytes of Korosi are consistently more siliceous than those of Paka, which is reflected in differences in normative mineralogy. The trachytes of Korosi are quartz-normative and show a trend towards more oversaturated compositions, whilst those of Paka include both weakly oversaturated and weakly undersaturated lavas.

The lavas of Silali consist mainly of basalts and trachytes with few rocks of intermediate composition. The majority of the trachytes define a trend of increasing alkalinity and undersaturation which extends into the phonolite field, although the trachytes of the Katenmening Lavas show a contrasting trend towards strongly oversaturated compositions.

Emuruangogolak lavas have the most pronounced bimodal compositional distribution of all the volcanic centres in the region. Only one lava of intermediate composition was found on the volcano, but this is in fact a mixed rock composed of commingled basalt and trachyte.

Only a limited number of analyses are available from the Namarunu area. The Pliocene lavas are bimodal, consisting of hypersthene and quartz-normative basalts and hawaiites, and oversaturated peralkaline trachytes associated with minor amounts of mugearite and benmoreite. The Quaternary lavas are strongly bimodal, consisting of undersaturated basalts and pantelleritic rhyolites and trachytes.

The lavas of the Barrier complex are bimodal, but show greater overall compositional variation than the other centres of the region, ranging from basanite through to trachyte and phonolite. In addition, there is a greater proportion of hawaiite and mugearite lavas than on the other centres. The trachyte lavas of the Kakorinya and Likaiu centres define trends of increasing undersaturation towards phonolitic compositions, whereas those of Kalolenyang show a contrasting trend towards strongly silica-oversaturated trachytes.

Attempts have been made to estimate the relative volumes of trachyte and basalt at each centre. These estimates are based on the geometry of the early volcanic shields, which are composed predominantly if not exclusively of trachytic rocks, and on the areas covered by younger lavas and pyroclastic deposits. The average thickness of the basalt lava fields at each centre is the most difficult parameter to estimate, but in most cases these are considered to be only a few tens of metres, as they only form thin coverings to the flanks of the volcanic shields. The volumetric ratios of trachyte to basalt estimated using this approach are 6:1 for Korosi-Paka, 4:1 for Silali, 10:1 for Emuruangogolak, and 9:1 for the Barrier complex. These estimates do not take into account the dense rock equivalent of pyroclastic material, nor the likelihood of basaltic dyke injection into the volcanic shields, both of which would tend to lower the ratios. On the other hand, the dispersion of tephra to the west of the volcanic centres by the prevailing wind will have resulted in the loss of trachytic material. This has occurred at all of the volcanic centres and in the case of Silali may have been significant. Despite these complicating factors, and also uncertainties regarding the average thicknesses of the basaltic fields, the estimated ratios are considered to be of the correct order of magnitude and serve to illustrate the overwhelming proportion of trachytic material relative to basalt. The exception to this is Namarunu, which during the Quaternary has erupted large volumes of basalt and relatively minor amounts of trachyte and rhyolite.

13.3 BASIC LAVAS

The Quaternary basic lavas within the inner trough consist predominantly of transitional alkaline basalts, with lesser volumes of hawaiite and mugearite, and minor occurrences of basanite.

Petrographic differences occur between the basalts of the various volcanic centres. The basalts of Korosi, Paka and Silali are predominantly weakly microporphyritic or aphyric rocks (generally <10% modal phenocrysts), whereas those of Emuruangogolak are almost all aphyric and glassy. On Namarunu the bulk of the Quaternary basalts are aphyric to weakly microporphyritic, but the youngest lavas are strongly porphyritic. On the Barrier complex most of the basalts

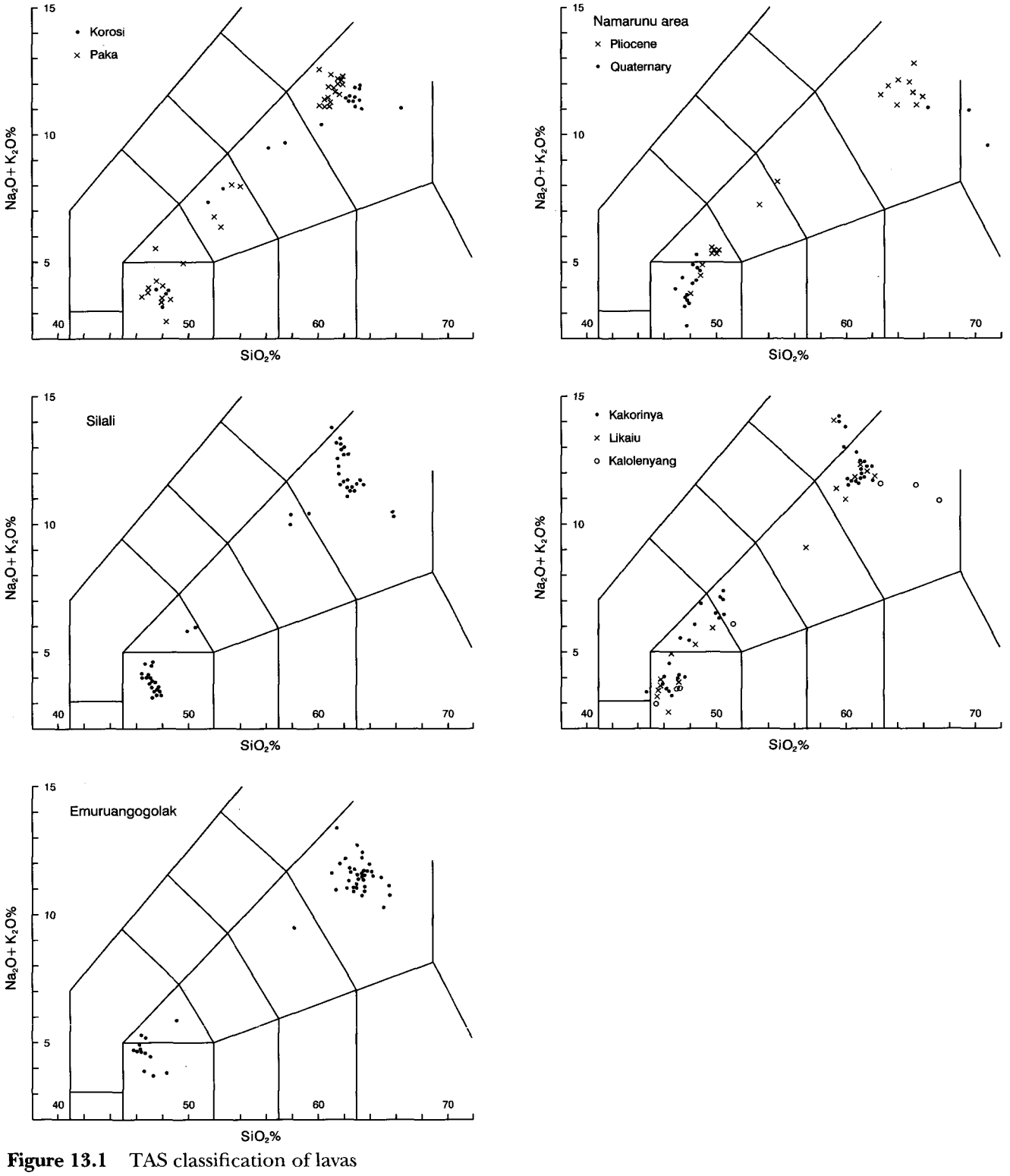

Figure 13.1 TAS classification of lavas

are porphyritic, some being strongly so, and aphyric types are uncommon.

Phenocryst assemblages include plagioclase, olivine, clinopyroxene, titanomagnetite and magnetite. Plagioclase is by far the most dominant phenocryst phase, but is absent in some of the porphyritic basalts of the Barrier complex. It is usually normally zoned, although reverse zoning is common, and mostly falls in the compositional range bytownite-sodic labradorite. In the more fractionated hawaiitic lavas, plagioclase phenocryst compositions range through to calcic oligoclase. Olivine is present in most basalts as subhedral-anhedral microphenocrysts and as skeletal crystals. Clinopyroxene occurs as subhedral to euhedral phenocrysts and is usually more dominant than olivine, although it is not always present, and in particular is absent as a phenocrysts phase in some of the Silali basalts. Compositionally it consists of augite or weakly pleochroic titanaugite.

In most basalts the groundmass is glassy or finely crystalline, although subophitic textures occur in some of the more coarsely crystalline examples. Groundmasses are composed predominantly of microlites and laths of plagioclase together with granular clinopyrox-

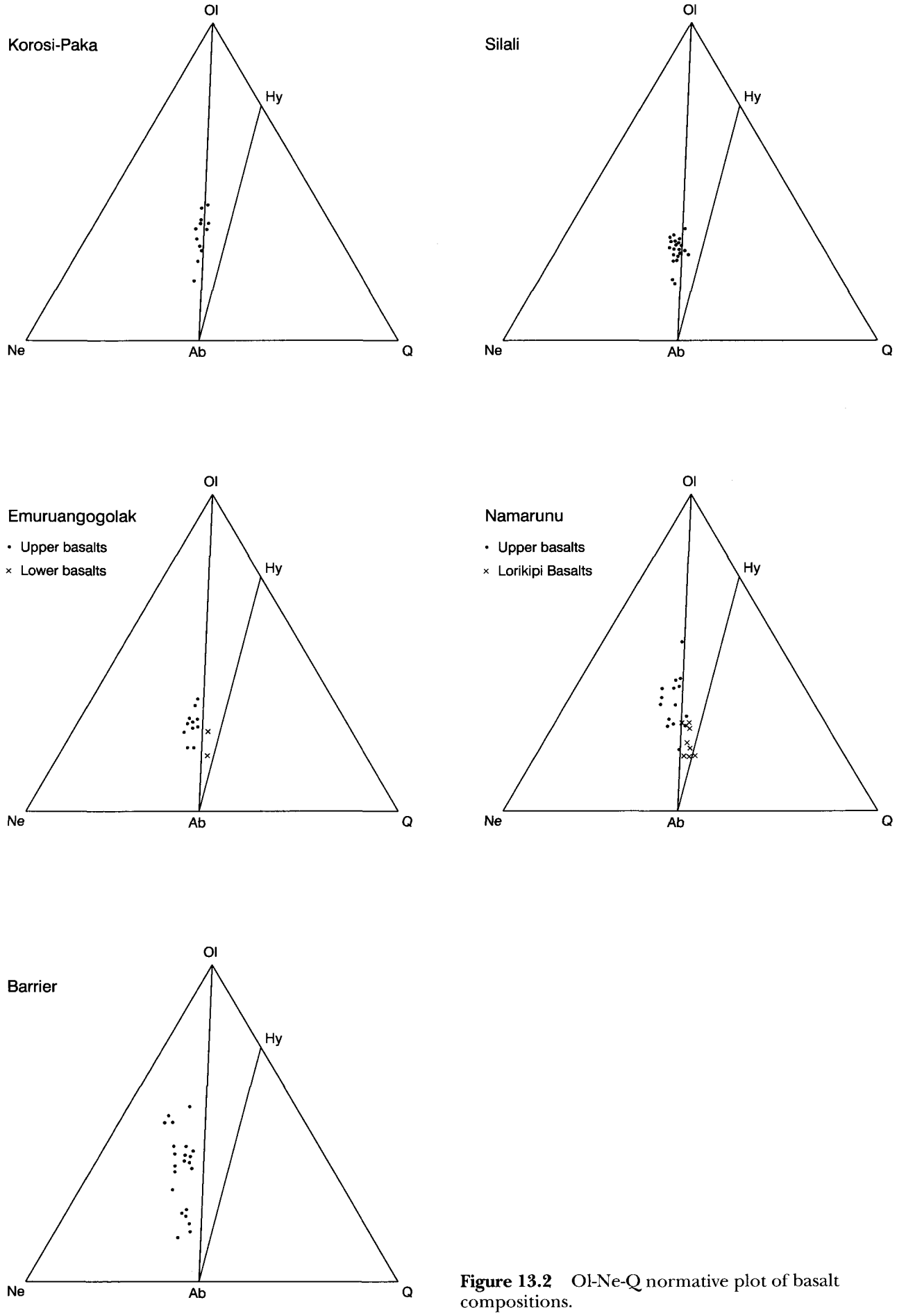

Figure 13.2 Ol-Ne-Q normative plot of basalt compositions.

ene, granular and skeletal olivine, oxide, and glassy mesostasis. The more fractionated basalts tend to contain a greater abundance of oxide in the groundmass.

Cumulophyric picrite basalts with gabbroic nodules are reported to occur on Emuruangogolak, 11 km north-west of Losetom (Weaver, 1977). During the present survey only aphyric basalts were observed in this area, although porphyritic basalts do occur 10 km north-east of Losetom and an occurrence of gabbroic nodules is marked at this locality on the EAGRU geology map (Truckle, 1979b). Weaver describes basalts with up to 40% euhedral phenocrysts of olivine, plagioclase and clinopyroxene, with basal zones containing up to 60% cumulus olivine. One flow is reported to contain abundant cognate xenoliths of gabbro in various stages of disaggregation, including one example of a layered gabbro. Weaver believed that these nodules provide evidence for layered gabbroic intrusive rocks at shallow levels beneath Emuruangogolak.

The composition of the Quaternary basalts changes progressively along the length of the rift, becoming increasingly undersaturated northwards (Table 13.1). At each volcanic centre the majority of basalts are nepheline-normative and only a small proportion are hypersthene-normative, with the exception of the Barrier complex where all are undersaturated. In the case of Paka, Emuruangogolak and Namarunu, the few examples of hypersthene-normative basalts that do occur are stratigraphically the oldest.

The basaltic rocks of all the centres are fractionated, having mg-numbers (Mol $Mg/Mg+Fe^{2+}$) that are mostly in the range 40–55, and Cr and Ni concentrations that are low to very low. On all of the centres, except for Silali, there are also occurrences of basalts with relatively high mg-numbers (60–74), but these are invariably strongly porphyritic, and their high magnesium contents probably result from cumulus enrichment of olivine and clinopyroxene. The least fractionated basalt discovered within the region is an aphanitic basalt from Namarunu, which has a relatively high *mg*-number of 61 and contains 114 ppm Cr and 70 ppm Ni.

Basalts containing relatively high Fe and Ti concentrations occur at each of the volcanic centres. In particular the Upper Basalts of Emuruangogolak and the Katenmening basalts of Silali show extreme enrichment with $FeO_T + TiO_2$ reaching 20% (Figure 13.3). These iron-rich basalts are characteristically very fine grained or glassy and are charged with finely disseminated oxide. Weaver (1977) used the term high-Ti ferrobasalt for these lavas on Emuruangogolak and pointed out that the peak of Fe-Ti enrichment coincided with the appearance of magnetite as a phenocryst phase. Weaver drew attention to the fact that similar high-Ti ferrobasalts are a feature of the early stages of fractionation of mildly alkaline rift-related basaltic magmas from Ethiopia (Barberi et al., 1971 and 1975) and the Azores (Self and Gunn, 1976).

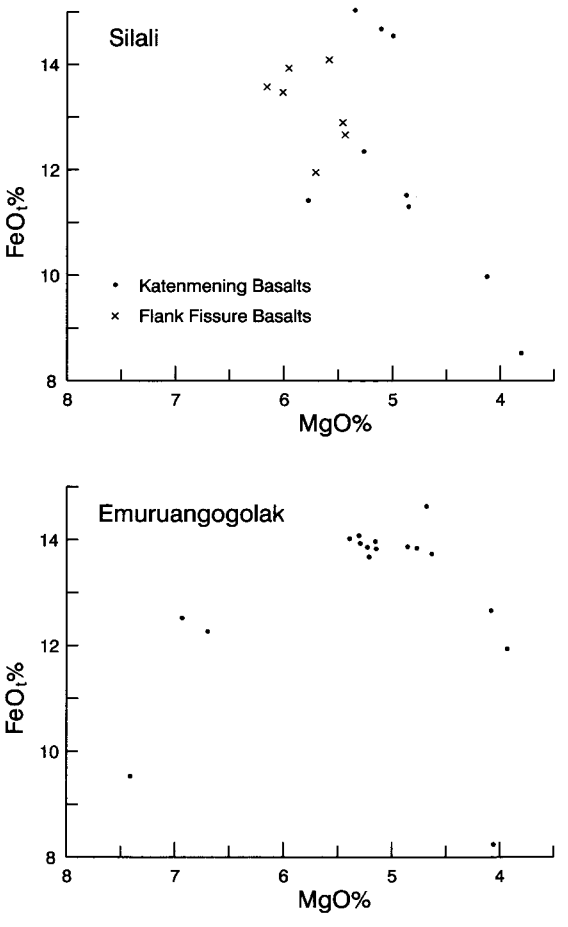

Figure 13.3 Plot of FeO against Mgo for the basalts of Silali and Emuruangogolak.

The origin of the basalts of the Kenya Rift is a controversial and speculative subject, which is outside of the scope of the present study. However, a brief summary of some current views is provided in the following paragraph as general background information.

In the light of rare earth element (REE) inversion modelling, Latin et al. (in press) favour an origin for the basalts by decompressional melting of an asthenospheric mantle plume underlying thinned lithosphere beneath the rift. Although geophysical evidence is compatible with the presence of a plume (Section 2.2), Macdonald (in press) argues on the basis of trace element signatures, that the basalts cannot have been derived directly from convecting asthenosphere, but must have been generated, or at least equilibrated within the lithosphere. Whilst trace element signatures may require lithospheric involvement, Macdonald et al. (in press) point out that the huge volumes of magmas erupted within the environs of the rift are far too great to have been derived from the lithospheric mantle alone, and therefore some asthenospheric mantle input would appear necessary. Regardless of the argument as to the extent of asthenospheric versus lithospheric mantle acting as a source for primary magmas, both Macdonald (in press) and Latin et al. (in press) infer from trace element evidence that the Quaternary basalts of the rift were generated in a melt zone extending across the transition from spinel to garnet peridotite.

Table 13.1 Normative compositions of basalts

	Normative range	Average	N
Korosi-Paka	4.93 *hy*–2.48 *ne*	0.27 *ne*	11
Silali	4.72 *hy*–2.42 *ne*	0.86 *ne*	23
Emuruangogolak	8.30 *hy* – 3.40 *ne*	1.47 *ne*	13
Namarunu	3.92 *hy*–5.07 *ne*	2.05 *ne*	15
Barrier	1.28 *ne*–6.94 *ne*	3.84 *ne*	21

As described above, the Quaternary basalts of the region show an increase in the degree of undersaturation towards the north. This is also matched by variations in REE patterns, which show an increase in the degree of LREE enrichment from south to north (Table 13.2, Figure 13.4). The basalts of Emuruangogolak are noticeably more LREE-enriched than those of the centres to the south, and the basalts of the Barrier are strongly LRRE-enriched. These variations suggest greater involvement of garnet in the mantle source of the basalts of the Barrier and to a lesser extent of Emuruangogolak, which in turn imply greater depths of partial melting beneath these areas compared with the volcanic centres further to the south.

Table 13.2 Chondrite normalised Ce/Yb ratios of Quaternary basalts

	Range	Average	N
Barrier	8.67–10.65	9.76	7
Namarunu	3.82–5.79	4.75	3
Emuruangogolak	5.04–5.99	5.42	4
Silali	3.63–4.11	3.90	7
Korosi-Paka	3.41–4.32	4.19	4

13.4 MUGEARITES AND BENMOREITES

Mugearites are relatively common on Paka, Korosi and the Barrier complex, although still only account for about 10% of the analyzed samples, whilst at the other centres they are rare or absent.

In appearance the mugearites resemble basalts. They are weakly microporphyritic lavas containing microphenocrysts of plagioclase, olivine and clinopyroxene, and in some examples accessory alkali feldspar. Groundmasses are fine-grained and are composed predominantly of feldspar laths and microlites showing strong pilotaxitic textures, with interstitial clinopyroxene, oxide and glassy mesostasis.

Lavas of benmoreitic composition are rare, accounting for less than 2% of the samples analyzed. Most resemble trachytes in appearance, although melanocratic benmoreites are found within the Pliocene succession of Namarunu. They contain microphenocrysts of sodic plagioclase and alkali feldspar, with or without clinopyroxene and olivine. Clinopyroxene microphenocrysts include colourless to weakly pleochroic augite-titanaugite, although aegerine-augite occurs in the more alkaline and undersaturated benmoreites of the Black Hills Lavas of Silali. Groundmasses are glassy or finely recrystallized, and contain fine laths and microlites of feldspar with accessory clinopyroxene, amphibole and oxide.

In addition to the limited number of 'true' benmoreites, there are lavas of overall benmoreitic composition which are the product of magma mixing. The clearest example of this is from Emuruangogolak, where the only benmoreitic lava from that centre is a porphyritic rock containing microphenocrysts of plagioclase, alkali feldspar and clinopyroxene in a trachytic groundmass containing abundant blebs of vesicular basalt glass (Section 9.3.2). The basalt blebs reach up to several centimetres in size and show all stages of resorbtion and commingling with the trachytic groundmass, indicating that they were liquid at the time of mixing. Similar mixed lavas of intermediate composition also occur within the Kapedo Tuffs exposed in the caldera wall of Silali. These contain fine-grained blebs and streaks of partially assimilated basaltic or mugearitic material, and gabbroic cognate xenoliths in a trachytic groundmass. Carney (1972) also describes trachymugearites (*sic*) from Korosi and Chepchuk which have disequilibrium phenocryst assemblages compatible with the mixing of trachytic and basaltic magma.

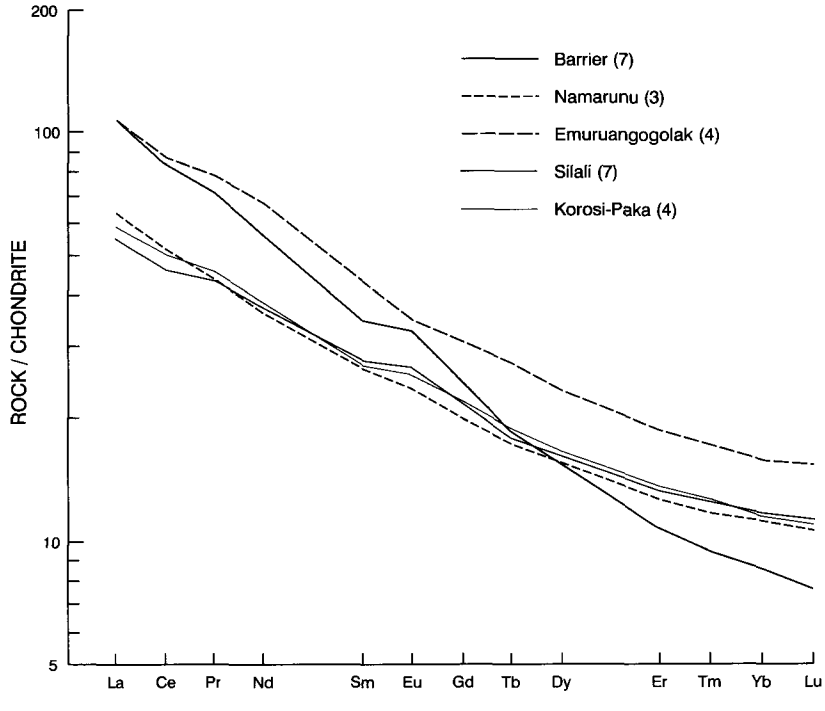

Figure 13.4 Average chondrite normalized rare earth element abundances of basalts from the Quaternary centres.

13.5 TRACHYTES

The majority of the trachytes are microporphyritic, although aphyric varieties are present at each of the volcanic centres. Anorthoclase is by far the most dominant phenocryst phase, whilst sanidine is rare and has only been observed in a few samples of undersaturated glassy trachytes from the Barrier complex and from the Black Hills Lavas of Silali. Sodic plagioclase phenocryst also occur in addition to anorthoclase in comenditic and metaluminous trachytes. Microphenocrysts of clinopyroxene are present in accessory amounts and consists of augite, or weakly pleochroic aegerine-augite which tends to be increasingly pleochroic in the more undersaturated trachytes. Fayalitic olivine microphenocrysts occur in accessory amounts, tending to be more common in trachytes of comenditic composition. Magnetite is present as small microphenocrysts which are generally more abundant in undersaturated trachytes. Small euhedral crystals of sodalite, variably altered to zeolite, occur in the trachytes of Paka and the Upper Trachytes of Kakorinya. Nepheline is rare and was only observed in accessory amounts in a single sample of trachyte collected from the Kapedo Tuffs in the caldera wall of Silali, although Sceal (1974) also reported a nepheline-bearing trachyte on Paka.

The groundmasses of the trachytes vary from being glassy to completely recrystallized. They are composed predominantly of skeletal laths and microlites of alkali feldspar with interstitial sodic amphibole (ferro-richterite-arfvedsonite-riebeckite), aegerine-augite, aenigmatite and oxide. Fine intergranular quartz is present in accessory amounts in some trachytes. Feldspar laths and microlites are commonly aligned to produce strong trachytic fabrics, although variolitic textures also occur.

The trachytes of the region vary in composition from centre to centre. Those of Korosi are all peralkaline, having agpaitic coefficients (Mol $(Na_2O + K_2O)/Al_2O_3$) in the range 1.01–1.41. They are oversaturated, containing normative quartz in the range 1.67–6.06%, and they form a single group that straddles the boundary between the fields of pantelleritic and comenditic trachytes as defined by Macdonald (1974).

On Paka there appears to be no systematic compositional variation between the lower, upper and post-caldera trachytes. As a single group they are critically saturated with respect to silica, and include both weakly nepheline-normative and weakly quartz-normative lavas, with a compositional range of 1.81% *ne* to 1.93% *q*. They are subaluminous to mildly peralkaline, having agpaitic indices of 0.99 to 1.17, and the oversaturated examples straddle the boundary between pantelleritic and comenditic compositions.

The trachytes of Silali are peralkaline to metaluminous and include undersaturated and oversaturated compositions. Only two samples of Lower Trachyte Lavas were analyzed and these are weakly undersaturated, having *ne* of 1.24% and 2.67%. The trachytes of the Kapedo Tuffs are peralkaline and include oversaturated and undersaturated compositions. Most are weakly oversaturated pantelleritic trachytes, containing *q* in the range 2.17–3.54%, although a moderately undersaturated trachyte containing modal and normative nepheline (5.56% *ne*) occurs within the tuffs in the southeast wall of the caldera. The Summit Trachytes are glassy or finely recrystallized pantelleritic trachytes that have agpaitic coefficients of 1.11–1.24 and *q* in the range 1.93–4.26%. The Katenmening trachytes cover a range of compositions but are all oversaturated. Most are weakly oversaturated pantelleritic and comenditic trachytes, having agpaitic coefficients of 1.10–1.20 and *q* 1.11–2.43%, although the 'Three Hills trachytes' are metaluminous and the most oversaturated lavas on Silali, having *q* in the range 11.32–11.41%. The Black Hills Trachytes are all undersaturated glassy rocks (*ne* 1.86–3.99%) that define a fractionation trend towards phonolitic compositions.

The trachytes of Emuruangogolak are virtually all oversaturated with the exception of a single sample of Middle Trachyte that is weakly nepheline normative (*ne* 0.31%). The Lower Trachytes are strongly peralkaline pantelleritic lavas, with agpaitic coefficients of 1.13–1.36 and *q* 1.72–12.75%. The Upper Trachytes are weakly oversaturated. They include strongly peralkaline pantelleritic trachytes with agpaitic coefficients of 1.16–1.57 and *q* 1.36–2.79%, and near-subaluminous to moderately peralkaline two-feldspar comenditic trachytes with agpaitic coefficients in the range 1.00–1.22 and *q* 0.84–3.51%.

At the Barrier complex the trachytes of Kalolenyang are oversaturated comenditic lavas containing *q* in the range 1.08–12.52%, whereas those of Likaiu are undersaturated and have *ne* ranging 0.01–4.59%. The trachytes of the younger Kakorinya centre are predominantly undersaturated, although two of the fifteen samples analyzed are weakly oversaturated, and the complete normative range for the trachytes of that centre is 0.89% *q* to 5.43% *ne*.

13.6 PHONOLITES

Phonolitic lavas are rare and only occur on the Barrier complex and Silali.

The most voluminous and best preserved phonolites are the young domes found around the caldera and on the northern flanks of Kakorinya. In the field these closely resemble trachytes in appearance. They are dark, vesicular, glassy rocks that contain abundant microphenocrysts of anorthoclase and accessory aegerine-augite aggregated with magnetite. The groundmass of these rocks is glassy or finely recrystallized with variolitic textures, and contains sparse to very abundant sub-millimetre size euhedral crystals of nepheline. These phonolites contain between 11.80% and 12.87% normative nepheline.

McCall and Hornung (1972) and Macdonald (personal communication, 1993) report the occurrence of phonolites within the Black Hills Trachyte Lavas of Silali.

13.7 PLUTONIC NODULES

Syenitic blocks, in some cases with dimensions of several metres, are present on all the volcanic centres and are particularly common in the Pyroclastic Deposits of Paka and the Upper Pyroclastic Deposits of Emuruangogolak. The analyses of Weaver (1977) indicate that on Emuruangogolak the syenitic nodules are compositionally similar to the trachyte lavas, with which they are assumed to be co-magmatic.

Abundant gabbroic blocks, many of which are large, occur within basalt lavas and cover the ground surrounding the Katenmening pit crater on Silali. These were described by McCall (1970) who suggested that they represent parts of a magma chamber brought to the surface by gas-coring during the terminal eruption of the Katenmening basalts. The nodules consist of olivine, titanaugite, plagioclase and Fe-Ti oxides with interstitial vesicular glass. The interstitial glass in these nodules is phonolitic and mugearitic in composition (Macdonald personal communication, 1993) and according to Macdonald (1987) represents fractionated liquid, possibly produced during side-wall crystallization. The vesicular nature of the matrix to these nodules suggests low-pressure conditions.

On Emuruangogolak, the presence of cumulophyric picrite basalts and cognate gabbro xenoliths, some of which have layered cumulate textures (Weaver, 1977) also strongly suggests that layered gabbro bodies exist at depth. Small gabbroic nodules are also found in the pyroclastic deposits of Paka.

13.8 THE RELATIONSHIP BETWEEN BASALTS, TRACHYTES AND PHONOLITES

An understanding of the relationship between basalts and trachytes is of fundamental importance, as this gives an insight into the nature of the magmatic plumbing systems within the volcanic centres of the region, which provide the heat for the high-level geothermal activity.

Linear correlations between pairs of incompatible trace elements (ITE), such as Zr and Nb, in the basalt-trachyte sequences of the rift's volcanic centres have been widely cited as evidence for derivation of the trachytes from basaltic magmas by fractional crystallization (Sceal and Weaver, 1971; Weaver et al., 1972; Weaver, 1977; Baker et al., 1977; Baker, 1987). Analyses obtained during the present survey confirm such linear correlations between ITE's for all of the volcanic centres of the northern sector of the rift, as illustrated for example by data for Emuruangogolak and for Kakorinya (Figure 13.5).

On the basis of Zr plotted against Nb, Weaver (1977) recognised three trachyte lineages on Emuruangogolak. These he attributed to changes in Zr/Nb ratios as a result of volatile degassing related to major pyroclastic events; during which Zr is assumed to have preferentially entered the vapour phase relative to Nb. However, given the prolonged evolutionary history of Emuruangogolak, and in particular the time gap of almost half a million years between the eruption of the youngest lower trachytes and the onset of upper trachyte activity, it is highly likely that more than one batch of magma was involved. Therefore the different

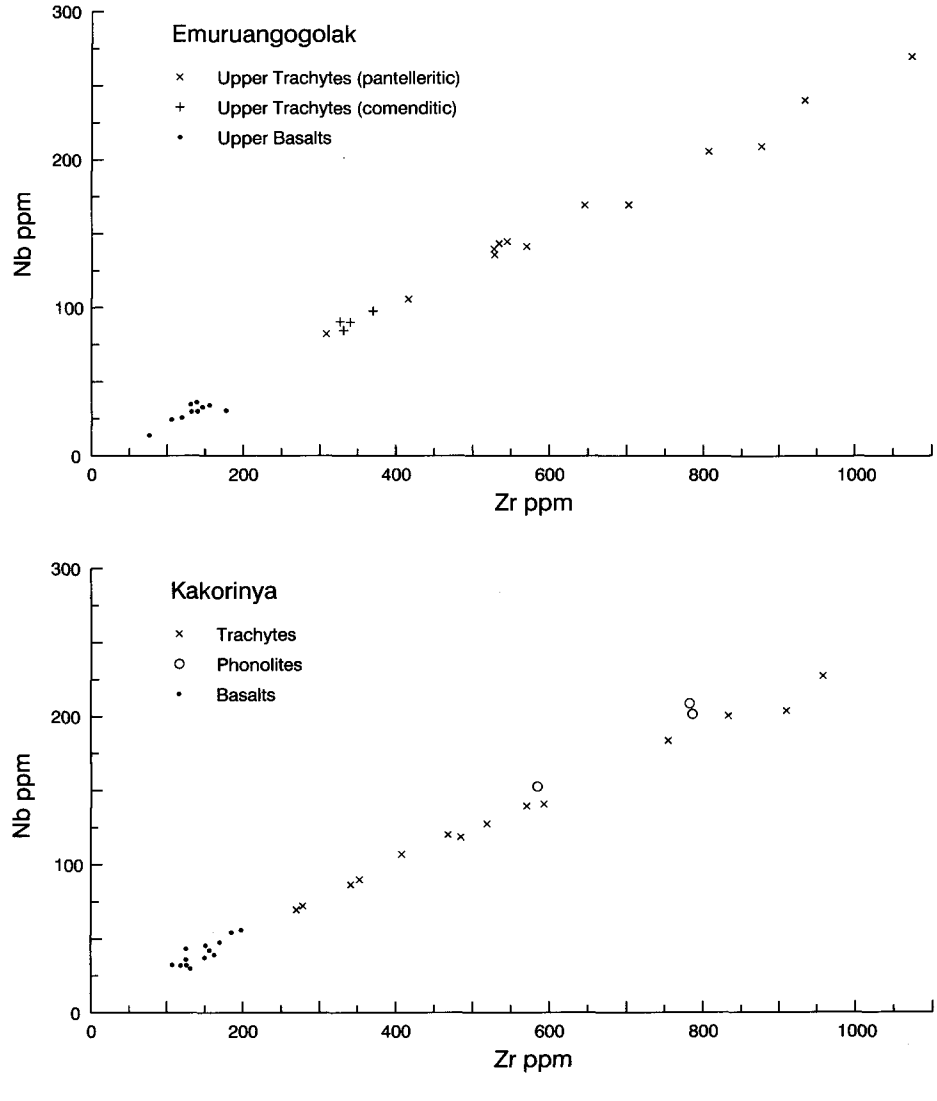

Figure 13.5 Plot of Nb against Zr for the younger lavas of Emuruangogolak and Kakorinya.

trachyte lineages defined by Weaver on the basis of Zr/Nb are more likely to reflect separate influxes of parental magma of slightly different compositions. In Figure 13.5 only data for the broadly coeval Upper Trachytes and Upper Basalts of Emuruangogolak are presented and these illustrate a single lineage.

On Silali, the Summit Trachytes, Katenmening trachytes and Black Hills Trachytes have different Zr/Nb ratios and appear to fall on separate but parallel lineages on a plot of Zr against Nb (Figure 13.6). However, the basalts do not plot on these lineages and have different Zr/Nb ratios to the trachytes. The basalts have a mean ratio of 6.07 and the trachytes of 3.95. These variations are probably too large to be explained by preferential loss of Zr by volatile degassing, and suggest that Silali trachytes could not have been derived by simple closed-system fractional crystallization of a single basalt parent magma.

The scarcity of intermediate lavas poses a problem regarding derivation of the trachytes by fractional crystallization of basaltic magma. Simple trace element modelling based on the assumption that Zr behaved completely incompatibly during fractional crystallization indicates that for Emuruangogolak the compositional gap between the most fractionated basalt and the least fractionated comenditic trachyte represents only 19% of the crystallization range, whilst for Kakorinya the compositional gap between hawaiite and trachyte represents an even smaller fractionation of about 14%. In a study of the similar basalt-trachyte suite of Reunion, Clague (1978) calculated that the compositional gap between 50–57% SiO_2 represents only 15% of the crystallization range. Both Clague and Weaver (1977) believed that the respective compositional gaps at Reunion and Emuruangogolak coincided with the precipitation of Fe-Ti oxides. If this is the case, then the position and size of the gap within a given basalt-trachyte series is likely to be a function of fO_2, which in turn may be related to the activity of H_2O.

Although benmoreites may represent a relatively small proportion of the total compositional range, the very low volume of benmoreitic lavas actually found within the volcanic succession at each centre is nevertheless considerably smaller than that predicted by fractional crystallization models; in the extreme case of Emuruangogolak they are completely absent. In order to explain this discrepancy several researchers have proposed that physical controls, resulting from viscosity and density variations within the differentiating magma chambers, have effectively discriminated against the eruption of benmoreitic compositions (Baker et al., 1977; Jones, 1979).

Isotopic analyses provide useful information bearing on the relationship between basalts and trachytes. Norry et al. (1980) presented a limited number of isotopic analyses for Emuruangogolak, and during the present survey representative suites of samples were analyzed from the younger lavas of Emuruangogolak and Kakorinya. Within each centre the basalts and trachytes have similar Pb and Nd isotopic compositions, which are consistent with derivation from a common source, but the trachytes at each centre have significantly higher $^{87}Sr/^{86}Sr$ than their related basalts (Figure 13.7). Norry et al. believed the trachytes were derived by fractional crystallization of the basalts, but interpreted the higher Sr isotope ratios as an indication of crustal contamination within the trachytes. Because the concentration of Sr is much lower in the trachytes than in the basalts, the Sr isotope ratio in the trachytes is much more sensitive to the effects of crustal contamination than in the basalts. Conversely, because Pb and Nd concentrations are much higher in the trachytes than in the basalts, the isotopic ratios of these two elements are less susceptible to the effects of crustal contamination in the trachytes.

The isotopic analyses obtained in the present survey also show a number of other significant features. On Emuruangogolak the comenditic trachytes have $^{86}Sr/^{87}Sr$ values intermediate between those of the basalts and pantelleritic trachytes. The comenditic trachytes are less fractionated than the pantelleritic trachytes, which may imply shorter residence times for comenditic trachyte melts and therefore less opportunity for crustal contamination. Evidence for the com-

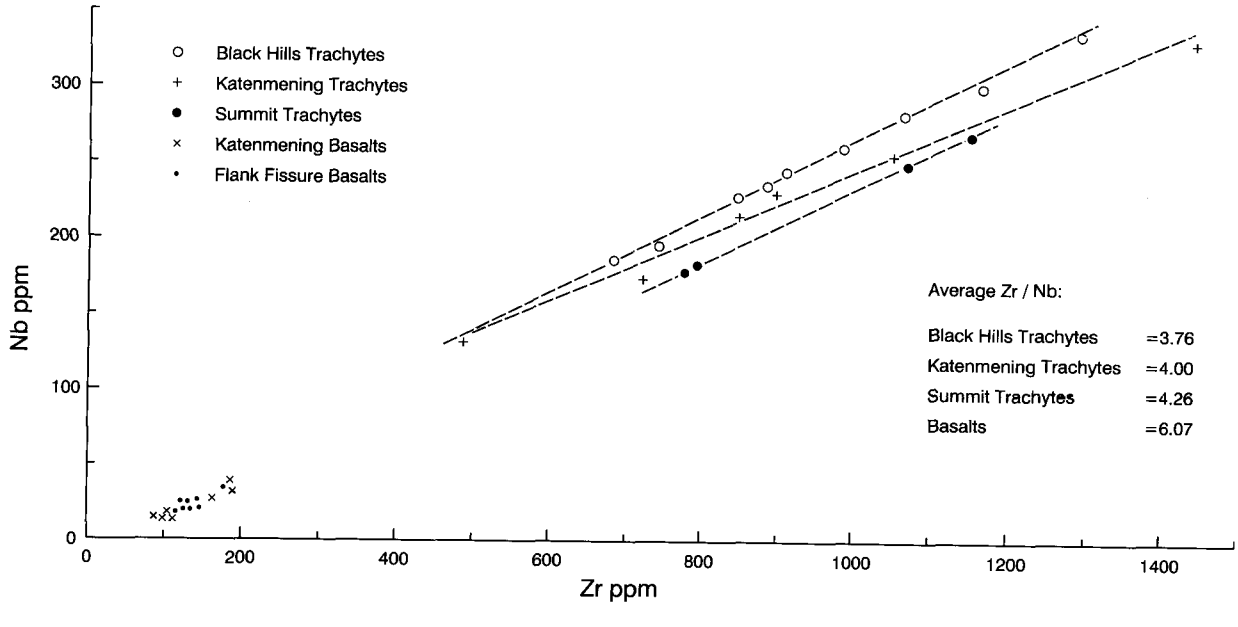

Figure 13.6 Plot of Nb against Zr for the lavas of Silali.

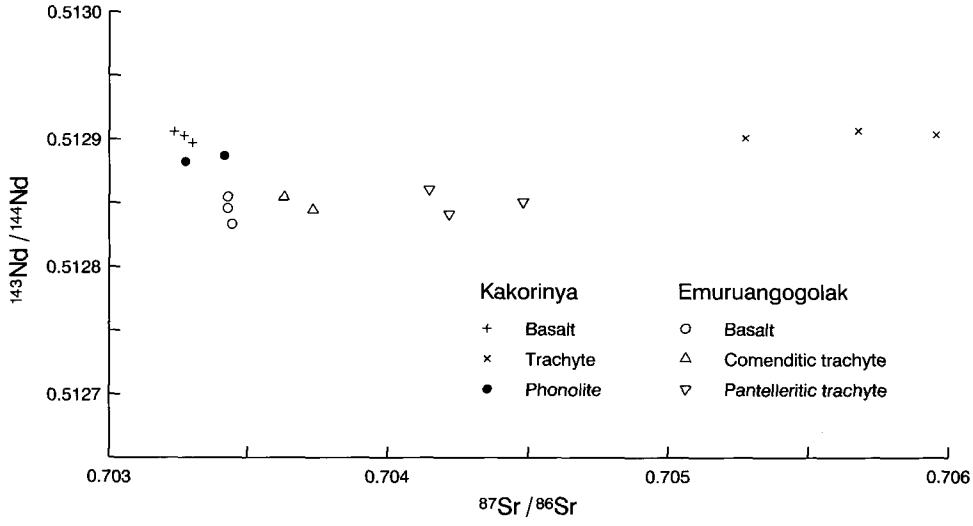

Figure 13.7 Plot of $^{143}Nd/^{144}Nd$ against $^{87}Sr/^{86}Sr$ for the younger lavas of Emuruangogolak and Kakorinya.

bined effects of assimilation and fractional crystallization (AFC) is provided in Figure 13.8, in which $^{86}Sr/^{87}Sr$ in the Emuruangogolak lavas increases linearly with Zr; the latter being taken as a fractionation index and a possible measure of residence time. However, when the age of the analyzed lavas is taken into account the situation appears to be more complicated. The least fractionated comenditic trachyte with the lowest $^{86}Sr/^{87}Sr$ is the youngest lava on the volcano. The variations in the degree of crustal contamination in the Emuruangogolak trachytes may be explained in a number of ways. The magma chamber may have been compositionally zoned, with an evolved cap of contaminated pantelleritic trachyte overlying a less contaminated zone of comenditic trachyte melt. Early eruptions could have been fed by the contaminated pantelleritic cap of the chamber, whilst later eruptions tapped deeper, less contaminated comenditic magmas. Alternatively, trachyte magmas may have fractionated and become contaminated in a high-level storage chamber, which has been periodically replenished with uncontaminated parental basaltic or less contaminated comenditic trachyte melt from deeper sources.

The interpretation of the Kakorinya data in Figure 13.7 is also complicated. On the basis of $^{86}Sr/^{87}Sr$ values the Kakorinya trachytes show evidence of crustal contamination relative to the basalts, but the phonolites show no sign of contamination and have virtually identical Sr, Pb and Nd isotopic compositions to the basalts. The phonolites of Kakorinya post-date the trachytes and with respect to trace element composition are generally more fractionated. This raises the question as to how evolved phonolitic liquids could have fractionated under closed-system conditions whilst less fractionated trachyte liquids became contaminated. On the strength of isotopic data it is unlikely that the trachytes and phonolites could have fractionated in the same magma chamber. The fact that they share similar ITE ratios (Figure 13.5) may be fortuitous, although it is more likely that they have fractionated (or melted) from a common primary source from which they have inherited similar ITE ratios.

Evidence presented in the next section (Section 13.9) strongly supports the presence of high-level trachyte magma bodies within the volcanic centres of the region. A plausible model for Kakorinya that may explain both trace element and isotopic compositions is that basaltic magma fractionated under closed-system conditions at depth to produce melts ranging in composition from basalt through trachyte to phonolite. High-level trachyte bodies could have formed in-situ by fractionation of basaltic magmas, or by the migration of trachytes from the deeper source. In either case, the high-level trachytes became crustally contaminated. In such a model, it is envisaged that phonolitic magmas from a deeper source would have been prevented from reaching the surface because of

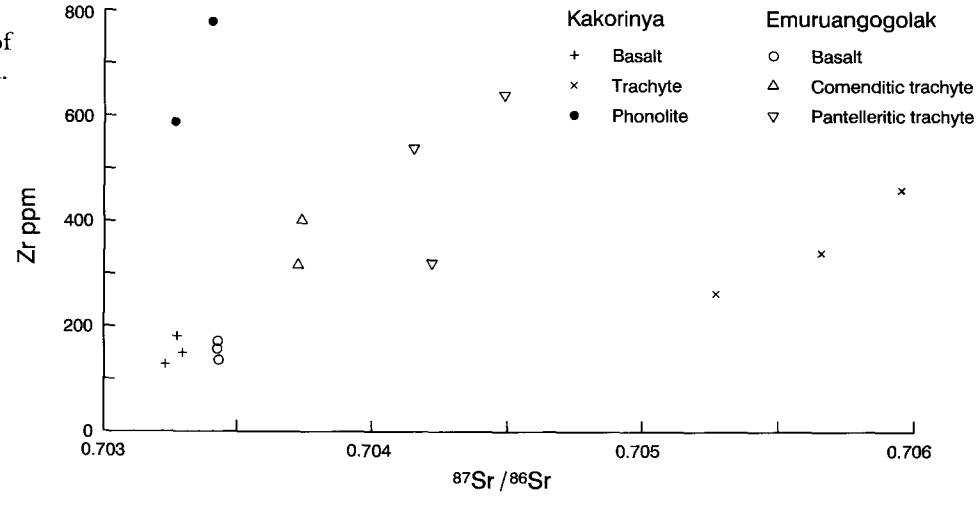

Figure 13.8 Plot of Zr against $^{87}Sr/^{86}Sr$ for the younger lavas of Emuruangogolak and Kakorinya.

the presence of the high-level trachytic magma bodies, which would have intercepted them. Only at a late stage in the evolution of Kakorinya, after caldera collapse and the evacuation (or solidification) of the high-level trachyte chamber, was it possible for uncontaminated phonolites and basalts to rise from deeper levels and erupt on the upper parts of the volcano. The depth of formation of the phonolites is open to speculation. Evidence from the nodules around the Katenmening pit crater of Silali (Section 13.7) suggests that phonolitic liquids may fractionate at shallow levels, whereas experimental evidence supports equilibration at depths equivalent to 7–8 kb (Section 13.9).

13.9 EVIDENCE FOR THE DEPTH OF MAGMA CHAMBERS

Direct evidence bearing on the depth of magma chambers within the volcanic centres is provided by the unroofed syenite on Namarunu (Section 10.4.9), which clearly indicates a high-level of intrusion into the volcanic pile. Additionally, recent drilling for geothermal energy at Eburru in the central sector of the Kenya Rift (Figure 1.1) penetrated a laterally extensive felsic intrusion or intrusion complex at depths of about 2 km beneath the summit, thus providing further evidence for high-level felsic intrusions within the volcanic centres of the rift. An abundance of syenitic nodules within the pyroclastic deposits on several of the volcanic centres in the project area may also be taken as evidence for shallow felsic intrusive bodies (cf. Mahood, 1984).

Additional evidence regarding the depth of magma chambers is provided by fracture patterns. At several of the volcanoes the intensity of faulting decreases and fault trends are refracted over summit regions, suggesting the presence of high-level magma bodies at the time of fracturing. Furthermore, Mahood (*op. cit.*) concluded that if magma chambers responsible for summit collapse are relatively deep, then subsidence is more likely to take place along regional faults producing graben structures, rather than upon ring fractures producing circular calderas. The presence of circular calderas within the project area therefore adds further weight to the notion of shallow magma chambers.

Basic intrusions are also thought to occur within the volcanic centres, as indicated by the presence of gabbroic nodules in the basalts and pyroclastic rocks of Emuruangogolak, Silali and Paka. The vesicular nature of the gabbroic nodules found around the Katenmening pit crater of Silali further suggests that such basic bodies may exist at relatively shallow levels.

Indirect evidence bearing on the depth of magma chambers is provided by the results of melting experiments on oversaturated peralkaline lavas. The melting experiments of Bailey and Cooper (1978) on a pantelleritic obsidian from Eburru indicate that under dry conditions alkali feldspar is the liquidus phase at pressures up to about 1 kb, where it is joined by quartz. Above 1 kb quartz is the liquidus phase and the temperature interval between the liquidus and the onset of alkali feldspar crystallization increases with increasing pressure. Alkali feldspar is by far the most dominant phenocryst phase in pantellerites and pantelleritic trachytes, but quartz phenocrysts are absent or rare, which suggests that pantellerites equilibrate at depths equivalent to less than 1 kb (3 km) (Mahood, 1984). Liquidii temperatures for pantellerites and trachytes converge at higher pressures (Bailey et al., 1974), supporting the view that the trachytes of the project area, which contain abundant alkali feldspar phenocrysts but no quartz phenocrysts, probably equilibrated at low pressures.

Melting experiments performed by Mahood and Baker (1986) on a mildly alkaline high-Ti ferrobasalt from Pantelleria, similar in composition to the basalts of the rift, also have bearing on the depth of fractionation beneath the volcanic centres of the surveyed area. During the initial stages of crystallization at pressures of 1 bar, liquids remained close to the critical plane of silica-undersaturation until, at lower temperatures the precipitation of Fe-Ti oxides drove the composition towards silica saturation. Thus the quartz-normative trachytes and pantellerites typically found in association with mildly undersaturated basalts in continental rifts, could be produced by low-pressure fractionation of basaltic magma. Mahood and Baker found that at pressures of 8 kb, liquids are driven to increasingly nepheline-normative compositions, suggesting that fractionation or partial melting of a basaltic source at higher pressures favours the production of phonolitic melts. The melting experiments of Hay and Wendlandt (1992) on Miocene flood phonolites from Kenya also support this interpretation, indicating depths of equilibration equivalent to a pressure of 7 kb.

13.10 THE FORM OF MAGMA CHAMBERS AND NATURE OF MAGMATIC PROCESSES

Although good evidence exists for magma chambers (or intrusions) at high structural levels within the volcanic centres of the surveyed area, the size, shape and configuration of these bodies remains speculative in the absence of detailed geophysical data.

Baker (1987) and Macdonald (1987) propose that compositionally stratified magma bodies have evolved within the rift's volcanic centres by a combination of crystal-fractionation and liquid-fractionation. In the process of liquid-fractionation, sidewall crystallization produces a fractionated liquid boundary layer adjacent to the wall. In magmas which decrease in density with differentiation, the fractionated boundary layer rises along the wall to accumulate as a separate zone in the upper parts of the chamber, but where fractionated liquids increase in density they descend to pond on the floor of the chamber (McBirney et al., 1985).

Density and temperature data derived from the lavas of Emuruangogolak and Paka led Baker (1987) to conclude that within the transitional-alkaline suites of the rift, density maxima occur within the ferrobasalt melts. Baker believed that in the basalt-ferrobasalt compositional range, ascent of differentiated dense ferrobasalt liquids would be impossible, and as long as the supply of replenishing basaltic magma was sufficient to offset solidification, the magma chamber could not differentiate past the density maximum and eruptions would therefore be of basalt. If replenishment was slow or ceased, the magma could fractionate past the density maximum and efficient liquid fractionation could take place, resulting in the ascent of a trachytic boundary layer and the accumulation of a strongly differentiated cap to the magma chamber.

Basaltic magma in the lower parts of such zoned magma chambers would be unable to penetrate upwards whilst the trachytic upper zones remain liquid. However, Baker (1987) suggested that replenishment of mafic magma could cause pressurization of the magma chamber and injection into surrounding tensile fissures, resulting in basaltic satellite eruptions. Such a mechanism may explain why trachytic rocks have been erupted from the upper parts of the volcanoes of the northern sector of the rift, but basalts were mainly erupted from fissures on the flanks. Basalts have only been erupted from the upper parts of the volcanoes at a late stage following caldera formation, presumably when liquid trachyte caps to the magma chambers had either been removed by eruption or had solidified.

Evidence for compositionally zoned magma chambers within the volcanic centres of the region is provided by the trachytic pumice lapilli tuffs on the east flank of Namarunu (see Section 10.4.6). These show a gradational transition from basal trachytic pumice deposits up into basaltic scoria, and are considered to represent the eruptive products of a zoned magma chamber, in which a fractionated trachytic cap was first erupted, followed by the evacuation of deeper basaltic zones.

The presence of compositionally zoned magma chambers or intrusions of the form proposed by Macdonald (1987) and Baker (1987) appears to fit many of the features of the volcanoes of the northern sector of the rift. However, isotopic data presented in Section 13.8 indicate that at Kakorinya the phonolites must have evolved in a separate magma chamber to that in which the trachytes equilibrated, and a two stage origin for the trachytes of that centre may have operated. The isotopic evidence from Emuruangogolak also suggests that the high-level Upper Trachyte magma storage system beneath the caldera has been replenished with fresh influxes of magma from time to time over the past 38 ka. Similarly, incompatible trace element data presented in Section 13.8 also indicate a number of trachyte lineages on Silali which are best explained in terms of several pulses of magma injection.

Supporting evidence for the form of zoned magma chambers, as envisaged by Baker (1987) and Macdonald (1987), may also be gained by drawing analogies with the eroded intrusive complexes of ancient rift systems. In petrological terms the best known ancient analogue for the Kenya Rift is probably the mid-Proterozic Gadar province of Greenland. This province contains rift-related transitional basalt and hawaiite dykes and lavas in association with central intrusive complexes composed predominantly of syenite (Upton and Emeleus, 1987). The syenitic intrusions are compositionally layered and were formed by fractional crystallization of the basaltic magmas. Individual complexes range in diameter from a few hundred metres up to tens of kilometres and typically have the form of steep-sided, quasi-cylindrical, composite intrusions. Giant dykes, composed predominantly of layered gabbroic and syenogabbroic cumulates form a link between simple dilational basaltic dykes and the central-type syenitic complexes.

In terms of size, it is considered a reasonable assumption that the high-level trachytic magma chambers within the volcanic complexes of the northern sector of the rift have, or had, diameters approximately the same as those of their associated calderas.

13.11 PETROLOGICAL SUMMARY

The volcanoes of the region are composed predominantly of trachyte and basalt, with trachyte being by far the most dominant rock type. Intermediate lavas of mugearitic and benmoreitic composition are scarce or at some centres absent. Minor amounts of phonolite are found at the Barrier complex and Silali.

The basalts are transitional alkali basalts which show a progressive increase in the degree of undersaturation northwards from Korosi to the Barrier. The basalts of the Barrier and to a lesser extent those of Emuruangogolak also show a marked increase in the degree of LREE enrichment when compared with the basalts of the other centres of the region. This is taken as evidence for greater involvement of garnet in the mantle source, implying greater depths of origin for the basalts of these two centres.

The trachytes are strongly peralkaline and include both undersaturated and oversaturated compositions. Good linear correlations are apparent between pairs of incompatible trace elements within the lavas at each centre and this is widely accepted as evidence for derivation of the trachytes by crystal fractionation of basaltic magmas. Simple trace element modelling based on Zr concentrations indicates that the transition between basalt and trachyte represents a relatively small proportion of the total compositional range. This partly explains the scarcity of intermediate lavas, although physical controls resulting from density and viscosity variations within the differentiating magma chambers are also thought to have discriminated against their eruption.

Field and structural observations strongly suggest that trachytic magma chambers have existed at high structural levels within the volcanic centres of the region. This is also supported by the results of melting experiments on peralkaline salic lavas which indicate that the trachytic magmas must have equilibrated under low pressures.

Pb and Nd isotopic analyses from Emuruangogolak and Kakorinya are compatible with derivation of the trachytes and basalts from a common source. However, Sr isotope ratios indicate that the trachyte magmas were contaminated by crustal material. On Emuruangogolak, $^{86}Sr/^{87}Sr$ values show a good linear correlation with the degree of fractionation, with comenditic trachytes having $^{86}Sr/^{87}Sr$ ratios intermediate between those of the basalts and pantelleritic trachytes. Although this provides strong evidence for AFC processes, the degree of fractionation and crustal contamination bears no relationship to the age of the lavas, and it is concluded that the high-level trachyte storage chambers have been periodically reinjected by fresh influxes of uncontaminated trachytic or parental basaltic magma from depth. Incompatible trace element data from Silali define several different trachyte lineages which also support a model of multi-phase injection of magma over prolonged periods.

On Kakorinya the youngest basalts, trachytes and phonolites appear to fall on a common fractionation trend, with the phonolites generally being more fractionated than the trachytes. However, Sr isotope ratios

indicate that the trachytes have suffered crustal contamination, whereas the phonolites are uncontaminated and isotopically similar to the basalts. From this it is concluded that although the trachytes and phonolites may have fractionated or melted from a common source, the trachytes resided within an open system whilst the phonolites evolved under closed system conditions. The fact that the phonolites are uncontaminated suggests that they are unlikely to have resided in a high-level magma chamber for any length of time.

No direct evidence is available regarding the form and configuration of the magma chambers that have existed or may exist within the volcanic centres of the region. However, by analogy with intrusion complexes exposed in eroded ancient rift systems, steep sided layered trachyte-basalt bodies are believed to underlie the volcanic centres. These are thought to be fed by basaltic melts which differentiate through a complex process of crystal-liquid and liquid-liquid fractionation to produce zoned chambers with trachytic caps. Trachytes and trachytic pyroclastic deposits were derived from the upper zones of the magma chambers and were erupted on the upper flanks and summit areas of the volcanoes. Basalts on the other hand were mainly erupted along fissures on the lower flanks and peripheral areas of the volcanoes. Only when the trachytic caps to the magma chambers were evacuated or had solidified sufficiently was it possible for basaltic lavas to erupt on the higher parts of the volcanoes. Similarly, at Kakorinya, phonolitic magmas were only able to reach the surface after caldera formation and trachytic activity had ceased.

14 Hydrogeology of the region

14.1 INTRODUCTION

Hydrogeological investigations, including both physical and chemical studies, were undertaken with reference to the geothermal potential of the area. The ultimate objective of these investigations was to obtain a conceptual model of the major hot and cold groundwater systems of the region. These studies have naturally concentrated on the geothermal systems associated with the volcanic centres, although the nature of the cold groundwater systems is also of interest, because these are the potential sources of recharge to the geothermal systems.

This chapter summarises the physical hydrogeological aspects of the Survey, whilst the geochemistry of the fluids is described in the following chapter (Section 15). Together these two chapters provide a synopsis of the work of Allen and Darling (1992) and Darling and Allen (1993), to which the reader is referred for more detailed accounts of the hydrogeology and hydrochemistry of the region.

In addition to work undertaken by the present survey, some information on the hydrology and hydrogeology of the southernmost part of the project area and the eastern margin of the Rift was obtained from an earlier water resource assessment project (WRAP) which investigated the Baringo and Laikipia areas (WRAP, 1987a and 1987b). Meteorological and hydrological information was also obtained from a study of Lake Turkana, carried out jointly by the Government of Kenya and the British Overseas Development Administration (Ferguson and Harbott, 1982).

Hydrogeological surveys normally rely on standard techniques involving the use of borehole data to provide information on aquifer properties and groundwater flow patterns. However, in the present study the paucity of borehole data has meant that greater reliance has had to be placed on indirect methods of assessing groundwater recharge, using meteorological and surface hydrological information.

It must be stressed that the hydrogeological interpretations contained in this report are not definitive. In an area of low rainfall, few boreholes and a low water table, interpretations must necessarily be somewhat speculative. The aim of the following account is therefore to provide a hydrogeological framework, which taken together with the geological and geochemical studies of this report will act as a guide for further investigations.

14.2 RECHARGE ESTIMATED FROM METEOROLOGICAL INFORMATION

14.2.1 Introduction

The extent of groundwater availability for recharge of geothermal systems depends primarily on hydrogeological factors such as transmissivity and storage. However, because groundwater data are few for the project area more emphasis is placed on the use of surface water data to estimate natural recharge.

14.2.2 Rainfall

Data were obtained from 45 rainfall stations situated within the Rift Valley and upon its margins, between Lake Bogoria in the south and Lake Turkana in the north. Figure 14.1 shows the distribution of the stations and indicates that much more data is available for the southern part of the area than for the north.

The map of mean annual rainfall (Figure 14.1) was produced using all the available data, including information from the WRAP rainfall maps for Baringo and Laikipia (WRAP, 1987a & 1987b). Within the area between Lake Baringo and Lake Turkana rainfall decreases in a northerly direction and generally increases with altitude. The floor of the Rift is appreciably drier than the margins and has mean annual rainfall ranging from about 650 mm around Lake Baringo to 166 mm at Loiyangalani on the south-eastern shores of Lake Turkana. The elevated ground of the western margin is generally wetter than the eastern margin, with mean annual rainfall reaching a maximum of more than 1400 mm in the Tugen Hills. Figure 14.2 illustrates the general dependence of rainfall on altitude, although the relationship is not simple; while data for the floor of the rift and western margin show a good linear relationship, with annual rainfall increasing by about 60 mm for each 100 m of ascent, rainfall for the eastern margin tends to be lower and more erratic for a given altitude.

Total annual rainfall varies considerably from year to year and the highest variability occurs in areas of lowest rainfall. Data obtained over a long period indicate that in the south of the area there are two rainfall peaks, which occur in April and August, and that the lowest rainfall occurs between December and February with January being the driest month. In the south of the area about 70% of the total annual rainfall occurs between March and August (WRAP, 1987a).

Information on rainfall for the northern part of the Suguta Valley and the region of Lake Turkana is sparse. The available data indicate that mean annual rainfall increases northwards along the shores of the lake, from 166 mm at Loiyangalani in the south-east to 360 mm at Todenyang in the north-east. Monthly rainfall variations are different to those in the south of the area. On the eastern side of the lake the mean monthly rainfall distribution is bimodal, with two roughly equal peaks in March–April and November, whereas on the western side there is a large peak in April and subsidiary peaks in July and November (Ferguson and Harbott, 1982).

14.2.3 Evaporation

Mean monthly potential evaporation data, measured using evaporation pans at 11 stations between Marigat

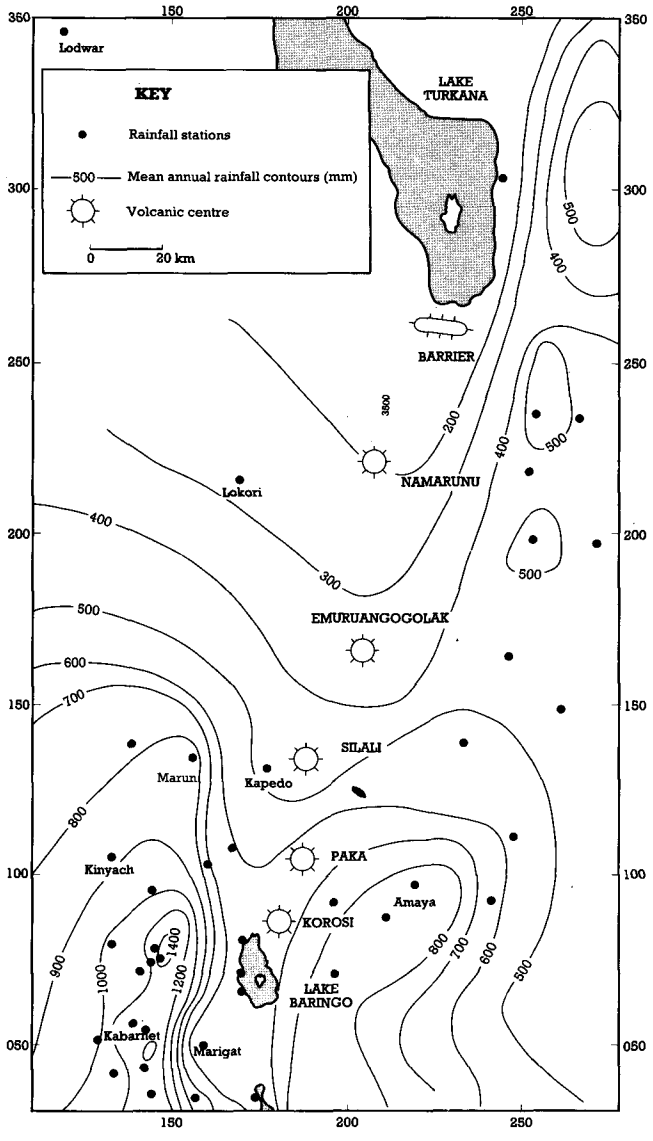

Figure 14.1 Mean annual rainfall distribution in the region between Lake Baringo and Lake Turkana.

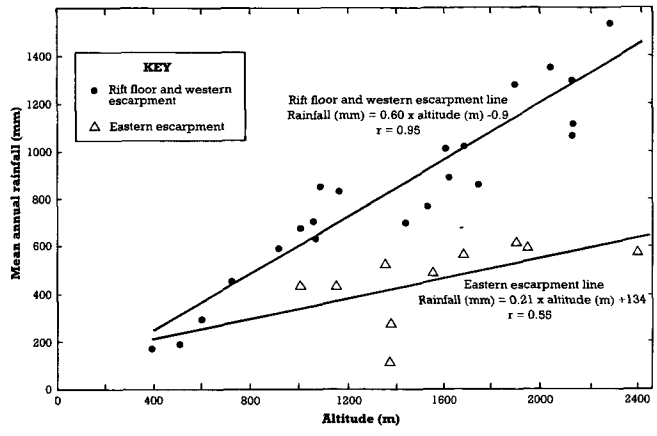

Figure 14.2 Plot of mean annual rainfall versus altitude for the region between Lake Baringo and Lake Turkana.

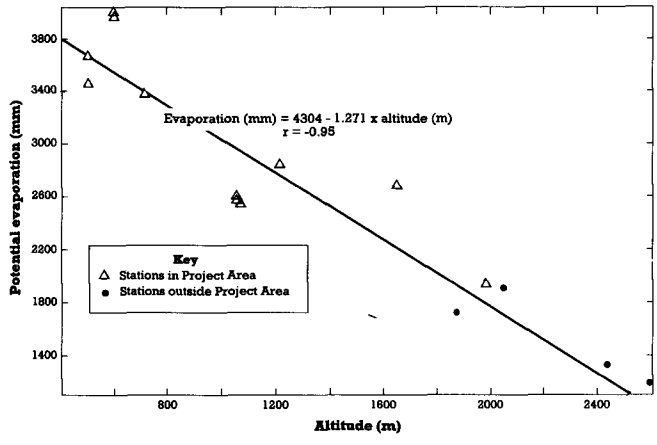

Figure 14.3 Plot of mean annual evaporation versus altitude for the region between Lake Baringo and Lake Turkana.

and Lodwar, were abstracted from records at the Meteorological Office and Ministry of Water Development. The location of these stations is shown in Figure 14.4, although where two stations are located near to each other a single site only is represented. For four stations, situated at Amaya, Kabarnet, Kapedo and Marigat, daily evaporation data were obtained over several years for comparison with daily rainfall values. In addition, data were obtained from the WRAP study for four other stations situated a short distance to the south of the project area (WRAP, 1987a).

Mean annual evaporation values vary from 1934 mm at Kabarnet to 3999 mm at Lokori. Average monthly evaporation rates vary most at high altitudes, where seasonal cloud cover is significant, and least in the arid low-lying areas in the northern part of the rift floor. The month of highest evaporation for most stations is March, although in some cases there is a January maximum, whilst the lowest evaporation rates occur between May and August.

Altitude exerts a major influence on evaporation rates. This is illustrated by Figure 14.3, which shows a very close inverse relationship between altitude and evaporation rate, with a correlation coefficient of-0.95. Because there are a limited number of evaporation stations within the project area it is not possible to draw a reliable map of potential evaporation. However, using the close relationship between altitude and evaporation rates it is possible to construct a map of estimated potential evaporation, and this is presented in Figure 14.4. This indicates that within the rift floor evaporation rates are high, being of the order of 3000 mm/yr or more.

Ferguson and Harbott (1982) estimated the average evaporation rate for the surface of Lake Turkana to be 2335 ± 347 mm/yr, based upon the rate of reduction in lake levels during periods of minimum inflow.

14.2.4 Recharge model

In broad terms, rainfall which does not evaporate or run off infiltrates the soil, and, if the soil moisture deficit is satisfied, may act as recharge to aquifers. Within the rift floor there is little evidence of significant surface runoff, presumably because the thin soils of the volcanic centres and surrounding sandy alluvial areas are permeable. The assumption is therefore made that rainfall that does not evaporate is available for recharge.

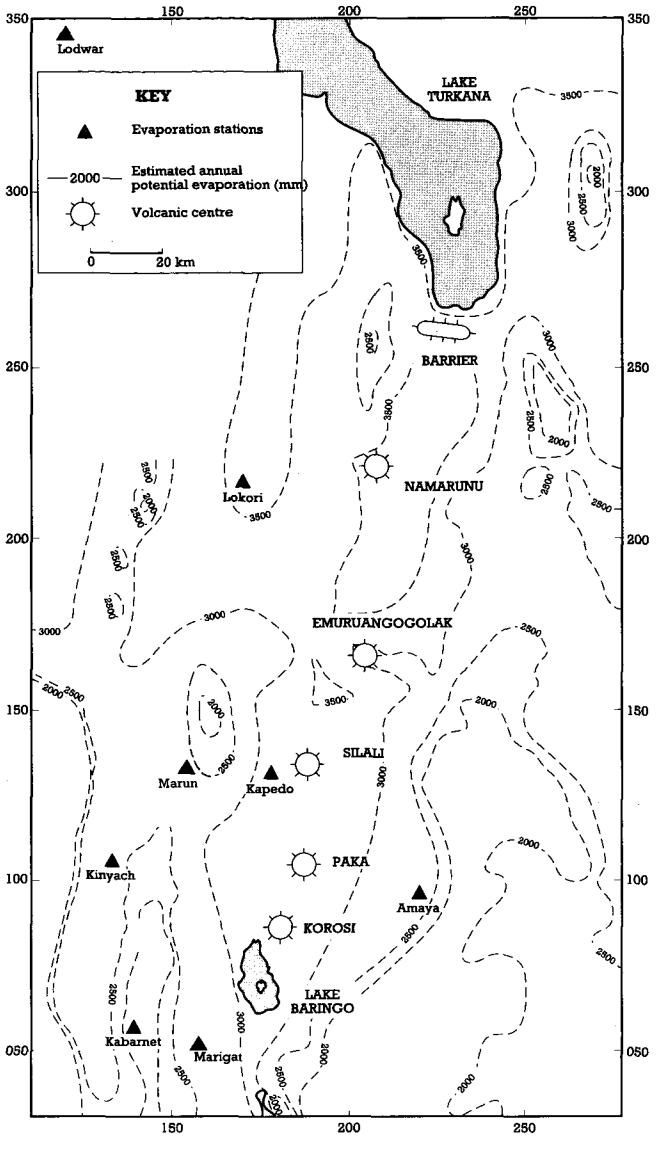

Figure 14.4 Map of estimated mean annual potential evaporation for the region between Lake Baringo and Lake Turkana.

If rainfall and potential evaporation rates are compared on an annual basis (Table 14.1) it is seen that in every case, including areas of high rainfall on the rift margins, potential evaporation exceeds rainfall. Even if mean monthly values are compared rainfall only exceeds evaporation at the Kabarnet site between April and August, with a total excess of 254 mm. However, this approach to estimating potential recharge is too crude for two reasons. Firstly, rainfall over the rift is generally concentrated into short periods of intense precipitation, during which precipitation greatly exceeds evaporation; but this difference is not apparent when monthly data are considered. Secondly, potential evaporation data only apply to freely evaporating surfaces, as measured using evaporation pans, but actual values of evapo-transpiration in an arid area will be much lower.

The first of these problems may be overcome by comparing rainfall and evaporation data on a time scale more appropriate to rainfall patterns. To this end, daily rainfall and potential evaporation data collected over several years were examined for the four

Table 14.1 Mean annual rainfall and potential evaporation

Station	Rainfall (mm)	Evaporation (mm)
Amaya	889	2698
Kabarnet	1357	1934
Kapedo Mission	445	3373
Kinyach Dispensary	875	2534
Lodwar MWD	–	3657
Lodwar Met	182	3488
Lokori MWD	–	3999
Lokori Met	295	3945
Marigat Pekerra MWD	–	2607
Marigat Pekerra Met	637	2559
Marun Mission	820	2824

meteorological stations of Amaya, Kabarnet, Kapedo and Marigat, which are at different altitudes around the project area.

The problem of estimating the actual amount of water lost by evapo-transpiration was considered using a computer model developed by Adams (1977), based upon a model of soil moisture deficit (SMD) proposed by Penman (1949). Soil moisture deficits occur when evapo-transpiration exceeds precipitation and vegetation has to draw on reserves of moisture in the soil to satisfy transpiration requirements. The SMD must be satisfied before rainfall infiltration can commence. When potential evaporation exceeds precipitation over a given period, SMD increases by the same amount and, up to a point, termed the Root Constant, the actual SMD increases by that amount. Once the Root Constant value of SMD has been reached it becomes increasingly difficult for evapo-transpiration to occur, and therefore subsequent increases in potential SMD (potential evaporation minus precipitation) lead to ever smaller increases in actual SMD. In practical terms this means that even for very arid areas there is an upper limit to SMD, taken to be 3.33 times the Root Constant by Adams (1977), and once this is satisfied infiltration can commence. The relationship between actual SMD and potential SMD used in the computer model is that proposed by Penman (1949).

For the computation an initial value of SMD, a Root Constant and daily values of rainfall and potential evaporation are required. Using this data the program calculates the actual SMD, the actual evaporation and the amount of infiltration on a daily basis.

Potential problems with the modelling are that neither values of initial SMD nor Root Constants are available for the four data sets. In practice it was found by running the program with different values of initial SMD that the model was very insensitive to this parameter. However, the problem regarding the choice of Root Constant is more serious since this has profound effects on the calculated amount of infiltration. Although precise values of Root Constants are unknown for the Rift Valley, estimated values were obtained from a recent hydrogeological study of the Chyulu Hills in south-eastern Kenya in which the Adams model was employed (Wright and Gunston, 1988). In this study various Root Constants were estimated for a range of vegetation types, ranging from

light scrub to intermontaine rain forest, underlain by young lavas and pyroclastic deposits. On this basis a range of root constants between 50–150 mm were considered appropriate for the four sites examined in the present study, with 50 mm being allotted to Marigat and Kapedo on the rift floor, 75 mm to Amaya on the eastern margin of the rift, and 150 mm to Kabarnet on the western margin.

For the rift floor stations the model predicts rapid increases to maximum SMD levels during the long dry periods, followed by occasional reductions towards zero deficits during periods of heavy rainfall. Infiltration is therefore predicted to occur on days when very heavy rainfall occurred, usually during a sequence of wet days. A similar pattern, although more subdued in nature, characterises the Kabarnet station.

Table 14.2 shows the long-term annual infiltration values obtained from the model for the four stations, using the whole range of Root Constants, but highlighting those considered most realistic for the particular vegetation cover at each site. The table shows that the SMD model predicts higher infiltration for the highest-rainfall station of Kabarnet than is suggested by taking potential evaporation values. In the low-rainfall areas of the rift floor the model also predicts that infiltration does occur for realistic root constants of 50–75 mm. For Marigat and Kapedo annual values of infiltration range between 21 and 38 mm, which is approximately 5% of the mean annual rainfall. Some support for this proportion of infiltration is provided by the WRAP study, which calculated from the analysis of baseflow hydrographs that average infiltration in the Baringo catchment is of the order of 1.5–3% of precipitation (WRAP, 1987a).

It is possible that the calculated infiltration for the rift floor is an underestimate, because the model assumes that recharge cannot occur until SMD is satisfied. However, when infiltration occurs in fractured aquifers, bypass mechanisms can operate, particularly during heavy rainfall. Thus, on the faulted and fissured volcanics of the rift floor percolating waters may enter aquifers directly via open fractures before the SMD is reduced to zero.

For an annual infiltration value of 30 mm, which is the average value predicted by the model for Kapedo and Marigat using realistic Root Constants (of 50–75 mm), an area of 100 km^2 would be sufficient to produce a recharge of 3×10^6 m^3/yr, which is equivalent to the discharge rate from the Olkaria geothermal power station (Allen et al., 1989). This calculated area should be viewed only as a rough estimate, given the relatively simplistic model assumptions and likely data errors. However, it is considerably smaller than the area of any of the volcanic centres in the region, suggesting that local recharge mechanisms would be sufficient to sustain geothermal production, even in the absence of recharge from the rift margins.

14.3 WATER BALANCE AND THE ESTIMATION OF GROUNDWATER OUTFLOW FROM LAKE BARINGO

14.3.1 Introduction

The soil moisture deficit model used in the previous section to estimate recharge by infiltration considers only the relationship between rainfall and evaporation. In this section the extent to which the analysis can be extended by considering water balance is examined.

14.3.2 The Problem of estimating groundwater flow in the Baringo catchment

The water balance equation for the Baringo catchment, excluding the lake, which may be considered as a separate but connected system, may be written as:

$$P_{basin} = E_{basin} + R_{out(Basin)} + G_{out(Basin)} + \Delta S_{total(Basin)} \quad (1)$$

Where:

P	=	Precipitation
E	=	Evaporation
R_{out}	=	Runoff (out of the catchment)
G_{out}	=	Subsurface flow (out of the catchment)
ΔS_{total}	=	Change in storage (surface water + groundwater)

The quantity of interest is $G_{out(Basin)}$ because this determines the theoretical long-term maximum value for groundwater abstraction for all purposes, including the exploitation of geothermal systems.

The rivers of the catchment flow into Lake Baringo, but there are no rivers flowing out of the lake, and therefore $R_{out(Basin)}$ is equal to $R_{in(Lake)}$ in equation (2). The groundwater inflow from Lake Baringo is transferred out of the catchment and therefore does not enter into the calculation. The S term (storage) may also be eliminated by considering long periods.

The problem with using equation (1) to estimate groundwater flow, is that this term is so small compared with the other terms. The analysis of section 14.2 indicates that most rainfall on the rift floor evaporates. The WRAP study considered that groundwater flow from the whole basin was at least one order of magnitude less than rainfall, evaporation or surface runoff, and in using equation (1) regarded the groundwater flow term as unimportant (WRAP, 1987a). The WRAP study therefore reduced equation (1) to:

Table 14.2 Long-term annual infiltration values predicted by the recharge model for different root constants (Rc).

Station	Altitude (m)	Infiltration (mm) Rc = 50	Rc = 75	Rc = 100	Rc = 150 (mm)
Kabarnet	1980	447	388	358	321
Amaya	1620	143	101	64	12
Marigat (MWD)	1060	36	21	9	0
Kapedo	720	38	22	13	0

Values of infiltration and root constants measured in mm. Infiltration values underlined are those calculated using the most realistic root constants for the station concerned.

$$P_{Basin} = E_{Basin} + R_{in(Lake)} \quad (2)$$

Using this equation (2) WRAP estimated that 95% of the rainfall evaporates, which agrees well with its baseflow hydrograph analysis, and also agrees with the results of Section 14.2.

It is apparent therefore that it is not possible to use a catchment water balance to determine groundwater flows in the Baringo catchment at present, because the volumes of flow lie well within the errors in precipitation, evaporation and runoff data.

14.3.3 Water balance model for Lake Baringo

Lake Baringo is a freshwater lake which is fed by several permanent rivers flowing in from the south. As there are no surface outlets from the lake, and because the area is one of very high evaporation, there must be a significant component of groundwater outflow, otherwise the lake would be salty. In this section the amount of groundwater outflow from the lake is estimated using a water balance model.

The water balance of Lake Baringo is best considered separately from the rest of the catchment, because a major factor in its water balance equation, evaporation, can be accurately estimated, since this is equal to the potential value at all times.

The WRAP study (WRAP 1987a) considered the water balance of Lake Baringo using the following equation:

$$P_{Lake} + R_{in(Lake)} = E_{Lake} + G_{out(Lake)} + \Delta S_{total(Lake)} \quad (3)$$

Where:

P_{Lake} = Precipitation over the lake
$R_{in(Lake)}$ = Runoff into the lake
E_{Lake} = Evaporation from the lake
$G_{out(Lake)}$ = Subsurface flow from the lake
$\Delta S_{total(Lake)}$ = Change in lake storage

Although estimates of annual precipitation (P) and evaporation (E) are reasonably well constrained by meteorological data, and the annual change in lake storage (ΔS) can be obtained from lake water-level measurements, the values of river discharge into the lake (R_{in}) are too poorly known to be used in equation (3). Therefore the WRAP study resorted to a salt balance approach to relate R_{in} to the subsurface outflow from the lake, G_{out}, using the following equation:

$$R_{in(Lake)} = G_{out(Lake)} \times TDS_{Lake}/TDS_{River} \quad (4)$$

Where:

TDS_{Lake} = Total dissolved solids of the lake
TDS_{River} = Total dissolved solids of rivers entering the lake

By combining equations (3) and (4) to eliminate R_{in}, and by using the resulting formula to calculate G_{out} on an annual basis, values for G_{out} ranging between 199 and 248 mm/yr were derived. For a mean lake area of 144 km^2 and an average G_{out} of 229 mm/yr this corresponds to a mean annual subsurface outflow from the lake of 33×10^6 m^3/yr.

While factors such as precipitation, evaporation and lake storage can be adequately assessed, there are problems in obtaining a reliable estimate of TDS in the relationship between groundwater flow and river runoff in equation (4). The WRAP study assumed a constant lake chemistry of 550 mg/l. The study noted that the average TDS of influent river water was difficult to determine, because it varied with discharge, but obtained a value of 70 mg/l from available data. The evaporative concentration factor (TDS_{Lake}/TDS_{River}) derived by WRAP from these data is therefore 7.9.

Subsequent work undertaken as part of the present survey shows that the chemistry of the lake is variable with time. A chloride balance study of the lake, using a time averaged Cl^- concentration indicates that the evaporative concentration factor may be as low as 2.5 (Section 15.2.1), which would suggest a subsurface outflow of 104×10^6 m^3/yr from the lake. Furthermore, an isotope balance suggests that subsurface outflow in excess of 150×10^6 m^3/yr may occur (Allen and Darling, 1992).

In conclusion, whilst it is difficult to calculate the amount of subsurface outflow from Lake Baringo, it does appear that groundwater recharge from the lake of at least several tens of millions of cubic metres per year is occurring, and data from the present survey suggests that outflow could exceed 10^8 m^3/yr. An analysis of borehole data (Section 14.5.3) indicates that this groundwater outflow will be directed northwards along the axis of the rift floor.

14.4 WATER BALANCE FOR LAKE TURKANA

Lake Turkana is by far the largest lake in the Kenya Rift, having a length of 250 km and a width of 15–30 km. Its total volume is thought to be about 245×10^9 m^3 (Yuretich and Cerling, 1983). The most important river flowing into Lake Turkana is the Omo, which enters at the northern end and according to Ferguson and Harbott (1982) supplies around 90% of the influent water to the lake. The Omo rises in the Ethiopian highlands where mean annual rainfall exceeds 1500 mm. Precipitation mainly occurs between April and September, but there is a lag of two months between the onset of the rains and the rise in lake level.

The Kerio and Turkwel rivers are the only other important rivers flowing into Lake Turkana. These enter at the south-western end and are estimated by Ferguson and Harbott to contribute less than 10% of the lake's inflow. Many minor water courses drain into the lake from the surrounding country, but they only flow intermittently and their contribution to the total water input to the lake is considered to be negligible.

The conductivity of Omo river water entering the lake is about 80 μS/cm, whereas that of the lakewater is generally around 3500 μS/cm. This disparity, caused by evaporation, has enabled the effects of Omo river water on the lake to be traced after the main discharge starts in June. As reported by Ferguson and Harbott (1982) the low salinity water in June is confined to the north-west corner of the lake. The effect spreads southwards until September when the southern part of the lake reaches its minimum salinity. Salinities then rise until March, when they are uniformly high over the lake, indicating no appreciable influence from the Omo.

In general Lake Turkana appears to be in a stable state, with annual inflows roughly equalled by water loss. There is no surface outflow from the lake and there is no evidence of substantial subsurface outflow (Section 15.2.3) and therefore water loss is likely to be almost entirely by surface evaporation. Subsurface inflows are unknown, but in such an arid area they are probably not large. Yuretich and Cerling (1983) suggest that, with a surface area of 7.5×10^9 m^2 and an annual evaporation rate of around 2300 mm/yr, total water loss by evaporation is about 17.5×10^9 m^3/yr. Input from rainfall, at around 180 mm/yr, is small, amounting to 1.5×10^9 m^3/yr. The balance, of about 16×10^9 m^3/yr inflow to the lake is provided by river inflows, with the main contribution from the Omo River.

A small amount of water seeps from Lake Turkana beneath the Barrier Volcanic Complex to Lake Logipi. Taking the elevation of Lake Turkana as 365 m and that of Lake Logipi as 270 m, the hydraulic gradient between the two, over a distance of 15 km, is about 0.006 m/m. Numerous hot seeps and small springs occur around the northern shores of Lake Logipi at the base of the southern flanks of the Barrier, and chemical evidence indicates that some of this flow originates in Lake Turkana. The total discharge of the springs is not large however, and while it is not possible to give a figure for the flow, it is estimated by Darling and Allen (1993) not to exceed 2000 l/s. Such a discharge only amounts to 10^6 m^3/yr, and even if all this was derived from Lake Turkana, it is insignificant when compared with other factors involved in the water balance of the lake. This conclusion would be unaltered even if the estimated spring discharge were increased by a factor of one hundred.

Given the above hydraulic gradient, the estimate of maximum subsurface outflow, and assuming that flow occurs at depths not exceeding 500 m over a width of 10 km, an approximate value may be obtained for the hydraulic conductivity of the material composing the Barrier Volcanic Complex. This is calculated to be around 0.04 m/day, and although it is a rough estimate, it is considered reasonable by comparison with the low permeability materials generally found elsewhere in the rift.

14.5 BOREHOLE DATA AND REGIONAL GROUNDWATER FLOW

14.5.1 Introduction

Data were obtained from records for a total of 70 boreholes, situated within the floor of the rift and on its bounding interfluves between Lake Baringo and Lake Turkana. These data have been used to gain information on aquifer properties and regional groundwater flow patterns.

It is important to stress that the borehole data set is very limited for such a large area. In particular, few boreholes are located within the rift floor, which is the area of greatest geothermal interest, and none has been drilled between Silali and the Barrier. It should also be emphasised that aquifer properties determined by the analysis of borehole records can only apply to the depths penetrated by the boreholes. Since these water boreholes only reach depths of a few hundred metres at most, it is not possible to predict the properties of potential geothermal reservoirs at greater depths, except by extrapolation. However, the regional groundwater flow systems inferred from examination of the water level data may persist to substantial depth.

14.5.2 Water level data

Water strike information is available for 66 of the boreholes, and the depths at which water was encountered in these ranges from a few metres to 206 m. Fifteen boreholes had water strikes at depths greater than 100 m, the majority of these being on the rift margins. Water rest levels range up to 146 m below ground level. Most rest levels (89%) are at depths of less than 100 m below the surface and a significant proportion (61%) are at depths of less than 50 m.

A combination of water strike and water rest level information is available for 63 boreholes. In 55 (87%) of these boreholes the final water rest levels are higher than initial water strike levels, suggesting confined aquifer conditions. The incidence of confined aquifer conditions may not be so common as these data suggest, because if drilling rates are high in aquifers of low permeability then water strikes may not be observed until boreholes have been deepened. However, when differences between rest levels and strike levels in excess of 5 m are considered, then 42 (67%) of the boreholes indicate confined conditions.

Records for 36 boreholes indicate that multiple aquifers were encountered. In 25 cases the rest water level after the first strike did not change after subsequent strikes and therefore hydraulic connection between aquifer-bearing layers can be assumed. In 11 boreholes the rest water level changed after the second water strike, indicating the presence of separate aquifers. These boreholes mainly occur on the margins of the rift to the east of Lake Baringo, and around Kabarnet to the west.

14.5.3 The potentiometric map and regional flow patterns

The potentiometric map shown in Figure 14.5 was constructed using borehole water rest level data and spring data. Where data are scarce contours have been estimated by assuming that the potentiometric surface is a subdued replica of the ground surface.

The depth to the water table beneath the rift floor probably varies from less than 50 m near Korosi to around 100 m near Silali. Depths to water under the volcanoes are unknown, although water rest altitudes may be higher than in the surrounding rift floor if recharge mounds exist (see below).

In broad terms groundwater flowlines are expected to be perpendicular to the groundwater contours shown in Figure 14.5, with recharge occurring at high groundwater altitudes and discharge at low altitudes. The figure therefore indicates areas of groundwater recharge on the east and west margins of the rift and a zone of discharge along the rift floor. Flows along the rift floor are directed northwards from Lake Baringo as far as Lake Logipi which is a regional discharge area with an approximate water surface level of only 270 m above mean sea level. Lake Turkana lies at an altitude of about 365 m and therefore subsurface drainage from the lake is directed southwards towards Lake

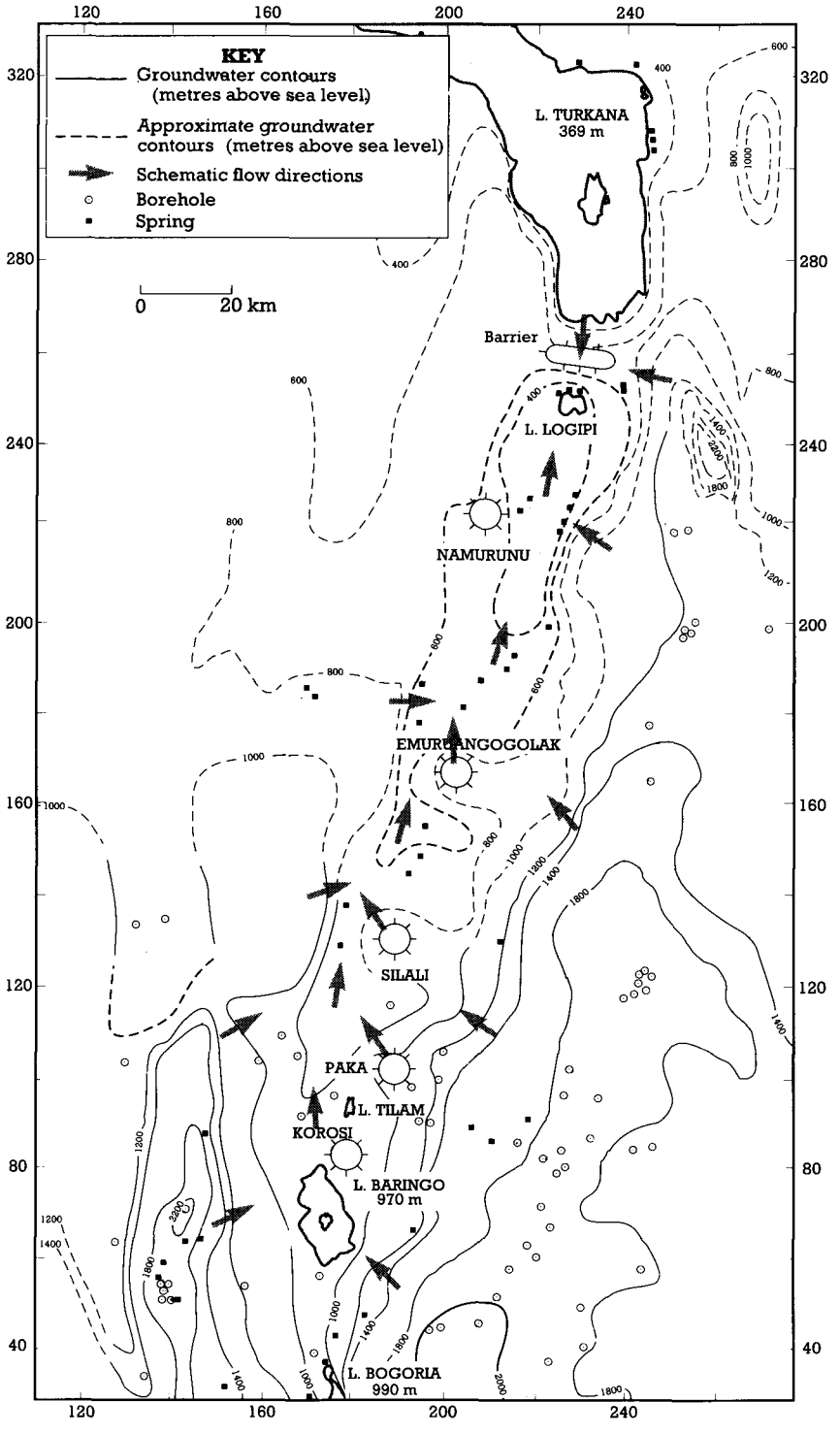

Figure 14.5 Potentiometric map of the region between Lake Baringo and Lake Turkana.

Logipi, passing beneath the Barrier Volcanic Complex.

The potentiometric data indicate that the regions around the volcanic centres of Korosi, Paka, Silali and Emuruangogolak are likely to be subject to groundwater flows both laterally from the rift margins and axially from the south. The rift margin component appears to be dominantly from the east for the Paka, Silali and Emuruangogolak areas, and perhaps also for Korosi. Lake Baringo water is likely to be the dominant component of axial flow within the rift floor in the south of the area, but decreases northwards. The potentiometric map (Figure 14.5) indicates that the axial flow is mainly directed along the western side of the inner trough as far north as Emuruangogolak. The Namarunu area appears to be one of easterly groundwater flow, with a component of axial flow, although it is unlikely that Baringo water persists in a readily identifiable form in this area. In the north of the area, around the Barrier Volcanic Complex, groundwaters are likely to be dominated by southerly subsurface flow from Lake Turkana with a strong component of easterly flow from the eastern margin of the rift around Ngirio.

The foregoing discussion does not imply that water encountered by drilling directly under the volcanic centres would necessarily be expected to derive solely from lateral rift margin or axial rift floor sources,

because the volcanoes form substantial topographic hills and should be the sites of local recharge mounds. Thus groundwater encountered beneath them to an unknown depth could be purely local in origin. Support for local recharge within the rift floor was presented in Section 14.2.4.

14.5.4 Effects of structure on regional flows

Hydrogeological investigations in the central sector of the Rift, undertaken during Phase I of the Project, considered that faulting had significant affect on regional flows (Allen et al., 1989). This was based upon a large amount of data obtained from more than 600 boreholes. In this central sector, flows across the rift are inhibited by major faults acting as zones of low permeability and in some areas the potentiometric surface is very deep. In addition, flows along the rift are affected by minor axial faults in the rift floor. These faults are considered to channel flows along the rift axis, either by acting as conduits if they are permeable, or by inhibiting lateral flow if they are of low permeability. In essence therefore, the effects of faulting in the central sector of the rift cause groundwater flows from the margins towards the axis to follow longer, deeper paths, which align with flows along the axis.

In hydrogeological terms the structure of the northern sector of the rift has similarities with the central sector, as investigated by the first phase of the project (Allen et al., 1989). In particular, both sectors are characterised by a preponderance of axial faults. Therefore, the same effects of structure on regional flows might be expected. Igneous dykes are also sporadically exposed within the volcanic centres of the region, and are believed to occur in axial swarms beneath the rift floor (Section 2.3). Such dyke swarms are likely to exert a similar influence to axial faults, acting as barriers to lateral flow and causing alignment of flow along the axis of the inner trough. The general paucity of borehole data make these suppositions regarding the effects of faulting and dyking difficult to prove or disprove, but some support for the inhibition of lateral flows is shown by borehole data in the Lake Baringo–Paka area. This region is heavily faulted by NNE-trending faults and the regional groundwater level gradient is roughly E–W across the fault trend. Several boreholes in the eastern part of this area show anomalously high hydraulic gradients in an E–W direction. For example, boreholes D1 and D7 (Figure 14.11) are only 6.25 km apart and have an altitude difference of only 55 m, yet water rest levels in these have a difference in altitude of 134 m. Similarly, although boreholes C3437 and C7122 are only 2.24 km apart and have an altitude difference of only 30 m, they have water rest levels that differ in altitude by 120 m. These figures strongly suggest that hydraulic barriers exist between these borehole pairs and the offset of aquifers by faults and, or, dykes is the most likely explanation.

14.6 AQUIFER PROPERTIES

14.6.1 Introduction

Hydraulic information relevant to the determination of aquifer properties is available to varying degrees for the 70 boreholes in the project area. Most of the borehole records have some productivity information, although less than half have data enabling specific capacity to be calculated, and only a quarter have enough information for an estimate of transmissivity to be made. This lack of transmissivity information means that more reliance must be placed on the less accurate, but more numerous, specific capacity and yield data as a guide to aquifer properties.

The available data from drillers' logs suggest that aquifer types include fractured volcanic rocks, sediments and weathered contacts between lithological units.

14.6.2 Yield

Information about yield is available for 63 boreholes within the area, of which 3 were dry.

Figure 14.6 shows the cumulative relative frequency curve of yields from the 60 productive boreholes. These data indicate that borehole yields are generally low throughout the region. The yields of 50% of the boreholes are less than 103 m^3/day and only 10% have yields in excess of 400 m^3/day, whilst the greatest frequency of borehole yields is in the range 40–60 m^3/day.

These yield estimates are only an approximate guide to aquifer properties because the values are influenced by factors other than the nature of the aquifer. For example, in a productive borehole the yield may be more a function of pump capacity than potential productivity. On the other hand, no account is taken of drawdown, and since production tests usually only last 24 hours, the long-term yield may be less than the stated value. However, the low values of the majority of borehole yields do suggest that regional permeabilities are low.

14.6.3 Specific capacity

The effects of different pump capacities and variations in drawdown between boreholes can be eliminated by using the concept of specific capacity (yield per unit drawdown), which allows borehole productivity to be compared on a more equal basis. Although specific

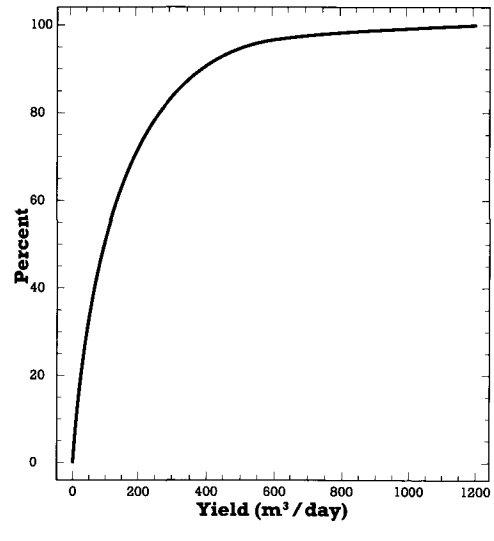

Figure 14.6 Cumulative relative frequency plot of borehole yields.

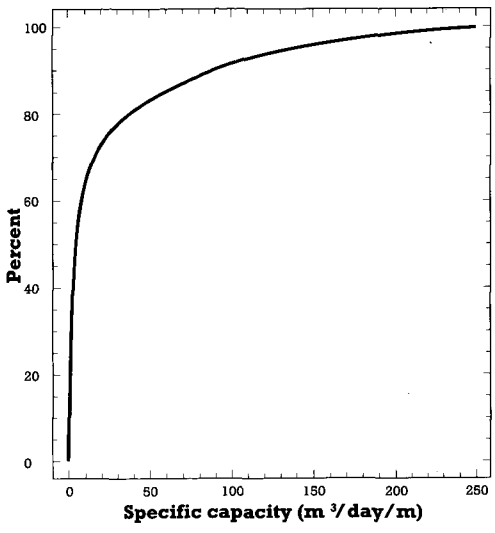

Figure 14.7 Cumulative relative frequency plot of borehole specific capacities.

capacity is not controlled solely by aquifer properties it is more closely related to them than yield alone.

Available data have enabled 32 specific capacity values to be calculated. The cumulative relative frequency curve of Figure 14.7 indicates that specific capacity values are generally low, with 50% of values falling below 4.5 m^3/day/m and only 10% exceeding 85 m^3/day/m. Those boreholes with high specific capacities include all three types of aquifer which are commonly found in the rift, namely sediments, weathered contacts between volcanic deposits and fractured volcanic rocks.

14.6.4 Transmissivity

Pumping test data from which aquifer transmissivity values may be calculated are severely limited for the area and data that does exist are of variable quality.

A total of 18 transmissivity values were obtained from pump test data and these are provided in Table 14.3, together with specific capacity values. Although transmissivity values range up to nearly 100 m^2/day, the data plotted in Figure 14.8 show that 75% of all values are less than 17 m^2/day, and 50% are less than

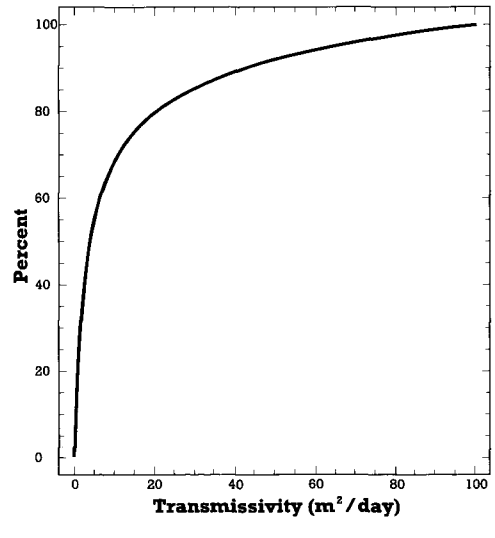

Figure 14.8 Cumulative relative frequency plot of borehole transmissivities.

Table 14.3 Specific capacity and transmissivity values for boreholes.

Borehole	Specific Capacity m^3/day/m	Transmissivity m^2/day
C1833	0.8	0.1
C3470	3.5	4.0
C3506	16.1	8.0
C3833	0.5	0.3
C3855	0.4	0.1
C3868	4.3	5.4
C3869	0.6	0.3
C4722	31.2	25.2
C4780	19.7	4.2
C4838	68.0	22.1
C5170	28.2	36.3
C5349	105.6	95.5
C5370	5.3	2.5
C5487	51.4	11.7
C6362	1.6	1.5
C6363	79.1	76.6
C6364	9.2	6.6
C6365	3.0	2.4

4.8 m^2/day. The greatest frequency of borehole transmissivities lies in the range 0–2 m^2/day, and although the average value of the data set is 17 m^2/day this is weighted by a few relatively high values for boreholes from the rift margins (C5348 and C6363).

The data of Table 14.3 are plotted in Figure 14.9, which illustrates that there is a good correlation between transmissivity and specific capacity, which conforms to the line:

$$T = 0.358 S_c^{1.175} \quad (5)$$

Where S_c = Specific capacity (m^3/day/m)

The good fit of the empirical equation (5) to the data suggests that there is some validity in using the equation to predict transmissivity values where only specific capacity data exist, thus enabling the transmissivity data set to be enlarged to 32 values.

The predicted transmissivity values are presented in Table 14.4, and have been used together with the original values of Table 14.3 to produce the cumulative relative frequency plot of Figure 14.10. The results suggest that borehole transmissivities are on average even lower than were indicated by the original transmissivity data, with 50% of values being less than 2.6 m^2/day.

The implication of the foregoing analysis is that aquifer transmissivities in the surveyed area are generally low. This in turn suggests that, in the absence of other factors the permeability at depth is also likely to be low, because generally permeability tends to decrease with depth as a result of diagenesis and fissure closure caused by overburden stress.

However, for various reasons the borehole data need to be treated with caution. Firstly, the data set is very small for such a large and hydrogeologically complex area, and no data are available at all for the geothermal prospects. Secondly, the borehole values only relate to the depth penetrated, which is much shallower than any geothermal reservoir. Thirdly, the volume of aquifer influencing a short-lived borehole produc-

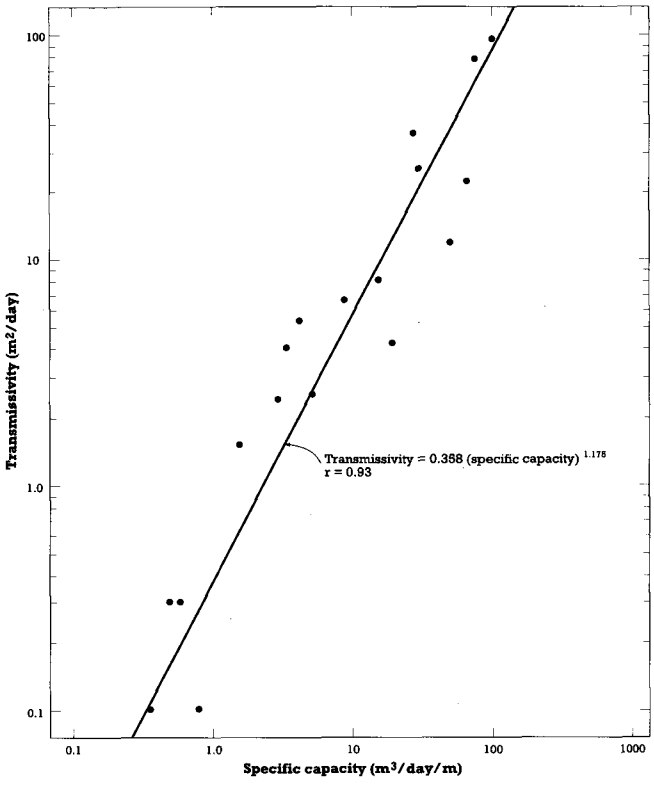

Figure 14.9 Plot of transmissivity versus specific capacity.

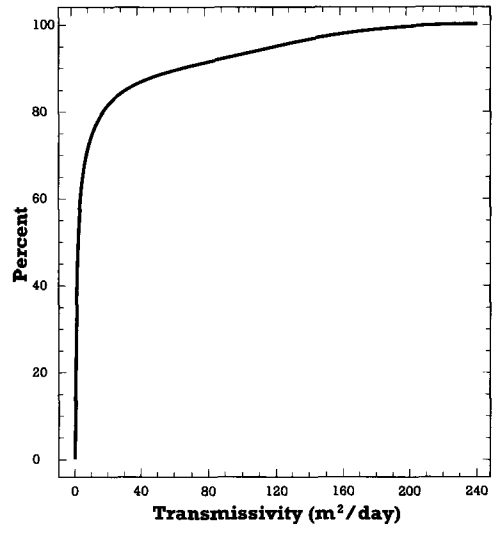

Figure 14.10 Cumulative relative frequency plot of actual and predicted borehole transmissivity values.

tivity test is very small, and therefore it is possible that the expected permeability enhancement caused by the considerable faulting in the rift is not reflected in the borehole pumping test data.

A more regional assessment of aquifer transmissivity may be gained by examination of the subsurface flow from Lake Baringo. In theory, if the volume of flow, the hydraulic gradient, and the cross-sectional area are known, then the average aquifer permeability can be calculated.

Assuming a hydraulic gradient of 0.01, a width of 15 km and an approximate flow from the lake of 100 × 10^6 m^3/yr (a rough average of the three estimates given in Section 14.3.3), the transmissivity is calculated to be 1800 m^2/day.

This figure is substantially greater than the 17 m^2/day average value calculated from borehole data. However, the boreholes only partially penetrate the aquifers and the average depth of penetration (taken crudely to be the distance between first water strike and the bottom of the borehole) is 74 m for the 18 boreholes for which transmissivity data are available. This would imply a full aquifer thickness of almost 8 km to give the transmissivity value estimated from lake discharge. Such a figure is unrealistically high by a factor of about 4, which in turn suggests that the borehole transmissivity values significantly underestimate regional values.

Naturally the above analysis based on lake discharge is very simplistic, given the available data. On the other hand the estimate does not include the unknown northward groundwater flow beneath the rift floor from sources other than the lake. All that can be concluded is that transmissivities are somewhat larger than those suggested by borehole data alone.

Table 14.4 Transmissivity data estimated from specific capacity values

Borehole	Specific Capacity m^3/day/m	Estimated Transmissivity m^2/day
C1018	4.83	2.3
C1785	1.55	0.6
C1882	1.48	0.6
C1896	5.59	2.7
C2345	18.14	10.8
C2434	1.97	0.8
C2844	8.91	4.7
C2847	0.48	0.2
C2972	0.23	0.1
C3055	224.68	208
C3119	1.39	0.5
C3456	0.64	0.2
C3461	3.99	1.8
D1	151.58	131

14.7 THERMAL SPRINGS AND BOREHOLES

14.7.1 Thermal springs

The following discussion is concerned only with the physical aspects of various warm and hot springs within the area.

The distribution of groundwater temperatures within the area is bimodal, with a distinct break between 39°C and 45°C. For the purpose of description hot springs are designated as having temperatures above 45°C. These occur widely within the inner trough between Lake Baringo and Lake Turkana (Figure 15.2). Their localities have been described in the previous chapters of this report covering the individual volcanic centres of the region, and their precise positions are shown on the accompanying 1:50 000-scale geothermal maps.

The springs on the rift margins generally have low flow rates and low temperatures, reaching up to 39°C.

These springs are not associated with high temperature geothermal activity, such as fumaroles and altered ground, and probably result from deep circulation of rift flank waters through marginal faults.

The hot springs within the inner trough have a wide range of flow rates and temperatures, and occur in several different structural and geomorphological settings.

As discussed in Section 14.5.3, the main direction of subsurface flow under the inner trough floor is along its axis from south to north, reversing north of Lake Logipi. This is modified by lateral flows off the rift margins and from local recharge mounds under the axial volcanic centres. Explanations for the origins of the springs within the inner trough must therefore be set in this context.

The Kapedo hot springs make up the largest spring system in the region. They issue at temperatures of around 50°C from fractured basalts along the base of the western flanks of Silali, where they act as the baseflow source of the Suguta River. Total flow from the springs, as estimated from gauging the Suguta River at Kapedo, is around 1 m^3/S. If a mean annual surface temperature of 25°C at Kapedo is assumed, this implies a heat flow from the springs of 100 Mw, indicating a significant heat source.

In a regional sense the Kapedo springs lie in an area of converging outflow waters from the western margin of the rift and from Silali, with axial flows along the rift, and on this scale the source of the springwaters is not apparent. The WRAP study of the Baringo catchment (WRAP, 1987a) concluded that the spring flow, of around 30×10^6 m^3/yr, is similar to its estimate for subsurface outflow from Lake Baringo, and therefore suggested that the lake could be the source of the Kapedo springs. This idea has the attraction that it appears to explain how the Kapedo springs have such a large discharge in an otherwise arid area. This explanation may be partly correct, in the sense that the outflow from Lake Baringo is large and is directed northwards. However, the potentiometric map (Figure 14.5) indicates that all groundwater flows between Lake Baringo and Silali are directed northwards, including local recharge and lateral flows from the rift margins, and that much of this water may move through the Kapedo area. It therefore seems more likely that the channelling of groundwaters from a variety of sources gives rise to the Kapedo springs, and that the component from Lake Baringo, 50 km to the south, is unlikely to be large.

If the average recharge in the rift floor is taken to be of the order of 30 mm/yr (Section 14.2.4), then the area required to support the Kapedo springs would be about 110 km^2. This is much smaller than the area of the rift floor between Lake Baringo and Kapedo and provides further evidence that subsurface flow from Lake Baringo is unlikely to be the only or even the major component of the spring discharge. Furthermore, stable isotope analyses suggest that it cannot exceed 30% (Section 15.4.1).

On a local scale, the position of the Kapedo springs on the western margin of Silali suggests that this volcano provides the source of the heat and perhaps a significant proportion of the water; bearing in mind that recharge on Silali is probably higher than on the rift floor because of its elevation. On the other hand it is possible that the heat output of the springs could be provided by regional groundwater flows causing convective movement of heat into the Kapedo area, although Silali is a much more obvious heat source.

In conclusion, the most likely hydrogeological explanation for the source of the Kapedo springs is that they are a mixture of outflow from the Silali recharge mound with groundwaters flowing axially northwards along the rift. The heat source is most likely to be Silali itself, possibly with a contribution from deeply circulating hot waters from the rift floor. However, chemical data presented in Section 15.4.1 provides little evidence for a high temperature contribution to the springs.

The Lorusio springs are situated a short distance to the north-west of Silali. They discharge at temperatures of up to 82°C as a series of pools and seepages 1.5 km to the west of the Suguta River at the base of the western margin of the rift. The source of the springwaters is not apparent from the potentiometric map (Figure 14.5) because the springs lie in an area where easterly groundwater flows from the western margin of the rift converge with westerly and northerly outflows from the Silali recharge mound and with northward directed flows along the axis of the rift floor. If the Lorusio springs were cold, then on a local scale their position near the foot of the western escarpment of the rift margin and at a higher elevation than the Suguta River would undoubtedly indicate an origin to the west. However, their high temperature and proximity to Silali, which is the most obvious heat source in the area, suggests that a connection between Lorusio and Silali cannot be discounted, although the waters do not have high temperature chemical characteristics (Section 15.4.1).

The hot springs immediately to the north of Emuruangogolak record a range of temperatures up to 70°C. From the orientation of the potentiometric surface in this area it is probable that these springs represent flow from Emuruangogolak.

The hot springs at Elboitong are located along the base of the escarpment of the eastern margin of the rift opposite Namarunu (Section 10.6.2). These constitute a large and vigorous system with temperatures exceeding the local boiling point and reaching up to 100.2°C. The total flow from the Elboitong springs has not been gauged, but is of a similar order to that of the Kapedo springs. Given their large discharge and high temperatures, the Elboitong springs clearly indicate a very significant heat flow. From their position at the base of the eastern escarpment of the rift margin and from the steep easterly-dipping potentiometric surface in this area (Figure 14.5) it would appear likely that rift margin waters make an important contribution to the springs. However, the inner trough in this area (the Gap) is very narrow and constricted, and axial groundwater flows in the floor of the rift are therefore likely to be an important source also. Other springs in the vicinity of the Gap, along the eastern side of Namarunu and around the Crescent, may have a similar origin. If an axial dyke swarm exists beneath the Gap, as suggested by the line of young basaltic centres, this could act as a barrier to deeply circulating waters from the eastern margin of the rift along major boundary faults.

At the northern end of the Suguta Valley the springs discharging around the shores of Lake Logipi almost

certainly have their origins to the north, where groundwater is driven southwards by the potentiometric head gradient of 0.08 m/m which exists between Lake Turkana and Lake Logipi. It is likely that this water from Lake Turkana becomes mixed to some extent with rift-margin waters and perhaps locally infiltrated water, and is heated by its passage through the Barrier Volcanic Complex.

14.7.2 Thermal boreholes

The average annual ground temperature in the floor of the rift is estimated to be 25°C using temperature data from Marigat. The temperatures of water discharges from boreholes is often higher than this, and in some boreholes is significantly so (Table 14.5).

Anomalously high borehole discharge temperatures do not in themselves imply either high geothermal gradients or high heat flows. However, in the absence of borehole temperature logs such data may be used as a guide to geothermal gradients if the producing aquifer level is known. Unfortunately aquifer level data are rarely available for boreholes within the rift, but a range of estimates may be made by assuming that all production occurs either where water is first struck or alternatively from the bottom of the borehole, which lead respectively to maximum and minimum estimates of geothermal gradient. The true value of geothermal gradient should therefore lie within this range.

Table 14.5 presents estimated geothermal gradients obtained by this method for boreholes with discharge temperatures in excess of 25°C. Twelve of the fifteen boreholes with anomalous temperatures lie in the rift floor. The three exceptions (C3855, C4417 and C3833) occur on the eastern margin of the rift but do not indicate particularly strong thermal anomalies.

Two of the thermal boreholes in the rift floor, C6362 and C6365, lie just to the south of the surveyed area, between Lake Baringo and Lake Bogoria. These partly penetrate a thick sequence of fluvio-lacustrine sediments between the two lakes. Temperature logs were run in these boreholes by the WRAP project (WRAP, 1987a). These indicate high temperature gradients between the surface and the water table, below which lower, but still high, gradients extend to the bottom of each hole at depths of 60 m. The explanation for the change in gradient at the water table is presumably that the thermal conductivity of the unsaturated material is lower than that of the saturated sediments. The source of the thermal water is unknown, but is likely to be to the south or south-west according to potentiometric gradients.

The remaining thermal boreholes all lie in the rift floor between Paka and Silali. Their locations, discharge temperatures and estimated geothermal gradients are shown in Figure 14.11. The highest borehole temperatures are found in the Nginyang-Kositei area (C3470, C3868 and C6363) and to the south-west of Paka. Estimated geothermal gradients are highest in the Nginyang-Kositei boreholes, where values greater than 100°C/km are suggested. When these thermal boreholes are considered with the regional potentiometric surface it is apparent that groundwater in the Nginyang–Kositei area probably originates to the south-west, rather than in the known geothermal centres of Korosi or Paka. It is uncertain whether this indicates an as yet unknown geothermal source, or is simply a reflection of widespread thermal waters within the rift.

The boreholes around the 1200 m potentiometric contour to the east of Paka intercept water flowing from the eastern margin of the rift and have less elevated temperatures than boreholes further to the west. Borehole D1, which is closer to the heat source of Paka is warmer and has a more elevated geothermal gradient. It probably receives heat and water fluxes from the volcano because although nominally at a higher potentiometric level than the Paka area, it is close to the likely recharge mound of Paka.

Morgan (1973) estimated heat flow values for three boreholes within the surveyed area. Two of these values were considered to be relatively reliable, and are 89.6 mW/m^2 at Chemolingot (C3470) and 111 mW/m^2 at Losikirimoi (C3461) on the periphery of the southern flanks of Silali. These values provide an additional indication of anomalously high heat flow in the floor of the rift within the project area (Section 2.2).

Table 14.5 Thermal borehole temperatures and geothermal gradient estimates.

Borehole	Location	Discharge Temperature (°C)	Estimated Geothermal Gradient (°C/km) Min	Max
C3437	Tangulbei	30.2	28	49
C3466	Nyunyau	'Hot'	–	–
C3470	Chemolingot	37.7	108	347
C3833	Sirata Oirobi	27	16	53
C3855	Baragoi	26	–	–
C3868	Nginyang	32.2	92	817
C4417	Baragoi	29	33	121
C6362	Salabani	45	220*	775*
C6363	Kositei	36.2	105	116
C6364	Chesirimion	34	75	85
C6365	Ngambo	45	185*	425*
D1	Katangora	36	69	87
D4a	Orus handpump	28	–	–
D4b	Orus solar	28	–	–
D7	Kokwototo	28	–	–

* values obtained from borehole temperature logs.

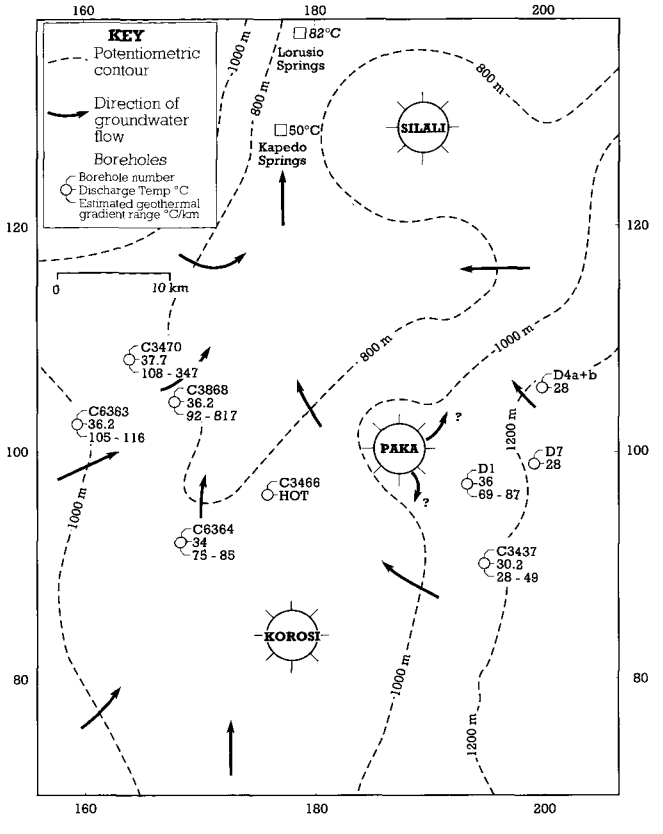

Figure 14.11 Thermal data for boreholes in the Korosi–Silali region.

14.8 CONCLUSIONS REGARDING THE HYDROGEOLOGY OF THE REGION

Groundwater flows in the region as far north as Lake Logipi are a combination of northerly axial flows along the rift floor, and lateral flows from the sides of the rift. Axial flow within the rift floor is generally directed along the western side of the volcanic centres. At the Barrier Volcanic Complex, axial flow is directed southwards from Lake Turkana towards Lake Logipi. The volcanic centres along the axis of rift may have local recharge mounds which will locally perturbate the regional flow systems. The interaction between lateral and axial flows is modified by faults and dykes trending along the rift. These cause lateral flows from the margins to follow longer and deeper paths, and to align with axial flow paths within the rift floor.

Groundwater within the rift is recharged from several sources as follows:

Lateral groundwater flows are recharged on the rift margins.

Lake Baringo recharges groundwaters in the floor of the rift.

Lake Turkana contributes towards the recharge of groundwaters beneath the Barrier Volcanic Complex

Local recharge on the rift floor by infiltration of rainfall is likely, particularly on the more elevated volcanic centres themselves.

The availability of local recharge, the magnitude of subsurface flow from Lake Baringo, and the availability of groundwater from the rift margins all suggest that geothermal production on a scale similar to the existing geothermal power station at Olkaria would not greatly affect regional water resources.

Borehole data for the area are limited, with information available for only 70 boreholes. None of these boreholes was drilled to depths much greater than 200 m and therefore there is no direct information on the physical properties of the underlying geothermal reservoirs. The available data from drillers' logs suggest that aquifer types are fractured volcanics, sediments and weathered contacts between different lithological units. Such aquifers may be discrete on a local scale, but on a regional scale hydraulic connections between aquifers are most probable. It is likely that geothermal reservoirs at depth are formed from these types of aquifers.

The hydraulic properties of aquifers, estimated from borehole data, are generally poor. It is estimated that the average value of transmissivity is only 17 m^2/day, with even lower values suggested by specific capacity data. However, regional estimates of aquifer properties, derived from subsurface flows from Lake Baringo suggest significantly higher values. It is almost certain that individual geothermal reservoirs will be substantially affected by local faulting.

15 Fluid geochemistry

15.1 INTRODUCTION

Samples of lake waters, river waters, hot and cold spring waters, steam condensates, and gases from fumaroles and hot springs were collected from representative sources for chemical and isotopic analysis. The sampling programme was designed to provide detailed information on the composition of geothermal fluids associated with the volcanoes within the inner trough, together with a more general appraisal of hydrochemical conditions in the region as a whole. This compositional data is used in conjunction with the physical hydrogeological information presented in Section 14 to obtain an understanding of the nature and the source of the fluids within the geothermal systems of the region.

The locations of sample sites are shown in Figures 15.1 and 15.2, and the results of the chemical and isotopic analysis of the fluids are presented in Tables 15.1 to 15.6. The salient features of these data are summarised in the following pages, but for a more detailed

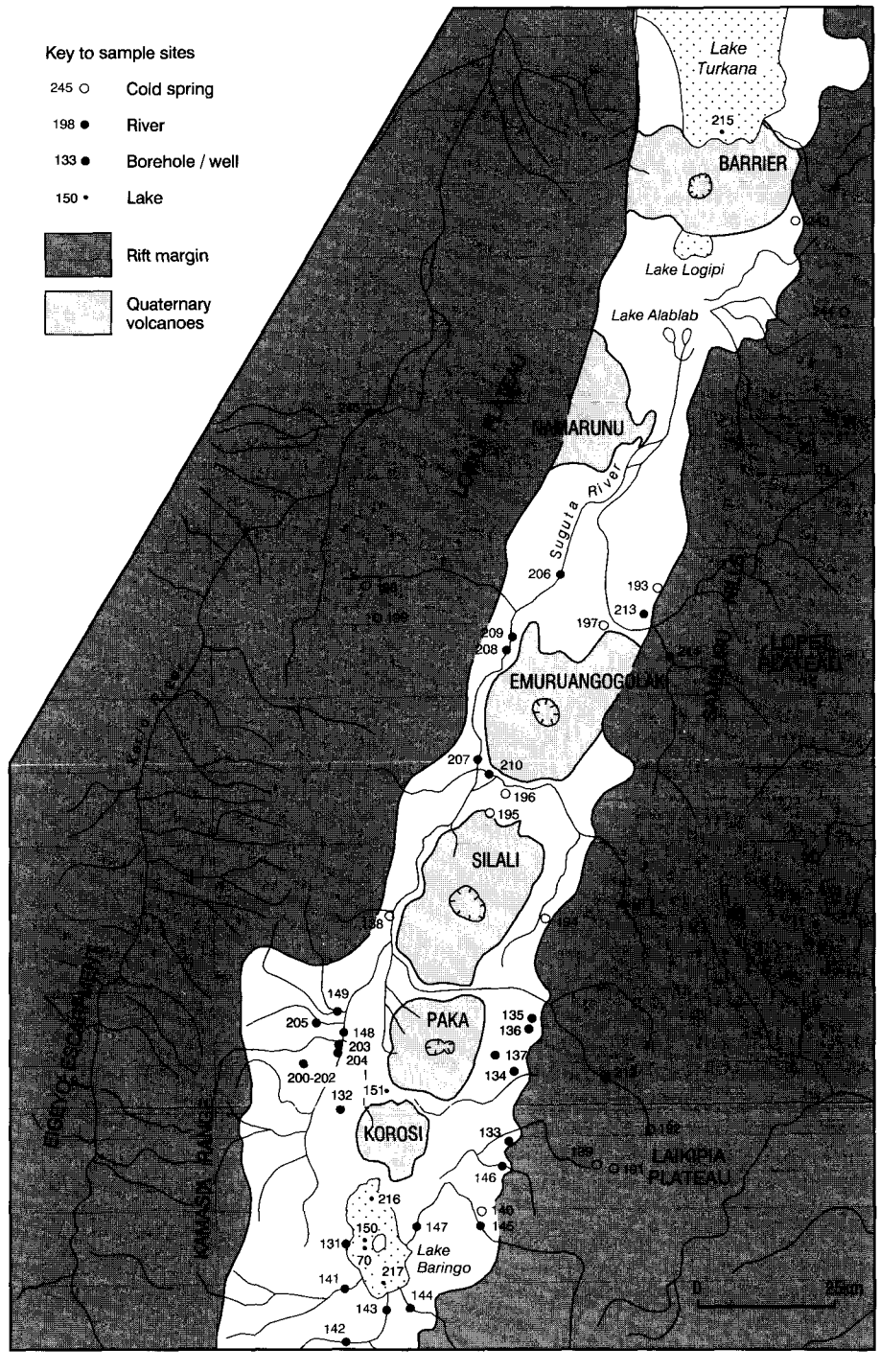

Figure 15.1 Map showing the location of ambient surface water and groundwater sample sites.

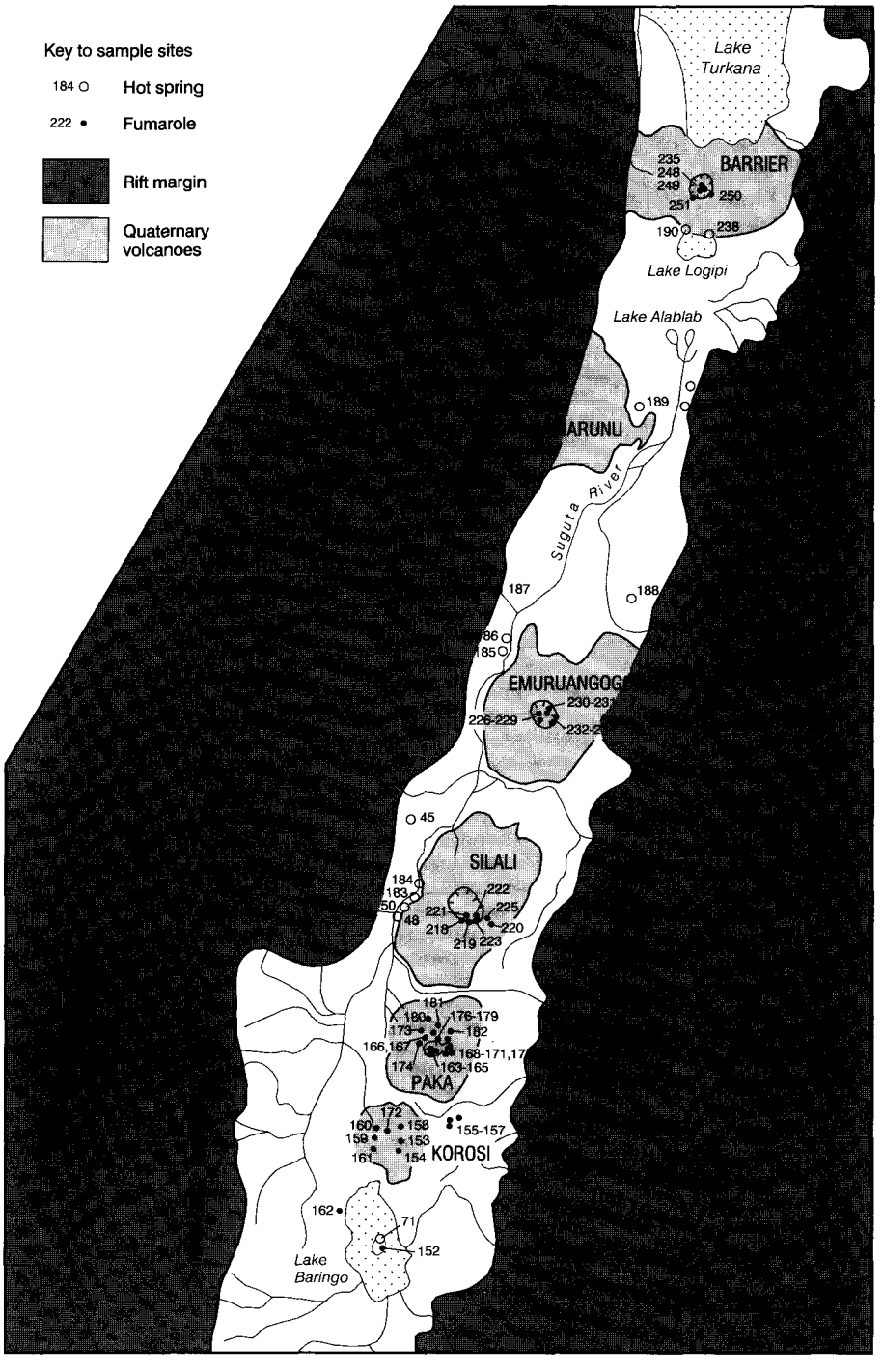

Figure 15.2 Map showing the location of hot spring and fumarole sample sites.

discussion the reader is referred to the reports of Allen and Darling (1992) and Darling and Allen (1993).

15.2 SURFACE WATERS

The surface waters within the northern part of the rift may be conveniently described in three separate groups, corresponding to the main drainage basins of the region. These are, Lake Baringo and its catchment, the rivers draining northwards into the Suguta Valley, and Lake Turkana.

15.2.1 Surface waters of the Baringo Basin

Rivers draining into Lake Baringo from the western margin of the rift have total dissolved solids (TDS) contents of 93–250 mg/l, whereas those from the eastern margin have a higher solute content of 218–655 mg/l. Comparison of the average Cl^- content of these rivers with the Cl^- content of Lake Baringo suggests an evaporative concentration factor within the lake of about 2.5 times. However, measurements of lake chemistry over a five-year period indicate that solute load varies significantly with seasonal fluctuations in rainfall and lake levels, having been 1.5 times higher when the lake was low in the dry years of 1986 and 1991, than in the intervening years.

The stable isotopic compositions of the rivers draining into the lake do not appear to be significantly affected by evaporation, except perhaps for that of the Mukutan (sample 147). Only a relatively small number of isotopic analyses of river samples are available for the Baringo catchment, but these appear, with the excep-

Table 15.1 Chemical composition of waters in mg/l

No.	Locality	Temp	pH	Na	K	Ca	Mg	HCO_3	Cl	SO_4	Si	Li	B	F
HOT SPRINGS														
45	Lorusio[a]	81.0	7.65	2150	57.0	3.0	0.2	4710	295	197	35.7	0.96	0.96	–
45	Lorusio[b]	82.2	7.45	2120	55.8	3.0	0.2	5000	300	200	33.2	0.96	0.92	48
48a	Kapedo[a]	50.0	8.25	988	22.0	1.6	0.6	2000	215	80.0	35.6	0.06	0.87	–
48a	Kapedo[b]	50.8	8.25	1020	22.7	1.6	0.5	2140	210	83.0	33.0	0.05	0.92	28
48a	Kapedo[c]	50.0	8.35	994	23.3	1.7	0.6	2110	240	83.4	36.1	0.05	0.88	27
71a	Ol Kokwe Island[b]	95.8	6.90	22.1	4.5	1.5	0.5	121	1.4	76.1	38.3	0.02	<0.06	0.42
71b	Ol Kokwe Island[a]	94.0	9.10	832	36.0	0.5	<0.7	1960	260	40.0	87.0	0.56	1.04	–
71b	Ol Kokwe Island[b]	96.0	9.05	922	39.3	1.0	<0.1	1980	260	30.5	126	0.61	1.19	19
71c	Ol Kokwe Island[b]	96.0	6.40	38.7	7.6	23.3	9.2	<1	6.2	1510	116	0.04	<0.06	5.4
183	Kapedo Spr SL26/2[c]	–	–	963	22.9	2.2	0.3	1900	250	84.9	41.0	0.07	0.94	28
184	Kapedo Spr SL27/5[c]	44.6	8.25	913	20.1	2.3	<0.1	1720	220	82.4	48.7	0.15	0.86	29
185	Suguta Spr SV3a[c]	68.4	8.25	1160	12.2	1.0	<0.1	2290	250	140	54.0	0.26	0.78	53
186	Suguta Spr SV3b[c]	64.0	8.30	1146	13.2	1.1	<0.1	2220	265	138	53.9	0.24	0.72	46
187	Kamuge Spr[c]	50.4	7.75	925	6.9	4.2	1.3	1930	160	100	38.4	0.22	0.47	37
188	Kageinya Spr[c]	67.8	9.50	5420	85.5	3.0	0.3	3350	2280	3700	81.5	0.23	13.6	190
189	Namarunu Spr[c]	66.2	8.80	5500	113	0.5	0.2	5860	3200	814	26.0	<0.01	6.53	140
190	Logipi NW	61.4	8.30	4170	79.4	0.5	0.1	5160	3420	590	18.5	0.05	5.11	110
236	Elboitong S	95.0	7.10	6770	129	0.82	<0.1	7940	4400	1070	46.2	0.307	6.78	87
237	Elboitong N	91.8	9.00	6690	126	1.40	0.5	8240	4500	1060	58.8	0.246	6.81	87
238	Logipi NE	69.8	8.85	6200	120	0.48	<0.1	5720	5250	920	30.8	0.149	6.39	82
239	Central Island	70.5	7.20	1550	78.9	13.9	25.2	2480	1059	30.8	95.7	0.414	4.45	4.2
COOL SPRINGS														
138	Nginyang-Kapedo[b]	36.0	8.30	991	21.3	2.8	2.1	2140	200	80.7	32.7	0.05	0.82	26
139	Churo[b]	28.0	7.20	131	4.5	1.7	0.3	326	13.9	4.8	24.9	<0.01	<0.06	1.2
139	Churo[c]	–	8.15	133	4.7	1.6	0.3	313	17.5	5.0	24.3	<0.01	<0.06	1.1
140	Ebirisat[b]	37.5	9.00	178	1.9	0.4	<0.1	435	23.0	7.1	19.3	<0.01	<0.06	0.14
191	Nangarwa Spr[c]	–	8.85	153	2.4	0.5	<0.1	340	30.0	8.5	18.4	<0.01	<0.06	2.1
192	Amaya Spr[c]	–	8.35	142	3.0	0.8	0.1	328	20.0	7.7	15.6	<0.01	<0.06	1.9
193	N Samburu Gates Spr[c]	–	8.85	638	4.7	4.9	1.2	1260	141	140	26.0	<0.01	0.53	19
194	Kachurkolh Spr[c]	31.0	9.15	1450	10.6	3.8	1.4	3370	191	126	10.0	0.61	0.06	18
195	Kalnangi Spr[c]	31.7	9.15	1040	18.0	0.5	<0.1	2880	260	102	36.0	0.16	1.04	35
196	Amakat Spr[c]	–	9.80	353	10.7	4.8	0.8	577	125	88	9.1	<0.01	1.09	16
197	S Nangarabat Sprs[c]	31.1	9.15	1680	24.9	0.6	0.2	3440	370	213	25.3	0.02	1.80	60
198a	Napeiton Sprs[c]	32.5	7.80	351	6.2	5.1	2.6	731	65.0	47.7	29.9	0.06	0.06	14
198b	Napeiton Well[c]	37.2	7.60	468	8.0	7.1	4.3	855	155	77.5	28.3	0.06	0.08	14
198b	Napeiton Well	36.8	7.80	471	7.8	7.1	4.2	899	156	79.7	27.2	0.061	0.08	–
199	Nasaken Spr[c]	31.0	7.50	104	6.6	15.6	1.6	260	15.0	16.6	28.0	0.06	0.04	7.7
08U*	Kanukurdio b/h	33	7.00	162	1.9	41.8	46.5	543	50	8.8	38.0	<0.01	0.09	<0.1
09U*	Eliye Springs	32	8.88	185	1.3	1.1	0.3	403	9.9	8.8	10.1	<0.01	0.08	0.1
240	Eliye Springs	35.4	9.00	142	0.6	0.97	0.2	344	5.5	11.8	9.7	0.007	0.04	2.0
241	Eliye North	37.3	8.75	110	0.8	1.39	0.3	267	3.5	6.5	9.0	<0.007	<0.03	2.2
242	Loyangalani	39.2	7.65	89	5.0	17.3	25.6	302	40	20.8	21.4	<0.007	0.07	0.3
243	Parkati Well	amb	7.50	244	22.8	104	45.7	262	217	306	56.6	0.013	0.03	1.3
244	Tum	amb	7.55	19.6	3.8	30.9	7.4	128	8.0	23.5	15.8	<0.007	<0.03	0.2
WELLS														
131	Kampi Ya Samaki[b]	–	7.70	263	21.0	18.8	16.7	727	55	22.7	31.1	0.05	0.13	43.0
131	Kampi Ya Samaki[d]	–	8.15	227	18.5	16.0	13.9	637	46.8	11.4	29.2	0.04	0.12	–
132	Chesirimion B/h[b]	–	7.20	94.8	7.4	2.2	1.1	199	14.4	9.6	43.1	0.03	0.06	3.60
132	Chesirimion B/h[c]	34.0	7.10	107	7.5	2.4	1.2	235	21.0	9.5	50.4	0.04	0.07	3.5
133	Tangulbei B/h[b]	30.2	7.70	164	5.4	27.0	21.3	556	26.5	11.7	23.7	<0.01	<0.06	0.90
134	Kokwo Toto B/h[b]	28.0	7.05	76.0	11.3	69.4	11.7	399	10.7	3.3	31.2	<0.01	<0.06	1.28
135	Orus Solar B/h[b]	28.0	7.00	139	10.5	37.6	12.3	483	31.7	–	27.8	<0.01	<0.06	1.40
136	Orus Hand B/h[b]	28.0	6.45	49.2	5.0	8.8	3.4	121	18.8	6.6	23.3	<0.01	<0.06	0.76
137	Katangora B/h[b]	36.0	8.30	122	10.9	7.2	3.3	266	48.2	12.7	13.7	<0.01	<0.06	3.76
200	Kositei Project Well[b]	–	7.35	104	6.1	28.9	6.9	360	17.5	7.5	40.7	0.01	<0.06	3.1
201	Kositei Mission Well[b]	–	7.25	168	6.2	26.9	7.6	478	12.5	33.9	33.0	0.04	<0.06	2.2
202	Kositei B/h[b]	35.8	8.95	224	1.8	0.8	<0.1	482	15.5	15.8	23.5	0.08	0.06	11
203	Nginyang School B/h[c]	–	–	893	4.7	1.4	1.1	1950	100	85	18.5	0.06	0.21	20
204	Nginyang Poly. B/h[c]	35.5	8.40	1500	10.4	2.4	1.1	3490	218	165	18.7	0.09	0.23	44
204	Nginyang Poly. B/h[d]	34.0	8.45	1500	8.1	2.03	0.9	3460	195	145	17.6	0.08	0.21	–
205	Chemolingot B/h[c]	37.7	8.35	269	3.1	2.9	0.5	614	20.5	27.1	24.1	0.04	0.06	5.4
RIVERS														
141	Ndau[b]	–	8.85	24.3	5.2	21.9	4.4	133	5.5	3.2	16.4	<0.01	<0.06	0.45
142	Tigeri[b]	–	7.65	10.7	4.9	7.2	1.4	483	3.7	1.9	14.3	<0.01	<0.06	0.40
144	Arabel[b]	–	8.55	47.1	7.4	8.0	2.7	101	37.0	1.8	13.2	<0.01	<0.06	0.52
145	Itwa[b]	–	8.60	91.2	8.2	5.5	2.3	500	25.3	2.5	18.8	<0.01	<0.06	0.86
146	Kabarmel[b]	–	8.05	45.4	10.0	16.8	3.9	135	26.4	8.6	18.8	<0.01	<0.06	0.35

Table 15.1 (*continued*)

No.	Locality	Temp	pH	Na	K	Ca	Mg	HCO_3	Cl	SO_4	Si	Li	B	F
147	Mukutan[b]	–	8.15	79.1	9.4	15.9	3.2	222	21.3	4.1	11.0	<0.01	<0.06	1.20
149	Cheptopokwo[b]	–	7.95	21.4	6.7	14.9	2.8	102	5.3	4.1	15.5	<0.01	<0.06	0.76
206	Suguta 1[c]	–	–	1150	21.6	3.1	1.9	2460	288	124	31.0	–	–	44
207	Suguta 2[c]	–	–	1030	24.0	3.9	1.9	2200	246	98.5	33.5	–	–	36
208	Suguta 3[c]	–	–	1104	20.3	3.4	1.7	2340	267	115	34.6	–	–	90
209	Suguta 4[c]	–	–	1093	22.4	3.8	2.1	2380	273	104	30.3	–	–	42
210	Suguta Trib.[c]	–	–	1340	20.1	1.6	0.3	2930	350	142	30.2	–	–	47
211	Gerau[c]	–	8.70	54	9.0	12.5	3.6	128	28.5	5.0	12.3	–	–	0.83
212	Amaya[c]	–	–	158	8.7	7.6	2.1	389	26.0	7.2	20.7	–	–	2.1
213	Namarangule[c]	–	8.30	–	–	–	–	–	–	–	–	–	–	–
214	Naliyo[c]	–	8.50	65	10.4	16.5	3.0	152	16.3	15.8	9.7	–	–	0.78
245	Kerio	–	8.65	12.3	10.4	29.0	10.7	58	2.8	2.1	80.6	0.01	<0.03	0.9
LAKES														
70	Baringo[a]	–	8.95	241	18.8	11.2	5.2	546	65	23	14.5	<0.01	0.15	–
150	Baringo[b]	–	9.05	192	15.4	9.2	2.5	384	48.5	19.7	15.2	0.01	0.14	6.40
150	Baringo[d]	–	9.00	231	18.0	12.3	4.3	495	54.8	20.1	14.9	<0.01	0.14	–
215	Lake Turkana[c]	–	–	985	20.5	3.8	2.5	1580	515	43.3	12.0	<0.01	0.72	21
216	Lake Baringo north[c]	–	8.85	192	14.3	11.0	3.5	399	46	17.0	12.9	<0.01	0.11	7.1
217	Lake Baringo south[c]	–	8.75	170	14.9	11.3	3.5	375	44	15.3	13.8	<0.01	0.10	6.3
246	Lake Turkana north	–	9.45	932	19.2	5.0	2.4	1580	446	40.0	11.8	<0.01	0.65	10
247	Lake Turkana central	–	9.45	909	18.8	5.2	2.4	1520	436	39.3	10.2	<0.01	0.63	11

Year of Sampling: a–1986, b–1988, c–1989, all other samples collected 1991, * data from Armannsson (1987)

tion of the Mukutan River, to fall into separate eastern and western groups (Figure 15.3). Since the catchment altitudes on both sides of the rift in the Baringo area are similar, the difference in isotope values may be attributable to movement of rain-bearing clouds from east to west. The waters of Lake Baringo are isotopically very heavy, as a result of the combined effects of high potential evaporation and the shallowness of the lake.

15.2.2 Surface waters of the Suguta River system

The Suguta River rises at the Kapedo hot springs and flows perennially through the area to the north. During wet periods it is also supplied with flood waters from the seasonal Nginyang River which drains the rift floor and rift margins to the south of Silali. Because of its hot spring source the Suguta has a high TDS content, and this increases progressively northwards as a result of evaporation and contributions from other thermal and ambient springs along its course. The increasing temperature and aridity towards the north raises the potential for evaporation and this is reflected in the isotopic composition of the rivers draining into the Suguta Valley from the eastern margin of the rift, which become progressively isotopically heavier northwards. As would be expected, the highest

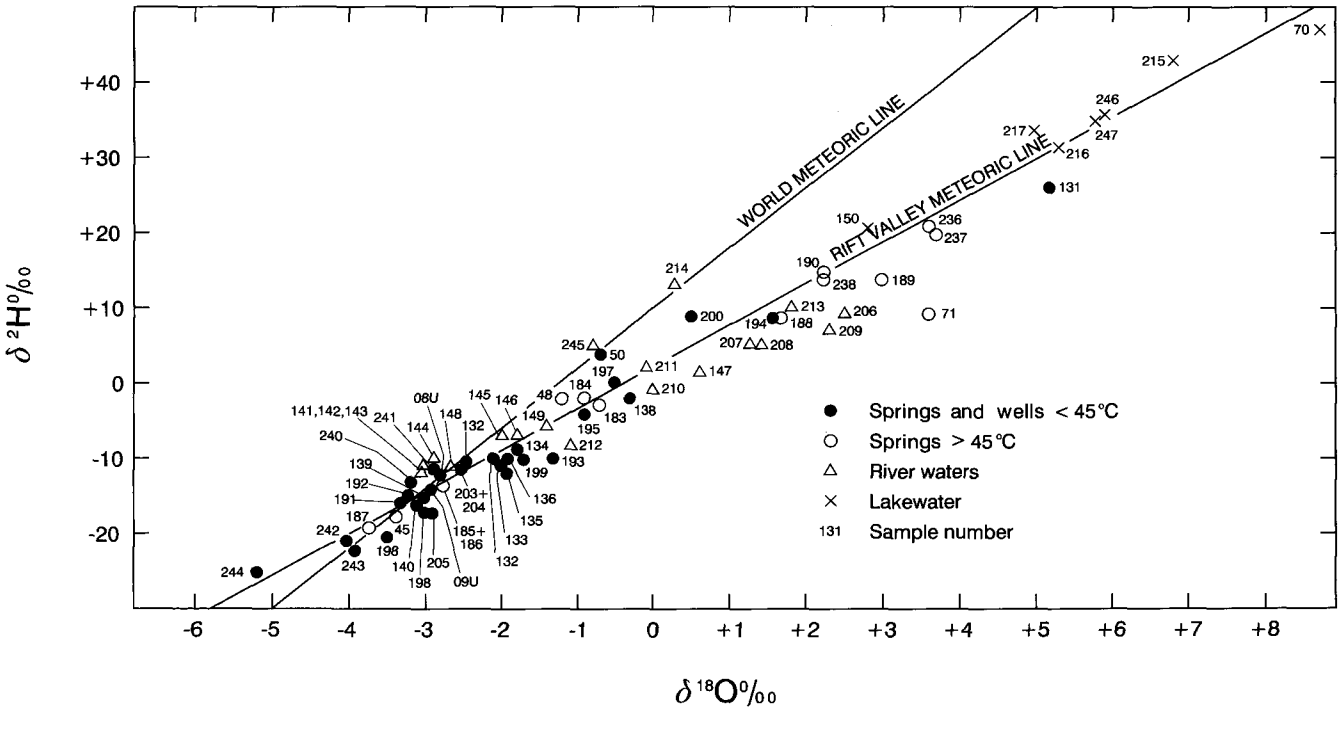

Figure 15.3 Plot of δ^2H against $\delta^{18}O$ for all water samples (values in permil with respect to SMOW).

solute loads and heaviest isotopic compositions of the Suguta occur in the north where the river breaks down into a series of distributaries which soak into the floor of the valley or feed into the ephemeral Lake Alablab.

The shallow ephemeral Lake Alablab and Lake Logipi in the north of the Suguta Valley are in part fed by hot springs. Both are highly saline and have surface encrustations of trona, and therefore no analyses were undertaken on these lakes because their chemistry has been excessively modified by evaporative processes.

15.2.3 Surface waters of the Turkana Basin

Much of the discussion that follows is based on the work of Yuretich and Cerling (1983).

The chemistry of Lake Turkana is mainly governed by input from the Omo River which drains large areas of the Ethiopian Highlands. While the lake is in a closed basin it is by no means as saline as other closed basin lakes within the rift to the south, such as Bogoria, Elmenteita-Nakuru and Magadi. This is because closure of the basin only occurred relatively recently, at about 3.5 ka (Butzer et al., 1972), and the large volume of the lake has not yet permitted the attainment of hypersaline conditions. Consideration of chloride concentrations suggest a lakewater to river water concentration factor of about 100. Other elements show lower concentration factors because of exchange and adsorption reactions. Yuretich and Cerling (*op. cit.*) conclude that the chemical balance of the lake rules out the possibility of any major subsurface outflow from the lake to the west or south, but minor outflow could be masked by various uncertainties attending the chemical balance.

Isotopic analyses of Lake Turkana waters are presented in Table 15.2 (samples 215, 246 and 247). These show that the lakewater is considerably evaporated, and this is confirmed by the isotopic crossplot of Figure 15.3, which also shows an analysis of the Kerio River (sample 245) sampled at Lokori, some 60 km upstream from the mouth, and of the Omo River made by Craig et al. (1977). Predictably both rivers show signs of isotopic enrichment, but compositions at their mouths are unknown, and therefore an isotopic balance for the lake cannot be attempted. Qualitatively the three sets of isotopic and chemical analyses made during the present study reveal that there was no significant difference between lakewater at North and Central islands, despite their separation by 60 km. Sampling took place in June 1991, when the annual flood from the Ethiopian Highlands via the Omo would have started, but there is no evidence of mixing in the vicinity of Central Island between waters from the south with those from the Omo as described by Yuretich and Cerling (1983).

Sample 215 from the southern end of the lake was collected in October 1989 and shows signs of chemical and isotopic enrichment. This would be expected for samples collected furthest from the main input to the lake, although the possibility of local nearshore evaporation cannot be wholly discounted. Assuming that there is minor subsurface outflow southwards from Lake Turkana into the topographically lower northern end of the Suguta Valley, it will be derived from this end of the lake, and therefore the composition of sample 215 is used in considering the implications of such underflow in Section 15.4.2.

15.3 AMBIENT AND NEAR-AMBIENT GROUNDWATER

The distribution of groundwater temperatures within the area is bimodal, with a distinct break between 39°C and 45°C. For the purpose of describing their geochemistry, groundwaters with ambient and near ambient temperatures are therefore defined as having temperatures below 39°C, whilst hot springs have temperatures above 45°C.

15.3.1 Ambient and near-ambient springs

The isotopic composition of rift-margin groundwaters in the south-east of the area is defined by a group of springs along the eastern margin of the rift (139, 140, 191, 192) which have δ^2H and $\delta^{18}O$ of around -16‰ and -3‰ respectively (Table 15.2). Such values are compatible with the meteoric line calculated for the whole of the Kenya Rift by Allen et al. (1989) and, if fed into the altitude/isotope correlation developed in that report give an average recharge altitude of about 1800 m.

Some springs on both margins of the rift are little more than seepages and their isotopic compositions may therefore be affected by evaporation. This could account for slightly enriched compositions at the Gates of Samburu (193) and Nasaken (199), although the seepages at Napeiton (198), to the north-west of Emuruangogolak, have similar isotopic compositions to the group of springs in the south-east. This suggests that the isotopic composition of meteoric waters is broadly similar throughout both rift margins of the surveyed area. However, there is a chemical difference, with Napeiton having about twice the level of TDS as the south-eastern group of springs, and also containing detectable Li, B and F (Table 15.1). Values of $\delta^{13}C$ in dissolved inorganic carbon (DIC) in the south-eastern springs are low (Table 15.2), averaging -12.3‰, and are typical of fairly unmodified meteoric water. No $\delta^{13}C$-DIC sample was collected at the Napeiton spring, although a sample from an adjacent well gave a value of -8‰. This together with other chemical indications of water-rock interaction suggests that the waters in the north-west around Napeiton may have circulated to greater depths, possibly along rift boundary faults, before rising to the surface and cooling.

Only three springs or groups of springs with cool or relatively cool temperatures occur on the rift floor between Lake Baringo and Lake Turkana. The Amakat pools (196) situated between Silali and Emuruangogolak are isotopically very enriched (Table 15.2) as a result of excessive evaporation, but TDS is low suggesting the pools consist largely of rainwater. The springs at Lake Kalnangi and South Nangarabat (195 and 197) occur where water flows out from beneath the basalt lava fields along the northern periphery of Silali and Emuruangogolak respectively. Both sets of springs have comparable TDS, chemical and stable isotopic compositions (Tables 15.1 and 15.2), and from their locations could be assumed to represent cooled outflow waters from the Silali and Emuruangogolak geothermal systems. However, such an interpretation is not supported by a detailed examination of their

Table 15.2 Hydrogen, oxygen and carbon stable isotope values for surface and groundwaters

No.	Locality	Temp °C	δ^2H	$\delta^{18}O$	$\delta^{13}C_{DIC}$
HOT SPRINGS					
45	Lorusio[a]	81.0	-23	-3.1	—
45	Lorusio[b]	82.2	-16	-3.4	-2.6
45	Lorusio[d]	81.0	-15	-3.6	—
48a	Kapedo[a]	50.0	-7	-3.5	—
48a	Kapedo[b]	50.8	+2	-0.5	-4.1
48a	Kapedo[c]	50.0	-2	-0.9	-3.3
48b	Kapedo[b]	50.0	-3	-0.6	—
48c	Kapedo[b]	50.0	-1	-0.5	—
71a	Ol Kokwe Island[b]	95.8	+15	+5.9	—
71b	Ol Kokwe Island[a]	94.0	+7	+1.3	—
71b	Ol Kokwe Island[b]	96.0	+4	+3.5	—
71c	Ol Kokwe Island[b]	96.0	+11	+3.7	—
183	Kapedo[c]	45.0	-3	-0.7	—
184	Kapedo[c]	45.0	-2	-0.9	—
185	Suguta SV3a[c]	68.4	-13	-2.7	-4.2
186	Suguta SV3b[c]	64.0	-14	-2.8	—
187	Kamuge[c]	50.4	-19	-3.7	-4.7
188	Kageinya[c]	67.8	+9	+1.7	-4.0
189	Namarunu[c]	66.2	+14	+3.0	-0.9
190	Logipi NW[c]	61.4	+15	+2.2	-1.2
236	Elboitong S[d]	95.0	+21	+3.6	-1.6
237	Elboitong N[d]	91.8	+20	+3.7	-1.5
238	Logipi NE[d]	69.8	+14	+2.3	-2.0
239	Central Island[d]	70.5	+36	+5.8	—
COOL SPRINGS					
50	Kapedob	27.0	+4	-0.7	—
138	Nginyang-Kapedo[b]	36.0	-2	-0.3	—
139	Churo[b]	28.0	-15	-3.0	-11.6
139	Churo[c]	—	-15	-3.1	-12.5
140	Ebirisat[b]	37.5	-16	-3.1	-14.9
191	Nangarwa[c]	—	-16	-3.3	-11.7
192	Amaya[c]	—	-15	-3.2	-10.6
193	N. Samburu Gates[c]	—	-10	-1.3	-6.6
194	Kachurkolh[c]	31.0	+9	+1.6	-0.5
195	Kalnangi[c]	31.7	. -4	-0.9	-2.7
196	Amakat[c]	—	+54	+12.0	-9.3
197	S. Nangarabat[c]	31.1	0	-0.5	-2.8
198a	Napeiton[c]	32.5	-17	-3.0	—
199	Nasaken[c]	31.0	-10	-1.7	-8.7
240	Eliye[d]	35.4	-13	-3.2	-10.1
241	Eliye North[d]	37.3	-11	-2.9	-10.6
242	Loyangalani[d]	39.2	-21	-4.0	-12.3
243	Parkati[d]	amb	-22	-3.9	-13.9
244	Tum[d]	amb	-25	-5.2	—
09U*	Eliye	32	-14	-2.9	—
WELLS					
131	Kampi Ya Samaki[b]	—	+27	+5.5	—
131	Kampi Ya Samaki[d]	—	+25	+4.9	-6.2
132	Chesirimion[b]	—	-11	-2.6	-14.9
132	Chesirimion[c]	34.0	-10	-2.3	-13.8
133	Tangulbei[b]	30.2	-11	-2.0	-13.7
134	Kokwo Toto[b]	28.0	-9	-1.8	-14.6
135	Orus solar[b]	28.0	-12	-1.9	-15.8
136	Orus hand[b]	28.0	-10	-1.9	-15.4
137	Katangora[b]	36.0	-10	-2.1	-9.6
198b	Napeiton[c]	—	-18	-3.3	-8.2
198b	Napeiton[d]	36.8	-23	-3.7	—
200	Kositei Project[c]	—	+9	+0.5	—
201	Kositei Mission[c]	—	-12	-2.7	—
202	Kositei[c]	35.8	-15	-2.9	-11.6
203	Nginyang Sch.[c]	—	-11	-2.5	-9.9
204	Nginyang Poly[c]	35.5	-11	-2.3	-10.0
204	Nginyang Poly[d]	34.0	-12	-2.8	-10.6
205	Chemolingot[c]	37.7	-17	-2.9	-11.7
08U*	Kankurdio	33	-12	-2.8	—
RIVERS					
141	Ndau[b]	—	-12	-3.0	—
142	Tigeri[b]	—	-12	-3.0	—
143	Molo[b]	—	-11	-2.9	—
144	Arabel[b]	—	-10	-2.4	—
145	Itwa[b]	—	-7	-2.0	—
146	Kabarmel[b]	—	-7	-1.8	—
147	Mukutan[b]	—	+1	+0.6	—
148	Nginyang[b]	—	-11	-2.7	—
149	Cheptopokwo[b]	—	-6	-1.4	—
206	Suguta 1[c]	—	+9	+2.5	—
207	Suguta 2[c]	—	+5	+1.3	—
208	Suguta 3[c]	—	+5	+1.4	—
209	Suguta 4[c]	—	+7	+2.3	—
210	Suguta Tributary[c]	—	-1	0.0	—
211	Gerau[c]	—	+2	0.1	—
212	Amaya[c]	—	-8	-1.1	—
213	Namarangule[c]	—	+10	+1.8	—
214	Naliyo[c]	—	+13	+0.3	—
245	Kerio[d]	—	+5	0.8	—
LAKES					
70	Baringo[a]	—	+47	+8.8	—
150	Baringo[b]	—	+21	+2.8	—
150	Baringo[d]	—	+40	+7.6	—
151	Tilam[b]	—	+7	+0.9	—
215	Turkana[c]	—	+43	+6.8	—
216	Baringo N.[c]	—	+32	+5.3	—
217	Baringo S.[c]	—	+34	+5.0	—
246	Turkana N.[d]	—	+36	+5.9	—
247	Turkana C.[d]	—	+35	+5.8	—

Values in permil with respect to SMOW or PDB as appropriate.
Year of sampling: a 1986, b 1988, c 1989, d 1991, *1986 data from Armannsson (1987).

chemical compositions. Figure 15.3 shows that both sets of springs have been modified by an evaporative process, and on a plot of δ^{13}C-DIC vs HCO_3^- (Figure 15.5) they fall on an evaporite dissolution trend, the implications of which are considered further in Section 15.4.1.

Stable isotope analyses show that the springs at Loyangalani (242), on the south-east shores of Lake Turkana, derive their water at least partly from a higher-than-local altitude, but not exclusively from Mt Kulal which rises to 3500 m. On the other hand the springs on the west side of the lake at Eliye Springs (240, 241) must be derived from a lower average altitude because they are relatively enriched. The similarity of the isotope ratios for the Eliye Springs with those of the Kankurdio borehole (08U), situated 30 km to the west of the lake, suggests that the springs do not derive their recharge locally.

15.3.2 Wells

Most of the wells and boreholes that were sampled are situated on the floor of the rift in the south of the area. These can be conveniently divided into two groups, one to the east of the volcanic centres and the other to the west. The shallow borehole on the edge of Lake Baringo at Kampi-ya-Samaki is not included in these groups but is considered separately.

Samples from the eastern group of wells (133, 134, 135, 136 and 137) present a coherent body of chemical and isotopic data (Tables 15.1 and 15.2). The isotopic compositions indicate that, unless the waters have suffered mixing, recharge has taken place at a lower average altitude than the rift-margin springs considered in the previous section. This would be consistent with recharge taking place on the lower slopes of the eastern margin of the rift, or upon the floor or the volcanic centres within the inner trough, as predicted in Section 14.2.4. The chemical analyses reveal good-quality drinking water low in F^-, and this together with low $\delta^{13}C$-DIC values indicates that the eastern wells in this area contain relatively unmodified meteoric water. Even the Katangora borehole (137), which is situated relatively close to the eastern flanks of Paka and has a slightly elevated temperature of 36°C, shows no geothermal influence other than higher than average F^- and $\delta^{13}C$-DIC values.

The compositions of water from the western group of wells are more variable. Samples from the Kositei and Chemolingot boreholes (202 and 205) are similar in chemical and isotopic composition, and the isotope values suggest an origin for the water on the higher western margin of the rift. Samples from the Chesirimion and Nginyang boreholes (132, 203 and 204) have isotopic compositions consistent with a greater contribution from rainfall on the rift floor, but resemblances end there. While Chesirimion water is similar to that from the eastern group of wells, the two Nginyang wells have very high HCO_3^- and F^- (Table 15.1). The reasons for this are probably related to mixing between groundwater and infiltrating river water (see Section 15.4.1 below).

The borehole at Kampi-ya-Samaki is situated very close to the edge of Lake Baringo. By virtue of its position, it might be expected that the isotopic composition of water from the borehole could represent a time-averaged composition for lakewater. This assumption is confirmed on a plot of $\delta^{18}O$ vs Cl^- (Figure 15.4), in which the borehole sample (131) and the averaged composition of lake samples collected between 1986 and 1991 are virtually coincident.

The composition of water from the hand-pumped well at Napeiton (198b), situated on the rift margin to the north-west of Emuruangogolak, is interpreted in a similar way to the spring at that locality (198a), which was considered in the previous section to be a deeply circulated rift margin groundwater.

The well at Parkati (243), situated at the base of the rift escarpment adjacent to the eastern end of the Barrier Volcanic Complex, has a stable isotope composition compatible with local recharge. The anions of this well are dominated by SO_4^{2-} rather than the more usual HCO_3^-. The source of this sulphate is not known; elevated Ca^{2+} suggests that gypsum is contributing, although it is equally likely that contamination from the concrete-based construction of the well may be responsible. The $\delta^{13}C$-DIC of this well plotted against HCO_3^- (Figure 15.5) is entirely consistent with a rift-flank groundwater unaffected by uptake of evaporites.

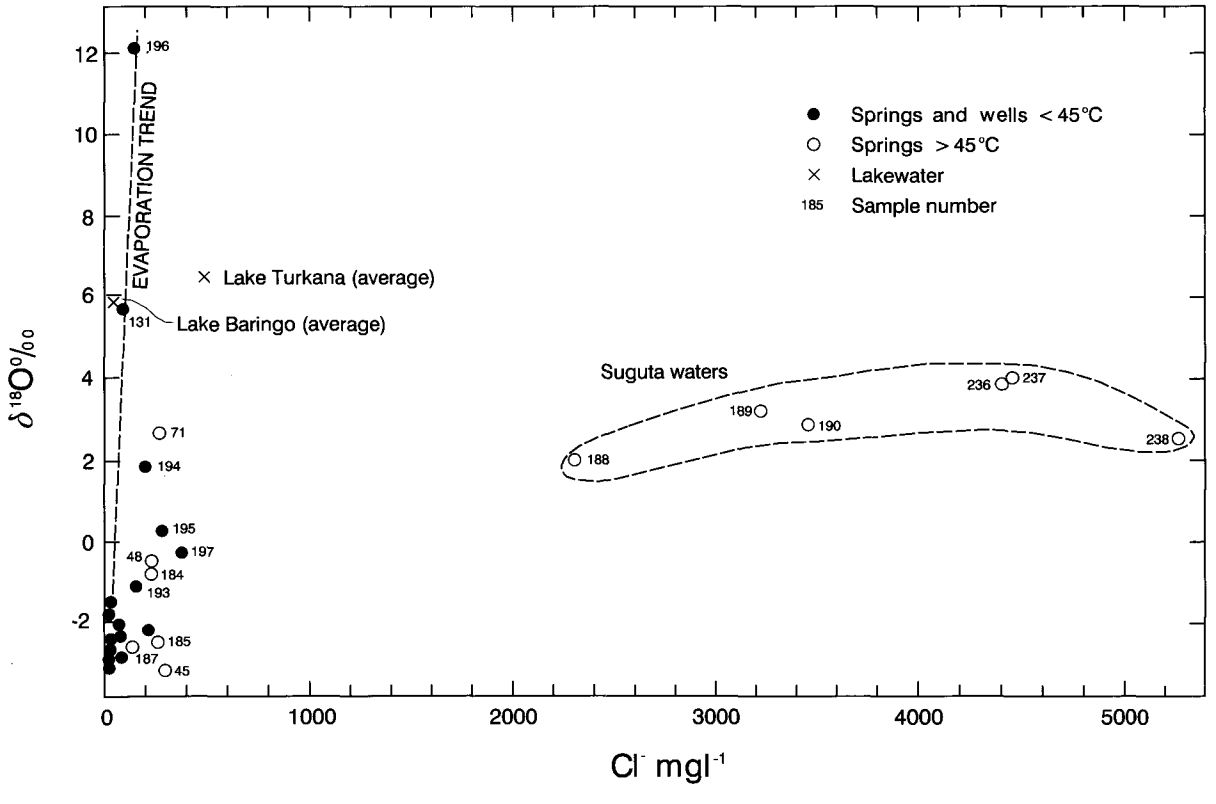

Figure 15.4 Plot of $\delta^{18}O$ against Cl^- for groundwaters (values of $\delta^{18}O$ in permil with respect to SMOW).

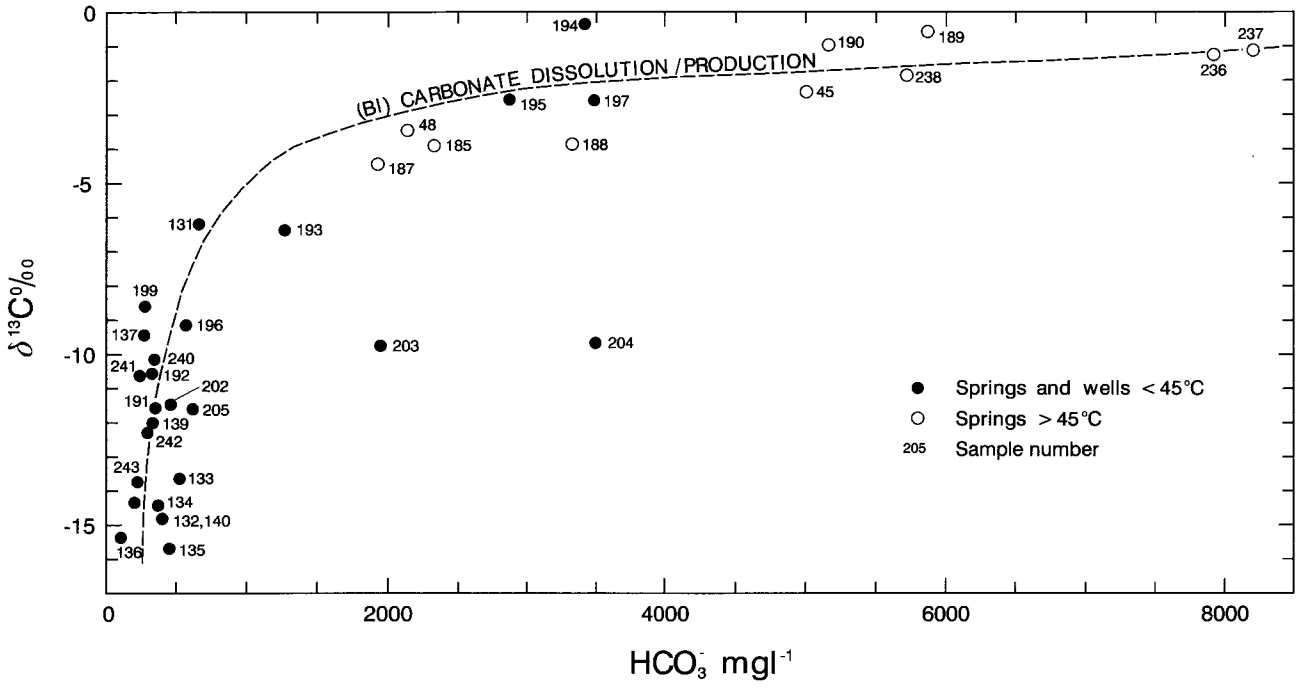

Figure 15.5 Plot of $\delta^{13}C$ against HCO_3^- for groundwaters (values of $\delta^{13}C$ in permil with respect to PDB).

15.4 THERMAL GROUNDWATER

Hot springs occurring within the inner trough of the rift are not necessarily found in close proximity to the volcanic centres. They have temperatures of 45°C and over, although cooler waters which have similar chemical characteristics to hot springs are also considered in this Section.

For the purpose of description the thermal groundwaters are conveniently divided into those of the Baringo–Emuruangogolak sector of the rift, the Suguta Valley, and Central Island of Lake Turkana.

15.4.1 Thermal groundwaters in the Baringo–Emuruangogolak sector of the Rift

Plots of HCO_3^- and SO_4^{2-} vs Cl^- provide a useful means of differentiating the various waters (Figure 15.6) These show that thermal waters are distinct from most ambient waters, and that there is no trend between the two groups, except for one example (Napeiton, 198a). Cool waters that plot in the hot spring field include the Nginyang wells (203, 204), and the springs of Kalnangi (195), South Nangarabat (197) and Kachurkohl (194). Each has an enriched $\delta^{13}C$-DIC value that fits the observed evaporite dissolution trend, except for the Nginyang wells, as noted previously in Section 15.3.2. The relationship of the various thermal waters and their links, if any, with the volcanically-driven hydrothermal activity is considered in the following paragraphs.

On the stable isotope plot of δ^2H vs $\delta^{18}O$ (Figure 15.3) the hot springs show a range from rift margin-like compositions (Lorusio, 45 and Kamuge, 187) to compositions enriched in heavy isotopes (Ol Kokwe Island, 71 and Kageinya, 188) which must contain a proportion of evaporated water. Of all the springs in the area, those of Ol Kokwe Island have the most enriched compositions, undoubtedly due to mixing with Lake Baringo water either before or after heating. The other thermal springs, and non-thermal springs with similar chemistry such as Kalnangi (195) and Nangarabat (197), are assumed to represent different amounts of mixing between subsurface outflow from Lake Baringo with meteoric water from the rift margins or from recharge on the volcanic centres. The percentage markings in Figure 15.9 refer to the calculated proportion of lakewater in the springs. It can be seen that the Kapedo hot springs (48) have about 30% lakewater, as do the cool springs of Kalnangi and South Nangarabat (195, 197). In contrast, hot springs situated on or close to the base of the rift margin escarpment appear to have little or no lakewater in their discharge, as for example those of Kamuge, SV3 and Lorusio (187, 185, 45).

The apparent mixing of water types is not reflected in chemical composition. All the thermal springs have TDS values in excess of 3000 mg/l which are dominated by Na^+ and HCO_3^-. Although concentrations can be very high, reaching ~7500 mg/l at Lorusio and are substantially higher in the Suguta Valley (Section 15.4.2), there is no evidence for chemical mixing between different bodies of groundwater. For example, a plot of δ^2H versus Cl^- (Figure 15.7) shows no particular trend. However, it does illustrate that while all waters have isotopic compositions within the range of a rift margin - lakewater mixing series they can have variable chemistry that is not the result of straightforward mixing.

All the thermal springs plot close to the theoretical evaporite dissolution trend of Figure 15.5. For the purpose of modelling this trend, it is assumed that unevolved post-recharge water with a typical initial composition of 250 mg/l HCO_3^- and -16‰ $\delta^{13}C$-DIC, progressively picks up evaporitic bicarbonate with a typical $\delta^{13}C$-DIC of -1‰, resulting in the plotted curve. The term 'evaporite' as used here also covers the possibility of local input of HCO_3^- from alteration

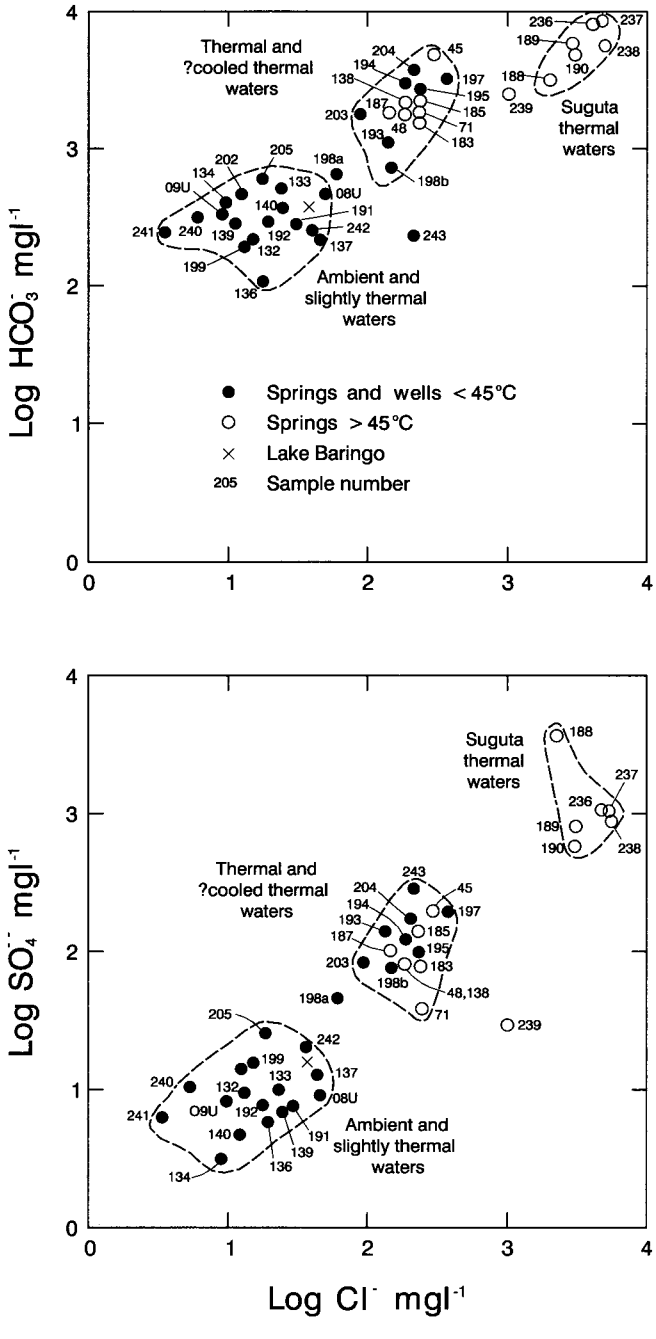

Figure 15.6 Plots of log HCO_3^- and SO_4^{2-} against log Cl^- for groundwaters.

of feldspars by CO_2 under conditions of low groundwater flow velocity. Since Na^+ and HCO_3^- are the dominant ions in virtually all waters from the rift it is reasonable to assume that sodium bicarbonate will dominate evaporitic deposits. This is supported by the presence of significant amounts of trona on and around lakes Alablab and Logipi, and thin but widespread surface encrustations over many of the alluvial flats on the floor of the inner trough extending northwards from Emuruangogolak. Although the bicarbonate has ultimately been derived from volcanism within the rift, its presence in the hot springs does not necessarily indicate a direct association with present high-temperature geothermal systems. All that can be concluded is that hotter waters are more effective at redissolving evaporites, which in most cases will result in significantly higher TDS and somewhat higher δ^{13}C-DIC values.

None of the thermal springs shows evidence of being an outflow from a high-temperature (>150°C) system except for those on Ol Kokwe Island. The other thermal springs are likely to be simply the result of deep circulation, although there may be local zones of higher heat flow which have some magmatic characteristics, such as at Lorusio with its abundant CO_2 gas and relatively high $^3He/^4He$ value.

There is no reason why the high bicarbonate content of certain cool springs, such as those at Kalnangi and Nangarabat (195, 197), should not be caused by the dissolution of evaporites. However, the rather anomalous position of the two Nginyang wells (203, 204) in Figure 15.5 requires a different explanation. Both sites lie on mixing trends between background bicarbonate water and water that has acquired evaporites. The simplest explanation is that water from the nearby Nginyang River is infiltrating and mixes progressively with a groundwater high in HCO_3^- and enriched in δ^{13}C. This would also account for the high concentrations of F^- recorded in the two wells.

15.4.2 Hot springs of the Suguta Valley

The hot springs in the Suguta Valley, such as those at Kageinya (188), Namarunu (189) Elboitong (236, 237) and Logipi (190, 238) have much higher TDS values (~15000 mg/l) than those within the inner trough further to the south. The Suguta Valley is the terminal drainage area for the northern half of the Kenya Rift and as such should have the greatest amount of salts available for recycling in thermal waters. In many respects this sump area, which terminates in the highly alkaline Lake Logipi, resembles the Magadi area which is the corresponding terminal drainage area for the southern half of the rift. It is anticipated that during passage to this sump area, evaporating waters would tend to precipitate bicarbonates first, which may explain why chloride increases relative to bicarbonate in the north of the area, as demonstrated in Figure 15.6.

The springs on the floor of the Suguta Valley are broadly associated with the volcanic centres of Emuruangogolak, Namarunu and Barrier, but despite this, they do not have any convincing indications of being high-temperature outflows, though the Namarunu and Logipi springs have high $^3He/^4He$ ratios (no He isotopic analyses are available for Elboitong at the time of writing).

Three sources of water could conceivably contribute to the hot springs in the northern part of the Suguta Valley. These are, infiltrating surface water derived from the south, meteoric water from the rift flanks, and subsurface leakage from Lake Turkana in the north. The first two categories are likely to apply to the Namarunu and Elboitong springs, whilst the last two could apply to the Logipi springs. Stable isotope data offer only a partial resolution of the sources. The crossplot of Figure 15.3 shows the compositions involved. The only obvious water source in the northern part of the Suguta Valley is the Suguta River. Samples 207–209 were taken from the river to the south, with 209 being collected nearest to Namarunu. The river waters show an evaporative trend, as would be expected for surface waters in a hot and arid area, but the hot spring samples are not aligned with this trend, suggesting that river waters do not make a major contribution to the springs. However, most recharge of groundwater may take place during the

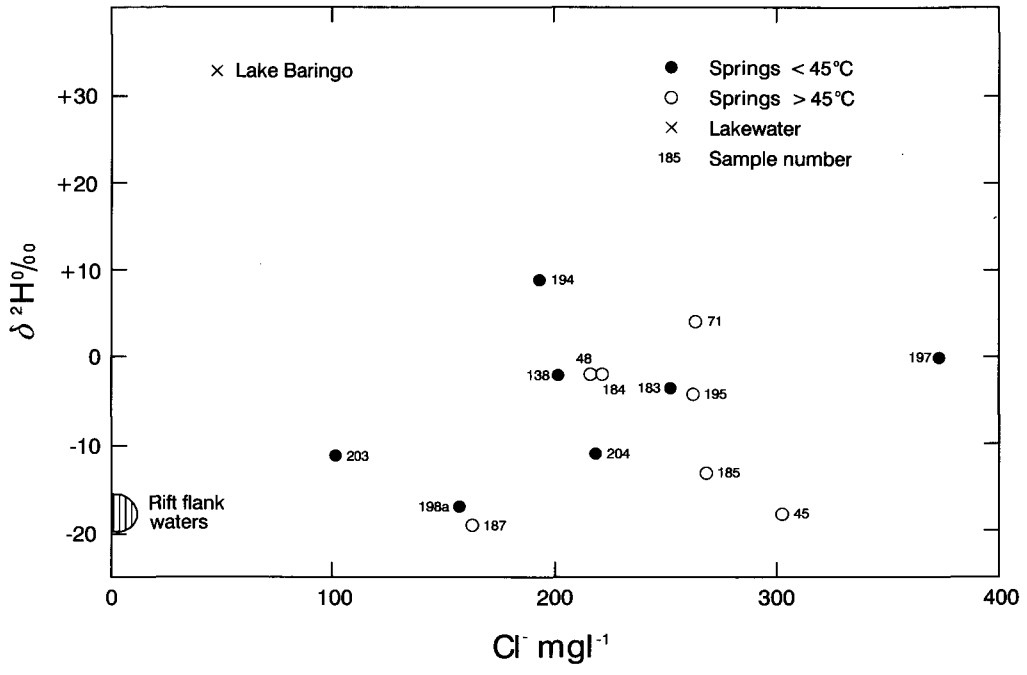

Figure 15.7 Plot of δ^2H against Cl^- for hot spring and associated waters (values of δ^2H in permil with respect to SMOW).

flood events to which the Suguta Valley is periodically subjected. Under these conditions the river and direct rainfall will deliver more isotopically depleted water, or at least water with a composition on or near the Rift Valley Meteoric Line, and it is conceivable that the springs at Namarunu and Elboitong derive their waters from such a source. There is likely to be considerable recycling of water by thermal springs in what is effectively a sump area, and this could result in the observed isotopic enrichments.

If, however, it is accepted that the river water analyses from sites 206–209 are indicative of the bulk of any recharge from the Suguta River, then it would appear that the river cannot be a major contributor to the springs. The springs might then consist of meteoric water from the rift flanks enriched by evaporation. While this is feasible for Elboitong it is less likely for the Namarunu springs because of their position on the eastern side of the Namarunu volcanic complex. An alternative explanation is that underflow from Lake Baringo may be contributing to the springs, although this is impossible to prove because of evaporative effects during recycling.

In the case of the Logipi hot springs there is every possibility that discharge from Lake Turkana may be contributing. It has been shown by Yuretich and Cerling (1983) on geochemical grounds that discharge cannot be significant in terms of the total lakewater budget, and this is supported by the small size of the Logipi springs. Furthermore, Lake Logipi tends to shrink considerably during periods of drought, which would probably not be the case if there were significant subsurface outflow from Lake Turkana towards the Logipe area. Isotopic considerations (Figure 15.3) show that a mixture of meteoric water and lakewater could be responsible for the observed isotopic ratios of the Logipe springs, although the exact proportions involved may be being masked by evaporative effects during recycling. However, an upper limit of about 70% can be put on a lakewater contribution, although the stable isotope compositions of steam from Kakorinya fumaroles suggest that 40% is a more likely figure for the actual contribution (Section 15.5.2). This indicates that even in this hot and arid part of the Suguta Valley there appears to be significant input of meteoric water from the rift flanks, or from the recharge mound of the Barrier Volcanic Complex itself. As with the Elboitong and Namarunu springs to the south, it is not possible to prove unequivocally that lakewater is involved at all; the springs have much the same isotopic composition and may simply represent discharges from various points of a rather homogeneous body of hot saline groundwater occupying the discharge area and fed mainly by meteoric waters which are then subject to evaporative enrichment. On balance, however, it would seem more likely that waters already enriched by evaporation, such as lake or river waters, must be contributing. Supporting evidence for this view comes from Lake Magadi in the southern part of the rift, where many hot saline springs peripheral to the lake retain isotopic compositions indicative of an origin on the rift flanks (Allen et al., 1989).

If the chemical composition of the hot springs of the Suguta Valley is considered, it can be demonstrated that they could be derived from ambient groundwaters by a simple process of evaporative concentration.

The analyses in Table 15.1 and Figure 15.6 show that the hot springs of the northern part of the Suguta Valley form a relatively restricted group. In keeping with the general composition of Rift Valley thermal waters they have extremely low Ca^{2+} and Mg^{2+}, high B^{3+} and F^-, and Na^+ and HCO_3^- are the dominant ions. However, compared with hot springs within the inner trough further to the south they have much higher TDS values (~15000 mg/l) which is most likely due to dissolution of evaporites. Though not particularly obvious from the log plots of Figure 15.6, both HCO_3^- and SO_4^{2-} decline relative to Cl^- within the Suguta Valley. It is anticipated that during passage northwards to the sump area of Lake Logipi, evaporating waters would tend to precipitate bicarbonates and sulphates first, which may explain why chloride increases relative to bicarbonate.

Under these circumstances, the increase in concentration of highly mobile elements such as F and Li is expected and is not necessarily indicative of high-temperature geothermal activity at depth. Heating by deep circulation of water down rift boundary faults is probably largely responsible for the boiling springs at Elboitong, although there is likely to be a local high heat flow and possibly some input of magmatic gas judging from the very high CO_2 concentration. The source of this heat may be related to the young basaltic volcanism that has taken place in the vicinity of the Gap. The springs of Namarunu (~66°C) are not so hot as those of Elboitong, although their high $^3He/^4He$ suggests some magmatic gas input, and isotope systematics indicate they may be the product of mixing between Elboitong and Suguta River-type groundwaters with some additional water-rock reaction.

Although Kakorinya (Barrier Volcanic Complex) is geothermally active and has been the site of significant volcanism in Recent times, there is no evidence of high temperature input into the Logipi hot springs (198, 238), such as high CO_2 and Si concentrations, as might be expected if water from Lake Turkana was passing beneath the volcanic edifice. It is therefore possible that the Barrier Volcanic Complex is damming Lake Turkana so effectively that there is little outflow from the lake, and the spring discharges on the northern shores of Lake Logipi are merely the product of relatively small-scale recycling of waters in the sump area of the Suguta in response to deep circulation or locally elevated heat flow.

In terms of their $\delta^{13}C$-DIC content plotted against HCO_3^- (Figure 15.5) the hot springs of the Suguta Valley obey the expected relationship for the dissolution of evaporites as described in Section 15.4.1.

15.4.3 Hot springs of Central Island

The only hot springs (>45°C) found within the vicinity of Lake Turkana occur around the main crater lake of Central Island (sample 239).

Isotopically the spring water is of similar composition to lakewater (Figure 15.10), which given the position of the island in the centre of the lake is the obvious source of any thermal fluid. The implication of the isotope analyses is that little or no shift in $\delta^{18}O$ has been caused by water-rock interaction. In chemical terms however, the spring fluid has evolved considerably from a lakewater composition, and is also unlike any of the hot springs in the northern part of the Suguta Valley. The analysis of sample 239 suggests genuinely high-temperature water-rock interactions, having high K^+ and Si, and Cl^- much greater than SO_4^{2-}, which implies that steam heating is not important. There is little doubt that this is one of the few examples in the Kenya Rift of a fluid derived from mixing with a high temperature geothermal outflow, as is also the case for the hot springs of Ol Kokwe Island, which are situated in an analogous position in the centre of Lake Baringo (Section 15.4.1).

15.5 FUMAROLE CONDENSATES

The fumaroles of the region are relatively weak and therefore only the strongest and hottest at each volcanic centre were sampled for chemical and isotopic analysis, the results of which are discussed separately.

15.5.1 Chemical composition of steam condensates

The chemical analyses of fumarole steam condensates are presented in Table 15.3. It should be noted that for the fumarole condensates from the project's Phase II area (Korosi–Emuruangogolak), several ions (K^+, Mg^{2+} and Li^+) were at or below detection limits in all the samples and are therefore not reported. In view of the low concentration of the analytes and the possibility that reaction with wall rocks may have altered the chemistry of the fumarole steam, it was decided to analyse the condensates from the project's Phase III area (Kakorinya and islands of Lake Turkana) for ammonia and stable isotopes only.

It is generally assumed that lower pH and solute contents of steam condensates indicate less interference by shallow groundwaters. This relationship is largely a reflection of the strength of steam flows, with weaker fumaroles being more prone to dilution and condensation. In terms of crude TDS averages for the fumaroles of each volcanic centre, the order from lowest to highest concentration is Paka, Emuruangogolak, Silali, Korosi and Chepchuk. By this criteria Korosi and Chepchuk fumaroles are therefore the weakest, and Paka fumaroles the strongest, which accords reasonably well with field observation.

Ammonium makes up a significant proportion of the ionic content of the fumarole condensates. Taking crude averages of the ammonium contents for each volcanic centre, the order from lowest to highest concentration is again Paka, Emuruangogolak, Kakorinya, Silali, Chepchuk and Korosi. Since NH_3 tends to partition into steam in inverse proportion to temperature, it would appear that the temperature order of the geothermal systems from highest to lowest is Paka, Emuruangogolak, Kakorinya, Silali, Chepchuk and Korosi.

However, the results from Ol Kokwe Island (152), Central Island and North Island (252–255), show that the interpretation of ammonia concentrations in fumarole condensates is not necessarily straightforward. The island fumaroles have very high concentrations of ammonia, most likely due to their proximity to lake sediments. Field observation and geochemical considerations suggest that the fumaroles on the islands represent more vigorous hydrothermal conditions than those on the main volcanic centres of Korosi through to the Barrier. However, it should be born in mind that the apparent relative strength of individual volcanic centres at the surface may not necessarily represent the situation at depth owing to the degree of sealing by hydrothermal alteration above deep reservoirs. The fumaroles of the islands are much nearer to their water tables than those of the main volcanic centres, where regional water tables are hundreds of metres below the surface. This alone could be responsible for differences in ammonia content, because of the opportunity afforded for gas-rock reaction during the upward passage through thick unsaturated zones.

15.5.2 Isotopic composition of steam condensates

Oxygen and hydrogen stable isotope data for fumarole condensates from the region between Lake Baringo and Emuruangogolak are plotted in Figure 15.8, to-

Table 15.3 Fumarole condensate chemistry, ions in mg l^{-1}, stable isotopes in permil vs SMOW.

No.	Locality	Temp °C	pH	Na	Ca	Cl	SO_4	Si	B	F	NH_4-N	δ^2H	$\delta^{18}O$
152	Ol Kokwe OK 1	95.8	5.90	0.89	0.21	1.60	1.1	0.5	1.03	<0.05	38.2	-18	-3.6
153	Korosi KR 10	85.5	5.60	—	—	—	—	—	—	—	—	-70	-10.6
157	Korosi KR 19	95.9	4.90	1.03	0.13	0.20	<0.8	0.2	0.20	<0.05	9.0	-50	-9.0
158	Korosi KR 21	90.1	6.00	1.97	0.43	<0.20	<0.8	3.0	<0.03	0.18	6.8	-51	-8.6
159	Korosi KR 23	95.4	3.60	1.58	0.10	0.40	<0.8	0.3	1.65	<0.05	8.5	-33	-6.5
159	Korosi KR 23*	96.0	5.70	0.56	0.08	0.55	<0.5	1.1	0.39	0.08	10.6	-42	-7.6
160	Korosi KR 24	82.5	6.45	—	—	—	—	—	—	—	—	-48	-8.4
172	Korosi KR 27	—	—	<0.05	0.07	0.20	<0.8	<0.1	<0.03	—	10.2	-60	-13.2
161	Korosi KR 32	91.5	6.05	—	—	—	—	—	—	—	—	-53	-9.6
162	Korosi KR 34	91.0	5.30	0.26	0.18	0.30	0.9	1.8	0.03	0.06	31.5	-112	-18.2
162	Korosi KR 34**	94.5	—	—	—	—	—	—	—	—	—	-99	-15.9
154	Chepchuk KR 12	95.7	5.05	12.2	0.17	1.60	1.5	4.2	0.04	0.24	4.0	-38	-7.1
155	Chepchuk KR 16	94.0	5.30	0.20	0.08	<0.20	0.8	<0.1	<0.03	<0.05	4.3	-48	-8.8
156	Chepchuk KR 18	96.4	—	6.3	0.23	1.10	<0.8	3.1	<0.03	0.34	5.2	-55	-9.5
163	Paka PK 1a	96.2	—	0.57	0.09	0.30	<0.8	1.3	0.49	0.05	0.08	+ 7	-2.3
163	Paka PK 1a*	95.0	4.10	0.24	0.13	<0.20	<0.5	0.4	<0.03	<0.05	0.09	+ 2	-2.4
164	Paka PK 1b	91.2	—	—	—	—	—	—	—	—	—	+10	-1.2
165	Paka PK 1c	91.0	—	—	—	—	—	—	—	—	—	+ 2	-2.8
173	Paka PK 3	—	—	0.15	0.08	0.40	<0.8	<0.1	0.12	—	2.5	-15	-2.4
166	Paka PK 4a	95.3	4.55	1.05	0.23	0.40	1.0	0.6	0.11	<0.05	1.3	-14	-4.3
167	Paka PK 4b	95.5	4.50	0.21	0.09	0.20	3.8	0.6	<0.03	<0.05	<0.05	-18	-4.0
174	Paka PK 6e	—	—	0.17	<0.05	<0.20	<0.8	<0.1	<0.03	—	0.34	-5	-2.8
168	Paka PK 7a	94.0	3.90	3.10	0.05	0.60	4.7	0.4	1.59	0.06	<0.05	-13	-3.5
169	Paka PK 7b	91.0	5.00	—	—	—	—	—	—	—	—	-22	-5.2
170	Paka PK 7c	91.0	5.25	—	—	—	—	—	—	—	—	-21	-4.8
171	Paka PK 7d	92.0	4.90	0.26	0.06	0.20	<0.8	<0.1	—	<0.05	0.15	-26	-5.7
175	Paka PK 7e	—	—	0.30	0.29	<0.20	<0.8	0.1	<0.03	—	0.30	-36	-7.1
176	Paka PK 20a	—	—	<0.05	<0.05	<0.20	<0.8	<0.1	<0.03	—	3.6	-17	-4.3
177	Paka PK 20b	—	—	0.08	<0.05	<0.20	<0.8	<0.1	<0.03	—	2.0	-17	-4.5
178	Paka PK 23	—	—	0.15	<0.05	<0.20	<0.8	<0.1	<0.03	—	1.1	-18	-4.9
179	Paka PK 31	—	—	0.79	0.06	0.20	<0.8	0.2	0.69	—	1.7	-21	-5.0
180	Paka PK 39	—	—	0.48	0.06	<0.20	<0.8	0.2	0.32	—	0.90	-69	-11.9
181	Paka PK 42	—	—	<0.05	<0.05	<0.20	<0.8	<0.1	<0.03	—	1.5	-52	-9.3
182	Paka PK 49	—	—	0.11	0.20	0.6	<0.8	0.3	<0.03	—	0.05	-76	-13.4

Table 15.3 *Continued*

No.	Locality	Temp °C	pH	Na	Ca	Cl	SO_4	Si	B	F	NH_4-N	δ^2H	$\delta^{18}0$
218	Silali SL4	96.5	6.25	0.18	0.06	<0.20	<0.8	0.7	0.21	<0.05	34.8	-28	-5.5
219	Silali SL7	95.3	3.90	<0.05	0.05	0.20	3.4	0.5	0.03	<0.05	0.03	-6	-2.6
220	Silali SL11	94.4	5.05	0.06	<0.05	<0.20	<0.8	0.3	0.05	<0.05	10.3	-52	-8.0
221	Silali SL14	95.8	4.15	<0.05	0.09	0.25	1.4	0.4	0.03	<0.05	1.42	-22	-5.8
222	Silali SL15	96.6	4.20	0.15	<0.05	0.30	0.9	0.4	0.13	<0.05	2.22	-18	-4.6
223	Silali SL16	96.1	4.55	0.14	0.07	<0.20	<0.8	0.5	0.11	<0.05	0.07	-27	-4.7
224	Silali SL19	95.7	4.70	0.06	<0.05	<0.20	<0.8	0.7	<0.03	<0.05	6.54	-50	-7.1
225	Silali SL22	92.3	4.05	0.33	0.12	0.65	0.5	0.7	0.35	<0.05	0.37	-86	-11.0
226	Emuruangogolak EM7	90.6	4.53	<0.05	0.11	<0.20	<0.8	0.9	<0.03	<0.05	0.53	-13	-6.1
227	Emuruangogolak EM9/23	92.6	4.30	0.21	<0.05	<0.20	<0.8	0.6	<0.03	<0.05	0.48	-10	-5.2
228	Emuruangogolak EM9/27	94.7	4.75	<0.05	0.35	<0.20	<0.8	0.7	<0.03	<0.05	0.70	-13	-5.4
229	Emuruangogolak EM9/40	90.6	5.85	0.49	0.10	0.20	<0.8	0.7	0.36	<0.05	0.47	-2	-3.3
230	Emuruangogolak EM16/2a	90.0	5.60	0.09	<0.05	<0.20	<0.8	0.6	<0.03	<0.05	1.35	-19	-4.4
231	Emuruangogolak EM16/2b	90.4	5.00	<0.05	0.06	<0.20	<0.8	0.4	<0.03	<0.05	0.66	-22	-5.0
232	Emuruangogolak EM20a	96.0	4.60	1.39	0.07	<0.20	<0.8	0.2	1.21	<0.05	1.98	-27	-6.0
233	Emuruangogolak EM20b	95.6	4.85	0.84	0.06	0.20	0.8	0.8	0.79	<0.05	1.89	-25	-5.8
234	Emuruangogolak EM20c	92.4	5.12	0.12	0.09	0.25	<0.8	1.0	<0.03	<0.05	2.32	-54	-9.2
235	Kakorinya BR11	96.0	—	0.66	0.16	<0.20	<0.8	1.2	0.04	<0.05	3.04	-5	-3.1
248	Kakorinya BR5	92.8	—	—	—	—	—	—	—	—	—	-30	-5.8
249	Kakorinya BR4	94.0	—	—	—	—	—	—	—	—	3.98	-19	-4.2
250	Kakorinya BR18	94.4	—	—	—	—	—	—	—	—	3.39	-17	-3.7
251	Kakorinya BR29	92.9	—	—	—	—	—	—	—	—	—	-22	-4.3
252	North Island	95.5	—	—	—	—	—	—	—	—	0.90	-18	+0.1
253	North Island-summit	95.9	—	—	—	—	—	—	—	—	204	-13	+1.3
254	Central Island	97.3	—	—	—	—	—	—	—	—	116	+11	+0.6
255	Central Island	97.4	—	—	—	—	—	—	—	—	108	+17	+0.9

NB: OK, KR and PK sites sampled in 1988 except * in 1989 and ** in 1991

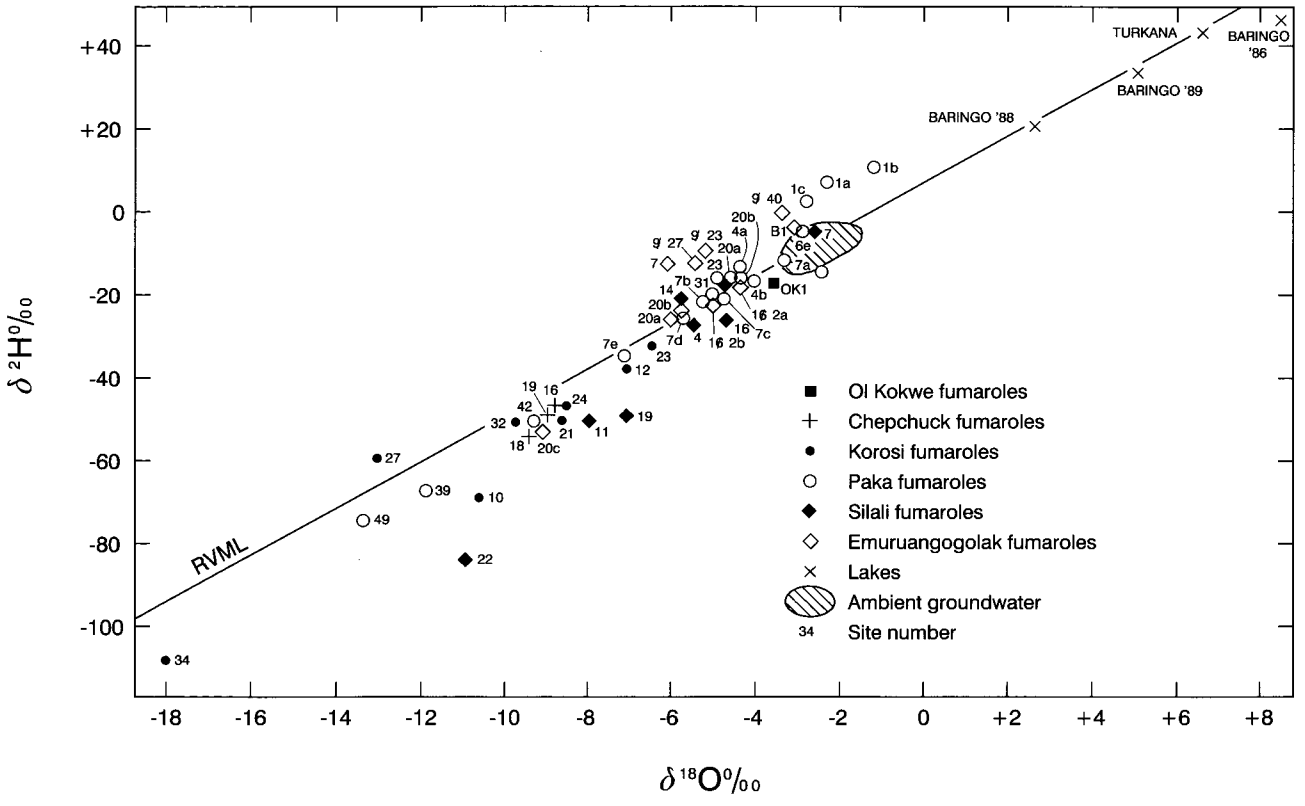

Figure 15.8 Plot of δ^2H against $\delta^{18}O$ for fumarole steam condensates from the southern volcanic centres of Korosi to Emuruangogolak (values in permil with respect to SMOW).

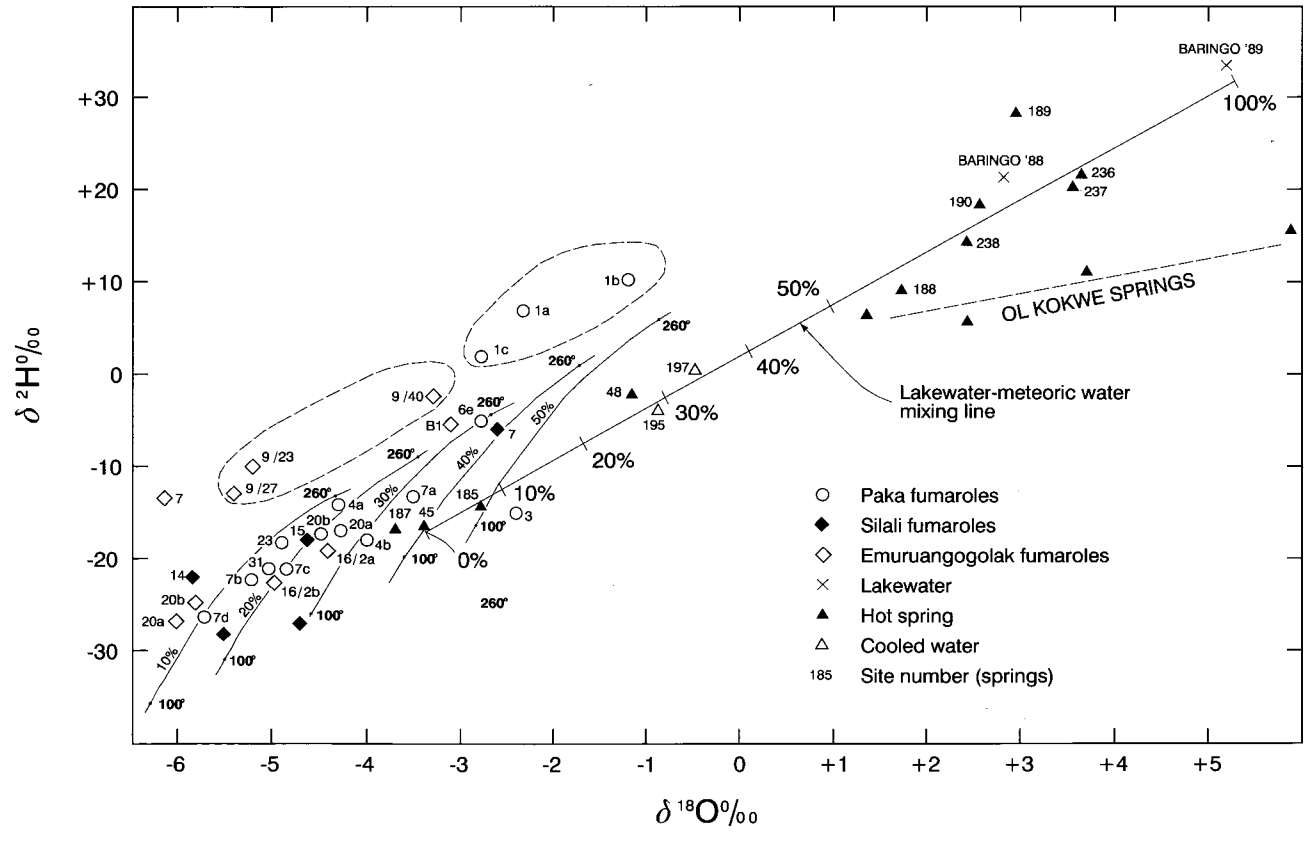

Figure 15.9 Plot of δ^2H against $\delta^{18}O$ for selected fumarole steam condensates (values in permil with respect to SMOW).

gether with data for ambient groundwaters and lakewaters. Similarly, stable isotope data for fumarole condensates from the Barrier and Central and North islands are plotted in Figure 15.10, together with data for ambient groundwaters and lakewaters from the Suguta Valley and Turkana basin. This demonstrates that the waters of the region have an extreme range of isotopic compositions, varying from about +50 to -110‰ δ^2H, and about +9 to -18‰ $\delta^{18}O$, and that the fumarole compositions cover more than two-thirds of each range.

The isotopic data indicate that there is insufficient variation in local groundwaters to account for all of the steam condensates by a simple process of primary steam separation from these waters. Firstly, there are fumarole samples more enriched in heavy isotopes than local ambient groundwaters, as for example the PK1 series (samples 163–165) collected from fumaroles in the caldera of Paka. Secondly, there are condensates that are so depleted that they could only be derived by primary steam separation if source waters were from very high altitudes.

Figure 15.9 shows an expanded portion of Figure 15.8 covering the main group of fumaroles and including the hot springs from the project's Phase II area. Primary steam condensate curves are shown on the diagram based upon 10% steps in a rift margin-lakewater mixing series, in a similar manner to the method employed by Darling et al. (1990). Using this scheme, most of the fumaroles in the main group can be explained by primary steam separation from varying mixtures of rift margin water and lakewater, except for the PK1 series of samples from Paka (samples 163–165) and the EM7 and EM9 series from Emuruangogolak. The EM7 and EM9 fumaroles (samples 226, 227, 228, 229) of Emuruangogolak caldera are not particularly strong, and may be explained in terms of a secondary origin, such as steam heating of groundwater. In contrast, the PK1 fumaroles of Paka caldera are strong and rich in CO_2 so a secondary origin is less likely for these. Only a water that has already lost steam could have a suitable isotopic composition to provide steam with the composition of these fumaroles, although other Paka fumaroles with more 'normal' isotopic compositions could be derived by primary steam separation, such as the PK4 series (samples 166–167) situated just outside the main caldera to the north and the PK7 fumaroles (samples 168–171 and 175) located in the eastern crater.

With the exception of the strongest and hottest fumarole on the Nakaporon fault zone (KR23), the Korosi and Chepchuk fumarole condensates are isotopically depleted and cannot be directly related to the proposed groundwater-lakewater mixing series. Some Paka, Silali and Emuruangogolak fumaroles also lie in the isotopically depleted area in Figure 15.8. These depleted compositions may be explained by subsurface steam condensation, which could have the effect of lowering the heavy isotope content of steam quite considerably. The Rayleigh process of condensation examined in Darling and Armannsson (1989) could account for quite large fractionations, particularly for weak fumaroles at a large distance from their upflow. A prime example of this is the very weak fumarole KR34 (162) at Loruk, which is a considerable distance from the nearest volcanic centres of Korosi or Ol Kokwe, and which has a highly depleted isotopic composition (site 34 in Figure 15.8). The isotopic data also indicate that even locally the process of subsurface condensation operates on a significant scale. This is exemplified by significant variations in the isotopic composition of fumaroles occurring within spatially constrained groups; for example, the PK1 group (samples 163a–b, 164, 165) from the main caldera of Paka, the PK7 group (samples 168, 169, 170, 171) from the eastern crater of Paka, and the EM9 group (samples 227, 228, 229) and EM20 group (samples 232, 233, 234) from the caldera of Emuruangogolak.

Given that significant subsurface condensation takes place even on a local scale, the safest option is to consider that the most enriched isotopic composition at any one volcanic centre is the most representative of the original steam. However, the possibility cannot be ruled out that even the most enriched fumarole is suffering from condensation, as is likely in the case of Korosi. The isotopic compositions of selected fumarole condensates are presented in Figure 15.9 together with the theoretical composition of steam compositions derived by single-stage separation from a lakewater-meteoric water mixing series. On the assumption that the most enriched fumarole condensates at each centre approximate to original steam compositions, it is apparent from Figure 15.9 that Paka, Silali and Emuruangogolak have fumaroles which indicate 45%, 25% and 10% of lakewater respectively in their source reservoirs, which is consistent with the progressive dilution northwards of outflow from Lake Baringo.

Other mechanisms may possibly operate and influence the isotopic composition of fumarolic steam within the area. For example, some very depleted isotopic compositions may result from the vaporisation of depleted meteoric water infiltrating after a single storm event. Another alternative mechanism, reflux condensation, might possibly give rise to significant isotopic variation also. Both these alternative mechanisms were considered in detail by Allen and Darling (1992) but are thought not to be important. The preferred model discussed above, of simple condensation of fumarolic steam derived from a lakewater-meteoric water mixing series, provides the simplest means of explaining the steam stable isotope compositions of most fumaroles in the region and is therefore retained for the purpose of interpretation in this report.

Figure 15.10 presents data obtained during phase III of the project for Kakorinya and the islands of Lake Turkana. This illustrates that the stable isotope compositions of the fumaroles of Central and North islands are markedly different from those of the Kakorinya centre. The fumaroles of Kakorinya resemble those of the volcanic centres to the south, notably Korosi, Paka and Silali, and their compositions can be satisfactorily explained by assuming single-stage steam separation from a relatively enriched water. Such a water need not be enriched beyond about 0‰ for both isotopes, and therefore could be produced from a mixture of Suguta Valley groundwater or Turkana lakewater with water from the rift flanks. In hydrogeological terms it appears more likely that Turkana lakewater must be contributing to the steam compositions rather than Suguta Valley groundwater, and an upper limit of less than 40% lakewater is indicated in Figure 15.10. The more depleted compositions may indicate a zoning of groundwater-lakewater mixing, or the effects of subsurface condensation. It should be noted that the most enriched steam is found

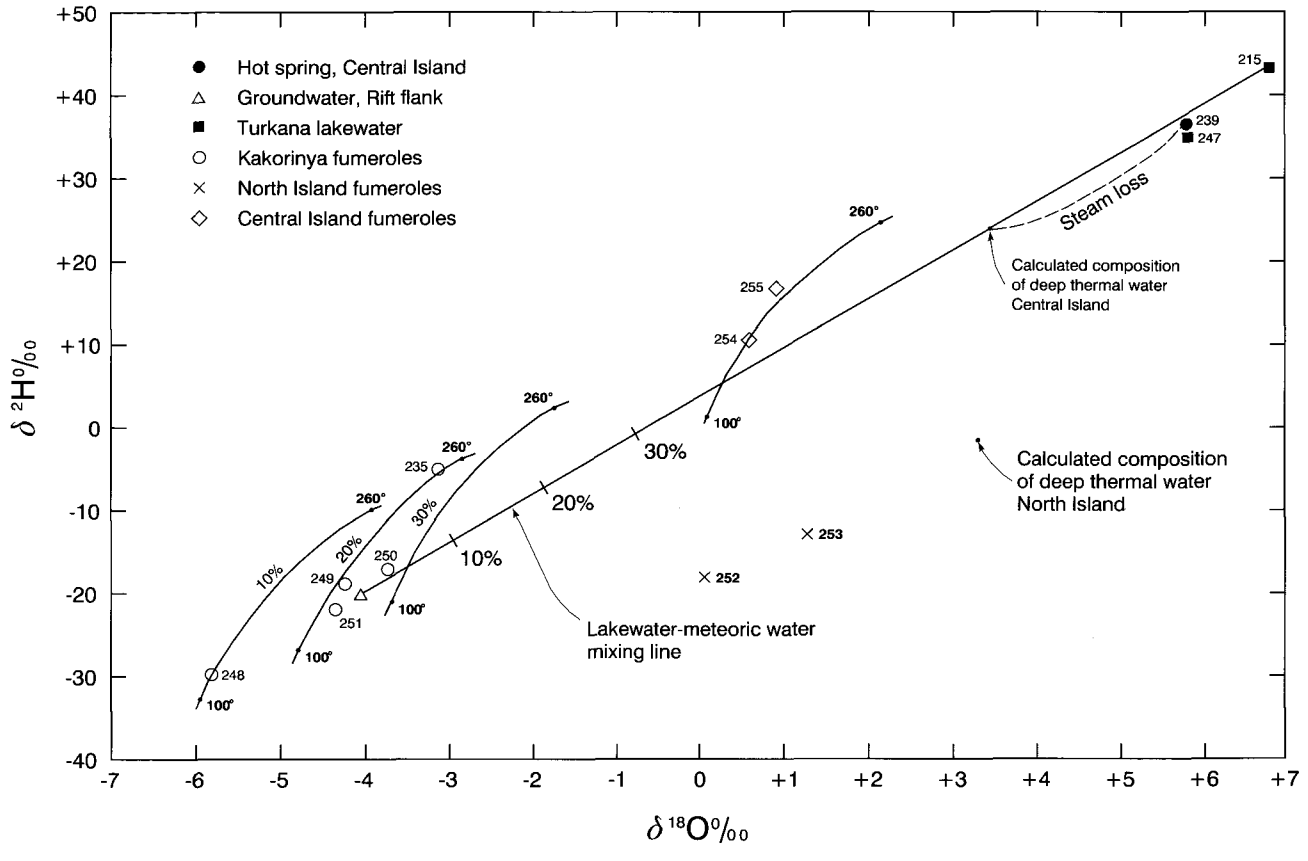

Figure 15.10 Plot of δ^2H against $\delta^{18}O$ for fumarole steam condensates from Kakorinya, Central Island and North Island (values in permil with respect to SMOW).

towards the centre of Kakorinya, where the hydrothermal plume is likely to be strongest.

The stable isotope compositions of steam condensates from Central and North islands require different explanations. Those of North Island fall significantly below the local meteoric line in Figure 15.10 and are dissimilar to fumaroles in the remainder of the Kenya Rift. Such compositions either require significant low-temperature subsurface condensation processes, which is unlikely because of the vigorous nature of these fumaroles, or are derived from a reservoir composition falling significantly off the meteoric line. Given the absence of suitable end-members for mixing, the only plausible way that such a composition could arise appears to be by oxygen isotope shifting by water-rock interaction. Figure 15.10 shows that a positive shift of about 4‰ is required. Such shifts caused by high-temperature water-rock interaction are known from various geothermal systems around the world, but have not been found within the Kenya Rift; unequivocal geothermal water from Olkaria has a $\delta^{18}O$ shift of only about 1‰. However, in the absence of contrary evidence, it is assumed that oxygen shifting of a greater order is occurring in the North Island hydrothermal system. The magnitude of oxygen isotope shifting is a function of the amount of water-rock contact, and relatively large shifts therefore imply that a system has either low permeability or is young, or has a combination of these features. Each case limits the amount of water that has passed through the rock, therefore limiting the extent to which rock and water can readjust towards isotopic equilibrium. If the assumption is made that all the rift's hydrothermal systems have roughly similar permeability, then a comparatively large $\delta^{18}O$ shift implies a young hydrothermal system. A difficulty with this interpretation is that the postulated deep fluid would consist of little more than 30% lakewater.

On Central Island, however, hot springs are available to test the validity of any assumptions made from consideration of fumarole steam analyses. The composition of fumarole condensates from Central Island, while more enriched than those found elsewhere within the rift, are compatible with derivation from a lakewater source without oxygen shifting. Figure 15.10 shows the likely relationship between steam and source water based on boiling off at ~280°C and cooling of steam to the local surface boiling point. The results indicate limited dilution of lakewater, perhaps resulting from direct infiltation of rainfall on the island.

15.6 FUMAROLE AND HOT SPRING GASES

Gas samples were collected from representative fumaroles on all of the volcanic centres of the region, and from gaseous hot springs. Details of the sampling methods employed were described by Darling and Talbot (1991).

15.6.1 Gas chemistry

The chemical compositions of the samples are presented in terms of mole percent in Table 15.4 and in m mole/kg of steam in Table 15.5.

Of the hot springs, Lorusio (45), Kageinya (188) and Elboitong (236, 237) have large amounts of gas.

Table 15.4 Gas compositions for springs and fumaroles in mole percent (except C_2-C_4 in ppmv).

Site	H_2	O_2+Ar	N_2	CO_2	CH_4	C_2H_6	C_3H_8	C_4H_{10}
HOT SPRINGS								
Lorusio (45)	0.79	2.3	13.3	83.6	0.11	1	nd	nd
Kapedo (48)	0.31	19.6	79.7	0.44	0.0008	nd	nd	nd
SV 3a (185)	nd	11.2	69.5	18.9	0.39	0.2	nd	nd
Kageinya (188)	0.003	1.08	97.5	nd	1.41	280	120	33
Namarunu (189)	nd	16.3	71.3	12.4	0.013	1	nd	nd
Logipi (190)	0.026	17.8	80.4	1.6	0.14	28	nd	nd
Elboitong (236)	nd	0.37	0.64	99.0	0.011	1.1	0.06	nd
Elboitong (237)	nd	1.33	3.35	93.4	0.004	5.0	0.06	nd
Logipe NE (238)	0.104	11.8	80.9	6.78	0.334	4.1	nd	nd
FUMAROLES								
OK 1 (152)	0.79	0.1	9.8	88.90	0.32	20	4	nd
KR 34 (162)	nd	11.4	45.9	42.3	0.35	44	17	6
KR 19 (157)	nd	0.05	1.0	97.6	1.3	290	130	21
KR 23 (159)	0.40	18.2	65.1	16.1	0.015	9	0.5	nd
KR 23 (159)*	0.0003	18.8	66.9	14.3	0.024	2.5	1.3	0.1
KR 12 (154)	nd	10.3	46.8	42.7	0.21	8	3	nd
KR 18 (156)	nd	0.3	1.9	96.3	1.5	340	130	43
PK 1a (163)	nd	3.4	11.3	83.8	1.5	1	nd	nd
PK 1a (163)*	nd	14.2	55.4	30.0	0.45	1	nd	nd
PK 4a (166)	4.1	0.61	2.1	91.8	1.3	1	nd	nd
PK 7a (168)	0.92	0.61	30.2	67.0	0.85	39	14	6
SL 7 (219)	0.87	0.09	0.34	98.4	0.25	0.7	nd	nd
SL 11 (220)	nd	10.4	37.1	52.0	0.48	18	4	nd
SL 14 (221)	0.65	0.05	0.29	98.7	0.25	0.6	0.1	nd
SL 15 (222)	0.93	0.06	0.22	98.6	0.24	1	0.1	nd
SL 16 (223)	0.044	15.7	58.2	26.0	0.026	0.3	0.2	nd
SL 19 (224)	0.0002	4.4	16.8	77.8	1.1	0.5	nd	nd
SL 22 (225)	0.0009	5.9	24.4	69.5	0.17	0.6	0.1	nd
EM 7 (226)	nd	16.0	61.3	22.2	0.51	nd	nd	nd
EM 9/27 (228)	0.001	13.4	57.1	28.8	0.64	2	nd	nd
EM 20a (232)	0.002	7.9	32.5	59.1	0.51	0.1	nd	nd
EM 20b (233)	nd	7.5	30.6	61.3	0.56	nd	nd	nd
BR 11 (235)	0.008	18.0	64.8	17.1	0.044	0.1	nd	nd
BR 5 (248)	nd	20.6	75.8	3.6	0.014	0.23	nd	nd
BR 4 (249)	0.038	19.8	73.3	6.92	0.023	0.84	nd	nd
BR 18 (250)	0.018	19.3	71.8	8.81	0.020	6.3	nd	nd
BR 29 (251)	nd	19.9	74.9	5.07	0.064	1.2	0.17	nd
N. Island (252)	0.660	13.6	46.0	39.3	0.470	29	5.5	0.71
N. Island (253)	0.053	1.22	8.55	89.0	1.19	80	10	1.1
C. Island (254)	1.75	nd	0.50	96.8	0.932	47	11	4.9
C. Island (255)	1.93	nd	0.59	96.6	0.930	48	9.8	3.9

* repeat sampling 1 year later, nd - below detection limit

At Lorusio the main gas is CO_2, but at Kageinya N_2 dominates, possibly because alkaline buffering prevents the existence of free CO_2. The Elboitong springs have the highest gas content of any springs in the region. The gas phase in these springs is dominated by CO_2 and has very low concentrations of CH_4 and other hydrocarbons. The high pCO_2 may be contributing to the elevated levels of HCO_3^- measured in the waters of Elboitong via interaction with feldspar. Springs without free gas bubbles at Kapedo, SV3 (north-west of Emuruangogolak), Namarunu and Logipi (48, 185, 189 and 238) are generally dominated by N_2, though they are generally depleted in O_2 and somewhat elevated in CO_2, which indicate that their gas compositions are at least partly original and not due simply to the introduction of air during sampling. The Logipi springs have CH_4 concentrations elevated by an order of magnitude compared with the Elboitong springs

Table 15.5 Amounts of fumarole gases in steam in m mole kg^{-1}

Site	H_2	O_2 + Ar	N_2	CO_2	CH_4	H_2S	NH_3
OK 1 (152)	11.1	138.2	138	1254	4.5	3.2	2.6
KR 34 (162)	—	426	1715	1580	13.0	0.81	2.0
KR 19 (157)	—	0.77	15	1494	20	0.79	0.60
KR 23 (159)	0.030	1867	6643	1420	2.4	0.15	0.56
KR 12 (154)	—	182	825	753	3.7	2.8	0.27
KR 18 (156)	—	3.7	23	1178	18	0.37	0.35
PK 1 (163)*	—	18	61	450	8.1	4.0	0.0056
PK 1 (163)**	—	423	1649	893	13	7.8	0.0059
PK 4 (166)	9.6	1.4	4.9	215	3.0	0.44	0.091
PK 7 (168)	9.4	6.2	308	684	8.7	3.9	0.0035
SL 7 (219)	3.0	0.31	1.2	336	0.85	2.4	0.0021
SL 11 (220)	—	67	240	336	3.1	57	0.72
SL 14 (221)	2.5	0.19	1.1	377	0.95	2.3	0.099
SL 15 (222)	1.3	0.086	0.32	142	0.35	0.84	0.16
SL 16 (223)	1.0	369	1368	611	0.61	12	0.0046
SL 19 (224)	0.014	298	1139	5273	75	16	0.36
SL 22 (225)	0.072	475	1963	5591	14	6.5	0.020
EM 9/27 (228)	0.079	1057	4505	2272	51	12	0.040
EM 20a (232)	0.052	207	850	1545	13	29	0.13
BR 11 (235)	0.097	219	788	208	0.54	0.23	0.21
BR 4 (249)	—	—	—	623	—	0.034	—
BR 18 (250)	—	—	—	3852	—	0.47	—
N. Island (252)	—	—	—	781	—	0.81	—
N. Island (253)	—	—	—	3070	—	0.26	—
C. Island (254)	—	—	—	950	—	38.4	—
C. Island (255)	—	—	—	987	—	39.6	—

* Sampled in 1988, ** sampled in 1989.

and they also have detectable H_2. This may indicate a small contribution to the Logipi springs from a magmatic source, which would be consistent with the possibility of limited underflow from Lake Turkana passing through the active zones of the Barrier Volcanic Complex. The gas composition of the Namarunu springs is similar to that of the Logipi springs, but with lower CH_4 concentrations. The proximity of Namarunu to Elboitong raises the possibility that CO_2-rich gas from Elboitong may be migrating to the Namarunu area and mixing with air. The relatively large amount of CH_4 at Kageinya is probably related to the absence of CO_2 due to alkaline buffering.

Table 15.4 shows that fumarole CO_2 values range between about 4% and 99%, depending on the amount of air contamination or entrainment. Most of the weaker fumaroles and also some of the stronger fumaroles issuing from large orifices are prone to air contamination. However, it is unlikely that all contamination occurs at the point of sampling, because air can penetrate the unsaturated ground, particularly where fumaroles occur on steep slopes as at KR23 (159), or can be dissolved in local perched aquifers which may affect the chemistry of weaker fumaroles. To avoid this problem as far as possible, O_2 and CO_2 were determined in many fumaroles using field-based analytical methods during the initial mapping phase of the survey. Subsequently only the stronger and hotter fumaroles with least air contamination (lowest O_2) were selected for sampling and detailed analysis, though on Kakorinya no very satisfactory fumaroles were found.

Hydrogen and methane are often taken as indicators of proximity to, or strength of hydrothermal upflows. Korosi fumaroles have least H_2 in keeping with other indicators of low potential as described in Section 15.5. Emuruangogolak and Kakorinya fumaroles are also low in H_2, as are the PK1 samples from the caldera of Paka. The latter is difficult to explain, because in all other respects Paka caldera appears to be a highly favourable locality. Methane was found in all samples, but no particular pattern is evident. The ratio of methane to higher alkanes is however of interest with respect to geothermometry, and is considered in more detail in Section 15.7.2. Hydrogen sulphide was found in all samples, generally in very low amounts, but other sulphur-bearing gases, such as COS, were below detection.

Table 15.5 gives gas data in the form of m mole per kg, which provides a measure of the relative amount of water vapour present. In general the strongest fumaroles (for example PK1, 4, 7, SL14, 15 and BR1) have the lowest amount of gas relative to water vapour. This is consistent, because the strongest fumaroles are probably hot enough to prevent excessive condensation of water, whereas the weaker and more distant fumaroles, such as KR34 (162), have relatively large gas contents because water has condensed out on the way to the surface. The highest relative gas contents (excluding air contamination) are seen on Silali,

where the fumaroles concerned, SL19 and SL22, also have stable isotope compositions indicative of subsurface condensation.

15.6.2 Gas isotopic compositions

The results of isotope analyses of fumarole and hot spring gases for $\delta^{13}C\text{-}CO_2$, $\delta^{13}C\text{-}CH_4$ and $^3He/^4He$ are presented in Table 15.6.

The results of $^3He/^4He$ analyses are reported in the form of R_A, which is the ratio of $^3He/^4He$ in the sample to that of the atmosphere (1.4×10^{-6}) corrected for air contamination on the basis of the Ne/He ratio. All samples have values in excess of 1, indicating enrichment to varying degrees in mantle He, and the maximum ratio of 8.0 is comparable with typical MORB values and with He issuing from the active carbonatite volcano of Oldoinyo Lengai in the rift in northern Tanzania (Javoy et al., 1989). In the case of fumaroles, high $^3He/^4He$ measurements may provide an indication of proximity to upflow, although as far as hot springs are concerned it is evident that high R_A values can occur at some distance from any presently active upflow (Allen and Darling, 1992).

There is no correlation between $\delta^{13}C$ values of CO_2 and CH_4 (Figure 15.11), neither is there a clear relationship of either with He isotope values (Allen and Darling, 1992). However, the bulk of the CO_2 is likely to come from deep crustal sources because samples consistently contain a relatively high ^{13}C content.

From its $\delta^{13}C$ values of approximately -20 to -30‰ it would appear that the methane cannot be of biogenic origin, but neither is it likely to be synthesised from CO_2 or H_2 at high temperatures because of the absence of alkene gases which are thought to be produced under such conditions. Allen and Darling (1992) point out that within the rift methane with similar $\delta^{13}C$ values may be produced by different types of hydrothermal systems, and they favour a relatively low-temperature thermogenic origin from organic matter entering the geothermal systems, perhaps dissolved in lake waters.

Figure 15.12 shows a good correlation between the ratios of methane to higher alkanes versus He R_A values for the volcanic centres of the Rift Valley as far north as Silali. Allen and Darling (1992) and Darling and Talbot (1991, 1992) conclude that this relationship is a function of temperature. In essence, with all other factors being equal, higher He R_A values are considered to occur closer to the centres of geothermal upflow zones. Mixtures of alkanes relatively rich in ethane and higher members of the series are thought to be produced from dissolved or sedimentary organic material of lacustrine origin in the warm outer regions of hydrothermal plumes. If these mixtures are drawn into the hotter parts of the plumes, progressive breakdown of the higher alkanes occurs resulting in an almost logarithmic increase in CH_4/C_2H_6, hence the relationship between this ratio and He R_A.

Table 15.6 Isotope analyses of gas phase components from hot springs and fumaroles ($\delta^{13}C$ in permil vs PDB, He ratio in R_A).

No.	Locality	$\delta^{13}C_{CO_2}$	$\delta^{13}C_{CH_4}$	$^3He/^4He$*
HOT SPRINGS				
45	Lorusio	-6.0	—	5.00
48a	Kapedo	—	—	3.92
185	SV 3a	-12.4	—	4.61
188	Kageinya	—	-31.8	—
189	Namarunu	-8.9	—	7.10
190	Logipi NW.	-14.6	—	6.50
236	Elboitong S.	-5.4	-28.3	—
237	Elboitong N.	-7.0	-28.3	—
238	Logipe NE.	-9.8	—	—
FUMAROLES				
152	OK 1	-3.5	-18.3	4.90
162	KR 34	-4.3	-27.6	3.17
157	KR 19	-3.9	-23.4	—
159	KR 23	-6.3	—	—
159	KR 23	-6.1	-19.7	1.63
154	KR 12	-4.3	—	3.90
156	KR 18	-3.9	-24.5	2.50
163	PK 1a	-2.9	-24.9	7.90
163	PK 1a	-3.2	-24.0	—
166	PK 4a	-3.4	-27.8	6.17
168	PK 7a	-2.7	-22.2	3.63
219	SL 7	-3.8	-23.0	7.52
220	SL 11	—	-24.3	—
221	SL 14	-3.7	-24.3	8.00
222	SL 15	-3.9	-25.0	—
223	SL 16/16	-4.7	-23.5	—
224	SL 19	-4.6	—	—
225	SL 22	-3.6	-21.7	7.86
226	EM 7	-3.9	-26.9	—
228	EM 9/27	-4.7	-20.7	4.16
232	EM 20a	-4.0	-22.5	6.02
235	BR 1	-3.3	-26.3	3.31
248	BR 5	-1.8	-26.0	—
249	BR 4	-5.7	-24.4	—
250	BR 18	-6.0	-25.8	—
251	BR 29	-4.0	-26.6	—
252	North Island	-5.2	-28.2	—
253	North Island	-5.4	-32.2	—
254	Central Island	-4.3	-32.2	—
255	Central Island	-3.8	-30.9	—

* Analyst Ms E Griesshaber at Cambridge University

15.7 GEOTHERMOMETRY

Geothermometry has been used to estimate temperatures at depth within the geothermal systems of the region. The methods employed rely on the fact or assumption that certain chemical equilibria between fluids and rocks are temperature dependent, and that the concentration of selected elements or gases in geothermal fluids are therefore related to temperature.

15.7.1 Hot spring geothermometry

The application of cation and silica geothermometers to the hot springs of the region is hampered by the fact that most of the solute content of these waters appears to have been acquired by a combination of evaporite dissolution, CO_2 metasomatism, or simple evaporative concentration, rather than by interaction

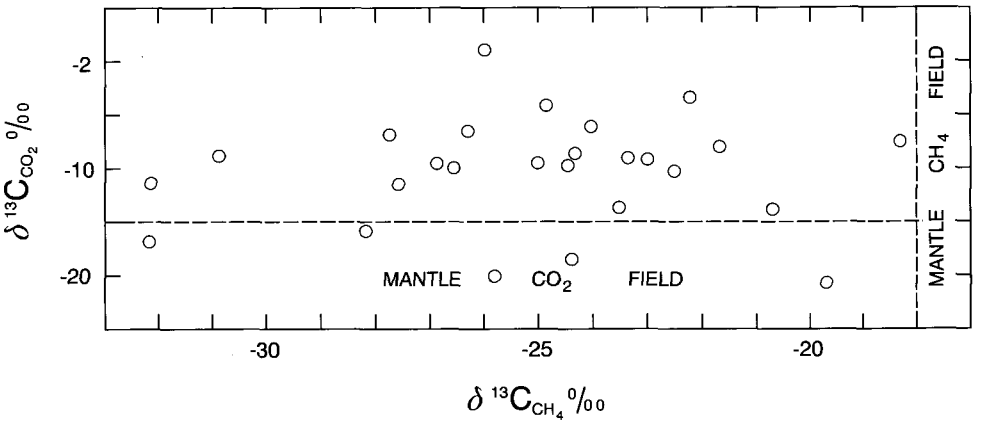

Figure 15.11 Plot of $\delta^{13}C_{CO2}$ against $\delta^{13}C_{CH4}$ for fumarole gases (values in permil with respect to PDB). Fields of mantle CO_2 and CH_4 based on Javoy et al. (1989) and Welhan and Lupton (1987).

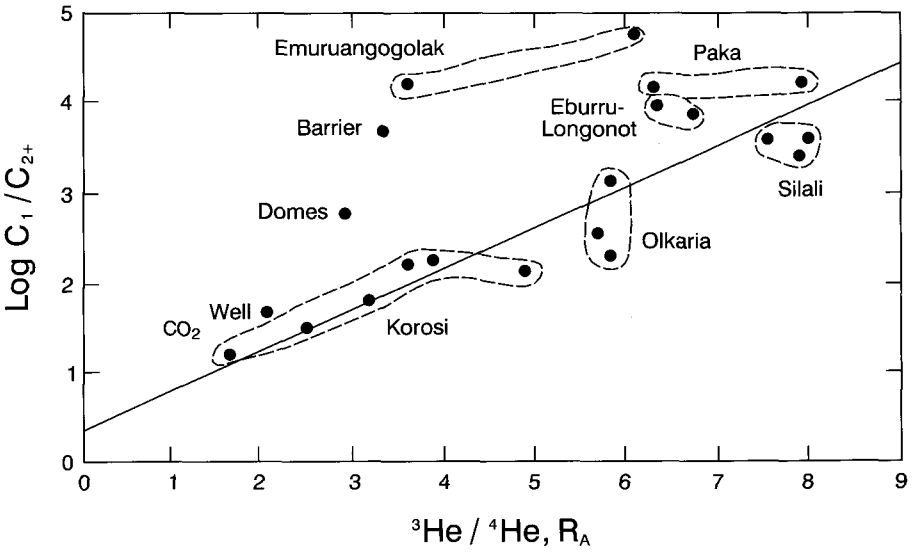

Figure 15.12 Plot of log C_1/C_{2+} alkanes against $^3He/^4He$. The figure includes data from the central sector of the rift. The best fit line is based on all data points excluding those for the Barrier and Emuruangogolak.

of water with rock in its more limited sense. Evidence to support this supposition is provided by Mg concentrations in the springs, which are mostly below the expected values for observed Na/K ratios if those ratios were the product of equilibration with feldspar at a particular temperature.

The calculated temperatures in Table 15.7 must therefore be treated with great caution. The Na/K geothermometer may overestimate temperatures by as much as 20°C. Similarly the highly alkaline nature of these waters may result in SiO_2 concentrations being much higher than they would be for the pH 7 water-rock equilibrium assumed for the purpose of silica geothermometry (Fournier, 1981). The effect of this would be to overestimate temperatures at typical thermal springs such as Kapedo (48) or the SV3 springs north-west of Emuruangogolak (185) by up to 15°C, and by as much as 25°C for the highly alkaline sites in the Suguta Valley, such as Kageinya (188), Namarunu (189) and Logipi (190, 238). These effects probably operate at all the sites to varying extent, although they will depend on how the observed surface silica concentrations and pH have arisen. For example, a high-temperature thermal water could become diluted by mixing with a high bicarbonate water on its way to the surface. Similarly, loss of CO_2 at the surface could lower pH significantly without causing an additional rise in SiO_2 concentration above that resulting from the original water-rock equilibration. The Elboitong springs (236, 237) are the most likely to have been affected in this way, and their temperatures for the adiabatic quartz geothermometer may be substantially correct.

The springs of Ol Kokwe (71) and Central Island (239) are likely to be the least affected by the processes outlined above, and may therefore be giving reasonably reliable temperature estimates. While there is good agreement between the Na/K and chalcedony version of the silica geothermometer, it is more likely that the quartz geothermometer is the correct version to use in this temperature range. To what extent the deep thermal waters at these sites may be mixing with cooler water is debatable. If such mixing is taking place, then silica would probably provide a more reliable index of higher temperatures, as it is less prone to re-equilibration at lower temperatures.

For the other lower temperature springs the chalcedony geothermometer is probably the most appropriate, while taking into account the limitations of silica-geothermometry outlined above. The chalcedony temperatures in Table 15.7 reveal that few of the thermal waters can have reached much more than 100°C. They do however show that the relatively cool springs at Kalnangi (195) and Nangarabat (197) could be cooled thermal waters.

15.7.2 Fumarole gas geothermometry

Temperatures calculated using the gas geothermometry equations of Arnorsson and Gunnlaugsson (1985), D'Amore and Panichi (1980) and the carbon isotope

Table 15.7 Geothermometry temperatures (°C) for hot springs.

No.	Locality	Temp. °C	Na/K	Qz	Qz-A	Ch	CO_2	H_2	CO_2/H_2	D-P	$\Delta^{13}C$
45	Lorusio	81	125	123	120	94	277	181	493	—	—
48	Kapedo	50	116	122	121	96	—	139	—	—	—
71	Ol Kokwe	94	155	175	176	170	—	—	—	—	—
183	Kapedo	45	120	129	130	106	—	—	—	—	—
184	Kapedo	45	114	140	135	114	—	—	—	—	—
185	SV 3a	68	79	145	139	119	—	—	—	64	—
186	SV 3b	64	83	145	139	119	—	—	—	—	—
187	Kamuge	50	64	126	124	100	—	—	—	—	—
188	Kageinya	68	98	171	161	148	—	205	—	426	260
189	Namarunu	66	112	106	108	78	—	—	—	85	—
190	Logipi NW	61	107	72	94	61	—	101	286	217	—
194	Kachurkolh	31	67	64	71	34	—	—	—	—	—
195	Kalnangi	32	103	125	121	96	—	—	—	—	—
197	S.Nangarabat	31	95	104	106	76	—	—	—	—	—
236	Elboitong S	95	107	137	133	111	—	—	—	—	—
237	Elboitong N	92	106	151	144	124	—	—	—	—	—
238	Logipi NE	70	108	115	—	87	—	—	—	—	—
239	Central Is.	71	166	182	—	161	—	—	—	—	—

Na/K and Qz (quartz), Qz-A (quartz, adiabatic) and Ch (chalcedony) based on Fournier (1981)
CO_2, H_2 and CO_2/H_2 gas geothermometers from Arnorsson and Gunnlaugsson (1985).
D-P from D'Amore and Panichi (1980). Δ13C from Panichi et al (1975).

geothermometer of Panichi et al. (1975) are presented in Table 15.8.

The application of these conventional geothermometers to the relatively weak fumaroles of the East African Rift system is generally considered to be inappropriate and to provide unsatisfactory results (Darling and Talbot, 1991). This is because the more reactive gases tend to disappear while traversing the often large distances from reservoir boiling zones to the surface, and also because subsurface condensation of steam changes the gas/water ratio. Furthermore, the mineral reactions assumed to control gas concentrations in the conventional gas geothermometers may not operate within the geochemical province of the rift.

Darling and Talbot (1991) discuss the application of the various gas geothermometers to the fumaroles of the region and show that generally they give unreliable results. Many of the geothermometers depend upon the concentration of H_2S and H_2, either singularly or together, and these suffer from the fact that in many fumaroles the concentrations of these two gases are near or below detection limits. The empirical geothermometer of D'Amore and Panichi has not been applied where H_2 is below detection limit, despite the authors' suggestion of using arbitrary concentration values under such circumstances. In in any case, this geothermometer has been found to be inconsistent and unreliable when used in the rift.

In most cases the CO_2 geothermometer gives unrealistically high temperature estimates because the concentration of CO_2 has been raised by subsurface condensation of steam. Only the strongest fumaroles are likely to give anything like realistic temperatures, as for example those from the summit area of Paka (PK1, 4, 7) (286–317°C) and the caldera floor of Silali (SL14, 15, 16) (274–315°C).

The carbon isotope geothermometer gives temperatures that are consistently much higher than are likely to be encountered. It is possible that the calculated temperatures are representative of conditions at depths greater than the other geothermometers can register, since CH_4-CO_2 isotopic equilibrium takes a very long time to become established at temperatures below 500°C, and fluids moving towards the surface may not have had time to re-equilibrate. However, this assumes that CH_4 is produced at depth by high-temperature inorganic synthesis, which according to Section 15.6.2 is unlikely, on the grounds that alkanes rather than the predicted alkenes are commonly detected in the fumaroles.

In view of the problems of applying the more conventional gas geothermometers to the weak fumaroles of the East African Rift System (EARS), Darling and Talbot (1991, 1992) developed a more appropriate geothermometer for use within the region. This is based upon the temperature dependence of the ratio of methane (C_1) to higher alkanes (C_{2+}) described in Section 15.6.2, and has been formalised into a methane/ethane (C_1/C_{2+}) geothermometer by calibration against geothermal wells throughout the EARS. Comparative studies indicate that for the rift system the new C_1/C_{2+} geothermometer outperforms the other gas geothermometers (Darling and Talbot, 1991). The methane/ethane relationship with temperature is unlikely to be controlled by mineral reaction, which largely explains why the C_1/C_{2+} geothermometer is so robust compared with other geothermometers when applied to the weak fumaroles of the rift.

Temperatures calculated using the C_1/C_{2+} geothermometer are given in Table 15.8. These are in good agreement with the field evidence and some of the other geochemical criteria. They indicate that Paka, Silali and Emuruangogolak all have similarly high temperature geothermal systems with temperatures around 300°C or higher. Kakorinya has slightly lower reservoir temperatures, averaging 263°C but with a maximum value still in excess of 300°C. Temperature estimates for Chepchuk are lower still, averaging 232°, whereas Korosi is by far the least good prospect with significantly lower temperatures averaging only 200°C.

The C_1/C_{2+} geothermometer provides consistent results for the islands of Lake Turkana. However, the

Table 15.8 Geothermometry temperatures (°C) for fumaroles.

No.	Locality	CO_2	H_2S	H_2	CO_2/H_2	H_2S/H_2	D-P	$\Delta^{13}C$	C_1/C_2
		----- Cl > 500 mgl -----							
152	OK 1	326	237	265	254	326	210	460	—
154	KR 12	320	253	—	—	—	164	—	261
156	KR 18	332	185	—	—	—	133	350	202
157	KR 19	354	204	—	—	—	139	390	203
159	KR 23	—	—	—	334	—	263	—	—
159	KR 23*	417	165	254	240	—	—	480	197
162	KR 34	346	205	—	—	—	142	215	224
163	PK 1a	306	243	—	—	—	164	340	—
163	PK 1a	380	259	—	—	—	110	370	323
166	PK 4a	286	191	274	222	357	237	300	329
168	PK 7a	317	243	274	187	319	221	380	256
219	SL 7	320	229	259	283	308	230	390	312
220	SL 11	320	307	—	—	—	131	—	261
221	SL 14	328	230	257	280	306	218	380	314
222	SL 15	265	206	249	285	313	256	370	306
223	SL 16	385	269	245	262	261	276	430	288
224	SL 19	492	278	208	183	183	206	—	335
225	SL 22	501	254	211	202	227	129	400	309
228	EM 9	440	269	212	215	218	143	340	310
232	EM 20	417	290	207	214	195	161	440	343
235	BR 11	290	175	215	247	290	197	400	314
248	BR 5	—	—	—	—	—	—	—	280
249	BR 4	316	181	288	277	383	218	—	262
250	BR 18	372	232	296	295	352	206	—	189
251	BR 29	—	—	—	—	—	—	—	271
252	N. Is.	322	243	301	291	352	281	—	241
253	N. Is.	364	220	283	249	337	76	—	244
254	C. Is.	327	318	303	292	290	257	—	253
255	C. Is.	325	318	303	293	290	263	—	251

All geothermometers except D-P and C_1/C_2 from Arnorsson and Gunnlaugsson (1985). D-P is the D'Amore-Panichi (1980) geothermometer. C_1/C_2 geothermometer of Darling and Talbot (1992).

average temperatures of 252°C for Central Island and 246°C for North Island are lower than those estimated for the main volcanic centres of Paka, Silali, Emuruangogolak and Kakorinya, despite the fact that the islands have far more vigorous surface activity than these centres. Some of the other geothermometers (H_2S, H_2, CO_2/H_2) give higher temperature estimates for the geothermal systems of the islands. It is possible that because of the high water tables, the island systems give less scope for alteration of gas concentrations and therefore the conventional geothermometers give more reliable results, whereas the C_1/C_{2+} geothermometer is possibly affected by a greater availability of organic material in lake sediments producing more C_{2+} gases, which causes a lowering of the indicated temperature. Nevertheless, it seems likely that the Central Island system has temperatures of 250–300°C, and that of North Island a little lower at ~250°C.

15.8 SUMMARY OF FLUID GEOCHEMISTRY

The interpretation of ambient and thermal fluid compositions must be made with reference to the regional groundwater flow patterns deduced from physical hydrogeological information in Section 14.5. Fortunately the main sources of groundwater within the inner trough, namely meteoric water from the rift margins and subsurface outflow from Lake Baringo, have distinctive isotopic signatures which are invaluable in modelling the origin of the geothermal fluids of the region.

Lake Baringo is a shallow lake fed by rivers flowing off the rift margins. High evaporation rates combined with the shallowness of the lake result in the lakewaters having relatively high TDS and strongly enriched isotopic compositions, which fluctuate seasonally.

Lake Turkana is by far the largest body of surface water in the area and is mainly fed by the Omo River which rises in Ethiopia. Although it is a closed basin lake, it has not yet become markedly saline because insufficient time has elapsed since its closure. Minor leakage from Lake Turkana southwards beneath the Barrier Volcanic Complex appears likely and contributes to Lake Logipi. Logipi itself appears to be largely the result of northward drainage from the Suguta Valley.

The compositions of ambient and near-ambient springs along the margins of the rift are consistent

with a relatively local and unmodified meteoric origin, with the exception of Napeiton on the western margin which shows indications of deeper circulation. The springs at Eliye Springs on the western shores of Lake Turkana have stable isotope compositions consistent with derivation from well to the west of the lake.

Wells in the rift floor are relatively shallow and are confined to the southern part of the area. Although there are indications that subsurface outflow takes place to the north from Lake Baringo, there is no evidence from stable isotopes that any of the wells within the floor of the inner trough penetrate the lakewater plume or mixing zone. Chemical and isotopic compositions indicate that wells to the east of the volcanic centres are recharged by meteoric waters falling locally on the floor of the trough and lower slopes of the rift margin escarpment. Well waters to the west of the volcanic centres have more variable composition. Those close to the base of the rift margin escarpment have isotopic compositions consistent with recharge at higher altitude on the rift margin, whereas wells further away from the escarpment at Nginyang and Chesirimion, show evidence of a greater contribution from rainfall on the rift floor. The two boreholes at Nginyang contain mixtures of river water with the type of high-HCO_3^- more usually found in warm springs.

Hot springs and cooler springs with similar chemical characteristics occur on the rift floor to the west and north of Silali and Emuruangogolak. The isotopic compositions of these may be explained in terms of mixing between meteoric waters and subsurface outflow from Lake Baringo, but their chemistry is primarily the result of varying amounts of evaporite dissolution and, or, CO_2 metasomatism, giving rise to high Na^+, HCO_3^- and to a lesser extent high SO_4^{2-} and Cl^-. Further to the north, hot springs along the margins of the inner trough at Namarunu and Elboitong and along the base of the southern flanks of the Barrier at Logipi, have even higher TDS and proportionally higher Cl^-, which is probably a reflection of evolution in an evaporite sequence towards the increasingly desiccated northern end of the Suguta Valley. There is no overt evidence of high temperature activity in any of these hot springs and it is therefore concluded that they do not represent outflow from high-temperature geothermal systems associated with the volcanic centres. The main heating agent is probably deep circulation, although Lorusio, with its 'magmatic' gas contents may indicate a locally higher heat flow. Only the hot springs of Ol Kokwe Island and Central Island show chemical evidence of a truly high temperature origin, and stable isotope compositions indicate that the circulating fluids at both localities are mainly derived from lakewater.

The alkali cation and silica geothermometers give results for the springs of the area which should be interpreted with caution, because of the effects of evaporite dissolution and high pH on water chemistry. Silica geothermometry indicates that the hot springs of Ol Kokwe Island and Central Island are the only springs of the region that represent outflow from high temperature geothermal systems (c.170°C), and also suggests that the cold springs at Kalnangi and South Nangarabat may be cooled low enthalpy thermal waters.

The chemical composition of steam condensates points to fumarole strength generally increasing in the order Korosi, Chepchuk, Silali, Kakorinya, Emuruangogolak and Paka, with Korosi and Chepchuk being very much the weakest systems. The stable isotope composition of fumarole steam accords with this, indicating that subsurface condensation takes place to varying degrees at all centres but is particularly prevalent at Korosi and Chepchuk.

Fumaroles with the least evidence of subsurface condensation have the most enriched isotopic compositions, and may be modelled in terms of derivation from a lakewater-meteoric water mixing series. This suggests that fumaroles on Paka, Silali and Emuruangogolak contain up to 45%, 25% and 10% lakewater respectively, which is consistent with a progressive northward dilution of groundwater outflow from Lake Baringo. Any isotopic evidence of lakewater being involved in the geothermal system of Korosi is obscured by subsurface condensation, which is a further reflection of the weakness of that system. The stable isotope composition of fumarolic steam at Kakorinya may be modelled in terms of derivation from a mixture of Turkana lakewater and meteoric water from the rift flanks, containing up to 40% lakewater. The isotopic composition of fumaroles on North Island indicates a reservoir source with a sizeable shift in $\delta^{18}O$, but direct evidence of such a water is lacking because no springs exist on the island. Springs are present on Central Island, but mainly consist of lakewater without any evidence of ^{18}O shifting. The isotopic compositions of nearby fumaroles on the island can be simply related to the spring composition by assuming boil-off at a typical geothermal reservoir temperature and cooling to the local surface boiling point.

Fumarole gases show no particular distribution pattern, although H_2, usually considered to be a good geothermal indicator, is least abundant at Korosi and Emuruangogolak. In terms of the ratio of gases to water vapour, Paka and Silali fumaroles show the least signs of subsurface steam condensation, and high $^3He/^4He$ values also suggest these are the most favourable sites. The fumaroles of Central and North islands are more vigorous than those on the other volcanic centres of the region and have much higher concentrations of geothermal gases. The presence of detectable H_2 and the widespread deposition of sulphur fit the obvious conclusion that the boiling zones are significantly closer to the surface beneath these island centres.

The application of gas geothermometry is hindered by the general weakness of the fumaroles of the region. Firstly, gases like H_2 and H_2S are only present in low concentrations, and secondly subsurface steam condensation alters the relative proportions of gas to water. This affects all the conventional gas geothermometers, although some do differentiate between the volcanic centres in relative terms. The new methane/ethane geothermometer, developed specifically for use within the East African Rift, appears to surmount certain of the difficulties of the conventional geothermometers and provides plausible results. This indicates that Paka, Silali and Emuruangogolak are all associated with high temperature geothermal systems (256–343°C). The Kakorinya system appears to have slightly lower temperatures (averaging 263°C) although has maximum values exceeding 300°C. Temperature estimates for Chepchuk are lower still (202–262°), and those for Korosi are by far the lowest, averaging only 200°C.

16 Summary and conclusions

16.1 INTRODUCTION

In this section the salient geological and hydrogeological features described in previous chapters are summarised and the underlying controls on the volcanism and geothermal activity of the region are examined. In conclusion to this summary the geothermal prospects of the region are ranked according to their considered potential, and recommendations are made regarding future exploration strategy.

16.2 STRUCTURAL EVOLUTION OF THE REGION AND TECTONIC CONTROLS ON THE LOCATION OF VOLCANIC CENTRES

Summaries of the regional structure and stratigraphy are shown in simplified form in Figure 16.1 and provide information on the interaction of tectonism and volcanism within the region.

Although a depression is inferred to have existed along the axis of the northern sector of the rift during the Pliocene, formation of the present inner trough did not take place until the Quaternary. In the north, faulting, inward tilting and landslipping of the rift margins to form the Suguta trough occurred during the uppermost Pliocene–early Pleistocene. This is constrained by radiometric dates from the rift margins of 2.3 ± 0.2 Ma and 1.86 ± 0.04 Ma for the youngest lavas of the Tirr Tirr and Loriu plateaux respectively, and of 1.37 ± 0.02 Ma for the oldest dated lavas at the Barrier Volcanic Complex (BVC) within the inner trough. In the south, faulting and formation of the inner trough took place at approximately the same time, as indicated by deposition of the Chemoigut sediments (1.9–1.3 Ma) and the construction of Chepchuk volcano (1.22 ± 0.06 Ma) within the Baringo basin.

In the south, the temporal and spatial association between volcanism and faulting during the period 1.2 to 0.5 Ma suggests that a syn-extensional volcanic belt had developed along the inner trough. This phase of faulting and intrusion may have been triggered by changes in orientation of the regional stress field (Section 2.5). Flood basalts were erupted within the inner trough during the period 1.2–0.8 Ma (Kasurein and Kwaibus basalts) and flood phonolites and trachyphonolites were erupted from centres to the south. Renewed faulting and subsidence of the Baringo basin was contemporaneous with major subsidence in the Bogoria region further south, and was associated with deposition of sediments of the Kapthurin and Chesowanja formations dated at about 0.75–0.65 Ma. Around 0.5 Ma the Loyamarok trachyphonolites were erupted on the floor of the trough, and the small phonolite-trachyphonolite volcanoes of Paratello, Karau and Erinei were active along its eastern margin. This activity was soon followed by a major phase of subsidence along the rift boundary faults, during which the western flanks of Paratello, Karau, Erinei and Chepchuk volcanoes were downfaulted into the inner trough, where they were buried by younger infill.

Flood eruptions of the Baringo and Mistoni basalts took place within the Baringo basin at about 0.5 Ma, and were followed closely by trachytic activity and the construction of the axial volcanoes of Ol Kokwe, Korosi, Paka and Silali. Initial activity at these volcanoes was broadly synchronous, with the construction of early trachyte shields taking place in the period 390–220 ka. Post-shield activity at these southern centres has been broadly contemporaneous and has continued to within the last few thousand years. The post-shield activity at Ol Kokwe, Korosi and Paka appears to have been largely synchronous, with all three centres having experienced a major phase of faulting and basaltic activity around 121 ± 37 ka, followed by voluminous trachytic activity within the past 100 ka on Korosi and Paka. Whilst Silali continued to be active during this same broad period, the timing of individual volcanic events was not synchronous with the activity of the centres to the south. In particular, the main phases of faulting and basaltic volcanism (of the Flank Fissure Basalts and Katenmening lavas) were younger than on Korosi and Paka.

Further north in the Suguta trough, large trachyte shield volcanoes were active at Emuruangogolak and the BVC during the period from at least 1.3 Ma to 0.5 Ma, and there were several phases of renewed trachytic and rhyolitic activity on the old Pliocene centre of Namarunu. At the BVC the locus of volcanism migrated from the margins of the rift towards the axis over time. Evidence for an early phase of basaltic flood lavas in the Suguta basin is provided by the Logipi and Latarr basalts (Section 11.4.2) and possibly the Suguta Basalts (Truckle, 1979a).

Over the last half million years, trachyte-basalt volcanism within the inner trough in the north continued to be focused on the three main volcanic centres of Emuruangogolak, Namarunu and the BVC. The construction of Kakorinya (200–0 ka) at the BVC effectively closed off the Suguta trough from the Turkana basin at around 100 ka. Unlike the southern centres, these northern centres evolved independently of one another, and major phases of basaltic activity have taken place during the Holocene with eruptions continuing through to historic times.

The change in both the timing and nature of tectonic and volcanic events between the Suguta trough in the north and the Baringo basin in the south, occurs in the vicinity of Emuruangogolak. This segmentation is also reflected by regional variations in basalt composition along the axis of the inner trough (Section 13.3). Any model seeking to explain the control of structure on the location of the central volcanoes along the axis of the inner trough should take the contrasts between the two rift segments into consideration.

The axial volcanoes of the inner trough are intersected or linked by linear or curvilinear fault zones which have been associated with basaltic fissure activ-

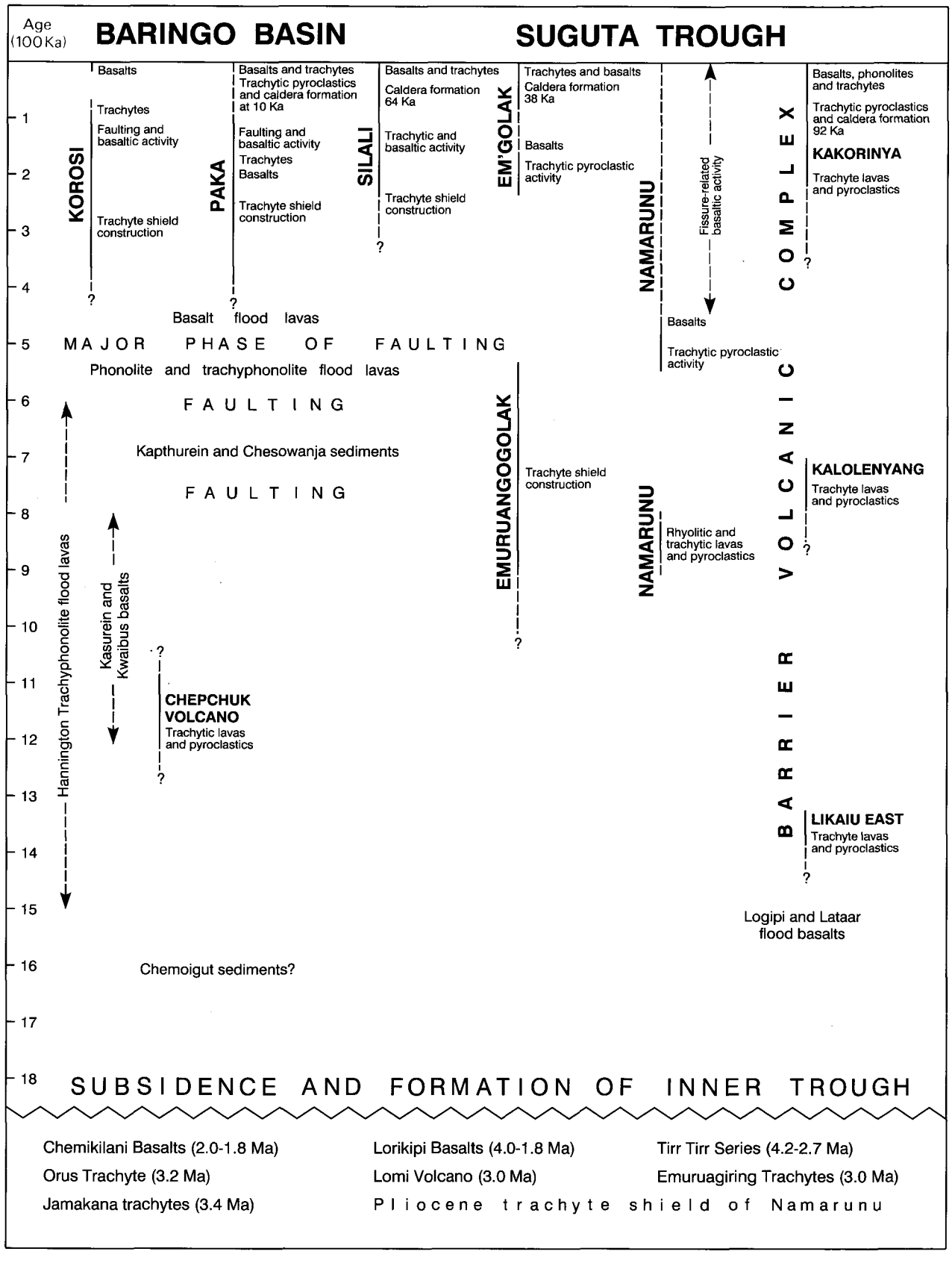

Figure 16.1 Summary of tectonic and volcanic events in the northern sector of the Rift.

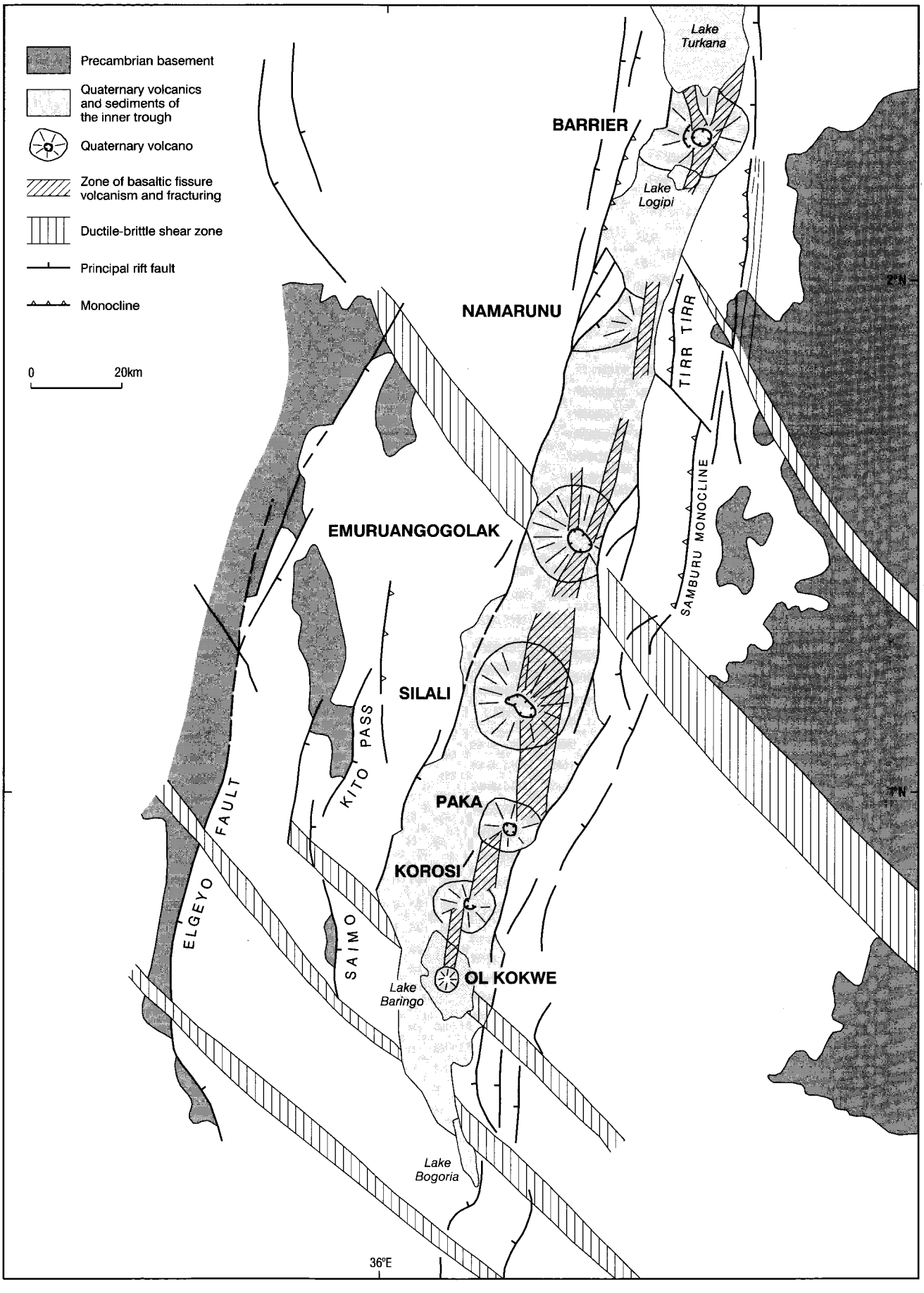

Figure 16.2 Simplified structural map of the region, showing major rift structures and the locations of volcanoes, in relation to basement shear zones.

ity. The location and arrangement of the centres in relation to these fracture zones varies between the southern and northern groups of volcanoes. In the south, the three broadly contemporaneous and almost contiguous centres of Korosi, Paka and Silali are linked by a right-stepping *en échelon* zone of N-trending fractures which has been the locus of basaltic activity and is broadly coincident with a positive Bouguer anomaly. Including the minor centre of Ol Kokwe, these volcanoes have an inter-centre spacing ranging between 17 and 25 km (average 20.5 km) and are offset laterally by 4 to 6 km. The northern centres of Emuruangogolak, Namarunu and the BVC are not linked to one another and have much larger spacings of between 40 and 50 km.

Previous attempts to explain the location of the Quaternary volcanoes of the rift propose that a gravitationally unstable layer in the asthenosphere may result in a series of relatively evenly spaced diapirs which rise to the base of the crust and feed volcanoes at the surface (Mohr and Wood, 1976; Karson and Curtis, 1989; Ten Brink, 1991). This simple model assumes a constant lithospheric thickness giving rise to a regular volcano spacing. However, there are problems in applying such a model to the rift. Firstly, the volcanoes of the rift are not regularly spaced. Secondly, studies of the basement geology indicate that there are likely to be complex variations in the nature and thickness of the lithosphere along the length of the rift (Mosley, 1993; Smith and Mosley, 1993). Thirdly, because the volcano spacing is greater in the north, the application of such a model would imply thicker lithosphere in this region, whereas considerations of the basement geology (Smith and Mosley, 1993) and geophysical data (KRISP, 1991) indicate that the converse is true.

An alternative explanation is that the reactivation of deep seated fractures or heterogeneities within the underlying Precambrian basement has influenced the ascent and emplacement of magma within the crust. The contrast in tectonic style and evolution of the two rift segments at the latitude of Emuruangogolak suggests the presence of a crustal discontinuity. Supporting evidence for such a discontinuity is provided by NW-trending lineaments and fault arcuations cutting the Miocene strata of the rift margins and an important NW-trending shear zone within the Precambrian basement outside the rift adjacent to Emuruangogolak. Such a basement structure may also explain why earlier Pliocene trachytic volcanism of the Emuruagiring Plateau was focused at the latitude of Emuruangogolak. Other important NW-trending lineaments or structural discontinuities cross the Baringo and Bogoria sectors of the rift and correlate with shear zones in the adjacent Precambrian basement.

In the south of the area between Lake Baringo and Emuruangogolak, the development of an *en échelon* array of volcanic centres linked by fracture zones oblique to the rift margins indicates that this segment developed within an oblique-shear regime. This is consistent with deformation between the two major basement shear zones positioned beneath Emuruangogolak in the north and Lake Baringo in the south, with a regional stress field (Pmin) orientated NW–SE. Under such a stress field strike-slip reactivation of basement shears is predicted with the development of pull-apart basins in the cover (Smith and Mosley, 1993). The zones of faulting and basaltic fissure activity are assumed to indicate the injection of dyke swarms into the crust. The manner in which these zones are offset between the volcanic centres may indicate separate dyke swarms, and the mechanism by which these overlap and interfere may have influenced the location of the volcanoes (cf Ryan, 1990). In such a model the central volcanoes are located in areas of enhanced tensile stress linking two *en échelon* zones of crustal spreading.

The underlying structural controls on the location of the two northern volcanic centres of Namarunu and the BVC are less clear. Both centres are characterised by right-stepping *en échelon* fracture systems which are oblique to the rift margins, indicative of an oblique rifting regime similar to that influencing the southern centres. The prolonged focusing of volcanism during the Pliocene and Quaternary at the latitudes of these centres may indicate a similar basement control to that of Emuruangogolak. However, whilst NW-trending shears are present within the basement to the east of Namarunu and the BVC, they converge into parallelism with the rift margin structures and do not appear to cut across the rift.

16.3 EVOLUTION OF THE VOLCANIC CENTRES

Each centre has been the site of large-scale volcanism during the last few hundred thousand years, with the three northern centres of Emuruangogolak, Namarunu and the BVC beginning their development much earlier than the three southern centres of Korosi, Paka and Silali.

Regardless of age all the centres show an early phase of trachyte shield construction. Where these shields are well-exposed, as at Korosi and Emuruangogolak, they are seen to be composed largely of trachyte lavas and show no evidence of basaltic activity.

During post-shield evolution each centre has experienced its own unique history of faulting and trachyte-basalt volcanism. Only at the contiguous centres of Korosi and Paka does there appear to have been anything like a common history, although even here there are important differences between the two centres.

The post-shield activity at each centre has been strongly influenced by N to NNE-trending faults. These have controlled the location of parasitic eruptive centres, and superimposed small-scale graben and horst topographies upon the gross morphology of the shields. The imposition of fault scarps upon the early shields has exerted topographic controls on the movement and accumulation of later lavas and pyroclastic flows. Basaltic activity has been closely associated with episodes of faulting and has been characterised by flank fissure eruptions of very fluid mildly alkaline lavas and scoria-spatter cones. Fault and fissure patterns are typical of those seen on large basaltic shield volcanoes (cf. Opheim and Gudmudsson, 1989) and are interpreted as the surface expression of dyke intrusion. Trachytic activity has been characterised by the eruption of peralkaline lavas and pumiceous pyroclastic deposits from parasitic cones and fissures on the upper flanks and summit areas. The main pyroclastic deposits are asymmetrically distributed on the western flanks of the volcanoes as a result of the prevailing wind direction from the east. At the three northern centres much of the youngest volcanism took place

within and around the shores of the former Lake Suguta, resulting in widespread subaqueous and phreatomagmatic activity.

Calderas formed on Paka, Silali, Emuruangogolak and the BVC at late stages in their evolution. These calderas are of different ages and their formations were triggered by various mechanisms. The caldera of Silali was formed by summit collapse induced by the lateral drainage of magma during flank eruption of the Katenmening basalts around 64 ka. The caldera of Emuruangogolak was formed as a result of the drainage of trachyte magma during initial flank eruptions of the Upper Trachyte Lavas at about 38 ka. Paka and Kakorinya calderas formed in response to major trachytic pyroclastic eruptions at around 10 ka and 92 ka respectively. Despite the variable triggering mechanisms of collapse, the calderas display a preferred NW–SE elongation, which is taken to imply a regional stress control on the shape and emplacement of the underlying magma bodies.

Resurgent trachyte lavas have been erupted within all of the calderas, and phonolite domes occur within the caldera of Kakorinya. Basaltic lavas have only been erupted within the calderas or upon the upper flanks of the volcanoes at a late stage, presumably when liquid trachyte caps to the magma chambers had either been removed or had solidified sufficiently so that basaltic conduits were able to propagate to the surface.

16.4 THE NATURE OF MAGMATIC HEAT SOURCES

In this section the nature of the magmatic plumbing within the volcanic centres is considered, and conclusions are drawn regarding the heat sources that drive the geothermal systems.

In Section 13.8 it was concluded that the trachytes were derived by fractional crystallization of basaltic magmas. Phase equilibrium studies suggest that fractionation probably occurred under low pressures, or that the trachyte magmas equilibrated at low pressures. Either case implies the presence of shallow trachytic (syenitic) magma chambers. Corroborative evidence for shallow intrusive bodies is provided by the unroofed syenite intrusion on Namarunu, and by the presence of abundant syenitic nodules within the pyroclastic deposits at several of the volcanic centres. The decrease in the intensity of faults and refraction of their orientations over the summit areas on several of the volcanoes may also indicate the existence of molten zones at high levels at the time of faulting.

In the absence of geophysical evidence, the form and configuration of the magmatic plumbing systems within the volcanic centres remains speculative. However, petrological and geochemical evidence combined with information from eroded intrusion complexes in ancient rift systems favour a model in which compositionally zoned magma chambers exist at relatively high structural levels, either within the volcanic edifices and, or, in the uppermost subvolcanic levels. Such chambers are inferred to have fractionated trachytic caps which pass down into basaltic lower levels, in turn fed by basaltic melts from a deeper source. Evidence for zoned chambers of this kind may be provided by the pumice lapilli tuffs and breccias of Namarunu (Section 10.4.6) which show a gradual change from trachytic to basaltic composition from the base to the top.

Individual trachytic intrusive complexes have been long-lived. In the case of Emuruangogolak, for example, radiometric dating indicates that the voluminous Upper Trachyte Lavas have been erupted over the past 38 ka, and chemical and isotopic data suggest that the intrusive system responsible for these lavas has been periodically replenished during this period (Section 13.8). Similarly, on Silali at least four main phases of trachytic activity have occurred over the last 130 ka, and trace element compositional differences between each of these phases indicate the injection of fresh batches of magma from depth. In the case of Kakorinya (BVC), isotopic data indicate that the young resurgent phonolites in the caldera must have fractionated in a separate magma chamber from the trachytes and were unlikely to have resided for any length of time at a high-level.

Basaltic rocks are volumetrically much less important than trachytes at the surface on all of the volcanic centres, although acceptance of a fractional crystallization origin for the trachytes implies that large volumes of basic and ultrabasic cumulate material must exist at depth (cf. Karson and Curtis, 1989). A significant proportion of this basic-ultrabasic material may occur in the lower parts or roots of the postulated high-level zoned intrusions or magma chambers.

Basaltic dykes are sporadically exposed within the volcanic centres and the floor of the inner trough, but are not common. However, the fracture patterns associated with the basaltic lava fields of the region, and their coincidence with positive Bouguer gravity anomalies suggest, by analogy with similar features on basaltic shield volcanoes elsewhere (Iceland and Hawaii), that dyke swarms exist at depth. In the case of the Kenya Rift, it is open to speculation as to how strongly developed such basaltic dyke swarms are likely to be, but if extension rates are low (Section 2.2) the volume of dyke material is likely to be correspondingly small, and is therefore unlikely to constitute a major source of heat.

The amount of heat that dyke swarms provide to the present day geothermal systems will also be dependent upon their age. At Korosi and Paka the main phase of fissuring and basaltic activity took place around 120 ka, and on Silali fissuring and eruption of the voluminous Flank Fissure Basalts and Katenmening Basalts was completed before 64 ka. Surface geothermal activity is virtually absent from the basalt fields of these centres, which is taken as an indication that the underlying dyke swarms no longer act as significant heat sources. On Kakorinya and Emuruangogolak, surface geothermal activity is virtually absent even from the young basalt fields that have erupted in historic times.

The most compelling evidence for basaltic fissure activity not providing long-lived heat sources is given by Namarunu. Here extensive basaltic activity has taken place over the past half million years, during which time there has been no trachytic activity. No surface geothermal activity is found on Namarunu itself, and only restricted occurrences of very feeble steam seepages are associated with the youngest zone of fissure-related activity in the vicinity of the Gap to the east. Although hot springs are spatially associated with

this youngest zone of basaltic activity they are not particularly hot and show no chemical signs of having been involved in a high-temperature geothermal system (Section 15.4.2).

In summary, it is concluded that the main heat sources for the geothermal systems of the region are trachyte or zoned trachyte-basalt central intrusions or intrusion complexes which extend to high structural levels within the volcanic centres. Depending on their age, these igneous bodies may be solid, partially solidified or liquid. Radiometric dating combined with information on the chemical and isotopic composition of the lavas indicates that these central intrusive bodies are long-lived features, having life-spans of tens of thousands of years or more, that have been reinjected from time to time by fresh pulses of magma from depth. The basaltic dykes of the region have not provided significant long-lived heat sources for the geothermal systems. At best they only act as auxiliary heat sources, which may currently contribute to the heating of low enthalpy spring waters.

16.5 HYDROGEOLOGICAL CONSIDERATIONS

Assuming that adequate heat sources exist at shallow levels within the volcanic centres, it is essential that sufficient groundwater is available to recharge the geothermal systems should they be exploited. This is particularly important bearing in mind the semi-arid to arid climate of the region.

In Section 14.5 it was concluded that the groundwater flow pattern within the region is a combination of northerly axial flows along the floor of the inner trough as far north as Lake Logipi and lateral flows from the rift margins. Minor axial flow is also directed southwards from Lake Turkana towards Lake Logipi. The interaction between lateral and axial flows is probably modified by faults and dykes, which cause lateral flows to follow longer, deeper paths and align with flow paths along the axis of the rift.

Recharge of groundwater occurs from several sources. Lateral groundwater flows are recharged from the higher and wetter rift margins. Lake Baringo recharges groundwaters in the floor of the rift, and Lake Turkana also contributes towards the recharge beneath the BVC. The analysis of meteorological data also indicates that direct infiltration of rainfall on the rift floor is likely to provide local recharge, especially on the higher ground of the volcanic centres themselves (Section 14.2).

It was concluded in Section 14 that geothermal exploitation on a scale similar to the existing geothermal power station at Olkaria would not greatly affect regional water resources. Despite the semi-arid to arid climate of the inner trough floor it was considered that direct infiltration of meteoric water, northward subsurface flow from Lake Baringo, and groundwater flows from the rift margins are likely to be individually sufficient to sustain such production.

Borehole data for the region are limited and restricted to shallow depths but suggest that the main aquifer types are fractured volcanics, sediments and weathered contacts between lithological units. Although such aquifers may be discrete on a local scale, on a regional scale hydraulic connections between aquifers are most probable. It is likely that geothermal reservoirs at depth are formed of these types of aquifers.

The hydraulic properties of aquifers estimated from borehole data suggest low permeability, although regional estimates of permeability derived from considering the subsurface flow from Lake Baringo suggest significantly higher values. One explanation for the different estimates is that older rocks buried at depth within the rift floor have been subjected to more prolonged histories of repeated faulting in response to rift tectonism, and are therefore more fractured than the younger lithologies penetrated by shallow boreholes drilled for water. Furthermore, no boreholes have been drilled within the volcanic centres themselves and few have been drilled along the axis of the inner trough. These areas are much more strongly fractured than the adjacent areas that have been drilled for water, and therefore may posses higher permeabilities than those suggested by shallow borehole data.

16.6 GEOTHERMAL ACTIVITY

Surface geothermal activity in the region occurs in two distinct settings. The most common manifestations are found on the Quaternary volcanic centres and consist of hot, hydrothermally altered ground with fumaroles. Of lesser importance are hot springs on the floor of the inner trough.

Fumarolic activity associated with hot, hydrothermally altered and steaming ground occurs on the upper flanks and summit areas of the volcanic centres. The location of this activity is strongly controlled by N- to NNE-trending faults and by caldera structures. Where calderas are developed these appear to overlie the upflow zones of the geothermal systems, and in the case of Emuruangogolak surface activity is exclusively confined to the caldera.

Surface geothermal activity on the volcanic centres is relatively weak by comparison with many other geothermal regions, but this does not necessarily indicate that the geothermal systems are of low potential; on the contrary, several lines of evidence suggest that relatively hot systems exist at depth. The general weakness of surface fumarolic activity is considered to be a function of deep water tables and the long paths that steam has to traverse to reach the surface from the zones of boiling, which in turn results from the semi-arid climate of the region. This point is well exemplified by the contrasting situation of North and Central Islands, which by virtue of their location in Lake Turkana have high water tables and are characterised by intense and vigorous surface geothermal activity including solfataras.

Silica sinters and silica veins related to former hot springs occur on the summit areas and upper flanks of several of the volcanic centres. U-series ages of the sinters correlate well with wetter climatic periods when lake levels within the rift were high (Sturchio et al., 1993). It is concluded that at various stages in the past elevated water tables and the increased availability of meteoric water associated with wetter climates, promoted greater transfer of heat and mass to the surface from the deep, long-lived heat sources within the volcanic centres. Variations in the intensity and vigour of geothermal activity within the region is therefore

not simply a function of the availability of heat, but is modulated by climatic and hydrogeological conditions.

The chemical and stable isotope compositions of fumarolic steam points to the vigour of the geothermal systems generally increasing in the order Korosi, Chepchuk, Silali, Kakorinya, Emuruangogolak and Paka, with Korosi and Chepchuk being very much the weakest systems. This accords moderately well with field observations on the intensity and vigour of the surface geothermal activity.

The stable isotope compositions of fumarolic steam may be modelled in terms of derivation from a lakewater - meteoric water mixing series. This suggests that the fumarolic steam on Paka, Silali and Emuruangogolak are derived from geothermal systems containing up to 45%, 25% and 10% lakewater respectively, which is consistent with the progressive northward dilution of subsurface outflow from Lake Baringo. Isotopic evidence for the involvement of Lake Baringo water in the geothermal system of Korosi is obscured by the effects of subsurface condensation, which is a further reflection of the weakness of that system. The stable isotope composition of steam at Kakorinya may be modelled in terms of derivation from a mixture of Lake Turkana water and meteoric water from the rift flanks, containing up to 40% lakewater.

The application of conventional gas geothermometry to the geothermal systems of the rift is considered to be generally inappropriate and unreliable. However, the methane/ethane geothermometer developed by Darling and Talbot (1992) for use within the East African Rift system does provide reliable and plausible temperature estimates (Section 15.7.2). Application of this geothermometer to the fumaroles of the region indicates that Paka, Silali and Emuruangogolak all have high temperature geothermal systems with temperatures around 300°C or higher (Table 15.8). The Kakorinya system appears to have slightly lower temperatures, averaging 263°C, although has maximum values exceeding 300°C. Temperature estimates for Chepchuk are lower still (202–262°C), and those for Korosi are the lowest, averaging only 200°C.

Almost all of the hot springs on the floor of the inner trough have temperatures well below the local boiling point, except for those at Elboitong which have temperatures reaching slightly over 100°C and include the hottest surface manifestations in Kenya. The isotopic compositions of the hot springs in the floor of the trough may be explained in terms of mixing between meteoric water and subsurface outflow from Lake Baringo, but their chemistry is primarily the result of evaporite dissolution and, or, CO_2-rock interaction, giving rise to high Na^+, HCO_3^-, SO_4^{2-} and Cl^-. There is no overt evidence for high temperature activity in any of these springs and it is concluded that they do not represent outflows from the high-temperature systems of the volcanic centres (Section 15.4). Heating of these waters probably results from deep circulation along rift boundary faults.

Only the hot springs of Ol Kokwe Island in Lake Baringo and Central Island in Lake Turkana show chemical evidence of truly high temperature origin, but these occur in a different structural setting to 'normal' hot springs of the rift floor. They occur upon small volcanic centres with high water tables, and geothermometry indicates reservoir temperatures of about 170°C.

16.7 RANKING OF THE GEOTHERMAL PROSPECTS

In this section the geothermal prospects of the region are ranked according to their considered potential. It must be stressed that this ranking is based entirely on geological, hydrogeological and fluid geochemical criteria and takes no consideration whatsoever of socio-economic factors.

A number of different criteria are used to rank the prospects. Taken individually these result in slightly different rankings. Equating these to obtain an overall ranking inevitably involves a degree of subjectivity.

In simple terms, a good geothermal prospect should have an adequate heat source and sufficient groundwater to recharge the system and act as a medium for transporting the heat. In Section 14.8 it was concluded that groundwater recharge within the region is sufficient to sustain geothermal exploitation, and therefore the ranking process described below is based largely on considerations of the nature of the heat sources.

In assessing the relative potential of the prospects it is assumed that by far the most important heat sources are trachyte or compositionally zoned trachyte-basalt cupolas, which exist at high structural levels within the volcanic centres or subvolcanic environment. Basaltic dykes are not considered to be good long-term heat sources, and at best the youngest dykes only provide auxiliary heat. Volcanic centres that have experienced prolonged trachytic activity with relatively young eruptions are therefore considered to be the best prospects.

As stated in the previous section, the intensity of surface geothermal activity is strongly dependent upon hydrogeological factors such as depth to water table and permeability, and therefore may not necessarily be a reliable indicator of the potential of a geothermal system at depth. Furthermore, in the extreme case, sealing of a good geothermal system by hydrothermal alteration may also result in reduced surface activity.

With the reservation that such complicating factors operate, Paka would appear to be by far the best prospect in the region in terms of areal extent, intensity and temperature of surface manifestations. Silali and Kakorinya are the next best prospects, having similar surface activity of almost the same areal extent; considerable activity on Silali may however be masked by the mantle of pumice in the caldera. Ranking Emuruangogolak on this criterion is problematical, because although surface manifestations are confined to a comparatively small area within the caldera, the fumarolic activity at this centre is relatively strong and visually the most impressive in the Kenya Rift. Although surface activity on Korosi is widespread it is relatively weak and temperatures are low, and it is therefore ranked fifth on this criterion. Chepchuk has similar style surface activity to Korosi, but this is of limited extent and the prospect is therefore ranked sixth. Activity on Namarunu is extremely weak and of very limited extent. Namarunu is therefore ranked last and is considered to be a very poor prospect indeed.

Considerations of the vigorousness of the geothermal systems based on chemical and stable isotope compositions of steam condensates suggest a similar ranking to that above (Section 15.5). On this criterion the order of decreasing vigour would appear to be Paka, Emuruangogolak, Kakorinya, Silali, Chepchuk and

Table 16.1 Summary of geothermal activity in the region

Locality	Relative strength and style of activity	Area of activity (km^2)	Max surface Temp (°C)	Geothermometry (°C) range	Geothermometry (°C) average	Age of last trachytic activity
North Is.	Vigorous fumaroles, solfataras and hot ground	0.5	96.3	241–244	243	–
Central Is.	Vigorous fumaroles, solfataras and hot springs	0.5	97.4	251–253	252	–
Kakorinya	Fumaroles of moderate strength and hot steaming ground	20	98.6	189–314	263	58 ± 4 ka
Em'gogolak	Moderately strong fumaroles and hot steaming ground	8	96.0	310–343	327	c.100 yr
Silali	Moderately strong fumaroles and hot steaming ground	20	96.8	261–335	304	4 ± 2 ka
Paka	Moderately strong fumaroles and hot steaming ground	32	97.8	256–329	303	11 ± 3 ka
Chepchuk	Weak fumaroles and hot, altered ground	2.5	96.1	202–261	231	1.13 Ma
Korosi	Weak fumaroles and hot, altered ground	33	95.7	197–203	200	104 ± 2 ka
Ol Kokwe Is.	Moderately strong fumaroles hot springs and solfataras.	<0.5	97.2	–	170	?300 ka

Geothermometry values are for the methane/ethane gas geothermometer of Darling and Talbot (1992), except for the value for Ol Kokwe Island which is for the chalcedony silica geothermometer.

Korosi, with the last two centres being of roughly equal standing.

In terms of likely reservoir temperatures, as estimated by the methane/ethane gas geothermometer, Emuruangogolak would appear to be the best prospect, followed closely by Silali and Paka (Table 16.1). All three have estimated temperatures in excess of 300°C, although it should be emphasised that in the case of Emuruangogolak only two temperature estimates were obtained, and the average value is therefore unlikely to be representative. Kakorinya is clearly fourth in this ranking, with an average estimated temperature of 263°C, although the maximum estimated value is in excess of 300°C. Chepchuk and Korosi are associated with the coolest systems although only two temperature estimates are available for each (Table 15.8). Taken at face value these suggest that Chepchuk has a hotter geothermal system than Korosi, with average temperature estimates of 232°C and 200°C respectively.

Ranking the prospects on the age and estimated size of their magmatic heat sources is somewhat subjective. With regard to size, it is assumed that caldera dimensions are likely to reflect the size of underlying trachytic intrusive bodies. On this criterion Silali is likely to have by far the largest heat source, followed by Emuruangogolak and Kakorinya on roughly equal terms, and finally by Paka which only has a small caldera. The lack of a caldera at Korosi may indicate that a sufficiently large central magma chamber did not develop at that centre, and the nature of the heat source at Chepchuk is unknown but is unlikely to be associated with a young trachyte system.

All of the volcanic centres have experienced prolonged phases of trachytic activity, and at several the youngest eruptions have occurred within the last few thousand years. As a result, a number of prospects are likely to have accumulated good magmatic heat sources which have had insufficient time to cool and which may continue to be recharged.

Emuruangogolak has experienced the most juvenile trachytic activity in the entire rift. It has been the site of repeated eruptions of large volumes of trachyte over the last 38 ka, with the youngest activity having taken place within the last hundred years. Replenishment of the magmatic system appears to have taken place during this prolonged period of activity, bringing additional heat to a high structural level. This phase of activity is related to the formation of the caldera.

Silali has also experienced repeated phases of voluminous trachytic activity over the past 130 ka, culminating in the collapse of the caldera at about 64 ka. The youngest trachytic activity has occurred on the eastern side of the caldera floor around 7±3 ka, and in the Black Hills to the east of the caldera over the period 10±2 ka–4±2 ka. Present day surface geothermal activity is confined to the eastern half of the caldera and to the Black Hills, suggesting that this latest phase of magmatism is providing the main heat source for the current geothermal system of Silali.

Paka has been the site of large-scale trachytic pyroclastic activity which triggered the formation of the caldera around 10 ka. This was followed by a final eruption of trachyte lava within the caldera shortly afterwards.

On Kakorinya major trachytic pyroclastic activity took place around 92 ka, resulting in the formation of the caldera, and this was followed by eruption of the youngest trachyte lavas in the caldera at about 58 ka. Young phonolite lavas have subsequently been erupted in the caldera and on the northern flanks. Isotopic evidence indicates that the phonolites are not crustally contaminated, suggesting that they were not stored for any length of time within high-level magma chambers. Whilst this phonolitic activity will undoubtedly have contributed heat to the geothermal system it is unlikely to have provided a major, long-lived heat source in the absence of high-level storage chambers.

On Korosi the last phase of trachyte activity took place around 100 ka, and has only been post-dated by minor basaltic activity. Korosi is therefore unlikely to have a juvenile magmatic heat source. Similar arguments apply to Chepchuk which is an early Pleistocene trachyte centre that has experienced basaltic activity within approximately the last 100 ka.

Namarunu is primarily a Pliocene volcanic centre which has experienced relatively minor rhyolitic and trachytic activity during the Quaternary, the last phase of which has an age of 509 ± 5 ka. Widespread and voluminous eruption of basalt has occurred subsequently, the latest of which appears to be very young. This basaltic activity is dyke-related and is therefore unlikely to have accumulated a significant amount of heat, a supposition that is supported by the virtual lack of surface geothermal manifestations on Namarunu.

On the basis of the age and intensity of the youngest phases of trachytic volcanic activity, Emuruangogolak is likely to have the hottest heat source, followed by Silali and Paka. Kakorinya is unlikely to possess such a good high-level heat source, and the magmatic heat source of Korosi is undoubtedly cooler still. Chepchuk is ranked sixth on this criterion, although its source of heat is speculative, and Namarunu is again considered to be a very poor prospect. This ranking is the same as that derived from gas geothermometry, with the exception of Chepchuk, and is therefore considered to hold some validity. However, in terms of the size of heat sources, as gauged from caldera dimensions, Silali is likely to have a considerably larger source than Emuruangogolak and Kakorinya, and Paka would appear to have a relatively small source.

Taking all the above factors into consideration the following overall ranking of the main geothermal prospects of the region is proposed:

1 Silali
2 Emuruangogolak
3 Paka
4 Kakorinya
5 Korosi
6 Chepchuk

On balance there is little to choose between the first three prospects, and therefore from a purely geological point of view Silali, Emuruangogolak and Paka should be given approximately equal status in future exploration.

Silali is ranked first because it is considered to have the largest and the second most juvenile magmatic heat source, and geothermometry indicates a geothermal system with temperatures in excess of 300°C.

Although Emuruangogolak has the most vigorous and juvenile trachytic magmatic system and geothermometry indicates reservoir temperatures to be the highest in the region, it is ranked second because it is likely to have a smaller heat source than Silali.

Paka is ranked third because geothermometry indicates it has reservoir temperatures that are slightly lower than those for Emuruangogolak. It also appears to possess a less juvenile trachytic heat source than Emuruangogolak, and on the basis of caldera size this is likely to be smaller than the heat sources of both Silali and Emuruangogolak. Although Paka has the most vigorous and widespread surface geothermal activity this may be misleading in terms of its potential. Gas compositions suggest that the upflow zone is restricted to a small area in the caldera and hydrogeological considerations indicate that the outflow is to the north. The northern flanks of the volcano are strongly fractured and the extensive and relatively strong surface manifestations in this area may simply result from the efficient loss of steam above the outflow zone. In this respect Paka resembles Eburru in the Naivasha sector of the rift.

Kakorinya is ranked fourth because its youngest trachytic activity was significantly older than the youngest activity of Emuruangogolak, Silali and Paka. Furthermore, reservoir temperatures estimated by geothermometry are also noticeably lower than at these three centres.

On all criteria, except for the extent of surface activity, Korosi is clearly ranked fifth.

Chepchuk is ranked sixth because although it has similar surface geothermal activity to Korosi in terms of strength and temperature, the area of activity is of very limited extent. Although geothermometry for Chepchuk suggests slightly higher reservoir temperatures than at Korosi, the nature of the heat source at Chepchuk is obscure. Given the regional groundwater flow paths and the pattern of faulting, it is unlikely that the activity at Chepchuk is related to outflow from the geothermal systems of Korosi or Paka, and it should therefore be treated as a separate prospect in future exploration programmes.

The geothermal system of Namarunu is very weak indeed and virtually extinct. For these reasons it does not merit further attention as a geothermal prospect.

16.8 RECOMMENDATIONS FOR FUTURE EXPLORATION

Silali, Emuruangogolak and Paka are considered to be good geothermal prospects. Despite ranking them in that order, there is little to choose between these three prospects, especially considering the subjective nature of the overall ranking process. Therefore, from a purely geological point of view they should be given roughly equal status in any future exploration programme. Kakorinya and Korosi are poorer prospects, but are still considered worthy of further exploration. Limited exploration should also be undertaken at Chepchuk to try to ascertain the subsurface extent of its geothermal system.

Future exploration should concentrate on three broad aspects, as described in the paragraphs below.

Regional geophysical surveys should be undertaken to investigate aspects of the broad structure, with par-

ticular regard to testing and refining the volcano-tectonic models of the volcanic centres. As a priority, regional gravity and low-level aeromagnetic surveys should be carried out to investigate the nature of the regional dyke swarms and the form of intrusive bodies within the volcanic centres. Microseismic monitoring should also be undertaken in the Korosi-Emuruan-gogolak sector, to ascertain if the fracture zones linking these centres are still active and to investigate the current sense of any movement on these fractures. Microseismic monitoring may also prove to be useful in detecting zones of geothermal boiling (cf. Tongue and Maguire, in press), and may possibly provide information on the presence of residual melt zones within the intrusive bodies beneath the volcanic centres. With regard to the latter point, seismic tomographic studies should also be undertaken at the three main prospects to ascertain whether molten zones exist beneath each and to try to delimit the form of such zones.

Detailed geophysical surveys should also be carried out on individual prospects to delimit subsurface zones of geothermal activity and hydrothermal alteration as targets for exploratory drilling. Resistivity techniques with appropriate electrode configurations should be applied wherever possible, although the remoteness of the centres, their rough terrain, and their extensive cover of young lava fields are likely to place severe operational constraints on the application of these techniques. In view of this, magneto-telluric and transient electromagnetic surveys should also be carried out to augment resistivity surveys.

At present there is an acute shortage of information on the hydrogeological conditions under, or in proximity to, the main geothermal areas. Ideally, boreholes should be drilled to depths of at least a few hundred metres within the more accessible volcanic centres in the south. These could give information on depth to the water table, on temperature and heat flow, on rock permeability from hydraulic tests, and indications of vertical flow from hydraulic head measurements. The boreholes should be logged with standard down-hole geophysical techniques and could also provide fluid samples for chemical analysis. The information obtained from sampling and borehole tests would greatly improve knowledge of the geothermal systems underlying the volcanic centres. If boreholes encounter potable water they could be exploited as valuable water sources once geothermal research has been completed.

The ultimate objective of these proposed follow-up geophysical and hydrogeological investigations should be to delimit sites for the drilling of exploration geothermal wells at the most suitable prospects.

REFERENCES

ACRES. 1987. Kenya National Power Development Plan 1986–2006. Prepared for joint World Bank/UNDP energy sector management assistance program by Acres International Ltd.

ADAMS, B. 1977. A simple program for the calculation of soil moisture deficits and actual evapotranspiration. *British Geological Survey Hydrogeological Report*, WD/ST/77/5.

ALLEN, D J, and DARLING, W G. 1992. Geothermics and hydrogeology of the Kenya Rift Valley between Lake Baringo and Lake Turkana. *British Geological Survey Reasearch Report*, SD/92/1.

— — and BURGESS, W G. 1989. Geothermics and hydrogeology of the southern part of the Kenya Rift Valley with emphasis on the Magadi-Nakuru area. *British Geological Survey Research Report*, SD/89/1.

ARMANNSSON, H. 1987. Studies on the geochemistry of steam in the Suswa and Longonot areas and water in the Lake Magadi, Kedong Valley and Lake Turkana areas, Rift Valley, Kenya. Final Technical Report. Project KEN/82/002. United Nations Department of Technical Co-operation for Development.

ARNORSSON, S, and GUNNLAUGSSON, E. 1985. New gas geothermometers for geothermal exploration—calibration and application. *Geochimica et Cosmochimica Acta*, Vol. 49, 1307–1325.

BAILEY, D K, and COOPER, J P. 1978. Comparison of the crystallization of pantelleritic obsidian under hydrous and anhydrous conditions. *Great Britain Natural Environment Research Council Publication*, Series D, Vol. 11, 637–652.

— — and KNIGHT, J L. 1974. Anhydrous melting and crystallization of peralkaline obsidians. *Bulletin Volcanologique*, Vol. 38, 653-665.

BAKER, B H. 1963. The geology of the Baragoi area. *Report Geological Survey of Kenya*, No. 53.

— 1987. Outline of the petrology of the Kenya rift alkaline province. 293–311 in *Alkaline Igneous Rocks*. FITTON, J.G. and UPTON, B G J (editors). Geological Society Special Publication. No. 30.

— GOLES, G, LEEMAN W P, and LINDSTROM, M M. 1977. Geochemistry and petrogenesis of a basalt-benmoreite-trachyte suite from the southern part of the Gregory Rift, Kenya. *Contributions to Mineralogy and Petrology*, Vol. 64, 303–332.

— MOHR, P A, and WILLIAMS, L A J. 1972. Geology of the eastern rift system of Africa. *Geological Society of America, Special Paper*, 136, 1–67.

— and WHOLENBERG, J. 1971. Structure and evolution of the Kenya rift valley. *Nature*, Vol. 229, 538–542.

— WILLIAMS, L A J, MILLER, J A, and FITCH, F J. 1971. Sequence and geochronology of the Kenya rift volcanics. *Tectonophysics*, Vol. 11, 191–215.

BANKS, R J, and BEAMISH, D. 1979. Melting in the crust and upper mantle beneath the Kenya rift: evidence from geomagnetic deep sounding experiments. *Journal of the Geological Society of London*, Vol. 136, 225–233.

BARBERI, F, BIZOUARD, H, and VARET, J. 1971. Nature of the clinopyroxene and iron enrichment in alkalic and transitional basaltic magmas. *Contributions to Mineralogy and Petrology*, Vol. 33, 93–107.

— FERRARA, G, SANTACROCE, R, TREUIL, M, and VARET, J. 1975. A transitional basalt-pantellerite sequence of fractional crystallization, the Boina centre (Afar Rift, Ethiopia). *Journal of Petrology*, Vol. 16, 22–56.

BATTICCI, G. 1987. Thermal conditions of the central-southern sector of the Kenyan rift valley from the data collected in the boreholes drilled for water. Unpublished Report. Project KEN/82/002. United Nations Department of Technical Co-operation and Development. 42 pp.

BELLIENI, G E, VICENTIN, J, ZANETTIN, B, and PICIRILLO, E M. 1981. Oligocene transitional tholeiitic magmatism in northern Turkana (Kenya): comparison with coeval Ethiopian volcanism. *Bulletin Volcanologique*, Vol. 44, 411–427.

BETCHTEL, T D, FORSYTH, D W, and SWAIN, C J. 1987. Mechanisms of isostatic compensation in the vicinity of the East African Rift, Kenya. *Geophysical Journal of the Royal Astronomical Society*, Vol. 90, 445–465.

BLOOMER, S H, CURTIS, P C, and KARSON, J A. 1989. Geochemical variation of Quaternary basaltic volcanics in the Turkana rift, Kenya. *Journal of African Earth Sciences*, Vol. 8, 511–532.

BOSWORTH, W. 1989. Basin and Range style tectonics in East Africa. *Journal of African Earth Sciences*, Vol. 8, 19–201.

— LAMBIASE, J J, and KEISLER, J A. 1986. A new look at Gregory's rift. The structural style of continental rifting. *EOS, Transactions of the American Geophysical Union*, Vol. 67, 577–582.

— and MAURIN, A. 1993. Structure, geochronology and tectonic significance of the northern Suguta Valley (Gregory Rift), Kenya. *Journal of the Geological Society*, Vol. 150, 751–762.

— STRECKER, M R, and BLISNIUK, P M. 1992. Integration of East African paleostress and present-day stress data: implications for continental stress field dynamics. *Journal of Geophysical Research*, Vol. 97, 11,851–11,865.

BROWN, F H, and CARMICHAEL, I S E. 1971. Quaternary volcanoes of the Lake Rudolf region: II. The lavas of North Island, South Island and the Barrier. *Lithos*, Vol. 4, 305–323.

BURGESS, W G. 1986. Report on a visit 17 March to 26 April 1986. *British Geological Survey Report*, WD/OS/86/4.

BUTZER, K W. 1971. Recent history of an Ethiopian delta, the Omo river and the level of Lake Turkana. *Research Paper of the University of Chicago, Department of Geography*, No. 136, 184 pp.

— ISAAC, G L, RICHARDSON, J L, and WASHBOURN-KAMAU, C. 1972. Radiocarbon dating of East African lake levels. *Science*, Vol. 175, No. 4027, 1069–1076.

CAMPBELL SMITH, W. 1938. Petrographic description of volcanic rocks from Turkana, Kenya Colony, with notes on their field occurrence from the manuscript of Mr A. M. Champion. *Quarterly Journal of the Geological Society*, Vol. 94, 507–553.

CARNEY, J N. 1972. The geology of the area east of Lake Baringo, Rift Valley Province, Kenya. Unpublished PhD thesis, University of London.

— HILL, A, WALKER, A, and MILLER, J.A. 1971. Late Australopithecine from Baringo District, Kenya. *Nature*, Vol. 230, 509–514.

CASANOVA, J. 1986. Les stromatolites continentaux: paleoecologie, paleohydrologie, paleoclimatologie. Application au rift Gregory. PhD thesis. Universite D'Aix-Marseille.

CAVENDISH, H S H. 1898. Through Somaliland and south of Lake Rudolf. *Geographical Journal*, Vol. 85, 323–341.

CCG. 1987. Aeromagnetic survey, Tertiary Rift Valley. Prepared for the National Oil Coporation of Kenya by Compagnie Generale de Geophysique.

CHADWICK, W W, and HOWARD, K A. 1991. The pattern of circumferential and radial eruptive fissures on the volcanoes

of Fernandina and Isabela islands, Galapagos. *Bulletin Volcanologique*, Vol. 53, 259–275.

CHAMPION, A M. 1935. Teleki's volcano and the lava fields at the southern end of Lake Rudolf. *Geographical Journal*, Vol. 85, 323–341.

— 1937. The volcanic region around the southern end of Lake Rudolf, Kenya Colony. *Zeitschrift fur Vulkanologie*, Vol. 17, 163–172.

CHAPMAN, G R. 1971. The geological evolution of the northern Kamasia Hills, Baringo District, Kenya. Unpublished PhD thesis, University of London.

— (Compiler) 1973. Geological map of the Northern Tugen Hills. 1:125 000. (Nairobi: Government of Kenya).

— and BROOK, M. 1978. Chronostratigraphy of the Baringo Basin, Kenya. 207–223 in *Geological background to fossil man.* BISHOP, W W (editor). (Scottish Academic Press, Edinburgh).

CHAPMAN, G R, LIPPARD, S, and MARTYN, J E. 1978. The stratigraphy and structure of the Kamasia range, Kenya rift valley. Journal of the Geological Society of London, Vol. 135, 265–281.

CLAGUE, D A. 1978. The oceanic basalt-trachyte association: an explanation of the Daly gap. *Journal of Geology*, Vol. 86, 734–743.

CLARKE, M C G, WOODHALL, D G, ALLEN, D J, and DARLING, W G. 1990. Geological, volcanological and hydrogeological controls on the occurrence of geothermal activity in the area surrounding Lake Naivasha, Kenya. *Report of the Ministry of Energy of Kenya.*

CRAIG, H, LUPTON, J E, and HOROWITZ, R M. 1977. Isotopic geochemistry and hydrogeology of geothermal waters in the Ethiopian Rift Valley. Scripps Institute of Oceanography. Reference Number 77-14, University of California, San Diego.

DAGLEY, P, MUSSETT, A E, and PALMER, H C. 1978. Preliminary observations on the palaeomagnetic stratigraphy of the area west of Lake Baringo, Kenya. 225–235 in *Geological background to fossil man.* BISHOP, W W (editor). (Scottish Academic Press, Edinburgh).

DAHLHEIM, H-A, DAVIS, P, and ACHAUER, U. 1989. Teleseismic investigation of the East African Rift-Kenya. *Journal of African Earth Sciences*, Vol. 8, 461–470.

D'AMORE, F, and PANICHI, C. 1980. Evaluation of deep temperatures in hydrothermal systems by a new gas geothermometer. Geochimica et Cosmochimica Acta, Vol. 44, 549–556.

DARLING, W G, and ALLEN, D J. 1993. Geothermics and hydrogeology of the Turkana region of the Kenya Rift Valley. *British Geological Survey Reasearch Report*, WD/93/21.

— — and ARMANNSSON, H. 1990. Indirect detection of subsurface outflow from a Rift Valley lake. *Journal of Hydrology*, Vol. 113, 297–305.

— and ARMANNSSON, H. 1989. Stable isotopic aspects of fluid flow in the Krafla, Namafjall and Theistareykir geothermal systems of northeast Iceland. *Chemical Geology*, Vol. 76, 197–213.

DARLING, W G, and TALBOT, J C. 1991. Evaluation and development of gas geothermometry for geothermal exploration in the East African Rift System. British Geological Survey Technical Report, WD/91/72.

— — 1992. Hydrocarbon gas ratio geothermometry in the East African Rift System. 1441–1444 in *Water-Rock Interaction.* KHARAKA, Y K. and MAEST, A S (editors) (Balkema, Rotterdam).

DEINO, A, and POTTS, R. 1990. Single-crystal $^{40}Ar/^{39}Ar$ dating of the Olorgesailie Formation, Southern Kenya. *Journal of Geophysical Research*, Vol. 95, No.B6, 8453–8470.

DODSON, R G. 1963. Geology of the South Horr Area. *Report of the Geological Survey of Kenya*, No. 60.

DUNKLEMAN, T J, ROSENDAHL, B R, and KARSON, J A. 1989. Structure and stratigraphy of the Turkana rift from seismic reflection data. *Journal of African Earth Sciences*, Vol. 8, 489–510.

FAIRHEAD, J D. 1976. The structure of the lithosphere beneath the eastern rift, East Africa, deduced from gravity studies. *Tectonophysics*, Vol. 30, 269–298.

FERGUSON, A J D, and HARBOTT, B J. 1982. Geographical, physical and chemical aspects of Lake Turkana. 1–107 in *Lake Turkana: a report on the findings of the Lake Turkana project 1972–75.* HOPSON, A J (editor). Report for the Overseas Development Administration, London.

FOURNIER, R O. 1981. Application of water geochemistry to geothermal exploration and reservoir engineering. 109–143 in *Geothermal systems: principles and case histories.* RYBACH, L, and MUFFLER, L J P (editors) (Wiley, New York).

FUCHS, V E. 1934. The geological work of the Cambridge expedition to the East African Lakes, 1930–31. *Geological Magazine*, Vol. 71, 97–112.

— 1939. The geological history of the Lake Rudolf Basin, Kenya colony. *Philosophical Transactions of the Royal Society of London*, Vol. 229, 219–274.

GICHURU, S K. 1992. Address by the Managing Director, Kenya Power and Lighting Co. Ltd. to the Geothermal Resources Council. *Geothermal Resources Council Bulletin*, Vol. 21, 388–390.

GOLDEN, M. 1978. The geology of the area east of Silale, Rift Valley Province, Kenya. Unpublished PhD thesis, University of London.

GREEN, V W, ACHAUER, U, and MEYER, R P. 1991. A three-dimensional seismic image of the crust and upper mantle beneath the Kenya rift. *Nature*, Vol, 354, 199–203.

GRIFFITHS, P S. 1977. The geology of the area around Lake Hannington and the Perkerra river, Rift Valley Province, Kenya. Unpublished PhD thesis, University of London.

GRIFFITHS, D H, KING, R F, KHAN, M A, and BLUNDELL, D J. 1971. Seismic refraction line in the Gregory Rift. *Nature*, Vol. 229, 66–71.

HACKMAN, B D. 1988. The geology of the Baringo–Laikipia area. *Report of the Mines and Geology Department of Kenya*, No. 104.

HAY, D E, and WENDLANDT, R F. 1992. Experimental results bearing on the origin of Kenyan Rift flood phonolites. *EOS, Transactions American Geophysical Union*, Vol. 73, Part 14, 337.

HENRY, W J, MECHIE, J, MAGUIRE, P K H, KHAN, M A, PRODEHL, C, KELLER, G R, and PATEL, J. 1990. A seismic investigation of the Kenya Rift Valley. *Geophysical Journal International*, Vol. 100, 107–130.

HILLAIRE-MARCEL, C, CARRO, O, and CASANOVA, J. 1986. ^{14}C and Th/U dating of Pleistocene and Holocene stromatolites from East African paleolakes. *Quaternary Research*, Vol. 25, 312–329.

HOEFS, J. 1987. Stable isotope geochemistry. (Springer Verlag, Berlin).

JAVOY, M, PINEAU, F, STAUDACHER, T, CHEMINEE, J L, and KRAFT, M. 1989. Mantle volatiles sampled from a continental rift: The 1988 eruption of Oldoinyo Lengai (Tanzania). *Terra Abstracts*, Vol. 1, No. 1, 324.

JOHNSON, T C, HALFMAN, J D, ROSENDAHL, B R, and LISTER, G S. 1987. Climatic and tectonic effects on sedimentation in a rift valley lake: evidence from high resolution seismic profiles, Lake Turkana, Kenya. *Bulletin of the Geological Society of America*, Vol. 98, 439–447.

JONES, W B. 1979. Mixed benmoreite/trachyte flows from Kenya and their bearing on the Daly gap. *Geological Magazine*, Vol. 116, 487–489.

— 1988. Listric growth faults in the Kenya rift valley. *Journal of Structural Geology*, Vol. 10, 661–672.

KARSON, J A, and CURTIS, P C. 1989. Tectonic and magmatic processes in the eastern branch of the East African Rift and implications for magmatically active continental rifts. *Journal of African Earth Sciences*, Vol. 8, 431–453.

KARSON, J A, and CURTIS, P C. 1990. Quaternary volcanic centres of the Turkana rift, Kenya. *Open file report of the Mines and Geology Department of Kenya.*

KELLER, R G, BRAILE, L W, DAVIS, P M, MEYER, R P, and MOONEY, W D. 1992. Kenya Rift International Seismic Project, 1989–1990 experiment. *EOS, Transactions of the American Geophysical Union*, Vol. 73, No. 33, 345–351.

KEMP, S J. 1989. X-ray diffraction studies of alteration/sinter samples from the Kenyan Rift Valley. *Mineral Sciences Brief Report, British Geological Survey.*

— 1990. Mineralogy and petrology of further alteration and sinter samples from the Rift Valley, Kenya. *British Geological Survey Technical Report*, WG/90/2R.

KEY, R M. 1987. The geology of the Maralal area. *Report of the Mines and Geology Department of Kenya*, No. 105.

— and WATKINS, R T. 1988. The geology of the Sabarei area. *Report of the Mines and Geology Department of Kenya*, No. 111.

KHAN, M A, and MANSFIELD, J. 1971. Gravity measurements in the Gregory Rift. *Nature*, Vol. 229, 72–75.

—and SWAIN, C J. 1978. Geophysical investigations and the rift valley geology of Kenya. 71–83 in *Geological background to fossil man.* BISHOP, W W (editor). (Scottish Academic Press, Edinburgh).

KING, B C. 1978. Structural Evolution of the Gregory rift valley. 29–54 in *Geological background to fossil man.* BISHOP, W.W. (editor). (Scottish Academic Press, Edinburgh).

KRISP WORKING GROUP. 1987. Structure of the Kenya rift from seismic refraction. *Nature*, Vol. 325, 239–242.

— 1991. Large-scale variation in lithospheric structures along and across the Kenya rift. *Nature*, Vol. 354, 223–227.

LATIN, D, NORRY, M J, and TARZEY, R J E. In press. Magmatism in the Gregory Rift, East Africa: evidence for melt generation by a plume. *Journal of Petrology.*

LE BAS, M J, LE MAITRE, R W, STREKEISEN, A, and ZANETTIN, B. 1986. A chemical classification of volcanic rocks based on the total alkali-silica diagram. *Journal of Petrology*, Vol. 27, 745–750.

LIPPARD, S J. 1972. The stratigraphy and structure of the Elgeyo escarpment, southern Kamasia hills and adjoining region, Rift Valley Province, Kenya. Unpublished PhD thesis. University of London.

MACDONALD, R. 1974. Nomenclature and petrochemistry of the peralkaline oversaturated extrusive rocks. *Bulletin Volcanologique*, Vol. 38, 498–516.

— 1987. Quaternary peralkaline silicic rocks and caldera volcanoes of Kenya. 313–333 in *Alkaline Igneous Rocks.* FITTON, J.G. and UPTON, B.G.J. (editors). Geological Society Special Publication, No. 30.

— In press. Petrological evidence regarding the evolution of the Kenya Rift Valley. *Tectonophysics.*

— WILLIAMS, L A J, and GASS, I G. In press. Tectonomagmatic evolution of the Kenya Rift Valley: some geological perspectives. *Journal of the Geological Society.*

MAHOOD, G A. 1984. Pyroclastic rocks and calderas associated with strongly peralkaline magmatism. *Journal of Geophysical Research*, Vol. 89, 8540–8552.

— and BAKER, D R. 1986. Experimental constraints on depths of fractionation of mildly alkalic basalts and associated felsic rocks: Pantelleria, Strait of Sicily. *Contributions to Mineralogy and Petrology*, Vol. 93, 251–264.

MAKINOUCHI, T, KOYAGUCHI, T, MATSUDA, T, MITSUSHIO, H, and ISHIDA, S. 1984. Geology of the Nachola area and the Samburu Hills, west of Baragoi, Northern Kenya. *African Study Monographs.* Supplementary Issue 2, 15–44.

MARTYN, J E. 1969. The geological history of the country between Lake Baringo and the Kerio River, Baringo District, Kenya. Unpublished PhD thesis, University of London.

MATSUDA, T, TORII, M, KOYAGUCHI, T, MAKINOUCHI, T, MITSUSHIO, H, and ISHIDA, S. 1984. Fission-track, K-Ar age determinations and palaeomagnetic measurements of Miocene volcanic rocks in the western area of Baragoi, Northern Kenya: Ages of hominoids. *African Study Monographs.* Supplementary Issue 2, 57–66.

MCBIRNEY, A R, BAKER, B H, and NILSON, R H. 1985. Liquid fractionation. Part 1: basic principles and experimental simulations. *Journal of Volcanology and Geothermal Research*, Vol. 24, 1–23.

MCCALL, G J H. 1968a. Silali, another major caldera volcano in the rift valley of Kenya. *Proceedings of the Geological Society of London*, No. 1644, 267.

— 1968b. The five caldera volcanoes of the central Rift Valley in Kenya. *Proceedings of the Geological Society of London*, No. 1647, 54–59.

— 1970. Gabbroic and ultramafic nodules: high level intracrustal nodular occurrences in alkalic basalts and associated volcanics from Kenya, described and compared with those of Hawaii. *Physics of the Earth and Planetary Interiors.* Vol. 3, 255–272.

— and HORNUNG, G. 1972. A geochemical study of Silali volcano, Kenya, with special reference to the origin of the intermediate-acid eruptives of the central Rift Valley. *Tectonophysics*, Vol. 15, 97–113.

MCCLENAGHAN, M P. 1972. The geology of the Ribkwo area, Baringo District, Kenya. Unpublished PhD thesis, University of London.

MOHR, P. 1987. Structural style of continental rifting in Ethiopia:reverse decollements. *EOS, Transactions of the American Geophysical Union*, Vol 68, 721, 729, 730.

— and WOOD, C A. 1976. Volcano spacings and lithopsheric attenuation in the Eastern Rift of Africa. *Earth and Planetary Science Letters*, Vol.33, 126–144.

MORGAN, P. 1973. Terrestrial heat flow studies in Cyprus and Kenya. Unpublished PhD thesis, University of London.

MORLEY, C K, WESCOTT, W A, STONE, D M, HARPER, R M, WIGGER, S T, and KARANJA, F M. 1992. Tectonic evolution of the northern Kenyan rift. *Journal of the Geological Society*, Vol. 149, 333–348.

MOSLEY, P N. 1993. Geological evolution of the Late Proterozoic 'Mozambique Belt' of Kenya. *Tectonophysics*, Vol. 221, 223–250.

NORDLIE, B E. 1973. Morphology and structure of the western Galapagos volcanoes and a model for their origin. *Bulletin of the Geological Society of America*, Vol. 84, 2931–2956

NORRY, M J, TRUCKLE, P H, LIPPARD, S J, HAWKESWORTH, C J, WEAVER, S D, and MARRINER, G F. 1980. Isotopic and trace element evidence from lavas, bearing on mantle heterogeneity beneath Kenya. *Philosophical Transactions of the Royal Society of London*, Vol. A297, 259–271.

NYBLADE, A A, POLLACK, H N, JONES D L, PODMORE, F, and MUSHAYANDEBU, M. 1990. Terrestial heat flow in East and Southern Africa. *Journal of Geophysical Research*, Vol. 95, 17371–17384.

OCHIENG', J O, WILKINSON, A F, KAGASI, J, and KIMOMO, S. 1988. Geology of the Loiyangalani area. *Report of the Mines and Geological Department of Kenya*, No. 107.

OPHEIM, J A, and GUDMUNDSSON, A. 1989. Formation and geometry of fractures, and related volcanism, of Krafla fissure swarm, northeast Iceland. *Bulletin of the Geological Society of America*, Vol. 101, 1608–1622.

PANICHI, C, FERRARA, G C, and GONFIANTINI, R. 1975. Isotope geothermometry in the Lardarello geothermal field. *Geothermics*, Vol. 5, 81–88.

PENMAN, H L. 1949. The dependence of transpiration on weather and soil conditions. *Journal of Soil Science*, Vol. 1, 74–89.

PICKFORD, M, ISHIDA, H, NAKANO, Y, and NAKAYA, H. 1984. Fossiliferous localities of the Nachola-Samburu Hills area, Northern Kenya. *African Study Monographs*, Supplementary Issue 2, 45–56.

POINTING, A J, MAGUIRE, P K H, KHAN, M A, FRANCIS, D J, SWAIN, C J, SHAH, E R, and GRIFFITHS, D H. 1985. Seismicity of the northern part of the Kenya Rift Valley. *Journal of Geodynamics*, Vol. 3, 23–37.

RHEMTULLA, S. 1970. A geological reconnaissance of South Turkana. *Geographical Journal*, Vol. 136, 61–73.

ROSENDAHL, B R, KILEMBE, E, and KACZMARICK, K. 1992. Comparison of the Tanganyika, Malawi, Rukwa and Turkana rift zones from analyses of seismic reflection data. *Tectonophysics*, Vol. 213, 235–256.

RUNDLE, C C. 1991. Potassium-Argon dating of trachyte lavas from the Emuruagiring Plateau, Kenya Rift Valley. *Report of the Natural Environment Research Council Isotope Geosciences Laboratory*, No. NIGL/26.

RYAN, M P. 1990. The physical nature of the Icelandic magma transport system. 175–224 in *Magma transport and storage*. RYAN, M P (editor). (John Wiley and Sons, Chichester).

SAVAGE, J E G, and LONG, R E. 1985. Lithopsheric structure beneath the Kenya dome. *Geophysical Journal of the Royal Astronomical Society*, Vol. 82, 461–477.

SCEAL, J S C. 1974. The geology of Paka volcano and the country to the east, Baringo District, Kenya. Unpublished PhD thesis, University of London.

— and WEAVER, S D. 1971. Trace element data bearing on the origin of salic rocks from the Quaternary volcano Paka, Gregory Rift, Kenya. *Earth and Planetary Science Letters*, Vol. 12, 327–331.

SELF, S, and GUNN, B M. 1976. Petrology, volume and age relations of alkaline volcanics from Terceira, Azores. *Contributions to Mineralogy and Petrology*, Vol. 54, 293–313.

SHACKLETON, R M. 1946. Geology of the country between Nanyuki and Maralal. *Report of the Geological Survey of Kenya*, No. 11.

SHOTTON, F, WILLIAMS, R E, and JOHNSON, A S. 1974. Birmingham University radiocarbon dates viii. *Radiocarbon*, Vol. 16, 285–303.

SIGURDSSON, H, and SPARKS, R S J. 1978. Lateral magma flow within rifted Icelandic crust. *Nature*, Vol. 274, 126–130.

SIMKIN, T. and HOWARD, K A. 1970. Caldera collapse in the Galapagos Islands, 1968. *Science*, Vol. 169, 429–437.

SKINNER, N J, ILES, W, and BROCK, A. 1975. The recent secular variation of declination and inclination in Kenya. *Earth and Planetary Science Letters*, Vol. 25, 338–346.

SMITH, M, and MOSLEY, P N. 1993. Crustal heterogeneity and basement influence on the development of the Kenya Rift, East Africa. *Tectonics*. Vol. 12, 591–606.

STRECKER, M R, BLISNIUK, P M, and EISBACHER, G H. 1988. Rotation of extension direction in the central Kenyan rift. *Geology*, Vol. 18, 299–302.

STURCHIO, N C. and BINZ, C M. 1988. Uranium-series age determination of calcite veins, VC-1 drill core, Valles caldera, New Mexico. *Journal of Geophysical Research*, Vol. 93, No. B6, 6097–6102.

— DUNKLEY, P N, and SMITH, M. 1993. Climate-driven variations in geothermal activity in the northern Kenya rift valley. *Nature*, Vol. 362, 233–234.

SWAIN, C J. 1976. Some gravity results from the northern Gregory Rift. 120–125 in Afar between continental and oceanic rifting. PILGER, A. and ROSSLER, A (editors). (Schweizerbart'sche, Stuttgart).

— 1979. Gravity and seismic measurements in Kenya. Unpublished PhD. thesis, University of Leicester.

— 1992. The Kenya rift axial gravity high: a re-interpretation. *Tectonophysics*, Vol. 204, 59–70.

— KHAN, M A, WILTON, T J, MAGUIRE, P K H, and GRIFFITHS, D H. 1981. Seismic and gravity surveys in the Lake Baringo–Tugen Hills area, Kenya Rift Valley. *Journal of the Geological Society*, Vol. 138, 93–102.

TATSUMI, Y, and KIMURA, N. 1991. Secular variation of basalt chemistry in the Kenya Rift: evidence for the pulsing of asthenospheric upwelling. *Earth and Planetary Science Letters*, Vol. 104, 99–113.

TEN BRINK, U S. 1991. Volcano spacing and plate rigidity. *Geology*, Vol. 19, 397–400.

THOMPSON, R C. 1991. Kenya geothermal prospects. Report of Unocal Geothermal Division, (Santa Rosa: Unocal Company Report)

TIERCELIN, J-J, and VINCENS, A. 1987. Le demi-graben de Baringo-Bogoria, Rift Gregory, Kenya. 30 000 ans d'histoire hydrologique et sédimentaire. *Bulletin Centres Recherche Exploration-Production, Elf Aquitaine*, Vol. 11, Part 2, 249–540.

TONGUE, J A, and MAGUIRE, P K H. In press. An earthquake study in the Lake Baringo Basin of the central Kenya Rift. *Tectonophysics*.

TRUCKLE, P H. 1976. Geology and late Cainozoic lake sediments of the Suguta Trough, Kenya. *Nature*, Vol. 263, 380–383.

— 1977a. The geology of the area to the south of Lokori, South Turkana, Kenya. Unpublished PhD thesis, University of Leicester.

— (Compiler). 1977b. Geological map of the Lake Baringo–Laikipia area. (Nairobi: Government of Kenya.)

— (Compiler). 1979a. Geological map of the Kapedo and Emuruangogolak area. (Nairobi: Government of Kenya.)

— (Compiler). 1979b. Geological map of the Southern Loriu area. (Nairobi: Government of Kenya.)

UPTON, B G J, and EMELEUS, C H. 1987. Mid-Proterozoic alkaline magmatism in southern Greenland: the Gadar province. 449–471 in Alkaline Igneous Rocks. FITTON, J.G. and UPTON, B G J (editors). Geological Society Special Publication. No. 30.

VON HÖNEL, L. 1894. *Discovery of Lakes Rudolf and Stephanie. Vol. II.* (London: Longmans Green & Co.)

WAGNER, M, ALTHERR, R, and VAN DEN HAUTE, P. 1992. Apatite fission-track analysis of Kenyan basement rocks: constraints on the thermotectonic evolution of the Kenya Dome. A reconnaissance study. *Tectonophysics*, Vol. 204, 93–110.

WEAVER, S D. 1973. The geology of the Nasaken area of the Rift Valley, South Turkana, Kenya. Unpublished PhD thesis, University of London.

— 1977. The Quaternary caldera volcano Emuruangogolak, Kenya Rift, and the petrology of a bimodal ferrobasalt-pantelleritic trachyte association. *Bulletin Volcanologique*, Vol. 40, 209–230.

— SCEAL, J S C, and GIBSON, I. 1972. Trace element data relevant to the origin of trachytic and pantelleritic lavas in the East African Rift System. *Contributions to Mineralogy and Petrology*, Vol. 36, 181–194.

WEBB, P K. 1971. The geology of the Tiati Hills, Rift Valley Province, Kenya. Unpublished PhD thesis, University of London.

— and WEAVER, S D. 1975. Trachyte shield volcanoes: a new volcanic form from South Turkana, Kenya. *Bulletin Volcanologique*, Vol. 39, 294–312.

WELBY, M S. 1900. King Menelek's dominion and the country between Lake Gallop (Rudolf) and the Nile Valley. *Geographical Journal*, Vol. 16, 292–306.

WELHAN, J A, and LUPTON, J E. 1987. Light hydrocarbon gases in Guaymas Basin hydrothermal fluids: Thermogenic versus abiogenic origin. *American Association of Petroleum Geologists*, Vol. 71, No. 2, 215–223.

WHEILDON, J, MORGAN, P, WILLIAMSON, K H, EVANS, T R, and SWANBERG, C A. In press. Heat flow in the Kenya Rift zone. *Tectonophysics*.

WILKINSON, A F. 1988. The geology of the Allia Bay area. *Report of the Mines and Geology Department, Kenya*, No. 109.

WILLIAMS, L A J. 1978. Character of Quaternary volcanism in the Gregory Rift Valley. 55–69 in *Geological background to fossil man*. BISHOP, W W (editor). (Scottish Academic Press, Edinburgh).

— and CHAPMAN, G R. 1986. Relationships between major structures, salic volcanism and sedimentation in the Kenya rift from the equator northwards to Lake Turkana. 59–74 in *Sedimentation in the African rifts*. FROSTICK, L E, RENAUT, R W, REID, I, and TIERCELIN, J J (editors). Special publication of the Geological Society, No. 25.

— MACDONALD, R, and CHAPMAN, G R. 1984. Late Quaternary caldera volcanoes of the Kenya Rift Valley. *Journal of Geophysical Research*, Vol. 89, No. B10, 8553–8570.

WORTHINGTON, E B. 1932. Scientific results of the Cambridge Expedition to the East African lakes, 1930–31. *Journal of the Linn. Society Zool.*, Vol. 38, 99–119.

WRAP (Water Resource Assessment Project). 1987a. Water resource assessment study in Baringo District. *Water Resource Assessment Division Report*. Ministry of Water Development, Nairobi, Kenya.

— 1987b. Water resource assessment study in Laikipia District. *Water Resource Assessment Division Report*. Ministry of Water Development, Nairobi, Kenya.

WRIGHT, E P, and GUNSTON, H (editors). 1988. The Chyulu Hills Water Resources Study, Kenya: 1984–1987. *British Geological Survey Technical Report*, WD/88/5C.

YOUNG, P A V, MAGUIRE, P K H, EVANS, J R, and LAFOLLEY, D D'A. 1991. Implications of the distribution of seismicity near Lake Bogoria in the Kenya Rift. *Geophysical Journal International*, Vol. 105, 665–674.

Yuretich, R F, and Cerling, T E. 1983. Hydrogeochemistry of Lake Turkana, Kenya: mass balance and mineral equilibria in an alkaline lake. *Geochimica et Cosmochimica Acta*, Vol. 47, 1099–1109.

SKETCH SECTIONS OF THE GEOLOGY OF SILALI CALDERA

(Drawn from oblique 35mm transparencies and photographs. Scales are approximate)
Vertical scale = horizontal scale

A. SOUTH WALL

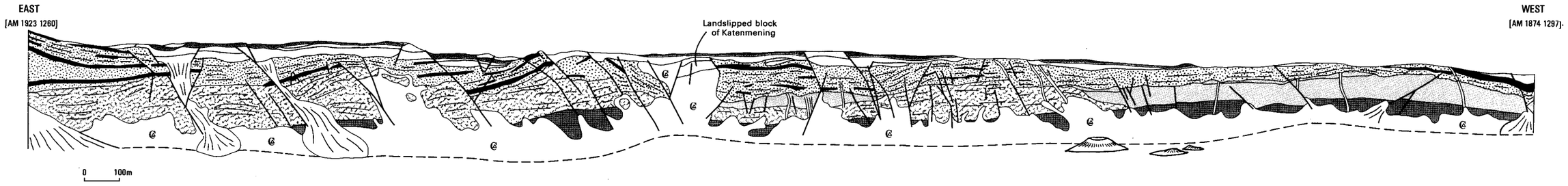

B. NORTH WALL

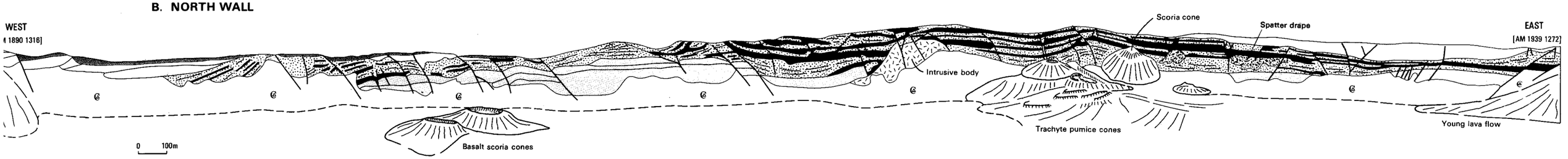

C. WEST WALL

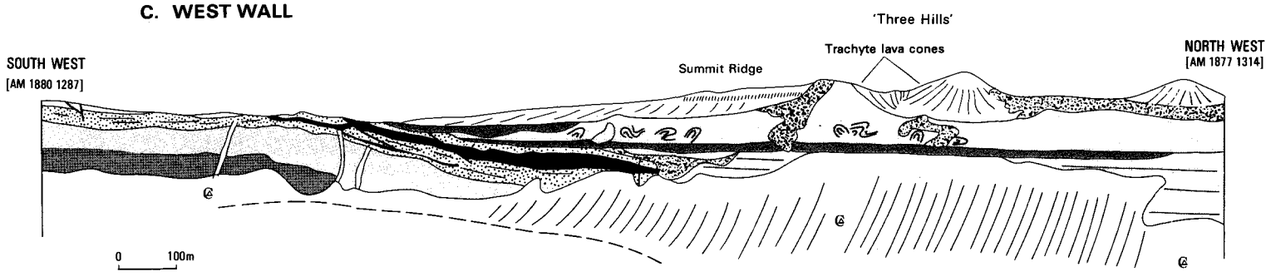

D. EAST WALL AND FAULTED PLATFORM

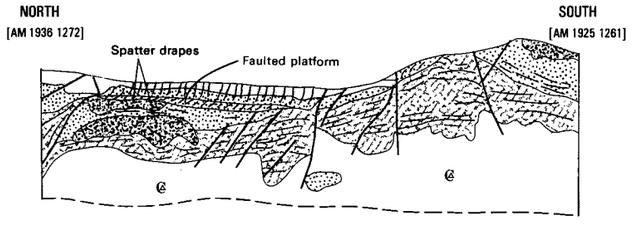

Intermediate Lavas

Lower Pyroclastic Deposits

Lower Trachyte Lavas

Katenmening Basalts

Katenmening Trachytes

Upper Pyroclastic Deposits

Scree and solifluction deposits

Basaltic spatter

Welded pyroclastic deposits including air-fall tuffs and pyroclastic flows

Fault

Dyke

Flow-fold

Location map